



Elucidating the Role of TGF β
Signalling in Drug Resistant Hh Driven
Cancers

Huw Morgan

Thesis submitted for the award of PhD

21st May 2018



CANCER
RESEARCH
WALES

Table of Contents

Table of Contents.....	i
Abstract.....	vii
Acknowledgements.....	ix
Declaration	x
List of Abbreviations	xi
Table of Figures.....	xv
Table of Tables.....	xix
Chapter 1 Introduction	2
1.1 Hallmarks of Cancer	2
1.1.1 Sustaining proliferative signalling	3
1.1.2 Evading growth suppressors	4
1.1.3 Resisting cell death	5
1.1.4 Enabling replicative immortality	6
1.1.5 Inducing Angiogenesis	7
1.1.6 Activating invasion and metastasis	8
1.1.7 Genome instability and mutation.....	9
1.1.8 Tumour-promoting inflammation	9
1.1.9 Reprogramming energy metabolism	10
1.1.10 Evading immune destruction.....	11
1.1.11 Therapeutic targeting.....	12
1.2 Cancer Driver Mutations.....	13
1.3 Targeted Therapies.....	18
1.3.1 BCR-ABL.....	20
1.3.2 Epidermal growth factor receptors	21
1.3.3 B-RAF.....	23
1.3.4 Hedgehog (see section 1.4)	24
1.3.5 Other targeted therapies	24
1.3.5.1 Epigenetic modification.....	25
1.3.5.2.....	25
Anti-angiogenesis therapy.....	25
1.3.5.3 Stress Response.....	26
1.3.5.4 Proteasome inhibitors.....	26
1.3.5.5 mTOR inhibitors	27
1.4 Hedgehog Pathway	28
1.4.1 Smoothened phosphorylation.....	28
1.4.1.1 Signalling downstream of mammalian SMO	29
1.4.1.2 Hedgehog signalling occurs in the primary cilium.....	32
1.4.2 Hh pathway physiological function	33
1.4.3 Hh pathway in cancer	36
1.4.4 Basal cell nevus (Gorlins) syndrome	39

1.4.5	Prototypic cancer: Basal Cell Carcinoma	39
1.4.5.1	Epidemiology.....	41
1.4.5.2	Pathogenesis.....	43
1.4.5.3	Molecular landscape of BCC.....	44
1.4.5.4	Management.....	45
1.4.5.4.1	Surgery.....	45
1.4.5.4.2	Topical Therapies.....	46
1.4.5.4.3	Radiotherapy.....	46
1.4.5.4.4	Photodynamic Therapy (PDT).....	47
1.4.6	Development of Hh antagonists	47
1.4.6.1	Natural Compounds (Alkaloids, sesquiterpenes and physalins).....	47
1.4.6.2	Synthetic Compounds.....	47
1.4.7	Development of resistance to Hh antagonists.....	49
1.4.7.1	Transformation of BCC into more aggressive phenotypes.....	49
1.5	Stem Cells	50
1.5.1	Haematopoietic SCs and Leukaemia initiating cells	51
1.5.3	Cancer Stem Cells and tumour heterogeneity	56
1.5.4	Clonal versus cancer Stem Cell theories	57
1.5.5	Cancer stem cells in solid malignancies	59
1.5.6	Keratinocyte cancer Stem Cells	61
1.5.7	Lineage tracing and lineage ablation of cancer stem cells	65
1.5.8	Cancer stem cells as mediators of drug resistance	66
1.5.9	Limitations of the cancer stem cell theory	68
1.5.9.1	Xenograft models.....	68
1.5.9.2	Stem cell and cancer stem cell plasticity.....	69
1.6	TGFβ Signalling Pathway	70
1.6.1	TGFβ Growth Factor Signalling Pathway	70
1.6.1.1	TGF β ligands and receptors.....	70
1.6.1.2	Mechanisms of receptor and SMAD activation/SMAD-dependent TGF β signalling.....	73
1.6.1.3	Target gene activation by SMADs.....	77
1.6.2	Non-canonical TGFβ Signalling	78
1.6.2.1	TGF β induced Erk activation and tyrosine phosphorylation.....	78
1.6.2.2	TGF β induced JNK/p38 activation.....	79
1.6.2.3	Rho-like GTPases in TGF β signalling.....	80
1.6.2.4	TGF β induced PI3K/Akt pathway activation.....	80
1.6.3	SMAD-dependent TGFβ signalling, independent of TGFβ receptor-ligand interactions	81
1.6.3.1	Cyclin-dependent kinases (CDKs).....	81
1.6.3.2	Mitogen-activated protein kinases (MAPK).....	82
1.6.3.3	Phosphoinositide 3-kinases (PI3K).....	83
1.6.3.4	Glycogen synthase kinase-3 (GSK-3).....	83
1.6.3.5	Rho-associated protein kinase (ROCK).....	84
1.6.4	Context dependent signal readout	84
1.6.5	Role of TGFβ signalling under physiological conditions	86
1.6.5.1	Embryonic development and homeostasis.....	86
1.6.5.1.1	Early Development: Axis Formation, and Patterning.....	86

1.6.5.1.2	Germ-Layer Specification, Patterning, and Gastrulation	87
1.6.5.1.3	Left-Right (L-R) Asymmetry.....	88
1.6.5.1.4	Organogenesis and Developmental Disease.....	88
1.6.5.2	Cell cycle progression and apoptosis	89
1.6.5.3	Epithelial-Mesenchymal Transition.....	90
1.6.6	TGFβ signalling in cancer	91
1.6.6.1	Points of disruption in the TGF β pathway in cancer	91
1.6.6.2	Tumourigenic Effects of TGF β : Tumour Growth, Invasion, and Immune Evasion	92
1.6.6.3	Epithelial-Mesenchymal Transition.....	92
1.6.6.4	Loss of TGF β mediated G ₁ arrest in cancer	93
1.6.6.5	Myofibroblast Generation.....	94
1.6.6.6	Production of Autocrine Mitogens.....	95
1.6.6.7	Evasion of Immunity.....	96
1.6.7	Changes in TGFβ and SMAD Protein Expression During Mouse Skin Carcinogenesis	97
1.6.8	Role of TGFβ signalling in Basal cell carcinoma.....	98
1.6.9	Crosstalk between the TGFβ and Hh signalling pathways.....	99
1.6.10	Role of TGFβ signalling in CSC.....	101
1.7	Aims and Objectives.....	106
Chapter 2	Materials and Methods	109
2.1	Human tissue Sample.....	109
2.1.1	Tissue Freezing and Cryosectioning.....	109
2.1.2	Tissue Dissociation.....	110
2.2	Cell Culture.....	111
2.2.1	Established Cell Lines	111
2.2.1.1	HaCaT	112
2.2.1.2	NIH-3T3	112
2.2.1.3	DAOY and UW228-2	112
2.2.1.4	SJSA-1	113
2.2.1.5	NIH3T3 (transduced with GLI-reporter construct)	113
2.2.2	Maintenance of Cell Lines	114
2.2.3	Sub-Culturing Cell Lines.....	115
2.2.4	Cryopreserving Cell Lines for Storage	116
2.2.5	Primary Cell Culture	116
2.2.5.1	BCC Cell Culture.....	116
2.3	Nucleic Acid Analysis.....	117
2.3.1	Gene Expression Analysis.....	117
2.3.2	RNA Extraction.....	117
2.3.2.1	BCC Tissue Samples	117
2.3.2.2	Cultured Cells	117
2.3.2.3	Homogenisation of Flow Sorted Cells	117
2.3.2.4	RNA Extraction	118
2.3.2.5	RNA Extraction from Flow Sorted Cells	118
2.3.3	Determination of RNA Quality	118
2.3.4	Preparation of cDNA for Quantitative Analysis.....	119

2.3.5	Quantitative real-time PCR (qPCR)	119
2.3.5.1	Gene Expression Analysis of qPCR Data	120
2.3.6	DNA Extraction	123
2.3.7	Microarray	123
2.3.7.1	RNA extraction	123
2.3.7.2	Determination of RNA quality	124
2.3.7.3	RNA amplification/cDNA library preparation	124
2.3.7.4	Applying samples to microarray chip	124
2.3.7.6	Bioinformatics analysis of the data	127
2.4	Cell Based Functional Assays	127
2.4.1	Cell Viability	128
2.4.1.1	Cell Titer Glo	128
2.4.2	Tumoursphere Forming Assay	128
2.4.3	Colony Forming Assay	129
2.4.4	siRNA transfection	130
2.4.5	Flow Cytometry and Cell Sorting	131
2.4.6	Annexin V apoptosis assay	131
2.4.7	GLI Reporter Experiments	133
2.4.7.1	Functional Validation and Luciferase Assay Performance	133
2.5	Tissue Analysis	134
2.5.1	Immunofluorescence on Frozen Tissue Sections	134
2.5.2	Immunofluorescent antibody labelling of Cultured Cells	135
2.6	Protein analysis	136
2.6.1	Protein Extraction	136
2.6.1.1	Total Cellular Proteins	136
2.6.1.2	Nuclear and Cytoplasmic Extracts	136
2.6.2	Quantifying protein concentration	138
2.6.2.1	BCA	138
2.6.2.2	Bradford	138
2.6.3	Western Blotting	139
2.6.3.1	Sample Preparation	140
2.6.3.2	SDS-PAGE	140
2.6.3.3	Western Transfer to Membrane	140
2.6.3.4	Confirming Protein Transfer	141
2.6.3.5	Blocking and Antibody Incubation	141
2.6.3.6	Detection	142
2.6.3.7	Stripping and Re-probing the Membrane	142
2.6.3.8	Quantitation by Densitometry	142
2.7	Statistical analysis	143
Chapter 3	Determination of TGFβ Signalling in Human Basal Cell Carcinoma	146
3.1	Introduction	146
3.2	Results	148
3.2.1	Microarray analysis of BCC identifies TGFβ signalling.	148
3.2.2	Volcano plots highlight the most significant genes within BCC	149
3.2.3	Unsupervised Clustering separates samples by disease status	154

3.2.4	Identifying differentially regulated pathways enriched in BCC	159
3.2.5	Identification of a TGF β responsive gene set panel	166
3.2.6	Determination of TGF β signalling in basal cell carcinoma	169
3.2.7	TGF β Signalling was not associated with proliferation.....	175
3.2.8	Analysis of EMT related gene expression in whole BCC tissue	177
3.2.9	Expression of TGF β pathway in BCC	179
3.3	Discussion	182
Chapter 4	Determination of TGF β Signalling in Human BCC CSC.....	190
4.1	Introduction.....	190
4.2	Results	191
4.2.1	CD200+ BCC cells are pSMAD3 positive in tissue sections.....	191
4.2.2	Isolation of CD200+ BCC cancer SCs by flow sorting.....	192
4.2.3	CD200 Expressing BCC CSCs are pSMAD3 positive	194
4.2.4	Obtaining RNA from low numbers of flow sorted cells	196
4.2.5	CD200 Expressing CSC Display EMT Gene Signature	197
4.3	Discussion	199
Chapter 5	Hedgehog and TGF β Pathway Antagonists in Hedgehog Driven Tumours 203	
5.1	Introduction	203
5.2	Results	207
5.2.1	Hedgehog agonist dose response curves	207
5.2.2	Hedgehog antagonist dose response curves.....	209
5.2.3	Identifying genes that are Hh regulated within Hh driven tumour cell lines 213	
5.2.4	Apoptosis after Hh antagonists	217
5.2.5	Hh antagonists in 2D culture do not reduce cell viability	222
5.2.6	Effect of Hh antagonist on 2D colony forming efficiency.....	224
5.2.7	Effect of Hh antagonist on 3D tumoursphere forming units.....	226
5.2.9	Hh antagonists induce SMAD3 phosphorylation and regulate TGF β gene expression.....	232
5.2.10	Blocking TGF β signalling.....	237
5.2.11	Effect of Blocking TGF β Signalling on Hh-regulated Genes in Hh Driven Tumours.....	240
5.2.12	Apoptosis after blocking TGF β signalling	243
5.2.13	Effect of Blocking TGF β signalling on cell viability.....	247
5.2.14	Effect of TGF β blockade on 2D colony formation	249
5.2.15	Effect of TGF β blockade on 3D tumoursphere forming units.....	251
5.2.16	Effect of combining TGF β and Hh antagonist on Hh- and TGF β -regulated genes	253
5.2.17	The effect of combining TGF β and Hh antagonists on apoptosis	263
5.2.18	Effect of Hedgehog and TGF β blockade on cell viability	272
5.2.19	Effect of TGF β and Hh blockade on 2D colony forming efficiency	275
5.2.20	Effect of TGF β and Hh blockade on 3D tumoursphere forming units.....	277
5.3	Discussion	281

Chapter 6 Defining the Basis for Nuclear Translocation of SMAD3 Following Hh Antagonist Treatment	292
6.1 Introduction.....	292
6.2 Results	294
6.2.1 TGFβ ligand expression is not induced by Hh antagonist	294
6.2.2 Nocodozaole induced microtubule collapse leads to nuclear accumulation of pSMAD3	296
6.2.3 Primary BCC treated with Hh antagonist reduce acetylated tubulin	299
6.2.4 Hh antagonists induce microtubule collapse and nuclear pSMAD3 accumulation	300
6.3 Discussion	303
Chapter 7 General Discussion	308
7.1 Discussion.....	308
7.2 Future Directions	315
Appendix One: Driver genes affected by subtle mutations	320
Bibliography.....	324

Abstract

Targeted therapies for cancer have been developed that block oncogenic pathways that drive tumour growth (e.g. hedgehog, mitogen-activated protein kinases, vascular endothelial growth factor, and the Abelson tyrosine kinase and the chromosome 22 break point cluster fusion gene). For inoperable metastatic disease, targeted therapies provide rapid response, but in most cases are associated with eventual relapse with more aggressive disease. Basal cell carcinoma (BCC) arises from keratinocytes with mutations leading to constitutively active sonic hedgehog (SHh) growth factor signalling. Unlike the multiple genetic lesions required during stepwise carcinogenesis in many other cancers, SHh signalling alone appears to be sufficient to cause BCC, which may explain the absence of precursor lesions and also why BCC is the most common malignancy in Caucasians. As expected hedgehog (Hh) antagonists lead to rapid involution of BCC, but also eventual relapse, and in some cases transformation to squamous cell carcinoma. Thus, BCC represent an ideal model to study relapse after targeted therapy.

We show that the TGF β signalling pathway constituents were amplified in BCC, consistent with increased signalling. TGF β signalling was evident in a third of untreated BCC cells at the tumour periphery. Cells at the tumour nodule periphery active for TGF β signalling demonstrated lower rates of proliferation, and upregulation of TGF β regulated epithelial mesenchymal transition (EMT) genes consistent with tumour invasion. Intriguingly, BCC cancer stem cells that have been previously identified at the tumour nodule periphery consistently demonstrated active TGF β signalling and enhanced expression of TGF β dependent EMT genes.

We show that as expected, addition of Hh antagonists (GANT-61, Vismodegib, Sonidegib) to primary BCC cells and three Hh driven tumour cell lines (DAOY, UW228-2, SJSA-1), had no significant impact on cell proliferation or survival *in vitro*. Interestingly, Hh antagonist treatment was associated with increased TGF β signalling activity as evidenced through nuclear accumulation of pSMAD3 and expression of TGF β regulated genes. However, blocking the TGF β signalling pathway, both on its own and in combination with Hh antagonists again had no significant impact on cell proliferation or

survival in the cell lines. When trying to elucidate the mechanisms that underlie tumour resistance, we found that Hh antagonist-induced TGF β signalling was accompanied by destabilisation of the microtubule network. This could subsequently lead to TGF β -induced EMT/invasion in either the general cell population or stem cell population, and may provide a mechanism through which tumours can promote relapse following treatment, and in rarer cases, induce transformation to more aggressive phenotypes such as SCC. However, additional studies are required to elucidate this mechanism of action further.

Acknowledgements

Firstly, I would like to thank Dr. Girish Patel for giving me the opportunity to undertake this PhD project, and for providing me with support, guidance, encouragement and enthusiasm throughout.

I would also like to thank my fellow lab colleagues, notably: Kate Powell, Simone Lanfredini, Carlotta Olivero, Abdullahi Mukhtar, and Elise Rees who have all contributed ideas and help throughout, and created an excellent working environment.

I would also like to thank all past and present members of the European Cancer Stem Cell Research Institute (ECSCRI), who have made the time spent doing my PhD an enjoyable one and have given me lots of good memories.

I would also like to thank Dr Katherine Tansey and Dr Robert Andrews for their advice/data processing and analysis of the microarray data set in the Data Clinic, College of Biomedical and Life Sciences, Cardiff University.

I would like to acknowledge the patients who have kindly donated tissue for me to conduct my research, and for the medical staff who have taken the time to prepare the tissue for me to collect. I am also incredibly grateful to Cancer Research Wales for funding my PhD project.

Finally, I would like to thank my mother, father, two sisters (Rach and Saz) and Liv for their constant love and support throughout this PhD.

Declaration

This work has not been submitted in substance for any other degree or award at this or any other university or place of learning, nor is being submitted concurrently in candidature for any degree or other award.

Signed (candidate) Date

STATEMENT 1

This thesis is being submitted in partial fulfillment of the requirements for the degree of PhD

Signed (candidate) Date

STATEMENT 2

This thesis is the result of my own independent work/investigation, except where otherwise stated. Other sources are acknowledged by explicit references. The views expressed are my own.

Signed (candidate) Date

STATEMENT 3

I hereby give consent for my thesis, if accepted, to be available for photocopying and for inter-library loan, and for the title and summary to be made available to outside organisations.

Signed (candidate) Date

STATEMENT 4: PREVIOUSLY APPROVED BAR ON ACCESS

I hereby give consent for my thesis, if accepted, to be available for photocopying and for inter-library loans after expiry of a bar on access previously approved by the Academic Standards & Quality Committee.

Signed (candidate) Date

List of Abbreviations

ABC ATP-binding cassette family of proteins

ALDH1 Aldehyde dehydrogenase 1

APC Adenomatous polyposis coli)

BCC Basal cell carcinoma

BCNS Basal cell nevus syndrome

BCR-ABL Break cluster region-abelson

BMP Bone morphogenetic protein

BSA Bovine serum albumin

CD45 Lymphocyte common antigen

CD200 OX-2 membrane glycoprotein

CD133 Prominin 1

CFE Colony Forming Efficiency

CDK Cyclin Dependent Kinase

CM Conditioned medium

CSC cancer Stem Cell

ECM Extracellular matrix

EGF Epidermal growth factor

EGFR Epidermal growth factor receptor

EMT Epithelial-mesenchymal transition

ERK Extracellular signal-regulated kinase

ESC Embryonic Stem Cell

FACS Fluorescence activated cell sorting

FBS Fetal bovine serum

FGF Fibroblast Growth Factor

Gsk3Beta Glycogen synthase kinase 3 beta

HGF Hepatocyte growth factor

Hh Hedgehog

IGF Insulin-like growth factor

IkB Inhibitors of NF-κB

IKK Inhibitor of KappaB kinase

IL-6 Interleukin 6

IL-8 Interleukin 8

JNK c-jun N-terminal kinase

K14 Keratin 14

MAPK Mitogen-activated protein kinase

MEKK1 MAP/ERK kinase kinase 1

MET Mesenchymal-epithelial transition

MMP Matrix metalloproteinase

mTOR Mammalian target of rapamycin

NF-κB Nuclear factor binding to the intronic kappa-lightchain enhancer element in B cells

PBS Phosphate-buffered saline

PCR Polymerase chain reaction

PI3k Phosphatidylinositol 3-kinase

PTCH Patched

qRT-PCR Quantitative reverse transcription PCR

Rb Retinoblastoma gene

RNAi RNA interference

ROCK Rho-associated protein kinase

SAHA Suberoylanilide hydroxamic acid

SBE SMAD binding elements

SC Stem Cell

SCC Squamous cell carcinoma

SDS-PAGE Sodium dodecyl sulphate polyacrylamide gel

SMAD Mothers against decapentaplegic

SNP Single nucleotide polymorphism

shRNA Short hairpin RNA

siRNA Small interfering RNA

SMO Smoothened

STATs Signal Transducer and Activator of Transcription proteins

TBS Tris buffered saline

TBS/T Tris buffered saline/tween

TFU Tumoursphere-forming unit

TGF β Transforming growth factor Beta

TGFBRI TGF Beta signalling type I receptors (ALK1-7)

TGFBRII TGF Beta signalling type II receptors

TIC Tumour initiating cell

TNF α Tumour necrosis factor alpha

VEGF-A vascular endothelial growth factor-A

Wnt Wingless-int

Table of Figures

Figure 1.1: Signal transduction pathways affected by Bcr-Abl and sites of inhibition. ...	21
Figure 1.2: ERK arm of the human epidermal growth factor receptor pathway and sites of inhibition	23
Figure 1.3: Hedgehog growth factor signalling pathway in vertebrate cells.	32
Figure 1.4: Three main categories of BCC.....	41
Figure 1.5: A timeline highlighting some of the major discoveries in stem cell research.	58
Figure 1.6: Receptor system for the TGF β signalling family.	73
Figure 1.7: Canonical TGF β signal transduction from the cell membrane to the nucleus. Adapted from Shi and Massague, 2003.....	76
Figure 1.8: Structure of SMAD proteins.	77
Figure 1.9: Crosstalk between TGF β and Hh signalling pathways.	100
Figure 2.1: Representative flow cytometry dot plot generated for Annexin V apoptosis assay	132
Figure 3.1. Volcano plots of differentially expressed genes.....	152
Figure 3.2. Heatmap from Unsupervised hierarchical clustering analysis.....	158
Figure 3.3. TGF β signalling in BCC.	160
Figure 3.4. Pathway enrichment observed in BCC compared to normal skin	163
Figure 3.5: Pathway enrichment observed in BCC compared to SCC.....	166
Figure 3.6: Defining a TGF β responsive gene panel	167
Figure 3.7: TGF β responsive gene panel in primary human BCC.....	168
Figure 3.8. pSMAD3 expression and localisation in TGF β 1treated HaCaT cells	171
Figure 3.9. pSMAD3 labelling of human hair follicles.....	171
Figure 3.10: pSMAD3 labelling of human BCC tumour tissues.....	173
Figure 3.11: pSMAD3 and MCM7 labelling of BCC	176
Figure 3.12: Expression of TGF β regulated EMT genes in BCC tissue	178
Figure 3.13: Expression of TGF β pathway ligands and receptors in BCC.....	181
Figure 4.1: CD200 expressing BCC CSC are active for TGF β signalling.....	192
Figure 4.2: CD200+ and CD200- BCC cells isolated using flow sorting.	193
Figure 4.3: CD200 expressing CSC display TGF β signalling pathway activation	195

Figure 4.4: Analysis of RNA integrity from flow sorted CSCs have good quality, but very low yields.....	196
Figure 4.5: CD200+ EPCAM+ CD45- BCC cells demonstrate TGFβ regulated EMT	198
Figure 5.1: Components of the canonical Hh signalling pathway and molecular sites targeted by Hh pathway inhibitors.....	205
Figure 5.2: Components of the canonical TGFβ signalling pathway and molecular sites targeted by TGFβ pathway inhibitors.....	206
Figure 5.3: mSHh induced GLI reporter assay dose response curve.	208
Figure 5.4: Inhibition of hedgehog signalling pathway by vismodegib	210
Figure 5.5: Inhibition of hedgehog signalling pathway by sonidegib	211
Figure 5.6: Inhibition of hedgehog signalling pathway by GANT-61	211
Figure 5.7: Identifying genes that are Hh regulated within Hh driven tumour cell lines.	216
Figure 5.8: Little or no impact on apoptosis in Hh driven tumour cell lines following Hh antagonist treatment	219
Figure 5.9: Hh Antagonists do not reduce cell viability in Hh Driven Cell Lines: Cell Titre Glo assay following 24hr treatment with Hh antagonists.	223
Figure 5.10: Colony forming cells are sensitive to GANT-61, but resistant to vismodegib.	226
Figure 5.11: Tumoursphere-forming cells are sensitive to GANT-61, but not to vismodegib and sonidegib in DAOY cells.....	227
Figure 5.12: Tumoursphere-forming cells are sensitive to GANT-61, but not to vismodegib and sonidegib in UW228-2 cells.....	228
Figure 5.13: Identifying genes that are TGFβ regulated within Hh driven tumour cell lines	231
Figure 5.14: The TGFβ signalling pathway is activated following treatment with Hh antagonists in Hh driven tumours	233
Figure 5.15: TGFβ-regulated genes are induced following treatment with Hh antagonists in Hh driven tumours.....	236
Figure 5.16: Blocking TGFβ signalling.	239
Figure 5.17: Effect of Blocking TGFβ Signalling on Hh-regulated Genes in Hh Driven Tumours.	242

Figure 5.18: Impact TGF β antagonist only treatment on apoptosis in Hh driven tumour cell lines	245
Figure 5.19: Blocking the TGF β signalling pathway at both the receptor and transcription factor level appears to have very little impact on relative cell viability in Hh driven cell lines.	248
Figure 5.20: Effect of TGF β blockade on 2D colony formation: Colony-Forming Assays.	250
Figure 5.21: Effect of TGF β blockade on tumoursphere-forming cells: Sphere-Forming Assays.	252
Figure 5.22: Effect of Blocking TGF β - and Hh-signalling on TGF β -regulated Genes in Hh Driven Tumours.	256
Figure 5.23: Effect of Blocking TGF β Signalling and Hh-signalling on Hh-regulated Genes in Hh Driven Tumours.....	261
Figure 5.24: Impact of SB431542 in combination with Hh antagonists on apoptosis in Hh driven tumour cell lines.....	264
Figure 5.25: Impact of SMAD4 siRNA in combination with Hh antagonists on apoptosis in Hh driven tumour cell lines	268
Figure 5.26: Effect of Combining TGF β and Hh Antagonist Treatment on Cell Viability in Hh Driven Tumours.....	274
Figure 5.27: Effect of TGF β and Hh blockade on 2D colony formation: Colony-Forming Assays.	276
Figure 5.28: Effect of TGF β and Hh blockade on tumoursphere-forming cells: sphere-forming assays.	280
Figure 6.1: Hedgehog antagonist treatment in Hh driven tumour cell lines does not increase the expression of TGF β ligands.	295
Figure 6.2: Nocodozaole induced microtubule collapse	297
Figure 6.3: Nocodozaole induced nuclear accumulation of pSMAD3 in Hh driven tumour cell line.	298
Figure 6.4: Hh antagonists induce microtubule destabilisation within primary human BCC	299
Figure 6.5: Hh antagonists induce microtubule changes in Hh driven tumour cell line.	302

Figure 6.6: Hh antagonists induce nuclear accumulation of pSMAD3 in Hh driven tumour cell line.	302
Figure 7.1: Microtubule destabilization can induce SMAD signalling through two potential mechanisms.	317

Table of Tables

Table 1.1: Driver genes affected by amplification or homozygous deletion (Taken from Vogelstein <i>et al.</i> , 2013).....	16
Table 1.2: Rearrangements in carcinomas (Taken from Vogelstein <i>et al.</i> , 2013).....	16
Table 1.3: Markers of Leukemia initiating cell populations (Taken from Stahl <i>et al.</i> , 2016)	52
Table 1.4: Cancer SC populations identified in a number of human cancers using <i>in vivo</i> assays (only cell surface markers are described)	59
Table 2.1: List of Hh driven cell lines along with their mutations and Hh signalling pathway profiles.....	111
Table 2.2: List of cell lines and passaging ratios	114
Table 2.3: Volumes of media used in cell culture.....	115
Table 2.4: Taqman Assay on Demand used for Taqman qPCR.....	120
Table 2.5: Drugs used in functional assays	127
Table 2.6: Concentrations used in siRNA knock down experiments	130
Table 2.7: Antibodies/Stains used in FACS experiments	131
Table 2.8: Primary antibodies used in immunofluorescence experiments	135
Table 2.9: Secondary antibodies used in immunofluorescence experiments	136
Table 2.10: Buffers used for protein extractions.....	137
Table 2.11: Buffers used in Western Blotting.....	139
Table 2.12: Primary antibodies used for Western Blotting	143
Table 2.13: Secondary antibodies used for Western Blotting.....	143
Table 3.1: List of significant genes highlighted identified by the volcano plot comparing BCC to NS.....	152
Table 3.2. List of significant genes highlighted identified by the volcano plot comparing BCC to SCC	153
Table 3.3 Top 20 processes (Gene Sets) enriched in BCC in comparison to normal skin	161
Table 3.4 Top 20 processes (Gene Sets) enriched in BCC in comparison to SCC.....	164
Table 5.1: Identifying genes that are Hh regulated within Hh driven tumour cell lines.	216
Table 5.2: The effect of Hh antagonists on apoptosis in Hh driven cell lines	220

Table 5.3: Identifying genes that are TGF β regulated within Hh driven tumour cell lines	231
Table 5.4: Impact of Hh antagonists on cell line specific TGF β regulated genes.....	237
Table 5.5: Impact of TGF β inhibition on cell line specific Hh regulated genes	243
Table 5.6: Effect of TGF β antagonist treatment on inducing apoptosis in Hh driven cell lines.	246
Table 5.7: Impact of SB431542 combinational treatments on cell line specific TGF β regulated genes.....	257
Table 5.8: Impact of SMAD4 siRNA combinational treatments on cell line specific TGF β regulated genes.....	258
Table 5.9: Impact of SB431542 combinational treatments on cell line specific Hh regulated genes.....	262
Table 5.10: Impact of SMAD4 siRNA combinational treatments on cell line specific Hh regulated genes.....	263
Table 5.11: Effect of Combining TGF β - and Hh-Antagonist Treatment on inducing apoptosis in DAOY cells.	265
Table 5.12: Effect of Combining TGF β - and Hh-Antagonist Treatment on inducing apoptosis in DAOY cells.	269
Table 5.13: Effect of Combining TGF β - and Hh-Antagonist Treatment on inducing apoptosis in UW228-2 cells.	270
Table 5.14: Effect of Combining TGF β - and Hh-Antagonist Treatment on inducing apoptosis in SJSA-1 cells.	271
Table 7.1: Summary of resistance mechanisms to some common molecular targeted agents	309

Chapter 1: Introduction

Chapter 1 Introduction

1.1 Hallmarks of Cancer

Throughout our lifetimes somatic mutations steadily accumulate within our cells, and although the vast majority of these are harmless, occasionally a mutation affects a gene or regulatory element, which leads to a phenotypic consequence. A fraction of these mutations are 'driver' mutations, in that they confer a selective advantage to the cell, which in turn lead to the preferential growth and/or survival of a clone (Stratton *et al.*, 2009). One of the end products of this evolution within somatic cells is cancer. In the UK, cancer represents the most common cause of death for males and females combined (Office for National Statistics: Deaths registered in England and Wales: 2015; National Records of Scotland. 2015 Births, Deaths and Other Vital Events; Northern Ireland Statistics and Research Agency. Registrar Northern Ireland Annual Report 2014), and accounts for roughly 28% of all deaths in the UK. In 2014, there were 163,444 cancer deaths in the UK (86,540 (53%) in males and 79,904 (47%) in females), with the crude mortality rate showing that cancer is responsible for 272 deaths for every 100,000 males in the UK, and 234 deaths for every 100,000 females (CRUK). However, cancer is a global problem, with cancer responsible for 25% of all deaths in the United States, and is second only to cardiovascular disease as the leading cause of death (Jemal *et al.*, 2008). Whereas in Canada, cancer is the number one cause of death, with roughly 45% of men and 39% of women shown to develop cancer within their lifetime, and about 1 in 4 Canadians will die from the disease (Marrett *et al.*, 2008). Furthermore, in other countries such as in India, the mortality rate attributed to cancer in 2014 was roughly 6% (Dikshit *et al.*, 2012); however in such rapidly developing countries the incidence of cancer will almost certainly increase as the average age of the population is set to increase, which in turn will result in more cancer related deaths.

Cancer in its very basic sense is a disease in which an autonomous clone of cells escape from the inbuilt cellular mechanisms that govern cell behaviour and proliferation. The

following section will give a brief description of the basic biological capabilities of cancer, termed 'hallmarks'. The 'Hallmarks of cancer' was a seminal peer-reviewed article published in *Cell* in January 2000 by Douglas Hanahan and Robert Weinberg (Hanahan and Weinberg, 2000), in which the complexity of cancer was reduced to six biological capabilities acquired during the multistep development of human tumours. The six hallmarks are as follows: 1) sustaining proliferative signalling, 2) evading growth suppressors, 3) resisting cell death, 4) enabling replicative immortality, 5) inducing angiogenesis, 6) activating invasion and metastasis. In 2011, Hanahan and Weinberg published an update (Hanahan and Weinberg, 2011), in which they proposed four new hallmarks: 1) genome instability and mutation, 2) tumour-promoting inflammation, 3) reprogramming energy metabolism and 4) evading immune destruction.

1.1.1 Sustaining proliferative signalling

One of the most important attributes of a cancer cell is its ability to sustain chronic proliferation. Normal cells are instructed to progress through the cell-growth-and-division cycle by the production and release of growth promoting signals, and thereby ensure cell homeostasis within the tissue. By deregulating these signals cancer cells acquire the ability to sustain proliferative signalling, which can be achieved in a number of ways (Lemmon and Schlessinger, 2010; Witsch *et al.*, 2010; Perona *et al.*, 2006). These include autocrine proliferative signalling, whereby cancer cells produce their own ligands, and can respond via upregulation of cognate receptors. Alternatively, cancer cells can send signals to neighbouring normal cells within the stroma, which reciprocate by supplying the cancer cells with growth factors (Cheng *et al.*, 2008; Bhowmick *et al.*, 2004). Deregulation of receptor signalling can also occur through the upregulation of receptor proteins at the cell surface or even through structural alterations within the receptors, which render the cells hyper-responsive to ligands. However more recently, other mechanisms have emerged allowing cells to be hyperproliferative. These include somatic mutations that serve to activate downstream pathways; an example of which can be seen in human melanoma, where 40% are found to have constitutive activation of the MAPK pathway through mutations within the B-Raf gene (Davies and Samuels, 2010). Defects in negative feedback-loops, which in normal tissues serve to dampen various types of signalling and thereby ensure homeostatic regulation (Wertz and Dixit,

2010), have also been linked to hyperproliferation within cancer cells. A classic example involves PTEN phosphatase, which counteracts PI3K by degrading its product PIP3. Loss-of-function mutations within this phosphatase amplify PI3K signalling and thereby promote tumour growth (Jiang and Liu, 2009; Yuan and Cantley, 2008).

1.1.2 Evading growth suppressors

Cancer cells must also be able to circumvent programs that negatively regulate cell proliferation. The two-prototypical tumour suppressor genes encode the proteins RB (retinoblastoma) and TP53, and are critical for controlling the decision for cells to proliferate, or activate senescence and apoptotic programs, respectively.

The RB protein integrates a diverse range of extracellular and intracellular signals and then decides whether to enter the cell division cycle (Deshpande *et al.*, 2005; Sherr and McCormick, 2002). As a consequence defects in the RB pathway permit persistent proliferation through the absence of this critical gatekeeper. TP53 receives and responds to stress and abnormality sensors within the cell, and can stop cell cycle progression until the conditions have been normalised (Zilfou and Lowe, 2009). Alternatively, if the signals received cannot be repaired or rectified, TP53 can trigger apoptosis (Zilfou and Lowe, 2009). Other mechanisms that cancer cells must overcome include contact inhibition. When normal cells are grown in 2D culture, the cell-cell contacts that form in dense populations provide cues that stop cell proliferation. This contact inhibition is also replicated *in vivo*, where it serves to maintain tissue homeostasis, however in cancer cells this contact inhibition is abolished (Wieser and Oesch, 1986). Recently mechanisms that underpin this abolition have begun to emerge. One such mechanism involves the product of the NF2 gene, Merlin, which has long been implicated as a tumour suppressor, and controls contact inhibition by coupling cell surface adhesion molecules to transmembrane receptor tyrosine kinases. This action has consequences that are two-fold: firstly Merlin strengthens cadherin-mediated cell-to-cell attachments; secondly, by sequestering growth factor receptors, Merlin restricts their ability to transduce mitogenic signals (Curto *et al.*, 2007; Okada *et al.*, 2005).

TGF β signalling is best known for its anti-proliferative effects under physiological conditions; however in late-stages of carcinogenesis TGF β signalling is found to activate a cellular program called epithelial mesenchymal transition (EMT) (Ikushima and Miyazono, 2010; Massague, 2008).

1.1.3 Resisting cell death

Cells undergoing programmed cell death via apoptosis have served as a natural barrier to cancer development (Adams and Cory, 2007; Lowe *et al.*, 2004), and function through two major mechanisms: first is the extrinsic apoptotic program involving the use of caspase 8; second is the intrinsic apoptotic program that involves the use of caspase 9. Both programs culminate in the activation of their respective proteases, which subsequently initiate a cascade of proteolysis involving caspases that are responsible for disassembling the cell (Elmore, 2007). The apoptotic trigger is controlled through a balance of pro- and anti-apoptotic members of the Bcl-2 family of regulatory proteins (Adams and Cory, 2007). Although the cellular conditions that underpin apoptosis remain to be fully elucidated, there are several abnormality sensors that play crucial roles in tumour development (Adams and Cory, 2007; Lowe *et al.*, 2004).

Tumour cells have acquired a number of strategies to restrict or circumvent apoptosis. The most common mechanisms through which tumour cells achieve this is by losing the tumour suppressor function of TP53 (Ozaki and Nakagawara, 2011). Alternatively, tumour cells can increase the expression of anti-apoptotic regulators (Bcl-2, Bcl-xL), and downregulate pro-apoptotic factors (Bax, Bim, Puma) (Kirkin *et al.*, 2004).

Other more recent advances in our understanding of resisting cell death pathways are beginning to be unravelled. One example of this includes the ability of autophagy to regulate both tumour cell survival and death. Autophagy, like apoptosis is an important physiological response that operates at low basal levels in cells, but has the capacity to be strongly induced under certain conditions of cellular stress, such as nutrient deficiency (Levine and Kroemer, 2008; Mizushima, 2007). Autophagy allows cells to break down cellular organelles including mitochondria and ribosomes, and subsequently recycle catabolites that are used for biosynthesis. Recent studies have

revealed that the regulatory circuits that govern autophagy and apoptosis are interconnected (Levine and Kroemer, 2008; Sinha and Levine, 2008; Mathew *et al.*, 2007). The protein, Beclin-1, has been shown by genetic studies to be necessary for the induction of autophagy and is a key protein for the interconnection between these two programs (Mizushima *et al.*, 2007). Mice with inactivating alleles for Beclin-1 from the autophagy machinery have been shown to exhibit increased sensitivity towards cancer (White and DiPaolo, 2009; Levine and Kroemer, 2008).

1.1.4 Enabling replicative immortality

In normal cell lineages, the number of successive cell growth and division cycles is limited by two distinct barriers: firstly, senescence, which is the entry into a non-proliferative state which is often irreversible, but still leaves the cell viable; and secondly, crisis, which involves cell death (Shay and Wright, 2011). When propagating cells in culture, the repeated cycles of cell division lead initially to senescence, and then for cells that cannot overcome this barrier, eventual cell death occurs through crisis. However, on rare occasions, cells can overcome the crisis phase and emerge with unlimited replicative potential, termed immortalisation. There are multiple lines of evidence showing that cells obtain the ability to endlessly proliferate through telomeres protecting the ends of chromosomes (Blasco, 2005; Shay and Wright, 2000). In non-immortalised cells that undergo propagation, the telomeres gradually shorten, until they are no longer able to protect the ends of chromosomes, which inevitably impacts on cell viability (Shay and Wright, 2011). Therefore, the length of telomeric DNA within a cell dictates how many cycles of proliferation it can undergo before the cell enters crisis. The enzyme telomerase is responsible for adding telomere repeat units to the ends of telomeric DNA and thereby lengthening it. In normal cells, the levels of telomerase are very low, however in spontaneously immortalised cells, roughly 90% are found to express functionally significant levels of telomerase (Shay and Bacchetti, 1997). Therefore one mechanism through which cancer cells maintain their telomere length and thereby bypass both senescence and crisis is through increased levels of telomerase. In fact experiments have shown that in mice lacking telomeres, premalignant cells can be forced into senescence, which ultimately contributes to attenuating tumourigenesis even in mice genetically pre-disposed to develop certain

cancers (Artandi and DePino, 2010). However, there are alternative mechanisms through which cancer cells can bypass cell senescence, including the alternative lengthening of telomeres (ALT) pathway, which is a homology-directed recombination-dependent replication pathway (telomere maintenance mechanism; TMM) that is frequently adopted by tumours from a mesenchymal and neuroepithelial origin (Sobinoff and Pickett, 2017).

1.1.5 Inducing Angiogenesis

In a similar manner to normal cells, tumour cells require nutrients and oxygen to grow as well as the ability to excrete metabolic wastes and carbon dioxide. Angiogenesis is the process by which tumour cells generate a neovasculature network in order to address these needs. Angiogenesis is a process that is adopted during embryogenesis where developing the vasculature involves the production of new endothelial cells and their subsequent assembly into tubes (Breier, 2000). Following this early development, the normal vasculature becomes mostly quiescent, and is only turned on in adult tissues, during times of the reproductive cycle for women, and for wound healing (Fraser and Lunn, 2000). However, this angiogenic switch is almost always active during tumour progression, and causes normally quiescent vasculature to help in sustaining the growing neoplasia through the sprouting of new vessels (Hanahan and Folkman, 1996).

The angiogenic switch is governed by a number of factors that either induce or oppose angiogenesis (Baeriswyl and Christofori, 2009; Bergers and Benjamin, 2003), and are usually signalling proteins that bind to either stimulatory or inhibitory receptors on the vascular endothelial cells. For example, one very well known inducer of angiogenesis is the vascular endothelial growth factor-A (VEGF-A), whereas thrombospondin-1 (TSP-1) is a well-established inhibitor of angiogenesis. The VEGF-A gene encodes ligands that are responsible for controlling the growth of new blood vessels during embryogenesis, homeostatic survival of endothelial cells, and the formation of blood vessels under physiological and pathophysiological conditions in the adult (Holmes and Zachary, 2005). VEGF signalling is transduced via three receptor tyrosine kinases (VEGFR-1-3), and due to its relative complexity, is regulated at multiple levels. The expression of VEGF can be upregulated by both hypoxic conditions and during oncogenesis (Ferrara,

2009; Gabhann and Popel, 2008). Furthermore, other factors responsible for stimulating angiogenesis, including the fibroblast growth factor (FGF) family, have been chronically upregulated during times of tumour angiogenesis (Baeriswyl and Christofori, 2009).

1.1.6 Activating invasion and metastasis

Invasion and metastasis is a multistep process, which can be broken down into a sequence of discrete steps, termed the 'invasion metastasis cascade' (Talmadge and Fidler, 2010; Fidler, 2003). This cascade involves a succession of cell biological changes that begin with local invasion, intravasation by cancer cells into the surrounding blood and lymphatic vessels, transit of these cells through the blood and lymphatic systems, escape of these cells from the lumina of the vessels into distant tissues, where they establish to form small tumours, before finally growing into a macroscopic tumour (colonisation). The best characterised alteration in this process is the loss of the key cell adhesion molecule, E-cadherin, in the cancer cells. Under physiological conditions, E-cadherin helps the formation of adherens junctions with adjacent epithelial cells, and thereby facilitates the assembly of epithelial sheets that maintain cell quiescence within these sheets (Pecina-Slaus, 2003). In cancer cells, E-cadherin is frequently found to either be downregulated or in rare instances contain loss-of-function mutations (roughly 4% of tumours), and thereby provides very strong evidence for its role in suppressing this hallmark capability (Berox and van Roy, 2009; Cavallaro and Christofori, 2004). The loss of E-cadherin is one of the hallmarks of EMT, a key transition process that gives cancer cells the ability to become more aggressive and migratory. A key regulator of EMT, notably during the later stages of carcinogenesis and tumour growth, is active TGF β signalling. EMT is characterised by loss of cell-to-cell contact and the poor correlation between the pattern of migration of a cell and its neighbour. However, cancer cells can also engage in amoeboid-like motility in which cells have a round cell-body phenotype and can dramatically differ in their protrusive activity. Amoeboid-like migration manifests itself in a number of different forms within cancer cells, ranging from cells that can achieve high migrating velocities through the presence of short thin protrusions and the absence of blebbing, to others that move more slowly and have blebbing morphology and are associated with chaotic movements (Clark and Vignjvic, 2015).

1.1.7 Genome instability and mutation

In order for cancer cells to acquire the multiple hallmarks outlined above, a succession of alterations within the genomes of neoplastic cells must occur. In its simplest form, certain mutant genotypes confer a survival advantage on subclones of cells, which enables them to eventually dominate in the local tissue environment. As a consequence, tumour progression can be depicted as a succession of clonal expansions, with each one triggered by the chance acquisition of a mutational genotype that confers an advantage over the other subclones (Diaz-Cano, 2012). However, the genome maintenance systems present within cells are extremely good at detecting and resolving defects within the DNA, therefore in order for tumourigenesis to be orchestrated through the accumulation of mutant genes, cancer cells often increase the rates of mutation (Negrini *et al.*, 2010; Salk *et al.*, 2010). Cancer cells achieve this through a break down in one or several components of the genome maintenance machinery, which increases the sensitivity of the cells to mutagenic effects, and thereby increase the rates of mutation. Furthermore, by compromising the surveillance systems that are responsible for assessing genome integrity and guiding damaged cells to senescence or apoptosis, cancers cells can accelerate the accumulation of these mutations (Jackson and Bartek, 2009; Kastan, 2008; Sigal and Rotter, 2000). Cancers have developed through a diverse range of defects affecting the DNA-maintenance machinery (Kinzler and Vogelstein, 1997). These defects have been shown to affect genes involved in: 1) the DNA damage detection and repair machinery, 2) the direct repair of DNA damage, and 3) the interception of molecules before they cause DNA damage (Negrini *et al.*, 2010; Ciccia and Elledge, 2010; Harper and Elledge, 2007; Friedberg *et al.*, 2006).

1.1.8 Tumour-promoting inflammation

It has long been recognised that some tumours contain immune infiltrate from both the adaptive and innate immune systems, which mirrors what is observed in normal tissue (Dvorak, 1986). However with the advent of improved cell-type markers, we have been able to show that nearly every tumour has immune infiltrate to some extent (Pages *et al.*, 2010). Such immune responses have largely been thought to be anti-tumourigenic,

and an attempt by the body to eradicate the tumour, however recent studies have shown that in some cancers the immune infiltrate can have pro-tumourigenic effects, and contribute to tumour progression (DeNardo *et al.*, 2010; Qian and Pollard, 2010; Colotta *et al.*, 2009). In fact, inflammation has been shown to promote tumour development by supplying the tumour microenvironment with growth factors, survival factors, pro-angiogenic factors, and extracellular matrix enzymes (DeNardo *et al.*, 2010; Karnoub and Weinberg, 2006-2007).

1.1.9 Reprogramming energy metabolism

Tumourigenesis is also associated with deregulation in the energy metabolism pathways in order to fuel growth and division. In normal cells under aerobic conditions, glucose is processed to pyruvate via glycolysis in the cytosol, and then to carbon dioxide in the mitochondria; whereas under anaerobic conditions, relatively little pyruvate is sent to the oxygen-consuming mitochondria, as glycolysis is the preferred form of energy metabolism. However, cancer cells have the capacity to reprogram their energy metabolism, and therefore their energy production, in the presence of oxygen, by limiting their energy metabolism to predominantly glycolysis, termed aerobic glycolysis (Warburg, 1930, 1956a, 1956b). However, this form of energy metabolism is rather counterintuitive, in that ATP production produced by glycolysis is roughly 18-fold less efficient than ATP produced through oxidative phosphorylation (Hanahan and Weinber, 2011). In order to compensate for this, cancer cells substantially increase the import of glucose into the cytoplasm through upregulation of glucose transporters, such as GLUT1 (Jones and Thompson, 2009; Hsu and Sabatini, 2008). This increased uptake and usage of glucose has been observed in many tumour types and can be visualised in a non-invasive way through positron emission tomography (PET) with a radiolabelled analogue of glucose as a reporter. The usage of tumour cells to adopt such a seemingly inefficient means for energy metabolism may also be explained in part by the fact that cancer cells are often under hypoxic conditions, particularly at the interior of the tumour, and the hypoxic response system induces the upregulation of glucose transporters and multiple enzymes of the glycolytic pathway (Semenza, 2010a; Jones and Thompson, 2009). Nevertheless, the functional rationale for cancer cells using glycolysis has remained unclear. However, one hypothesis is that the process of glycolysis allows the

intermediates of the pathway to be diverted into a variety of biosynthetic pathways, including those involved in generating nucleosides and amino acids, which in turn can be used to generate macromolecules and organelles required for the production of cells (Potter, 1958; Vander Heiden *et al.*, 2009). However, not all cancer cells are found to use glycolysis for their energy production. Interestingly, studies have shown that cancers can contain two subpopulations that are distinguished from one another by their ability to metabolise energy. In this manner, the two subpopulations function symbiotically, with the one subpopulation generating lactate through the glycolytic pathway, and in turn the lactate is then used by the second subpopulation as its main energy source in the citric acid cycle (Kennedy and Dewhirst, 2010; Feron, 2009; Semenza, 2008).

1.1.10 Evading immune destruction

The long-standing theory of immune surveillance is that the cells and tissues within our body are constantly being monitored by our immune system, and is responsible for recognising and destroying the majority of cancer cells and therefore tumour initiation. However, if this is true, then any tumours that do appear have successfully evaded the immune system or have limited the extent of immunological killing. The role of the immune system may be seen by the significant increases observed in some tumours in patients with compromised immune systems (Vajdic and van Leeuwen, 2009); however the majority of these are virus-induced. However, even in non-viral induced tumours, there is a growing body of evidence mostly generated from mouse genetic studies and clinical epidemiology to suggest that the immune system does in fact serve as a significant barrier to the formation and progression of tumours. For example in mice genetically engineered to lack various cell populations of the immune system, tumours were shown to arise more frequently, and grew more rapidly in comparison to the immunocompetent mice (Shankaran *et al.*, 2001; Kim *et al.*, 2007). In particular, deficiencies in both the T- and NK-cell populations were linked to an increased risk of cancer development, and therefore indicate in part the reliance on both the innate and adaptive arms of the immune system for immune surveillance and as a consequence tumour eradication (Teng *et al.*, 2008; Kim *et al.*, 2007). Furthermore, both of these studies highlighted a process known as immune editing, whereby in an immune

competent host, highly immunogenic cancer clones are eradicated, leaving behind the weakly immunogenic clones that are capable of growing in both immunocompetent and immunodeficient mice; conversely when such cancer clones arise in immunodeficient mice, the highly immunogenic clones are not selectively destroyed, and therefore prosper along with the weakly immunogenic clones. However, when these clones are transplanted into a syngeneic host they are immediately rejected as they encounter a fully functioning immune system for the first time and therefore do not develop (Smyth *et al.*, 2006; Teng *et al.*, 2008; Kim *et al.*, 2007).

Cancers can also co-opt immune-checkpoint pathways as a mechanism of evading immune responses, particularly against T cells, which are specific for tumour antigens. With regard to T cells, the quality and amplitude of the immune response is governed through the recognition and binding of a T cell receptor (TCR) to an antigen displayed in the major histocompatibility complex (MHC) on the surface of an antigen presenting cell. Under physiological conditions immune checkpoints are essential for maintaining self-tolerance (preventing autoimmunity) and serve to protect the tissue from harm when the immune system is responding to infection. However, some cancers can acquire immune system resistance through the deregulation of immune-checkpoint proteins. In the context of clinical cancer therapy, the two immune checkpoint receptors that have been most intensely studied are the cytotoxic T-lymphocyte-associated antigen 4 (CTLA4) and programmed cell death protein 1 (PD1), which are negative regulators of T cell immune function. Therefore inhibition of these immune checkpoint inhibitors has led to the approval of several new drugs, which have in some instances proven to be effective in cancer treatment (Pardoll, 2016).

1.1.11 Therapeutic targeting

The description of hallmark principles has and is continuing to inform the development of therapies and will likely continue to do so in the future. The vast majority of drugs targeting cancer have been directed towards specific molecular targets that are involved in one or at most only a few of the hallmark processes outlined above. Targeted therapies have their advantages in that they present inhibitory activity towards a target, while at the same time having very few off target effects which as a

consequence limits non-specific toxicity. However, resulting clinical responses of targeted therapies have been largely transitory, followed by an almost-inevitable relapse of the tumour. One reason for this relapse however is that a targeted therapeutic agent may not be capable of completely inhibiting a hallmark capability, since each of the core hallmark processes are regulated by partially redundant signalling pathways. This therefore allows some cancer cells to survive with residual function until they or even their progeny adapt to the selective pressure applied through therapy, by mutation, epigenetic reprogramming or remodelling of the surrounding stroma, thereby permitting growth and subsequent relapse. Since the number of parallel signalling pathways driving tumour growth is limited, it is likely that future therapeutic strategies will target all of the supportive pathways and thereby prevent this resistance.

1.2 Cancer Driver Mutations

Cancer is a genetic disease caused by inherited and or somatic DNA mutations, of which the latter can be triggered by endogenous or exogenous carcinogens. The number of DNA mutations required to transform cells was initially debated in the 1990's. Carl Nordling, who had shown that cells can acquire mutations during normal cell division, proposed that more rapidly dividing tissues acquire the necessary mutations quicker and hence cancers develop earlier in life (Nordling, 1953). In 1971 Alfred Knudson proposed the 'two-hit hypothesis', in which the potent tumour suppressor gene, RB1 required two mutational events and therefore inactivation in both alleles (Knudson, 1971). Much later, it was realised that retinoblastoma progression also requires additional mutations consistent with Nordling's proposal (Laurie *et al.*, 2006). This is consistent with epidemiological studies that suggest that cancers ordinarily require between 5-8 genomic hits (Armitage and Doll, 2004).

The progression to cancer through acquisition of multiple DNA mutations is best observed in the colon, wherein screening colonoscopy allowed for determination of mutation in pre-malignant and malignant lesions. Vogelstein proposed a multistep basis for colon cancer, which included the following salient features: firstly, colorectal tumours arise initially from a combination of mutational activation of oncogenes

coupled with the loss of tumour suppressor genes; secondly, for a tumour to become malignant, mutations in at least four to five genes are required; thirdly, the tumours biological properties are determined by the total accumulation of changes, rather than the order of changes with respect to one another; and fourthly, in some instances, tumour suppressor genes may not be recessive at the cellular level, and therefore appear to exert a phenotypic effect even when present in a heterozygous state (Fearon and Vogelstein, 1990).

Comparative cancer genome sequencing has revealed that common solid tumours, such as those derived from the colon, breast, brain, or pancreas, harbour on average 33 to 66 gene mutations that would be expected to alter their protein products, with the vast majority of these found to be single base substitutions (~95%) (Vogelstein *et al.*, 2013). However, some tumours have been shown to contain over 200 non-synonymous mutations, most notably melanoma and lung cancer, which are likely associated with exposure to potent environmental carcinogens, such as ultraviolet light and cigarette smoke, respectively. Consequently, lung cancers from patients who smoked have 10 times as many somatic mutations as those from non-smokers. In contrast, paediatric tumours and leukaemia on average harbour 10 mutations per tumour. These observations are consistent with Norling's earlier prediction, whereby the number of mutations in certain tumours of self-renewing tissues is directly correlated with age (Tomasetti *et al.*, 2013).

The rate-limiting step in the acquisition of DNA mutations for lesions to evolve from benign to malignant tumours is determined by the timing of "gatekeeper mutations", for example the RB1 gene. Gatekeeper mutations provide a selective growth advantage over the surrounding normal tissue cells, allowing for expansion into a microscopic clone (Nowell, 1976; Kinzler and Vogelstein, 1997). In the colon, APC (Adenomatous polyposis coli) is the tumour suppressor gene that is the gatekeeper mutation, after which a second mutation in the KRAS gene unleashes a second round of clonal expansion. However, there are many mutations within the tumour that do not influence protein structure and so have no functional significance, these are called "passenger mutations". Even within genes that confer a selective growth advantage, so called

“driver genes”, passenger mutations occur frequently so as not to interfere with the gene function. For example, driver mutations in the APC gene result in N-terminus protein truncation. These driver mutations initially however, only provide a small selective advantage to the cell, with an increase in the difference between cell birth and death in the order of 0.4%. However, through cell divisions, this slight increase can result in a large mass, containing billions of cells (Bozic *et al.*, 2010).

Tumour suppressors are proteins that normally function to limit cell proliferation, for example cell cycle checkpoint proteins, and cancer driver mutations cause their functional loss. Oncogenes encode proteins in growth factor signal transduction pathways and so promote cell proliferation, therefore oncogene driver mutations result in increased activity. As many amino acids and their configuration are required for function of a protein, driver mutations in tumour suppressor genes, such as in the gene patched (PTCH), occur throughout the gene length and result in protein-truncating alterations (Nanni *et al.*, 1999). In contrast, driver mutations in oncogenes, for example in the gene smoothed (SMO), occur at fixed positions within the gene. Using this knowledge Vogelstein *et al.* sought to determine a list of oncogenes and tumour suppressors from the Catalogue of Somatic Mutations in Cancer (COSMIC) database based on the principles that; (1) for oncogenes that >20% of the recorded mutations in the gene are at recurrent positions and are missense and (2) for tumour suppressor genes >20% of the recorded mutations in the gene are inactivating (Vogelstein *et al.*, 2013) (Appendix; Table 1). This analysis identified 54 oncogenes and 71 tumour suppressor genes. The key growth factor pathways perturbed in cancer identified were: Wnt, hedgehog, Notch, RAS-MAP kinase, PI3K, STAT and TGF β . Additionally there were 13 genes not found to be point mutated, but were associated with amplifications for 10 oncogenes (e.g. MYC family genes) while the remaining three were tumour suppressor genes containing homozygous deletions (e.g. MAP2K4) (Table 1.1). However, for some cancers fusion genes are found to be important drivers (Table 1.2). Thus, a limited number of cellular signalling pathways confer a growth advantage, which can be broadly divided into those that influence cell fate, cell survival and genome maintenance.

Table 1.1: Driver genes affected by amplification or homozygous deletion (Taken from Vogelstein *et al.*, 2013)

Gene Symbol	Genetic alteration	Classification	Core Pathway	Process
CCND1	Amplification	Oncogene	Cell Cycle/Apoptosis	Cell Survival
CDKN2C	Homozygous deletion	TSG	Cell Cycle/Apoptosis	Cell Survival
IKZF1	Homozygous deletion	TSG	Transcriptional Regulation	Cell Fate
LMO1	Amplification	Oncogene	Transcriptional Regulation	Cell Fate
MAP2K4	Homozygous deletion	TSG	MAPK	Cell Survival
MDM2	Amplification	Oncogene	Cell Cycle/Apoptosis	Cell Survival
MDM4	Amplification	Oncogene	Cell Cycle/Apoptosis	Cell Survival
MYC	Amplification	Oncogene	Cell Cycle/Apoptosis	Cell Survival
MYCL1	Amplification	Oncogene	Cell Cycle/Apoptosis	Cell Survival
MYCN	Amplification	Oncogene	Cell Cycle/Apoptosis	Cell Survival
NCOA3	Amplification	Oncogene	Chromatin Modification	Cell Fate
NKX2-1	Amplification	Oncogene	PI3K; MAPK	Cell Survival
SKP2	Amplification	Oncogene	Cell Cycle/Apoptosis	Cell Survival

Table 1.2: Rearrangements in carcinomas (Taken from Vogelstein *et al.*, 2013)

Gene Fusion	Tumour type	Core Pathway	Process
TMPRSS2:ERG	prostate	Transcriptional Regulation	Cell Fate
CRTC1:MAML2	salivary gland	NOTCH	Cell Fate
PAX8:PPARG	thyroid	Transcriptional Regulation	Cell Fate
SLC45A3:ERG	prostate	Transcriptional Regulation	Cell Fate
TPM3:NTRK1	colon	MAPK	Cell Survival
TMPRSS2:ETV1	prostate	Transcriptional Regulation	Cell Fate
BRD4:C15orf55	midline organs	Cell Cycle/Apoptosis	Cell Survival
CD74:ROS1	lung	PI3K; RAS	Cell Survival
CRTC3:MAML2	salivary gland	NOTCH	Cell Fate
MYB:NFIB	salivary gland	Transcriptional Regulation	Cell Fate
PRCC:TFE3	kidney	TGF-b; APC	Cell Fate/Cell Survival
FGFR1:PLAG1	salivary gland	Transcriptional Regulation	Cell Fate
TMPRSS2:ETV4	prostate	Transcriptional Regulation	Cell Fate
SLC45A3:ELK4	prostate	MAPK	Cell Survival
HMGA2:WIF1	salivary gland	APC	Cell Fate
TPR:NTRK1	thyroid	MAPK	Cell Survival
PTPRK:RSPO3	large intestine	APC	Cell Fate

SLC34A2:ROS1	lung	PI3K; RAS	Cell Survival
CHCHD7:PLAG1	salivary gland	Transcriptional Regulation	Cell Fate
LIFR:PLAG1	salivary gland	Transcriptional Regulation	Cell Fate
TFE3:ASPSCR1	kidney	TGF-b; APC; PI3K	Cell Fate/Cell Survival
VTI1A:TCF7L2	large intestine	APC	Cell Fate
NDRG1:ERG	prostate	Transcriptional Regulation	Cell Fate
SDC4:ROS1	lung	PI3K; RAS	Cell Survival
SFPQ:TFE3	kidney	TGF-b; APC	Cell Fate/Cell Survival

The vast majority of genetic alterations within cancer disrupt the precise balance between differentiation and division, favouring the latter process, which ultimately confers a selective growth advantage, as differentiating cells eventually die or become quiescent. Cell fate pathways that function through this process, include APC, Hh (Hedgehog), and NOTCH, and are well known to control cell fate in organisms ranging from worms to mammals (Perrimon *et al.*, 2012). Signalling through these pathways allows cancer cells to maintain a proliferative state and in the context of the cancer SC theory (discussed later) maintenance of SC fate is essential for the growth of cancer.

Cell survival is maintained by receiving growth signals and through cell cycle progression. Although cancer cells divide in an uncontrolled manner, the surrounding stromal cells are normal and therefore are unable to match the demand for nutrients. In order to compensate for this, tumour cells have abnormal vasculature. The vasculature in normal tissues is well ordered and can tightly control nutrient concentrations, however the vasculature associated with tumours is tortuous and lacking in structural uniformity (Kerbel, 2008, Chung and Ferrara, 2011). In normal tissues cells tend to always be within 100uM of blood vessels for their nutrient supply, however this isn't the case in cancer cells (Baish *et al.*, 2011). As a consequence cancer cells that acquire mutations that permit them to proliferate under nutrient deficient conditions will have a selective growth advantage. Mutations that support cell survival in cancers include EGFR, HER2, FGFR2, PDGFR, TGFBR2, MET, KIT, RAS, RAF, PIK3CA, and PTEN (Hynes and Lane, 2005; Turner and Grose, 2010). For example, KRAS and BRAF mutations provide

cells with a survival advantage by allowing them to grow in glucose concentrations that would be too low for normal cells or cancer cells lacking these mutations (Yun *et al.*, 2009; Ying *et al.*, 2012). Also included in this category are genes that promote cell cycle and simultaneously block apoptosis, such as CDKN2A, MYC, and BCL2. Finally, VHL stimulates angiogenesis by inducing vascular endothelial growth factor secretion.

Genome maintenance is essential for cancer cell survival as they must reside in a genotoxic environment and acquire additional mutations from constant proliferation (Kwak *et al.*, 2004). Thus, mutations in genes such as TP53 and ATM, abrogate checkpoints that would otherwise stop the cell from entering the cell cycle and induce apoptosis, (Derheimer and Kastan, 2010). There is also an indirect advantage that is conferred to cells harbouring mutations within these genes, as they allow cells that have a gross chromosomal change favouring growth, to survive and divide. Unsurprisingly, mutations within genes that control point mutation rates, such as MLH1 and MSH2, are also found in cancer, and serve to accelerate the acquisition of mutations within genes that function to regulate cell fate and/or survival.

In summary, the cancer hallmarks discussed earlier are the result of DNA mutations in key genes that allow cells to proliferate and survive, hence providing a growth advantage over their normal tissue cell counterparts. These mutations are acquired from environmental factors and during cell division through imperfect DNA replication. Mutations in gatekeeper genes facilitate this process by initiating a local growth advantage, with subsequent mutations influencing cell fate, cell survival and genome maintenance.

1.3 Targeted Therapies

The advance in next generation sequencing has helped define driver mutation, most notably in oncogenes. The term "oncogene addiction" has been used to describe tumours that are dependent on a continued activity of a mutated constitutively activated oncogene for their maintenance (Weinstein, 2002). The identification of oncogenic drivers of cancer has led to the development of targeted therapies. In some

cases, the drug target is a specific mutated protein; such as drugs that block the BRAFV600E mutation. More commonly, targeted therapies have successfully blocked oncogenic pathways at multiple different levels: at the receptor (e.g. trastuzumab (herceptin) HER2 receptor antagonist), receptor tyrosine kinase (e.g. imatinib mesylate (gleevec) the *BCR-ABL* oncogene), and signal transduction intermediaries (e.g. vismodegib (Erivedge) a smoothed antagonist). Despite their advance and successes, targeted therapies have not been a cancer cure (discussed in detail below sections); although, immunotherapies may prove to be an exception. Briefly, the field of cancer immunotherapy has been re-energized by the development of immune checkpoint inhibitors and chimeric antigen receptor (CAR) T cell therapies, which have yielded very promising results and will be described briefly.

As highlighted both CTLA4 and PD-1 are immune checkpoint receptors that negatively regulate T cell function and have been the subject of much interest for the development of drugs that block CTLA-4 and PD-1 binding and thereby stimulate a T cell response and target cancer cells for destruction. The rationale for investigating immune checkpoint inhibition has been provided by pre-clinical studies showing a reduction in tumour growth and improved survival following blockade of the CTLA-4 and PD-1 pathways (Leach *et al.*, 1996; Hirano *et al.*, 2005). Monoclonal antibodies that block these pathways have now been approved for the treatment of melanoma (Nivolumab and Pembrolizumab) and lung cancer (Ipilimumab). Perhaps even more exciting is the use of peripheral blood T cells that have been genetically modified to express CAR genes and are subsequently infused into patients and are directed against specific antigens that can mount an immune response against a cancer. This adoptive transfer of CAR T cells has demonstrated remarkable success when treating haematologic cancers such as acute and chronic B cell leukaemia (Davila and Sadelain, 2016). This proof of principle has led to intense focus on the treatment of solid cancers using this approach. However solid tumours present barriers that are not present in haematologic malignancies, in that CAR T cells must be able to exit the blood and access the tumour in spite of potential mismatches between T cell chemokine receptors and tumour-derived chemokines. Furthermore, even if these barriers are overcome the CAR T cells must then be able to infiltrate the stromal elements of the tumour in order to elicit cytotoxicity, and tolerate the potentially hostile tumour microenvironment

characterised by oxidative stress, nutritional depletion, acidic pH and hypoxia (Buchbinder and Desai, 2016; Newick *et al.*, 2017).

1.3.1 BCR-ABL

The germline chromosome translocation t(9;22), known as the Philadelphia chromosome, is associated with the development of leukaemia, and is the hallmark of chronic myeloid leukaemia (CML). The Philadelphia chromosome is also observed in acute myelogenous leukaemia (occasionally) and adult and childhood acute lymphoblastic leukaemia (ALL), 25–30% and 2–10% respectively (Kurzrock *et al.*, 2003). The Philadelphia chromosomal translocation results in a fusion gene BCR-ABL, which encodes an oncogenic protein Bcr-abl fusion protein. The p190 and p210 variants are unregulated tyrosine kinases that have the capacity to transform cells (Lichty *et al.*, 1998) (Figure 1.1).

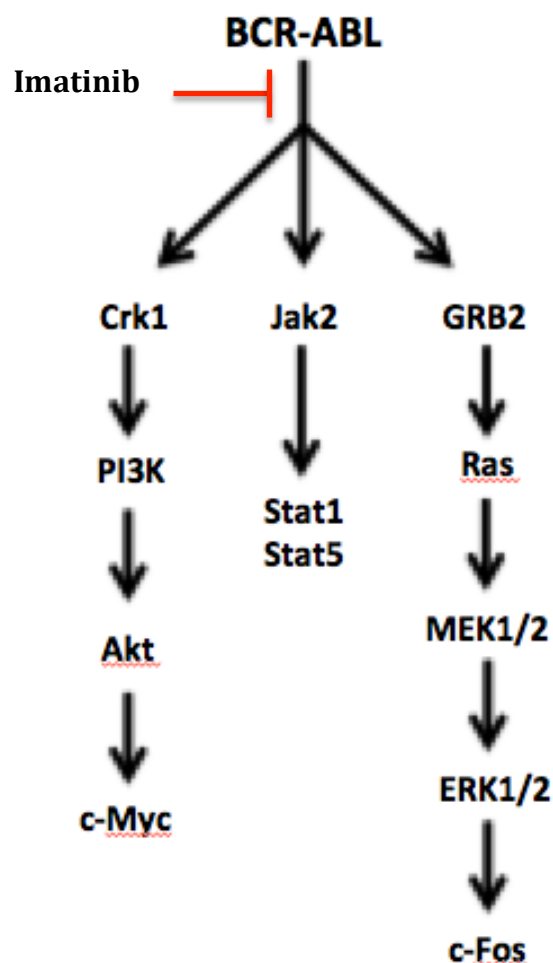


Figure 1.1: Signal transduction pathways affected by Bcr-Abl and sites of inhibition.

Imatinib mesylate (Gleevec, Novartis) is a small molecule inhibitor that binds the inactive form of the enzyme and has significantly improved survival in CML (Deininger *et al.*, 2005). Although developed to target the BCR-ABL tyrosine kinase domain, imatinib has a small effect on other tyrosine kinases. A second-generation small molecule inhibitor BCR-ABL, dasatinib (Sprycel, Bristol-Myers Squibb) has much broader tyrosine kinase inhibition including the Src family, c-Kit, platelet-derived growth factor receptor and EphA2 (Zhang *et al.*, 2009). Tyrosine kinase inhibitors (such as imatinib and sunitinib) are important drugs against a variety of cancers including CML, renal cell carcinoma (RCC) and gastrointestinal stromal tumours (GISTs), hypereosinophilic syndrome, systemic mastocytosis, and dermatofibrosarcoma protuberance.

Imatinib does not appear to cure the disease with eventual relapse of the disease. Mechanisms for resistance and relapse include: mutations within BCR-ABL, overexpression of BCR-ABL by amplification, and enrichment of CML SC progenitors that are resistant to BCR-ABL directed therapies (Deininger, 2008). As with imatinib resistance in CML, GIST patients also develop drug resistance (Mahadevan *et al.*, 2007).

1.3.2 Epidermal growth factor receptors

The human epidermal growth factor receptors (HER1, 2, 3, and 4) are receptor kinases belonging to the epidermal growth factor receptor (HER/EGFR/ERBB) family (Coussens *et al.*, 1985). Approximately 30% of breast cancer patients demonstrate HER2 amplification or over-expression of this oncogene, which is often associated with aggressive and progressive disease (Burstein, 2005). Trastuzumab (Herceptin) binds the extracellular domain of HER2 to block signalling and is approved for the treatment of

HER2+ metastatic breast cancer and HER2+ metastatic gastric or gastroesophageal junction adenocarcinoma (Brand *et al.*, 2006) (Figure 1.2).

Other HER family members are overexpressed (HER1, 2, and 3; lung, head and neck, breast, and prostate cancers) or mutated (HER1 and 2; lung cancer and glioblastoma multiforme [GBM]), leading to constitutive activation in multiple malignancies. The HER1/HER2 heterodimer strongly activates RAS-MAPK and STAT pathways (Yarden and Sliwkowski, 2001). In contrast, the HER3 receptor activates the PI3K/AKT survival pathway (Yarden and Sliwkowski, 2001). A second HER2-targeting monoclonal antibody, pertuzumab, binds the HER2/HER3 heterodimer and also inhibits HER3 overexpressing tumours (ovary, breast, prostate, colon, lung) by abrogating the activation of the PI3K/AKT pathway (Johnson and Janne, 2006). HER2 antagonists originally developed for the treatment of breast cancer appear to also be effective at treating other cancers, most notably non-small cell lung cancer.

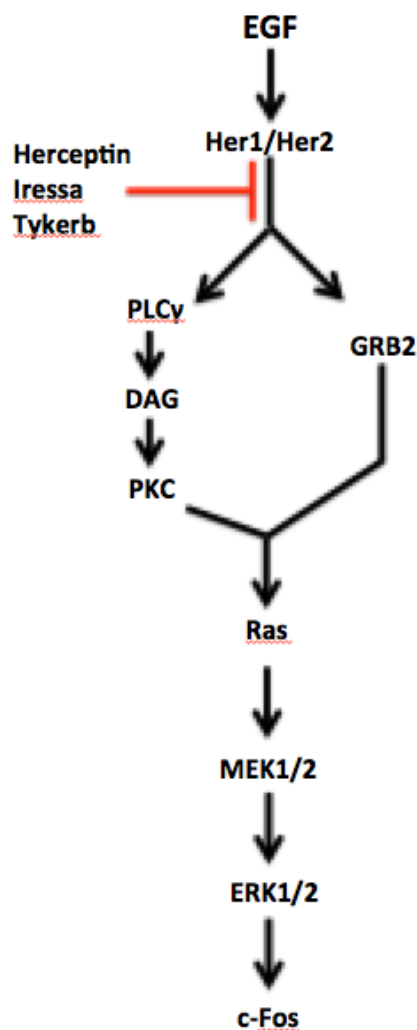


Figure 1.2: ERK arm of the human epidermal growth factor receptor pathway and sites of inhibition

The human epidermal growth factor receptor-signalling pathway is one of the most important pathways for the regulation of cell growth, survival, proliferation and differentiation. This signalling pathway is comprised of four tyrosine kinase receptors, however this schematic only outlines EGFR (Her1) and ErbB-2 (HER2), along with the Ras/Raf/MEK/ERK and phospholipase C γ signalling arms downstream of these receptors. In reality this pathway is far more complex and has other signalling arms, including the PI3K/AKT, STAT and Nck/PAK signalling cascades, which are not outlined in this schematic.

Gefitinib (Iressa, AstraZeneca) is a small molecule inhibitor that specifically targets the HER1 ATP-binding site, leading to inhibition of the Ras signal transduction cascade and subsequent cell growth (Ma *et al.*, 2015). It is currently approved for NSCLC with mutations in the EGFR tyrosine kinase domain (Rusnak *et al.*, 2001).

However, HER targeted therapy eventually leads to drug resistance, from secondary mutations in the HER1 TK domain (T790M, D761Y) (Sharma *et al.*, 2007), KRAS mutations (Van *et al.*, 2015), and amplification and overexpression of c-Met (Bean *et al.*, 2007) and HER3 (Sergina *et al.*, 2007). In summary, HER antagonists although effective, eventually are associated with resistance and relapse.

1.3.3 B-RAF

The RAS/RAF/MEK/ERK proteins represent an important signal transduction pathway that is activated by a number of growth factor receptors through RAS phosphorylation. Oncogenic mutations, most notably the BRAF V600E mutation, constitutively activate ERK signalling that induces proliferation and promotes transformation (Davies *et al.*, 2002). The BRAF V600E driver mutation is detected in melanoma (50-70%), primary thyroid carcinoma (36-69%), clear renal cell carcinoma (5-12%), and NSCLC (1-4%) (Davies *et al.*, 2002).

Sorafenib targets multiple tyrosine kinases, with binding to B-RAF, VEGFR-2/3, c-Kit, PDGFR, Flt-3, and FGFR1. It is approved for advanced RCC and HCC (Ma and Adjei, 2009; Halilovic and Solit, 2008). However, sorafenib only showed modest activity in melanoma, with no correlation to BRAF mutational status (Halilovic and Solit, 2008).

Vemurafenib (Zelboraf) inhibits the active "DFG-in" form of the kinase; firmly anchoring itself in the ATP-binding site, thus selectively inhibits the proliferation of cells with unregulated BRAF (Bollag *et al.*, 2012). Vemurafenib is approved for the treatment of metastatic melanoma. In a Phase III clinical study, it improved survival to 53%, compared to 7-12% with the former best chemotherapeutic treatment, dacarbazine (Chapman *et al.*, 2011). In spite of the high efficacy, all tumours eventually develop resistance to vemurafenib.

1.3.4 Hedgehog (see section 1.4)

Sonic hedgehog ligand binding of the patched receptor leads to translocation of SMO from the cell membrane to the primary cilium, where it replaces patched (Rohatgi *et al.*, 2007). After cellular delocalisation, SMO must additionally be activated by a distinct mechanism in order to stimulate hedgehog signal transduction, but that mechanism is unknown (Arensdorf *et al.*, 2016; Rohatgi *et al.*, 2009). Mutations in SMO itself can mimic the ligand-induced conformation of SMO and activate constitutive signal transduction (Arensdorf *et al.*, 2016). In addition to Patched mutations, activating SMO mutations can lead to unregulated hedgehog signalling in cancers such as medulloblastoma, basal-cell carcinoma, pancreatic cancer, and prostate cancer (Wang *et al.*, 2009; Xie *et al.*, 1998).

1.3.5 Other targeted therapies

There are number of targeted therapies in development targeting individual aspects of the cancer hallmarks: epigenetics, angiogenesis, cell stress, neovascularisation, apoptosis, cell cycle, tumour invasion and immunity. Below I have discussed those with established therapies.

1.3.5.1 Epigenetic modification

Tumour suppressors within cancers are frequently silenced by epigenetic modification of the DNA and/or histones.

DNA methyltransferase (DNMT) enzymes cause covalent modification of DNA by methylation at the 5-position of cytosine bases after DNA synthesis reaction (Bird *et al.*, 2002). Thus, aberrant DNA methylation is associated with gene silencing in malignancies (Issa *et al.*, 2005). Two DNA hypomethylating agents, 5-azacytidine (azacitidine) and 5-aza-2'-deoxycytidine (decitabine) have been approved for the treatment of higher-risk myelodysplastic syndrome (MDS) (Silverman *et al.*, 2002; Kantarjian *et al.*, 2006; Steensma *et al.*, 2009).

Histone acetyltransferases (HATs) and histone deacetylases (HDACs) catalyse the reversible acetylation of histones. In malignancies, HDACs drive the equilibrium of this reaction in favour of deacetylation, causing tightening of histones and epigenetic silencing (Marson, 2009). Vorinostat (suberoylanilide hydroxamine acid) is a HDAC inhibitor to be approved for the treatment of advanced cutaneous T-cell lymphoma (CTCL) (Mann *et al.*, 2007). However, more recently the HDAC inhibitors, decitabine (Kantarjian *et al.*, 2006), belinostat (O'Connor *et al.*, 2015), and panobinostat (San-Miguel *et al.*, 2014) have been approved for the treatment of multiple myeloma and T cell lymphoma, and have also shown to be effective in the treatment of solid tumours (San-Miguel *et al.*, 2014).

1.3.5.2 Anti-angiogenesis therapy

Angiogenesis defines the growth of new blood vessels, a hallmark of cancer. The controlled physiological development of new blood vessels, such as after injury, reflects a balance between proangiogenic and antiangiogenic factors. However, cancers also rely on angiogenesis for growth and therefore therapies have been developed targeting this process.

The vascular endothelial growth factor (VEGF, previously known as vascular permeability factor) family is composed of 6 secreted ligands (VEGF-A, B, C, D, and E and placental growth factor) and 3 receptor tyrosine kinases (VEGFR-1, 2, 3). Ligand

receptor interaction results in changes to the endothelial cell cytoskeleton, facilitating migration and proliferation (Dvorak *et al.*, 1995). VEGF-A is the main factor in cancer angiogenesis and the targeting monoclonal antibody bevacizumab is licensed for the treatment of renal cancer, NSCLC, breast cancer and glioblastoma multiforme (Ferrara *et al.*, 2003). Platelet-derived growth factor also plays a significant role in the formation of blood vessels and is a potent mitogen for cells of mesenchymal origin. Several VEGFR antagonists have been developed and FDA approved, including pazopanib for the treatment of renal cell carcinoma in 2009 (Hurwitz *et al.*, 2009), and regorafenib for the treatment of colorectal cancer in 2012 (Mross *et al.*, 2012).

1.3.5.3 Stress Response

DNA damage and replication stresses add to cancer cell mutagenesis, but can be therapeutically exploited and two approaches are currently licensed for the treatment of cancer: proteasome inhibitors and mTOR inhibitors.

1.3.5.4 Proteasome inhibitors

The proteasome complex is a multi-subunit 4 ring structure responsible for intracellular proteolysis. Unfolded or mis-folded intracellular proteins become ubiquitinated and thus targeted for proteasomal degradation (Adams, 2002). Cancer cells exhibit increased amounts of abnormal cellular proteins, thus inhibition of this pathway can cause selective cancer cell killing (Adams, 2004). Bortezomib is a proteasome inhibitor licenced for the treatment of multiple myeloma and mantle cell lymphoma in combination with melphalan and prednisolone (San Miguel *et al.*, 2008). Although bortezomib has been associated with good clinical responses in the treatment of multiple myeloma, it has been associated with resistance and tumour relapse. Furthermore, up to 80% of patients with the disease develop any grade neuropathy (Richardson *et al.*, 2010), and thrombocytopenia (Lonial *et al.*, 2005). These issues have led to the development of second-generation proteasome inhibitors, such as the epoxyketones, which unlike boronates such as bortezomib, can form irreversible bonds with the N-terminal threonine residues within catalytic proteasome subunits responsible for the cleavage of peptide bonds, and therefore have longer durations of inhibition One such epoxyketone is carfilzomib, which has shown to be both tolerable

and active against relapsed and/or refractory multiple myeloma, even in patients who have previously received bortezomib (O'Connor *et al.*, 2009; Alsina *et al.*, 2012; Manasanch and Orlowski, 2017).

1.3.5.5 mTOR inhibitors

Expression of the hypoxia inducible factor HIF-1a is upregulated in many cancers, most notably in renal cell carcinoma (Otrock *et al.*, 2009). HIF-1a is a downstream target of the PI3K-AKT cell survival pathway. Downstream of AKT in the PI3K pathway is mTOR, a cytosolic serine threonine kinase that can exist in two complexes: TORC1 (mTOR, raptor PRAS40, mLst8) and TORC2 (mTOR, rictor, Sin1, mLst8, mAv03) (Bhaskar and Hay, 2007). The TORC1 complex is regulated by cellular stress, controls the G1 to S phase transition, cap-dependent translation, membrane trafficking, protein degradation, ribosome biogenesis, proliferation, and survival. Importantly, the TORC1 complex regulates transcription of HIF-1a (Dowling *et al.*, 2009). Several TORC1 inhibitors are licenced for the treatment of renal cell carcinoma: rapamycin, everolimus and temsirolimus (Meric-Bernstam and Gonzalez-Angulo, 2009). However, recently mTOR resistance mutations have been identified in both rapalogs (rapamycin and its derivatives) and kinase inhibitors of mTOR (Rodrik-Outmezguine *et al.*, 2016). To overcome this resistance, a third generation of mTOR inhibitors have been developed, called Rapalink, which are single molecules containing both rapamycin crosslinked with a kinase inhibitor of mTOR (Rodrik-Outmezguine *et al.*, 2016). Rapalink is still only in its experimental stages but has however been shown to have better efficacy than rapamycin, and potentially block cancer-derived, activating mutants of mTOR in glioma mouse models (Fan *et al.*, 2017).

Over the last decade there have been many targeted therapies in early-phase clinical trials, including those targeting oncogene and non-oncogene addicted signalling pathways. While the advent of growth factor/oncogene driven targets has led to dramatic anti-cancer response, as illustrated above eventual relapse and resistance is common. Determining the basis for resistance and utilising synergistic killing may prove a useful strategy to improve the efficacy of oncogene targeting therapies.

1.4 Hedgehog Pathway

Hedgehog (Hh) was initially identified as a 'segment-polarity' gene (Nusslein-Volhard and Wieschaus, 1980). The human homologue Hh was identified in the early 1990s (Echelard *et al.*, 1993; Krauss *et al.*, 1993; Riddle *et al.*, 1993; Chang *et al.*, 1994; Roelink *et al.*, 1994). The Hh signalling pathway is evolutionary conserved and is essential during development (Ingham and McMahon, 2001; Weedon *et al.*, 2008; Zhao *et al.*, 2009).

In vertebrates the pathway is activated by three secreted hedgehog ligands: Sonic Hedgehog (SHh), Indian Hedgehog (Ihh) and Desert Hedgehog (Dhh), with SHh being the key morphogenetic factor (Mann and Beachy, 2004). All three ligands bind a single twelve-transmembrane receptor protein, Patched (PTCH), on the recipient cell (Hooper and Scott, 1989). In the absence of ligand binding, PTCH acts as a negative regulator of a seven-transmembrane G-protein coupled receptor (GPCR) smoothed (SMO) (Alcedo *et al.*, 1996; van-den-Heuvel and Ingman, 1996; Stone *et al.*, 1996; Ingman *et al.*, 1991). However upon binding of Hh, PTCH relinquishes inhibition of SMO leading to SMO phosphorylation by CK1 and GRK2, which is aided by the co-receptor Cdo (Denef *et al.*, 2000; Zheng *et al.*, 2010).

1.4.1 Smoothed phosphorylation

Mammalian SMO is regulated through multi-site phosphorylation in a dose-dependent manner, which regulates both the subcellular localization and conformation (Chen *et al.*, 2011). The kinases CK1 and GRK2 are both required for the phosphorylation and activation of SMO at six Serine/Threonine clusters found in the SMO C-terminus (Chen *et al.*, 2004, Meloni *et al.*, 2006, Chen *et al.*, 2011). This phosphorylation induces the ciliary localization of SMO through the recruitment of β -arrestins that link SMO to the anterograde kinesin-II motor (Chen *et al.*, 2011, Kovacs *et al.*, 2008). However, pathway activation also induces a conformational switch, which is governed by CK1/GRK2-mediated phosphorylation of the C-terminus that results in dimerization/oligomerisation of the SMO C-tail (Zhao *et al.*, 2007). In the absence of

ligand, SMO adopts an inactive conformation, which masks the kinase binding sites from CK1/GRK-2 (Chen *et al.*, 2011). A possible explanation for observing much higher levels of Hh signalling activity in the primary cilia is that fact that CK1 is accumulated in the primary cilia in response to Hh ligand, and therefore enhances the phosphorylation of SMO (Chen *et al.*, 2011).

1.4.1.1 Signalling downstream of mammalian SMO

The negative regulator, suppressor of fused (Sufu), forms complexes with GLI proteins to inhibit their ability to localize within the nucleus and drive gene transcription (Barnfield *et al.*, 2005; Ding *et al.*, 1999; Cheng and Bishop, 2002; Merchant *et al.*, 2004). However, upon Hh ligand binding, this complex dissociates and thereby relinquishes the full-length GLI proteins (Humke *et al.*, 2010, Tukachinsky *et al.*, 2010). Several kinases have been implicated in the regulation of GLI activity, including Cdc211, which acts upstream of GLI and downstream of Smo, and is a positive regulator of Hh signalling capable of associating with Sufu and thereby repressing its inhibitory actions (Evangelista *et al.*, 2008). An additional mechanism, through which SHh can regulate Sufu and its complex with Gli, is through the ubiquitin/proteasome pathway (Yue *et al.*, 2009), and also through phosphorylation at Serine342/346 by PKA (Chen *et al.*, 2011). Kif7 on the other hand plays both a positive and negative role in Hh signalling (Cheung *et al.*, 2009; Endoh-Yamagami *et al.*, 2009; Liem *et al.*, 2009). Studies have shown that Kif7 can be a positive regulator of the pathway by destabilizing Sufu and limiting its ciliary accumulation (Hsu *et al.*, 2011); and also be a negative regulator by inhibiting the transcriptional activity of Gli, independent of Sufu (Liem *et al.*, 2009; Hsu *et al.*, 2011).

The Hh signal transduction pathway culminates in the activation of GLI zinc-finger transcription factors. In vertebrates, there are three GLI proteins. GLI2 and 3 are activated by SMO, while GLI1 is transcriptionally induced by pathway activation and therefore acts in a positive feedback loop to reinforce GLI activity (Hui and Angers, 2011). Both GLI2 and 3 contain activator and repressor domains and in the absence of

ligand, undergo proteolytic processing into a truncated form (Gli^R), which also functions as a transcriptional repressor (Figure 1.3A). This proteolytic processing is achieved through the phosphorylation of GLI2 and 3 which promotes the recognition by the F-box protein β -TRCP which targets them for proteasome processing (Wang *et al.*, 2006; Bhatia *et al.*, 2006). The processing of GLI2 is very inefficient, with the small amount that is processed rapidly degraded, resulting in very little cleaved GLI2 within the cell. Conversely, GLI3 is very efficiently processed into its repressor form, and as a consequence GLI2 functions predominantly as an activator, while GLI3 is predominantly a repressor. GLI1 does not harbour the same domains and therefore does not undergo the same processing as GLI2 and 3, but is instead regulated by sequestration (Kogerman *et al.*, 1999; Liu *et al.*, 2014; Ding *et al.*, 1999). In the absence of ligand, SuFu complexes with GLI1 and prevents it from entering the nucleus, however upon signal activation this complex dissociates allowing GLI1 to enter the nucleus and drive gene transcription (Tukachinsky *et al.*, 2010). Hedgehog signalling inhibits GLI processing and converts the full length Gli^F into the active form Gli^A, which then acts as a transcription factor inducing downstream target genes (e.g. GLI 1, GLI2, K17, PDGFR α , PTCH1, BCL2) (Figure 1.3B). Furthermore, GLI activation is prevented by a complex consisting of Kif7, Sufu, and several Serine/Threonine kinases, which include PKA, GSK3 and CK1 (Chen and Jiang, 2013). In the mammalian system GLI activity is mostly blocked by Sufu and to a lesser extent Kif7 (Svard *et al.*, 2006; Chen *et al.*, 2009).

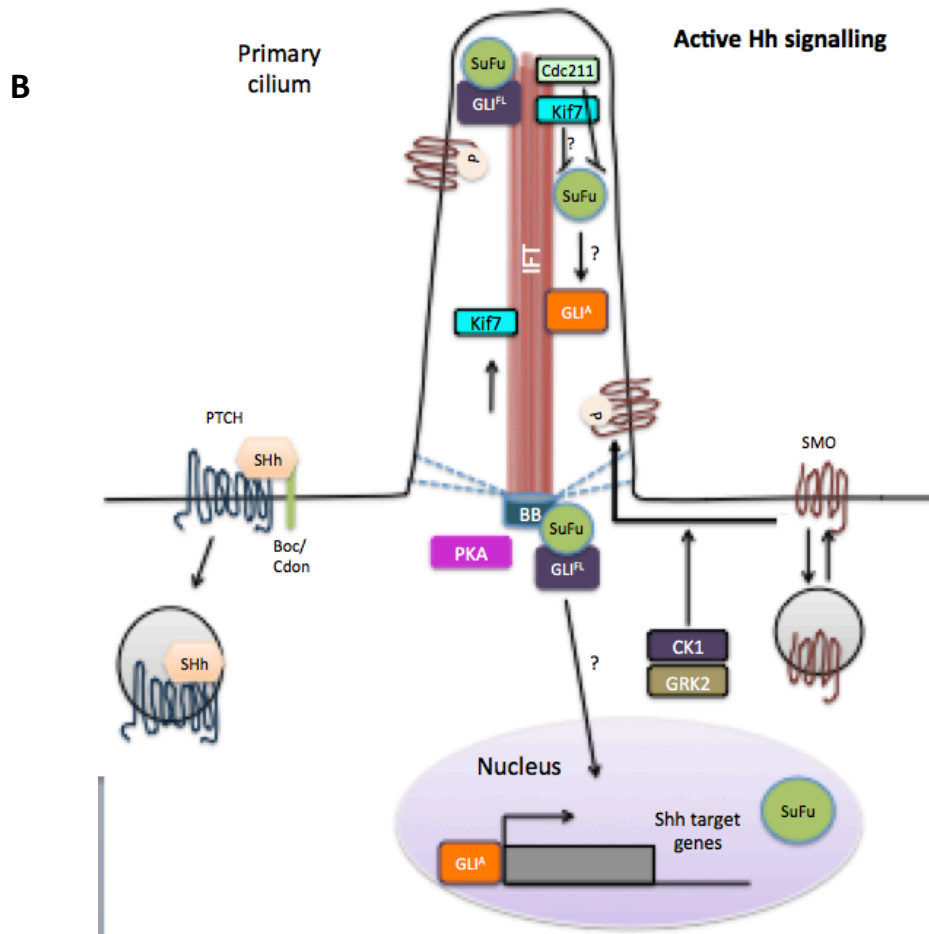
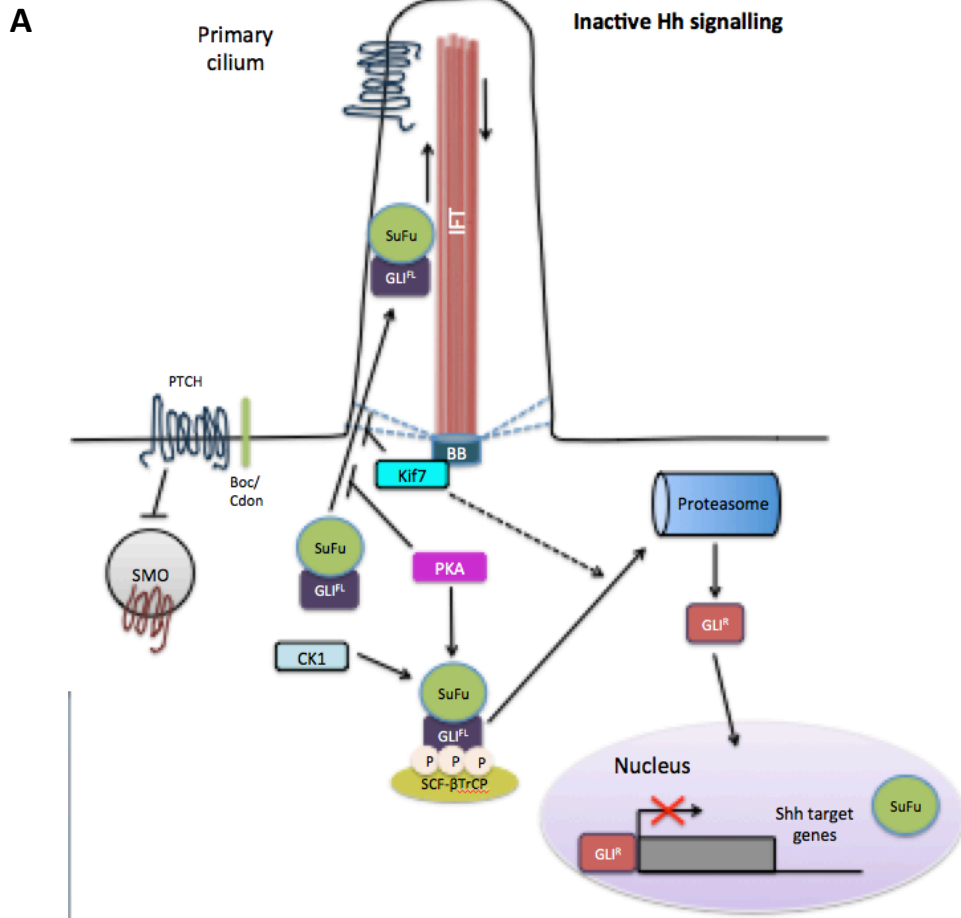


Figure 1.3: Hedgehog growth factor signalling pathway in vertebrate cells.

(A) Core Hh components localize to the primary cilium. In the absence of Hh ligand, PTCH localizes to the primary cilium where it prevents activation of SMO, which is sequestered into endocytic vesicles (circle). Microtubule motors within the cilium form the intraflagellar transport (IFT) machinery responsible for shuttling components of the Hh signalling pathway, including small amounts of GLI, in and out of the cilium. At the base of the cilium in this inactive state, protein kinase A (PKA), kinesin family member 7 (Kif7), and casein kinase 1 (CK1) promote the proteolytic processing of GLI3 into its repressive form GLI^R , which serves to suppress the expression of Hh target genes within the nucleus. In addition to this, SuFu stabilizes GLI proteins thereby inhibiting the transcriptional activity of GLI2, while PKA and Kif7 prohibit the accumulation of GLI^{FL} within the cilium. **(B)** Hh ligand binds to PTCH and its co-receptors Boc/Cdon, leading to the internalisation of PTCH which stops PTCH inhibition of SMO through phosphorylation, and results in SMO accumulation within the cell membrane through both lateral transport and the secretory pathways. Loss of PTCH inhibition on SMO leads to a conformational change within SMO causing it to reveal sites that are subsequently phosphorylated by CK1 and G-protein coupled receptor 2 (GRK2). This in turn leads to the abrogation of PKA function and promotes the movement of the SuFu-GLI complex and Kif7 to the ciliary tip where dissociation of SuFu and GLI^{FL} is thought to occur. The accumulation of GLI^{FL} in the ciliary tip is associated with the production of GLI activators (GLI^A), which are the processed forms of GLI^{FL} . GLI^A can then accumulate within the nucleus to drive transcription of Hh target genes.

1.4.1.2 Hedgehog signalling occurs in the primary cilium

In the mammalian systems Hh signalling is dependent on the primary cilium, a microtubule based membrane protrusion that is present in almost all vertebrate cells (Goetz and Anderson, 2010). Major Hh signalling components are present within the primary cilia complex, including PTCH, Smo, Kif7, Sufu, PKA and GLI proteins (Chen *et al.*, 2009; Corbit *et al.*, 2005, Haycraft *et al.*, 2005, Rohatgi *et al.*, 2007, Tuson *et al.*,

2011, Tukachinsky *et al.*, 2010). Hh-PTCH binding, promotes ciliary exit of PTCH and accumulation of SMO from the cell surface. Pathway activation also results in accumulation of GLI proteins at the cilium tip (Huangfu and Anderson, 2005; Haycraft *et al.*, 2005; Liu *et al.*, 2005). Thus, the primary cilium functions as a signalling centre to control the molecular events that lead to GLI processing.

Disruption of primary cilia prevents the formation of Gli^R and Gli^A. Furthermore, GLI phosphorylation by PKA occurs within the cilia base (Tuson *et al.*, 2011).

GLI3 is a negative regulator of the Hh pathway. Both Sufu and Kif7 are required for GLI3 processing, with Sufu phosphorylating GLI3 through recruitment of GSK3 (Kise *et al.*, 2009). The formation of this complex is inhibited upon activation of Hh signalling by SHh (Humke *et al.*, 2010; Tukachinsky *et al.*, 2010, Kise *et al.*, 2009).

1.4.2 Hh pathway physiological function

The hedgehog pathway has important functions in cell growth, survival and fate; and is also essential during development, and in SC maintenance. Under physiological conditions paracrine signalling is essential for development and for maintaining various epithelial tissues (Ingham and McMahon, 2001; Vheunissen and de Sauvage, 2009).

Hh proteins act as morphogens and are responsible for controlling multiple developmental processes. All three mammalian Hh proteins, *Sonic*, *Indian*, and *Desert Hh*, have similar physiological effects in development, with the differences in their roles due to the diverse patterns of expression (McMahon *et al.*, 2003; Sagai *et al.*, 2005). The expression of Dhh is predominantly found within the gonads, including the sertoli cells of the testis and the granulosa cells of ovaries (Bitgood *et al.*, 1996; Yao *et al.*, 2002; Wijgerde *et al.*, 2005). As a consequence of this restricted expression, mice deficient in Dhh do not show any noticeable phenotypic effects, with the exception of males being infertile due to the absence of mature sperm (Bitgood *et al.*, 1996). Like Dhh, Ihh is also expressed in specific tissue types, including the primitive endoderm (Dyer *et al.*, 2001), gut (van den Brink, 2007) and chondrocytes within the growth plates of bones (Vortkamp *et al.*, 1996). In humans, hypomorphic mutations within Ihh cause

acrocapitofemoral dysplasia, which is a congenital condition characterised by bone defects (Hellemans *et al.*, 2003). SHh on the other hand is broadly expressed, and has a crucial role in early embryogenesis. For example, SHh is responsible for the development of midline tissue, such as the node, notochord, and floor plate, and controls patterning of the L-R and A-V axes of the embryo (Sampath *et al.*, 1997; Pagan-Westphal and Tabin, 1998; Schilling *et al.*, 1999). SHh is also expressed within the zone of polarising activity of the limb bud and is pivotal in patterning of the distal elements of the limbs (Riddle *et al.*, 1993; Marti *et al.*, 1995). SHh also has an important role in later stages of development, particularly in organogenesis where it affects the development of most epithelial tissues. Due to its important role in development, loss of SHh can lead to cyclopia, along with defects in ventral neural tube, somite and foregut patterning.

Therefore, Hh signalling is essential during embryogenesis but is mostly quiescent during adulthood, and in adult tissues remains active in discrete populations of SCs found within a number of organs including the skin (Brownell *et al.*, 2011), muscle (Koleva *et al.*, 2005) and gut (van Dop *et al.*, 2009; Kang *et al.*, 2009) (Saqui-Salces & Merchant, 2010). Normal skin contains multiple populations of phenotypically distinct lineage-restricted SCs (Solanas and Benitah, 2013). SHh is the main Hh ligand that predominates within postnatal skin. During the anagen phase (growth) of the hair cycle, the lower end of the hair follicle can be found to express SHh, whereas the downstream effectors PTCH and GLI1 are more broadly expressed (Brownell *et al.*, 2011; Oro and Higgins, 2003). As a consequence, it has been demonstrated that anagen progression and subsequent hair growth can be blocked in mice using an anti-SHh blocking antibody (Wang *et al.*, 2000), which suggests that SHh is required for adult bulge SC regeneration. Conversely, the opposite has also been shown, whereby anagen can be stimulated in resting hair follicles following exogenous administration of SHh (Sato *et al.*, 1999). A recent study has revealed a positive feedback mechanism in the hair follicle, whereby SHh⁺ progenitor cells signal to the parental quiescent SC located in the bulge region and trigger SC activation and proliferation (Hsu *et al.*, 2014). Although, during the telogen phase (rest) of the hair cycle SHh expression is not detected at significant levels, additionally, both GLI2 and 3 are broadly expressed both in the follicle and the neighbouring dermis. In contrast, the expression of GLI1 and PTCH1 is found to be

restricted to two distinct SC domains: a K15-negative domain within the upper bulge region, and a K15/LGR5-positive domain within the lower bulge region (Brownell *et al.*, 2011). Finally, consistent with the role of Hh signalling in stimulating cell proliferation, loss-of-function mutations within SMO, or gain-of-function mutations within PTCH1 can give rise to BCC-like skin lesions when induced in hair follicle SCs (discussed in more detail later on) (Youssef *et al.*, 2010; Youssef *et al.*, 2012).

Skeletal muscle is almost unique in that it is one of the few adult mammalian organs capable of almost complete regeneration following injury, which is made possible through the presence of satellite cells (muscle SC population) (Lepper *et al.*, 2011). Under normal conditions these cells remain largely inactive, however upon injury, they can give rise to myogenic cells that are capable of reconstituting the myofibrils of the muscle (Yin *et al.*, 2013). Hh signalling has been shown to function as a pro-survival and proliferation factor in adult mouse satellite cells (Koleva *et al.*, 2005). Intriguingly, in adult fully differentiated muscle, both SHh and PTCH upregulation has been observed upon the induction of regeneration following ischemic injury. During this process of regeneration, Hh plays a pivotal role in promoting both angiogenesis and increasing the number of satellite cells at the affected site (Pola *et al.*, 2001; Pola *et al.*, 2003; Straface *et al.*, 2009). As a result, inhibiting Hh signalling has been shown to induce muscle fibrosis and increase inflammation in injured animals (Straface *et al.*, 2009).

Throughout the adult GI tract of both humans and rodents, the expression of SHh and IHH is expressed, and has been shown to signal to the Gli-expressing mesenchyme (Kolterud *et al.*, 2009; van den Brink *et al.*, 2002; van Dop *et al.*, 2009). Within the adult colonic mesenchyme, activation of Hh signalling through the conditional removal of PTCH1 results in the depletion of the epithelial precursor cell pool due to premature differentiation (van Dop *et al.*, 2009). Furthermore, during repair following the induction of gastric ulcers, Hh signalling has been shown to be downregulated, whereas SMO inhibition via an antagonist has shown to further inhibit gastric progenitor cell differentiation within these mice (Kang *et al.*, 2009). Finally, mouse models of Hh pathway inhibition have demonstrated the loss of villus smooth muscle cells, which caused atrophy of the small intestine villi, accompanied with inflammation and an

increase in the proliferation of the epithelial compartment (van Dop *et al.*, 2010; Zacharias *et al.*, 2010).

In summary, Hh signalling is essential not only during early embryogenesis, but also in adult tissue homeostasis, where high levels of Hh signalling are observed within specific cell populations, many of which have stem and progenitor cell properties. Following injury, Hh signalling is capable of stimulating SCs and other resident cells to contribute to the repair of the tissue; however, given its essential role in SC maintenance, perturbations within the Hh signalling pathway can contribute to disease states such as cancer.

1.4.3 Hh pathway in cancer

One quarter of all cancers exhibit activation of the Hh growth factor pathway, of which the archetypal cancer is BCC. Constitutive activation of the Hh pathway has been identified in multiple tumour types, including lung (Watkins *et al.*, 2003), stomach (Berman *et al.*, 2003), pancreas (Thayer *et al.*, 2003), prostate (Karhadkar *et al.*, 2004) and the brain (Clement *et al.*, 2007). There are three basic models for Hh signalling activity in cancer: 1) Type I – ligand independent, mutation driven; 2) Type II – autocrine, ligand dependent; 3) Type III – paracrine, ligand dependent.

The type I model for Hh signalling activity drives many cancers. For example, mutations have been identified in a small percentage of BCC (discussed in more detail later), medulloblastoma, rhabdomyosarcoma and osteosarcoma. Loss-of-function mutations within the negative regulators, PTCH and Sufu have been identified in cancer formation, with Sufu mutations identified in medulloblastoma patients (Taylor *et al.*, 2002), and PTCH mutations found in patients with basal-cell-nevus syndrome (discussed in more detail later) (Johnson *et al.*, 1996; Hahn *et al.*, 1996). Furthermore, sporadic BCC and medulloblastoma are often characterised by inactivation of PTCH1 or constitutive activation of SMO (Wolter *et al.*, 1997; Xie *et al.*, 1997; Xie *et al.*, 1998; Riefenberger *et*

al., 1998). However, mutations within the Hh signalling pathway have only been identified in BCC, medulloblastoma and rhabdomyosarcoma.

Most Hh driven epithelial malignancies demonstrate elevated levels of Hh ligand and/or ectopic PTCH and GLI expression. This ectopic ligand production can either occur within all tumour cells or a subset of tumour SCs and serve to support tumour growth and survival of surrounding cells. However, it is important to note that the exact mechanisms by which this pathway affects tumour survival and growth are not fully understood. The autocrine model of tumour growth occurs through the production of Hh ligands by tumour cells which act on neighbouring tumour cells to stimulate their growth and survival. This mode of Hh pathway activation is found in breast cancer (Mukherjee *et al.*, 2006), NSCLC (Singh *et al.*, 2011), and colorectal cancer (Gulino *et al.*, 2009). However, some groups have identified potential mechanisms involved in Hh driven tumours. For example, Chan *et al.* (2014) used a mouse model with partial upregulation of Hh signalling in mature osteoblasts, and found that it was capable of inducing osteosarcoma development through the overexpression of Yap1 (Chan *et al.*, 2014).

Paracrine Hh signalling is also an important mechanism in cancer and comprises tumour cells secreting Hh ligands that bind to receptors on the neighbouring stroma and thereby activate stromal Hh signalling (Jiang and Hui, 2008; Yauch *et al.*, 2008). Paracrine signalling functions to stimulate mesenchyme proliferation. The paracrine mechanism for Hh signalling was originally shown in prostate cancer; wherein patient derived xenografts induced elevated levels of PTCH and GLI1 within the murine stroma (Fan *et al.*, 2004). Hh ligand expressing cancers are refractory to the ligand, whereas the surrounding stroma is responsive (Nolan-Stevaux *et al.*, 2009; Theunissen and de Sauvage, 2009; Tian *et al.*, 2009; Yauch *et al.*, 2008). Furthermore, paracrine signalling has also been identified in pancreatic cancer, where it regulates metastasis and lymphogenesis (Tian *et al.*, 2009).

Another alternative mechanism by which Hh signalling can induce tumour development is through its ability to act on cancer stem cells (CSCs) that have the capability of not

only self-renewal, but also differentiation among multiple lineages, that enables them to potentially repopulate a tumour following treatment. CSCs have been identified in a wide range of solid tumours, including breast, pancreas, skin, and brain (discussed in more detail later) (Al-Hajj *et al.*, 2003; Ignatova *et al.*, 2002; Singh *et al.*, 2004; Collins *et al.*, 2005; Fang *et al.*, 2005; Li *et al.*, 2007; Colmont *et al.*, 2013). Sustained Hh-GLI signalling has shown to be required for the clonogenicity and tumorigenicity of human glioma CSCs (Clement *et al.*, 2007). Furthermore, the role of Hh signalling in CSCs has also been suggested in other tumours such as breast (Liu *et al.*, 2006) and multiple myeloma (Peacock *et al.*, 2007).

Although there are only a limited number of autocrine and paracrine signalling mechanisms that have been elucidated to date in tumour development, the role of Hh driven tumour cell lines has been a valuable tool for beginning to unravel the underlying mechanisms. There are a number of cell lines that have been characterised as Hh driven (Arnhold *et al.*, 2016). Hh signalling has been shown to be a key contributor in many of the paediatric tumours mentioned previously; notably medulloblastoma, rhabdomyosarcoma and osteosarcoma, and although to date there is no cell line known to stem from tumours with activating Hh mutations they have nevertheless been shown to have high levels of Hh signalling activity. There are 44 medulloblastoma cell lines, and only 18 of these have been subtyped. Through gene expression profiling, four main subtypes of medulloblastoma were identified: WNT, SHH, group 3 and group 4. The SHH group of medulloblastoma is driven by aberrantly activated Hh signalling, and is composed of four cell lines: DAOY, UW228-2, ONS-76 and UW426, with DAOY (Jacobsen *et al.*, 1985; Saylor *et al.*, 1991; Triscott *et al.*, 2013; Lacroix *et al.*, 2014) and UW228-2 (Keles *et al.*, 1995; Triscott *et al.*, 2013; Kunkele *et al.*, 2012; Lacroix *et al.*, 2014) being the most extensively used for research (Ivanov *et al.*, 2016). qPCR analysis of osteosarcoma cell lines revealed an overexpression of the key Hh pathway components, PTCH1, SMO, and GLI (Hirotsu *et al.*, 2010). The SJSA-1 cell line in particular has a 15-fold upregulation of GLI1 (Khatib *et al.*, 1993). Other cell lines with notable Hh activity include the Ewing sarcoma tumour cell lines, CADO-ES1, STA-ET1, and VH-64 (Arnhold *et al.*, 2016; Spaniol *et al.*, 2011), along with the rhabdomyosarcoma cell lines RD and RH-30 (Arnhold *et al.*, 2016; Spaniol *et al.*, 2011).

1.4.4 Basal cell nevus (Gorlins) syndrome

Basal cell nevus syndrome (BCNS) is an autosomal dominant disorder, and predisposes individuals with the disease to craniofacial and skeletal abnormalities (Gorlin and Goltz, 1960; Kimonis *et al.*, 1997). Patients with basal cell nevus syndrome are at increased risk of developing BCC and medulloblastoma. Basal cell nevus syndrome is caused by a germline mutation in the PTCH1 gene resulting in active Hh signalling (Aszterbaum *et al.*, 1998; Hahn *et al.*, 1996). Within basal cell nevus syndrome, tissue specific somatic mutations within the normal PTCH1 allele leads to the development of BCCs, medulloblastomas, meningiomas, and rhabdomyosarcomas (Colmont *et al.*, 2013). The incidence of BCC in individuals with BCNS is about 50% in patients >20 years, and up to 90% by the age of 40 (Evans *et al.*, 1993; Endo *et al.*, 2012). As mentioned previously, SMO is a GPCR and represents the obligatory signal transducer in the canonical Hh signalling pathway. Therefore it comes as no surprise to find that constitutively activating mutations within SMO contribute to the development of carcinomas, namely BCC (Hahn *et al.*, 1996; Johnson *et al.*, 1996) and medulloblastoma (Jiang and Hui, 2008; Xie *et al.*, 2008). More recently, mutations of PTCH1, SMO, and SUFU have been identified in sporadic BCC and medulloblastoma (Epstein, 2008; Kool *et al.*, 2008). In the case of sporadic BCC, nearly all tumours show evidence of constitutive Hh pathway activity, with 90% exhibiting loss of PTCH1 (Gailani *et al.*, 1996; Kim *et al.*, 2002) and 10% with activating mutations in SMO (Xie *et al.*, 1998; Reifenberger *et al.*, 1998).

1.4.5 Prototypic cancer: Basal Cell Carcinoma

BCC was first described in 1827 by Jacob (Jacob, 1827). BCC keratinocytes morphological resemble epidermal basal layer keratinocytes. BCC lesions, particularly in the early stages, appear as small, translucent or pearly lesions, with the distribution of small-dilated blood vessels over their surface. The development of BCC can occur at different anatomical sites, however 80% are found on the head and neck, (particularly the face), with the remainder found on the trunk and limbs (Rubin *et al.*, 2005). BCC usually manifests as an asymptomatic slow growing translucent raised nodule, which over the

period of 1-2 years may reach a diameter of half a centimetre before more rapid growth occurs leading to central ulceration.

BCC is classified based on the pattern of growth into four main categories: Nodular, superficial, infiltrative and morphoeic (Figure 1.4) (Rippey and Rippey, 1997; Lang and Maize, 1986). Nodular BCC is the most common type (50% of cases), and presents as a raised nodule with dilated blood vessels on the surface, which sometimes forms a central depression that may ulcerate, bleed or scab. Under the microscope, nodular BCC can be seen to have both small and large nests of tumour cells, with peripheral palisading growth from the epidermis to the dermis. Superficial BCC represents 15% of the cases, and is mainly found on the trunk. They are characteristically slow growing, and are often scaly, flat erythematous plaques which can easily be mistaken for psoriasis, discoid eczema, or Bowen's disease. Histologically, they are confined to the papillary dermis and are found to have numerous small islands of basaloid cells attached to the epidermis. In fact patients that present with BCC on the trunk, are usually more prone to developing multiple BCCs which are seen to develop at a faster rate than BCCs found on other regions of the body (Lear *et al.*, 1998). Morphoeic BCC represents 10% of the cases, and presents as a flat, atrophic, hard white or red plaque. The edges are not clear and are often much larger than what is seen on the surface. Histologically, morphoeic BCC has small root-like projections that extend deep into dermis, and are surrounded by a dense cellular stroma.

BCC rarely metastasize, with estimations showing that it occurs less than 0.0028% of the time, which as a consequence means the overall mortality from BCC remains very low (Rubin *et al.*, 2005). However, BCC is associated with significant morbidity, through its ability to invade locally into vital structures such as cartilage and bone, thereby causing cosmetic disfigurement. However, in instances where BCCs are neglected, they have the potential to grow very large, and have been known to invade into the orbit and cranium (Madan *et al.*, 2010).

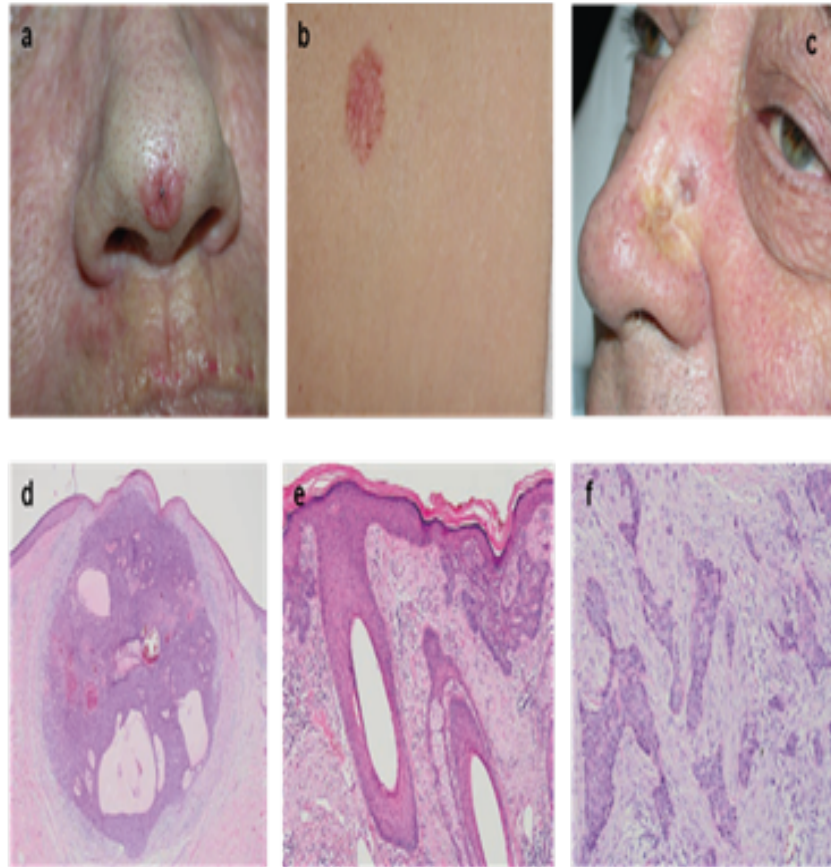


Figure 1.4: Three main categories of BCC.

Clinical and histological appearances of (A, D) nodular, (B, E) superficial, and (C, F) morpheiform BCCs. Taken from online source (GERIATRICS & AGING, September 2009, Volume 12, Number 8)(SCRIPTA MEDICA (BRNO) – 79(5-6):261-270, December 2006)

1.4.5.1 Epidemiology

Amongst fair-skin coloured individuals BCC is the most common skin cancer, which is in contrast to black-skinned individuals, where NMSC is rarely seen to develop (Halder and Bang, 1988). The estimated lifetime risk of developing BCC in Caucasians is between 28-33%. Men are shown to have a slightly higher incidence of BCC, which maybe because there is a statistically increased likelihood of working outdoors, and therefore becoming exposed to UV (Miller and Weinstock, 1994). In the UK, 56% of men, and 44% of women

will develop BCC, a male:female ratio of 1.5:1 (Lear *et al.*, 2007). While elderly men represent the highest rates of BCC, there is a trend over the past decade towards increasing BCC incidence among young women who use sunbeds or tan excessively (Christenson *et al.*, 2005; de Vries *et al.*, 2004; Epstein, 2008; Karagas *et al.*, 2002). For BCC and SCC, the average age-standardised rate per 100,000 is 98.6 and 22.7% respectively, however as many as one third of diagnoses may go unregistered (Andl *et al.*, 2004; Lomas *et al.*, 2012; Musah *et al.*, 2013). Between 2000-2002 and 2008-2010, the recorded incidence of BCC increased by around a third in England, Scotland, Northern Ireland, and Ireland combined (National Cancer Intelligence Network (NCIN). Non-melanoma skin cancer in England, Scotland, Northern Ireland, and Ireland: London: NCIN; 2013). This is in contrast to the overall cancer diagnoses over the past decade, where there was only a modest increase of 3% men and 6% in women observed. Thus the true socioeconomic burden of BCC is not known, as the cancer registry does not collect data pertaining to BCC (Goodwin *et al.*, 2004).

The main causative factor in the pathogenesis of BCC is exposure to UV radiation, consistent with this is the observation that the incidence of BCC varies geographically and globally, with Australia having the highest rates of BCC in the world (Gallagher *et al.*, 1995; Marks *et al.*, 1993). BCC development is also linked to exposure to other well-known carcinogens, including arsenic, coal tar, and ionizing radiation (Diepgen and Mahler, 2002). Furthermore, there is an association between smoking and the development of skin cancer, particularly amongst young women (Boyd *et al.*, 2002). However, although cumulative carcinogen exposure (i.e UV light) in adulthood is an important factor contributing to BCC, intrinsic factors to the individual are equally important. Intrinsic factors such as fair skin, red or blonde hair, light coloured eyes, and childhood freckling, are all factors that are associated with greater risk towards BCC development (Daya-Grosjean and Couve-Privat, 2005; Rubin *et al.*, 2005; Wong *et al.*, 2003). Also there is a strong relationship between BCC development and individuals with a positive family history of skin cancer (Corona *et al.*, 2001). BCC can also be seen more frequently amongst individuals with a high dietary intake coupled to low vitamin intake (Gallagher *et al.*, 1996; Yamada *et al.*, 1996). The incidence of BCC has been reported to be much higher in patients who have been on long-term

immunosuppressive therapy when compared to the general population, with renal transplant and heart transplant patients shown to be 10 and 21 times more likely to develop BCC than their normal counterparts (Ong *et al.*, 1999). It is believed that this increase is due to the immunosuppressive drugs dampening down the immune surveillance and thereby allowing mutated cells to progress to cancer (Tilli *et al.*, 2005).

Meta-analyses have shown that patients who have developed a BCC are at increased risk of developing further BCCs, with three-year cumulative risks varying from 33-77% (Stern and Lang, 1988). Additionally, studies have shown that the risk of developing SCC and malignant melanoma are also increased in individuals who have developed BCC (Boyd *et al.*, 2002; Gallagher *et al.*, 1995).

1.4.5.2 Pathogenesis

Mouse models of BCC support the role of the Hh pathway in the pathogenesis. Wild type mice rarely develop BCCs even following treatment with UV or ionizing radiation. However, when applying UV radiation to a mouse with a PTCH^{+/-} genetic background, BCC development is common (Aszterbaum *et al.*, 1999). Interestingly, if these mice are kept under normal conditions, they rarely develop BCCs, thereby showing the importance of UV exposure in generating additional PTCH mutations in the normal allele in the development of BCC (Mancuso *et al.*, 2004). Furthermore, overexpression of Hh signalling pathway members (Hh, SMO, GLI1 and GLI2) has been shown to result in BCC development in murine skin and/or in human skin grafted onto mice (Fan *et al.*, 1997; Oro *et al.*, 1997; Grachtchouk *et al.*, 2000). The situation in medulloblastoma is less uniform, with up to 30% of tumours showing a gene expression signature that is indicative of hedgehog pathway activation, but only 50% of these were associated with loss of PTCH1, loss of SUFU or gain-of-function SMO mutations.

The vast majority of BCCs occur sporadically, however, as mentioned earlier Gorlin's syndrome is a rare inherited disorder that predisposes these individuals to BCC development. For many years it has been thought that the development of BCC occurs through a combination of mutations tumour suppressor genes, p53 and PTCH via the

targeting of UV. A mutation within these genes drives cell proliferation and subsequent BCC development (Kastan *et al.*, 1991).

Even though BCC is the most common neoplasm in humans, its precise origins are still unknown. Recent publications suggest that it develops from keratinocyte SCs of the hair follicle bulge (Youssef *et al.*, 2010; Wang *et al.*, 2011), however this will be discussed in more detail in section 1.5.

1.4.5.3 Molecular landscape of BCC

Exposure to UV is the most important risk factor in BCC, and as mentioned previously, the Hh signalling pathway is essential for its development. Numerous studies have reported point mutations, copy-loss of heterozygosity and copy-neutral loss of heterozygosity within PTCH1 in sporadic BCC (Teh *et al.*, 2005; Santos *et al.*, 2011). However, the mutation of the gene TP53 is an equally important event in the pathogenesis of BCC, with mutations found anywhere from 30-70% of BCCs (Lacour, 2002; Reifenberger *et al.*, 2005; Tang, 2011). In spite of this there are only a limited number of key mutations found to be required for the development of BCC, and yet of all the tumours, BCC has been found to have the highest mutation rate (65 mutations/Mb) (Jayaraman *et al.*, 2014; Bonilla *et al.*, 2016). Beyond both PTCH/SMO and TP53 mutations, other tumour suppressor genes and proto-oncogenes have been implicated in the pathogenesis of BCC including members of the RAS proto-oncogene family (van der Schroeff *et al.*, 1990; Pierceall *et al.*, 1991; Jayaraman *et al.*, 2014). In a recent study by Bonilla *et al.* (2016), 293 BCC tumours were genetically profiled and additional driver mutations were identified in other cancer-related genes including MYCN (30%), PPP6C (15%), PTPN14 (23%), STK19 (10%), and LATS1 (8%) (Bonilla *et al.*, 2016). Furthermore, consistent with these mutational profiles, both N-Myc (MYCN) and Hippo-YAP (PTPN14 and LATS1) pathway target genes were upregulated. Recent studies have also shown, in approximately 50% of BCC the presence of UV-induced somatic mutations within the telomerase reverse transcriptase (TERT) gene, which leads to increased expression of telomerase, thereby allowing cells to divide indefinitely, and avoid senescence and apoptosis (Griewank *et al.*, 2013; Scott *et al.*, 2014). Therefore,

although aberrant activation of Hh signalling is a hallmark of BCC development, recent genomic studies have discovered additional signalling pathways associated with the pathogenesis of BCC.

1.4.5.4 Management

Non-melanoma skin cancers (NMSC), including BCC are usually treated at the early stages. BCC management is usually surgical excision (Ceilley and Del Rosso, 2006).

1.4.5.4.1 Surgery

Due to it being a highly effective form of therapy for primary BCC, surgical excision is the preferred method of treatment, and it gives surgeons the opportunity to confirm complete excision by studying the histology of the tumour. Providing surgery is performed with clear histological margins, there is a <2% recurrence rate after 5 years, with increasing peripheral margins found to increase the cure rate further (Griffiths *et al.*, 2005; Walker and Hill, 2006). However, incomplete excision or border that are very close to the tumour, are frequently associated with recurrence (Sussman and Liggins, 1996). This is seen frequently in sites where skin preservation is important, such as the 'T' zone of the face, as there is often a balance between excising the tumour completely so that it doesn't grow back, and ensuring that the patient isn't left too disfigured due to skin removal (Kumar *et al.*, 2000). In the instances where re-excision is necessary, Mohs micrographic surgery (MMS) is the treatment most often adopted. Although MMS is an excellent treatment for high risk BCC with very high cure rates, it remains very costly to perform and time consuming and is therefore reserved for managing high-risk sites. In contrast, in other modes of surgery in which histology is not used to demonstrate eradication, such as cryosurgery, curettage, and photodynamic therapy, higher recurrence rates are observed (Chiller *et al.*, 2000; Holt, 1988; Johnson *et al.*, 1991).

1.4.5.4.2 Topical Therapies

The immune-modulator imiquimod stimulates toll like receptors and thereby activates the immune system and subsequently release of pro-inflammatory cytokines (Vidal *et al.*, 2004). More than 90% clearance of superficial BCC has been achieved following bi-daily treatment of imiquimod for 6-12 weeks (Marks *et al.*, 2001). However, its use is often limited due to potentially serious side effects such as marked inflammatory reaction, and although it has proven useful for the treatment of superficial BCC, it is not suitable for invasive BCC. Furthermore, a number of Hh pathway inhibitors are currently in clinical trials for a variety of malignancies, and this year the National Institute of Clinical Excellence (NICE) approved the SMO inhibitor, vismodegib for the treatment of inoperable and metastatic BCC. However, clinical studies already suggest that a BCC sub-population is resistant to vismodegib, discussed later (Von Hoff *et al.*, 2009; Metcalfe & de Sauvage, 2011; Skvara *et al.*, 2011; Sekulic *et al.*, 2012). Of note the relapse is associated with regrowth of the original tumour nodules, suggesting the presence of a residual and resistant tumour cell population that is able to repopulate the tumour; by definition CSC (discussed later).

1.4.5.4.3 Radiotherapy

In the case of primary and metastatic BCC, radiotherapy has been shown to be an effective therapy, and in some instances even against recurrent BCC (Al-Othman *et al.*, 2001; Caccialanza *et al.*, 2001). The overall 5-year cure rates being 91.3% for primary BCC and 90.2% for recurrent disease (Rowe *et al.*, 1989). This form of treatment is very helpful for people who are unable to tolerate surgery. For lesions up to 6 mm in depth, 170KV may be used, and for tumours invading deeper, electron beam radiotherapy may be used. However, in order to avoid radionecrosis of underlying tissues (particularly at the eyelids and bridge of the nose where the skin is thin), the dose has to be carefully titrated (Telfer *et al.*, 2008). An important point to make is that radiotherapy induces mutations in surrounding tissues, and as such should be avoided in patients with xeroderma pigmentosa and basal cell nevus syndrome (Caccialanza *et al.*, 2004).

1.4.5.4.4 Photodynamic Therapy (PDT)

PDT is a medical therapy based on the activation of chemical substances called photosensitizers by a light source emitting radiation of an appropriate wavelength, which have the capacity to selectively concentrate in neoplastic cells, and allow the energy they capture to pervade into surrounding tumour tissue (Matei *et al.*, 2013). This triggers photodynamic changes that result in the destruction of the tumour. BCC responds very well to this form of therapy (Matei *et al.*, 2013).

1.4.6 Development of Hh antagonists

1.4.6.1 Natural Compounds (Alkaloids, sesquiterpenes and physalins)

Cyclopamine and jervine (steroidal alkaloids) are naturally occurring Hh inhibitors, isolated from the corn lily *Veratrum californicum*. Cyclopamine blocks the Hh pathway at the level of SMO and inhibits the transcription of Hh target genes (Chen *et al.*, 2002). Following oral administration of cyclopamine, the growth of UV-induced BCCs in PTCH1^{+/-} mouse model was reduced by 90% and also there was a 50% reduction in new tumours (Athar *et al.*, 2004). However, due to its poor pharmacokinetic properties, low potency (EC₅₀ 300nM) and cytotoxicity, cyclopamine has never been developed in clinical trials. Other natural compounds that inhibit Hh signalling include: zerumbone, physalin B, physalin F and staurosporine (Stanton *et al.*, 2009).

1.4.6.2 Synthetic Compounds

Vismodegib is licenced for the treatment of locally aggressive BCC that are not amenable to surgical resection and metastatic disease. Von-Hoff and colleagues conducted a two-stage phase 1 trial on 33 patients with metastatic or locally advanced BCC, and assessed the response of these tumours to the small-molecule inhibitor of

SMO, vismodegib (Von-Hoff *et al.*, 2009). They found that of 33 BCC patients treated, only two had a complete response, while 18 had an objective response, and the remaining 15 had either stable disease or progressive disease (Von-Hoff *et al.*, 2009). They later performed a larger 2-cohort nonrandomized study on 104 patients (71 locally advanced BCC and 33 metastatic BCC), and found that vismodegib treatment was associated with tumour responses in 43% of patients with locally advanced BCC, and 30% of patients with metastatic BCC (Sekulic *et al.*, 2012). The efficacy of vismodegib was also evaluated in patients with BCNS in a randomised, double blind, placebo-controlled trial, and was shown to reduce the tumour burden and block growth of new BCCs; however drug treatment was discontinued in 54% of patients due to adverse effects of the drug (Tang *et al.*, 2012).

When assessing the efficacy of vismodegib on medulloblastoma, Von-Hoff and colleagues presented a case report of a 26-year-old man diagnosed with medulloblastoma confined to the cerebrum, at the age of 22. The patient demonstrated a good initial response to the drug, although this was only transient, and the tumour rapidly developed resistance to the drug and relapse occurred approximately 3 months after the initiation of the therapy and the patient died a further 2 months after this (Rudin *et al.*, 2009). A biopsy of one of the tumours revealed that resistance was attributed to D473H mutation within SMO (Yauch *et al.*, 2009; Dijkgraaf *et al.*, 2011).

LDE-225/Sonidegib (Novartis) is a recently licenced potent, orally bioavailable SMO antagonist. Sonidegib was found to impair medulloblastoma cell growth when combined with PI3K inhibitors (Buonamici *et al.*, 2010), and was also found to reverse Taxane resistance in a model for ovarian cancer (Steg *et al.*, 2012). However, in phase II trials, Sonidegib showed only a partial response to treatment with Gorlin syndrome and BCC (Skvara *et al.*, 2011).

Therefore, taken together Hh/SMO antagonists have shown some reasonable responses to the treatment of Hh driven tumours, but have also been faced with tumour unresponsiveness and even relapse/resistance (Skvara *et al.*, 2011; Sekulic *et al.*, 2012).

Therefore it will be important to better understand the mechanisms of resistance that underlie the failure of the drugs.

1.4.7 Development of resistance to Hh antagonists

Vismodegib inhibits SMO and despite it being active in advanced BCC, more than 50% of such lesions have demonstrated resistance to vismodegib (Ransohoff *et al.*, 2015; Metcalfe and de Sauvage, 2011); the mechanisms of such resistance will be discussed. Atwood *et al.* (2015) and Sharp *et al.* (2015) used a large collection of tumour samples to identify specific mutations within SMO that were responsible for conferring resistance to vismodegib (Atwood *et al.*, 2015; Sharpe *et al.*, 2015). A similar mechanism for resistance was also identified in medulloblastoma treated with vismodegib (Yauch *et al.*, 2009). Both studies demonstrated similar findings in that in spontaneous BCCs, 15-33% were found to have SMO mutations, whereas this rose to 69-77% in resistant tumours. The authors were also able to separate the resistance-associated mutations into two groups by aligning the mutations with the crystal structure of the SMO transmembrane domain. Group 1 mutations were found within or immediately adjacent to the ligand/drug-binding pocket, whereas the group 2 mutations were found at more distant sites within SMO.

1.4.7.1 Transformation of BCC into more aggressive phenotypes

Several cases of SCC arising from the same tumour bed as the original BCC during and after treatment have been documented (Ransohoff *et al.*, 2015; Mohan *et al.*, 2016; Aasi *et al.*, 2013; Orouji *et al.*, 2014; Zhu *et al.*, 2014; Chang *et al.*, 2012; Zhu *et al.*, 2014). Whether the SCC is related to the BCC clone or simply rose independently in the same stroma bed is not always determined in many of these clinical reports. However, Ransohoff *et al.*, (2015) provided genetic evidence of phenotype switching from BCC to SCC during vismodegib treatment. In this instance DNA was obtained from the primary basal-cell lesion before vismodegib therapy, and from the recurring squamous cells, and underwent exome sequencing. Sequencing identified identical PTCH1 and TP53 mutations within both tumours sequenced, with the recurrent SCC found to have a very

similar mutation rate of 35 mutations per mega-base and shared a 90% genomic identity with the original BCC (Ransohoff *et al.*, 2015). In an attempt to identify the mechanisms underpinning this conversion following treatment, they found that the recurrent SCC showed no signs of acquired SMO mutations but still demonstrated maintained Hh signalling pathway activity. Another study identified the onset of keratoacanthomas (KAs) in two patients with no history of developing KAs or SCCs, following treatment of locally advanced BCC with vismodegib (Aasi *et al.*, 2013). Furthermore in a study by Mohan *et al.* (2016) on a cohort of 180 patients (BCC=55 cases; Controls=125 cases), patients exposed to vismodegib had an increased risk of developing cutaneous SCC (Mohan *et al.*, 2016).

1.5 Stem Cells

Tissues such as the skin epidermis continuously self-renew through the dedicated activity of adult tissue-specific SCs (SC) (Fuchs and Chen, 2013). Adult tissue SCs are long-lived and produce progeny that are function-specific and short-lived. SCs represent a rare population of cells, which in mammals can be divided into two main categories: i) embryonic SCs and ii) adult SCs. Embryonic SCs are capable of giving rise to all cell lineages, and under normal conditions are unable to revert back to a pluripotent state (Mitalipov and Wolf, 2009). Following embryonic development, embryonic SCs lose their plasticity, however tissue specific adult SCs remain. These adult tissue SCs are responsible for the maintenance and repair of many tissues, including the skin, brain, digestive tract and haematopoietic system (Wagers and Weissman, 2004). Within these tissues, SCs are found at the top of the cellular hierarchy, and are defined by their long-term self-renewal capacity, and ability to produce cells capable of differentiation, which ensure the specific functions of the tissue. Self-renewal is the cardinal property of a SC, in which cell division produces one (asymmetric) or two (symmetric) daughters that retain the ability to self-renew, and thereby maintain and/or expand the SC population (Yamashita *et al.*, 2010; Fuchs and Chen, 2013). Schofield *et al.* (1978) proposed that SCs reside in a specific anatomical compartment within the tissue that promotes the maintenance of SC properties, termed the 'SC niche'. These niches are essential for normal SC function, and are as varied as the SCs they support, with studies showing that

tissues contain distinct functional SC niches, each designed to support the specialized role of that tissue (Morrison and Spadling, 2008; Plaks *et al.*, 2015; Lane *et al.*, 2014). Interestingly, there is increasing evidence to show that deregulation of these SC niches is implicated in numerous pathologies associated with tissue degeneration and tumourigenesis (Plaks *et al.*, 2015).

1.5.1 Haematopoietic SCs and Leukaemia initiating cells

In 1961, Till and McCulloch published the first in a series of groundbreaking experiments that went on to demonstrate that: 1) the existence of clonal haematopoietic cells in the bone marrow could give rise to mixed myeloerythroid progeny, 2) some of these cells had the capacity to make more of themselves, and 3) in the spleens of these mice, there were cells that had the capacity to make lymphocytes (Till and McCulloch, 1961; Becker *et al.*, 1963; Siminovitch *et al.*, 1963; Wu *et al.*, 1967; Wu *et al.*, 1968). In the early 1990's Dick and colleagues utilising a similar approach found that most subtypes of acute myeloid leukaemia (AML) could engraft reliably in immunodeficient mice (Lapidot *et al.*, 1994; Bonnet and Dick, 1997). They successfully showed that leukaemia-initiating cells (LICs) were enriched within the CD34⁺ CD38⁻ fraction and that the leukaemia initiating cell frequency was approximately 1 per 250,000 tumour cells. Transcriptional profiling of these LICs revealed that they were similar to normal haematopoietic SCs (Eppert *et al.*, 2011). However studies have shown that by transplanting sorted fractions of primary *NPM*-mutated AML into immunodeficient mice, LICs were present in the CD34⁻ fraction also (Taussig *et al.*, 2008). Table 1.3 outlines the multiple cell fractions that have been identified as capable of initiating leukemia in both primary and secondary recipients. Interestingly, the cell of origin for most LICs is not entirely clear (Dick, 2008; Clarke *et al.*, 2006), with one hypothesis that LICs only arise from normal haematopoietic SCs (HSCs) and not from committed progenitors, whereas the other is that transformation may occur in a variety of cell types within the haematopoietic hierarchy. LICs derived from HSCs is supported by the observation that they both share numerous characteristics such as their capacity to self renew and be quiescent (Terpstra *et al.*, 1996; Lessard and Sauvageau, 2003; Yilmaz *et al.*, 2006). However, there is experimental evidence in mice to support the alternative hypothesis, with LSCs shown

to arise from a variety of target cell populations following neoplastic changes (Wang *et al.*, 2010; Huntly *et al.*, 2004; Kvinlaug *et al.*, 2011). However some neoplastic changes including those in MOS-TIF, MLL-AF9 and MLL-ENL are capable of inducing LICs when expressed in both HSC and progenitor cell populations (Krivstov *et al.*, 2006; Cozzio *et al.*, 2003), whereas other neoplastic changes such as those in BCR-ABL, FLT3-ITD, Hoxa9 and Meis1 have only been found to induce LICs when expressed in HSCs only (Wang *et al.*, 2010; Kvinlaug *et al.*, 2011).

Table 1.3: Markers of Leukemia initiating cell populations (Taken from Stahl *et al.*, 2016)

Cell Surface Markers	Patient Samples Used	Mouse Model	References
CD34+CD38-	FAB M1, M4, M5	NOD/SCID	Bonnet and Dick, 1997; Lapidot <i>et al.</i> , 1994
CD34+CD38+	CN-AML, MLL-ENL	NOD/SCID+IVIG or anti-CD122	McKenzie <i>et al.</i> , 2006; Taussig <i>et al.</i> , 2008; Civin <i>et al.</i> , 1996; Hogan <i>et al.</i> , 2002
CD34-CD38+	AML with NPM1 mutation	NOD/SCID IL2 receptor	Taussig <i>et al.</i> , 2008
CD34+CD123+	FAB M1, M2, M4	NOD/SCID	Jordan <i>et al.</i> , 2000
CD34+CD38-CD96+	CK-AML, CBF-AML	Rag2 ^{-/-} , IL2RG ^{-/-}	Hosen <i>et al.</i> , 2007
CD34+CLL1+	AMLs with FLT3-ITD	NOD/SCID	van Rhenen <i>et al.</i> , 2007
TIM3+	FAB-M1, M2, M4	NOD/Rag1 ^{-/-} , IL2RG ^{-/-}	Kikushige <i>et al.</i> , 2010
CD34+CD38-	CN-AML	NOD/SCID	Taussig <i>et al.</i> , 2005
CD33+CD13+	CBF-AML, MLL-ENL	NOD/SCID	Taussig <i>et al.</i> , 2005

1.5.2 Keratinocyte SCs

The concept that the epithelium of the skin contains SCs arose from the patterns of proliferation observed within the morphological units of structure, termed epidermal proliferative units (EPUs) (Mackenzie *et al.*, 1969; Mackenzie *et al.*, 1985; Potten *et al.*, 1974). Within the epidermis, tissue homeostasis and wound repair is governed by these adult SCs, which as previously described are found within a specific niche known as the microenvironment, responsible for hosting and maintaining SCs. It is thought that the stemness of SCs is preserved through their infrequent cycling, and ability to self-renew and remain undifferentiated over time. The epidermis is able to achieve this homeostasis when the number of cell divisions within the tissue compensates the number of cells that are lost (Xie & Spradling, 2000). Two distinct models have been proposed to explain the behaviour of basal cells. In the hierarchical model, the epidermis is organized into discrete proliferative units, containing slow-cycling SCs that give rise to transit-amplifying cells capable of departing the basal layer after several divisions, to subsequently generate columnar units of differentiating cells. Whereas in the stochastic model, a single type of proliferative progenitor comprises the basal layer, whose daughter cells randomly choose one of two fates, either to remain as a progenitor, or to differentiate.

In early studies, [3H] thymidine labelling was used to show that basal cells located at the periphery of the EPU were readily labelled, and were frequently shown to have mitotic figures, whereas the central cells within the EPU required continuous labelling and were termed label retaining cells (LRCs) because they were seen to persist within the EPU for weeks to months after labelling (Mackenzie *et al.*, 1969; Mackenzie *et al.*, 1985). These observations suggested that the central cells have SC properties. However, more recently when evaluating the contribution of SCs to tissue homeostasis, lineage tracing has proven a very powerful method. Lineage tracing involves the genetic marking of one or even a group of cells, such that their progeny retain marker expression and can be subsequently followed over time. Numerous groups have used this method to study the fate of cells within the epidermis, and have generated conflicting results. For example some groups have generated clonal fate data, from the

long term labelling of basal cells in tail, ear, or hind paw epidermis in mice, and found that it was compatible with the stochastic model (Fuchs, 2016; Clayton *et al.*, 2007; Doupe *et al.*, 2010; Lim *et al.*, 2013). However, one important unresolved issue with these aforementioned studies is whether they randomly or selectively mark the basal cells. In contrast, other studies who have generated data to support the hierarchical model. An example includes the study by Mascre *et al.* (2012), where they used two inducible Cre-Lineage tracers, the first of which was driven by the K14 promoter and was active in all basal cells, while the second was driven by an Involucrin promoter, which was present in a distinct subset of K14+ basal cells (Mascre *et al.*, 2012). They demonstrated that basal cells marked by K14-CreER behaved like long-lived SCs, which subsequently gave rise to a subset of more committed basal progenitors marked by Involucrin-CreER (Mascre *et al.*, 2012). Although the exact number and characteristics of epidermal SCs is still not known, their reliance on the surrounding niche is beginning to be unravelled. Epidermal SCs were first functionally demonstrated in the 1970s through *in vitro* studies, which showed that human keratinocytes could be successfully maintained and propagated for many generations without losing stemness (Rheinwald and Green, 1975). Furthermore when expanding epidermal cultures from an unaffected region of a burns patient, it was found that they could be engrafted onto the damaged skin, which some 30 years on have not developed cancer or other abnormalities, thereby indicating that under the right conditions SC expansion and differentiation could be achieved without deleterious consequences, when co-culturing with irradiated dermal fibroblasts (Gallico *et al.*, 1984). This requirement for surrounding dermal cells highlighted the need for SCs to crosstalk with their niche.

Under physiological conditions, active hair growth takes place in the lower hair follicle (HF) through cycles of hair growth (anagen), destruction (catagen), and rest (telogen) (Alonso and Fuchs, 2006). The emergence of the new hair follicle takes place next to the old hair, which persists into the next cycle, thereby creating a protrusion or bulge. Cotsarelis *et al.* (1990) extended the LRC concept to the HF, and found that LRCs were present in the bulge (Cotsarelis *et al.*, 1990). Studies have shown that the bulge contains slow cycling label retaining cells, which sometime later were isolated and characterized, and shown to be capable of long-term self-renewal, contributing to the HF cell lineages

and wound repair (Cotsarelis *et al.*, 1990; Morris *et al.*, 2004; Blanpain *et al.*, 2004; Claudinot *et al.*, 2005). Furthermore, SCs within the bulge region of the HF are responsible for driving hair growth. Such studies include Oshima *et al.* (2001) who through a combination of micro-dissecting hair follicles and grafting techniques, demonstrated that within the cutaneous epithelium, bulge cells were capable of differentiating into all cell types (Oshima *et al.*, 2001). Within the HF there exist multiple cell populations with SC properties, with each having distinct cell surface markers and locations within the follicle (Singh *et al.*, 2012). FACS along with cell culture have been very important techniques for identifying keratinocyte SCs within the cutaneous epithelium. A number of studies have adopted these approaches, including Jones and Watt (1993), who demonstrated that keratinocyte SCs could be isolated by their relatively high levels of $\beta 1$ integrin expression (Jones and Watt, 1993). $\beta 1$ integrin expression was also used by Bickenbach and Chism (1998) to enrich LRCs due to their greater adhesiveness to type IV collagen (Bickenbach and Chism, 1998). Small and relatively undifferentiated keratinocytes that later turned out to be LRCs, were identified by Tani *et al.* (2000) based on $\alpha 6$ integrin expression along with a reduction in the expression of CD71 (Tani *et al.*, 2000). $\alpha 6$ integrin expression has also been used alongside CD34 (a haematopoietic stem and progenitor marker), by Trempus *et al.* (2003), to identify cells within the hair follicle bulge that were enriched for LRCs in culture (Trempus *et al.*, 2003). Another group also isolated hair follicle bulge cells, but this time used a strategy that enriched the cells based on histone H2b-Green Fluorescent Protein expression. CD34 was used by Blanpain *et al.* (2004) for FACS sorting, and identified two cell populations based on the presence or absence of immunoreactivity with $\alpha 6$ -integrin (Blanpain *et al.*, 2004).

Furthermore, within the bulge region of the HF, a population has been identified expressing both CD34 and Lgr5 (originally identified as an intestinal SC marker), and is capable of, reconstituting all of the epidermal lineages in reconstitution assays and maintaining HF lineages under steady state conditions (Jaks *et al.*, 2008). Located just above the CD34+ bulge region are quiescent, clonogenic LRCs that express the MTS24 epitope and $\alpha 6$ integrin (but not K15 or CD34) (Nijhof *et al.*, 2006). There exists yet another SC population between the bulge region and infundibulum, that expresses

MTS24, and $\alpha 6$ integrin, but lacks CD34 and sca-1 expression, and is capable of reconstituting the interfollicular epidermis, HF, and sebaceous glands (Jensen *et al.*, 2008). Flow sorting has proven very successful for isolating SCs within the bulge region of the HF; however, sorting interfollicular SCs has proven more difficult. Nevertheless, Lrig1 is another SC marker that has been used to characterize adult interfollicular SCs in humans, and the HF junctional zone adjacent to the sebaceous glands and infundibulum in mice (Jensen *et al.*, 2009).

Finally lineage-tracing strategies as mentioned earlier, have also been very useful for visualising the fate of cells from the HF bulge. Both Tumber *et al.* (2004) and Morris *et al.* (2004) found that bulge cells contributed towards HF cycling, but made much less of a contribution towards epidermal and sebaceous gland homeostasis. Furthermore, the Tumber *et al.*, 2004 found that the bulge environment was growth and differentiation restricted. Levy *et al.* (2005) used a different transgenic mouse model, and found that follicular cells expressing SHh contributed to the epidermis and sebaceous gland. This finding was expanded by Ito *et al.* (2005), and found that K15 expressing SCs contributed to early phase of wound healing, but did not persist in the wound when it was healed, thereby indicating no or little involvement in epidermal homeostasis.

1.5.3 Cancer Stem Cells and tumour heterogeneity

The cancer SC (CSC) theory states that tumour growth has a similar hierarchy, in which tumour growth is maintained by a small population of long-lived cells called CSCs. Recent papers have shown the presence of CSCs through lineage tracing and cell ablation in intact tumours (Driessens *et al.*, 2012; Schepers *et al.*, 2012; Kozar *et al.*, 2013; Zomer *et al.*, 2013; Chen *et al.*, 2012). In this section I discuss the basis for the cancer SC theory and its relevance to therapy.

Tumour heterogeneity was first observed by pathologists over a century ago and is often the basis for pathological diagnosis (Heppner, 1984). Cutaneous squamous cell carcinoma (SCC) demonstrates keratinisation or stratification and thus tumours contain so called “keratin pearls”(Petter *et al.*, 1998). Even BCC consists of HF outer root sheath

basaloid cells, albeit representing a more subtle histological feature (Colmont *et al.*, 2013; Morgan *et al.*, 2018 (Manuscript under review)). The tumour heterogeneity associated differentiated cells are of prognostic value, since tumours that maintain normal tissue architecture are classed as “well differentiated” and so have a good prognosis (Brantsch *et al.*, 2008; Cox *et al.*, 2006). Conversely “poorly differentiated” tumours with loss of normal tissue architecture are associated with a worse clinical outcome. In this static view of cancer growth all histologic features of their parent tissue maybe lost resulting in “de-differentiated” tumours, leading some to suggest that the tumour tissue has regressed to a more primitive cell type (Morgan *et al.*, 2008). Consistent with the poor prognosis associated with poor or de- differentiated cancers, these tumours have a high mitotic rate while at the same time switch off the mutually exclusive process of terminal differentiation (Brantsch *et al.*, 2008; Cox *et al.*, 2006).

Interrogation using molecular biology has demonstrated heterogeneity in the expression of cell surface markers (Dexter *et al.*, 1978; Poste *et al.*, 1980) and the presence of multiple sub-populations within many cancers, such as melanoma (Gray and Pierce, 1964), breast cancer (Dexter *et al.*, 1978) and intestinal cancer (Dexter *et al.*, 1979). These sub-populations exhibit unique DNA aberrations (Mitelman *et al.*, 1972; Shapiro *et al.*, 1981), growth rates (Danielson *et al.*, 1980) and relevant to this thesis response to therapeutics (Barranco *et al.*, 1972). As such, tumour heterogeneity aids diagnosis and may account for variable response to conventional anti-cancer therapies.

1.5.4 Clonal versus cancer Stem Cell theories

Using radiolabelling of mouse squamous cell carcinoma, Pierce and Wallace in 1971 showed that pulse radiolabelling occurred almost exclusively within undifferentiated cells. At later time points, the DNA label appeared also within the well-differentiated cells, suggesting that they were derived from undifferentiated cells. These well-differentiated cells did not form tumours when transplanted into compatible hosts, only the undifferentiated cells could reform SCC (Pierce and Wallace, 1971). These and other

experimental findings led Pierce to frame the CSC concept: “a concept of neoplasms, based upon developmental and oncological principles, states that carcinomas are caricatures of tissue renewal, in that they are composed of a mixture of malignant SCs, which have a marked capacity for proliferation and a limited capacity for differentiation under normal homeostatic conditions, and of the differentiated, possibly benign, progeny of these malignant cells.” (Pierce and Speers, 1971). This and other such similar findings raised concern over the pervading theorem of clonal evolution of cancer (Figure 1.5).

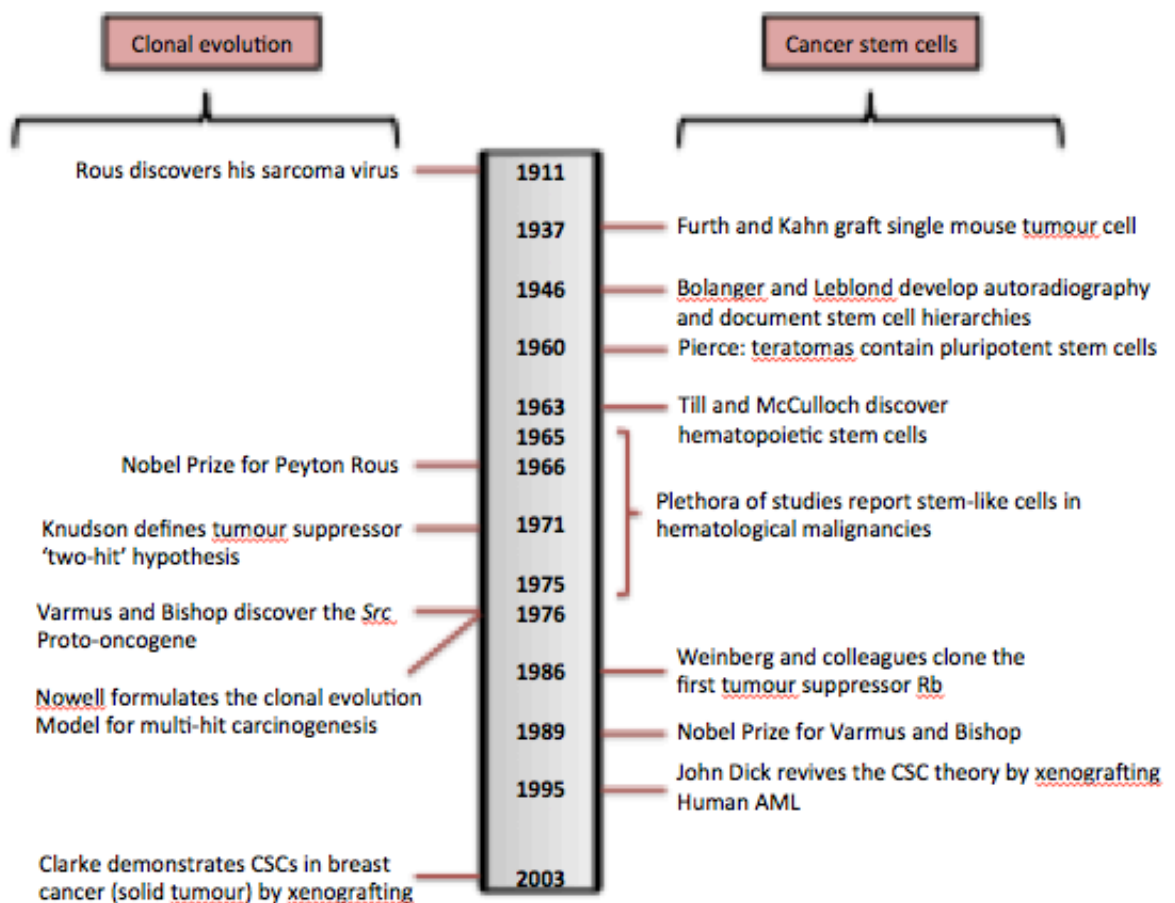


Figure 1.5: A timeline highlighting some of the major discoveries in stem cell research.

A timeline highlighting some of the major discoveries in the fields of clonal evolution (shown on the left) and cancer SCs (shown on the right). Adapted from Clevers, 2013.

The central tenets of the CSC theory of tumour growth based on existing assays are:

1. Tumour heterogeneity arises from hierarchical growth.
2. CSC's are a rare self-renewing population at the hierarchical apex. CSC's have long-term proliferative capacity, usually quiescent, while progeny undergo short-term proliferation prior to terminal differentiation.
3. Differentiation is unidirectional, with limited plasticity.
4. CSC's are resistant to conventional treatment, radiotherapy and chemotherapy, which preferentially target fast dividing cells i.e. progeny. Thus CSC's are the basis for relapse and metastasis.

The CSC hypothesis was developed to distinguish between the clonal and CSC models of tumour growth. The CSC hypothesis is used to test the presence of tumour initiating cells and states that only a small population of cancer cells have the capacity to recreate tumour growth *in vivo*. Implicit in this is that the remaining tumour cells regardless of how many cells are implanted do not have the capacity to recreate tumour growth. In the clonal (stochastic) model of tumour growth, the majority of the cells would be expected to be able to recreate tumour growth.

1.5.5 Cancer stem cells in solid malignancies

Many solid cancers have been identified as exhibiting CSCs, utilising *in vivo* xenograft assays to demonstrate self-renewal (Table 1.4). In their landmark paper in 2003, Clarke and colleagues were able to demonstrate CSCs in breast cancer, with as few as 100 CD44+CD24-/low cells able to demonstrate mammary fat pad engraftment, whereas the bulk population was unable to do so (Al-Hajj *et al.*, 2003). Hence using immunodeficient mouse assays, multiple solid cancers have been found to demonstrate CSC dependent growth.

Table 1.4: Cancer SC populations identified in a number of human cancers using *in vivo* assays (only cell surface markers are described)

Human tumour	Normal adult tissue SC marker	Tumour initiating cell marker	Model used for validation	Percentage of marker +ve cells in tumour	References
Acute Myeloid Leukaemia	CD34+ CD38- CD90+ CD45RA-	CD34+ CD38-	SCID & NOD SCID	0.1%	Lapidot <i>et al.</i> , 1994; Bonnet and Dick, 1997; Doulatov <i>et al.</i> , 2012
Chronic Myeloid Leukaemia	Lin-	CD34+ CD38-	NOD SCID	0.1%	Doulatov <i>et al.</i> , 2012; Wang <i>et al.</i> , 1998
Breast Cancer	CD49f+ CD24-	ESA+ CD44+ CD24-/low	NOD SCID	12-35%	Al-Hajj <i>et al.</i> , 2003; Peterson and Polyak, 2010
Meduloblastoma	CD133+	CD133+	NOD SCID	6-21%	Singh <i>et al.</i> , 2004; Uchida <i>et al.</i> , 2000
Glioblastoma Multiforme		CD133+		19-29%	
Colon Cancer	Lgr5+	CD133+	NOD SCID	1.1-24.5%	O'Brien <i>et al.</i> , 2007, Ricci-Vitiani <i>et al.</i> , 2007, Barker <i>et al.</i> , 2007
Colorectal Cancer		EpCAM ^{hi} CD44+	NOD SCID	0.03-38.7%	Dalerba <i>et al.</i> , 2007; Barker <i>et al.</i> , 2007
Pancreatic Cancer	Not defined	ESA+ CD44+ CD24+	NOD SCID	0.2-0.8%	Kajstura <i>et al.</i> , 2011
Head and Neck SCC	CD29 ^{hi} CD44+	CD44+ Lin-	NOD SCID	<10%	Prince <i>et al.</i> , 2007, Jensen <i>et al.</i> , 2008
Melanoma	Not defined	ABC5 CD271+ CD20+HMW-	NOD SCID & Rag2-/-	1.6-20.4% 2.5-41%	Schatton <i>et al.</i> , 2008; Boiko <i>et al.</i> , 2010;

		MAA+	γ c-/-		Boonyaratanakornkit <i>et al.</i> , 2010; Schmidt <i>et al.</i> , 2011
Lung	CD117+	CD133+	NOD SCID	0.3-22%	Eramo <i>et al.</i> , 2008; Li <i>et al.</i> , 2007
Ovarian	Not defined	CD133+	NOD SCID	0.3-35%	Curley <i>et al.</i> , 2009
Hepatocellular Cancer	CD90+ CD34+	CD90+ CD45-	SCID beige	0.03-6.2%	Yang <i>et al.</i> , 2008; Masson <i>et al.</i> , 2006
SCC	CD49 ^{hi} CD71 ^{lo}	CD133+ CD45-	Nude with stromal bed	0.1-1.7%	Patel <i>et al.</i> , 2012; Kaur and Potten, 2011
BCC	CD200+	CD200+	Nude with stromal bed	0.1-3.9%	Colmont <i>et al.</i> , 2013

1.5.6 Keratinocyte cancer Stem Cells

The concept that CSC are the cancer initiating cells in skin cancer is not new, however, there is now specific evidence to show that this is indeed the case in the cutaneous epithelium. A small number of cells were identified in the middle, permanent region of hair follicles by Morris and Potten (1999), and shown to retain [3H] thymidine label for more than a year and remained following plucking, and even proliferated in response to it. A previous study by Morris *et al.* (1986) found that the central [3H] thymidine LRCs within the EPU were capable of retaining the carcinogen label [14C] benzo[a]pyrene for up to a month. These observations identified the SC populations as potentially relevant to the initiation of two-stage carcinogenesis. Further studies provided more evidence to suggest that LRCs are important players in skin cancer, in that LRCs were shown to proliferate in response to the mouse skin tumour promoter 12-O-tetradecanoylphorbol-13-acetate (TPA), whereas the more mature keratinocytes did not (Morris *et al.*, 1985).

They also observed that following their division, LRCs and their daughters remained on the basal layer to again take up a central position within the EPU, whereas pulse-labelled cells rarely divided and instead underwent displacement and subsequent terminal differentiation from the basal layer. These findings showed that LRCs were not only capable of retaining carcinogen-DNA adducts, but also responded to TPA treatment by proliferating, which is a necessary event for tumour promotion. Further findings included the study by Morris *et al.* (1991) where through the use of density gradient sedimentation of freshly harvested keratinocytes into heavy and light populations, they found that the smallest and most dense subpopulation was enriched for clonogenic keratinocytes *in vitro*. These findings were important as they demonstrated that the cells relevant to skin carcinogenesis differed from the other less dense keratinocytes both *in vitro* and *in vivo* (Morris *et al.*, 1991). A later study by Morris *et al.* (1997) investigated the SC properties of initiated keratinocytes through the treatment of mice both before and after exposure to 5-fluorouracil (an agent known to kill cycling but not quiescent cells). Due to its effects on cycling cells, treated mice experienced profound epidermal atrophy, but despite this damage, both papilloma and carcinoma responses were surprisingly similar between treated and vehicle controls, suggesting that the initiating cells were quiescent rather than cycling (Morris *et al.*, 1991). Although previous studies suggest that keratinocyte SCs are quiescent or slow cycling, more recent evidence is suggesting the co-existence of two distinct SC populations: i) quiescent cells and cells with a low metabolic state, and ii) active SCs, such as those entering the cell cycle that are unable to retain the DNA label. This co-existence has been observed in a number of tissues including HF, intestine and bone marrow (Li and Clevers, 2010). In particular the HF has been shown to contain both slow cycling (CD34+Lgr5-) and actively cycling (CD34+Lgr5+) cell populations next to the bulge area, which is consistent with Lgr5+ SCs (actively cycling) located adjacent to the LRCs (slow cycling) (Jaks *et al.*, 2008; Zhang *et al.*, 2006). Therefore it seems that the hair follicle contains both quiescent and actively cycling cells in distinct yet adjacent locations.

The precise identification of CSCs along with the mechanisms that underlie tumour initiation in the non-melanoma skin cancers, SCC and BCC has remained largely unknown. However, more and more evidence is showing that in both of these

malignancies the major target cell for carcinogenesis lies in the epithelial SC compartment (Gerdes and Yuspa, 2005; Perez-Losada and Balmain, 2003; Kangsamaskin *et al.*, 2007; Singh *et al.*, 2012). Primary human SCC is a heterogeneous tumour organized in a hierarchy of both proliferating and differentiating keratinocytes that recapitulates normal epidermal development. Since keratinocyte SCs are responsible for reconstituting the cellular hierarchy within the normal epidermis, it is highly possible that SCCs are also initiated by CSCs. For primary human SCC, *in vivo* tumour growth demonstrated dose dependent tumour growth, with assured engraftment if $> 3 \times 10^6$ SCC cells were implanted, irrespective of the original SCC histological grade (Patel *et al.*, 2012a; Patel *et al.*, 2012b). Based upon a limiting dilution calculation, it was possible to estimate the tumour initiating cell frequency within the unsorted SCC cell suspension was 1 in 10^6 . After CD133 sorting, the CD133+ CD45- population could recreate SCC growth *in vivo* with as few as one hundred cells, albeit reproducibly with 10^4 CD133+ CD45- sorted SCC cells. Intriguingly once tumours had formed from the CD133+ CD45- sub-population the CD133+ fraction remained at 1%, similar to the original SCC. Yet despite implanting over 3 million CD133- CD45- SCC cells, this subpopulation was unable to give rise to tumour growth. In line with other human tumour initiating cell studies, tumour cells derived from CD133+ CD45- had recreated the original tumour heterogeneity, including the requisite CD133- cells (Patel *et al.*, 2012a; Patel *et al.*, 2012b). Additional studies include Li *et al.* (2013) who observed the ability of K15 expressing bulge SCs within the hair follicle towards the development of squamous papilloma in a Krt1-15CrePR1;R26R bigenic mouse model. Firstly, they found that K15 expressing cells contributed to papilloma development following TPA promotion; secondly, the K15 cells were shown to persist in papillomas for many months following the induction of the reporter gene (Li *et al.*, 2013). These findings indicated that these K15 expressing hair follicle cells contributed to the development of these papillomas. However, the contribution of SCs cannot be ignored in other NMSC such as BCC.

The identity of the disease-initiating cells and the compartments has been controversial; however recent publications are shedding more light on these matters. In particular, there have been a number of publications that have demonstrated the pivotal contribution of SCs in BCC development. A recent study by Peterson *et al.* (2015)

used several inducible Cre drivers to delete PTCH in different cellular compartments within mice skin, and found that there were a number of SC populations within the HF that were capable of driving tumour growth. Conversely, these SCs located within the interfollicular epidermis were unable to drive tumour growth. In particular they found that Gli-expressing progenitors within mechanosensory touch dome epithelia were highly tumourigenic. However, these findings are in contradiction to that observed by Youssef *et al.* (2010), who constitutively activated Hh signalling in mice by conditionally expressing an active Smoothed mutant (SmoM2) in different cellular compartments of the skin epidermis. Here they found that SCs within the bulge region were unable to drive tumour growth, whereas long-term progenitor cells within the interfollicular epidermis and upper infundibulum did. Therefore, both studies present data with conflicting views on where BCC originates, but both are unanimous in relaying the need for SCs in BCC tumour initiation. Whereas the previous studies were undertaken in the mouse system, Colmont *et al.* (2013) used human BCC samples to demonstrate the need for SCs to initiate tumour growth by using the cell surface marker, CD200, to identify CSCs. They showed that all BCC samples contain a small CD200+ tumour cell population, $1.63 \pm 1.11\%$ (range 3.96 to 0.05% (n=21)), irrespective of the histological type (Colmont *et al.*, 2013). When 10^5 flow-sorted cells were plated from five different BCC samples, CD200+ CD45- sorted cells gave rise to 3-fold more colonies than the CD200- CD45- subpopulation ($p < 0.005$), which also gave rise to fewer colonies than unsorted cells ($p < 0.01$). Most BCC cells, defined by a CD200- CD45- phenotype, also expressed the transcription factor KLF4 and were therefore considered committed to terminal differentiation. Using a novel reproducible *in vivo* xenograft growth assay, they determined that CSC frequencies are approximately 1 per 1.5 million unsorted BCC cells. Their findings establish that CD200+ CD45- BCC subpopulations are enriched for BCC CSC. In summary, both cutaneous keratinocyte tumours, similar to the normal epidermis and hair follicle, demonstrate hierarchical growth with the presence of rare CSC. Therefore, although unsubstantiated it may be that these TIC originated from the bulge region of the HF also.

CSC have also been identified in melanoma with the first marker identified in 2005 by Fang *et al.* (2005) who showed that a subpopulation of CD20+ cells harboured stem-like properties in metastatic human melanoma (Fang *et al.*, 2005). Schatton *et al.* (2008)

later used the expression of the ATP-binding cassette (ABC) transporter, ABCB5, to characterise the melanoma SC population, which demonstrated the capacity to self-renew and differentiate following serial transplantation in NOD/SCID mice (Schatton *et al.*, 2008). CD271 (Boiko *et al.*, 2010; Civenni *et al.*, 2011) and ALDH (Boonyaratanakornkit *et al.*, 2010; Luo *et al.*, 2012) have also been used to identify melanoma SC populations with the capacity to self-renew and differentiate.

1.5.7 Lineage tracing and lineage ablation of cancer stem cells

Lineage tracing has allowed visualisation of CSC enriched populations and has provided us with a tool to explore the fate of tumour cells in their native microenvironment. Using the same principles of label retaining cells, three papers have used mouse genetics to determine the presence of quiescent long-lived CSC in skin, intestine and breast cancers. Blanpain and colleagues combined inducible clonal tracing using *K14CREER/Rosa-YFP* mice to study the effect on two-step chemical carcinogenesis (Driessens *et al.*, 2012). Only a small fraction of tumour cells could propagate tumours upon serial passage and these label retaining cells behaved similar to normal epidermal keratinocyte SCs. Similarly, Clevers and colleagues used an *Lgr5CREER/APC-Rosa-Confetti* mouse to study intestinal cancer (Schepers *et al.*, 2012; Kozar *et al.*, 2013). They showed that *Lgr5* identified 20% of tumour cells and that only these cells were able to repopulate tumour growth. Lineage tracing of breast cancer in the *MMTV-PyMT* mouse also demonstrated dominant clones consistent with the CSC theory (Zomer *et al.*, 2013). Hence, mouse genetics have conclusively shown that oncogene driven tumour growth results in tumour heterogeneity that is consistent with the CSC model of tumour growth.

Mouse models that enable lineage ablation have been used to demonstrate tumour growth dependence on a small sub-population of CSC. Ablation of the Nestin+ sub-population within glioblastoma multiforme using the *HSV tyrosine kinase* suicide gene significantly improved survival, demonstrating the importance of Nestin+ CSC (Chen *et al.*, 2012). Intestinal tumour deleting of *Dcl1+*, a putative marker of CSC, using diphtheria toxin, led to tumour regression (Nakanishi *et al.*, 2013). A recent study by

Sanchez-Danes *et al.* (2016) used lineage tracing to assess the impact of Hh signalling in distinct cell populations and their capacity to induce BCC. They found that only CSCs and not committed progenitors were capable of initiating tumour formation upon constitutive activation of Hh signalling, which was attributed to a higher p53-dependent resistance to apoptosis in the SC population (Sanchez-Danes *et al.*, 2016).

In summary, both mouse genetics in established tumour models has demonstrated the presence of CSC based tumour growth by both lineage tracing and ablation.

1.5.8 Cancer stem cells as mediators of drug resistance

It follows therefore that cancer relapse after therapy would be dependent upon CSC survival and proliferation. It has been argued that conventional therapies that target rapidly dividing cancer cells, such as radiotherapy and chemotherapy, fail to eradicate CSC.

Like their normal tissue SC counterparts, CSC are resistant to the DNA damaging effects of radiotherapy as a consequence of lower levels of induced reactive oxygen species, activation of DNA checkpoints and efficient DNA repair (Diehn *et al.*, 2009; Sotiropoulou *et al.*, 2010; Bao *et al.*, 2006). As a consequence, after radiotherapy there has been a relative increase in CSC, for example in breast cancer and glioblastoma multiforme (Diehn *et al.*, 2009; Bao *et al.*, 2006). Intrinsic resistance to conventional radiotherapy may allow CSC to survive and proliferate, resulting in disease relapse.

CSCs also demonstrate chemotherapy resistance through a variety of mechanisms, including expression of multidrug resistance cell surface proteins or detoxification proteins. The drug efflux ability of CSC has been utilised to isolate enriched populations of normal tissue SCs and CSC by flow sorting Hoechst dye. Gliomas that exhibit PI3K pathway activation express the ABCG2 protein leading to resistance to temozolomide (Bleau *et al.*, 2009). Our group has previously shown that BCC CSC both constitutively and induce ABCG2 expression (Colmont *et al.*, 2014). Likewise, the enzyme that catalyses aldehyde oxidation, ALDH, has also been used to define CSC enriched

populations most notably in the breast (Ginestier *et al.*, 2007). As such, ALDH positive cells have been shown to effectively demonstrate drug resistance in lung and breast cancers (Huang *et al.*, 2013; Cojoc *et al.*, 2015). As alluded to earlier (section 1.3), CSCs may also resist killing by growth factor pathway inhibitors, and subsequently expand and cause tumour relapse. For example, Shlush *et al.* (2014) showed that highly purified HSC, progenitor and mature cell fractions obtained from the blood of AML patients harboured recurrent DNMT3a mutations (DNMT3a^{mut}), and demonstrated that in xenograft experiments, DNMT3a^{mut}-bearing HSC were capable of repopulating multiple lineages in comparison to non-mutated HSC, thereby establishing their identity as pre-leukemic-HSC. Importantly, these pre-leukemic-HSCs were found in remission samples indicating that they survive chemotherapy (Shlush *et al.*, 2014). Lung CSC are enriched and expanded after gefitinib (Shien *et al.*, 2013). Glioblastoma multiforme CSC were similarly enriched and expanded after bevacizumab (Hamerlik *et al.*, 2012). We have previously observed that BCC CSCs are resistant to treatment with Hh antagonists, cyclopamine and vismodegib (Colmont *et al.*, 2013). In summary, CSC exhibit intrinsic modes of resistance to therapies and importantly their subsequent enrichment may result in relapse with potential for more aggressive disease.

TGF β associated EMT is a phenotype associated with more invasive malignancies. Cancer cells that have undergone EMT are often more likely to demonstrate resistance to therapy (Cojoc *et al.*, 2015). TGF β signalling, a hallmark of EMT, in CSC increases their resistance to cisplatin via the Nrf2/p21 pathway, by enhancing glutathione metabolism of the drug (Oshimori *et al.*, 2015). A downstream target of TGF β is an EMT inducing transcription factor Zeb1, which increases stemness and also promotes drug resistance (Oskarsson *et al.*, 2014; Siebzehnrubl *et al.*, 2013). Interestingly, Zeb1 is regulated by miR-203 and the histone deacetylase inhibitor mocetinostat restores miR-203 expression that in turn represses Zeb1 and restores treatment sensitivity (Meidhof *et al.*, 2015). Our microarray analysis of BCC treatment with Hh antagonists demonstrated an increase in TGF β regulated genes, suggesting that this pathway maybe responsible for EMT and drug resistance in BCC.

1.5.9 Limitations of the cancer stem cell theory

1.5.9.1 Xenograft models

In the absence of homotransplantation, the identification of human CSC is reliant on mouse xenograft models; as such xenografting is central to the CSC model. Murine lineage tracing and ablation experiments outlined above obviate the need for xenografting and support the existence of CSC. In the case of solid cancers, such tumour initiating experiments also rely on tumour dissociation with the added risk that stromal context is lost. Moreover, prolonged exposure to dissociation enzymes may lead to cell surface protein expression change. Therefore, one potential concern is that the harsh processes involved in generating single cells from whole tissue may select for only robust cells and not faithfully recreate the *in situ* biology.

The xenograft assay raises concerns relating to host specific selection bias. For example the tumour microenvironment maybe significantly different and some murine growth factors are not cross-species reactive, as is the case of tumour necrosis factor (Bossen *et al.*, 2006). Orthotic transplantation is important, for example breast cancers are grafted into the mammary fat pad (Kuperwasser *et al.*, 2004) although this is relatively easy for skin cancer (Morgan *et al.*, 2018b; Olivero *et al.*, 2018). The importance of which was evident in the identification of leukaemia initiating cells, where intra-femoral injection of tumour cells was important (Eppert *et al.*, 2011). In addition, models have necessitated the creation of a tumour specific stromal bed to facilitate engraftment (Kuperwasser *et al.*, 2004; Patel *et al.*, 2012; Colmont *et al.*, 2013). Thus careful attention to the tumour microenvironment is often required for accurate recreation of *in situ* tumour growth.

Quintana *et al.* (2010) showed that melanoma growth could be achieved from 1 in 4 melanoma cells without sorting in a “permissive” xenograft model (Quintana *et al.*, 2010). Growth of melanoma cells in this *in vivo* model was facilitated by use of severely immunodeficient mice, growth factor laden cell matrix, and the duration the xenograft

was allowed to grow. In the absence of immune editing, tumour cells that are passaged in highly immunocompromised (NOD/SCID/IL2ry (null) mice, or in natural killer cell-depleted nude or NOD/SCID mice lose their original markers, and no longer phenocopy the original tumour, and become more readily propagated through *in vivo* selection (Civenni *et al.*, 2011; Boiko *et al.*, 2010). Therefore, the use of mouse models, such as the one we have described, remains a necessary evil in CSC research that has to be factored into the interpretation of findings (Eaves, 2008; Fukunaga-Kalabis *et al.*, 2011).

1.5.9.2 Stem cell and cancer stem cell plasticity

Lineage tracing and ablation studies have revealed the potential for committed cells to move both up and down the differentiation hierarchy and so undergo de-differentiation. This plasticity has been observed following the deletion of intestinal crypt LGR5+ SCs, which was found to stimulate the establishment of multipotent SCs from the secretory and enterocyte lineages to subsequently re-occupy the niche (Tian *et al.*, 2011; van Es *et al.*, 2012; Buczacki *et al.*, 2013; Tetteh *et al.*, 2016). To understand this phenomenon the SC niche theory of neutral competition has been proposed in which SC progeny compete to occupy the niche (Clayton *et al.*, 2007; Doupe *et al.*, 2010; Lopez-Garcia *et al.*, 2010). Plasticity has also been observed in breast CSC (Gupta *et al.*, 2011) and colon cancer (Shimokawa *et al.*, 2017; Gupta *et al.*, 2011). Although in glioblastoma multiforme the hierarchy appears to be more rigid (Chen *et al.*, 2012). Other studies have shown through a combination of genetic lineage tracing and targeted expression of oncogenes and/or deletion of tumour suppressor genes in different cell lineages within the same tissue, that SCs and not transit amplifying cells are capable of tumour formation when targeted with particular oncogenic hits (Blanpain, 2013). In the skin epidermis, studies have shown that targeted deletion of Kras and p53 to short lived rapidly proliferating matrix cells of the HF did not lead to tumour formation, whereas when these same genes were deleted in the SC population, rapid tumour formation occurred (Lapouge *et al.*, 2011; White *et al.*, 2011). As mentioned previously, one of the essential properties that a CSC exhibits is its ability to reform a tumour that exhibits the same heterogeneity as the primary tumour. Therefore, in theory, if CSC differentiation is unidirectional, then the progeny should

have limited capacity if any to give rise to tumour populations. However, experimentally this situation is frequently not observed, with a number of papers demonstrating a certain degree of cell plasticity within tumours (Gupta *et al.*, 2011). In some instances cellular markers can be reversibly expressed by tumour cells with CD271⁻ cells shown to give rise to CD271⁺ cells in melanoma mouse models (Boiko *et al.*, 2010; Civenni *et al.*, 2011), and CD34⁻ cells found to reform secondary tumours with both CD34⁺ and – cells in SCC mouse models (Malanchi *et al.*, 2008; Beck *et al.*, 2011). Thus, a major limitation of the CSC theory is that xenografting experiments rely on a fixed CSC, wherein plasticity is not evaluated and may account as to why not all cancers contain CSC.

1.6 TGF β Signalling Pathway

TGF β signalling is responsible for controlling a diverse set of functions notably in cell proliferation, development, differentiation, during adult homeostasis and disease. The TGF β superfamily of cytokines are secreted by many cell types and the pathway has overlapping receptor usage, which means the role of this pathway is long reaching and complex (Massague, 1998). However, it is important to note that TGF β signalling is context dependent, in that at the transcriptional level, the collaboration of SMADs (which are signal driven TFs), and lineage-determining TFs (LDTF) (which specify cell identity and determine the binding of SMADs to loci within the genome). Therefore, by sensing the chromatin status at these loci along with the cooperation of other signal driven TFs, SMADs are capable of integrating these inputs to produce a contextual response to TGF β family signals (David and Massague, 2018).

1.6.1 TGF β Growth Factor Signalling Pathway

1.6.1.1 TGF β ligands and receptors

In mammals the TGF β superfamily of growth factors contains over 30 members including TGF β s, BMPs, GDFs, Activins, and Nodal, and is vital for the development and

homeostasis of metazoans (Massague, 1998; McCartney-Francis *et al.*, 1998; Feng & Derynck, 2005). The ligands and their downstream pathway components regulate diverse cellular functions including growth, adhesion, migration, apoptosis, and differentiation. TGF β is a pleiotropic growth factor responsible for the regulation of a wide variety of fundamental biological processes including cell growth, differentiation, ECM remodelling, migration and apoptosis (Matsuura *et al.*, 2010; Burch *et al.*, 2011). Cytokines that are part of the TGF β superfamily of ligands are initially secreted as precursor proteins, which undergo proteolytic cleavage and subsequently reach maturation to create a functional form. Within mammals there are three related ligands, termed TGF β 1, 2, and 3, which contain 390, 412, and 412 amino acids respectively, and are 70-80% similar in their sequence homology. The active form of the TGF β ligand is a 12-15 kDa homo-dimer stabilized by a 'cysteine knot', which is a hydrophobic disulfide-rich core (Sun and Davies, 1995). The next step is the cleavage of covalent bonds between the pro-peptide and the mature ligand, which is facilitated by a furin-like convertase (Derynck *et al.*, 1985; Miyazono *et al.*, 1988). The resulting two polypeptides formed by cleavage remain intact through non-covalent interactions, and are subsequently secreted as a latent complex. The propeptide portion of this complex, termed the latency-associated protein (LAP) keeps the mature propeptide biologically inactive by restricting its access to membrane receptors (Lee and McPherron, 2001). In some instances, the LAP remains the predominant non-covalent partner in the secretory pathway of the TGF β ligand. However, the alternative route is that the LAP complex binds to large secretory glycoproteins known as latent TGF β binding proteins (LTBPs), which have been shown to aid the secretion and/or activation of the LAP-ligand complex. Proteolytic processing of the LAP is responsible for the release of biologically active TGF β ligands from latent complexes (Massague and Chen, 2000).

There are a variety of membrane proteins that enhance the binding of ligands to their receptors. In particular, TGFBRIII (membrane-anchored proteoglycan) binds and presents TGF β to the TGFBRII, and also mediates the binding of the activin antagonist, inhibin, to activin receptors (Wrana *et al.*, 1992). TGFBRIII is generally considered to be inhibitory towards the TGF β signalling pathway (Lewis *et al.*, 2000). Whereas there are proteins that facilitate the binding of ligands to receptors, there is also a structurally

diverse group of proteins that 'trap' members of the TGF β family, and limit their access to membrane receptors. Examples include the previously mentioned latency-associated protein (LAP), which sequesters TGF β to the extracellular matrix in the form of a complex using latent TGF β -binding proteins (LTBP1-4). Furthermore, other proteins are capable of trapping ligands, including noggin, chordin, gremlin, and follistatin, which trap BMP ligands, and nodals, which trap activins by DAN/Cerberus (Shi and Massague, 2003).

The receptor system for the entire TGF β family is made up of combinations of seven type I receptors (TGF β RI, also known as activin receptor-like kinase (ALK1-7)) and five type II receptors (TGF β RII) (Manning *et al.*, 2002), whose differential affinities for individual ligands contributes to signalling specificity (Figure 1.6) (Nickel *et al.*, 2009). Most members of the TGF β superfamily share several type I and II receptors, with TGF β being the exception, in that among the type II receptors, only the constitutively active transmembrane serine/threonine kinase, TGFBR2, can bind to TGF β (Lin *et al.*, 1992). The TGFBR2-TGF β interaction then recruits and activates one of three potential TGFBR1, including ALK1, 2, or 5 (Kang *et al.*, 2009). This complex, which is composed of two receptor type I (TGF β RI, also known as ALK5) and two receptor type II family members has serine/threonine kinase activity which initiates intracellular signalling through the phosphorylation of the GS regulatory domain of TGFBR1 by TGFBR2 (Wrana *et al.*, 1994; Wieser *et al.*, 1995). This active form of TGFBR1 is the principle component of the receptor complex and downstream signals can be transmitted in a manner that is dependent on SMAD transcription factors (canonical TGF β signalling) (Heldin and Moustakas, 2012) or independent of SMAD transcription factors (non-canonical TGF β signalling) (Mu *et al.*, 2012).

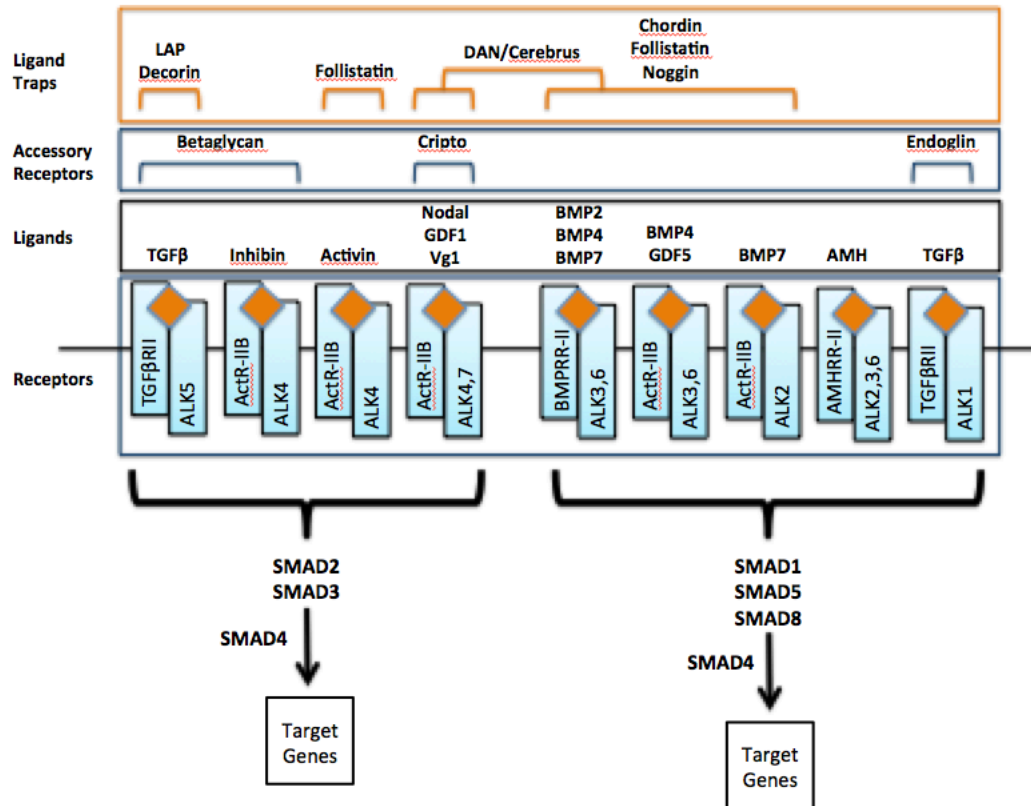


Figure 1.6: Receptor system for the TGF β signalling family.

Complex relationship between TGF β ligands, ligand-binding traps, accessory receptors, with type I and II receptors in vertebrates. Adapted from Shi and Massague, 2003.

1.6.1.2 Mechanisms of receptor and SMAD activation/SMAD-dependent TGF β signalling

The human genome encodes for eight SMAD proteins, which can be subdivided into three classes; receptor regulated SMADs (R-SMADs), SMAD1, 2, 3, 5 and 8, which are the substrates for the TGF β family of receptors (Massague *et al.*, 2005); the common mediator, SMAD4 (Co-SMAD) (Shi *et al.*, 1997); and the inhibitory SMADs (I-SMADs), SMAD6 and 7 (Itoh *et al.*, 2001). Following activation of TGFBR1, this receptor recognizes receptor regulated SMADs (RSMADs) with the aid of the adaptor protein SARA (SMAD

anchor for receptor activation) (Wu *et al.*, 2000), and subsequently phosphorylates the serine residues located at the carboxy terminus end of the SMAD proteins in order to transmit the signal (Attisano and Wrana, 2000). Once activated SMAD2 and/or 3 form a heterodimeric or heterotrimeric complex with SMAD4, also known as the cooperating-SMAD (Co-SMAD), before subsequently accumulating in the nucleus where they regulate the transcription of a large set of target genes (Figure 1.7) (Chen *et al.*, 2002; Derynck *et al.*, 1998; Derynck and Zhang, 2003; Gomis *et al.*, 2006). SMAD proteins are 400-500 amino acids in length and are composed of three distinct regions (Shi and Massague, 2003). R-SMADs are composed of two highly conserved domains that are separated from one another by a less conserved proline-rich region (Shi *et al.*, 1998; Martin-Malpartida *et al.*, 2017), and are termed the MAD-homology 1 (MH1) and MAD-homology 2 (MH2) domains (Figure 1.8). The MH1 domain is found at the N-terminus and harbours a DNA-interaction region while the MH2 domain is found at the C-terminus and is responsible for mediating subcellular localization and transcriptional regulatory activity (Hill, 2009; Wu *et al.*, 2000). The MH1 domains within SMAD3 and 4 allow for binding to the specific DNA sequences containing 5'-AGAC-3', termed SMAD-binding elements (SBE) (Zawel *et al.*, 1998). The C-terminal MAD-homology 2 (MH2) domain binds to the TGFBR1, which enables SMAD homo- and hetero-oligomerisation along with transactivation of nuclear SMAD complexes (Moustakas and Heldin, 2009). SMAD proteins exist in a very dynamic activation-deactivation cycle, which is as a consequence of the opposing actions of kinases and phosphatases. In a steady state, R-SMADs are found predominantly in the cytoplasm in their inactive forms, whereas SMAD4 is distributed throughout the cytoplasm and nucleus. Unlike the R-SMADs, SMAD2, and 3, SMAD6 and 7 are inhibitory SMADs (I-SMADs) that in response to feedback loops and antagonistic signals, control TGF β pathway activity. SMAD6 has been found to compete with SMAD4 for the receptor activated SMAD1, and SMAD7 is capable of recruiting ubiquitin ligase-Smurf to TGF β and BMP receptors for inactivation (Kavsak *et al.*, 2000). This shuttling of R-SMADs between the cytoplasm and the nucleus following their activation is controlled by the reciprocal functions of importin. Importin is a transporter that binds to nuclear localization sequences (NLS) and subsequently carries cargo into the nucleus. CRM1 is an importin-like adaptor protein which binds nuclear export sequences present on SMAD4 to mediate their export from the nucleus

(Xiao *et al.*, 2000; Xiao *et al.*, 2003). Both SMAD2 and 3 do not require CRM1 for nuclear export (Pierreux *et al.*, 2000; Xu *et al.*, 2002). However, it is important to note that the dynamics of SMAD shuttling between the nucleus and cytoplasm is far more complex. For example, sorting nexin 9 (SNX9) is a structurally related trafficking protein that is required for SMAD3-dependent responses, with SNX9 shown to interact with pSMAD3 independent of SMAD2 or 4 and mediate the association of pSMAD3 with importin 8 (Imp8) (Wilkes *et al.*, 2015). Inman *et al.* (2002a) showed that, following the nuclear accumulation of R-SMAD-SMAD4 complexes (due to TGF β pathway activation), the export of SMAD4 could be blocked when using the CRM1 blocker, LMB, whereas SMAD2 could still be redistributed to the cytoplasm when using the receptor blocker, SB431542 (Inman *et al.*, 2002a). Furthermore, since the stabilisation of R-SMAD-SMAD4 complexes occurs through the C-terminal phosphorylation of R-SMADs, the data suggests that these complexes dissociate in the nucleus as a result of R-SMAD dephosphorylation, and that the resulting monomeric R-SMADs and SMAD4 are exported via separate mechanisms. Importantly, recent evidence has challenged the linear view of the TGF β signalling pathway, with studies showing that even in an unstimulated cell, SMAD2 and 4 are continuously shuttled between the cytoplasm and nucleus, and in the case of SMAD2 and 3 can even freely diffuse in and out of the nucleus (Inman *et al.*, 2002a; Xu *et al.*, 2002; Schmierer and Hill, 2005). The accumulation of SMAD 2, 3 and 4 in the nucleus occurs at a relatively slow rate and reaches a maximum level at approximately 45 min after pathway activation (Inman *et al.*, 2002a), which, once accumulated, will mostly remain for roughly 4 – 5 hours, after which they begin to relocalise to the cytoplasm (Pierreux *et al.*, 2000). Following inhibition of the pathway using the ALK5 inhibitor, SB-431542, they showed an immediate decrease in the nuclear levels of SMADs, resulting in the bulk of SMADs relocating to the cytoplasm (Inman *et al.*, 2002b). In order to explain how nuclear SMADs could detect the inactivation of the receptor, photobleaching and photoactivation experiments using GFP fusion of SMAD2 directly demonstrated the continuous shuttling of SMADs in and out of the nucleus even in active cells, which serves to connect events at the plasma membrane with the nucleus (Batut *et al.*, 2007; Nicolas *et al.*, 2004; Schmierer and Hill, 2005).

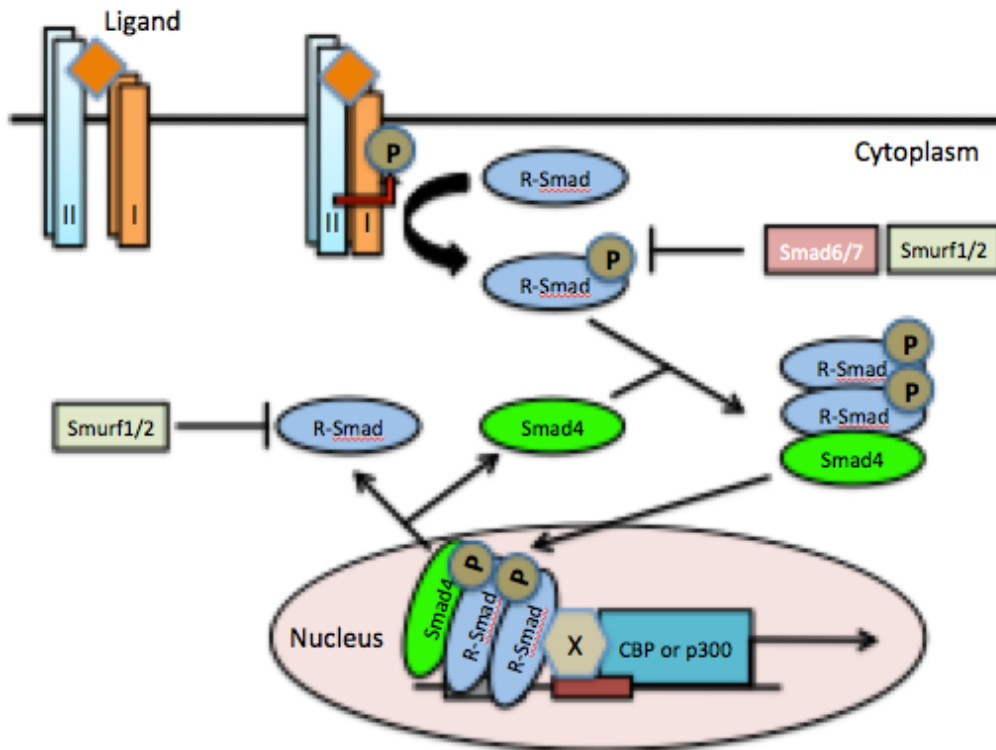


Figure 1.7: Canonical TGFβ signal transduction from the cell membrane to the nucleus.
Adapted from Shi and Massague, 2003.

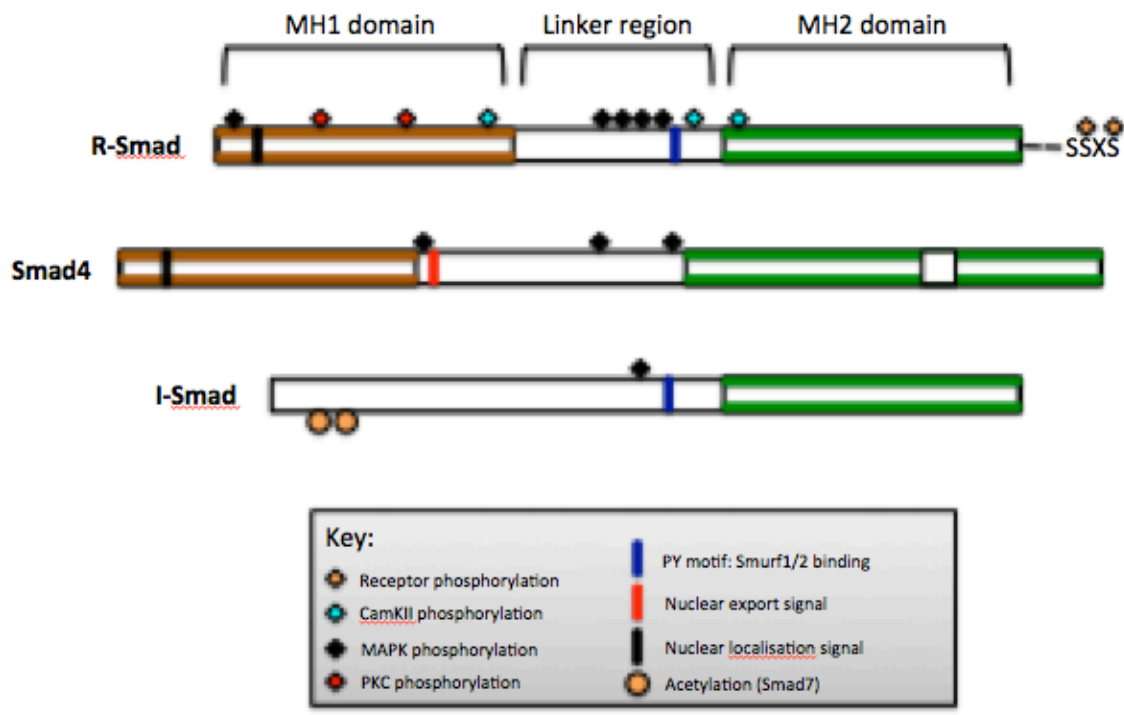


Figure 1.8: Structure of SMAD proteins.

Structural organisation and role of the SMAD domains, along with candidate target sites for kinase pathways (e.g. Erk MAPK and JNK, as well as CamKII and PKC). Adapted from Shi and Massague, 2003.

1.6.1.3 Target gene activation by SMADs

The recruitment of R-SMADs to DNA is the crucial step in the modulation of gene transcription following TGF β induced pathway activation. This activation of transcription through TGF β proteins occurs through the physical interaction of SMADs along with the functional cooperation of sequence-specific transcription factors and the coactivators CBP and p300 (Massague, 2000; Itoh *et al.*, 2000; Moustakas *et al.*, 2001; and Zawel *et al.*, 1998). R-SMADs (with the exception of SMAD2) and SMAD4 bind to specific DNA sequences at an affinity 100-fold lower than the DNA transcription factors (which is required for transcriptional activation) (Derynck and Zhang, 2003). SMADs are capable

of functionally interacting with a vast number DNA-binding transcription factors, and to add an extra layer of complexity, multiple signalling pathways often regulate them. Furthermore, aside from the main coactivators, CBP and p300, the level of transcriptional activation can be defined by other coactivators and corepressors interacting with SMADs. Even SMAD4 can act as a coactivator by stabilizing the interaction of R-SMADs with DNA and CBP/p300 to enhance ligand-induced transcription (Massague, 2000; Itoh *et al.*, 2000; Moustakas *et al.*, 2001).

1.6.2 Non-canonical TGF β Signalling

In addition to the canonical SMAD-driven side of TGF β signalling, TGF β is capable of transducing the signal in a SMAD-independent manner (Zhang, 2009). TGF β is capable of activating various branches of the MAP kinase pathways, Rho-like GTPase signalling pathways, and phosphatidylinositol-3-kinase/AKT pathways.

1.6.2.1 TGF β induced Erk activation and tyrosine phosphorylation

MAPKs comprise a large family of serine/threonine kinases, that make up at least 11 members which can be subdivided into 6 main groups: 1) ERK (ERK1 and 2); 2) JNK (JNK1, 2, and 3); 3) p38 (p38 α , β , γ and δ); 4) ERK5; 5) ERK3 (ERK3, p97 MAPK and ERK4); and 6) ERK7 (ERK7 and 8) (Teramoto and Gutkind, 2013). The most prominent members of the MAPK pathway are ERK1/2, JNK and p38 (Johnson and Lapadat, 2002), with ERK implicated in cell growth responses (Kamimura *et al.*, 2004), while JNK and p38 are traditionally linked with stress related signalling that involves apoptosis and inflammatory cytokines (Zhou *et al.*, 2007; Yogi *et al.*, 2006). The ability of TGF β to induce rapid activation of p21 (Ras) in rat intestine (Mulder *et al.*, 1992) and mink lung epithelial cells (Yan *et al.*, 1994) was the first indication that TGF β can activate the Erk MAPK pathway. Engel *et al.*, 1999 performed studies using SMAD4-deficient cells, or dominant-negative SMADs to support the ability of TGF β signalling to activate the MAPK pathway independently of the SMADs. Although TGFBR1 and II are very well defined serine-threonine kinases, TGF β RII is capable of undergoing auto-phosphorylation on the tyrosine residues: Y259, 336 and 424 (Lawler *et al.*, 1997). Src, a non-RTK, is capable

of phosphorylating TGFBRII on Y284, which can serve as a docking site for the recruitment of the signalling molecules growth factor receptor binding protein 2 (Grb2) and Shc (Gallagher *et al.*, 2007). TGFBR I can also be tyrosine phosphorylated upon TGF β stimulation, and subsequently recruit and directly phosphorylate ShcA on tyrosine and serine residues, which promotes the formation of an ShcA/Grb2/Sos complex. The formation of this complex leads to the sequential activation of c-Raf, MEK, and Erk through the activation of Ras at the plasma membrane (Lee *et al.*, 2007).

1.6.2.2 TGF β induced JNK/p38 activation

Of all the non-SMAD pathways, it is the JNK/p38 MAPK signalling cascades that are the best characterized. Similar to Erk, JNK and p38 represent the tertiary layer of MAPK cascades, and are activated by the MAP kinase kinases (MKK), MKK4 and MKK3/6, respectively (Weston and Davis, 2007). In various cell lines, TGF β is capable of activating JNK through MKK4 (Frey and Mulder, 1997; Engel *et al.*, 1999; Hocevar *et al.*, 1999), and p38 MAPK through MKK3/6 (Hanafusa *et al.*, 1999; Sano *et al.*, 1999; Bhowmick *et al.*, 2001). A demonstration of SMAD-independence was observed through the use of a mutant TGFBR I, which rendered the receptor unable to bind and activate SMADs, but still retain an intact kinase activity. This mutant type I receptor was still capable of activating JNK and p38 MAPK in a TGF β induced manner (Yu *et al.*, 2002; Itoh *et al.*, 2003). MKKs can also be activated further upstream by the MAP3Ks, which in the cases of MKK3/6 and MKK4 is performed by TGF β -activated kinase 1 (TAK1), a kinase found to activate and be activated by TGF β signalling (Yamaguchi *et al.*, 1995). The physiological significance of this kinase in TGF β signalling was elucidated in mouse genetic studies, whereby TAK1-deficient embryos exhibited phenotypes strikingly similar to that of loss-of-function mutations in genes encoding the type I receptor, ALK1 (Jadrich *et al.*, 2006). TAK-1 has also been shown to be required for TGF β -induced JNK and NF κ B activation (Shim *et al.*, 2005), and shortly after a direct interaction between TAK-1 and TGFBR II was identified (Watkins *et al.*, 2006).

1.6.2.3 Rho-like GTPases in TGF β signalling

The Rho-like GTPases, including RhoA, Rac and Cdc42, have important roles to play in cytoskeletal organization, cell motility, and gene expression through a wide variety of effectors (Jaffe and Hall, 2005). In a similar manner to MAPK pathways, TGF β is capable of activating RhoA-dependent signalling pathways to induce the formation of stress fibres and mesenchymal characteristics in epithelial cells and primary keratinocytes (Bhowmick *et al.*, 2001; Edlund *et al.*, 2002). TGF β stimulation is capable of inducing the assembly and accumulation of TGFBR1-TGFBR2 complexes at tight junctions, where the scaffolding protein that regulates epithelial cell polarity, Par6, gets phosphorylated by TGFBR2 at serine residue 345 (Ozdamar *et al.*, 2005). Following this phosphorylation Par6 recruits Smurf1 to the activated TGFBR1 and II complex at tight junctions in polarized epithelial cell sheets. The Par6-Smurf1 complex then enables TGF β -dependent dissolution of tight junctions (a pre-requisite of EMT), by mediating the localized ubiquitination and turnover of RhoA at cellular protrusions (Ozdamar *et al.*, 2005). TGF β can also induce the activation of the Cdc42 GTPase (Wilkes *et al.*, 2003), and physical interactions between Cdc42 and cell surface TGF β receptor complexes have been identified (Barrios-Rodiles *et al.*, 2005).

1.6.2.4 TGF β induced PI3K/Akt pathway activation

There have been a large number of findings to support the ability of TGF β signalling to induce PI3K/Akt activation. Firstly, TGF β is capable of activating the PI3K pathway, through the phosphorylation of Akt, which is downstream (Bakin *et al.*, 2000; Shin *et al.*, 2001; Vinals and Pouyssegur, 2001; Lamouille and Derynck, 2007), and appears to be independent of SMAD2/3 activation (Wilkes *et al.*, 2005). Secondly, immunoprecipitation experiments have shown that TGFBR2 was constitutively associated with the regulatory subunit of PI3K, p85, while association between TGFBR1 and p85 required TGF β stimulation (Yi *et al.*, 2005). Consequently chemical inhibition of TGFBR1 activity was found to prevent TGF β -induced activation of Akt by PI3K (Bakin *et al.*, 2000; Lamouille and Derynck, 2007). Furthermore, the PI3K/Akt pathway is another

non-SMAD dependent pathway that is capable of contributing to TGF β -induced EMT. Studies using chemical inhibitors have shown that PI3K is implicated in TGF β mediated actin filament reorganization and cell migration (Edlund *et al.*, 2004; Bakin *et al.*, 2000). Evidence suggests that the involvement of the PI3K/Akt pathway in TGF β -mediated EMT could in part be due to mammalian target of rapamycin (mTOR), which is a downstream effector of Akt, and a key regulator of protein synthesis via phosphorylation of S6 kinase (S6K) and eukaryotic initiation factor 4E-binding protein 1 (4E-BP1) (Lamouille and Derynck, 2007).

1.6.3 SMAD-dependent TGF β signalling, independent of TGF β receptor-ligand interactions

C-terminal phosphorylation by the TGFBR1 is the key event in SMAD activation; however other kinase pathways are capable of regulating SMAD signalling further. In some instances, SMAD transcription factors are capable of transducing signal via gene transcription and regulation in a manner that is independent of the upstream TGF β -TGFBR interaction. There are a number of non-SMAD signalling proteins/kinases that have the ability to modulate SMAD activity through phosphorylation of the SMAD linker region.

1.6.3.1 Cyclin-dependent kinases (CDKs)

Cyclin-dependent kinases (CDK) comprise a family of multifunctional serine/threonine kinase enzymes involved in cell cycle progression and transcription. CDK has been shown to phosphorylate the SMAD linker regions in bovine endothelial cells (Kamoto *et al.*, 2014), while SMAD3 is phosphorylated by CDK2 and 4 in Mv1Lu mink lung epithelial cells, acting as a key regulator in the anti-proliferative effects of TGF β (Matsuura *et al.*, 2004). In the case of SMAD3, CDK2 and 4 are capable of phosphorylating 9 of 14 residues, and inhibiting SMAD3 anti-proliferative function (Matsuura *et al.*, 2004; Liu and Matsuura, 2004). CDK8 and 9 have also been shown to phosphorylate the SMAD

linker region at Thr179, Ser208 and Ser213 in SMAD2 and 3 which targets these activated SMADs for proteosomal degradation through the recognition of the E3 ubiquitin ligase, Nedd4L with the phospho T-P-Y motif in the linker region of SMAD2/3 (Gao *et al.*, 2009). However, CDK8 and 9 can also phosphorylate the linker region of SMAD1, which results in the recruitment of YAP, which enhances SMAD-mediated transcription via interaction with the cofactor, Pin1, until this phosphorylated linker region is ultimately recognised by Smurf1 and subsequently degraded (Alarcon *et al.*, 2009; Aragon *et al.*, 2011). Therefore, there is a functional switch from initial SMAD activation to subsequent degradation, which occurs following a switch in the recognition between SMAD phosphoserines of both transcription factors and E3 ubiquitylating ligases. For example, SMAD3 phosphorylation by CDK8/9 following TGF β pathway activation creates binding sites for WW domains of Pin1, and subsequent phosphorylation by GSK3, adds binding sites for Smurf1 WW domains, thereby switching off Pin1 binding and targeting SMAD3 for degradation (Aragon *et al.*, 2011).

1.6.3.2 Mitogen-activated protein kinases (MAPK)

Numerous studies have identified the crosstalk that exists between the TGF β and MAPK pathways (Wrighton *et al.*, 2009; Burch *et al.*, 2010; Yue and Mulder, 2001). One of the first instances of such regulation was the ability of the ERK-mediated phosphorylation of specific serine residues in the linker domain of R-SMADs, which blocked their nuclear translocation and transcription (Kretschmar *et al.*, 1997). In addition MSK1 kinase, which is a p38 substrate, was shown to regulate SMAD3 transcriptional activity by promoting its association with co-activator p300 (Abecassis *et al.*, 2004). Massague and colleagues (Kretschamer *et al.*, 1997) demonstrated the ability of EGF, an activator of MAPK, to phosphorylate cluster sites within the linker regions of SMADs. Interestingly, tyrosine kinase receptors for EGF and hepatocyte growth factor signalling are capable of inducing SMAD2 phosphorylation and transcription (de Caestecker *et al.*, 1998).

1.6.3.3 Phosphoinositide 3-kinases (PI3K)

PI3K are a highly conserved family of kinases harbouring dual protein and lipid kinase activity, and can be subdivided into three main groups (I, II and III). Class I PI3Ks are heterodimers composed of a catalytic (p110 α , β , γ and δ) and regulatory subunit (p85 or p101 family) (Morello *et al.*, 2009). Studies using chemical inhibitors of the PI3K-Akt pathway were shown to affect SMAD-dependent transcriptional responses in mouse mammary epithelial cells (NMuMG), suggesting a potential involvement of PI3K and/or Akt in TGF β signal transduction (Sansal and Sellers, 2004). Furthermore, studies in mesangial cells, have demonstrated the ability of phosphoinositide-dependent kinase 1 (PDK1), a member of the PI3K pathway, to phosphorylate SMAD3 and enhance its transcriptional activation of the collagen I gene following TGF β activation of the PI3K signalling pathway (Runyan *et al.*, 2004).

1.6.3.4 Glycogen synthase kinase-3 (GSK-3)

In 1980, Embi *et al.* identified a proline-directed serine/threonine kinase, designated glycogen synthase kinase 3, which was shown to have the ability to phosphorylate and subsequently inactivate the enzyme glycogen synthase, therefore giving it the ability to regulate glycogen metabolism. Within mammals, there are two isoforms of GSK3, GSK3 α (51KDa), and β (47KDa), with both isoforms shown to be highly conserved and widely expressed (Yao *et al.*, 2002). In fact, more recently GSK3 has established itself as a multi-faceted kinase, with functions in many signalling pathways, including the insulin, Wnt/ β -catenin, Notch, and Hedgehog pathways which are capable of determining cellular fate and morphology (Doble and Woodgett, 2003). A number of studies have demonstrated the ability of GSK3 to interact with SMADs. For example, in the heart, pro-fibrotic TGF β 1-SMAD3 signalling is inhibited through the ability of GSK3 β to interact with the SMAD3 linker region and c-terminus (Lal *et al.*, 2014). In this study, inhibition of GSK3 β was shown decrease phosphorylation at the linker region (Ser204), and increase phosphorylation at the c-terminus (Ser423/425).

1.6.3.5 Rho-associated protein kinase (ROCK)

Rho-associated protein kinase (ROCK) is a kinase that belongs to the AGC (PKA/PKG/PKC) family of serine/threonine kinases, and in mammals there are two forms (ROCK1 and 2). ROCK1 has a molecular weight of 158 kDa and is the main downstream effector of the small GTPase RhoA (Hahmann and Schroeter, 2010). One of the primary functions of ROCK is to regulate the shape and movement of cells by interacting with the cytoskeleton (Riento and Ridley, 2003). A couple of studies have highlighted the ability of Rho/ROCK to regulate SMAD activity through linker region phosphorylation (Chen *et al.*, 2006A; Kamaraju and Roberts, 2005). The regulation of SMAD activity by Rho/ROCK was first established by Chen *et al.*, following TGF β -induced smooth muscle differentiation (Chen *et al.*, 2006B). Furthermore, during EMT and cytoskeletal arrangements, the induction of TGF β signalling has been shown to greatly influence activation of the Rho/ROCK pathway (Bhowmick *et al.*, 2003; Lee and Helfman, 2004). In fact, a study demonstrated the ability of the microtubule disruptor, colchicine, to stimulate the phosphorylation of SMAD2 and 3 in a Rho/ROCK-dependent mechanism that is independent of TGF β ligand and/or receptor activity (Samarakoon *et al.*, 2009). Conversely, the inverse has also been demonstrated, with p38 and Rho/ROCK pathways found to greatly impact the anti-proliferative effects of TGF β signalling (Kamaraju and Roberts, 2005).

1.6.4 Context dependent signal readout

Although the identification and structural characterisation of the core components of the TGF β signalling pathway have been important for developing our understanding of the signal transduction process, it is insufficient in explaining how TGF β ligands activate different genes within the same cell or how the same SMADs can activate different genes in different contexts. The concepts that provide the basis for explaining the versatility of the TGF β signalling pathway will be briefly discussed. One example of this is the ability of SMADs to bind to common DNA motifs. As mentioned previously, both TGF β and BMP initiate direct responses by the activation of different SMADs. SMAD3 and 4 bind the palindromic duplex 5'-GTCTAGAC-3', and X-ray crystal structures of the

SMAD1, 3 and 4 MH1 domains shown to be bound to this sequence showed that all three SMADs recognised the GTCT motif or its complementary extended sequence CAGAC (Shi *et al.*, 1998; BabuRajendran *et al.*, 2010). SMAD1 and 4 were also found to bind to GC-rich motifs (Kusanagi *et al.*, 2000; Labbe *et al.*, 1998; Morikawa *et al.*, 2011), which led to the proposal that these GC-rich motifs serve as BMP response elements, whereas the CAGAC motifs functioned as SBE for the TGF β family. Therefore, there appears to be a dichotomy between the SMADs, given the sequence identity of the MH1 domain β -hairpin (an element required for DNA binding). More recent studies have shown that SMAD1, 3, 4 and 5 recognise the common consensus sequence GGCGC, referred to as the 5GC SBE motif (Martin-Malpartida *et al.*, 2017). X-ray crystallography on SMAD MH1 domains bound to these 5GC SBEs has shown that the β -hairpin has a high degree of conformational flexibility, and that in target genes, the SMAD binding promoter and enhancer elements are enriched in clusters of 5GC SBEs. Therefore, it appears that TGF β induced SMAD3 and BMP induced SMAD1/5 recognise common DNA motifs but yet regulate different target genes.

Since the differential DNA binding activity of SMAD1/5 and SMAD2/3 does not appear to be a major factor of TGF β vs BMP subfamily specificity in the recognition of target genes, then other factors must determine this specificity. Early work on the two LDTFs, forkhead box protein H1 (FOXH1) and zinc finger protein 423 (ZFP423), provided examples of the pivotal role of these factors as contextual determinants of TGF β and BMP induced responses. FOXH1 directs Nodal-activated SMAD2/3 to target promoters during the formation of the mesendoderm (Yoon *et al.*, 2015; Zhang and Glass, 2013; Chen *et al.*, 1996; Chen *et al.*, 1997), whereas ZFP423 directs BMP-activated SMAD1 to target promoters during ventral mesoderm specification in *Xenopus laevis* (Hata *et al.*, 2000). Therefore, in this instance, the specificity was defined by FOXH1 and ZFP423, which discriminately bind to SMAD2/3 and SMAD1/5, respectively, and form resulting complexes which target gene regulatory regions containing FOXH1 and ZFP423 binding elements coupled with SBEs. The analysis of genome bound SMADs in various cell types shed more light onto how cells read TGF β family signals. Mullen *et al.* (2011) showed that the binding pattern of signal-activated SMAD2/3 was different to ESCs, myoblast precursors and pro-B cells, and that these binding patterns closely aligned with binding

of highly expressed LDTFs within each cell lineage (Mullen *et al.*, 2011). This paradigm was also demonstrated for the binding patterns of BMP-activated SMAD1 (Trompouki *et al.*, 2011), and in sum demonstrates that the cell type-specific and pathway-specific activity of SMADs is determined by LDTFs. However, this does not mean that SMADs are passive participants, since LDTF guided SMADs can regulate the expression of other LDTFs. Furthermore, SMADs do not always form exclusive partnerships with a master TF, and LDTFs are not obligatory partners of SMADs.

SMADs integrate inputs from multiple signalling pathways, and are broadly separated into two categories: i) regulating the strength and duration of SMAD signalling activity through signal-dependent post-translational modifications, and ii) the response of signal-driven TFs to specific cytokines which cooperate with both SMADs and LDTFs at target gene loci. The latter ties to recent studies that have identified the concept of super-enhancers, which compared to regular enhancers are rare and are strongly enriched at LDTF loci (Whyte *et al.*, 2013). Furthermore, upon examination of the DNA elements that comprise super-enhancers, there was an enrichment in both LDTF and signal-driven TF binding sites (Hnisz *et al.*, 2015). Furthermore, the TFs were associated with multiple pathways, which overall suggests that the control of cell identity is a process that is highly cooperative, and involves LDTFs and multiple signal-driven TFs, with SMAD proteins being prominent among them.

1.6.5 Role of TGF β signalling under physiological conditions

1.6.5.1 Embryonic development and homeostasis

1.6.5.1.1 Early Development: Axis Formation, and Patterning

In early development (embryogenesis), members of the Nodal/Activin and BMP families have pivotal roles in the generation of axes and in the subsequent patterning of tissues across these axes. These morphogens are capable of providing positional information through the formation of concentration gradients in a dose-dependent manner, which initiate downstream molecular programs to fields of cells (Wu and Hill, 2009). In

Drosophila embryos, dorsal-ventral (D/V) axis specification and patterning is achieved through the BMP orthologs Decapentaplegic (Dpp), and Screw (Scw) (Morisato and Anderson, 1995). Cells along this D-V axis respond differently depending on the levels of Dpp signalling, with high levels of signalling specifying the amnioserosa, lower levels of signalling specifying the dorsal ectoderm and the lack of signalling permitting neural ectoderm formation (O'Connor *et al.*, 2006). In contrast, unlike in *Drosophila*, the first zygotically induced axis in mice is the anterior-posterior (A-P) axis, however, again, Nodal is a key player. Nodal, whose initial expression occurs within the epiblast, is involved with A-P formation in three-key steps (Schier, 2003; Yamamoto *et al.*, 2004). First, is its requirement for induction of the distal visceral endoderm (DVE); second, cells within the visceral endoderm secrete Nodal antagonists (in response to Nodal), which results in the inhibition of Nodal-induced proliferation within cells close to these antagonists; and third, nodal induces cells of the DVE to migrate towards the anterior and thereby create an A-P axis. Despite these slight differences, the molecular requirements for defining and patterning the D/V axis are highly conserved between vertebrates and *Drosophila*.

1.6.5.1.2 Germ-Layer Specification, Patterning, and Gastrulation

Along with its pivotal involvement in axis specification, Nodal is also required in vertebrates of the three germ layers: endoderm, mesoderm, and ectoderm (indirectly). Firstly, different levels of Nodal signalling are required for further patterning, with high levels inducing endoderm and lower levels inducing the mesoderm (Zorn and Wells, 2007). The third layer, ectoderm, is considered a default tissue type, as tissues absent from Nodal signalling become ectoderm, with active inhibition of Nodal signalling required in the embryo (Zhang *et al.*, 1998). Without the appropriate specification of the three germ layers, normal gastrulation cannot occur, and therefore there is no surprise that severe gastrulation and primitive streak defects can occur following loss-of-function mutations within Nodal signalling (Zorn and Wells, 2007).

1.6.5.1.3 Left-Right (L-R) Asymmetry

After the formation of A-P and D-V axes, the L-R axis is specified, which is important for organ positioning and the directional looping of tubules in the body (Wu and Hill, 2009). Yet again Nodal plays a key role, and during L-R axis specification, is dynamic, both spatially and temporally. BMP signalling is also involved in L-R patterning, with evidence from mouse and chick revealing BMP ligands to have differing roles, with BMP4 repressing Nodal expression in the right lateral plate mesoderm (LPM) in mouse (Mine *et al.*, 2008) and BMP2 inducing Nodal expression on the left side in chick (Schlange *et al.*, 2002). Experiments in zebra fish suggest that BMP signalling can temporally regulate these two separate events (Chocron *et al.*, 2007).

1.6.5.1.4 Organogenesis and Developmental Disease

So far only a few key players, mainly Nodal and several BMPs that are required for early embryogenesis, and their ligands are deployed in later developmental processes in tissue morphogenesis and homeostasis. In vertebrates the role in morphogenesis of most organs is played by a number of TGF β superfamily ligands. Examples include anti-mullerian hormone (AMH), which is a highly specialized member of the TGF β family, and is required for a number of processes, including follicular development in females, whose expression is used as a marker for follicular reserve in women, and excessive amounts can cause polycystic ovary syndrome (Wang *et al.*, 2007).

Family members of the TGF β signalling pathway are well known for their ability to induce epithelial-mesenchymal transition (EMT) (Yang and Weinberg, 2008), which allows polarized cells within an epithelial sheet to assume a spindle-like mesenchymal shape, migrate from site of origin and invade/colonise surrounding tissue. The process of EMT is essential under physiological conditions for a variety of developmental processes, with a classic example being the invasion of endocardial cells from the

atrioventricular (AV) canals into the heart cushion, which eventually gives rise to heart valves (Mercado-Pimentel and Runyan, 2007).

1.6.5.2 Cell cycle progression and apoptosis

In response to TGF β ligands many genes are activated, whereas others are transcriptionally repressed. Under physiological conditions TGF β signalling is responsible for G1-phase arrest of the cell cycle (Ewen *et al.*, 1995; Geng and Weinberg, 1993; Herrera *et al.*, 1996; Zhang *et al.*, 1999). There are multiple mechanisms that control TGF β mediated anti-proliferative responses. Various studies have shown TGF β is capable of inducing TGF β signalling and inhibits cell-cycle progression by regulating the transcription of cell growth arrest through the upregulation p^{15Ink4b} and p21^{Cip1} (Polyak *et al.*, 1994; Senturk *et al.*, 2010), which subsequently inhibit cyclin-dependent kinase (CDK)-mediated phosphorylation of the retinoblastoma protein (pRb) (Florenes *et al.*, 1996; Rich *et al.*, 1999; Robson *et al.*, 1999). TGF β signalling is also capable of inducing cell cycle arrest through the upregulation of p27^{Kip1} or through the inhibition of CDK tyrosine phosphatase cdc25A (Iavarone and Massague, 1997). TGF β impacts other cell cycle regulators; among them include c-Myc and Id family members, which are downregulated by TGF β (Chen *et al.*, 2002; Kang *et al.*, 2003). In TGF β induced c-Myc downregulation, SMAD3 represses its transcription in association with the transcription factors E2F4, E2F5 and co-repressors p107. This complex is assembled in the cytoplasm before being translocated into the nucleus (in response to TGF β treatment), where, in association with SMAD4, it binds to the SMAD-E2F-binding site in the c-Myc promoter and represses c-Myc expression (Chen *et al.*, 2002). TGF β -activated SMAD3 also downregulates Id1 activity by directly inducing ATF3 expression, before forming a complex with ATF3 and repressing the Id1 promoter (Kang *et al.*, 2003).

TGF β family members can also induce cell apoptosis, which is typically accompanied by growth arrest. One mechanism by which TGF β induces apoptosis is through the JNK and p38 pathways, mediated through the adaptor protein Daxx (Edlund *et al.*, 2003; Perlman *et al.*, 2001). TGF β can also induce programmed cell death, usually through the accumulation of reactive oxygen species (Langer *et al.*, 1996), downregulation of Id2

(Cao *et al.*, 2009), and transcriptional regulation of apoptotic proteins BIK and BCL-XL (Spender *et al.*, 2009). Recent work on pre-malignant pancreatic progenitor cells harbouring mutant KRAS has shown that TGF β induced apoptosis occurs through the altered regulation of SOX4 (directly) and Krueppel-like factor 5 (KLF5) (indirectly) through activation of the EMT programme (David *et al.*, 2016).

1.6.5.3 Epithelial-Mesenchymal Transition

EMT is a well-coordinated process during embryogenesis and a pathological feature in neoplasia and fibrosis. Cells that undergo EMT begin to lose apical-basolateral cell polarity, undergo actin reorganization, and lose the expression of E-cadherin and ZO-1, which in turn causes them to become more motile and invasive through the production of a mesenchymal cell cytoskeleton (Kalluri and Weinberg, 2009; Levayer and Lecuit, 2008). TGF β induced EMT has been demonstrated in a wide variety of cell types, including keratinocytes, mammary epithelial cells and hepatocytes (Cui *et al.*, 1996; Davies *et al.*, 2005; Miettinen *et al.*, 1994; Sheahan *et al.*, 2008). EMT is driven by a set of transcription factors including Snail and Slug (zinc-finger proteins), Twist (bHLH factor) (Mani *et al.*, 2007; Thuault *et al.*, 2006), ZEB-1 and -2 (zinc-finger-homeodomain proteins), and FoxC3 (forkhead factor) (Xu *et al.*, 2009). Through a combination of direct association with DNA and recruitment of a complex consisting of HDAC, the expression of various target genes are regulated (e.g E-cadherin) by TGF β -induced Snail family transcription factors (Dhasarthy *et al.*, 2007; Zavadil and Bottinger, 2005). In a similar fashion to Snail family members, Zeb family transcription factors recognize E-box elements on regulatory regions of target genes, and are capable of repressing E-cadherin through the recruitment of the transcriptional co-repressor C-terminal binding protein (CtBP) (Vandewalle *et al.*, 2005).

1.6.6 TGF β signalling in cancer

1.6.6.1 Points of disruption in the TGF β pathway in cancer

Due to the diverse role of TGF β signalling in cellular functions, disruption of this pathway has been associated with a diverse range of diseases including cancer, atherosclerosis, and renal fibrosis (Derynck *et al.*, 2001; Massague and Wotton, 2000). There is a growing body of evidence that implicates the TGF β signalling pathway as a point of disruption in cancer. Bi-allelic inactivation of TGF β RII mutations that either truncate the protein or inactivate its kinase domain have been shown in many carcinomas including colon, gastric, biliary, pulmonary, ovarian, esophageal, and head and neck (Levy and Hill, 2006). Also, germline mutations in the BMP type I receptor BMPRIA in a subset of individuals with the autosomal dominant disease, Juvenile Polyposis Syndrome (JPS), predisposes them to gastrointestinal polyps and cancer (Zhou *et al.*, 2001). There have been a number of instances whereby the ligand trap proteins are linked to carcinogenesis, including the overexpression of follistatin and gremlin-1 that have been implicated in breast cancer metastasis (Kang *et al.*, 2003) and skin basal cell carcinomas (Sneddon *et al.*, 2006) respectively. Surprisingly, even though R-SMADs have such a pivotal role in connecting signalling pathways, they are rarely mutated in cancer, with only a limited number of cases including intragenic mutations in SMAD2 present in a small proportion of colorectal cancers (Sjoblom *et al.*, 2006), and the loss of SMAD3 expression being found in gastric cancer and T cell lymphoblastic leukemia being reported (Levy and Hill, 2006). Unlike SMAD2 and 3, SMAD4 is a notable target for inactivation in cancer (Ryan *et al.*, 2014). Including, SMAD4 mutations, which are present in more than half of pancreatic carcinomas (close in prevalence to KRAS, p53, and p16INK4A mutations) (Jaffee *et al.*, 2002); SMAD4 is also mutated in more than half of sporadic colorectal tumours, and in a high proportion of esophageal tumours (Sjoblom *et al.*, 2006). Finally, some cancers have also been associated with changes in I-SMADs. For example, in endometrial carcinomas and thyroid follicular tumours, SMAD7 overexpression and therefore suppression of TGF β signalling has been found (Cerutti *et al.*, 2003; Dowdy *et al.*, 2005). Under physiological conditions SMAD function is directly inhibited by transcriptional repressors such as Ski (SKI) and SnoN (SKIL). As a

consequence SKI and SKIL deletions as well as amplifications have been observed in colorectal and esophageal cancers, which interestingly raises the possibility that these genes can act as either oncogenes or tumour suppressor genes depending on the context (Zhu *et al.*, 2007).

1.6.6.2 Tumourigenic Effects of TGF β : Tumour Growth, Invasion, and Immune Evasion

Although implicated in tumour progression, the role of TGF β throughout the development of a cancer is one that is complex and context dependent, with TGF β shown to be anti-tumourigenic at early stages of tumourigenesis, and pro-tumourigenic at later stages (Cui *et al.*, 1996; Mao *et al.*, 2006; Pierce *et al.*, 1995). These anti-tumourigenic effects deployed by TGF β are the aforementioned roles of this pathway under physiological conditions, including inhibition of cell cycle progression and proliferation, as well as even inducing apoptosis (Pardali and Moustakas, 2007; Siegel and Massague, 2003) in addition to senescence in certain cell types such as keratinocytes (Shukla *et al.*, 2008; Vijayachandra *et al.*, 2003).

However, the pro-tumourigenic effects of TGF- β signalling in cancer are typically associated with increased invasiveness and an aggressive phenotype. This is predominantly achieved through (1) induction of epithelial-mesenchymal transition (Heldin *et al.*, 2012), (2) increased proliferation arising from retinoblastoma gene inactivation (Donovan & Slingerland, 2000), (3) autocrine growth factor signalling (TGF-beta itself and PDGF), (4) release of osteoclastic proteins, and (5) immunosuppressive effects (Tian *et al.*, 2011).

1.6.6.3 Epithelial-Mesenchymal Transition

In transformed epithelial progenitor cells with tumour-propagating abilities, TGF β -induced EMT is observed, and as such contributes to tumour invasion and dissemination owing to the cell junction-free, motile phenotype the cells acquire (Nieto *et al.*, 2016;

Mani *et al.*, 2008; Puram *et al.*, 2017; Ye and Weinberg, 2015; Diepenbruck and Christofori, 2016). Tumour cells with such mesenchymal traits are often found to be CSCs, and are observed at the invasion front/edge, which is a region that is rich in stromal TGF β and other cytokines that may play a part in EMT induction. TGF β is a potent inducer of EMT (Derynck and Ackhurst, 2007; Thiery, 2003), and its role in human cancer has been reported in tumour-propagating breast cancer cell populations expressing the cell surface markers, CD44+/CD24^{low} (Shipitsin *et al.*, 2007). The gene expression pattern of these cells compared to the bulk population suggested the presence of an active TGF β signalling pathway, and that when these cells were exposed to a TGFBR1 blocker, they were induced to adopt a more epithelial phenotype. These cells, therefore, may represent a population that has undergone EMT. The ability of TGF β to induce EMT occurs through a combination of SMAD-dependent transcriptional events and SMAD-independent effects of cell junctional complexes. The transcriptional events include the induction of Snail, Slug, and Twist through SMAD-mediated expression of HMGA2 (high-mobility group A2) (Thuault *et al.*, 2006), while independent of SMAD activity, the dissolution of cell junction complexes occurs through T β RII-mediated phosphorylation of Par6 (Ozdamar *et al.*, 2005). Of further note, in mouse tumours and cell lines, Ras signalling has been shown to enhance SMAD-dependent TGF β -induced EMT (Derynck and Akhurst, 2007).

1.6.6.4 Loss of TGF β mediated G₁ arrest in cancer

As previously described under physiological conditions, TGF β induces G₁ arrest through the downregulation of c-Myc, inhibition of CDKs, and hypo-phosphorylation of pRb (Fyfan and Reiss, 1993). The cyclin D1 genes have been shown to contribute to TGF β resistance, with overexpression and/or amplification of this gene seen in 40% of breast cancers (Lammie *et al.*, 1991; Buckley *et al.*, 1993). Increased expression of the cyclin E protein has also been observed in cancers (Porter *et al.*, 1997). Amplifications and activating mutations in the Cdk4 gene have also been associated with cell cycle progression, with amplifications observed in primary breast cancers (An *et al.*, 1999), and dominant active mutations observed in individuals with malignant melanoma (Bates and Peters, 1995). There are a number of mechanisms by which c-Myc can

contribute to cell cycle arrest. Overexpression of c-Myc is capable of increasing G1 cyclin levels, and may indirectly regulate the expression of cyclins D1, E and A (Jansen-Durr *et al.*, 1993; Shibuya *et al.*, 1992), which in turn leads to the sequestration of the cell cycle inhibitor p27 away from cyclin E-cdk2, which subsequently activates cell cycle progression (Perez-Roger *et al.*, 1991; Bouchard *et al.*, 1999).

1.6.6.5 Myofibroblast Generation

There are numerous publications that have highlighted the role of TGF β signalling in landscaping the tumour microenvironment during tumour progression, with particular attention to its impact on stromal fibroblasts. A large proportion of colorectal and pancreatic cancers avoid TGF β -mediated growth arrest by completely abolishing the pathway; however, this apparent paradox between high levels of TGF β and poor prognosis can be explained in part by the fact that the tumour microenvironment is responsive to TGF β signalling. Calon *et al.* (2012) used an orthotopic mouse model for colorectal cancer to show that colorectal cancer cells increased the efficiency of organ colonisation due to the activity of TGF β on stromal cells, and that mice treated with a TGFBR1 receptor demonstrated resilience to metastasis (Calon *et al.*, 2012). In a breast cancer metastasis model a complementary finding was also observed where TGF β signalling was used by tumour SCs to infiltrate the lungs and create a metastatic niche (Malanchi *et al.*, 2011). Therefore these findings support the notion that at early time points of the metastatic process the TGF β activated stroma is crucial to facilitate the colonisation of cancer cells.

Another significant component of the pro-invasive action of TGF β is the mobilization of myofibroblasts. Myofibroblasts are highly motile and have features of fibroblasts and smooth muscle cells, and their presence in the tumour stroma (aka cancer-associated fibroblasts; CAFs) facilitates tumour development (Allinen *et al.*, 2004; De Wever and Mareel, 2003). CAFs may arise from TGF β driven differentiation of resident tissue fibroblasts into activated fibroblasts (Evans *et al.*, 2003), a process that requires chloride intracellular channel 4 (CLIC4) (Shukla *et al.*, 2014). *In vitro* myofibroblasts are capable of guiding colon cancer cell invasion into a collagen matrix, and is a process that is

constantly reliant on TGF β . Myofibroblasts promote cancer cell proliferation, tumour invasion, and neo-angiogenesis through the production of matrix metalloproteases (MMPs), cytokines, such as IL-8 and VEGF, and chemokines including CXCL12 (Massague, 2008). The crosstalk that exists between cancer cells and CAFs can occur through either cell-cell contact or through the release of soluble factors. Epithelial tumours such as prostate cancer cells have been shown to secrete sufficient amounts of TGF β to activate primary fibroblasts (Grubisha *et al.*, 2012). Furthermore, treatment with tumour cell-derived conditioned media induced TGF β signalling in CAFs, including proteinases that mediate cell invasion, which was subsequently abolished following TGFBR1 blockade, thereby indicating a strong TGF β dependency (Hawinkels *et al.*, 2014). A study by Calon *et al.* (2015) has even identified the role of CAFs in increasing the frequency of tumour-initiating cells, and the fact that TGF β signalling dramatically enhances this process. Furthermore, through the use of patient derived organoids and xenografts, they found that TGF β inhibitors blocked the crosstalk between cancer cells and the microenvironment and thereby halted disease progression (Calon *et al.*, 2015).

1.6.6.6 Production of Autocrine Mitogens

Tumour cell proliferation is promoted by TGF β through the stimulation of the production of autocrine mitogenic factors. An example of this can be seen in glioma, where the loss of the TGF β tumour suppressor arm, due to PI3K hyperactivation, loss of p15INK4b, or mutational inactivation of RB, allows these tumour cells to profit from TGF β -induced mitogen production (Jennings and Pietenpol, 1998). The production of autocrine mitogenic factors has also been observed in a number of other tumour types, including leukemia inhibitor factor (LIF) and platelet-derived growth factor (PDGF) production in glioblastoma (Penuelas *et al.*, 2009), angiopoietin-like 4 (ANGPTL4) production which serves as a mediator of infiltration of circulating breast cancer cells into the lungs (Padua *et al.*, 2008), and expression of osteoclast stimulating genes (i.e. CTGF) for bone colonisation by breast cancer cells (Kakonen *et al.*, 2002; Kang *et al.*, 2005; Sethi *et al.*, 2011).

1.6.6.7 Evasion of Immunity

A net pro-tumourigenic advantage may result when the immunosuppressive effects of TGF β outweigh the tumour-suppressive benefits of its anti-inflammatory action. Examples of this have been shown in mouse studies, where T-cell specific expression of a dominant-negative form of TGFBR2 prevented the growth of inoculated melanoma (Gorelik and Flavell, 2000). This effect has also been demonstrated in glioma patients, whereby TGF β has been shown to decrease the expression of the activating immunoreceptor NKG2D in CD8 $^+$ T cells and NK cells, but represses the expression of the K+NKG2D ligand MICA (Friese *et al.*, 2004). Furthermore knocking down the synthesis of TGF β in glioma cell lines prevented NKG2D downregulation and subsequently enhanced the killing of glioma cells by CTL and NK cells. Therefore both the immunosuppressive action of TGF β and the TGF β -induced production of PDGF may be essential for glioma development. Therefore TGF β signalling has a critical role in regulating the adaptive immune system. TGF β signalling has been shown to suppress the expression of interferon- γ , restrict the expression of T_H1 cells, inhibit the development of memory T cells, and attenuate the activation and cytotoxic effects of CD8 $^+$ effector cells (Li and Flavell, 2008; Gorelik and Flavell, 2000; Thomas and Massague, 2005; Takai *et al.*, 2013). However, more significantly TGF β has been shown to induce the differentiation of regulatory T cells (Tregs), which are a sub-population of CD4 $^+$ T cells that express CD25 and the forkhead box P3 (FOXP3) transcription factor (Chen *et al.*, 2003; Liu *et al.*, 2007; Liu *et al.*, 2009; Chen *et al.*, 2005). FOXP3 is the signature transcription factor that maintains the functional program of the Treg lineage, and TGF β has been shown to induce the expression of FOXP3 on Tregs (Tone *et al.*, 2008; Hori *et al.*, 2003). Following induction by TGF β , FOXP3 induces the expression of CTLA4 and the ligand Galectin-9 (GAL-9), with CTLA-4 shown to restrain co-stimulation of T cells and GAL-9 that triggers exhaustion or apoptosis of effector T cells through engaging the T-cell immunoglobulin domain and mucin domain-3 (TIM-3) immune-inhibitor receptor (Wing *et al.*, 2008; Oida *et al.*, 2006; Zhu *et al.*, 2005). The induction and maintenance of Tregs is strengthened in an autocrine positive feed-forward loop, with GAL-9 shown to interact with TGF β receptors in order to drive more FOXP3 expression (Wu *et al.*, 2014). The functional orientation of tumour-infiltrating immune

cells has a major impact on a patient's outcome with cancer, with T_H1 cells, cytotoxic CD8⁺ T cells and memory T cells expression associated with longer disease-free survival and tumour-infiltrating Tregs associated with poor prognosis in numerous cancer types (Dranoff, 2005; Curiel, 2008; Tosolini *et al.*, 2011). Therefore the ability of TGF β to skew CD4⁺ T cell differentiation away from a T_H1 phenotype towards a Treg lineage has significant clinical implications. As highlighted previously, clinical efforts used to counteract tumour-induced immune tolerance have focused on the use of monoclonal antibodies, which are designed to attenuate T-cell inhibitory receptors that function as immune checkpoints (e.g. CTLA4 and PD-1/PD-L1). One potential limitation of using immune checkpoint inhibitors is in the case of tumours enriched for TGF β , and therefore FOXP3 expression, as autocrine and paracrine signalling within the tumour microenvironment could skew tumour-infiltrating T cells towards a Treg lineage and away from T_H1 and CD8⁺ immune effector cell response. A recent study by Ravi *et al.* (2018) used bifunctional antibody-ligand traps, containing an antibody capable of targeting CTLA4 or PD-L1, and a TGFBRII ectodomain, which can sequester and inactivate TGF β within the local tumour microenvironment (Ravi *et al.*, 2018). They found that in comparison to the CTLA4 antibody, Ipilimumab, the bifunctional antibody-ligand traps inhibited tumour progression as a consequence of a significant reduction in tumour-infiltrating Tregs, and activating antitumour immunity (Ravi *et al.*, 2018). The role of TGF β signalling in the ineffectiveness of immune checkpoint inhibitors has been reported by Mariathasan *et al.* (2018) who found that in metastatic urothelial carcinoma, an increased TGF β signature was associated with resistance to PD-L1 blockade (Mariathasan *et al.*, 2018). Another recent study by Tauriello *et al.* (2018) used a mouse model of metastatic colon cancer to show that in cooperation with PD-L1 blockade, TGF β inhibition promoted T cell-mediated clearance of liver metastases (Tauriello *et al.*, 2018).

1.6.7 Changes in TGF β and SMAD Protein Expression During Mouse Skin Carcinogenesis

Significant alterations in the expression of TGF β growth factors (along with other TGF β components) have been reported in several laboratories during mouse skin carcinogenesis. Early mouse studies showed the localized production of TGF β in tumour promoter-stimulated mouse epidermis (Akhurst *et al.*, 1988), and that papillomas and carcinomas induced *in vivo* had elevated levels of TGF β 1 RNA within the basal keratinocyte compartment (Fowlis *et al.*, 1992). Furthermore, Kane *et al.* (1991) found that following cutaneous injury and subsequent physiological changes during wound healing, changes in the structure or conformation of TGF β 1, its localization and perhaps its activity vary in a spatial and temporal manner (Kane *et al.*, 1991). Studies have also shown that the Ras signalling pathway is required for TGF β 1 stimulation of invasiveness and metastasis in keratinocytes (Santibanez *et al.*, 2000). Furthermore, crosstalk between Ras and SMAD signalling pathways, whereby SMAD4 attenuates the activity of Ras in keratinocytes expressing the Ras oncogene, and blockade of SMAD4 function led to the progression to undifferentiated carcinomas due to hyperactivation of the Ras/ERK pathway. The reliance of Ras signalling for TGF β 1-induced EMT has been reported in a number of epithelial cells. Interestingly, Oft *et al.* (2002) showed that elevated H-Ras levels were required for nuclear translocation of SMAD2, therefore inducing EMT as a consequence.

1.6.8 Role of TGF β signalling in Basal cell carcinoma

BCC represents the most common cancer in humans, which as previously mentioned places a significant strain on healthcare services worldwide. There is increasing evidence to suggest that cutaneous epithelial tumours such as BCC are linked to deregulation of the TGF β signalling pathway. When taking a whole genome approach, a number of groups have performed microarray analysis on human basal cell carcinoma in an attempt to enhance our understanding of the genetic and molecular basis of BCC (Heller *et al.*, 2013; Pellegrini *et al.*, 2017). The microarray study performed by Heller *et al.*, 2013, compared human BCC tissue against site-matched control samples, and found several pathways to be significantly overrepresented in BCC, including PPAR- γ , TGF β signalling, lipid metabolism along with the previously well established roles of SHh and

p53. Other groups have studied the levels of mRNA and protein expression in BCC samples and found a significant overexpression of TGF β 1, SMAD3, and SMAD7 mRNA levels, and marked protein overexpression of SMAD3 (Gambichler *et al.*, 2007). BCCs are unusual in that they rarely metastasize, although they can be locally invasive. However, BCC is unique in that the vast majority of mutations responsible for driving tumour growth are found solely within the Hh signalling pathway, and as a consequence when discussing the role of TGF β signalling in BCC, it is important to consider its interaction with Hh signalling.

1.6.9 Crosstalk between the TGF β and Hh signalling pathways

In both normal and malignant tissues, the Hh and TGF β pathways have been shown to directly regulate key components of each other (Guo and Wang, 2009). TGF β has been shown to induce Hh expression, which in turn activates GLI1 and GLI1-dependent epithelial mesenchymal transition in non-small cell lung cancer cells (Maitah *et al.*, 2011). SHh ligand has been shown to promote an invasive phenotype within human gastric cancer cells, mediated through the SHh-induced expression of TGF β ligand and TGF β RI (Yoo *et al.*, 2008). The SMAD transcription factors within the TGF β pathway have been shown to interact with the GLI transcription factors in the Hh pathway, where in several cell types, TGF β /SMAD3 has been demonstrated to directly induce the transcription of GLI2, which in turn upregulates GLI1 (Dennler *et al.*, 2007) (Figure 1.9). Of clinical relevance is that TGF β blockade has been shown to attenuate Gli-mediated Hh signalling and reduce cell growth in pancreatic cancer cells that were resistant to Hh inhibition (Dennler *et al.*, 2007). Several SMAD proteins have been shown to interact with truncated form of GLI3 (which is a repressor of Hh signalling), and thereby serve to sequester this repressor and activate Hh signalling. Furthermore, this SMAD-GLI3 complex was shown to dissociate following TGF β /BMP treatment, and therefore be free to suppress Hh signalling (Liu *et al.*, 1998). In BCC in particular, the most significant pathogenic event is the upregulation of Hh signalling. This crosstalk has been observed in BCC, and has led to the identification of increased expression of TGF β signalling in untreated BCC (Heller *et al.*, 2013; O'Driscoll *et al.*, 2006). Furthermore, TGF β signalling activation is required for tumour progression in a mouse model of BCC development where it may exert immunosuppressive activities (Fan *et al.*, 2010). Furthermore,

clinical benefit of blocking the TGF β pathway was demonstrated as BCC development was prevented in this model upon the use of a TGFBR1 small molecule blocker (Fan *et al.*, 2010). Therefore, while TGF β likely contributes to the biological effects imparted by Hh signalling, it is apparent that the opposite is also true, and as a consequence these two pathways appear to demonstrate a reciprocal cycle of activation.

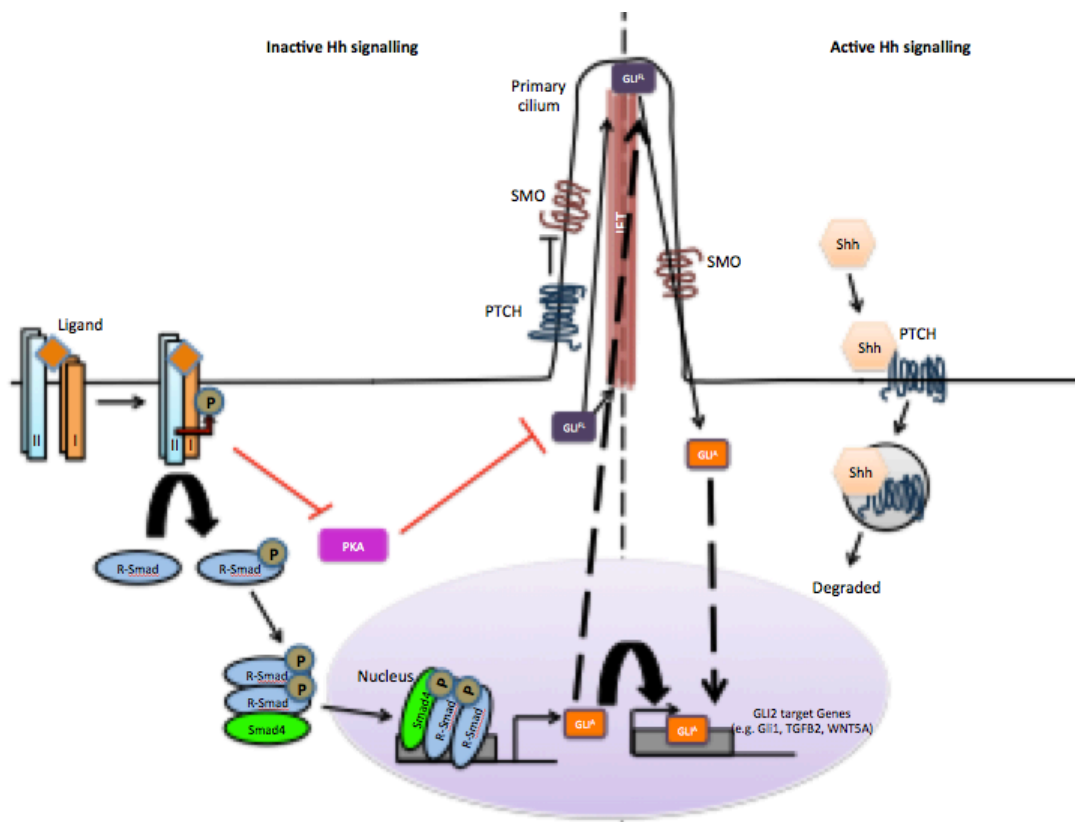


Figure 1.9: Crosstalk between TGF β and Hh signalling pathways.

*TGF β ligands stimulate the formation of heteromeric serine/threonine kinase receptor complexes, which subsequently phosphorylate and activate R-SMAD proteins, which are capable of inducing GLI2 expression. GLI2 is then capable of inducing the expression of genes including those involved in EMT. Adapted from Javelaud *et al.*, 2012.*

1.6.10 Role of TGF β signalling in CSC

There are multiple lines of evidence supporting the role of TGF β signalling in the regulation and maintenance of SCs. More specifically, TGF β signalling has been recognized for its role in the maintenance of embryonic stem (ES) cells, adult/somatic SCs (in a select number of tissues), and more recently in CSCs.

ES cells are derived from the inner cell mass of blastocysts, which are multicellular structures derived from multiple divisions of fertilized eggs. One of the most defining features of ES cells is their ability to produce identical progeny through symmetric cell divisions. Mouse embryos deficient in the common mediator SMAD, SMAD4, have been shown to have abnormal epiblast proliferation and a delay in the outgrowth of the inner cell mass (Sirard *et al.*, 1998). Furthermore, pSMAD2 has been observed within undifferentiated human ES cells, and was found to decrease upon early differentiation (James *et al.*, 2005). As a consequence, use of the ALK5 inhibitor, SB431542 (Inman *et al.*, 2002b), has shown a decreased expression of the markers of undifferentiated states (James *et al.*, 2005; Vallier *et al.*, 2005). SB431542 was also shown to dramatically reduce the proliferation of mouse ES cells without impacting on their pluripotency, suggesting that TGF β signalling is essential for the proliferation of mouse ES cells (Ogawa *et al.*, 2007). Therefore, TGF β signalling plays an important role in maintaining self-renewal and pluripotency in human and mouse ES cells.

The signals transduced by TGF β family members have been implicated in various types of somatic/adult SCs (e.g. intestinal SCs, HF epidermal SCs, neural SCs) (Watabe and Miyazono, 2008).

In intestinal SCs, it is predominantly the BMP axis of the TGF β /BMP signalling pathway that plays a role in regulating this SC population. Within the intestinal crypts, BMP signalling acts as a negative regulator of the SC population. BMP-4 is highly expressed within the intravillus mesenchyme, while in differentiated villus epithelial cells and intestinal SCs phosphorylation and nuclear accumulation of BMP-specific R-SMADs has been observed (Haramis *et al.*, 2004). This suggests that there is paracrine BMP

signalling from the mesenchyme to the neighbouring SCs. Exogenous expression of the BMP ligand Noggin within the mouse intestine lead to the ectopic formation of normal crypt-villus units, and eventual formation of a complex architecture which was similar to human juvenile polyposis (Haramis *et al.*, 2004). Furthermore, mouse studies have shown that deletion of the gene *Bmpr1a* within the crypts disturbs intestinal epithelial regeneration and causes an expansion in the stem and transient amplifying cells, leading to a type of polyposis (He *et al.*, 2004). Balancing the control of SC self-renewal occurs through BMP signalling inhibiting the Wnt signalling pathway, which it achieves through the activation of PTEN, which in turn decreases the level of nuclear β -catenin through inactivation of the PI3k-Akt signalling pathway (He *et al.*, 2004).

The role of TGF β signalling in skin SCs is well documented, with studies showing that if you compromise the pathway is comprised through loss of TGFBRII, epidermal homeostasis is maintained, but the basal cell layer containing SCs undergoes increased proliferation and apoptosis (Guasch *et al.*, 2007). TGF β signalling is a key pathway involved in the formation of the HF, where exogenous TGF β 2 has been shown to induce dermal papilla formation, which is sufficient to promote SC driven hair growth (Fuchs and Nowak, 2008). TGF β signalling is also found to be upregulated in the bulge cells of the hair follicle (Tumbar *et al.*, 2004), and is known to dampen the cell cycle (Massague, 2007). To produce new hairs, existing HFs must undergo cycles of growth (anagen), regression (catagen) and rest (telogen), with the new growth phase driven by SCs. As a consequence, the HF represents an excellent model for looking at the regulation of SC quiescence and activation (Alonso and Fuchs, 2006). Importantly, TGF β signalling is found to be a key player in the control of this cycle, with elevated TGF β 1 levels shown to perpetuate catagen, while the transition from catagen to telogen is linked to a fall in TGF β 1 (Foitzik *et al.*, 2000). Whereas during telogen, factors associated with anagen, such as FGF18 (Greco *et al.*, 2009) and TGF β 2 (Oshimori and Fuchs, 2012) are simultaneously downregulated. Oshimori and Fuchs, (2012) went on to demonstrate that TGF β 2 is critical for inducing hair follicle SCs (HFSC) at the bulge base, through antagonizing BMP signalling and thereby lowering BMP thresholds within the niche (Oshimori and Fuchs, 2012). They also demonstrated the presence of nuclear pSMAD2+ cells within the HFSC located at the bulge base.

In early development, the inhibition of TGF β family signalling results in the formation of embryonic neural SCs from ES cells (Temple, 2001). These ES SCs are then capable of differentiating into complex arrays of neurons and glia within the central nervous system. The maintenance and growth of these neural SCs is controlled through TGF β signals (Falk *et al.*, 2008). Within the mid/hind brain, enhancement of self-renewal but not multipotency was observed in neural SCs following the ablation of the TGF β RII gene, resulting in the enlargement of the midbrain. Within mutant brains, both FGF and Wnt signalling components have been observed, which suggests that TGF β signalling serves to negatively regulate these pathways and therefore self renewal of neural SCs in order to control the size of a specific area of the brain (Falk *et al.*, 2008).

Similar to its complex role in cancer, TGF β signalling has been shown to have a dual role in the biology of CSCs, whereby it seems to be capable of inhibiting or sustaining their function in a context dependent manner (Bellomo *et al.*, 2016). An example of TGF β signalling inhibiting CSC function can be seen in breast cancer whereby it adopts two independent mechanisms: 1) reducing the CSC pool, and/or 2) by promoting the differentiation of a highly proliferative committed progenitor population to a more differentiated less proliferative state (Tang *et al.*, 2007). Cammareri *et al.* (2016) found that in vemurafenib-induced skin lesions and sporadic cSCC, both TGFBR1 and TGFBR2 were frequently mutated. They found that these mutations eradicated TGF β signalling in the bulge SCs in both normal human and murine skin, and that through targeted ablation of TGF β signalling in combination with MAPK pathway hyperactivation to the LGR5+ SC population enabled the development of cSCC in the mouse (Cammareri *et al.*, 2016). Therefore under these circumstances the loss of TGF β signalling in combination with MAPK pathway activation in the LGR5+ SC population is key for driving skin carcinogenesis. However, the role of TGF β signalling in CSC promotion and maintenance is well documented and has been demonstrated in a number of cancer types, including breast cancer (Bruna *et al.*, 2012; Lo *et al.*, 2012; Bholra *et al.*, 2013; Shipitsin *et al.*, 2007), liver cancer (You *et al.*, 2010; Mima *et al.*, 2012), glioblastoma (Ikushima *et al.*, 2009; Penuelas *et al.*, 2009) and skin cancer (Oshimori *et al.*, 2015) to name just a few. For example in liver cancer, TGF β has been shown to increase the expression of the SC

marker CD133, through promoting the demethylation of the CD133 promoter, and thereby enhancing the tumourigenic potential of the population *in vivo* (You *et al.*, 2010). In breast cancer, a strong TGF β pathway signature was identified within metastatic breast CSCs (CD44^{high}, CD24^{low}), which were subsequently shown to adopt an epithelial-like structure following TGF β pathway inhibition (Shipitsin *et al.*, 2007). In glioblastoma, a SMAD-dependent induction of leukaemia inhibitory factor (LIF) along with the sequential activation of the LIF-Janus kinase-STAT pathway was shown to induce self-renewal of CSC but not normal glial progenitors (Penuelas *et al.*, 2009). Studies have also shown that the relationship between TGF β and SOX4 is also important in glioblastoma CSC, with TGF β shown to induce expression of SOX2, which is mediated by the TGF β target gene SOX4 (Ikushima *et al.*, 2009). They found that TGF β signalling inhibitors drastically reduced the tumourigenicity of glioma-initiating cells by promoting their differentiation, a process that could be attenuated when these cells were transduced with SOX2 or SOX4 (Ikushima *et al.*, 2009). Furthermore, a study by Anido *et al.* (2010) found that the treatment of GBM neurospheres with TGF β increased the levels of ID1, ID2, LIF, SOX2 and SOX4, and thereby indicates the importance of TGF β signalling in the self-renewal of a glioblastoma CD44^{high}/ID1^{high} CSC population (Anido *et al.*, 2010). Furthermore, they demonstrated that knocking-down SOX 2 or 4 induced a decrease in the CD44^{high} population, indicating that these proteins are responsible for the maintenance of this population (Anido *et al.*, 2010). Finally in squamous cell carcinoma (SCC), Oshimori *et al.* (2015) identified a non-genetic mechanism for the role of TGF β signalling in driving heterogeneity within SCC-CSCs, which impacted on drug resistance. Here TGF β supplied from the tumour-vasculature bestowed slow cycling properties to SCs nearby; and further played a role in giving these TGF β responsive cells resistance towards anticancer drugs through transcriptional activation of p21, which in turn stabilized NRF2, and subsequently enhanced glutathione metabolism (Oshimori *et al.*, 2015). A more recent study by Brown *et al.* (2017) highlighted the role of TGF β signalling in mediating chemoresistance in 'tumour-propagating cells (TPCs)' in SCC (Brown *et al.*, 2017). In this study, Brown *et al.* (2017) were able to distinguish between quiescent and proliferative TPCs using a combination of H2B-GFP based pulse-chasing with cell surface markers, and found that quiescent TPCs resist DNA damage and have enhanced tumourigenic potential following chemotherapy (Brown *et al.*, 2017). This

quiescence was regulated by TGF β signalling and they found that TGF β inhibition prevented TPC entry into a quiescent state and thereby increased their susceptibility to chemotherapy (Brown *et al.*, 2017). As previously described, numerous publications have supported the notion that BCC is a follicular disease and is derived from SCs (Wong and Reiter, 2011; Colmont *et al.*, 2013; Wang *et al.*, 2011; Grachtchouk *et al.*, 2011), and more specifically derived from the bulge region of the hair follicle (Colmont *et al.*, 2013; Wang *et al.*, 2011; Grachtchouk *et al.*, 2011). Our lab identified a CD200+ CSC population within BCC that was resistant to chemotherapy, which was intriguing as CD200 is also a marker of SCs located within the bulge region of the HF (Colmont *et al.*, 2013).

Although highlighted previously, it is important to note the role of EMT in the context of CSC. During cancer progression, EMT confers malignant properties, such as invasiveness and motility to tumour cells. TGF β signalling plays an important role in inducing EMT, most notably through the ability of SMADs to interact with Zeb proteins to repress the expression of E-cadherin (Comijn *et al.*, 2001; Postigo *et al.*, 2003; Verschueren *et al.*, 1999). Mani *et al.* (2008) found that SCs isolated from both normal and cancerous mammary glands exhibited EMT properties with decreased expression of E-cadherin and increased expression of mesenchymal markers, such as vimentin (Mani *et al.*, 2008). Therefore the connection between EMT and epithelial SC properties highlights how malignant CSCs can be generated in cancer and raises the possibility that pharmacological intervention regulating the process of EMT may have a role in regenerative medicine through the generation of normal epithelial SCs.

1.7 Aims and Objectives

One quarter of all cancers are dependent upon the hedgehog growth factor signalling pathway to drive tumour growth, including: breast, pancreas, gastrointestinal, prostate, haematological, and neural malignancies. Activating mutations can be identified in 100% of basal cell carcinoma (BCC), 50% of medulloblastoma, 29% of rhabdomyosarcomas, and 19% of breast cancers..

In 2012 the National Institute of Clinical Excellence (NICE) approved vismodegib, a potent hedgehog pathway inhibitor, for the treatment of inoperable and metastatic BCC. Vismodegib inhibits SMO and, despite it being active in advanced BCC, more than 50% of such lesions have demonstrated resistance to vismodegib. Atwood *et al.* (2015) and Sharp *et al.* (2015) used a large collection of tumour samples to identify specific mutations within SMO that were responsible for conferring resistance to vismodegib (Atwood *et al.*, 2015; Sharpe *et al.*, 2015). A similar mechanism for resistance was also identified in medulloblastoma treated with vismodegib (Yauch *et al.*, 2009). However, the development of resistance towards Hh pathway inhibition is attributed to SMO mutations in roughly 50% of the cases studied (Ransohoff *et al.*, 2015; Metcalfe and de Sauvage, 2011). Therefore, the mechanism that underlies resistance in the rest of Hh-driven resistant tumours remains to be determined. As previously mentioned, there have been several clinical cases reporting the transformation of BCC into a more aggressive phenotype, such as an SCC, following treatment (Ransohoff *et al.*, 2015; Mohan *et al.*, 2016; Aasi *et al.*, 2013; Orouji *et al.*, 2014; Zhu *et al.*, 2014; Chang *et al.*, 2012; Zhu *et al.*, 2014). Preliminary microarray data already generated by our lab has shown the enrichment of TGF β signalling pathway components in BCC samples treated with vismodegib. Given these findings along with the well-established crosstalk between the Hh and TGF β signalling pathways in malignant tissues (Guo and Wang, 2009; Maitah *et al.*, 2011; Yoo *et al.*, 2008; Dennler *et al.*, 2007), TGF β signalling is clearly an important pathway that must be explored for drug resistance in Hh driven tumours.

This project will build on our studies that demonstrate the presence of BCC CSC and show that they are both resistant to conventional chemotherapy and vismodegib, which is sufficient to sustain tumour recurrence (Colmont *et al.*, 2014; Colmont *et al.*, 2013). Therefore, in this study we will utilise primary human BCC samples along with a panel of Hh driven tumour cell lines in order to explore relevance of TGF β signalling in both the whole and CSC populations following treatment with a panel of Hh antagonists. The four overarching aims of this project are highlighted below.

Aims:

1. Identify differentially regulated pathways in BCC and normal skin
2. Define the expression of the TGF β pathway in human BCC CSC
3. Characterise the induction of TGF β signalling in BCC and Hh driven tumour cell lines resulting after Hh antagonist treatment
4. Determine the effect of blocking TGF β signalling in these Hh driven tumours

Chapter 2: Materials and Methods

Chapter 2 Materials and Methods

2.1 Human tissue Sample

Normal human skin and human BCC tissue was obtained after approval by the NHS R&D (Project ID: 08/DMD/4425) and ethics committee (Reference: 09/WSE02/10). After gaining informed written consent, excess tumour tissue or normal skin was placed into a tissue collection tube containing media and labelled with the patients' age, sex, body site and tissue type. The samples were then either immediately snap frozen and stored at -80°C (for immunolabelling) or placed in keratinocyte-serum free media (Gibco) and placed in the refrigerator at 4°C until transported to the laboratory. All samples entering the laboratory were logged in accordance with the Human Tissue Act. All human tissue was processed within 4 hours in one of six potential ways: **1)** Frozen for immunolabelling (Section 2.1.1), **2)** RNA extraction using the Qiagen RNeasy Mini Kit (Section 2.3.2), **3)** DNA extraction using the Qiagen Blood and Tissue Kit (Section 2.3.6), **4)** Tissue dissociation for subsequent primary culture (Section 2.1.2), **5)** Tissue dissociation and Fluorescent Activated Cell Sorting (Section 2.4), or **6)** Discarded if sample too small or infected.

2.1.1 Tissue Freezing and Cryosectioning

Tissue samples were trimmed, orientated in plastic moulds and embedded in Tissue-Tek OCT™ compound on dry ice. Frozen samples were logged in accordance with the Human Tissue Act and stored in a freezer at -80°C until use.

Samples were cryosectioned using the Leica Cryostat CM1860 UV (Leica Systems, England). The cryostat chamber was cleaned with 70% ethanol; frozen samples were placed into the chamber (set at -20°C) and allowed to acclimatize for 10 minutes. Frozen sample was removed from its plastic cryomould and attached to a metal chuck using OCT compound. The chuck was then attached to the instrument, and tissue sectioned to a thickness of 10 µm onto ThermoScientific superfrost ultra plus glass slides (#1014356190) and allowed to air-dry at room temperature. The slides with tissue sections were wrapped in aluminium foil and stored in a freezer at -80°C until

use. Upon completion, the cryostat chamber was once more cleaned with 70% ethanol, and exposed to DNA damaging UV irradiation for one-hour.

2.1.2 Tissue Dissociation

Tissue was dissociated into a cell suspension in a laminar flow class 2 tissue culture hood for cell culture, flow cytometric analysis, or flow sorting, as previously described (Colmont *et al.*, 2013). Briefly, 2 mL of Medium 199 was pipetted into the centre of a sterile 10 cm² petri dish. Using sterile forceps the tissue specimen was dipped in povidene iodine and then rinsed in HBBS before placing it into the medium 199 in the petri dish. The tissue was then finely minced with sterile iris scissors, then transferred into a 100 mL sterile conical flask, containing 25 mL medium 199 with 200U/ml Dispase (Gibco) and 200U/ml Ultrapure Collagenase Type IV (Worthington), together with a magnetic stir bar.

The flask containing the tissue was placed onto a magnetic stir plate in a tissue culture CO₂ incubator and incubated for 2 hours at 37°C. The semi-dissociated mixture was pipetted into a sterile 50 mL conical centrifuge tube and centrifuged at 200xg for 5 minutes. The enzyme mixture was aspirated and replaced by 10 mL of trypsin 0.05% with EDTA (Gibco) and incubated for 5 minutes in a water bath at 37°C. During this time the tube was shaken every 2 minutes. The tube contents were pipetted through a 40 µm cell strainer directly into a sterile 50 mL conical centrifuge tube containing 30 mL of Medium 199 with 5% FBS. 40 µL of the cell suspension was added to a haemocytometer for enumeration of viable cells by addition of trypan blue. The remaining contents of the 50 mL conical centrifuge tube were centrifuged at 200xg for 5 minutes. 1 mL of red cell lysis buffer (SC Technologies) was added and incubated at room temperature for 2 minutes, then diluted out with 9 mL of PBS, and contents pelleted once more by centrifugation at 200xg for 5 minutes. Cells were then resuspended for downstream applications.

2.2 Cell Culture

2.2.1 Established Cell Lines

The cell lines have been utilized for this project and are summarised in Table 2.1, murine NIH-3T3 fibroblasts (with and without transduced GLI-reporter construct), the human keratinocyte cell line, HaCaT, the osteosarcoma cell line, SJSA-1, and two medulloblastoma cell lines, DAOY and UW228-2. NIH-3T3, HaCaT, SJSA-1 and DAOY cell lines were purchased from American Type Culture Collection (ATCC; HTB-186), while the UW228-2 cell line was kindly provided by the laboratory of Prof. Martin Baumgartner (Zurich, Switzerland with permission from Professor John Silber). UW228-2 and DAOY cell lines were chosen as they are both well-characterized cell lines, and represent two sides of the spectrum of medulloblastoma tumours that are driven by hedgehog signalling, termed the 'SHh' subtype (Table 2.1). Furthermore, both of these cell lines have been well characterized with regard to SC assays, allowing us to explore the effects of Hh antagonists not only on the whole cell population but also on the SC population. The SJSA-1 cell line is not as heavily reliant on Hh signalling for its growth, but it nevertheless does have GLI amplifications, which mean that it in part is driven by Hh signalling (Table 2.1). Furthermore, this cell line allows us to explore the effects of these Hh antagonists in another tumour type, and also is wild type for p53 unlike the previous two-cell lines that have mutant p53. Finally, mouse NIH-3T3 fibroblasts have biological relevance to our studies and are a murine cell line, and therefore can be used as a negative control in some of our experiments. Conversely, HaCaT cells are a very well characterized cell line in skin cancer research and are frequently used as positive controls in publications related to our research.

Table 2.1: List of Hh driven cell lines along with their mutations and Hh signalling pathway profiles

Cell Line	Mutations	Hh signalling components (mRNA)	Sensitive to recombinant SHh	References
DAOY	TP53; MYC amplification	High levels: SHh, PTCH1, SMO, GLI1,	Yes	Arnhold <i>et al.</i> , 2016

		GLI2		
UW228-2	TP53; MYC amplification	Low Levels: SHh, PTCH1, GLI2	Yes	Arnhold <i>et al.</i> , 2016
SJSA-1	Mutant P53	High levels: GLI	N/A	N/A

2.2.1.1 HaCaT

HaCaT cells represent a spontaneously immortalized human keratinocyte cell line. The cells were obtained in 1988 from histologically normal skin, distal to an excised melanoma (Boukamp *et al.*, 1988). HaCaT cells get their namesake from the fact they are human adult skin keratinocytes, and were grown in low Ca²⁺ medium at an elevated temperature. HaCaT cells have been shown to be non-tumourigenic and non-invasive, and like normal keratinocytes, they grow into a well-structured epidermis when transplanted onto mice, and display normal differentiation, which was maintained at higher passages (Fusenig *et al.*, 1988).

2.2.1.2 NIH-3T3

The NIH-3T3 cells are an adherent fibroblast cell line established by George Todaro's group at the National Cancer Institute in Bethesda, Maryland from the NIH Swiss mouse embryo in 1969. Since then the NIH-3T3 cell line has become a standard fibroblast cell line used in research. Since they have the ability to secrete growth factors that are favourable for the growth they have been used as a feeder layer for the cultivation of normal keratinocytes, BCC and squamous cell carcinoma (Morgan *et al.*, 2018).

2.2.1.3 DAOY and UW228-2

DAOY are an adherent human primary medulloblastoma cell line, established from the cerebellum of a 4-year old boy in 1985, and has a polygonal morphology. UW228-2 is an

adherent cell line established alongside two other cell lines (UW228-1, and -3) from a posterior fossa medulloblastoma in the laboratory of Professor John Silber in 1995. Many publications have investigated the proteome and phenotype of both these cell lines. In fact, the subtype and molecular classification of over 40 medulloblastoma cell lines has been compiled, with less than half of these being sub grouped (18/44). Of these 18 cell lines, 4 have been classified as SHh-cell lines, and comprise the DAOY, UW228-2, ONS-76, and UW426 cell lines. Both DAOY and UW228-2 cell lines harbour TP53 mutations, and represent high-risk aggressive medulloblastoma (Ivanov *et al.*, 2016). Although both cell lines are 'SHh-subtype', they differ with regard to their mRNA expression of Hh signalling components and sensitivity to recombinant SHh, such that DAOY cells are characterized as having high levels of SHh, PTCH1, SMO, GLI1, and 2 and were stimulated to grow with SHh ligand (Arnhold *et al.*, 2016); whereas UW228-2 cells have low levels of SHh, PTCH1 and 2, and was also shown to increase cell viability upon addition of SHh ligand (although at a higher rate than DAOY cells). Therefore we have utilised well-established SHh-subtype cell lines that have slightly different Hh signalling characteristics.

2.2.1.4 SJSA-1

SJSA-1 is an adherent osteosarcoma cell line established from the primary tumour of a 19-year-old male with primitive multipotential sarcoma of the femur in 1982. It has fibroblast morphology and is characterized with expressing wild-type TP53 but also displaying amplifications in MDM2 and MDMX. Furthermore, this cell line also exhibits a 15-fold amplification of the GLI proto-oncogene within the Hh signalling pathway.

2.2.1.5 NIH3T3 (transduced with GLI-reporter construct)

The Gli-Reporter NIH-3T3 cell line (Amsbio, UK) was designed for monitoring the activity of the Hh signalling pathway. The reporter cell line contains the firefly luciferase gene under the control of GLI responsive elements stably incorporated into NIH-3T3 cells. Luciferase activity correlates with Hh signalling pathway activity.

Cells were thawed at 37°C in a water bath, re-suspended in a falcon tube containing 10 mL of pre-warmed DMEM (Hyclone #SH30243.01), 10% FCS, but without Geneticin (Gibco, UK), spun down at 300×g for 5 min to pellet cells. Cell pellet was re-suspended in 5 mL in media described above and placed into a T25 tissue culture flask. Cells were grown to first passage, where they were switched to DMEM with 10% FCS, and 500µg/mL of Geneticin (Gibco, UK). Cells were sub-cultured (Section 2.2.2) and cryopreserved (Section 2.2.3) as described.

2.2.2 Maintenance of Cell Lines

All cell lines were thawed at 37°C in a water bath, transferred to a 15 mL falcon tube (Corning) and 9 volumes of pre-warmed media supplemented with 10% fetal bovine serum (FBS). Cells were pelleted at 300 × g for 5 min at room temperature (RT) and supernatant discarded. Cell pellets were re-suspended in 15 mL of aforementioned media and incubated at 37°C (5% CO₂) in a T75 culture flask. Media was changed every 2-3 days, and cells were sub-cultured (described in Section 2.2.2) at high confluence (80-90%).

The media used to maintain the cell lines and the passaging ratio are described in table 2.2.

Table 2.2: List of cell lines and passaging ratios

Cell Line	Growth Media	Passaging Ratio
NIH-3T3	DMEM, 4.5 g/L glucose, 2 mM L-glutamine, 10% FBS, 50U/ml penicillin (All Gibco)	1:15
HaCaT	DMEM, 4.5 g/L glucose, 2 mM L-glutamine, 10% FBS, 50U/ml penicillin	1:15
DAOY	MEM, 2 mM L-glutamine, 10% FBS, 50U/ml penicillin	1:10
UW228-2	DMEM, 4.5 g/L glucose, 2 mM L-glutamine, 10%	1:5

	FBS, 50U/ml penicillin (All Gibco)
SJSA-1	RPMI, 2 mM L-glutamine, 10% FBS, 50U/ml penicillin 1:15
NIH-3T3 (GLI Reporter Transduced)	DMEM, 4.5 g/L glucose, 10% FCS, and 500µg/ml of Geneticin (Gibco, UK). 1:5

2.2.3 Sub-Culturing Cell Lines

For all cell lines, media was aspirated and cells were washed once with pre-warmed PBS (Gibco, UK), before adding 0.05% trypsin-EDTA (Gibco, UK). Cells were incubated at 37°C for 5 min, or until cells detached from the culture flask. Four volumes of media with 10% FBS or FCS (GLI-Responsive NIH-3T3) was added to inhibit trypsin activity, and cell suspension transferred to a 15mL falcon tube. Cells were centrifuged for 300 × g for 5 min at RT, supernatant was removed and cell pellets re-suspended in media required for their maintenance, and counted using a haemocytometer. Cells were seeded into appropriate cell culture plates/flasks (Table 2.3) depending on the assay being performed. Cells were incubated at 37°C (5% CO₂) until 80-90% confluent (3-5 days).

Table 2.3: Volumes of media used in cell culture

Plate	Relative Surface Area (cm ²)	Volume (µL)
T-25	25	5,000
T-75	75	15,000
T-150	150	30,000
96-well	0.3	100
48-well	1.0	250
24-well	2.0	500
12-well	4.0	1,000
6-well	10.0	2,000

2.2.4 Cryopreserving Cell Lines for Storage

All cell lines were prepared for cryopreservation in the same manner as sub-culturing, with the exception that they were re-suspended in freezing medium following centrifugation. For all cell lines, recommended cell concentrations for freezing was 1.5×10^6 cells/mL.

A specialized freezing medium is required in order to keep cells preserved for a long period of time in liquid nitrogen. Both NIH-3T3 and HaCaT cells were stored in a mixture of DMEM with 10% FBS and 10% v/v DMSO. GLI-Responsive NIH-3T3 cells were stored in a mixture of 90% FBS and 10% DMSO. In all instances freezing medium was thoroughly mixed with the cells in 2mL cryovials, and placed in a CoolCell Biocision cryopreservation container (Dutscher Scientific) and stored at -80°C overnight, before being transferred to liquid nitrogen.

2.2.5 Primary Cell Culture

2.2.5.1 BCC Cell Culture

BCC tissue was dissociated as previously described (Section 2.1.2), single cells resuspended, and either plated onto a feeder layer (50 Gy irradiated NIH-3T3 murine fibroblasts) in a tissue culture flask (T75) or cultured without irradiated 3T3s (depending on duration of culture) in keratinocyte serum free media (Gibco, UK) supplemented with 20ng/mL EGF (Peprotech), 10ng/mL FGF-basic (Peprotech), 25 $\mu\text{g}/\text{mL}$ of bovine pituitary extract (Gibco, UK), 25 units/mL of penicillin (Gibco, UK), 25 $\mu\text{g}/\text{mL}$ of streptomycin (Gibco, UK) and 10 $\mu\text{g}/\text{mL}$ of Amphotericin (Gibco, UK). If necessary, every three days, the media was replaced and the irradiated NIH-3T3 murine fibroblasts were replenished, and after 2 weeks BCC colonies could be visualized under an inverted microscope. BCC colonies were passaged following trypsinisation, onto a fresh irradiated NIH-3T3 murine fibroblast feeder layer or frozen down in cell freezing media and stored in liquid nitrogen (Section 2.2.4). BCC cells were then exposed to drugs for either 24 or 48 hours, before being processed for downstream applications.

2.3 Nucleic Acid Analysis

2.3.1 Gene Expression Analysis

During procedures involving RNA extraction and handling, care was taken to ensure that all plastic-ware (i.e. pipettes), glassware, and work surfaces were RNase-free by spraying them with RNaseZAP. Sterile RNA and DNA free filter tips were used to carry out all procedures involving RNA work.

2.3.2 RNA Extraction

2.3.2.1 BCC Tissue Samples

Extraction of total RNA from BCC tumour tissue was achieved firstly by removing the epidermis and any underlying dermis using a sterile scalpel under sterile conditions in a tissue culture hood. Samples were placed in screw-cap tubes containing 600 μ l of RLT buffer (approx. 20-30 mg of tissue) with 1.4 mm ceramic beads (Lysing matrix D tubes, MP Biomedical), and subsequently homogenized using Precellys24 homogeniser (Bertin Technologies) at 6,500 rpm for 2 \times 45-second cycles. To pellet the beads and any cellular debris, tubes were spun at 11,000 \times g for 5 min. Following homogenization RNA was isolated using the Qiagen RNeasy Plus Mini kit (Qiagen, UK) per manufacturers instructions (Section 2.3.2.4).

2.3.2.2 Cultured Cells

Firstly, adherent cell lines were trypsinised and pelleted at 300 \times g for 5 min to pellet the cells. Supernatant was removed and pellet re-suspended in 600 μ l of RLT buffer (per 1 \times 10⁶ cells) and disrupted by passing through a 23-gauge needle 8-10 times. Following homogenization RNA was isolated using the Qiagen RNeasy Plus Mini kit (Qiagen, UK) per manufacturers instructions (Section 2.3.2.4).

2.3.2.3 Homogenisation of Flow Sorted Cells

FACS was carried out as described in Section 2.4. Cell populations were sorted directly into 1.5 mL Eppendorff tubes containing, 350 μ L of RLT buffer if there were fewer than 50,000 cells present, or PBS with 20% BSA, if the number of cells was considerably larger (i.e. >50,000 cells). Cell populations sorted into PBS+20% BSA were subsequently centrifuged at 400 \times g for 5 min and re-suspended in 350 μ L of RLT Plus Buffer. Lysates were passed through a 23-gauge needle 8-10 times. Extraction of total RNA was achieved using the Qiagen RNeasy Micro Kit for <50,000 cells, or the Qiagen RNeasy Mini Kit for >50,000 cells (Section 2.3.2.5).

2.3.2.4 RNA Extraction

Lysates were transferred to a gDNA eliminator spin column together with a 2 mL collection tube and centrifuged for 30 s at 8,000 \times g. One volume of 70% ethanol was added to one volume of flow-through, and transferred to an RNeasy spin column and spun for 30 s at 8,000 \times g. Spin column membrane was then washed with 700 μ L of Buffer RW1 and spun for 30 s at 8,000 \times g, followed by two washes with 500 μ L of Buffer RPE with subsequent spins at 8,000 \times g for 30 s and 2 min, respectively. RNA was eluted by adding 50 μ L of RNase-free water, and centrifugation for 1 min at 8,000 \times g.

2.3.2.5 RNA Extraction from Flow Sorted Cells

RNA extraction from flow-sorted cells was undertaken using the Qiagen RNeasy Plus Micro Kit (Qiagen, UK). The protocol was similar to the Qiagen RNeasy Plus Mini Kit (above), with the exceptions that the final spin column membrane wash uses 500 μ L of 80% ethanol at 8,000 \times g for 2 min, and the RNA was eluted in a smaller volume of RNase-Free water, 14 μ L.

2.3.3 Determination of RNA Quality

The quality of the extracted RNA was assessed using the Agilent RNA 6000 Nano and Pico kits. The Nano kit assesses RNA quality quantitatively within the range of 25-500 ng/ μ L of total RNA (i.e. RNA from whole tissue or cell cultures), whereas the Pico kit

assesses RNA quality quantitatively within the range of 50-5,000 pg/ μ L, which was therefore chosen for samples with lower RNA concentrations (i.e. RNA from flow sorted samples). RNA concentration was determined using a NanoDrop 2000 (Thermo Scientific). Both Agilent Nano and Pico chips were run on the Agilent 2100 Bioanalyzer according to manufacturers guidelines. RNA integrity was assessed on the 28S to 18S rRNA ratio, and several other characteristics of the RNA electropherogram trace, to generate an RNA Integrity Number (RIN). RIN assigns an electropherogram a value of 1 to 10, with 10 being the least degraded.

2.3.4 Preparation of cDNA for Quantitative Analysis

cDNA synthesis was performed using the Quantitect Reverse Transcription Kit (Qiagen, UK) in 0.2ml PCR tubes as per manufacturers guidelines. cDNA synthesis reaction comprised two steps: 1) gDNA removal, and 2) reverse transcription (RT) reaction. Firstly, any contaminating gDNA was removed by adding 500ng of total RNA to 2 μ L of gDNA wipeout, and made up to a final volume of 14 μ L with RNase-free water, and incubated at 42°C for exactly 2 min in a thermocycler (Biorad). Then 1 μ L of reverse transcriptase, 1 μ L of primer mix, and 4 μ L of RT buffer was added to the 14 μ L of aforementioned solution, and incubated at 42°C for 15 min and then 95°C for 3 min.

2.3.5 Quantitative real-time PCR (qPCR)

For qPCR gene expression studies, all reactions were performed using the TaqMan assay. Pre-designed TaqMan primer/probes were obtained from Applied Biosystems. A number of conditions were considered when obtaining the primers. Primers were human specific, and did not cross react with mouse. Primers resided across exon boundaries to avoid amplification of gDNA. Gene symbols and primer accession IDs are specified in Table 2.4 below.

All reactions were run on the QuantStudio 7 Flex Real-Time PCR system (Applied Biosystems) supplemented with the QuantStudio software. All reactions were run in three technical triplicates. Housekeeping genes (usually GAPDH, beta actin) were used as a reference gene for each plate run. Reactions were run using the TaqMan Universal

Master Mix II, with UNG (Applied Biosystems) according to the manufacturers guidelines. qPCR reactions were assembled in 96- and 384-well plates to a final reaction volume of 15 μ L and 10 μ L, respectively. The amount of cDNA used was such that each well would contain 20 ng of RNA/cDNA. Reactions were run using the following conditions: 50°C for 2 min, 95°C for 10 min, followed by 40 cycles (95°C for 15 seconds, 60°C for 1 min).

2.3.5.1 Gene Expression Analysis of qPCR Data

Samples with reproducible cycle time (Ct) values were analysed using the $2\Delta\Delta C_t$ method. The ct value of the reference gene (i.e. GAPDH) from the same sample was used to calculate the ΔC_t values. Average ΔC_t values were calculated for all control samples and $\Delta\Delta C_t$ value was calculated for each individual sample in reference to the average control ΔC_t .

Table 2.4: Taqman Assay on Demand used for Taqman qPCR

Gene Symbol	Assays on demand reference	Dye
ACTB	Hs00357333_g1	FAM-MGB
ADAM19	Hs00958320_m1	FAM-MGB
ADRB2	Hs00240532_s1	FAM-MGB
ANGPTL4	Hs01101127_m1	FAM-MGB
ARHGEF18	Hs01547795_m1	FAM-MGB
ATF3	Hs00231069_m1	FAM-MGB
AURKA	Hs01582072_m1	FAM-MGB
BMP4	Hs03676628_s1	FAM-MGB
CDH1	Hs01023894_m1	FAM-MGB
CDH2	Hs00983056_m1	FAM-MGB
CDKN2A	Hs00923894_m1	FAM-MGB
CDKN2B	Hs00394703_m1	FAM-MGB
CEBPD	Hs00270931_s1	FAM-MGB
COL6A1	Hs01095585_m1	FAM-MGB
CTGF	Hs01026925_g1	FAM-MGB
DUSP6	Hs04329643_s1	FAM-MGB
DUSP7	Hs00997002_m1	FAM-MGB
EPHB2	Hs01031829_m1	FAM-MGB
ETS2	Hs00232009_m1	FAM-MGB
FSTL3	Hs00610505_m1	FAM-MGB
GAPDH	Hs02758991_g1	FAM-MGB
GLI1	Hs00171790_m1	FAM-MGB
GLI2	Hs01119974_m1	FAM-MGB
ID1	Hs03676575_s1	FAM-MGB
ID2	Hs04187239_m1	FAM-MGB
ID3	Hs00171409_m1	FAM-MGB
IL1B	Hs00174097_m1	FAM-MGB
ITGA5	Hs01547673_m1	FAM-MGB
ITGB6	Hs00982350_m1	FAM-MGB
JUN	Hs01103582_s1	FAM-MGB

JUNB	Hs00357891_s1	FAM-MGB
KLF10	Hs00921811_m1	FAM-MGB
LDLR	Hs01092524_m1	FAM-MGB
MAP3K4	Hs01104570_g1	FAM-MGB
MEIS2	Hs01035448_m1	FAM-MGB
MN1	Hs00159202_m1	FAM-MGB
MXI-1	Hs00365648_m1	FAM-MGB
MYC	Hs00905030_m1	FAM-MGB
NEDD9	Hs00610590_m1	FAM-MGB
PIM1	Hs01065498_m1	FAM-MGB
PLAU	Hs01547054_m1	FAM-MGB
PTCH1	Hs00970968_m1	FAM-MGB
PTGER4	Hs00964382_g1	FAM-MGB
RUNX1	Hs01021970_m1	FAM-MGB
RUNX2	Hs00231692_m1	FAM-MGB
SERPINE1	Hs01126606_m1	FAM-MGB
SKIL	Hs01045418_m1	FAM-MGB
SLUG	Hs00950344_m1	FAM-MGB
SMO	Hs01090242_m1	FAM-MGB
SMURF1	Hs00905769_m1	FAM-MGB
SMURF2	Hs00224203_m1	FAM-MGB
SNAIL	Hs00195591_m1	FAM-MGB
ST3JAL1	Hs00161688_m1	FAM-MGB
TAp63	Hs00978340_m1	FAM-MGB
TBX3	Hs01105635_g1	FAM-MGB
TGFB1	Hs00998133_m1	FAM-MGB
TGFB2	Hs00234244_m1	FAM-MGB
TGFB3	Hs01086000_m1	FAM-MGB
TWIST1	Hs01675818_s1	FAM-MGB
VDR	Hs00172113_m1	FAM-MGB
VEGFA	Hs00900054_m1	FAM-MGB
Vimentin	Hs00958111_m1	FAM-MGB

XIAP	Hs00745222_s1	FAM-MGB
ZEB1	Hs00232783_m1	FAM-MGB
ΔNp63	Hs00978337_m1	FAM-MGB

2.3.6 DNA Extraction

DNA isolation was performed using the DNeasy Blood & Tissue kit (Qiagen, UK) per manufacturers guidelines. Briefly, human BCC tissue was homogenized as described in section 2.3.2.1, with the exception that 180 μ L of Buffer ATL was used for tissue lysis instead of RLT Plus buffer as for RNA extraction. Following homogenization, lysate and any tissue was transferred to a fresh Eppendorff tube where 20 μ L of proteinase K solution was added, mixed thoroughly by vortex, and incubated at 56°C in a shaking hot block until the tissue was completely lysed (usually 10-16 hours). Tube was vortexed for 15 sec, and then 200 μ L of Buffer AL was added and mixed thoroughly, followed by 200 μ L of ethanol (96-100%) again mixing thoroughly by vortexing. Mixture was pipetted into DNeasy Mini spin column and centrifuged at 8,000 \times g for 1 min. Flow through was discarded and column membrane was washed by firstly adding 500 μ L of Buffer AW1, and centrifuging at 8,000 \times g for 1 min; secondly, 500 μ L Buffer AW2, and centrifuged at 20,000 \times g for 3 min to dry the membrane. Finally, DNA was eluted by adding 200 μ L of Buffer AE directly onto the column membrane, left to incubate at RT for 1 min, and centrifuged at 8,000 \times g for 1 min. DNA concentration was determined using NanoDrop 2000 (Thermo Fisher Scientific).

2.3.7 Microarray

2.3.7.1 RNA extraction

Homogenization of primary human BCC, SCC, and normal skin (NS) samples using the method described in section 2.3.2.1, RNA extracted as outlined in 2.3.2.4.

2.3.7.2 Determination of RNA quality

RNA concentration was performed in the same manner as outlined in section 2.3.3.

2.3.7.3 RNA amplification/cDNA library preparation

The standard approach for the preparation of RNA samples for array analysis is RNA amplification, which is what was used in this project. The Illumina TotalPrep RNA Amplification Kit is a complete system for generating biotinylated amplified RNA for hybridization with Illumina Sentrix arrays. Briefly, 500 ng of RNA/sample was brought up to 11 μL by addition of nuclease-free water, and 9 μL of Reverse Transcription Master Mix, then placed in a PCR hot block for 2 hr at 42°C. Then 80 μL of Second Strand Master Mix was added to each sample and incubated for a further 2 hr at 16°C. The next step was cDNA purification, which was achieved by adding 250 μL of cDNA Binding Buffer to each sample and passing the mixture through a cDNA filter cartridge, before finally washing with 500 μL of Wash buffer, and eluting the cDNA with 20 μL of nuclease free water (preheated to 55°C). The penultimate step in the process was the synthesis of cRNA, which was achieved by adding 7.5 μL of *in vitro* transcription master mix to each cDNA sample, incubating for 4-14 hr at 37°C, before adding 75 μL of nuclease free water to each sample to stop the reaction. Finally, the cRNA was purified by adding 350 μL of cRNA binding buffer to each sample, along with 250 μL of 100% ethanol, and pipetted to mix. The mixture was passed through a cRNA filter cartridge, and the flow through discarded. The filter contents were washed by passing 650 μL of wash buffer, before finally eluting the cRNA with 200 μL of 55°C nuclease free water to yield purified cRNA.

2.3.7.4 Applying samples to microarray chip

The chip used for the microarray was the Illumina HumanHT-12 v4 Expression BeadChip, which provided genome-wide transcriptional coverage of well-characterized human genes. 12 samples (6 BCC, 3 SCC, and 3 NS) were applied to the chip using the Direct Hybridization assay protocol. The first step in this process was the hybridization of the labelled cRNA generated earlier in section 2.3.7.3 on the BeadChip containing the

complementary gene specific sequence. We firstly preheated the cRNA sample tube at 65°C for 5 mins, vortex and briefly centrifuge tubes at 250xg. The sample was allowed to cool down to room temperature and the appropriate amount for each cRNA sample was added into each hybridization tube (750ng worth of cRNA for 12-sample chip), and made up to 5 µL using nuclease free water. Finally to each cRNA sample tube, 10 µL of HYB solution was added (15 µL total). Next 15 µL of sample was loaded onto the centre of each inlet port on the BeadChip, which was loaded into a Hyb chamber insert (full details of assembly can be found in the manufacturers guidelines), ensuring the barcode end of the chip was over the ridged part of the Hyb chamber. Finally, the BeadChip chamber lid was closed, locked, checked to ensure that the Hyb chamber was completely closed as any gap in the seal would result in evaporation during hybridization and therefore ruin the results. The Hyb chamber was placed into a 58°C Illumina Hybridization Oven on a rocker at speed 5 and incubated for at least 14hr (but no more than 20hr). In preparation for the next day, preheated 500 mL of 1x High-Temp Wash Buffer (made from 10x stock with nuclease free water) to 55°C using the Hybex water bath.

Following incubation in the Hyb Chamber the next step was to wash the BeadChip. Firstly, the wash E1BC solution was made by adding 6 mL E1BC buffer to 2 mL nuclease free water. Next the Hyb Chamber was removed from the oven, disassembled, and BeadChip removed before being submerged face down in a beaker containing 1 L of the E1BC solution. Once submerged the cover seal on each BeadChip was removed, while ensuring the Chip remained submerged, so as to ensure it didn't dry out. Then using tweezers the BeadChip was transferred to a slide rack and submerged in a staining dish containing 250 mL wash E1BC solution. Then using the slide rack handle, the rack containing the BeadChips was transferred to the water bath containing High-Temp wash buffer (prepared the previous day) and incubated for 10 min. After incubation the slide rack was transferred back into a staining dish containing 250 mL of fresh Wash E1BC Buffer, and using the slide rack handle the rack was plunged in and out of the solution 5-10 times. The staining dish containing the slide rack was placed back onto an orbital shaker and allowed to shake at room temperature for 5 min, before being transferred to a new staining dish containing 250 mL fresh 100% ethanol where it was plunged in

and out of the solution 5-10 times, before finally being placed back onto the orbital shaker at room temperature for 10 min. The final wash involved a second incubation in fresh 250 mL of wash E1BC buffer using the same methods deployed in the first wash.

Following incubation in the wash E1BC buffer the BeadChip was blocked as follows. The BeadChip was washed in a tray on the rocker mixer, before 4 mL Block E1 buffer was added to the wash tray. Then using tweezers the BeadChip was transferred face up from the rack in the staining dish into the wash tray containing blocking buffer. The wash tray was gently tilted to ensure the block solution was covering the entire chip, then placed back onto the rocker platform and allowed to rock for 10 min.

The final stage before scanning the BeadChip was detection of the signal, which was achieved as follows. This process involved the addition of Cy3-SA to bind to the analytical probes that were hybridized to the BeadChip, which allowed for differential detection of signals when the BeadChip was scanned. Firstly Cy3-Streptavidin was removed from the freezer and allowed to acclimatize to room temperature for 10 min. Once acclimatized 2 mL Block E1 Buffer was prepared with a 1:1,000 dilution of Cy3-Streptavidin for each BeadChip, and 2 mL of the prepared buffer was added into a fresh wash tray. Using tweezers, the BeadChip was transferred into the wash tray containing the Block solution, and again gently tilted until the buffer was entirely covering the chip, before covering the wash tray with the flat lid provided so that it was not exposed to the light. The tray was placed on the rocker mixer and incubated at room temperature for 10 min. After the incubation the BeadChip was inserted into a slide rack and placed into a staining dish containing fresh 250 mL Wash E1BC buffer, before washing the slide in the same manner as the previous two Wash E1BC buffer steps. After incubation, the BeadChip was dried by placing it in a centrifuge and spinning at 1,400 rpm for 4 min at room temperature. After the centrifuge was complete, the dried BeadChip was stored in a dark environment until ready to be scanned.

The last step in the process was to image the BeadChip on the iScan system. The steps involved in scanning the BeadChip can be found on the Illumina website.

2.3.7.6 Bioinformatics analysis of the data

The resulting data were analysed using the Bioconductor packages in the R statistical program for data processing for all the subsequent steps. For analysing Illumina microarray data, the ‘Lumi’ package was used for assessing quality control of the samples, and remove outliers, before transforming the data using variance stabilizing transformation (vst), and normalizing using the conditional quantile normalization method. Finally, genes were annotated and mapped at the probe level using ‘lumiHumanAll.db’ and ‘luminHumanIDMapping’ programs respectively. We then filtered out the genes/probes whose expression was absent between the samples. Next we performed comparisons between the tumour groups and the normal group by using the Limma program again in the Bioconductor package to calculate the level of gene differential expression. Briefly, to estimate the fold changes and standard errors, a linear model was fitted for each gene using ‘lmFit’ and the empirical Bayes smoothing was applied to the standard errors using ‘eBayes’, before finally showing the statistics for the top genes using ‘topTable’ (e.g. tumour vs normal). We obtained a list of differentially expressed genes (DEGs) at a p value < 0.05. Following this, we used the expression values of DEGs to perform pathway analysis using NIH DAVID Tools (NCBI), and Gene Set Enrichment Analysis (GSEA; Broad Institute) by exporting our DEGs in a format accepted by GSEA software.

2.4 Cell Based Functional Assays

Table 2.5 outlines the drugs that were used in our functional assays

Table 2.5: Drugs used in functional assays

Drug	Stock (mM)	Cat. #	Source	Solvent
GANT-61	10	S8075	Selleckchem	Ethanol
Vismodegib	25	S1082	Selleckchem	DMSO
Sonidegib	50	S2151	Selleckchem	DMSO
SB431542	50	S1067	Selleckchem	DMSO
Etoposide	10	S1225	Selleckchem	DMSO

2.4.1 Cell Viability

2.4.1.1 Cell Titer Glo

The Cell Titer Glo assay (Promega, Southampton, UK) is used to determine the number of viable cells in culture based on the quantitation of the ATP present, which is an indicator of metabolically active cells. Cultured cells were seeded into white-sided 96 well flat-bottomed plates (Greiner Bio One), and allowed to adhere overnight. Once adhered, cultures were exposed to a variety of treatment conditions for 24 or 48 hr before performing the experiment to assess the impact of these agents on cell viability. Experiment was performed by adding the single reagent (Cell Titer-Glo Reagent) directly to the cells cultured in media supplemented with serum in a 1:1 ratio (100 μ L reagent to 100 μ L media) and plate was placed on an orbital shaker for 2 min in order to lyse the cells, before being placed in a dark environment for 20 min at room temperature in order for the signal to stabilise. The Cell Titer-Glo reagent contains lysing reagents, which lyse the cells, and the enzyme Ultra-Glo rLuciferase, which requires ATP from the lysed cells to convert luciferin into oxyluciferin, to subsequently generate the luminescent output. Following incubation the luminescent signal produced was measured using the CLARIOstar plate reader (BMG Labtech) by setting the excitation/emission wavelengths to 560/590 nm.

2.4.2 Tumoursphere Forming Assay

The tumoursphere-forming assay is a functional assay that is designed to isolate SCs from a bulk population of cells by exploiting their capacity to resist anoikis. Cell lines initially grown in 2D adherent culture are trypsinised and plated into non-adherent culture conditions, which has the capacity to induce anoikis in the bulk tumour cell population and since the SCs are resistant to anoikis they remain. The remaining cells then self renew and form small colonies of cells termed tumourspheres. Furthermore, these tumourspheres once formed can be dissociated into single cells and replated or passaged for a second time in the same culture conditions, a process which assays for the ability of these cells to self renew, and therefore whilst primary tumoursphere

formation is a measure of both SC and early progenitor cell activity, secondary tumoursphere formation allows their self renewal to be quantified, which is a key property of CSCs. Therefore quantifying tumoursphere number is indicative of SC number. Tumoursphere assays were carried out in non-adherent culture conditions using a serum free epithelial growth medium (MEM, Gibco) supplemented with 1xN-2 (Invitrogen), 1xB27 (Invitrogen), 20ng/mL FGF (Peprotech), and 20 ng/mL EGF (Peprotech) and 1% Penicillin/Streptomycin (Gibco). Depending on the experiment performed, tumoursphere experiments were conducted following a 24 hr or 48 hr treatment in adherent culture (MEM with 10% FBS, 2 mM L-Glutamine and 1% Penicillin/Streptomycin). Cells were trypsinised and plated in ultra-low attachment 96-well plates (Costar, Corning) at a seeding density of 5,000 cells/mL. After 7 days in non-adherent culture conditions, tumourspheres were counted, then collected by centrifugation (300 x g for 5 min at room temperature), and dissociated in 0.05% trypsin with 0.25% EDTA and subsequently counted and re-seeded at the same density of 5,000 cells/mL. Cells were left to form tumourspheres for another 7 days and again counted for each condition.

2.4.3 Colony Forming Assay

The colony-forming assay assesses the ability of individual cells to survive, proliferate, and expand to form small colonies (Locke *et al.*, 2005). Cells were seeded at a low density of 300 cells/well in a 12-well plate, allowed to adhere overnight and then subsequently drugged (ensuring drugging occurs before cells begin to divide) and left for 7 days in normal growth media to allow colonies to form. Colonies were quantified by removing the media, washing with PBS and subsequently staining with a crystal violet/ethanol solution for 15-30 min on a rocker at room temperature, before finally washing off solution by gently running the plates under tap water. Plates were allowed to dry and colonies containing 32 or more cells were enumerated either manually or automatically using a GelCount plate reader (Oxford Optronix) to detect colonies (Shaw *et al.*, 2012).

2.4.4 siRNA transfection

Short interfering RNA (siRNA) was transfected in our cell lines to transiently knock-down the transcription factor, co-SMAD4 (ON-Target plus SMART pool, GE Dharmacon, Bucks, UK; #L-003902-00). SMAD4 is required by the other SMADs for nuclear translocation and subsequent activation of downstream target genes following TGF β signalling pathway activation. In all siRNA experiments an irrelevant scrambled control was also used (ON-Target plus SMART pool, GE Dharmacon, Bucks, UK; #D-001810-10-05). Each siRNA pool was re-suspended according to the manufacturer's guidelines. Transfection was conducted by firstly diluting stock siRNA in Opti-MEM (Gibco) to achieve a final concentration, which was cell line dependent, and was left to incubate for 5 min at room temperature. Finally, the transfection reagent, Lipofectamine 3000 (Invitrogen) was added to the siRNA/Media mix and left to incubate for a further 5 min at room temperature before being diluted in a well containing cells and standard culture media (with serum). The typical reagent concentrations used for different plate formats can be found in Table 2.6 below.

Table 2.6: Concentrations used in siRNA knock down experiments

Plate Format	Volume of Media/Well	Volume of Opti-MEM (μL)	Volume of siRNA (μL)	Volume of Lipofectamine	Final Volume of Media/Well
96-Well	87.5 μL	12.125	0.125	0.25	100 μL
48-Well	218.75 μL	30.3125	0.3125	0.625	250 μL
24-Well	437.5 μL	60.625	0.625	1.25	500 μL
12-Well	875 μL	121.25	1.25	2.5	1,000 μL
6-Well	1,750 μL	242.5	2.5	5.0	2,000 μL

2.4.5 Flow Cytometry and Cell Sorting

All antibody incubations were carried out for 30 min at 4°C. All centrifugations were performed at 400 × g for 5 min at 4°C. For routine cell sorting, human BCC tissue was dissociated as described (Section 2.1.2), and subsequent cell suspensions at 10⁶ cells/ml were stained with anti-CD200-BV421, anti-CD45-FITC, and the live-dead stain, 7AAD (Table 2.7). Cells were sorted at low pressure (20 psi) using a 100 µm nozzle on a FACSAria (Becton Dickinson, Oxford, UK). Cells were sorted into 1.5 mL Eppendorf tubes maintained at 4°C. Single stained samples were used as compensation controls. Samples were gated on the basis of forward- and side-scatter. Doublets, dead cells, and pan-leukocytes (CD45+) were excluded.

Table 2.7: Antibodies/Stains used in FACS experiments

Antibody	Dilution	Cat. #	Source
CD200 (BV421/DAPI)	1:1000	564114	BD Pharmingen
CD45 (FITC)	1:1000	341071	BD Pharmingen
EpCAM (APC)	1:1000	347200	BD Pharmingen
Annexin V (APC/647)	1:1000	A23204	ThermoFisher
7-AAD	5µL/1x10 ⁶ cells	559925	BD Pharmingen
DAPI	1µL/1x10 ⁵ cells		

2.4.6 Annexin V apoptosis assay

The Annexin V apoptosis assay was used to determine the proportion of cells undergoing early or late apoptosis following drug treatment, by detecting/studying the externalization of phosphatidylserine, one of the earliest indicators of apoptosis. On the day of analysis, media containing dead cells was removed from cultured cells and kept, cells were washed with PBS, trypsinised and trypsin inactivated using the media that was stripped off the well earlier. Cells were pelleted, supernatant was removed, and each sample/condition was resuspended in 100 µL of 1xAnnexin V Binding Buffer (Biolegend) and 1 µL of Annexin V, Alexa Fluor 647 conjugate (ThermoFisher Scientific) was added to the suspension and incubated for 20 min at room temperature in a dark environment. 100 µL of Annexin V buffer was used for every 100,000 cells, and volumes

were scaled up according to cell number. Following incubation, a further 400 μL of Annexin V binding buffer was added to each sample to inactivate the reaction. Just before each sample was analysed, 1 μL of DAPI (20 $\mu\text{g}/\text{mL}$) was added. Samples/cells were analysed using a BD LSRFortessa flow cytometer (BD Biosciences), and were gated by first selecting the cell population using FSC-area/SSC-area, and then by obtaining a single cell population by removing doublets using FSC-area/FSC-height, before finally gating this single cell population based on the intensity of the far-red APC dye conjugated to Annexin V, and DAPI to identify cells that are either early or late apoptotic, and live or dead. Data was processed using FlowJo analysis software (Figure 2.1).

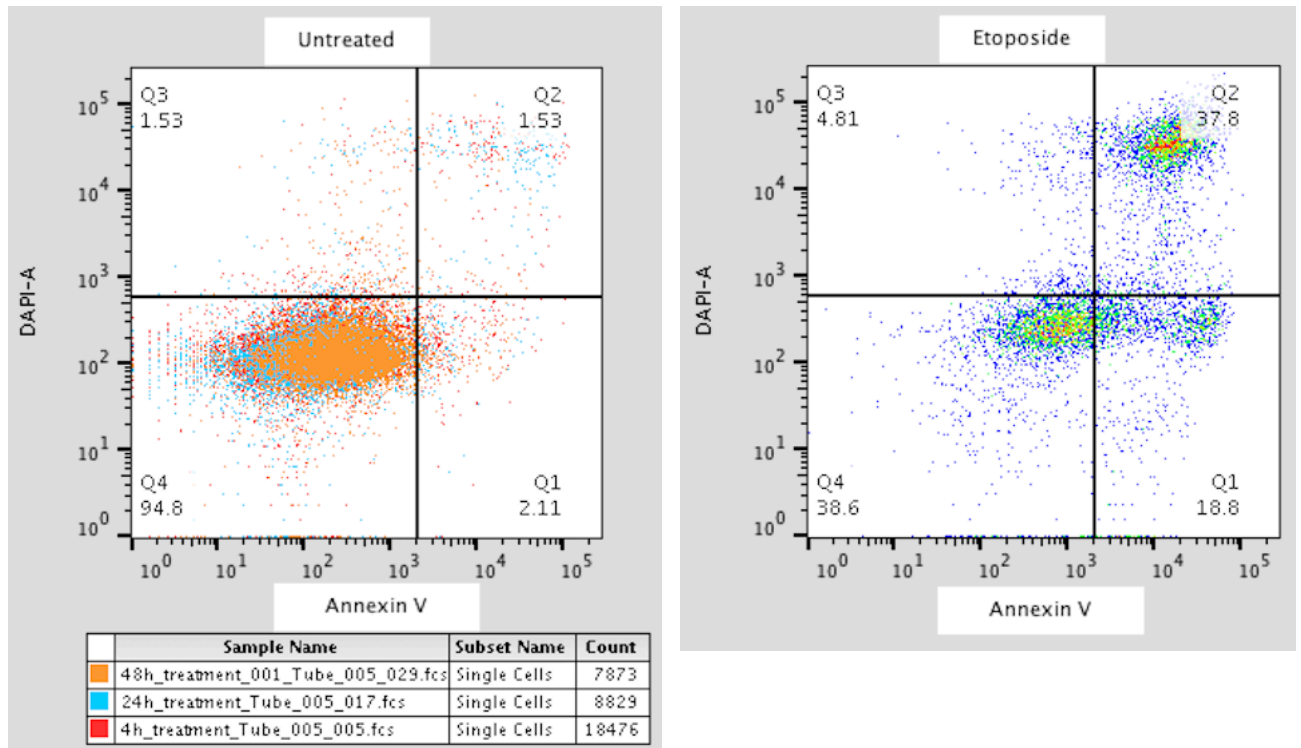


Figure 2.1: Representative flow cytometry dot plot generated for Annexin V apoptosis assay

Flow cytometry dot plot depicts: Q1) cells entering early apoptosis, Q2) cells entering late apoptosis, Q3) cells that have necrosed/died, and Q4) cells that are viable. Left dot plot shows untreated cells, whereas the right dot plot shows the etoposide treated cells (+ve).

2.4.7 GLI Reporter Experiments

2.4.7.1 Functional Validation and Luciferase Assay Performance

The following assays were carried out in white clear-bottom 96-well microplates (Sigma Aldrich, UK). Dose response of GLI Reporter NIH-3T3 cells to mouse Sonic Hedgehog (mSHh) was performed by seeding 40,000 cells per well in 100 μ L of DMEM +10% FBS, without Geneticin. Each treatment was set up in triplicate. Cells were plated and incubated at 37°C (5% CO₂) for 24 hours. Cells were incubated at 37°C (5% CO₂) for 16-20 hours, or until cells reached confluence. Once confluent, the growth media was carefully removed using a pipette (not an aspirator) so as not to disrupt the, monolayer. 50 μ L of three-fold serial dilution of mSHh in assay medium was added to stimulated wells, and 50 μ L of assay medium without mSHh was added to untreated (control) wells and cell-free (control) wells (for determining background luminescence). The Luciferase assay was performed by adding 50 μ L of ONE-Step Luciferase reagent to the assay media per well, and then gently rocked for 20-30 min at RT. Following incubation luminescence was measured using the CLARIOstar High Performance Monochromator Multimode Microplate Reader (BMG LABTECH).

Values were obtained by subtracting the average background luminescence from the average obtained for each treatment. Raw luminescence values were then plotted against logged mSHh dose ranges.

Inhibition of mSHh-induced reporter activity by inhibitors of Hh signalling pathway was determined by first seeding cells as previously described. Stock solutions of Hh pathway inhibitors, vismodegib (Selleckchem), cyclopamine (Selleckchem), sonidegib, (Selleckchem) and GANT-61 (Selleckchem) were prepared in DMSO and diluted in assay medium. 45 μ L of diluted inhibitor in assay medium was added per well, along with 45 μ L of assay medium with the same concentration of DMSO but without inhibitor, and 45 μ L of assay medium with DMSO to cell-free wells. Plate was incubated at 37°C (5% CO₂) for 1-2 hours. 5 μ L of diluted mSHh in assay medium was added to the stimulated wells

(final [mSHh]= 3.3 μ g/mL), along with 5 μ L of assay medium to untreated control wells (determining basal activity), and cell-free control wells. Each treatment was set up in triplicate. Plate was incubated at 37°C (5% CO₂) for 24 hours, and luciferase assay performed as described above. Luminescence was measured using the CLARIOstar High Performance Monochromator Multimode Microplate Reader (BMG LABTECH).

Values were obtained by subtracting the average background luminescence from the average obtained for each treatment. The results are shown as a percentage of luminescence. The background-subtracted luminescence of cells stimulated with mSHh in the absence of Hh inhibitors was set at 100%.

2.5 Tissue Analysis

2.5.1 Immunofluorescence on Frozen Tissue Sections

Indirect immunofluorescence was performed, where a primary antibody binds specifically to tissue antigens and the secondary antibody is labelled with a fluorochrome, which binds to the primary antibody for visualization. Cryostat tissue sections were removed from storage, allowed to air-dry for 15 min, and circled with a hydrophobic marker pen (ImmuneEdge, VectorLabs). Tissue was fixed by incubating with 4% PFA for 15 min. Tissue was permeabilised using TBS with 0.5% TritonX-100 (Sigma Aldrich) for 10 min. To prevent non-specific binding of primary antibodies, all tissue epitopes were blocked by using TBS with 10% donkey serum (DS) and 0.1% Triton X-100, and incubating for 1 hour at RT. Slides were washed with TBS three times for 5 min each wash. The equivalent of 1 μ g of primary antibody protein in TBS with 10% DS and 0.05% Triton X-100 was added to each tissue section over night at 4°C, then the slides were washed with TBS four times for 5 min each wash. Tissue sections were then incubated with species-specific conjugated fluorochrome antibodies used as per manufacturer's instructions together with 5 μ L of the nuclear stain, DAPI (1mg/mL), in the dark for 45 min at RT. Finally slides were washed with TBS three times for 5 min each wash, before being mounted with coverslips using fluorosave aqueous mounting media. Slides were stored at 4°C and then examined using a Leica DMI6000B Inverted fluorescent microscope (Leica Biosystems, England).

2.5.2 Immunofluorescent antibody labelling of Cultured Cells

Glass coverslips were first sterilized with 100% ethanol; air dried, and placed into the wells of a 6-well culture plate, before cells were seeded into the plate at a density of 100,000 cells/mL and allowed to adhere overnight. With the exception of primary and secondary antibody incubations, all steps were carried out with the coverslips still in the culture plate. On the day of analysis, cells were washed with PBS, and fixed with 4% PFA for 10 min, and then washed 3x5min in PBS. Cells were then permeabilised with 0.25% Tween-20 (Sigma) in PBS, and then blocked with 3% BSA in PBS for 1 hr at room temperature. Coverslips were then placed on parafilm and incubated with primary antibody (Table 2.8) in 3% BSA in PBS and incubated overnight at 4°C. Following incubation, coverslips were placed back into a 6-well culture plate and washed 3x5min with PBS, and then subsequently incubated with fluorescence-conjugated secondary antibody (Invitrogen, Table 2.9) diluted 1:400 in PBS containing DAPI nuclear stain (1:1000) for 1 hr at room temperature. Coverslips were then washed 3x5min in PBS and mounted in Vectashield mounting solution (Vector Labs). Cells were visualized and pictures acquired on a Leica confocal microscope.

Table 2.8: Primary antibodies used in immunofluorescence experiments

Antibody	Dilution	Species	Cat	Source
pSMAD3	1:100	Rabbit	ab52903	Abcam
Total p63	1:500	Mouse	ab735	Abcam
ΔNp63	1:500	Mouse	619002	BioLegend
K14	1:500	Chicken	906001	Biolegend
Alpha-Tubulin	1:100	Mouse	T6074	Sigma
Phalloidin-488	1:100	N/A	A12379	ThermoFisher

Table 2.9: Secondary antibodies used in immunofluorescence experiments

Secondary Antibody	Fluorochrome (nm)	Dilution	Source
Dk α-Rb (H&L)	488	1:400	ThermoFisher
Gt α-Ms (H&L)	568	1:400	ThermoFisher
Gt α-Ck (H&L)	647	1:400	ThermoFisher

2.6 Protein analysis

2.6.1 Protein Extraction

2.6.1.1 Total Cellular Proteins

Cells in culture were trypsinised, centrifuged for 5 min at 1,400 rpm and the resulting pellet was washed with PBS, and again pelleted. PBS was removed and resuspended in 100 μ L of RIPA buffer containing complete protease inhibitors (1 tablet/5 mL RIPA buffer; Roche). Samples were passed through a 23-gauge needle in a 1 mL syringe 6-8 times before being placed into a 1.5 mL microcentrifuge tube and incubated on ice for 30min. Following incubation samples were centrifuged at 13,000 rpm for 10 min at 4°C, and the supernatant collected and placed into a fresh microcentrifuge tube and stored at -80°C. Composition of RIPA buffer can be found in table 2.10.

2.6.1.2 Nuclear and Cytoplasmic Extracts

Cells in culture were trypsinised, centrifuged for 5 min at 1,400 rpm and the resulting pellet was washed with PBS, and again pelleted. PBS was removed and re-suspended in 200 μ L of NEBA containing complete protease inhibitors (Roche), and transferred to 1.5mL microcentrifuge tubes. Resuspension was performed by gently pipetting up and down, before placing on ice for 15 min. Following incubation 25 μ L of 10% NP-40 was

added to the samples and vortexed vigorously for 30 seconds, before being centrifuged at 10,000 rpm for 30 seconds, with the resultant supernatant (cytoplasmic proteins) transferred to a fresh microcentrifuge tube. The next step was to remove any additional contaminating cytoplasmic proteins from the pellet (nuclear proteins), which was achieved by adding 200 μ L of NEBA to the pellet (being careful not to disturb the pellet too much) and then centrifuging again at 10,000 rpm for 30 secs. The supernatant was removed and discarded, and NEBC buffer containing complete protease inhibitors was added to the resultant pellet and subsequently vortexed for 30 seconds and placed on ice for a further 30 min. Following incubation, samples were centrifuged at 13,000 rpm for 5 min at 4°C and the supernatant (nuclear proteins) transferred to a fresh tube before being stored at -80°C (Compositions of NEBA and NEBC buffer can be found in table 2.10).

Table 2.10: Buffers used for protein extractions

RIPA Buffer	NEBA	NEBC
<ul style="list-style-type: none"> • 5 mL 1M Tris pH7.4 • 10 mL 10% Nonidet-P40 (Sigma) • 0.25 g Sodium Deoxycholate • 3 mL 5M NaCl • 0.4 mL 0.25M EGTA • Made up to 100 mL with H₂O and to pH 7.4 	<ul style="list-style-type: none"> • 10mM HEPES pH7.9 • 10mM KCl • 0.1mM EDTA pH8.0 • 0.1mM EGTA pH8.0 	<ul style="list-style-type: none"> • 10% glycerol • 20mM HEPES pH7.9 • 0.4M NaCl • 1mM EDTA pH8.0 • 1mM EGTA pH8.0

2.6.2 Quantifying protein concentration

2.6.2.1 BCA

The BCA assay kit (Pierce, ThermoFisher Scientific) was used to determine protein concentrations of total proteins or cytoplasmic extracts. BCA assay was set up in a 96-well clear flat bottomed plate with each sample run in duplicate for accuracy. 5 μ L of sample or BSA standard was added to 25 μ L BCA reagent (BCA reagent was made using 50 parts of BCA reagent A to 1 part of BCA reagent B) and incubated at 37°C for 30 min then kept at 4°C. Standards of 25, 125, 250, 500, 750, 1000, 1500, 2000 μ g of BSA per mL were diluted in RIPA or NEBA buffer to produce a standard curve from which sample protein concentration could be extrapolated. Following incubation, protein concentrations were determined by running the plate on a CLARIOstar plate reader, and software used to determine protein concentration.

2.6.2.2 Bradford

The Bradford assay reagent was used to determine the protein concentrations of cytoplasmic and nuclear protein extracts. Again, the assay was carried out in a 96-well plate. 10 μ L of sample or BSA standard was added to 290 μ L Bradford assay reagent and incubated at room temperature for 5-10 min. Standards of 1.25, 2.5, 5 and 10 mg/mL BSA (Sigma) in NEBC buffer were used to produce a standard curve from which the protein concentration could be extrapolated. Again following incubation, protein concentrations were determined by running the plate on a CLARIOstar plate reader, and software used to determine protein concentration.

2.6.3 Western Blotting

Table 2.11 outlines the solutions prepared for use during Western blotting.

Table 2.11: Buffers used in Western Blotting

Solution	Composition
4x Laemmli (Loading) Buffer	60 mM Tris-Cl pH 6.8, 2% SDS, 10% glycerol, 5% β -mercaptoethanol, 0.01% bromophenol blue
TBST	1xPBS solution: 5 tablets 500 mL dH ₂ O with 0.5 mL Tween (Sigma)
Resolving Gel Buffer	Made using TGX™ FastCast™ Acrylimide Kit, 7.5% #161-0171
Stacking Gel Buffer	Made using TGX™ FastCast™ Acrylimide Kit, 7.5% #161-0171
1x SDS-PAGE Running Buffer	3.62 g Trizma (Sigma), 14.4 g Glycine (Sigma) pH6.8 and add H ₂ O up to 1 L
Trans-Blot Turbo Transfer Buffer	Add 200 mL 5x Trans-Blot Turbo Transfer Buffer to 800 mL of dH ₂ O
Blocking Buffer	5% w/v non-fat dry milk powder (Marvel): 0.75 g in 15 mL TBST 5% w/v BSA powder (Sigma): 0.75 g BSA in 15 mL TBST
Antibody Dilution Buffer	5% w/v non-fat dry milk powder (Marvel): 0.1 g in 2 mL TBST 5% w/v BSA powder (Sigma): 0.1 g BSA in 2 mL TBST
Stripping Buffer	62.5 mM Tris-HCl (pH6.8, 2% w/v SDS, 100 mM 2- β -mercaptoethanol

2.6.3.1 Sample Preparation

Samples were diluted in the correct protein extraction buffer (RIPA, NEBA, or NEBC) plus 1x Laemmli buffer at a concentration no less than 1 $\mu\text{g}/\mu\text{L}$, and subsequently heated to 95°C for 5 min and used immediately.

2.6.3.2 SDS-PAGE

To prepare the resolving gel, 30 μL 10% APS (Sigma) plus 3 μL TEMED (Sigma) were added to the resolving gel buffer (3 mL Resolver A and 3mL Resolver B) and immediately poured. dH_2O was immediately added on top of the stacking solution to ensure that the gel front was even. The resolving gel was allowed to set for 15-20 min at room temperature. While the resolver gel was setting, the stacking gel was prepared by adding 10 μL 10% APS and 2 μL TEMED to the stacking solution (1 mL Stacker A and 1mL Stacker B), and immediately poured on top of the resolving gel once the dH_2O had been poured off. Finally, combs were inserted into the top of the gel and allowed to set for 15-20 min more. Once set, the gels were placed into the electrophoresis gasket, which itself was placed into a gel running tank (BioRad), and the centre of the gasket was filled to the top with SDS running buffer, while the outer compartment of the tank was filled with the same buffer to a depth of 3-4 cm. The plastic comb was then removed from the gel and 20-30 μL of prepared samples were loaded into the wells in addition to a molecular weight marker (PageRuler, ThermoFisher). Once the samples were loaded, the electrophoresis tank was connected to a power pack and gels were run at 300 V for 20-30 min or until desired marker separation was achieved.

2.6.3.3 Western Transfer to Membrane

The Trans-Blot Buffer was prepared by mixing 200 mL of 5X Trans-Blot Turbo Buffer with 200 mL of 100% ethanol and 600 mL of dH_2O . The transfer stacks were wet and equilibrated by immersing in 1x Trans-Blot Turbo Buffer for 2-3 min. For the PVDF membrane, we firstly immersed in 100% methanol for 2-3min until the membrane was translucent, and then transferred to 1x Trans-Blot Turbo Buffer for 2-3 min before allowing to equilibrate for 2-3 min. Western blot transfer was achieved using the Trans-

Blot Turbo RTA Mini PVDF Transfer Kit using the Trans-Blot Turbo Blotting System. Briefly, the ion reservoir stack with the membrane (anode stack) was laid in the centre of the cassette base, ensuring that the stack was not overlapping the green rubber moulding in the base. The PVDF transfer membrane was placed directly onto the ion reservoir stack, and the gel was carefully aligned on top of the PVDF membrane. The second ion reservoir stack (cathode stack) was then placed on top of the gel, and the blot roller used to remove any air bubbles in the assembled transfer pack. Once the gel stack was placed in the cassette base, the cassette lid was placed on the base and locked. The cassette was slid into the Trans-Blot Turbo instrument bay until a hear click could be heard, and then the transfer protocol was run (refer to manufacturers guidelines).

2.6.3.4 Confirming Protein Transfer

Once membrane transfer was complete, we examined protein transfer by washing the PVDF membrane for 5 min in TBST, and then rinsing under tap water. Ponceau red solution was poured on top of the membrane and allowed to incubate for 2 min in the ponceau until bands (protein binding) began to appear on the membrane. To keep a record of the protein transfer and loading, the membrane was placed between two acetate sheets and photocopied. The membrane was then washed 3x5 min in TBST before blocking.

2.6.3.5 Blocking and Antibody Incubation

Following the confirmation of protein transfer, PVDF membrane was incubated in blocking buffer for 1 hr at room temperature with shaking. Following incubation, the membrane was then transferred to a 30 mL universal tubes (Fisher) containing 4-5 mL of the desired primary antibody diluted in 5% BSA or Milk (depending on the antibody used; Table 2.12) in TBST, and incubated overnight at 4°C on a roller.

2.6.3.6 Detection

Following overnight incubation, the membrane was washed 3x5 min in TBST (all washes were performed in a universal tube) and 4-5 mL of appropriate (Table 2.13) horseradish peroxidase (HRP)-conjugated secondary antibody (Abcam) diluted 1:2000 in 5% Milk in TBST. Membranes were incubated in the secondary antibody for 1 hr at room temperature on the roller, before being washed 3x5 min in TBST. Following washes antibody binding was detected by incubating Illumina Forte chemiluminescence reagent (Millipore) on the membrane for 30-60 seconds (less for endogenous controls) and membrane transferred to the ChemiDoc MP Imaging System (BioRad) and chemiluminescence was detected and imaged.

2.6.3.7 Stripping and Re-probing the Membrane

Membrane was placed in a 30 mL universal tube and incubated in the presence of stripping buffer (ThermoFisher) at RT for 10-15 min on a roller. Membrane was washed 3x5 min in TBST on a roller. The membrane was then blocked and again re-probed with primary antibody as described before.

2.6.3.8 Quantitation by Densitometry

To quantitate Western blotting data by densitometry, the ImageLab software (BioRad) was used. The pixel density over the selected areas was quantified and compared.

Table 2.12: Primary antibodies used for Western Blotting

Antibody	Dilution	Diluted in	Source	Cat #	Species	Target Si
pSMAD3 (mAb)	1:500	10% BSA	Cell Signalling	9520	Rabbit	55 kDa
Total SMAD3 (mAb)	1:500	10% BSA	Cell Signalling	9523	Rabbit	55 kDa
PARP	1:1000	10% Non-fat milk	Cell Signalling	9532	Rabbit	110 kDa
ΔNp63	1:500	10% Non-fat milk	Biolegend	619002	Rabbit	70 kDa
Alpha-Tubulin	1:1000	10% Non-fat milk	Sigma	T6074	Mouse	55 kDa
Acetylated Alpha-Tubulin	1:1000	10% Non-fat milk	Sigma	T6793	Mouse	55 kDa
GAPDH	1:5000	10% Non-fat milk	Millipore	MAB374	Mouse	35 kDa
LAMIN A/C	1:1000	10% Non-fat milk	Cell Signalling	2032	Rabbit	65-70 kDa

Table 2.13: Secondary antibodies used for Western Blotting

Secondary Antibody	Dilution	Source	Cat #
Goat pAb to Rb IgG (HRP)	1:2000	Abcam	ab97051
Goat pAb to Ms IgG1 (HRP)	1:2000	Abcam	ab98693
Goat pAb to Ms IgG2a (HRP)	1:2000	Abcam	ab97245

2.7 Statistical analysis

Error bars on graphs represent standard error values. In the vast majority of cases, an unpaired student's T-test was used to establish if there was statistical significance between experimentally treated samples and control samples. All tests assumed unequal variance and in most cases were carried out on data sets with samples sizes of $n=3$ unless otherwise stated. Tests were carried out using Microsoft Excel 2010 software and Graphpad Prism software, and results were taken to be significant if the calculated p value was equal to or less than 0.05.

Chapter 3: Determination of TGF β Signalling in Human Basal Cell Carcinoma

Chapter 3 Determination of TGF β Signalling in Human Basal Cell Carcinoma

3.1 Introduction

One quarter of all cancers exhibit activation of the hedgehog growth factor pathway to drive tumour growth, including: breast, pancreas, gastrointestinal, prostate, haematological, and neural malignancies. The archetypal cancer for Hh signalling is BCC, with activating mutations found in nearly 100% of tumours studied. As a consequence of this, a number of hedgehog pathway inhibitors are currently in clinical trials for a variety of these malignancies, and in 2012 the drug vismodegib became the first Hh signalling pathway targeting agent to gain U.S. Food and Drug Administration (FDA) approval for the treatment of inoperable and metastatic BCC. However, clinical studies already suggest that a BCC sub-population is resistant to vismodegib (Von Hoff *et al.*, 2009; Metcalfe & de Sauvage, 2011; Skvara *et al.*, 2011; Sekulic *et al.*, 2012), with growing numbers of case reports showing an initial regression of BCC after vismodegib treatment, followed by an inevitable relapse of the tumour, or even progression of the tumour into a more malignant phenotype (Hausauer *et al.*, 2013). Studies have now demonstrated resistance towards these growth factor inhibitors. Research from our lab, has shown that vismodegib was ineffective against the treatment of primary human BCC cells in an *in vitro* SC assay (Colmont *et al.*, 2013).

Therefore this raises the question as to how these tumours are capable of resisting such therapies. One essential factor that has long been contributed to drug resistance is the cross talk that exists amongst the signalling pathways, which serves to provide tumour cells with the opportunity to circumvent other pathways to enhance their survival (Sun *et al.*, 2016; Prahallad and Bernards, 2015). In particular, the crosstalk that exists between the TGF β and Hh signalling pathways is very well documented whereby in both normal and malignant tissues, they have been shown to regulate key components of each other (Dennler *et al.*, 2007; Mauviel *et al.*, Javelaud *et al.*, 2011; Javelaud *et al.*, 2012). TGF β signalling in cancer is typically associated with increased invasiveness and aggressiveness through the two key mechanisms: (1) increased proliferation arising

from retinoblastoma gene inactivation, and (2) induction of epithelial-mesenchymal transition.

Under physiological conditions TGF β signalling is responsible for cell cycle arrest, however, proliferation can occur after concomitant inactivation of the retinoblastoma gene (Laiho *et al.*, 1990; Herrera *et al.*, 1996). Whereas EMT is a biological process in which a non-motile epithelial cell undergoes changes to a mesenchymal phenotype and possesses invasive capacities (Weinberg *et al.*, 2008). TGF β signalling is associated with epithelial cell migration during wound healing and facilitates the egress of adult tissue SCs from the HF bulge (Oshimori *et al.*, 2012), and has a pivotal role in inducing EMT. This is achieved by regulation of a well-established EMT core signature (Derynck *et al.*, 2014; Taube *et al.*, 2010), whereby TGF β 1 induced TGF β signalling enhances the expression of EMT inducers, including the transcription factors (TFs) Goosecoid, Snail, and Twist. The overexpression of these EMT inducers then in turn upregulates a subset of other EMT-inducing TFs, with Twist, Zeb1, Zeb2, Runx1 and Runx2 being commonly induced. These TFs are capable of transforming cells into ones that display classic hallmarks of EMT, such as the loss of epithelial cell surface markers, most notably E-cadherin, whose transcriptional repression is mediated through the binding of the aforementioned TFs to E-boxes present within the E-cadherin promoter, and the acquisition of mesenchymal markers such as N-cadherin (CDH2) and vimentin.

TGF- β was recently shown to induce Hh expression, which in turn activates GLI1 and GLI1-dependent EMT in non-small cell lung cancer cells (Maitah *et al.*, 2011). For instance, there are multiple lines of evidence showing that crosstalk exists between the Hh and TGF β pathway, which has led to the identification of increased expression of TGF β signalling observed in untreated BCC (Heller *et al.*, 2013; O'Driscoll *et al.*, 2006). For example, TGF β signalling activation is required for tumour progression in a mouse model of BCC development where it may exert immunosuppressive activities. Hh signalling has been shown to promote motility and invasiveness in human gastric cancer cells through TGF β mediated activation of the TGF β receptor 1 pathway. Furthermore, there is a non-canonical Hh cascade that is capable of activating GLI transcription factors independently of Hh ligands or PTCH/SMO. Activation of GLI transcription

factors is positively regulated by a number of pathways including KRAS, TGF β , PI3K-AKT, and PKC α (Pellegrini *et al.*, 2017).

It is this crosstalk that led to our laboratory performing microarray analysis and generating preliminary data showing an increased expression of TGF β signalling following exposure of our primary human BCC cells, established *in vitro* to vismodegib. We found that exposure to vismodegib was associated with expression of TGF β pathway genes (increase: TGF β , ACVR1, E2F4, ID1, RUNX2, JunB, Snail1, Snail2, Zeb2 and decrease: SMURF1 and SMURF2) and concomitant up-regulation of TGF β target genes (Sox4, Lif, Hey1, Jagged11, CXXC5 and ID1). Therefore, in BCC, where the most significant pathogenic event is the upregulation of Hh signalling, an enrichment of the TGF β signalling pathway was observed when treating with the commercially available drug vismodegib.

3.2 Results

3.2.1 Microarray analysis of BCC identifies TGF β signalling.

I undertook microarray analysis of untreated BCC, normal skin and an alternative cutaneous keratinocyte carcinoma (squamous cell carcinoma, SCC). Normal human skin, BCC and SCC samples were obtained for this study within 8 hours of cutaneous surgery, from dermatology departments in two University Health Boards, as part of an ethics committee and NHS approved clinical study (09-WSE02-1). Samples were collected directly from the surgeon during the procedure and sterilely placed into a prepared transportation tube containing keratinocyte media and were then transported to the laboratory on ice. Tissue samples were processed immediately upon receipt and messenger RNA (mRNA) was extracted within 24 hours using established protocols and stored at -20 °C. In the case of keratinocyte tumours, histological confirmation was sought from the sample submitted for the pathologists report before the RNA was used. The quantity and quality of the RNA was determined by nanodrop™ and Bioanalyser™, respectively. A total of 10 BCC, 10 normal skin and 10 SCC samples were processed in this way. Of these, 6 BCC, 3 SCC, and 3 normal skin samples were determined to be of

sufficient quantity (100-200 ng/ μ L) and quality (RIN 9-10) for gene profiling by Illumina HT-12 v4 bead microarray chips. The raw microarray data was then transformed and normalised using the Bioconductor packages in the R statistical program (Section 2.3.7.6). Based on the box plot distributions, two out of the six BCC samples were identified as outliers and were therefore removed from the analysis. Therefore, the microarray analysis was performed on four BCC, three SCC and three normal skin samples.

3.2.2 Volcano plots highlight the most significant genes within BCC

The Illumina platform allowed for gene expression analysis of 24,329 genes, utilising multiple probes for each gene. Following transformation and normalisation of our samples, we identified differentially expressed genes using an $FDR > \pm 2.0$, and a $p < 0.05$: 1,424 genes that were differentially expressed between BCC and normal skin and 1,664 genes between BCC and SCC. Volcano plots using a cut off of $> \pm 2.0$ fold difference in expression and a $p\text{-value} < 0.01$, identified 24 up-regulated and 21 down-regulated genes (in BCC tissue compared to NS; Fig. 3.1A; Table 3.1). In keeping with the prominent stroma around BCC and the fact that is a very invasive and locally aggressive carcinoma, 16 of the 24 genes demonstrating increased expression were associated with proteins in the extracellular matrix. Of note were 7 collagen genes (COL1A1, 1A2, 1A2, 3A1, 5A1, 5A2 and 6A3), a group of proteoglycans and glycoproteins (VCAN, FBN3, TNC, CSPG4 and LUM), other extracellular proteins (SPON2 and CALD1), and genes involved in remodelling the extracellular matrix (MMP11).

BCC compared to SCC identified 20 up-regulated and 3 down-regulated genes (in; Fig. 3.1B; Table 3.2). Ten genes demonstrated increased expression in both analyses, and were therefore found to be highly upregulated in BCC when compared to both normal skin and SCC. Surprisingly none of these ten genes were found to be the collagens, which also highlight the similarity in the stroma of both BCC and SCC. However, the proteoglycans and glycoproteins were still found to be elevated in BCC when compared to SCC (VCAN, FBN3, CSPG4), along with the additional extracellular matrix protein SPON2. The remaining genes were the proto-oncogene MYCN, the Cre-dependent

trans-activator, CREB5, and the mitogenic factor PDGFA. The remaining two genes were APCDD1L and SLC39A14, however, very little is known about their function. Although not found to be upregulated in BCC when compared to normal skin, some of the remaining upregulated genes also have involvement in regulating the extracellular matrix, including MT1F, which is associated with collagen deposition, MARCKSL1, which affects the formation of adherens junctions, GPC4, which is a proteoglycan, and LCE2B, which is associated with epidermal differentiation. Another notable gene was the 7-transmembrane domain receptor, FZD7, which is involved in the Wnt signalling pathway (highlighted in gene set enrichment analysis later on).

Only three genes were significantly downregulated in BCC compared to SCC, and they were the type I cytokeratin, KRT13, IGFL1 and the subunit of NADH dehydrogenase located in the mitochondrial inner membrane, NDUFA4L2.

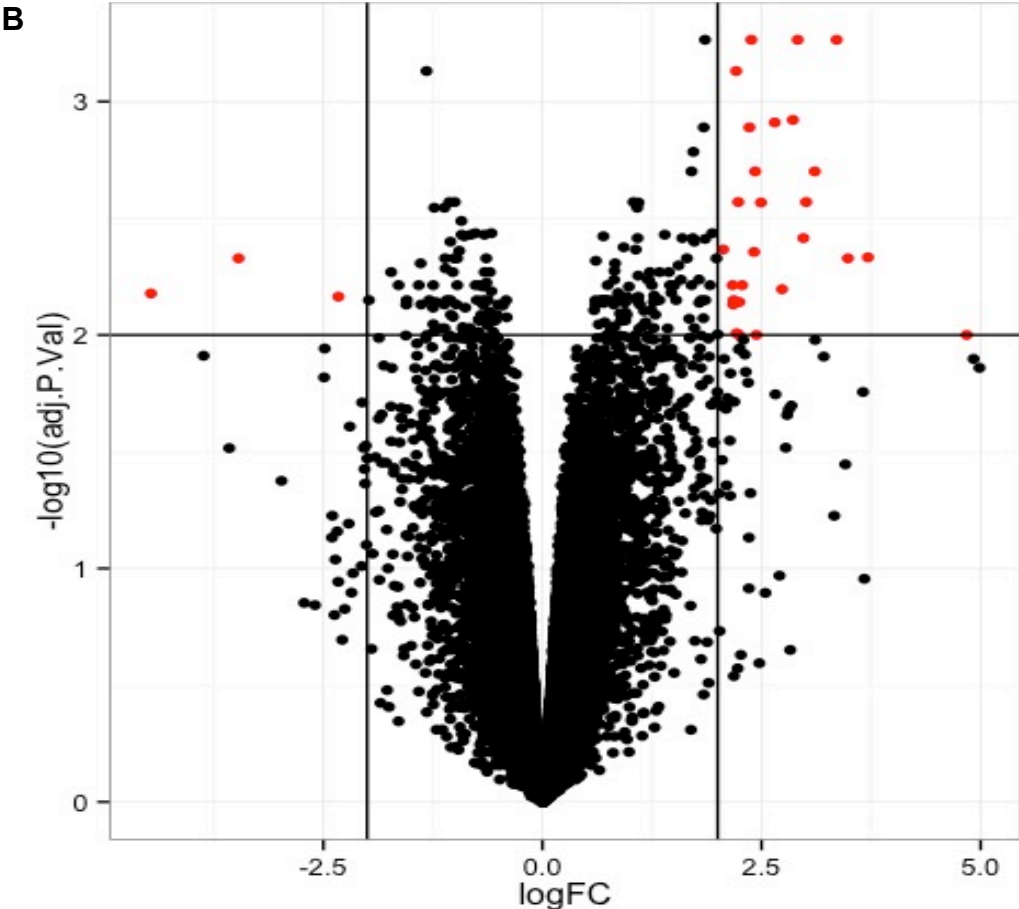
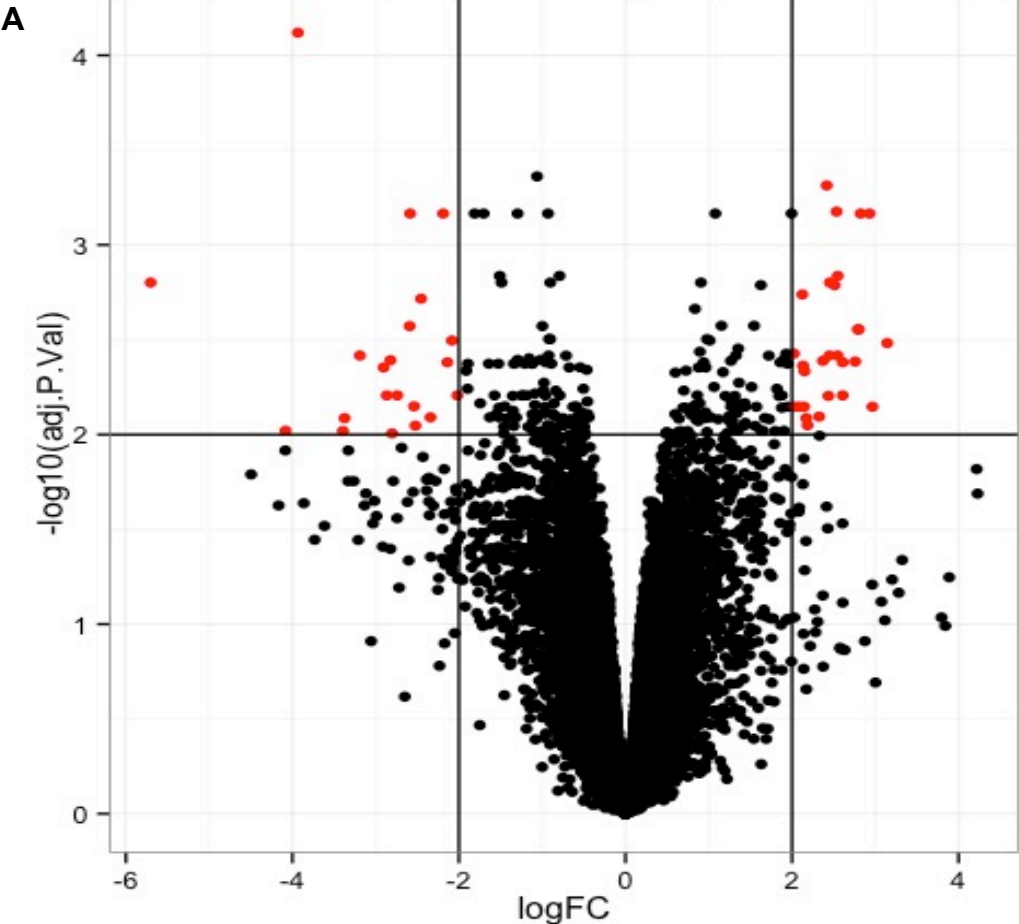


Figure 3.1. Volcano plots of differentially expressed genes

Volcano plot representation of the differentially expressed genes with visualised genes on the right and left corresponding to 2.0-fold upregulation and downregulation respectively, at $p < 0.01$: **(A)** Statistically significant genes observed when comparing BCC to normal skin (NS), **(B)** Statistically significant genes observed when comparing BCC to SCC.

Table 3.1: List of significant genes highlighted identified by the volcano plot comparing BCC to NS

#	Gene	Fold Change	Gene	Fold Change
1	VCAN	3.14	DCD	-5.70
2	APCDD1L	2.97	PIP	-4.08
3	MYCN	2.93	SCGB2A2	-3.93
4	SLC39A14	2.82	ALOX15B	-3.39
5	FBN3	2.80	MUC1	-3.37
6	TNC	2.79	ACTA1	-3.19
7	COL1A1	2.76	TMEM91	-2.91
8	FLJ22536	2.61	KIA18881	-2.87
9	MMP11	2.61	SCGB1D2	-2.82
10	COL5A1	2.55	MUCL1	-2.80
11	COL1A2	2.55	CFD	-2.74
12	CHCHD7	2.54	GPT	-2.59
13	COL5A2	2.51	HMGCS2	-2.59
14	GJB6	2.46	UBIAD1	-2.54
15	PDGFA	2.45	FCGBP	-2.52
16	LUM	2.44	PSAPL1	-2.45
17	CSPG4	2.42	BRI3BP	-2.34
18	IGF2BP2	2.37	AZGP1	-2.19
19	SPON2	2.33	CHCHD10	-2.14
20	CREB5	2.19	PROL1	-2.08
21	CALD1	2.17	FCGBP	-2.01
22	COL6A3	2.15		
23	COL1A2	2.15		
24	COL3A1	2.13		

Table 3.2. List of significant genes highlighted identified by the volcano plot comparing BCC to SCC

#	Gene	Fold Change	Gene	Fold Change
1	LHX2	3.71	KRT13	-4.47
2	APCDD1L	3.49	IGFL1	-3.47
3	MYCN	3.36	NDUFA4L2	-2.33
4	FBN3	3.01		
5	CREB5	2.98		
6	CHCHD7	2.91		
7	SLC39A14	2.86		
8	PELI2	2.73		
9	TMEM98	2.65		
10	FZD7	2.49		
11	LCE2B	2.44		
12	GPC4	2.43		
13	PDGFA	2.42		
14	CSPG4	2.38		
15	TSPAN18	2.36		
16	MT1F	2.28		
17	VCAN	2.24		
18	SPON2	2.22		
19	MARCKSL1	2.21		
20	IRX2	2.18		

3.2.3 Unsupervised Clustering separates samples by disease status

Unsupervised hierarchical clustering of 235 significant differentially expressed genes ($p < 0.01$), identified 6 clusters (Figure 3.2 A). Cluster 1 identified genes that were over expressed in keratinocyte carcinoma more than NS. While cluster 2, identified genes under expressed in BCC relative to SCC and NS. Clusters 3, 4 and 5 represented genes that were overexpressed in BCC much more than in SCC or NS. Cluster 5 represented genes that were overexpressed in NS but not in BCC and SCC.

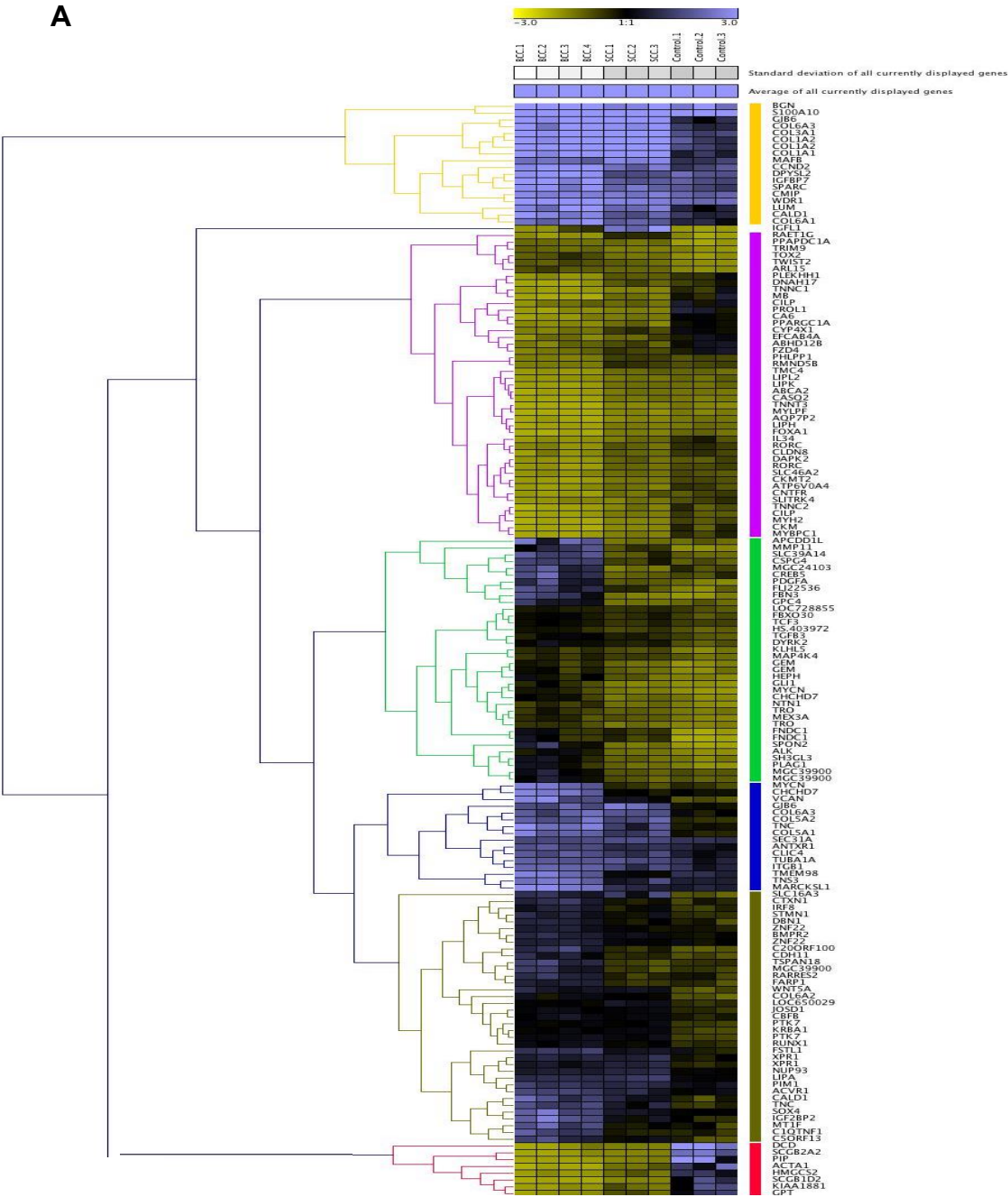
Cluster 1 predominantly contained genes involved in the extracellular matrix. In particular the collagen proteins, COL1A1, 1A2, 3A1, and 6A3, were all shown to be highly upregulated in both BCC and SCC tissue when compared to normal skin. This pattern of collagen gene expression observed between the tissue groups is consistent with other microarray studies on BCC tissue (Heller *et al.*, 2013). This is interesting, as collagens are regulated by TGF β and Hh signalling pathways, which may possibly give further insight into the pathways involved in these tissues (Zunich *et al.*, 2012).

There are a number of different genes that can be observed within Cluster 2 (Figure 3.2C), with 19/46 of these genes concordantly downregulated in both BCC and SCC in comparison to normal skin. This group consisted of genes with indeterminate functions in BCC and SCC, including PROL1, CA6, PPARGC1A, and CYP4X1, while the remaining 27 genes were highly downregulated in all three-tissue groups including transcription factors: TOX2, TWIST2, and FOXA1; and genes involved in lipid metabolism (LIPL2, LIPK, and LIPH), and skeletal muscle formation (TNNT3, MYLPP, and TNNC2).

Gene cluster 3 (Fig. 3.2D) contained genes that are upregulated in BCC when compared to SCC and normal skin, whose expression levels are found to be similar between both tissue groups. The genes APCDD1L, MMP11, SLC39A14, CSPG4, MGC24103, and FBN3 were all highly upregulated in BCC, and again are genes integral to the maintenance and remodelling of the extracellular matrix. Other genes shown to have increased expression included GLI1, which is to be expected since the Hh signalling is constitutively activated in BCC.

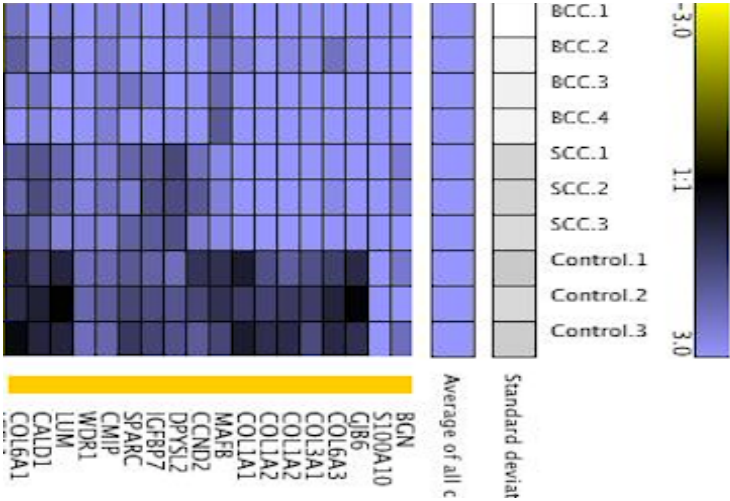
Gene cluster 4 (Figure 3.2E) is subdivided into blue and brown clusters. Genes in the blue cluster were predominantly found to be concordantly expressed in all three-tissue groups, with the highest increases in expression found in BCC tissue. These genes are involved in the extracellular matrix/stroma, including *VCAN* (proteoglycan), *COL6A3*, *COL5A2*, *COL5A1*, *ANTXR1* (type I transmembrane protein involved in cell attachment and migration), and *TUBA1A* (encodes α -Tubulin, which is responsible for the formation of microtubules within cells). Again all of these genes have important roles in maintaining the functionality/integrity of the extracellular matrix and the cells themselves. Genes in the brown cluster were all highly upregulated in BCC, in comparison to both SCC and normal skin, where no change in gene expression, and downregulation was observed respectively. Interestingly the genes upregulated in BCC are regulated or induced by TGF β signalling including *CDH11*, *RUNX1*, *SOX4* (regulators of EMT), and *FSTL1*.

A



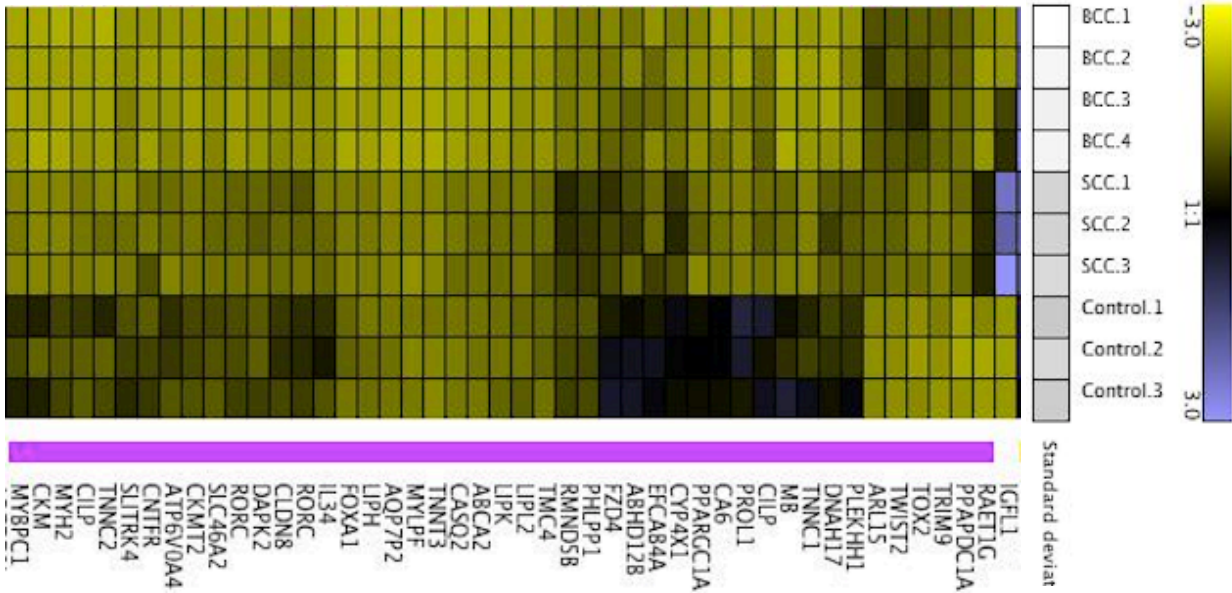
Cluster 1

B



C

Cluster 2



3.2.4 Identifying differentially regulated pathways enriched in BCC

As BCC expression could be differentiated from SCC and normal skin with respect to volcano plots and hierarchical clustering, differentially expressed genes were then functionally annotated and pathway analysis was performed by: 1) DAVID (Database of Annotation (p<0.05), Visualization and Integrated Discovery; NCBI) and 2) gene set enrichment analysis (GSEA, <http://www.broadinstitute.org/gsea/index.jsp>).

DAVID is a bioinformatics resource providing functional annotation of gene expression data to identify enriched biological pathways/functional processes. DAVID pathway analysis of differentially expressed genes in BCC revealed enrichment in 21 pathways (p < 0.01). The enriched pathways included 'metabolic pathways' (p < 0.01; 131 genes), 'ECM-receptor interactions' (p < 0.01; 17 genes), 'tight junctions' (p < 0.01; 20 genes), and 'PPAR signalling pathway' (p < 0.01; 12 genes). Unsurprisingly also enriched were 'cancer' (p < 0.01; 43 genes), and 'basal cell carcinoma' (p < 0.01; 11 genes). Importantly, the enrichment of these pathways has been documented in other BCC microarray studies (Heller *et al.*, 2013), strengthening the reliability of our microarray dataset.

DAVID pathway analysis also highlighted the enrichment of some key functional processes in BCC, including 'SMAD binding sites' that were highly regulated in BCC when compared to normal skin (Figure 3.3A). Furthermore, in BCC, when analysing the gene expression levels within our dataset, increases were observed in the SMAD transcription factors, SMAD2, 3, and 4, when compared to normal skin (Figure 3.3B). Therefore it appeared that TGF β signalling was enriched in BCC when using basic pathway analysis.

When comparing BCC to SCC a total of 16 pathways were found to be statistically significant (p < 0.05). As expected there was enrichment of 'basal cell carcinoma' (p < 0.01; 11 genes) and the 'hedgehog-signalling pathway' (p < 0.05; 6 genes). However there were a number of other pathways significantly enriched including the TGF β (p < 0.01; 15 genes), Hippo (p < 0.01; 21 genes) and PI3K-AKT (p < 0.01; 37 genes) signalling pathways.

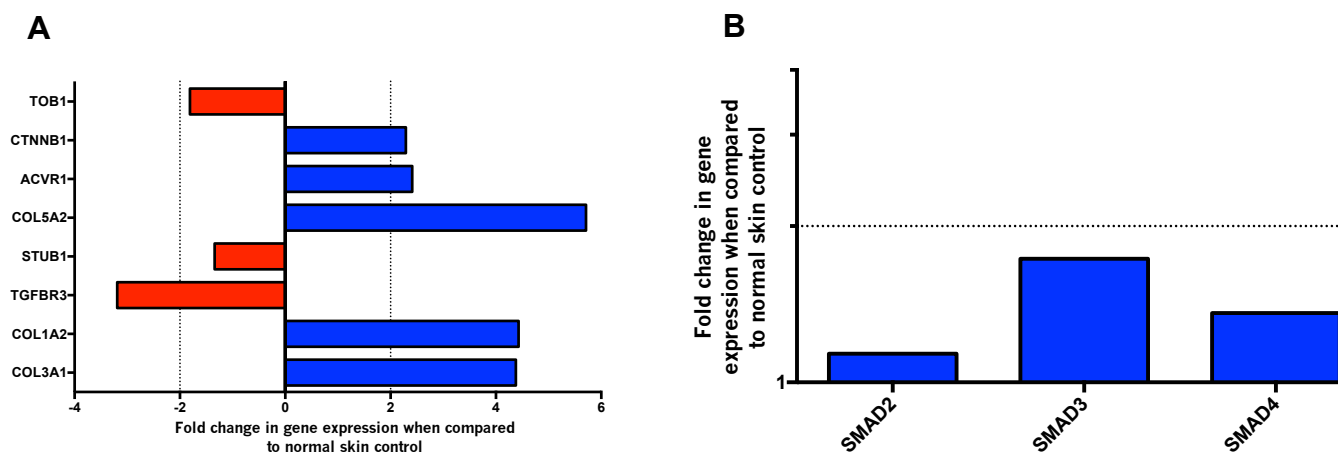


Figure 3.3. TGF β signalling in BCC.

When comparing BCC to normal skin there were 1,664 significant differentially expressed genes ($p < 0.05$). These were annotated using DAVID functional pathway analysis. **(A)** Gene expression profile showing fold change of genes involved in the Gene Ontology (GO) process 'SMAD Binding' obtained through DAVID pathway analysis. **(B)** Gene expression levels of SMAD transcription factors in BCC.

Next we performed more detailed pathway analysis using GSEA (<http://www.broadinstitute.org/gsea/index.jsp>), to correlate expression patterns with a phenotype. GSEA differs from DAVID pathway analysis, in that expressed genes are ranked by their correlation with a phenotype, and then this ranked list is compared to curated gene sets, which are downloaded from the Broad Institutes Molecular Signatures Database (MSigD).

When using GSEA to identify the enrichment of pathways/processes between BCC and NS (Table 3.3), and BCC and SCC (Table 3.4), considerable overlap between these two comparison groups was observed. As expected the Hh signalling pathway was enriched in BCC, when compared to both NS (ES=0.52, $p > 0.05$), and SCC (ES= 0.64, $p < 0.01$) (Figure 3.4A and 3.5A, respectively). Similarly, EMT was significantly enriched in comparison to NS (ES=0.77; $p < 0.05$; Figure 3.4B) and SCC (ES=0.66; $p > 0.05$; Figure 3.5B).

Angiogenesis was relevant in BCC compared to SCC (Figure 3.5C), which is used as a clinical feature in BCC with the presence of peripheral vessels being a common diagnostic finding. Of the other signalling pathways that were observed, the TGF β signalling pathway was enriched in BCC (ES=0.56; Figure 3.4C) when compared to normal skin, where it was the most enriched signalling pathway. TGF β signalling is often implicated in EMT, suggesting that these two profiles may be linked. Another notable pathway enriched was the KRAS signalling pathway (ES=0.55; Figure 3.4D), which has been shown to interact with TGF β signalling in a number of carcinomas (Adorno *et al.*, 2009; Vasilaki *et al.*, 2016). In addition, the Wnt/ β -catenin pathway was also enriched in BCC compared to SCC. Nuclear staining with β -catenin, a feature of Wnt activation, is more frequent in BCC when compared to SCC (Doglioni *et al.*, 2003). In summary, both DAVID and GSEA support the role of TGF β signalling in BCC, a pathway that has previously been considered only relevant for SCC development.

Table 3.3 Top 20 processes (Gene Sets) enriched in BCC in comparison to normal skin

Enrichment results report generated on the Broad Institute website

(<http://www.broadinstitute.org/gsea/index.jsp>), listing the top 20 gene sets enriched in BCC when compared to normal skin, along with the size of each gene set and the enrichment score (ES), which reflects the degree to which the gene set is overrepresented at the top or bottom of a ranked list of genes in the expression dataset. Gene sets are ordered by normalized enrichment score (NES), which accounts for the differences in gene set size and in correlations between gene sets and the expression data set.

	Gene Sets	Size of Gene Set	Enrichment Score	Normalized Enrichment Score	Nominal p-value
1	G2M CHECKPOINT	178	0.54	1.44	0.059
2	E2F TARGETS	179	0.51	1.39	0.120
3	EPITHELIAL MESENCHYMAL TRANSITION	185	0.77	1.34	0.045
4	TGFB SIGNALLING	48	0.56	1.34	0.092

5	KRAS SIGNALLING	179	0.55	1.33	0.140
6	ALLOGRAFT REJECTION	165	0.56	1.29	0.146
7	MITOTIC SPINDLE	180	0.51	1.29	0.000
8	UV RESPONSE (DOWN)	129	0.48	1.23	0.109
9	ANGIOGENESIS	32	0.80	1.23	0.050
10	APOPTOSIS	149	0.46	1.22	0.106
11	PANCREAS BETA CELLS	19	0.54	1.21	0.317
12	MYC TARGETS	191	0.38	1.18	0.205
13	COMPLEMENT	173	0.45	1.17	0.146
14	IL6 JAK STAT3 SIGNALLING	75	0.53	1.16	0.202
15	IMFLAMMATORY RESPONSE	173	0.53	1.14	0.213
16	HEDGEHOG SIGNALLING	30	0.52	1.14	0.112
17	IL2 STAT5 SIGNALLING	180	0.41	1.13	0.153
18	WNT BETA CATENIN SIGNALLING	38	0.48	1.09	0.278
19	APICAL SURFACE	35	0.50	1.09	0.119
20	DNA REPAIR	146	0.29	1.08	0.182

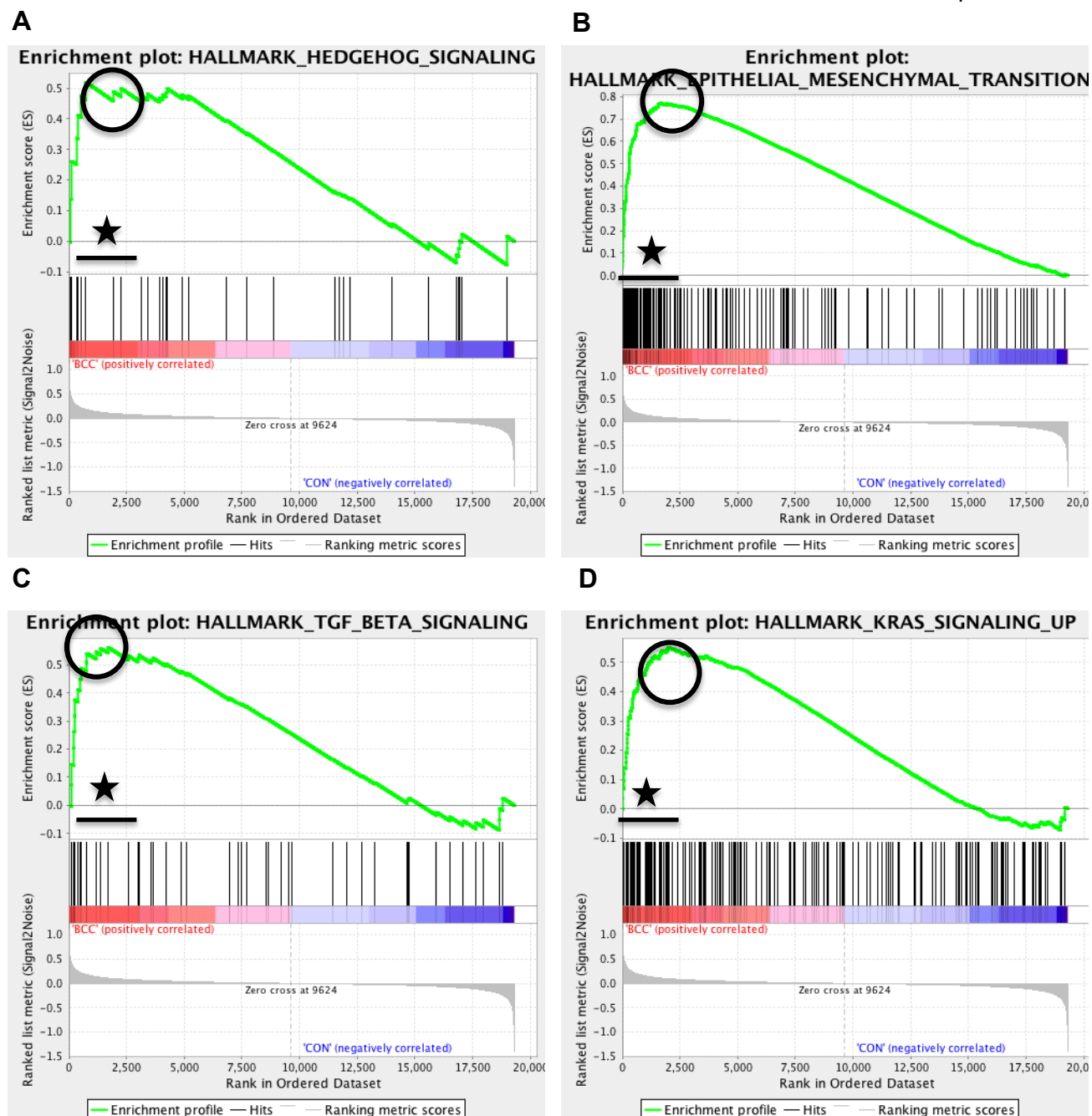


Figure 3.4. Pathway enrichment observed in BCC compared to normal skin

Gene Set Enrichment Analysis reveals enrichment of **(A)** Hh signalling, **(B)** EMT, **(C)** TGF β signalling, and **(D)** KRAS signalling. On the x-axis, the human genes are ranked from the most upregulated (left end) to the most downregulated (right end) between BCC and normal skin. The 'barcode' indicates the position of the genes from the biological gene set within that particular pathway. The y-axis shows a running enrichment score (ES), which increases when genes are encountered within that particular pathway, leading to an assessment of the gene distribution within a set of genes. Black circles show the enrichment score. Black star symbols showing the leading edge subset, which represents

the subset of gene members within that gene set which contributed to the ES.

#	Gene Sets	Size of Gene Set	Enrichment Score	Normalized Enrichment Score	Nominal p-value
1	WNT/BETA CATENIN SIGNALLING	38	0.58	1.32	0.043
2	HEDGEHOG SIGNALLING	30	0.59	1.25	0.075
3	ANGIOGENESIS	32	0.69	1.22	0.239
4	EPITHELIAL MESENCHYMAL TRANSITION	185	0.66	1.21	0.175
5	UV RESPONSE DN	129	0.53	1.19	0.000
6	MITOTIC SPINDLE	180	0.36	1.16	0.187
7	MYOGENESIS	167	0.34	1.12	0.208
8	APOPTOSIS	149	0.40	1.10	0.245
9	KRAS SIGNALLING	179	0.47	1.08	0.212
10	COAGULATION	105	0.47	1.07	0.335
11	NOTCH SIGNALLING	32	0.33	1.06	0.390
12	ANDROGEN RESPONSE	97	0.31	1.05	0.250
13	SPERMATOGENESIS	82	0.28	1.04	0.416
14	DNA REPAIR	146	0.23	1.00	0.244
15	APICAL JUNCTION	177	0.36	0.96	0.471
16	TNFA SIGNALLING	189	0.44	0.96	0.506
17	PANCREAS BETA CELLS	19	0.40	0.92	0.535
18	APICAL SURFACE	35	0.32	0.92	0.627
19	PROTEIN SECRETION	92	0.25	0.91	0.605
20	IL2/STAT5 SIGNALLING	180	0.37	0.89	0.697

Table 3.4 Top 20 processes (Gene Sets) enriched in BCC in comparison to SCC

Enrichment results report generated on the Broad Institute website

(<http://www.broadinstitute.org/gsea/index.jsp>), listing the top 20 gene sets enriched in BCC when compared to SCC, along with the size of each gene set and enrichment score (ES), which reflects the degree to which the gene set is overrepresented at the top or bottom of a ranked list of genes in the expression dataset. Gene sets are ordered by

normalized enrichment score (NES), which accounts for the differences in gene set size and in correlations between gene sets and the expression data set.

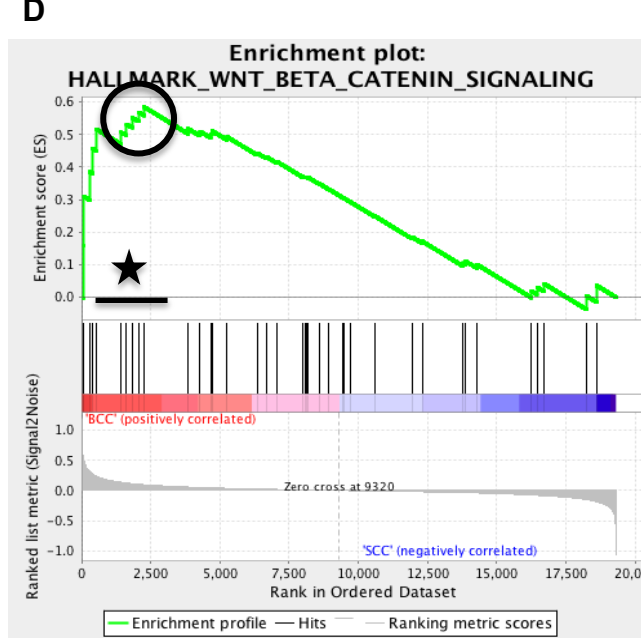
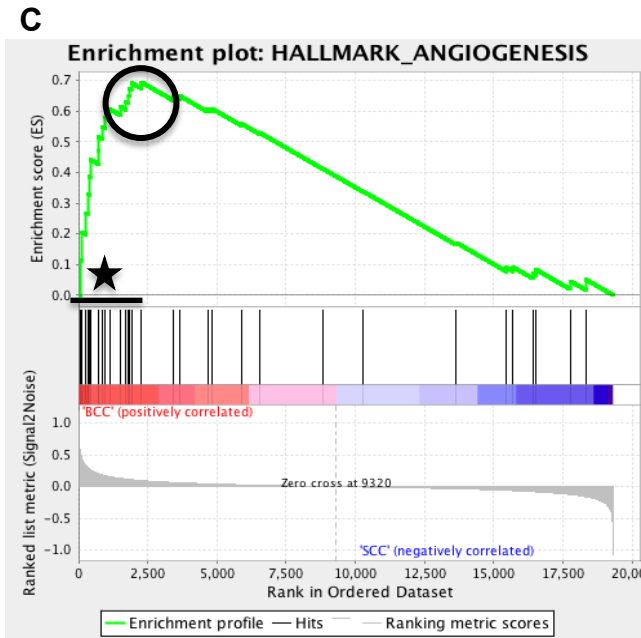
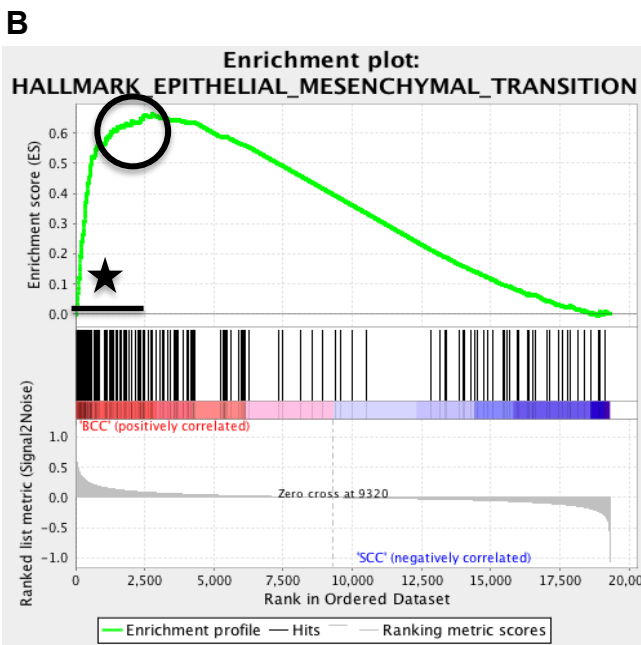
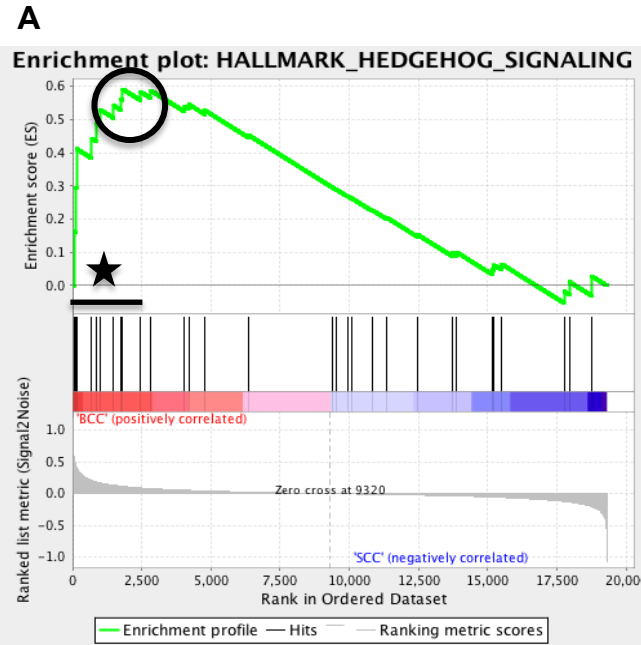


Figure 3.5: Pathway enrichment observed in BCC compared to SCC.

Gene Set Enrichment Analysis reveals enrichment of (A) Hh signalling, (B) EMT, (C) Angiogenesis, and (D) WNT/ β -Catenin signalling. On the x-axis, the human genes are ranked from the most upregulated (left end) to the most downregulated (right end) between BCC and normal skin. The 'barcode' indicates the position of the genes from the biological gene set within that particular pathway. The y-axis shows a running enrichment score (ES), which increases when genes are encountered within that particular pathway, leading to an assessment of the gene distribution within a set of genes. Black circles show the enrichment score. Black star symbols showing the leading edge subset, which represents the subset of gene members within that gene set which contributed to the ES.

3.2.5 Identification of a TGF β responsive gene set panel

We sought to define a panel of TGF β signal responsive genes that could be used to define TGF β signalling. Numerous laboratories have performed and published microarray analysis on a variety of different epithelial cell lines comparing TGF β 1 treated and untreated gene sets (Ranganathan *et al.*, 2007; Xie *et al.*, 2003, Moustakas *et al.*, 2002; Zavadil *et al.*, 2001). These studies sought to determine genes regulated by TGF β signalling in a wide range of cell lines; including lung (A549 cells; Ranganathan *et al.*, 2007), HNSCC (Xie *et al.*, 2003), and skin (HaCaT; Zavadil *et al.*, 2001) for defined periods of time (range from 30 min to 4 hours). We identified a panel of 27 candidate TGF β regulated genes from these reported microarray studies. To generate a comprehensive panel of genes relevant for our studies, we treated the HaCaT cell line with TGF β 1 ligand, as reported previously and interrogated our panel of genes. As expected, all the genes demonstrated TGF β responsive changes (Figure 3.6) when compared to untreated controls, which is consistent with what was observed in the literature.

To define whether the 27 TGF β responsive genes showed similar expression in BCC, we next ran the 27 genes against primary BCC tissue (n=5) and compared to normal skin

(Figure 3.7). Of the 27 genes within the panel, 19 were found to have expression that was concordant with what was observed in the TGF β 1 treated HaCaT cells. Of these 19 genes, a panel of 9 were found to be either highly up or down regulated in concordance with the HaCaT TGF β 1 treated cell line data (Figure 3.6). This smaller subset of genes was selected as a refined panel of TGF β -responsive genes and was used to define TGF β response in BCC and the Hh driven tumour cell lines (chapter 5). Furthermore, when performing a chi-square test, there was no significant difference in the expression of the TGF β gene panel between the TGF β 1 treated HaCaT cell line and the primary BCC tissue ($p > 0.05$), thereby confirming that this panel of TGF β regulated genes is relevant in BCC. Therefore we have identified a refined panel of genes that are highly regulated and responsive in BCC.

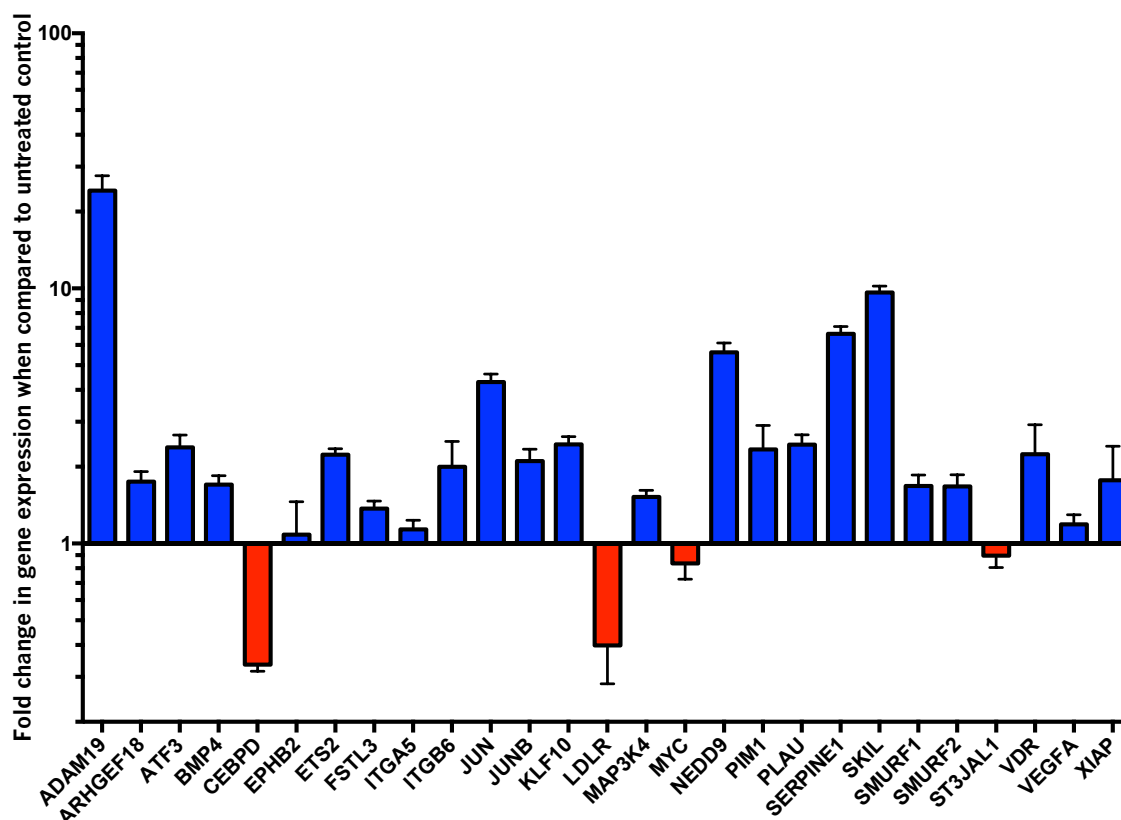


Figure 3.6: Defining a TGF β responsive gene panel

HaCaT cells were cultured on glass coverslips treated for 1hr with 20 ng/mL TGF β 1 and then assayed for expression of 27 TGF β -responsive genes in comparison to an untreated control. Fold change in gene expression was compared to untreated HaCaT cells. Experiment was performed in duplicate ($n=2$), with each experiment containing three

internal technical replicates for each gene, along with two endogenous controls (β -Actin, and GAPDH). Blue bars indicate genes that were upregulated in response to TGF β 1. Red bars indicate genes that were downregulated in response to TGF β 1. Error bars represent SE of the mean.

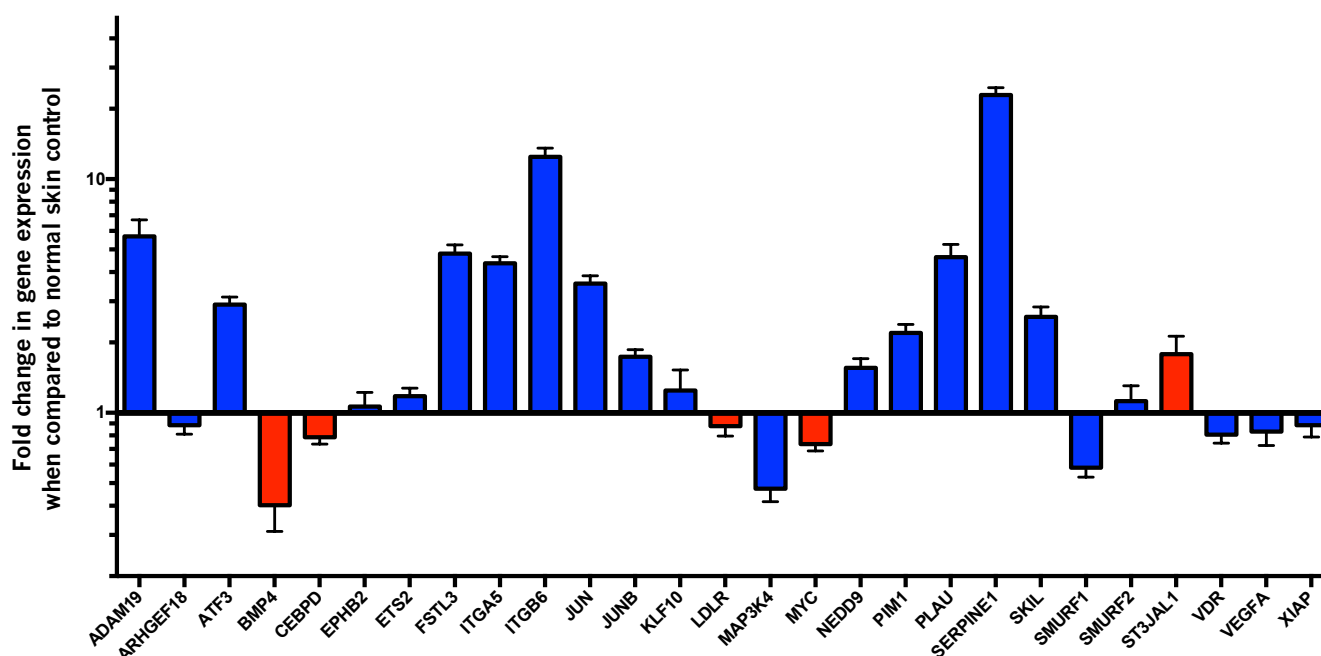


Figure 3.7: TGF β responsive gene panel in primary human BCC

RNA was extracted from primary human BCC tissue ($n=5$) and subsequently assayed for the expression of a TGF β -responsive gene set. Fold change in gene expression was compared to normal skin control ($n=3$). Each experiment contained three internal technical replicates for each gene, along with two endogenous controls (β -Actin, and GAPDH). Blue bars indicate genes that were upregulated in HaCaT cells following TGF β 1 treatment (Figure 3.6). Red bars indicate genes that were downregulated in HaCaT cells following TGF β 1 treatment (Figure 3.6). Error bars represent SE of the mean.

3.2.6 Determination of TGF β signalling in basal cell carcinoma

TGF β 1 induced pathway activation uses the nuclear accumulation of phosphorylated forms of the TFs SMAD2 and 3 to drive gene transcription. I therefore used a phosphorylated SMAD3 (pSMAD3) specific antibody to detect TGF β signalling in BCC. BCC samples were collected and processed within 4 hours of surgery. As a positive control, HaCaT cells were grown on glass coverslips and treated with TGF β 1 for 30 min at a concentration of 20 ng/mL. As expected, TGF β treatment led to increased pSMAD3 nuclear accumulation (n=3; Figure 3.8). Therefore, activation of the TGF β signalling pathway by TGF β 1 could be detected by immunofluorescence using pSMAD3 antibody labelling.

As BCC are derived from the HF, we also used HF tissue as a positive control during telogen, as TGF β signalling is active in the HF bulge SCs (Cammaraeri *et al.*, 2016). In the HF, nuclear pSMAD3 labelling was evident within the scalp HF bulge keratinocytes only (n=5 samples, Figure 3.9), and was not uniformly expressed by all cells, which suggests that it is limited to a specific cell population. Nuclear pSMAD3 labelling was not evident within the interfollicular epidermal keratinocytes (Figure 3.9). Consistent with mesenchymal dermal papilla signalling to the HF bulge, TGF β signalling was restricted to the hair follicle bulge keratinocytes within normal skin.

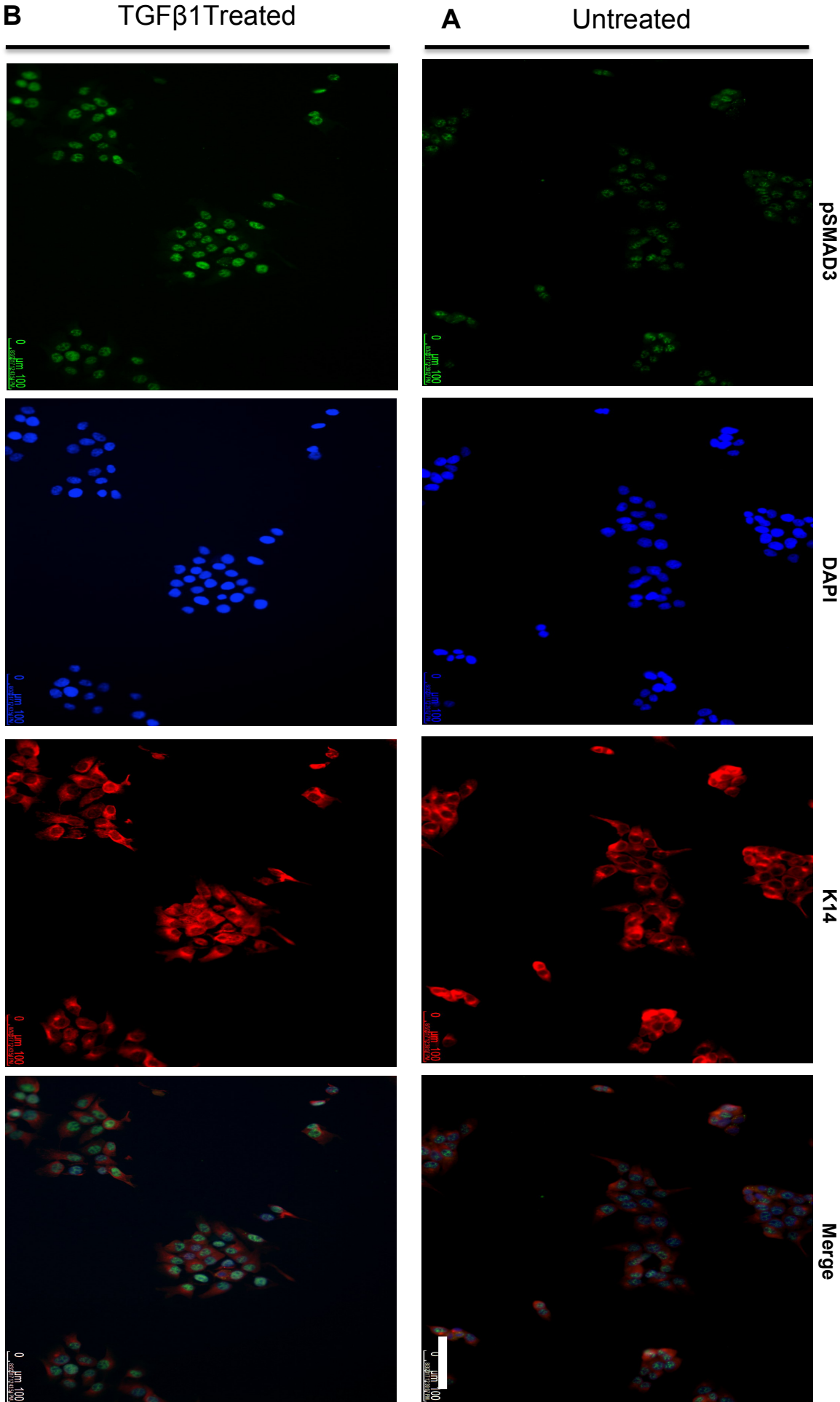
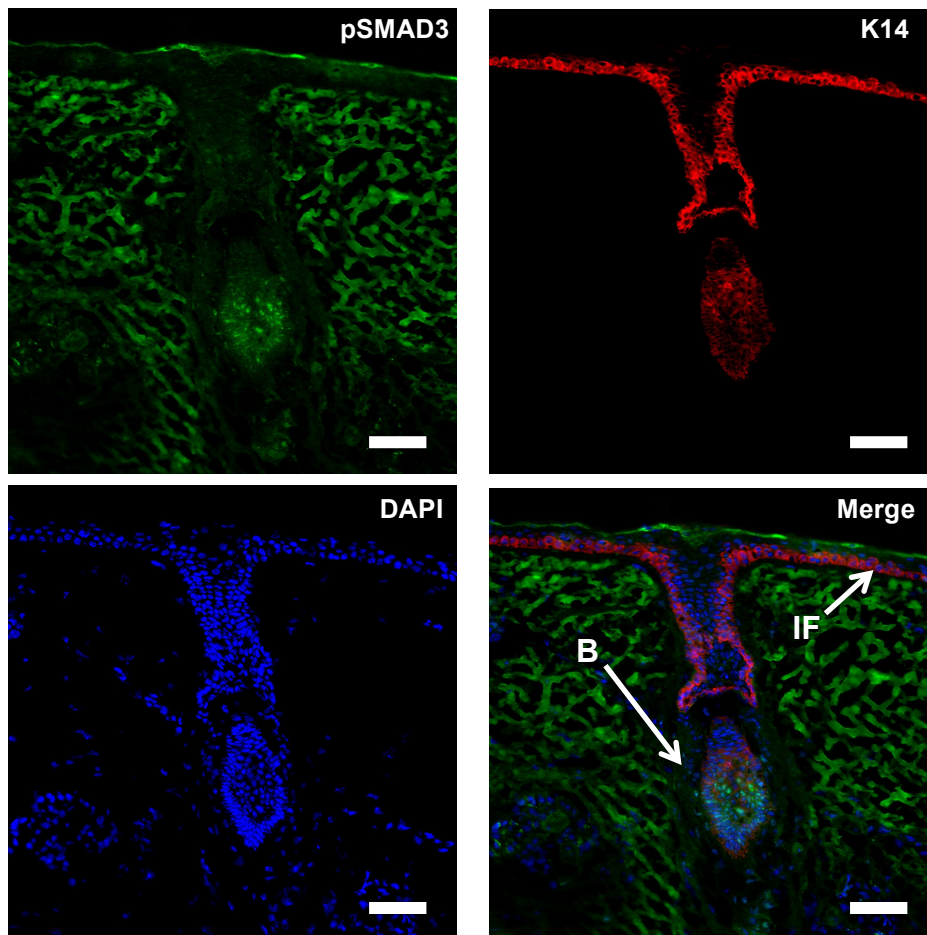


Figure 3.8. pSMAD3 expression and localisation in TGFβ1 treated HaCaT cells

Positive control experiment was performed by culturing HaCaT cells onto glass coverslips and treating with 20 ng/mL TGFβ1 ligand for 30 min, before performing immunofluorescence to detect the presence of nuclear pSMAD3, DAPI, and K14. **(A)** Untreated HaCaT cells, **(B)** TGFβ1 treated HaCaT cells. Scale bars represent 100 μM for all. (n=3)

**Figure 3.9. pSMAD3 labelling of human hair follicles**

Primary human non-lesional telogen scalp hair was frozen with embedding medium and sectioned before performing immunofluorescent staining for pSMAD3, K14, and DAPI. All three stains were merged. Fluorescent microscopy revealed the presence of nuclear pSMAD3 (green) within the bulge region (B) of the hair follicle, but not within the interfollicular epidermis (IF). Scale bars represent 100 μM. (n=5)

Next, 14 BCC tumour sample sections were labelled with pSMAD3, together with K14 and DAPI. All BCC tissue had been collected and frozen with embedding medium. All 14 independently collected BCC samples immunolabelled with pSMAD3 antibody demonstrated nuclear expression, using keratin 14 co-labelling to identify BCC tumour cell nodules within the tissue sections. However, nuclear pSMAD3 and therefore active TGF β signalling was not uniform throughout the tumour nodules, instead expression was preferentially localised towards the tumour periphery (Figure 3.10A). When enumerated, $74.09\pm 2.30\%$ (n=14) of all nuclear pSMAD3 positive cells within K14 positive BCC tumour nodules were located within the basal layer and immediate two suprabasal cell layers (Figure 3.10B). Furthermore, when enumerating all of the DAPI positive cells at the tumour nodule periphery, $31.77\pm 1.86\%$ (n=14) were positive for pSMAD3 staining (Figure 3.10C). Thus similar to the HF bulge keratinocytes, BCC pSMAD3 labelling was restricted to a sub-population of keratinocytes at the tumour periphery.

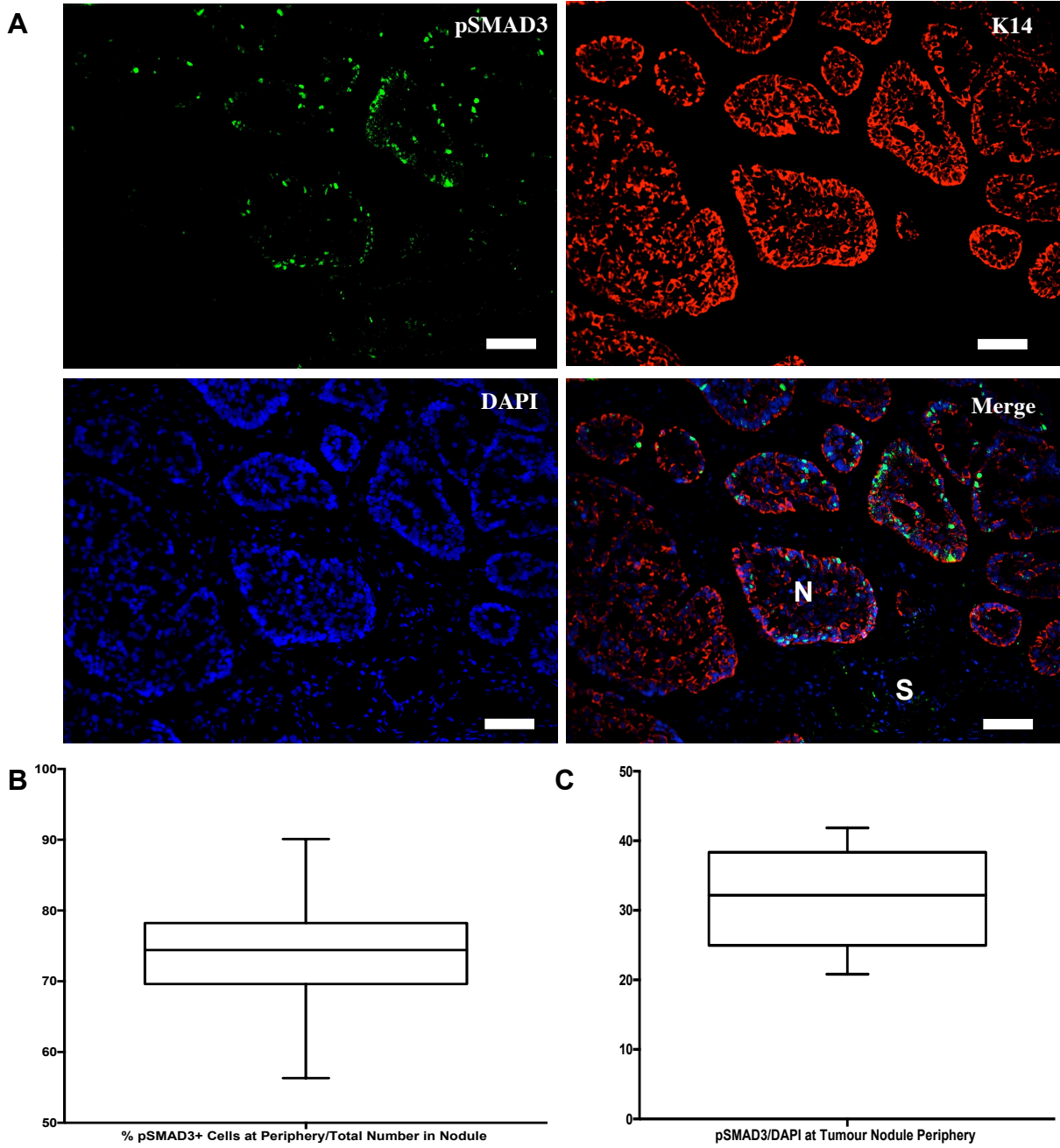


Figure 3.10: pSMAD3 labelling of human BCC tumour tissues

Primary human BCC tissue was frozen with embedding medium and sectioned before performing immunofluorescent staining for pSMAD3, K14, and DAPI (A) Immunofluorescent microscopy of human BCC tissue revealed the presence of nuclear pSMAD3 (green) within the BCC tumour nodules (N) marked with keratin14 (red) and predominantly around the periphery, with very little staining in the stroma (S). Scale

bars represent 200 μM **(B)** Box and whisker plot showing the percentage of pSMAD3-positive cells found at the tumour nodule periphery when compared to the total number of DAPI positive nuclei at the tumour nodule periphery over 14 independent BCC samples ($n=14$) **(C)** Box and whisker plot showing the % of pSMAD3-positive cells found at the tumour nodule periphery when compared to the total number of DAPI-positive nuclei over 14 independent BCC samples ($n=14$). For each BCC sample the number of positive cells enumerated was based on the number of tumour nodules present within that sample; however over the 14 BCC samples, an average of five tumour nodules were enumerated per sample.

3.2.7 TGF β Signalling was not associated with proliferation

TGF β signalling in the human HF is associated with anagen, thus proliferation and egress of HF bulge keratinocytes (Oshimori *et al.*, 2012). I next hypothesised that the TGF β signalling in BCC may be similarly responsible for BCC keratinocyte proliferation and migration/invasion. Our group has previously shown that proliferation, invasion and BCC CSCs are all present at the tumour periphery (Colmont *et al.*, 2013), similar to where nuclear pSMAD3 positive keratinocytes were visualised. While the centre of BCC nodules undergoes terminal differentiation akin to the terminal differentiation consistent with telogen HF growth (Morgan *et al.*, 2018, manuscript submitted).

We sought to determine the frequency of BCC pSMAD3 positive keratinocytes that were proliferating by immunofluorescence co-labelling with an s-phase marker of proliferation, MCM7. For each section of tissue (n=14; Figure 3.11), I enumerated the number of pSMAD3 positive only cells, MCM7 positive only cells, and pSMAD3/MCM7 double positive cells (yellow). Of the tumour keratinocytes with nuclear pSMAD3 positivity, only 17.49% \pm 4.63% were positive for MCM7 (Figure 3.11C). Similarly, of all of the MCM7 positive cells, nuclear pSMAD3 was evident in 10.92% \pm 2.50% (Figure 3.11C). Finally, of all the cells present within a tumour nodule, 13.98% \pm 2.18% were found to be proliferating (Figure 3.11C). This is in line with normal physiological effects, and therefore TGF β signalling in BCC is not associated with proliferation of BCC keratinocytes.

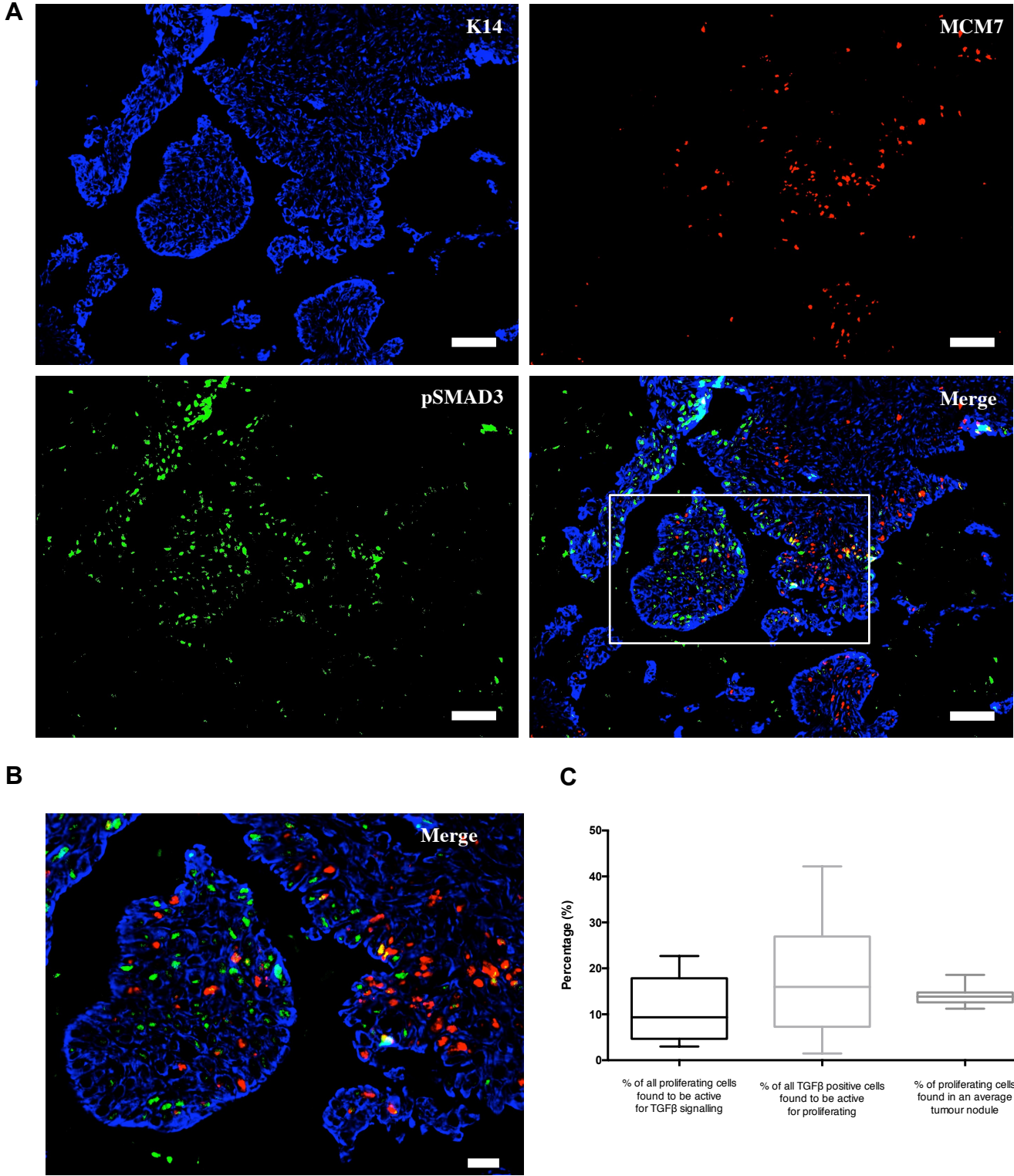


Figure 3.11: pSMAD3 and MCM7 labelling of BCC

Whole primary human BCC tissue was frozen with embedding medium and sectioned before performing immunofluorescent staining for pSMAD3, MCM7, K14, and DAPI. **(A)** Fluorescent microscopy of human BCC tissue (n=14) shows that very little co-localisation

(yellow) is observed between pSMAD3 (Green) and the cell cycle marker, MCM-7 (Red). (B) 40x magnification of (A). (C) Box and Whisker plot enumerating the percentage of TGFB pathway active cells shown to be proliferating (left box plot), and the percentage of proliferating cells shown to be active for TGFB signalling (right box plot) in 14 independent BCC samples. For each BCC sample the number of positive cells enumerated was based on the number of tumour nodules present within that sample; however over the 14 BCC samples, an average of five tumour nodules were enumerated per sample. Scale bar = 200 μ M.

3.2.8 Analysis of EMT related gene expression in whole BCC tissue

We next hypothesized that TGF β signalling may be involved in BCC tumour cell invasion into the stroma, consistent with our microarray findings. To confirm this we used the EMT core gene signature to define EMT within whole BCC (n=5) and normal skin (n=5) (Figure 3.12). In the 5 individual BCC samples studied, consistent with TGF β signalling induced EMT, there was concordant downregulation of E-Cadherin (CDH1) in 4/5 BCC samples tested, along with the upregulation of Runx1 (4 of 5 BCC), Runx2 (4 of 5 BCC), Slug (all 5 BCC), Snail (2 of 5 BCC), Twist1 (all 5 BCC) and vimentin (3 of 5 BCC) when compared to normal skin. However, there was discordant regulation of CDH2 and Zeb1, which showed downregulation rather than upregulation in 4 of 5 and 3 of 5 samples respectively. However when all 5 BCC samples were averaged together all of the genes described were not statistically significant in comparison to the control tissue, which is suggestive of the pattern of TGF β regulated EMT genes being unique between BCC tumours. With the exceptions of CDH2 and Zeb1, these findings suggest that BCC demonstrate TGF β dependent EMT.

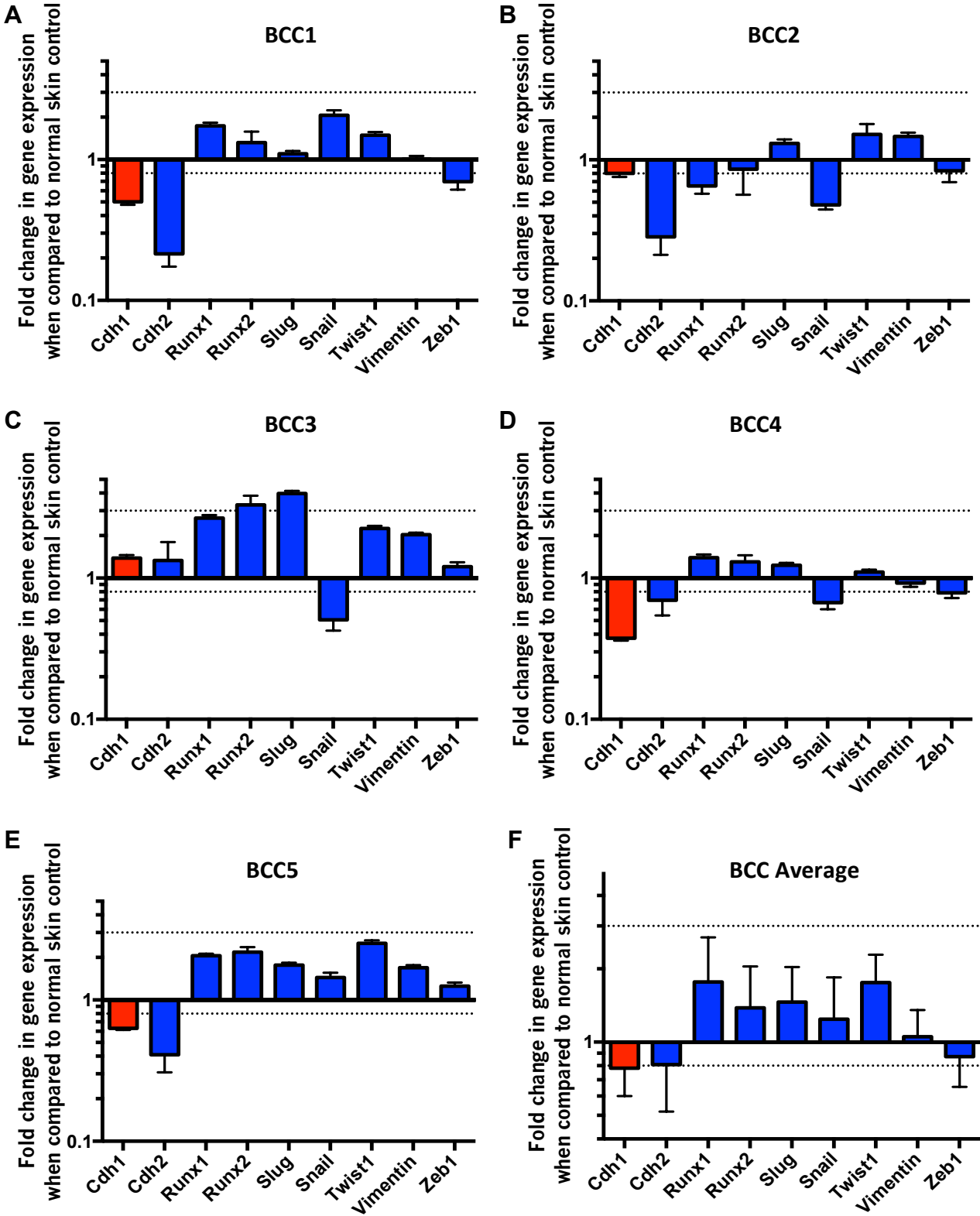


Figure 3.12: Expression of TGFβ regulated EMT genes in BCC tissue

RNA was extracted from whole primary human BCC tissue (n=5) and subsequently assayed for the expression of a panel of 9 TGFβ-associated EMT genes in order to identify an EMT profile within whole BCC tissue. Five individual BCC samples: (A) BCC1,

(B) BCC2, (C) BCC3, (D) BCC4, and (E) BCC5 were analysed by qPCR for the expression of these EMT genes in comparison to normal skin (n=5). **(F)** Represents the average expression over the 5 independent BCC samples relative to 5 normal skin samples. Red bars indicate genes that are expected to be downregulated in EMT, while the blue bars indicate genes that are expected to be upregulated in EMT. Dotted lines represent 2-fold changes in gene expression. Each experiment contained three internal technical replicates for each gene, along with two endogenous controls (β -Actin, and GAPDH).

3.2.9 Expression of TGF β pathway in BCC

To support our findings, qPCR was performed using the TGF β /BMP signalling RT(2) Profiler PCR Array (Qiagen, UK) containing primers for 84 genes related to TGF β /BMP-mediated signal transduction. This array allowed the expression of a focused panel of genes related to TGF β /BMP signalling to be analysed, from members of the TGF β superfamily of cytokines (Figure 3.13A) and their receptors (Figure 3.13B), along with SMAD (Figure 3.13C), and SMAD target genes (Figure 3.13D). Gene expression profiles shown in Figure 3.13 A-D were categorised by Qiagen using their online software to process the qPCR results. The ligands responsible for driving the canonical Activin/TGF β signalling side of the pathway, notably TGF β 1, 2, and 3, were all elevated by two-fold or more, with TGF β 1 and 3 found to be statistically significant ($p < 0.05$; and $p < 0.01$, respectively). In contrast, the ligands responsible for driving signalling down the BMP side of the pathway were mostly down regulated (Figure 3.13A). All receptors involved in both sides of the pathway were up regulated, most by two-fold or greater, with the exception of the negative regulator of canonical Activin/TGF β signalling, TGFBR111, whose expression was over three-fold lower than that of the control (Figure 3.13B). In a similar manner to the microarray data, the expression of SMAD transcription factors was increased, in particular SMAD2 ($p < 0.05$), 3, and 4, whose expression was found to be 1.5-fold or greater in both the microarray and qPCR data sets (Figure 3.13C). Nearly 70% (18/26) of the Activin/TGF β -responsive genes were up regulated, while the inverse was observed for the BMP-responsive genes where 4/7 genes were found to be downregulated (Figure 3.13D). Therefore the expression levels obtained from the qPCR array mirrored the microarray results to a high degree, confirming canonical TGF β

signalling pathway activation in BCC, with prominent increased expression observed in the ligands, receptors, transcription factors, and genes regulated downstream.

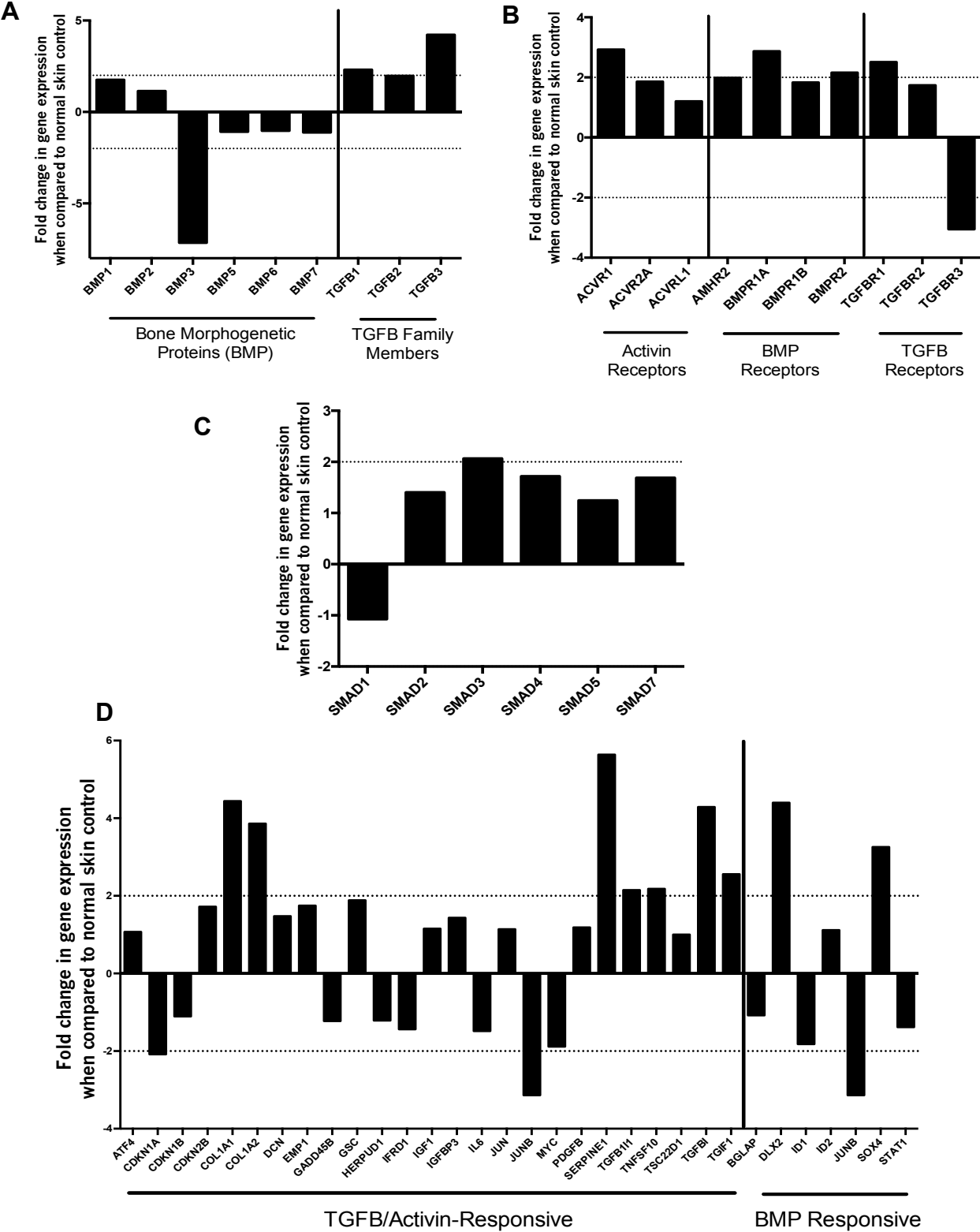


Figure 3.13: Expression of TGF β pathway ligands and receptors in BCC.

A qPCR array (Qiagen, UK) was performed on whole BCC RNA ($n=5$) in comparison to normal skin ($n=3$) to evaluate the expression of 84 genes related to the TGF β /BMP-signalling pathways. Gene expression values and profiles **(A-D)** were generated by Qiagen using their online software. **(A)** TGF β superfamily of cytokines, **(B)** Receptors, **(C)** Transcription factors, and **(D)** SMAD target genes. Dotted lines represent 2-fold changes in gene expression. Two endogenous controls were used for each sample studied (β -Actin, and GAPDH).

3.3 Discussion

In this chapter we performed microarray analysis on primary human BCC, SCC and normal skin samples to assess the relevance of TGF β signalling in BCC. When taking a whole genome approach comparing BCC to normal skin, a number of studies have performed microarray analysis in an attempt to enhance our understanding of the genetic and molecular basis of BCC (Heller *et al.*, 2013; Pellegrini *et al.*, 2017; Jayaraman *et al.*, 2014; Bonilla *et al.*, 2016). When studying the most highly significant genes within BCC tissue compared to normal skin, a large number of collagens and matrix remodelling enzymes were found to be highly upregulated. This observation is consistent with the pathogenesis of sporadic BCC as exposure to UV is the most important risk factor, and many of the collagens and MMPs are upregulated following exposure to UV light (Pittayapruek *et al.*, 2016). Furthermore, BCC has a high propensity to be locally invasive and destructive, therefore the remodelling and degradation of the ECM is a hallmark of both BCC and SCC development. Since BCC has the highest mutation rate of any cancer (closely followed by SCC) (Jayaraman *et al.*, 2014; Bonilla *et al.*, 2016), there was no surprise that in comparison to normal skin, BCC was found to have 1,664 significant differentially expressed genes ($p < 0.05$). As there were so many differentially expressed genes found to be significant, we began expression profiling in order to extrapolate pathways and processes relevant in BCC. To do this, functional pathway analysis using DAVID and GSEA was performed, and several pathways/processes were found to be significantly over-represented in BCC compared to normal skin, including: i) EMT, ii) TGF β signalling, iii) KRAS signalling, iv) WNT signalling, v) Hh signalling, and vi) MYC target genes. As alluded to earlier, the significant enrichment of EMT observed in BCC is to be expected due to the upregulation of collagens and proteins involved in ECM maintenance and remodelling. TGF β signalling was found to be the most significantly over-represented signalling pathway in BCC when compared to normal skin. This finding is in concordance with a study by Heller *et al.* (2013) who compared human BCC tissue against site-matched normal skin control samples and found several pathways to be significantly overrepresented in BCC, including TGF β signalling along with the previously well established roles of SHh and p53 (Heller *et al.*, 2013). The enrichment of the KRAS signalling pathway has also been

identified in other studies as being implicated in the pathogenesis of BCC (van der Schroeff *et al.*, 1990; Pierceall *et al.*, 1991; Bonilla *et al.*, 2016). Interestingly 'MYC target' genes, were also enriched in BCC tissue, which is consistent with a recent study by Bonilla *et al.* (2016), who performed genetic profiling of 293 BCC samples in comparison to normal skin and found that 85% of BCCs harbor additional driver mutations in other cancer-related genes, including recurrent mutations in MYC (30%) along with the upregulation of MYC target genes following GSEA (Bonilla *et al.*, 2016). Furthermore, although beyond the scope of their paper, Bonilla *et al.* (2016) identified 10 pathways/processes that were significantly over-represented in BCC tissue when compared to normal skin, with one of them being the TGF β signalling pathway (Bonilla *et al.*, 2016). A limitation of our microarray study however is the small sample size, with only four BCCs, three SCCs, and three normal skin samples processed, which can lead to poor random error estimates and inaccurate statistical tests of differential gene expression. Another limitation of using low BCC sample numbers is the inability to compare gene expression profiles/pathway enrichment profiles between histological subtypes of BCC, which would be possible if the sample size was larger. Comparing histological subtypes could potentially be of interest as some subsets of BCC have been associated with higher risks of recurrence than others, and therefore identifying what pathways predominate in these subtypes in comparison to others is important. However, in spite of this, the pathways that were found to be significantly over-represented in our study using GSEA were similar to that observed in a number of studies, including the study by Bonilla *et al.* (2016), who used a much larger sample size. Another potential factor that needs to be considered is the control samples used for the experiment. In this instance we used normal skin samples, which is in accordance with the vast majority of studies. However, evaluating the roles of SCs within BCC/Hh driven tumours is within the scope of this project, and there is significant evidence both by studies from our lab (Colmont *et al.*, 2013), and others (Youssef *et al.*, 2010; Wang *et al.*, 2011), to suggest that BCC has a follicular SC origin. Therefore, using follicular SCs may serve as a more accurate control sample for comparing gene expression profiles in microarray studies. One important consideration is the fact that the HF contains several distinct SC populations, therefore for the purposes of our research, the CD200+ bulge stem cell population could be used a control, since previously published papers from

our lab indicate BCC may be derived from this population (Colmont *et al.*, 2013; Colmont *et al.*, 2014).

Our microarray results highlight that, although the most significant pathogenic event in BCC is the constitutive activation of the Hh signalling cascade, BCC has a much more complex genetic network of cancer-related genes. Numerous studies have shown that GLI activity can be positively regulated by a number of pathways including TGF β , KRAS, PI3K-AKT, and PKC (Seto *et al.*, 2009; Rajurkar *et al.*, 2012; Ramaswamy *et al.*, 2012; Deng *et al.*, 2015), and therefore are involved in BCC tumour progression. In particular, crosstalk between TGF β and Hh signalling pathways is well established, with TGF β signalling shown to induce Hh expression, which in turn activates GLI1 and GLI1-dependent EMT in non-small cell lung cancer cells (Maitah *et al.*, 2011). Furthermore, SMAD TFs have been shown to interact with the GLI TFs, where in several cell types, TGF β /SMAD3 has been demonstrated to directly induce the transcription of GLI2, which in turn upregulates GLI1 (Dennler *et al.*, 2007). Therefore, our microarray data supports the role of TGF β signalling in Hh-driven BCC. Given the fact that TGF β signalling enrichment has also been observed in other BCC studies (Bonilla *et al.*, 2016; Heller *et al.*, 2013), and that the crosstalk between Hh and TGF β signalling pathways is very well established (particularly in BCC) (Dennler *et al.*, 2007; Javelaud *et al.*, 2012), we then explored the role of TGF β signalling in BCC further using immunofluorescence and qPCR.

We confirmed TGF β signalling by labelling BCC samples with the TGF β associated transcription factor pSMAD3, using nuclear localisation of the pSMAD3 protein as evidence of active TGF β signalling. The pSMAD3 antibody was optimized by treating the human keratinocyte cell line, HaCaT, with and without TGF β 1 at a concentration of 20 ng/mL for 1hr before performing immunofluorescence. Nuclear pSMAD3 levels were shown to increase in the HaCaT cell line following treatment; however, an important point to note is that the experiment performed in Figure 3.8 lacked a true negative control, in that the cells were not treated with a receptor kinase inhibitor such as SB431542 and therefore pSMAD3 staining was not shown to be truly negative. Nevertheless, in BCC, 74% of all nuclear pSMAD3 positive cells within K14 positive BCC

tumour nodules were located within the basal layer and immediate two suprabasal cell layers. Furthermore, when enumerating all of the DAPI positive cells at the tumour nodule periphery, 31% were positive for pSMAD3 staining. This is important since it is where proliferation and invasion occur and is where our lab previously identified the CSC population in BCC using immunofluorescence. The presence of cells active for TGF β signalling at the invasive tumour edge has been observed in SCC (Oshimori *et al.*, 2015). In this study, Oshimori *et al.* (2015) observed intense pSMAD2 staining in a subset of basal tumour cells at the invasive tumour front, which were identified as being slow cycling SCs responsible for fueling tumour heterogeneity and drug resistance (Oshimori *et al.*, 2015). A previous study by the same group used CD34 to identify in SCC, two highly tumourigenic CSC populations that were enriched for integrins. These populations co-existed together at the tumour-stroma interface and were reliant on TGF β /focal adhesion kinase signaling for their growth (Schober and Fuchs, 2011). Other cancer types have also demonstrated the presence of CSC at the invasive tumour edge, including a study by Ye *et al.* (2012) on glioma who demonstrated the presence of CD133+ glioma stem-like cells at the invasive front which became more invasive following treatment with TGF β 1 (Ye *et al.*, 2012). Finally, a study by Stankic *et al.* (2013) demonstrated in breast cancer that the expression of ID1 (a gene responsible for breast cancer colonization) was regulated by TGF β signalling in mesenchymal-like breast cancer cells at the invasive edge (Stankic *et al.*, 2013). BCC CSC population is studied in more detail in chapter 4.

Another important consideration for future work is assessing the role of pSMAD2 rather than solely pSMAD3. SMAD2 and 3 are mostly considered to be equally important in mediating TGF β signals and are functionally interchangeable (Souchelnytskyi *et al.*, 1997; Brown *et al.*, 2007; Massague *et al.*, 2005; Liu *et al.*, 2004), which as a consequence means the vast majority of studies use either pSMAD2 or 3 as an output for active TGF β signalling. However, it is important to note that their roles are context dependent, and at the biochemical level, several lines of evidence have demonstrated obvious differences between SMAD2 and 3, including the observation that in a basal state, SMAD2 is found as a monomer, whereas SMAD3 exists in oligomeric states (Jayaraman and Massague, 2000). Other differences include the fact that SMAD3 can

bind DNA through its β -hairpin DNA-interaction motif within the MHI region, whereas SMAD2 cannot (Shi *et al.*, 1998; Dennler *et al.*, 1999; Yagi *et al.*, 1999); and that SMAD2/4 or SMAD3/4 oligomers enter the nucleus with assistance from different proteins, where SMAD3/4 can enter through importin- β 1 and a Ran dependent mechanism, whereas the SMAD2/4 oligomer cannot (Xiao *et al.*, 2000; Kurisaki *et al.*, 2001). Finally, a recent study by Liu *et al.* (2016) found that SMAD2 and 3 had differential sensitivity in transducing TGF β signalling and have functionally distinct roles in regulating early developmental events (Liu *et al.*, 2016).

As the BCC tumour periphery contains both dividing and invading cells, whereas the inner cell mass is associated with differentiation, we next sought to determine the functional role of TGF β signalling at the invasive edge. In normal cells, the TGF β signalling pathway exerts tumour suppressor effects by regulating cell growth, death, and immortalization. However, the protective and cytostatic effects offered by TGF β are often lost as a tumour begins to develop and progress. As a consequence, TGF β signalling then switches to promote tumour progression, invasion, and metastasis. Two major ways TGF β signalling achieves this are: 1) progression through the cell cycle, achieved through inactivation of the retinoblastoma gene, and 2) EMT. When evaluating the role of TGF β signalling in cell proliferation, we found that only 10% of pSMAD3 positive BCC cells were proliferating, which is suggestive of TGF β signalling-induced G1 arrest; thus, TGF β was therefore not considered to have a role in proliferation. As a consequence, we next hypothesized that TGF β signalling may be involved in tumour cell invasion into the stroma. EMT has been implicated in both the progression and metastasis of tumours. Epithelial cells that undergo EMT lose contact with their neighbouring cells and rearrange their cytoskeletons, which contribute to them becoming more motile and invasive. Therefore, we analysed EMT related gene expression in whole BCC tissue, and although BCC do not frequently metastasize, consistent with TGF β signalling, upregulation of EMT related genes, notably Runx1, 2, Slug, Snail and Twist, along with the downregulation of E-Cadherin was observed in BCC when compared to normal skin. This is consistent with the microarray data, where enrichment in EMT was observed in BCC in comparison to normal skin following GSEA. The slight variation in EMT gene expression observed between all five BCC samples

could potentially be explained by the samples being of different subtypes (subtype information was not provided), as some subtypes have been shown to be more infiltrative and therefore more aggressive than others, which could impact on the expression of the genes studied. As alluded to earlier the presence of EMT related genes within BCC is not unusual as it is locally invasive and highly destructive. For example, CAFs within the stroma have been shown to have involvement in BCC tumour progression (Sasaki *et al.*, 2018; Omlandet *et al.*, 2017; Mickeet *et al.*, 2007), and given our observation that cells at the tumour nodule periphery are active for TGF β signalling, focusing on the tumour-stroma interface in BCC may be interesting for potential future work.

Finally, to determine at what level the TGF β signalling pathway was perturbed in BCC, we determined the gene expression of an array of TGF β and BMP pathway genes captured in a 384 well plate qRT-PCR array (Qiagen, UK). We identified increased expression of TGFBR1 and II, added to which was the increased expression of the transcription factors, SMAD3 and 4. Conversely, ligands responsible for activating the BMP side of the pathway, such as GDF5, 7 and BMP3 were found to be downregulated along with TGFBR3, which is a negative regulator of the TGF β signalling pathway. These observations support findings in the literature that have shown BMP signalling to be a potent tumour suppressor in the epidermis and HF (Blessing *et al.*, 1995; Sharov *et al.*, 2009). Other observations included the upregulation of SerpinE1 and DLX2, both of which are SMAD2/3 regulated, and have been shown to drive tumour invasion in a number of cancers (Choi *et al.*, 2016; Klein *et al.*, 2012; Samarakoon *et al.*, 2009). Thus the TGF β signalling pathway constituents were amplified in BCC, consistent with increased signalling.

In summary we have shown that TGF β signalling is enriched/over-represented in BCC tissue compared to normal skin when studying gene expression profiles through microarray and qPCR. We have shown that the tumour nodules within BCC are active for TGF β signalling, and that the majority of these cells are found at the invasive edge of the tumour nodules. This is important, as our lab has previously shown that BCC growth is dependent on CSCs and that they reside at the tumour nodule periphery (Colmont *et*

al., 2013; Colmont *et al.*, 2014). We found that these cells were not involved in proliferation, but rather may be associated with invasion. Therefore, we next hypothesised that BCC CSCs may be active for TGF β signalling, which is addressed in the following chapter.

Chapter 4: Determination of TGF β Signalling in Human BCC CSC

Chapter 4 Determination of TGF β Signalling in Human BCC CSC

4.1 Introduction

The human HF undergoes cyclical growth in response to mesenchymal signals (Alonso and Fuchs, 2006; Hsu and Fuchs, 2012). Upon receiving mesenchymal TGF β 1, CD200+ HF cells in the outer layers of the hair bulge become activated, heralding the onset of anagen (Oshimori *et al.*, 2012). During anagen, HF bulge keratinocytes proliferate and egress from the bulge during expansion of the HF. The human BCC cell of origin is thought to be the long-lived HF bulge SC population, which are sufficiently long lived to acquire mutations that enable transformation (Wang *et al.*, 2011; Seykora and Cotsarelis, 2011). Once BCC is established, we have shown that CD200+ CSC are capable of maintaining and propagating tumour growth, while the bulk population undergoes terminal differentiation (Colmont *et al.*, 2013).

It has been shown that CSC population may be responsible for resistance to conventional chemotherapies and subsequent relapse, both during and after treatment (Holoan *et al.*, 2013). For example, in a mouse model of glioblastoma, a population of quiescent tumour cells survived treatment with temozolomide and were found to be capable of regenerating the tumour (Chen *et al.*, 2012). Moreover, targeted therapies that block oncogenic pathways that drive tumour growth (e.g. Hh, mitogen-activated protein kinases, vascular endothelial growth factor, and the Abelson tyrosine kinase and the chromosome 22 break point cluster fusion gene) have also been associated with resistance and relapse. Notably, a number of case reports show an initial regression of BCC following vismodegib treatment, followed by an inevitable relapse of the tumour (Von Hoff *et al.*, 2009; Skvara *et al.*, 2011; Sekulic *et al.*, 2012).

Our preliminary data suggest that BCC cells demonstrate increased expression of TGF β pathway genes upon exposure to vismodegib *in vitro* based on preliminary microarray (Affymetrix) analysis. Consistent with TGF β responsiveness, I have found active TGF β signalling within a sub-population of BCC cells located at the tumour periphery, wherein

reside BCC CSC. These observations support our hypothesis that TGF β signalling provides a cell survival signal for BCC CSC.

4.2 Results

4.2.1 CD200+ BCC cells are pSMAD3 positive in tissue sections

To define TGF β signalling within the BCC CSC population, I sought to determine pSMAD3 presence and localisation by immunofluorescent staining within the CD200 and keratin 14 expressing BCC CSC population. As previously described, CD200 expression was observed in a select subset of tumour cells within BCC nodules at the tumour periphery. In all the BCC tissue sections where BCC CD200 and K14 co-expression was observed, we simultaneously observed nuclear accumulation of pSMAD3 (Figure 4.1) (n=2). Due to the paucity of the CD200+ cells within BCC tissue, it was difficult to visualize and identify this population when studying whole tissue by immunofluorescence. However, these findings support our hypothesis and show that BCC CSC demonstrate active TGF β signalling that may be relevant for CSC maintenance.

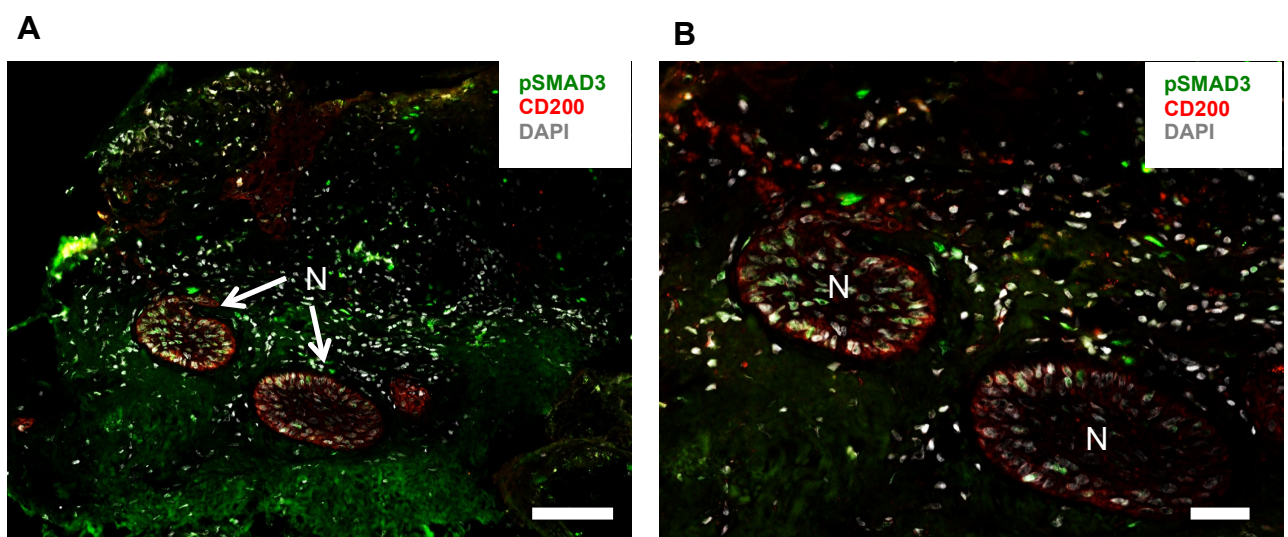


Figure 4.1: CD200 expressing BCC CSC are active for TGF β signalling

Primary human BCC tissue sections were labelled for immunofluorescence with antibodies to pSMAD3, CD200, and keratin 14 (not shown), then stained with DAPI. Immunofluorescent microscopy (10x image A and 20x image B) revealed the presence of CD200 (red) expressing BCC cells within the tumour nodule (N) at the periphery. Scale bars represent 200 μ M. (n=2)

4.2.2 Isolation of CD200+ BCC cancer SCs by flow sorting

To further characterize the BCC CSC population, we optimized flow cytometry and FACS to isolate CD200+ CD45- cells (CSCs) to determine active TGF β signalling (Figure 4.2). BCC samples obtained within 8 hours of cutaneous surgery, from dermatology departments in two University Health Boards as part of an approved clinical study, were dissociated as outlined in section 2.1.2, and single cells labelled for flow sorting (Section 2.4.5).

All BCC samples contained a small CD200⁺ tumor cell population (1.63 \pm 1.11%; range, 3.96–0.05%; n=21; Figure 4.2A, population Q4), irrespective of the histological type (Colmont *et al.*, 2013). BCC also contained CD45⁺ tumour-associated leukocytes that accounted for 13.81 \pm 10.84% (n=21) of all cells and included a subpopulation of CD200⁺ CD45⁺ cells (0.66 \pm 0.7%; Figure 4.2A, population Q1). Thus, CD200⁺ BCC tumour cells could be distinguished by flow cytometry with the pan-leukocyte marker CD45 to exclude tumour-infiltrating leukocytes. BCC CD200⁺ CD45⁻ and CD200⁻ CD45⁻ subpopulations were isolated by flow cytometry with greater than 86% and 98% purity, respectively (Figure 4.2B).

To confirm active TGF β signalling we undertook immunofluorescence by flow sorting individual cells onto a glass slide (see section 4.2.3), and qPCR analysis by flow sorting directly into RLT buffer for RNA extraction (see section 4.2.4).

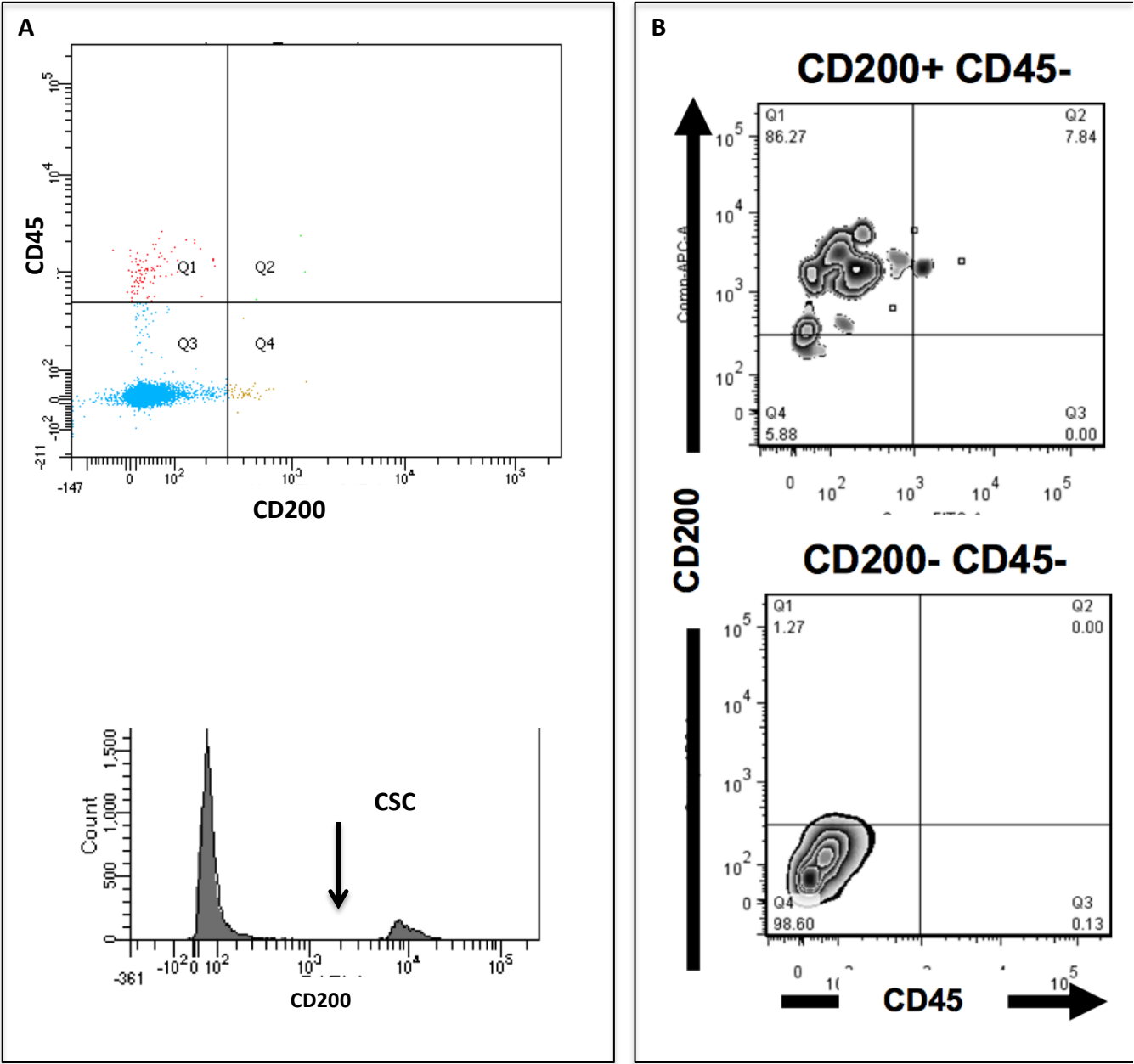


Figure 4.2: CD200+ and CD200- BCC cells isolated using flow sorting.

Enzymatically dissociated BCC tissue labelled with the cell surface markers CD200 and CD45 were flow sorted using a FACS ARIA. (A) FACS dot plot (top plot) and histogram (bottom plot) profiles were determined using unlabelled and isotype controls. The pan-leukocyte marker CD45 was used to eliminate tumour-infiltrating leukocytes (Q1). CD200+ CD45- represented the BCC CSC population (Q4), while CD200- CD45- represented the non-CSC BCC population (Q3). A representative single parameter

histogram, right hand side plot, shows the selected CD45⁻ population with a distinct CD200⁺ CSC population. **(B)** A density plot to show that the CD200⁺ CD45⁻ (top plot) and CD200⁻ CD45⁻ (bottom plot) subpopulations were isolated with greater than 86% and 98% purity, respectively (Taken from Colmont et al., 2013). Dead cells were excluded using 7-AAD.

4.2.3 CD200 Expressing BCC CSCs are pSMAD3 positive

To determine pSMAD3 labelling and therefore active TGF β signalling within the BCC tissue CD200⁺ BCC cells, we sought to determine pSMAD3 expression. Based on the literature and our own experimental findings, the available reagents did not allow for flow cytometric determination of pSMAD3 expression. Instead, we undertook immunofluorescent labelling of flow sorted CD200⁺ versus CD200⁻ BCC cells using cell surface proteins CD200, Epcam and CD45. Flow sorted CD200⁺ Epcam⁺ CD45⁻ and CD200⁻ Epcam⁺ CD45⁻ subpopulations were directly placed onto a glass slide via the FACS Aria, (n=3, with an average of 50 cells counted per sort for each cell population). Each droplet was allowed to dry and was then immunofluorescence labelled for pSMAD3 (Figure 4.3). Nuclear labelling of pSMAD3 was evident within a greater proportion of the CD200⁺ population, with 56.4 \pm 2.7% of the total BCC CSC population (Figure 4.3A&C), compared to non-CSC BCC keratinocytes, which had 16.8 \pm 5.2% nuclear pSMAD3 positivity (p<0.05) (Figure 4.3 B&C). Quantification of the relative intensity of nuclear pSMAD3 staining, the relative fluorescent intensity (RFI) of the CD200⁺ population was also greater, 33,699 \pm 6,524, compared to the CD200⁻ population, which was 8,011 \pm 1,471 (Figure 4.3D), however this increase did not reach statistical significance. In summary, nuclear pSMAD3 and therefore active TGF β signalling was observed in CD200⁺ BCC CSC and also demonstrated a 4-fold increase in staining intensity.

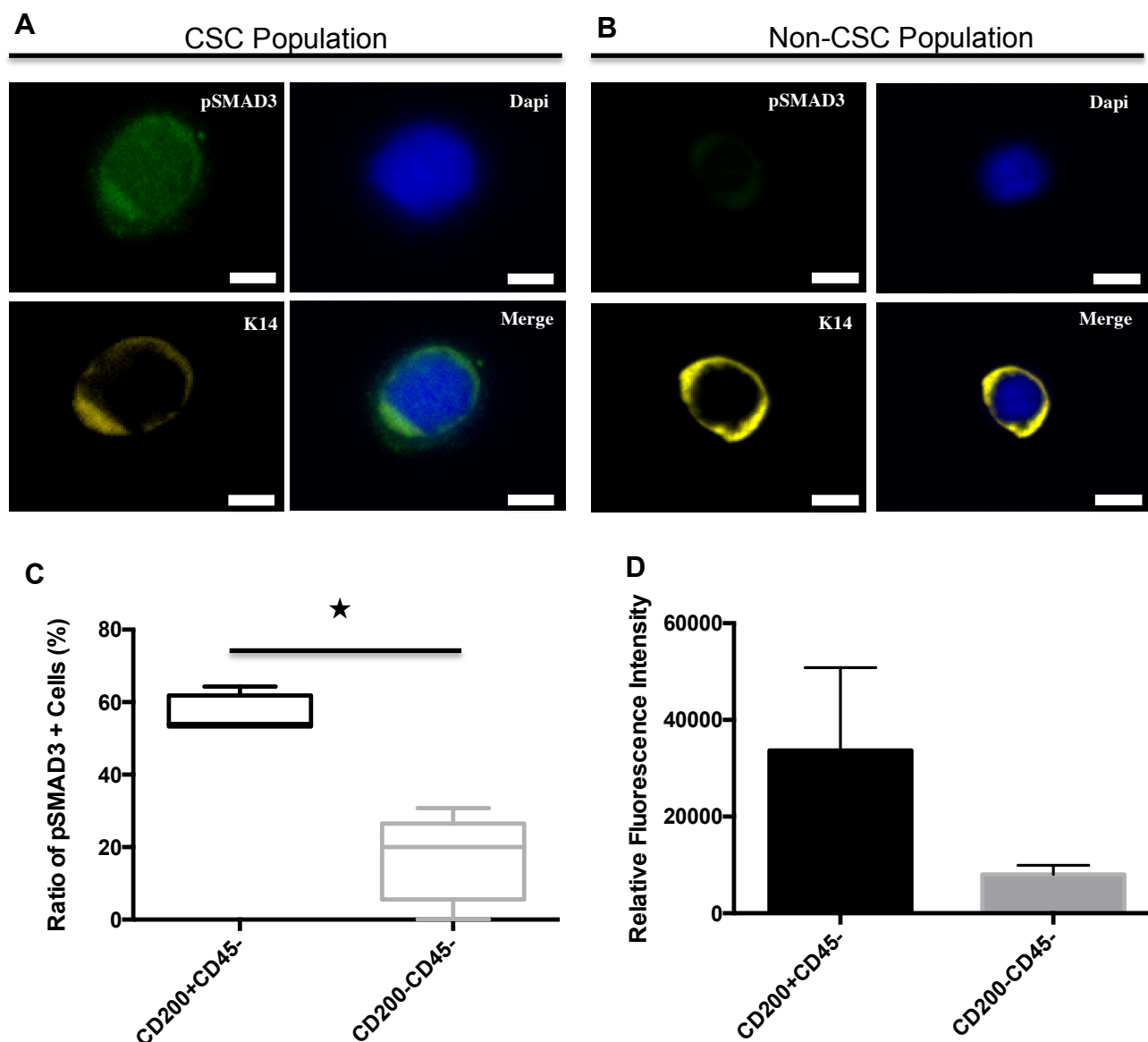


Figure 4.3: CD200 expressing CSC display TGF β signalling pathway activation

Enzymatically dissociated BCC tissue were labelled with the cell surface markers CD200, EPCAM and CD45, then flow sorted directly onto glass slides. The sorted cells were fixed then labelled for immunofluorescence with antibodies to pSMAD3 and K14, and stained with DAPI. (A&B) Immunofluorescent microscopy demonstrated the presence of nuclear pSMAD3. (C) Bar graph shows the percentage of cells found to be positive for pSMAD3 relative to the total number of cells stained in both cell populations. (D) Bar graph shows the average level of nuclear pSMAD3 fluorescent intensity for each cell population. The relative fluorescent intensity was quantified using ImageJ software and values were

obtained from an average over 3 independent experiments ($n=3$). Performed two-tailed *T*-test to determine statistical significance. * represents $p<0.05$. Scale bar = 10 μ M.

4.2.4 Obtaining RNA from low numbers of flow sorted cells

A number of issues arose when isolating RNA from cell populations using this approach. In BCC samples the CD200+CD45- population represents 1.63% \pm 1.11% of the total cell population (Colmont *et al.*, 2013). As BCC tumour samples tended to be small, we typically obtained 10 ng/ μ L of RNA per population per sort. The quality of the RNA was verified using a Bioanalyser™, with an RNA Agilent 6000 Pico Chip. Although the RNA yield was very low, the RNA quality was excellent, with RNA Integrity Numbers (RIN) in the range of 9-10 frequently being obtained, which represents near perfect RNA (Figure 4.4). Therefore, the RNA achieved from our flow sorting was of sufficient quality to run qPCR analysis on this population for a small number of genes.

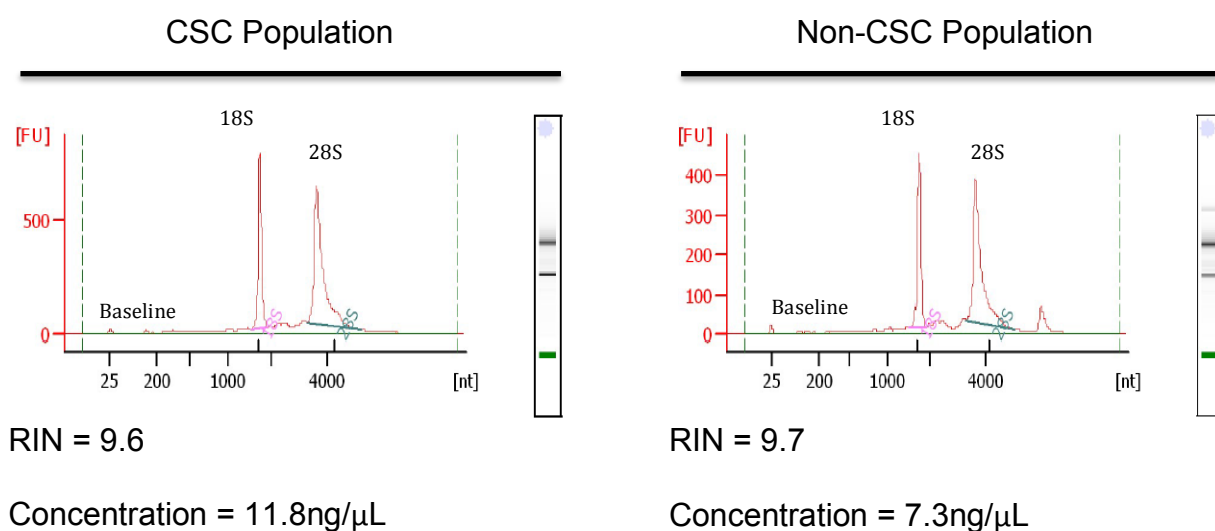


Figure 4.4: Analysis of RNA integrity from flow sorted CSCs have good quality, but very low yields.

Electropherogram generated from and Agilent 2100 Bioanalyzer showing good integrity of RNA in both flow sorted populations, as shown by a flat baseline and distinct peaks of both 18S and 28S ribosomal RNA. Left panel: CD200+CD45- population. Right panel: CD200-CD45- population.

4.2.5 CD200 Expressing CSC Display EMT Gene Signature

To confirm active TGF β signalling in BCC CSC, I performed RT-PCR on flow sorted CD200+ EPCAM+ CD45- and CD200- EPCAM+ CD45- cells (CSCs) using a panel of TGF β regulated EMT genes. All genes studied in this panel have well-established roles in the process of EMT (Kalluri and Weinberg, 2009; Lamouille *et al.*, 2014). Concordant regulation of TGF β regulated EMT genes was observed within BCC CSC compared to the non-CSC population (Figure 4.5). There was a 7.5 ± 0.5 -fold reduction in expression of E-cadherin. Increased expression genes driving EMT were also observed, including Runx1 (20.2 ± 3.0), Slug (1.8 ± 0.5), Snail1 (454.0 ± 22.0), Twist 1 (6.4 ± 1.8), vimentin (5.8 ± 0.3), and Zeb1 (2.3 ± 0.3). These findings support the role of TGF β signalling within BCC CSC, moreover the levels of EMT expression suggest that these cells at the tumour periphery are actively involved in tumour invasion.

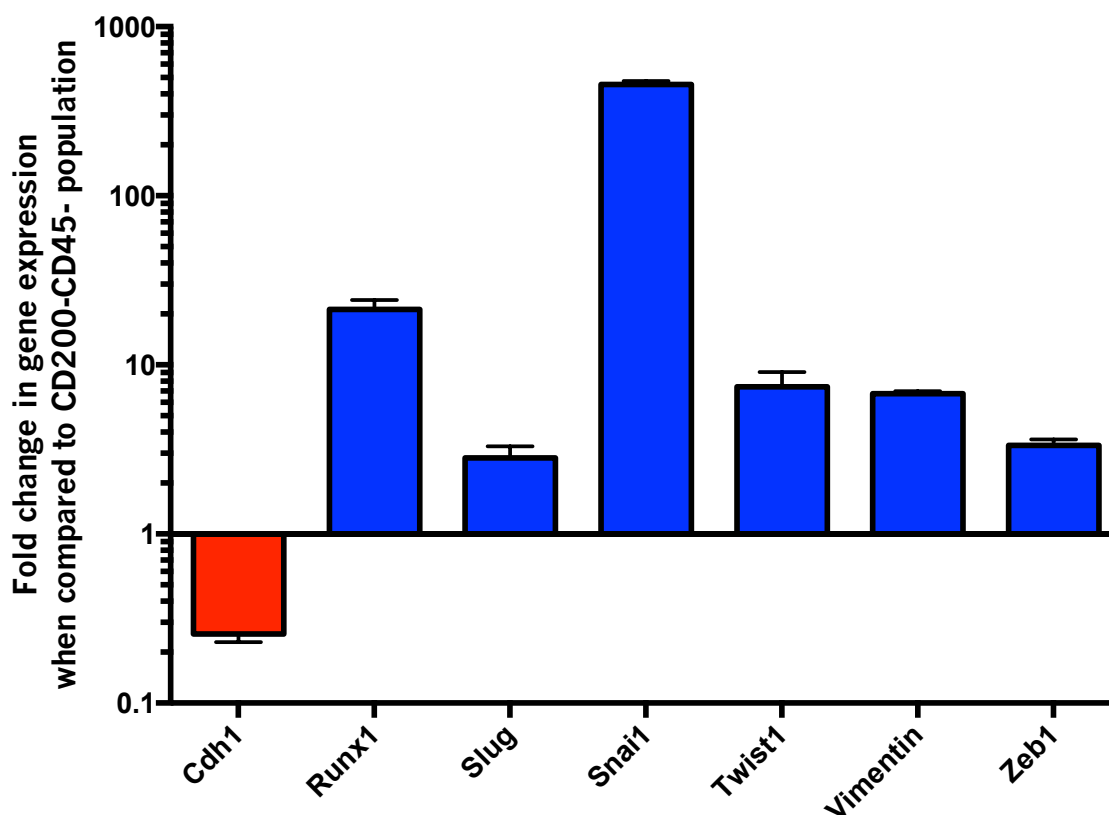


Figure 4.5: CD200+ EPCAM+ CD45- BCC cells demonstrate TGF β regulated EMT

CD200+ BCC cells (CSC) were sorted directly into RLT buffer and RNA extracted before being assayed for the expression of a panel of 7 TGF β -associated EMT genes in order to identify an EMT profile within the CSC population. BCC CSC display a distinct TGF β regulated gene signature in comparison to normal skin keratinocytes (n=1). Red bars indicate genes that are downregulated in EMT, while the blue bars indicate genes that are upregulated in EMT. This experiment (n=1) contained three internal technical replicates for each gene, along with two endogenous controls (β -Actin, and GAPDH).

4.3 Discussion

In this chapter, we have isolated CSCs from whole BCC tissue in an attempt to elucidate the mechanisms of resistance in Hh driven cancers. We have shown that CSCs isolated from the Hh driven cancer, BCC, were active for TGF β signalling. Immunofluorescent labelling of BCC tissue confirmed the presence of BCC CSC at the tumour periphery, and were shown to be positive for nuclear pSMAD3, which is consistent with what is observed in the HF SCs from which BCC are thought to be derived (Youssef *et al.*, 2010; Wang *et al.*, 2011; Colmont *et al.*, 2013). This was verified and enumerated within the CD200+ flow sorted population, demonstrating that 56% of all cells exhibit nuclear pSMAD3, compared to their negative counterparts, which was at 17%. This observation is consistent with other cancer types, where the role of TGF β signalling has also been identified in the CSC population (Bruna *et al.*, 2012; Lo *et al.*, 2012; Bhola *et al.*, 2013; Shipitsin *et al.*, 2007, You *et al.*, 2010; Mima *et al.*, 2012, Ikushima *et al.*, 2009; Penuelas *et al.*, 2009, Oshimori *et al.*, 2015), with some of these studies highlighting the existence of CSC at the tumour-stroma interface (Oshimori *et al.*, 2015; Schober and Fuchs, 2011; Ye *et al.*, 2012; Stankic *et al.*, 2013). Furthermore, some of these studies have implicated the CSC population at the leading edge as being responsible for drug resistance and/or tumour relapse (Oshimori *et al.*, 2015; Schober and Fuchs, 2011; Colmont *et al.*, 2013; Stankic *et al.*, 2013). Importantly, the role of CSC in Hh antagonist resistance has been suggested in BCC within the clinic (Von-Hoff *et al.*, 2009; Skvara *et al.*, 2011; Sekulic *et al.*, 2012; Tang *et al.*, 2012). In fact, our group has previously shown that BCC CSCs both constitutively express and induce ABCG2 expression following etoposide treatment (Colmont *et al.*, 2014), and are resistant to vismodegib treatment (Colmont *et al.*, 2013). Furthermore, our group demonstrated that this CD200+ population was capable of recreating BCC tumour growth *in vivo* (Colmont *et al.*, 2013). Therefore, this CD200+ BCC CSC population demonstrates resistance towards Hh antagonists, and we have shown in this chapter that this same CSC population has increased TGF β signaling activity, and is located at the tumour nodule periphery. We also demonstrated in the previous chapter that cells at the tumour nodule periphery active for TGF β signalling were not associated with proliferation, which raised the possibility that they may be involved with invasion. Our microarray analysis on whole

BCC tissue identified an enrichment for EMT related genes, and gene expression analysis using a panel of TGF β -related EMT genes showed that there was significant enrichment in the BCC CSC population, suggesting that these cells may be involved in EMT. The link between EMT and SCs/CSCs was highlighted by Mani *et al.* (2008) and has important implications in tumour heterogeneity, therapeutic resistance, and disease progression. EMT-TFs have been shown to bestow cancer cells with the capacity to adapt to environmental stresses and resistance to apoptosis. EMT-TFs render cancer cells resistant to chemotherapy and radiotherapy (Sanchez-Tillo *et al.*, 2012). For example, the aberrant expression of Slug and Snail has been shown to alter the response to DNA damage induced by doxorubicin treatment in cancer cells (Kajita *et al.*, 2004), and has also been shown to contribute directly to cisplatin resistance in ovarian cancer (Haslehurst *et al.*, 2012). Furthermore, the expression of EMT related genes has been shown to correlate with sensitivity towards growth factor targeted therapies. For example, the sensitivity of lung cancer cells towards the EGFR tyrosine kinase inhibitor, gefitinib, has been shown to correlate with the expression of E-cadherin (Witta *et al.*, 2006), and knockdown of Snail has shown to increase the sensitivity of these lung cancer cell lines to cisplatin (Zhuo *et al.*, 2008). This therefore raises the possibility that CSCs may be involved not only with BCC tumour development/invasion, but also in the refractory response observed following Hh antagonist treatment.

The link between EMT and GLI-dependent gene regulation has already been established (Li *et al.*, 2006), which when coupled with TGF β being a prototypic cytokine capable of inducing the phenotypic switch in EMT (Zavadil and Bottinger, 2005), has led to suggestions that GLI-dependent mechanisms take place downstream of TGF β in connection with EMT. In fact this crosstalk has already been implicated in EMT/invasion in a number of other cancer types, including bladder cancer, where in a series of bladder cancer cell lines it was found that Hh-independent GLI2 expression and function was linked to invasiveness, with suggestions that this non-canonical Hh activity was contributed by RAS and TGF β signalling (Mechlin *et al.*, 2010). Furthermore, in a breast cancer progression mouse model, TGF β 1 has shown to be responsible for both increased GLI2 expression and GLI-dependent transcription in MCFDCIS cells (Hu *et al.*, 2008), and upon implantation into mice, ductal carcinoma in situ (DCIS) tumours were

shown progress to invasive tumours (Miller *et al.*, 2000). In this paper, the authors found that TGF β -dependent GLI2 expression was capable of promoting myoepithelial cell differentiation and progression to invasion. Finally, it was reported that in recurrent ovarian tumours, CSCs overexpressed GLI1 and 2 together with effectors of the TGF β pathway when compared to the primary tumours, and that the recurrent tumours demonstrated resistance to cisplatin (Steg *et al.*, 2012). Therefore it is possible that there is crosstalk between the TGF β and Hh signalling pathways in the BCC CSC population and that this crosstalk may be implicated in EMT/invasion.

Given our ability to isolate excellent quality RNA from the BCC CD200+ CSC population, one important future experiment would be to evaluate this population using RNA sequencing in order to explore the transcriptional profiles of this population further and develop a better understanding of its role in tumour progression and drug resistance by comparing treated and untreated populations. Furthermore, sequencing will allow us to identify what gene signatures are enriched within the CSC population, which has been used to good effect in other studies, such as Schober and Fuchs (2011), who used RNA sequencing to show that the CD34 CSC population within SCC was enriched for genes involved in the cell cycle, mitosis, epithelial morphogenesis and apoptosis, along with the involvement of signaling pathways including MAPK4, FAK, and TGF β , relative to wild-type SCs. They further showed that these cells had a down-regulation of cell-cell adhesion genes including E- and α -cadherin, suggestive of cytoskeletal and adhesion remodeling within this population, which they concluded was correlated with the features that typify the CSC microenvironment at the edge of the tumour-stroma interface (Schober and Fuchs, 2011).

The findings within this chapter raise two important questions: (1) is TGF β signalling an important CSC survival pathway?; and (2) alternatively, after Hh antagonist treatment is there an enrichment of active TGF β signalling? Therefore, in order to explore this further we recruited the use of three well-established Hh driven tumour cell lines to address these questions in the next chapter.

Chapter 5: Hh and TGF β Pathway Antagonists in Hh Driven Tumours

Chapter 5 Hedgehog and TGF β Pathway Antagonists in Hedgehog Driven Tumours

5.1 Introduction

25% of all cancer types demonstrate constitutive activation of the Hh growth factor signalling pathway including breast, pancreas, gastrointestinal, prostate, mesenchymal, haematological, and neural malignancies. BCNS as previously mentioned is an autosomal dominant disorder that is caused by a germline mutation in the PTCH1 gene resulting in active Hh signalling (Aszterbaum *et al.*, 1998; Hahn *et al.*, 1996). This predisposes individuals with the disease to craniofacial and skeletal abnormalities (Gorlin and Goltz, 1960; Kimonis *et al.*, 1997), and greatly increases their risk of developing BCC and medulloblastoma. Therefore, although BCC is the archetypal tumour for Hh driver mutations, medulloblastoma is also strongly linked with Hh driver mutations and pathway activation. One of the limitations of using BCC as a model for studying Hh signalling is that the number of cell lines available in both human and mouse is very limited, and the cell lines that are available (e.g. TE 354.T; ATCC CRL-7762) are notoriously slow growing and cannot be used in stem cell assays since they do not form spheres in non-adherent culture conditions. Therefore, the assays performed in this chapter will be carried out using medulloblastoma cell lines as they are still highly relevant to this project and there are over 40 medulloblastoma cell lines currently available, with approximately half of these being sub-grouped and characterised (18/44) (Ivanov *et al.*, 2016); furthermore, these cell lines can be used in stem cell-based assays. Of the 18 cell lines that have been characterised, four have been classified as SHh-cell lines, and comprise the DAOY, UW228-2, ONS-76, and UW426 cell lines. Both DAOY and UW228-2 cell lines harbour TP53 mutations, and represent high-risk aggressive medulloblastoma (Ivanov *et al.*, 2016), and were therefore used in our experiments. The osteosarcoma cell line, SJSA-1, was also used in our experiments, but was chosen as osteosarcoma is also associated with Hh driver mutations and/or pathway activation, and this cell line is well documented as having a 15-fold GLI amplification (Khatib *et al.*, 1993). Therefore, although the SJSA-1 cell line is not considered to be as dependent on

Hh signalling for its growth as the DAOY and UW228-2 cell lines, it does nevertheless have some reliance on the pathway, and might serve as a good reference in our experiments. Hence all cell lines used in this chapter should respond to the two-targeted therapies that block the Hh pathway, notably vismodegib and sonidegib, which, have both been approved for clinical use by the Federal Drug Administration and European Medicines Agency (Figure 5.1).

The steroidal alkaloids cyclopamine and jervine are naturally occurring Hh pathway antagonists, which act to inhibit SMO and have formed the basis for targeted therapy development (Chen *et al.*, 2002). Vismodegib (GDC-0449, Genentech/Curis Inc.), a small-molecule SMO antagonist belonging to the 2-arylpyridine class, was the first SMO antagonist to be approved for clinical use in the treatment of BCC (Sekulic *et al.*, 2012; Tang *et al.*, 2012). Clinical studies have shown that vismodegib treatment is associated with therapeutic response in 43% of patients with locally advanced BCC, and 30% for metastatic BCC (Von-Hoff *et al.*, 2009; Sekulic *et al.*, 2012). Furthermore, vismodegib was shown to reduce the tumour burden and block growth of new BCCs in individuals with basal cell nevus syndrome (Tang *et al.*, 2012). LDE-225/Sonidegib (Novartis) is a potent, oral, SMO antagonist (Buonamici *et al.*, 2010). Patients with Gorlin syndrome and sporadic BCC showed a response to treatment with sonidegib (Skvara *et al.*, 2011). GANT-61 is a small molecule inhibitor that directly inhibits GLI1 and 2 (Mechlin *et al.*, 2010; Kawabata *et al.*, 2011; Yan *et al.*, 2011).

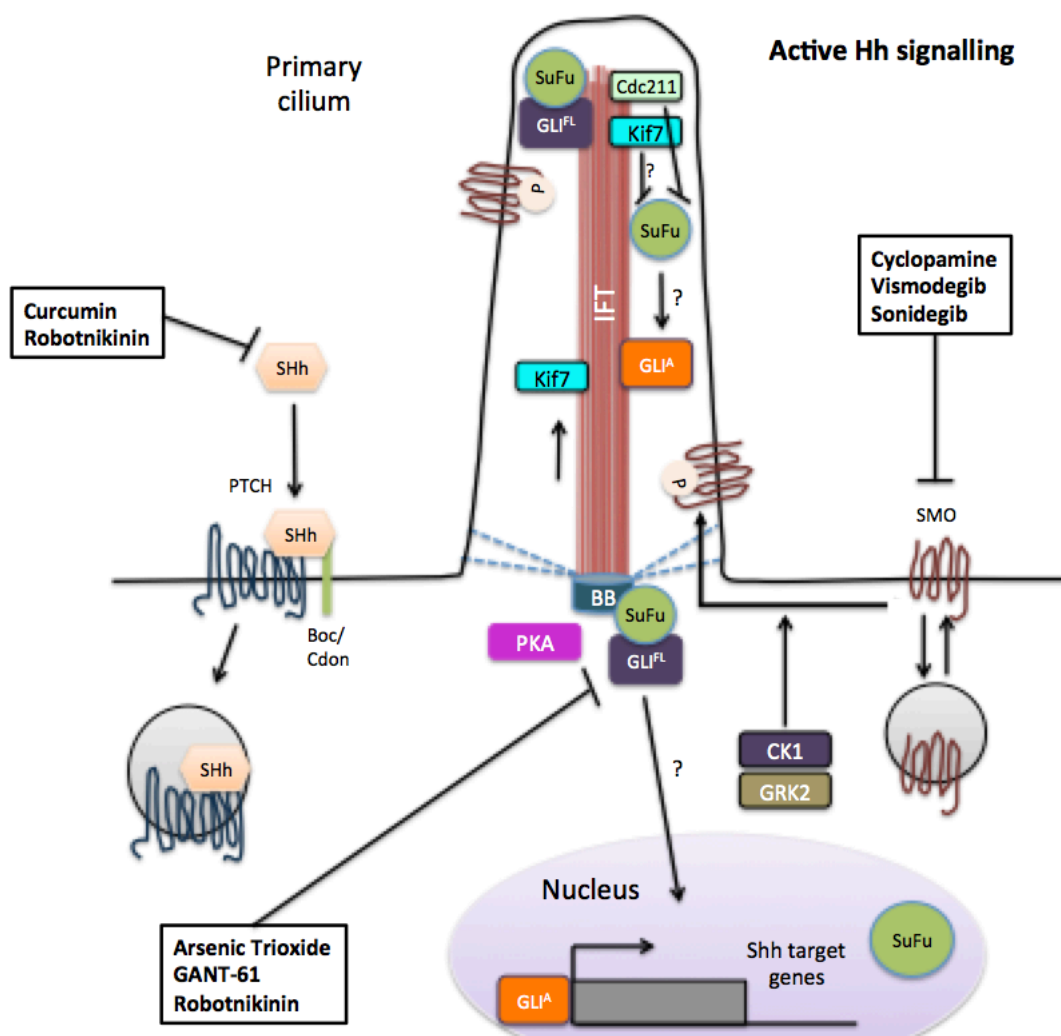


Figure 5.1: Components of the canonical Hh signalling pathway and molecular sites targeted by Hh pathway inhibitors.

Crosstalk exists between Hh and TGF β signalling pathways. Hh signalling has been found to induce the expression of TGF β family members in human cancer cell lines (Yoo *et al.*, 2008) and murine models (Fan *et al.*, 2010). Primary and recurrent and metastatic medulloblastoma tumour tissue microarray analyses demonstrated increased TGF β gene expression that correlated with positive nuclear staining of pSMAD3 (Aref *et al.*, 2013). Similarly TGF β signalling can induce SHh and GLI1 expression, resulting in SMO-independent Hh signal transduction (Javelaud *et al.*, 2011; Dennler *et al.*, 2007). SHh-induced cell motility and invasiveness requires activation of the TGF β -driven SMAD

pathway; it is likely that these family members are involved in SMO-dependent tumourigenesis (Yoo *et al.*, 2008). Thus, the crosstalk between Hh and TGF β signalling pathways is amplified in malignancy and promotes tumour invasion.

TGF β signalling pathway can be inhibited at the level of the: 1) ligand with a TGF β receptor blocking antibody (research only, TGF-beta 1, 2, 3 Antibody, R&D Systems), 2) receptor using a TGFBR1 tyrosine kinase phosphatase small molecule inhibitor (SB431542, GlaxoSmithKline) (Inman *et al.*, 2002b), 3) transcription factors using siRNA targeting co-SMAD4 (Figure 5.2). In transgenic mice with Hh resistant SMO, activation of TGF β signalling and tumour development could be inhibited by the TGFBR1 SB431542 inhibitor (Fan *et al.*, 2010).

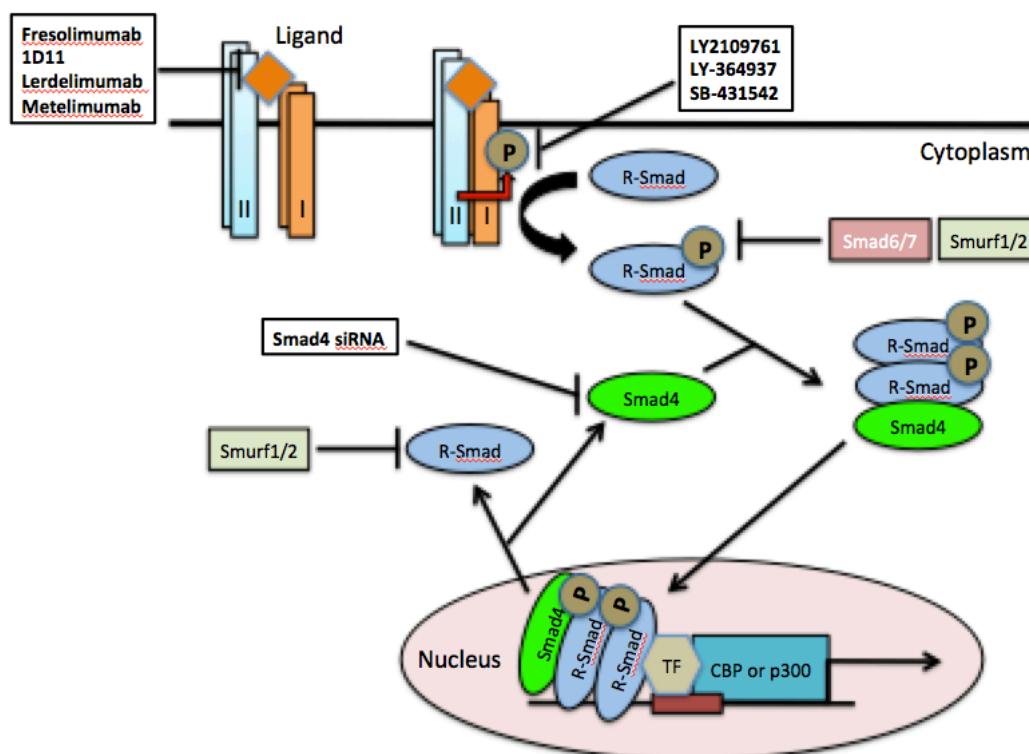


Figure 5.2: Components of the canonical TGF β signalling pathway and molecular sites targeted by TGF β pathway inhibitors.

Treatment of Hh driven tumours with currently available Hh pathway antagonists, vismodegib and sonidegib, has been disappointing. In 33 cases of metastatic or locally advanced BCC oral vismodegib demonstrated an objective response in 18 patients, with 2 complete responses and 16 partial responses (Von Hoff *et al.*, 2009). Eleven other patients had stable disease with 4 patients having progressive disease. Similarly, although there is a case report of medulloblastoma responding to vismodegib, the subsequent clinical trial failed to demonstrate clinical benefit (Rudin *et al.*, 2009; Von Hoff *et al.*, 2009). Therefore we hypothesised that the TGF β pathway may be responsible for Hh driven treatment resistance after Hh inhibition.

5.2 Results

5.2.1 Hedgehog agonist dose response curves

To determine the optimal *in vitro* dose of Hh signalling antagonists, we utilised an *in vitro* reporter assay in which NIH 3T3 cells were transduced with a luciferase GLI reporter construct (Taipale *et al.*, 2000). I first had to determine the dose of the Hh agonist, sonic Hh (SHh) that would reproducibly induce downstream Hh signalling. The Hh agonist protein targets are conserved between mouse and human. GLI reporter NIH 3T3 cells were plated at 10^4 cells per well in a 96 well clear-bottomed white-walled plate. The cells were allowed to establish growth for up to 24 hours, before stimulation with increasing concentrations (0.01 to 30 μ M) of murine SHh (mSHh) in quadruplicate. After 24 hours, bioluminescence readouts relative to unstimulated cells were determined using a ONE-Step Luciferase reagent and CLARIOstar High Performance Monochromator Multimode Microplate Reader. The experiment was performed in triplicate (n=3). Consistent with the literature, the peak response was determined as 3.3 μ g/ml resulting in an 11.96 fold increase in bioluminescence in comparison to unstimulated (Figure 5.3). Hence in our *in vitro* assays, we used 3.3 μ g/ml of mSHh, to define the optimal dose of hedgehog signalling inhibitors.

Dose Response of Gli Reporter - NIH3T3 Cells to mShh

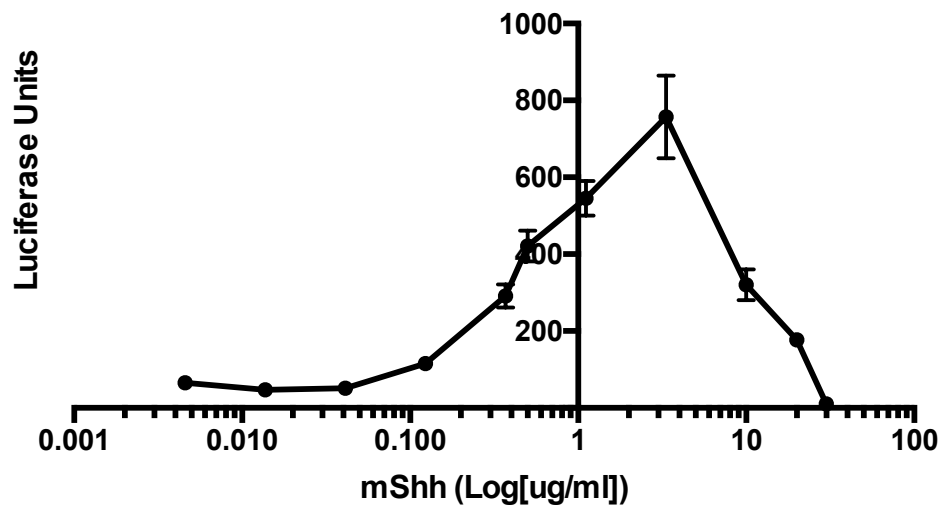


Figure 5.3: mSHh induced GLI reporter assay dose response curve.

Fold induction in bioluminescence from GLI reporter NIH 3T3 cells treated with varying Log concentrations of mSHh for 24 hr. Experiment was performed in triplicate, with four internal technical replicates for each condition (n=3). Error bars represent SE of mean.

5.2.2 Hedgehog antagonist dose response curves

Vismodegib is a currently licensed SMO antagonist for the treatment of inoperable BCC at a dose of 150 mg daily. The optimal *in vitro* dose varies according to the cell line, ranging from an IC_{95} for patient derived colorectal cancer xenograft (0.068 μ M) to a PTCH allograft model of medulloblastoma (0.042 μ M) (Wong *et al.*, 2011). In the presence of 3.3 μ g/ml of mSHh, Gli-reporter NIH 3T3 bioluminescence was determined upon addition of increasing vismodegib concentrations (0.01-30 μ M) (Figure 5.4). There was negligible reduction in bioluminescence with the addition of vismodegib at a concentration below 1 μ M in our assay. At a dose of 10 μ M of vismodegib, there was a maximal 30% reduction in luminescence (Figure 5.4). There was no further reduction in luminescence, despite concentrations of vismodegib up to 30 μ M. Numerous studies have also used 10 μ M in their functional assays using the same or similar cell lines (Infante *et al.*, 2016; Laressergues *et al.*, 2016; de la Rosa *et al.*, 2017; Pambid *et al.*, 2014). Therefore a concentration 10 μ M of vismodegib was used for our experiments.

Like vismodegib, sonidegib is a licensed SMO antagonist for the treatment of adult patients with locally advanced BCC who are not amenable to curative surgery or radiation therapy. In the presence of 3.3 μ g/ml of mSHh, we determined the bioluminescence change in GLI reporter NIH 3T3 cells with co-administration of increasing sonidegib concentrations from 0.01-30 μ M (Figure 5.5). There was a progressive reduction in bioluminescence with the addition of sonidegib, with a 70% reduction in luminescence when 10 μ M of sonidegib was co-administered (Figure 5.5). Sonidegib at a concentration of 20 μ M and higher was associated with cell death, therefore a 10 μ M concentration of sonidegib was used for experiments, which mirrors concentrations used in other studies on similar cell lines (Infante *et al.*, 2016; Pambid *et al.*, 2014).

GANT-61 inhibits GLI1 and GLI2-induced transcription, and is currently in clinical development. In the presence of 3.3 μ g/ml of mSHh, we determined the bioluminescence change in GLI reporter NIH 3T3 cells with co-administration of increasing GANT-61 concentrations from 0.01-30 μ M (Figure 5.6). There was a

progressive reduction in bioluminescence with the addition of GANT-61, with a 50% reduction in luminescence when 10 μM of GANT-61 was co-administered. Again studies have used 10 μM and above in their functional assays for treating these Hh driven cell lines (Arnhold *et al.*, 2016). Therefore, 10 μM was the concentration used in later experiments.

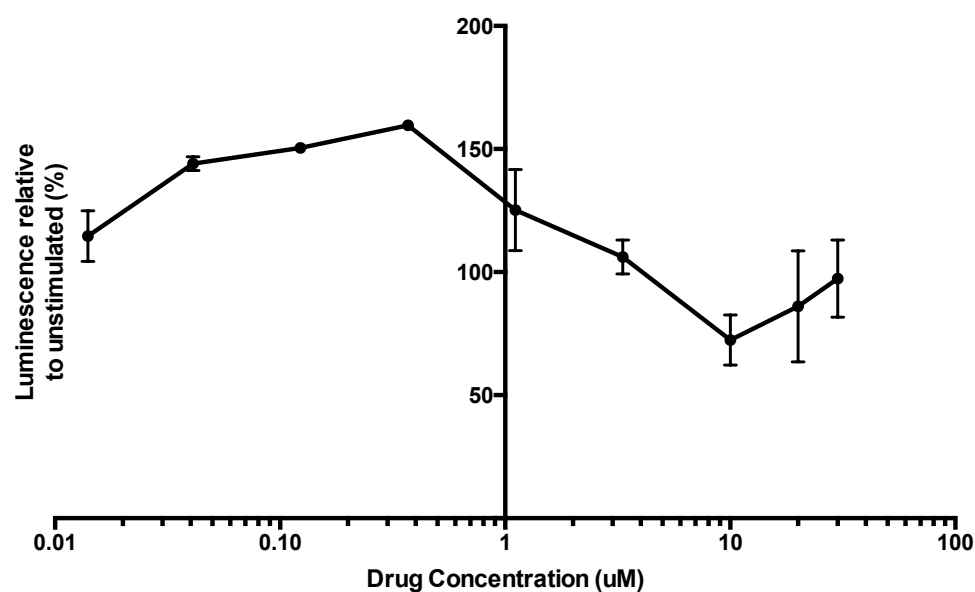


Figure 5.4: Inhibition of hedgehog signalling pathway by vismodegib

Fold change in bioluminescence from GLI reporter NIH 3T3 cells treated with 3.3 $\mu\text{g/ml}$ of mSHh varying and Log concentrations of vismodegib for 24hr. Experiment was performed in triplicate, with four internal technical replicates for each condition. (n=3). Error bars represent SE of mean.

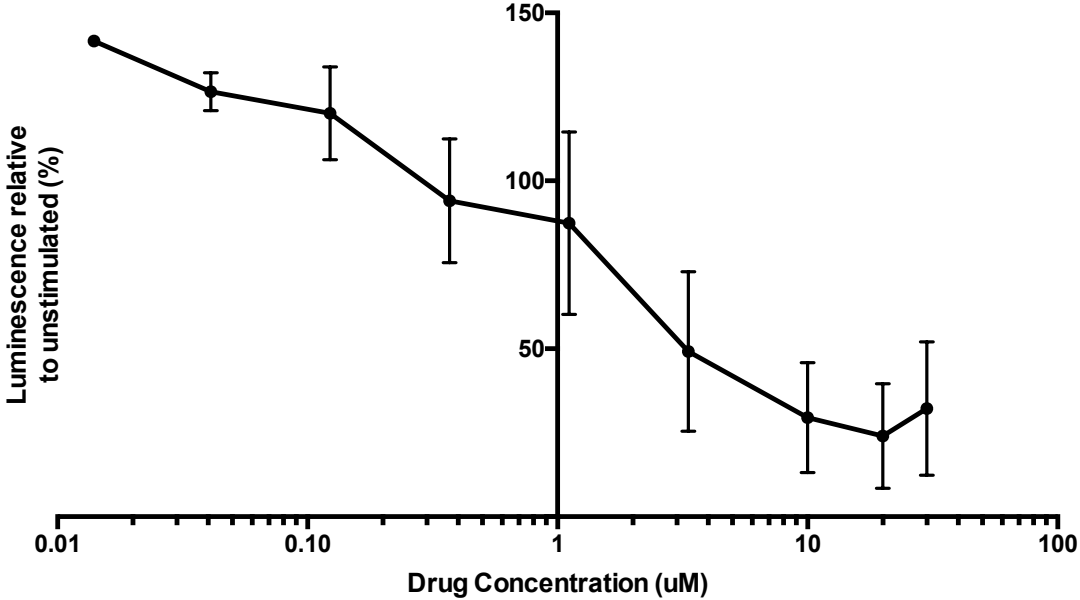


Figure 5.5: Inhibition of hedgehog signalling pathway by sonidegib
Fold change in bioluminescence from GLI reporter NIH 3T3 cells treated with 3.3 µg/ml of mSHh varying and Log concentrations of sonidegib for 24hr. Experiment was performed in triplicate, with four internal technical replicates for each condition. (n=3). Error bars represent SE of mean.

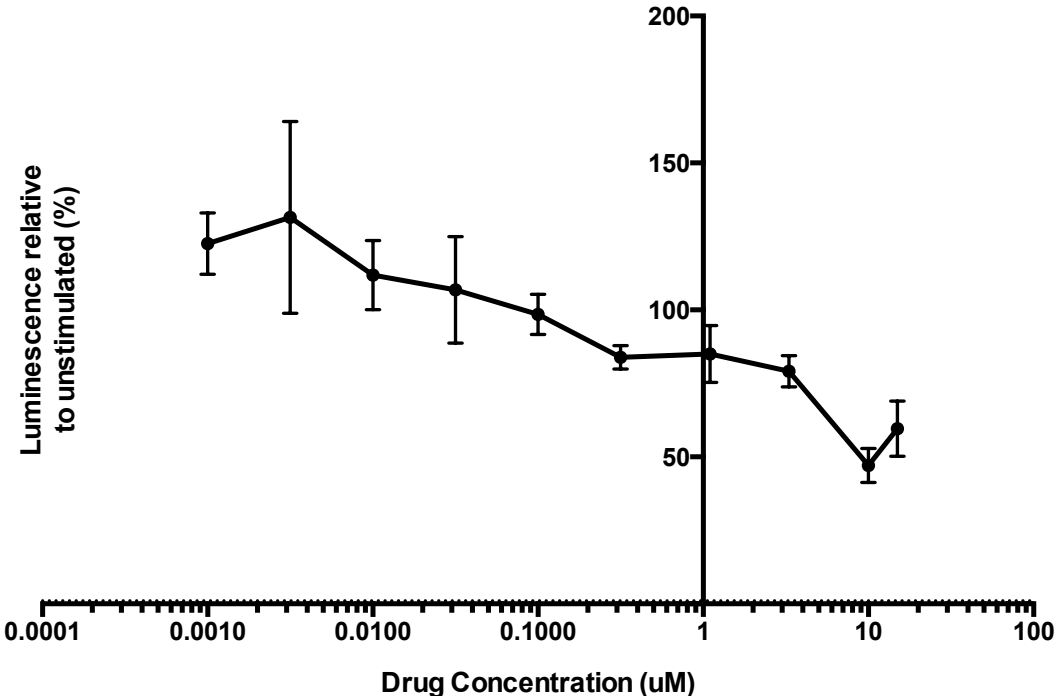


Figure 5.6: Inhibition of hedgehog signalling pathway by GANT-61

Fold change in bioluminescence from GLI reporter NIH 3T3 cells treated with 3.3 µg/ml of mSHh varying and Log concentrations of GANT-61 for 24hr. Experiment was performed in triplicate, with four internal technical replicates for each condition. (n=3). Error bars represent SE of mean.

5.2.3 Identifying genes that are Hh regulated within Hh driven tumour cell lines

The DAOY and UW228 cell lines are derived from children with paediatric medulloblastoma (Jacobsen *et al.*, 1985; Keles *et al.*, 1995). The UW228 cells are diploid and the DAOY cells are tetraploid. As is common with Hh driven growth in medulloblastoma, both cell lines harbour MYC amplification and p53 mutation (Higdon *et al.*, 2017). DAOY cell line exhibits high levels of SHh, PTCH1, GLI1, and GLI2 expression. While UW228-2, demonstrate low levels of SHh, PTCH1 and GLI2. DAOY remain responsive to Hh signalling, while UW228-2 cells are less responsive (Arnhold *et al.*, 2016; Götschel *et al.*, 2013). SJSA-1 cells demonstrate GLI amplification (Khatib *et al.*, 1993).

All three-tumour cell lines were treated with Hh ligand and/or Hh antagonists (10 μ M) for 24 hr before performing qPCR on a panel of Hh regulated genes in order to determine which genes are truly Hh regulated (a response following agonist treatment which can be subsequently reversed following antagonist treatment) within each of the cell lines (Figure 5.7A-C). Summarised in Table 5.1.

In DAOY cells, following Hh agonist treatment, an increased expression was observed for GLI1 (0.74 ± 0.26), GLI2 (0.15 ± 0.09), and SMO (0.44 ± 0.18), whereas a decrease in expression was observed for PTCH (-1.03 ± 0.10) when compared to the untreated control (Figur 5.7A). Following Hh antagonist treatment in comparison to Hh agonist treatment: a reduction in GLI1 expression was found following treatment with vismodegib (0.06 ± 0.14), sonidegib (-8.63 ± 0.14) and GANT-61 (0.38 ± 0.40), with the greatest reduction observed for sonidegib; a reduction was observed in GLI2 expression following sonidegib (-2.85 ± 0.12) and GANT-61 (-1.54 ± 0.08) treatment, whereas no change was observed for vismodegib (0.01 ± 0.09); finally, a reduction was observed in SMO expression following vismodegib (0.14 ± 0.07) and GANT-61 (0.08 ± 0.06), whereas sonidegib was shown to greatly reduce the expression of SMO (-6.65 ± 0.05). Therefore, in the DAOY cell line, GLI1, 2 and SMO will be classified as Hh regulated genes, with sonidegib shown to have the most pronounced effect in their expression.

In UW228-2 cells, following Hh agonist treatment, an increased expression was observed for GLI1 (0.56 ± 0.14), no change was observed for PTCH, whereas a decrease was seen for GLI2 (-4.86 ± 0.12) and SMO (-2.39 ± 0.09) when compared to the untreated control (Figure 5.7B). Following Hh antagonist treatment in comparison to Hh agonist treatment: an even greater increase in GLI1 expression was found following treatment with vismodegib (2.43 ± 0.59), sonidegib (1.77 ± 0.44) and GANT-61 (3.49 ± 0.79); a reduction was observed in GLI2 expression following sonidegib (-8.58 ± 0.12) and GANT-61 (-6.36 ± 0.09) treatment; mixed results were observed for PTCH expression, with a reduction observed for sonidegib (-2.36 ± 0.14), whereas an increase was found for GANT-61 (0.82 ± 0.25) (vismodegib data was not available); finally, a further reduction was observed in SMO expression following vismodegib (-6.13 ± 0.08), sonidegib (-5.70 ± 0.11) and GANT-61 (-5.10 ± 0.15). Therefore, in UW228-2 cells, Hh antagonists did not reverse this expression, but rather enhanced the effects observed in the Hh agonist treated cells by further downregulating GLI2, PTCH, and SMO, and upregulating GLI1. Although none of the four genes conform to the criteria GLI1, 2 and SMO will be used as a Hh output for this cell line, as their expression changed upon both the addition of Hh agonist and antagonist in comparison to the untreated cells, whereas PTCH expression didn't change upon addition of agonist.

In SJSA-1 cells, following Hh agonist treatment, a small increase in expression was observed for GLI1 (0.10 ± 0.09), whereas a decrease was seen for GLI2 (-5.89 ± 0.06), PTCH (-3.83 ± 0.11) and SMO (-3.00 ± 0.15) when compared to the untreated control (Figure 5.7C). Following Hh antagonist treatment in comparison to Hh agonist treatment: an even greater increase in GLI1 expression was found following treatment with vismodegib (0.15 ± 0.08), sonidegib (0.30 ± 0.14) and GANT-61 (0.19 ± 0.06); an increase was observed in GLI2 expression following vismodegib (0.26 ± 0.19), sonidegib (0.24 ± 0.17) and GANT-61 (0.45 ± 0.26) treatment; an increase was observed for PTCH expression following sonidegib (0.38 ± 0.10) and GANT-61 (0.39 ± 0.12) treatment; finally, an increase was also observed for SMO expression following vismodegib (0.10 ± 0.09), sonidegib (0.31 ± 0.21) and GANT-61 (0.23 ± 0.15) treatment. Therefore, in the SJSA-1 cell line GLI2, PTCH and SMO were classified as being Hh regulated, and appear to be negatively regulated.

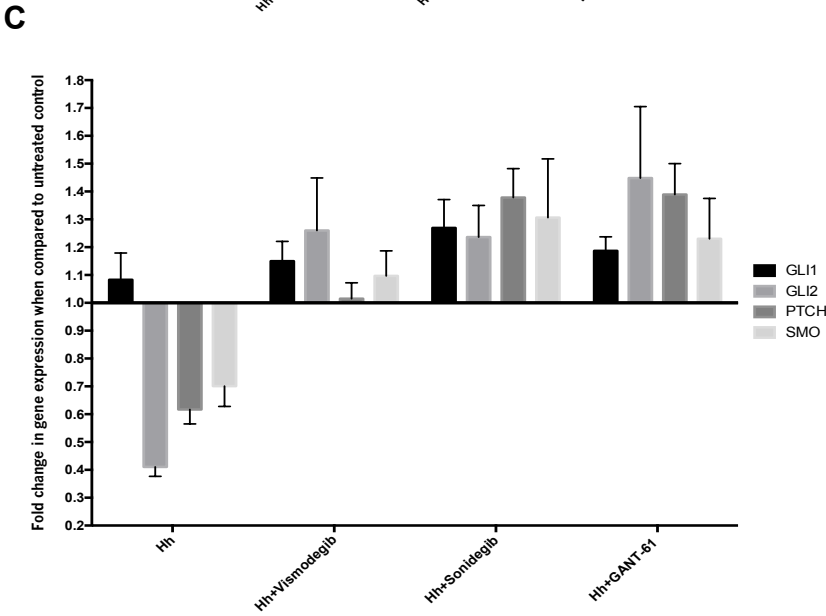
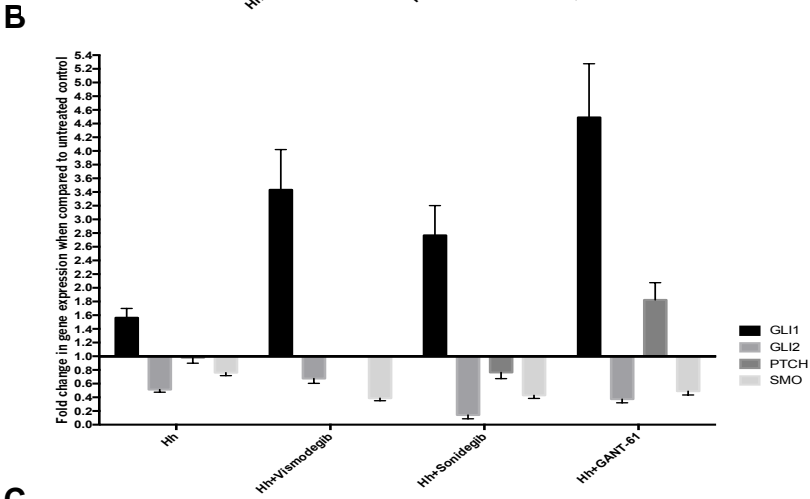
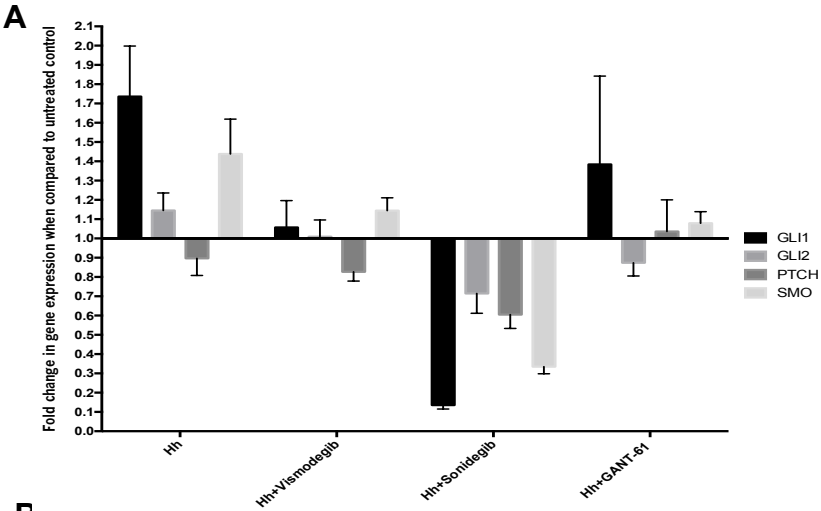


Figure 5.7: Identifying genes that are Hh regulated within Hh driven tumour cell lines.

Hh driven cell lines were cultured in the presence of Hh antagonists (vismodegib, sonidegib and GANT-61) for 24hr. RNA was extracted and assayed for a panel of Hh-regulated genes by qPCR in (A) DAOY, (B) UW228-2, and (C) SJSA-1 cell lines. Expression values are based on the Log_{10}RQ , where a value of 1.0 represents a fold change of +10, and 0.1 represents a fold change of -10. All results are an average of two independent experiments. The qPCR assay was performed with three internal technical replicates and two endogenous controls. (n=2).

Table 5.1: Identifying genes that are Hh regulated within Hh driven tumour cell lines.

*UP, represents genes that are upregulated; DOWN, represents genes that are downregulated; NC, represents no change in gene expression. All changes stated are in comparison to the untreated control. *=moderately up/downregulated; **=highly up/downregulated. ?=cannot determine based on the available data.*

Cell Line	Hh Regulated Genes	Hh Agonist	Hh Antagonists	Hh Regulated
DAOY	GLI1	UP**	Vismodegib – UP*	YES
			Sonidegib – DOWN**	
			GANT-61 – UP*	
	GLI2	UP*	Vismodegib - NC	YES
			Sonidegib – DOWN**	
			GANT-61 – DOWN*	
	PTCH	DOWN*	Vismodegib – DOWN*	NO
			Sonidegib – DOWN**	
			GANT-61 - NC	
	SMO	UP**	Vismodegib – UP*	YES
			Sonidegib – DOWN**	
			GANT-61 – UP*	
UW228	GLI1	UP*	Vismodegib – UP**	NO
			Sonidegib – UP**	

			GANT-61 – UP**	
	GLI2	DOWN*	Vismodegib – DOWN*	NO
			Sonidegib – DOWN**	
			GANT-61 – DOWN**	
	PTCH	NC	Vismodegib – N/A	?
			Sonidegib – DOWN	
			GANT-61 – UP	
	SMO	DOWN*	Vismodegib – DOWN**	NO
			Sonidegib – DOWN**	
			GANT-61 – DOWN**	
SJSA	GLI1	UP*	Vismodegib – UP*	NO
			Sonidegib – UP**	
			GANT-61 – UP**	
	GLI2	DOWN**	Vismodegib – UP*	YES
			Sonidegib – UP*	
			GANT-61 – UP*	
	PTCH	DOWN**	Vismodegib – NC	YES
			Sonidegib – UP*	
			GANT-61 – UP*	
	SMO	DOWN**	Vismodegib – UP*	YES
			Sonidegib – UP*	
			GANT-61 – UP*	

5.2.4 Apoptosis after Hh antagonists

To determine whether Hh antagonist treatment for 4, 24, and 48 hours resulted in apoptosis of Hh driven cell lines, we undertook flow cytometric analysis of annexin V and DAPI labelled cells; allowing detection of early and late apoptotic events.

For the positive control, when compared to the total cell population (100%) all three cell lines demonstrated an increase in the percentage of apoptotic cells (Annexin V positive) between untreated and 24 hour etoposide treatment: DAOY 0.93% vs 6.97%,

UW228-2 1.65% vs 17.1%, and SJSA-1 cells 2.11% vs 18.8%. All three cell lines demonstrated an increase in the percentage of dead cells (AnnexinV/DAPI positive) between untreated and etoposide treatment: DAOY 2.37% vs 20.9%, UW228-2 1.28% vs 12.2%, and SJSA-1 cells 1.53% vs 37.8%. Therefore we were able to detect a change in the level of apoptotic and dead cells in our Hh driven cell lines following etoposide treatment.

Figure 5.8 shows representative dot plots between untreated and Hh antagonist treated cell lines over three time-points. Table 5.2 outlines the effect of Hh antagonist only treatments on early apoptosis (Annexin V^{pos}/DAPI^{neg}), late apoptosis (Annexin V^{pos}/DAPI^{pos}) or necrosis (Annexin V^{neg}/DAPI^{pos}) over three time-points (4, 24 and 48 hr) in our three Hh driven cell lines.

In the DAOY cell line, following 4, 24 and 48 hr of vismodegib treatment, no significant effect was observed on early apoptosis, late apoptosis or necrosis when compared to the untreated control. Following sonidegib treatment, no significant effect was observed on early apoptosis, late apoptosis or necrosis at any of the three time points when compared to the untreated control. Finally, following GANT-61 treatment no significant effect was observed on early and late apoptosis over 4, 24 and 48 hr of treatment; however a significant increase in the % of necrotic cells was observed after 48hr of treatment when compared to the untreated control (5.95% vs 14.31%; $p < 0.05$).

In the UW228-2 cell line, following 4, 24 and 48 hr of vismodegib treatment, no significant effect was observed on early apoptosis, late apoptosis or necrosis when compared to the untreated control. Following sonidegib treatment, no significant effect was observed on early apoptosis, late apoptosis or necrosis at any of the three time points when compared to the untreated control. Finally, following GANT-61 treatment no significant effect was observed on early apoptosis, late apoptosis or necrosis over 4, 24 and 48 hr of treatment.

In the SJSA-1 cell line, following 4, 24 and 48 hr of vismodegib treatment, no significant effect was observed on early apoptosis, late apoptosis or necrosis when compared to

the untreated control. Following sonidegib treatment, no significant effect was observed on early apoptosis at any of the time points, whereas an increase in the % of cells in late apoptosis was observed at all time points, although only the 24 hr time-point was significant (1.78% vs 9.75%; $p < 0.05$). Marginal increases were also observed in the % of necrotic cells at all time points although none were found to be significant. Finally, following GANT-61 treatment no significant effect was observed on early and late apoptosis over 4, 24 and 48 hr of treatment; however a significant increase in the % of necrotic cells was observed after 48hr of treatment when compared to the untreated control (2.03% vs 10.21%; $p < 0.05$).

In conclusion, Hh antagonists have minimal effect on short-term viability. Only sonidegib treated SJS-1 cells and GANT-61 treated UW228-2 cells, showed an increase in dead and apoptotic cells respectively.

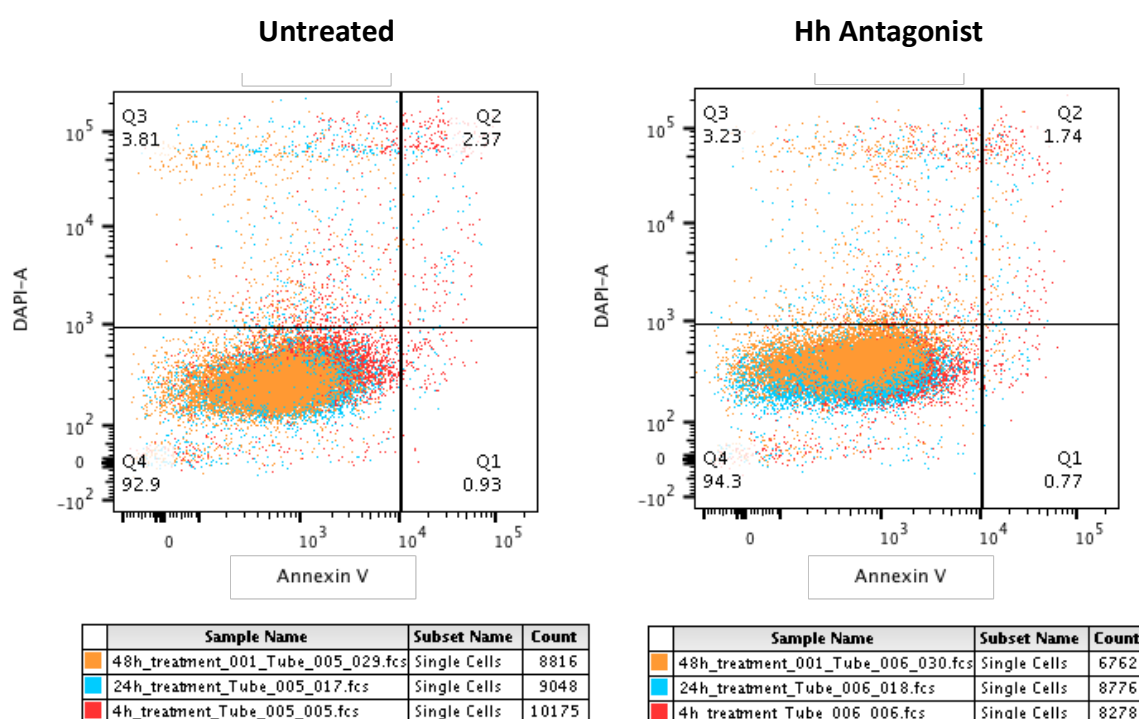


Figure 5.8: Little or no impact on apoptosis in Hh driven tumour cell lines following Hh antagonist treatment

Representative dot plot showing the effect of Hh antagonists over the three time periods 4, 24, and 48 hr in Hh driven tumour cell lines. 4hr (red population), 24hr (blue population), and 48hr (orange population) treatments are merged on top of each other

*in order to display any shifts following treatment over the three time periods. Annexin V (apoptosis marker) and DAPI (dead cell marker) are on the X- and Y-axis, respectively. Each quadrant represents as follows: Q1) early apoptosis, Q2) late apoptosis, Q3) necrosis, Q4) viable cells. Experiments were performed in triplicate (n=3), * represents $p < 0.05$, t-test.*

Table 5.2: The effect of Hh antagonists on apoptosis in Hh driven cell lines

Cell Line	Drug	Time Points (hr)	% Live Cells	% Early Apoptosis	% Late Apoptosis	% Necrosis
DAOY	Untreated	4	86.25	2.99	2.76	8.01
		24	93.30	1.23	1.92	3.54
		48	92.20	0.44	1.42	5.95
	Vismodegib	4	92.60	1.38	1.73	4.30
		24	94.15	0.63	0.92	4.29
		48	93.75	0.74	0.84	4.69
	Sonidegib	4	86.70	4.63	3.86	4.79
		24	93.60	0.53	0.89	5.01
		48	92.60	0.45	1.28	5.69
	GANT-61	4	90.00	3.88	2.93	3.17
		24	94.85	0.73	0.97	3.58
		48	83.20	0.67	1.79	14.31
UW228-2	Untreated	4	89.25	1.44	3.25	6.11
		24	84.45	2.57	8.99	4.00
		48	86.75	3.12	5.65	4.53
	Vismodegib	4	93.75	3.82	0.96	1.43
		24	96.15	1.68	0.58	1.60
		48	94.75	1.62	0.72	2.91
	Sonidegib	4	91.05	1.05	2.45	5.48
		24	91.40	1.07	2.08	5.46
		48	86.50	2.93	5.03	5.53
	GANT-61	4	92.20	5.20	1.27	1.33
		24	92.15	4.15	1.10	2.59
		48	80.40	5.84	6.48	7.30
SJSA-1	Untreated	4	94.55	1.90	1.39	2.18
		24	94.95	1.60	1.78	1.64
		48	95.85	1.41	0.72	2.03
	Vismodegib	4	92.70	1.93	2.83	2.52
		24	93.15	2.29	2.48	2.09
		48	96.60	0.98	0.83	1.64
	Sonidegib	4	85.40	1.16	6.87	6.57
		24	83.70	1.81	9.75	4.79
		48	94.25	0.87	1.95	2.96

		4	94.60	1.91	1.59	1.91
	GANT-61	24	89.50	3.43	2.89	4.18
		48	86.75	1.47	1.58	10.21

5.2.5 Hh antagonists in 2D culture do not reduce cell viability

To determine if Hh antagonists resulted in loss of cell culture viability, 10,000 cells per well in a 96-well flat-bottomed white-walled plate were cultured overnight, before the addition of 10 μ M Hh antagonists for 24 hours. Cell viability was determined by Cell Titre Glo assay by comparing untreated and treated cells. HaCaT cells were used as a non-Hh driven cell line control. As expected since HaCaT cells are not driven by Hh signalling, no reduction in cell viability was observed for vismodegib 98.7% \pm 4.5%, sonidegib 91.9% \pm 15.3% or GANT-61 96.4 \pm 3.6% treatments (Figure 5.9A). As a positive control, cell lines were treated with the chemotherapeutic agent docetaxyl resulting in a reduction in cell viability to 36.1% \pm 19.0% (DAOY), 58.1% \pm 13.0% (UW228-2), and 49.3% \pm 11.4% (SJSA-1), respectively (Figure 5.9B).

In all three-cell lines, the addition of 10 μ M vismodegib or sonidegib resulted in no significant reduction in cell viability (Figure 5.9C, D). GANT-61 at a concentration of 10 μ M for 24 hours reduced UW228-2 cell viability to 81.5% \pm 4.35%, but with no effect on DAOY or SJSA-1 viability (Figure 5.9E). In summary, 24 hr treatment with antagonists of the Hh-signalling pathway did not adversely affect cell viability and proliferation, with the exception of GANT-61 treatment of UW228-2 cells.

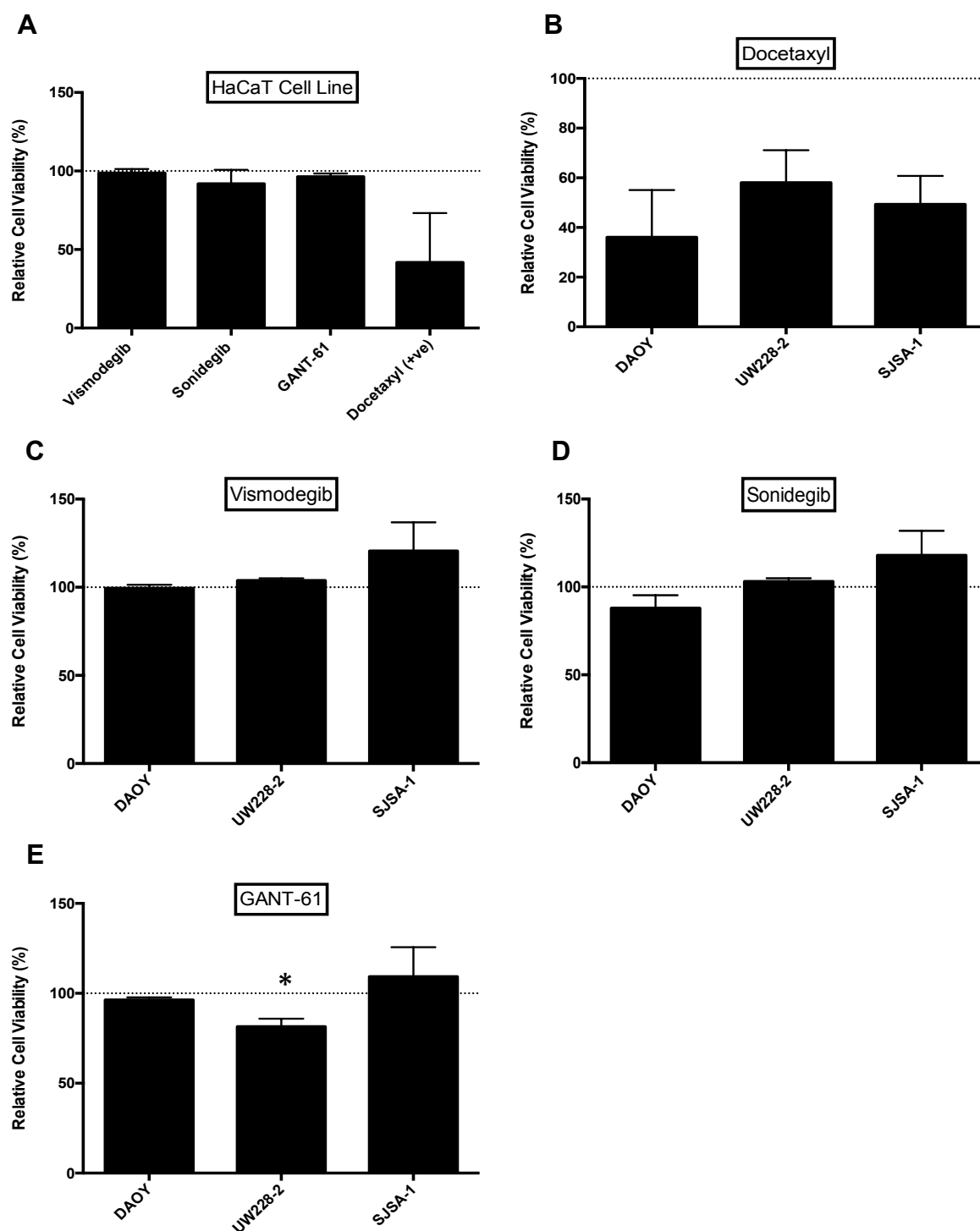


Figure 5.9: Hh Antagonists do not reduce cell viability in Hh Driven Cell Lines: Cell Titre Glo assay following 24hr treatment with Hh antagonists.

(A) All three Hh antagonists, vismodegib, sonidegib and GANT-61 were ineffective in the non HH-driven HaCaT cell line (-ve). All three-cell lines (DAOY, UW228-2, and SJSA-1) were treated with (B) Docetaxyl (+ve), (C) vismodegib, (D) sonidegib, and (E) GANT-61. Graphs represent an average over three independent experiments, with each

experiment having four internal technical replicates for each condition. ($n=3$), Error bars represent SE mean, * represents $p<0.05$, t-test.

5.2.6 Effect of Hh antagonist on 2D colony forming efficiency

We previously determined the inability of Hh signalling pathway antagonism to influence BCC colony forming efficiency (Colmont *et al.*, 2013). We next sought to determine if Hh antagonists could influence CFE in other tumours with Hh pathway activation. The three cell lines were plated at a density of 75 (DAOY), 125 (UW228-2), and 125 (SJSA-1) cells/cm² and allowed to adhere overnight (in a total of 1mL of media), and then subsequently treated with Hh antagonists. Colonies were established over 7-12 days (cell line dependent) in the presence of the drug, with colonies needing to reach a cut-off of at least 32 cells (5 cell divisions) to be counted (Harrison, 2012).

Vismodegib did not influence CFE in DAOY and UW228-2 cell lines (Figure 5.10B and C), but reduced CFE in SJSA-1 (77.1%±1.2%) although this was not significant (Figure 5.10D). Sonidegib demonstrated reduced CFE in all cells lines: DAOY (63.2%±1.9%, $p<0.05$), UW228-2 (25.1%±0.07%, $p<0.01$) and SJSA-1 (31.6%±0.2%, $p<0.01$). GANT-61 significantly reduced CFE in all three cell lines (Figure 5.10A-D), when compared to the unstimulated control: DAOY (<1%, $p<0.01$), UW228-2 (0%, $p<0.01$), SJSA-1 (22.6%±0.30%, $p<0.01$). Hence Hh driven tumour cells appeared sensitive to GANT-61, followed by sonidegib, with the least effective demonstrated to be vismodegib.

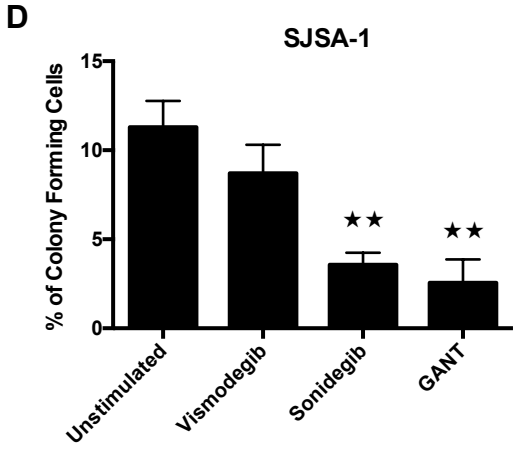
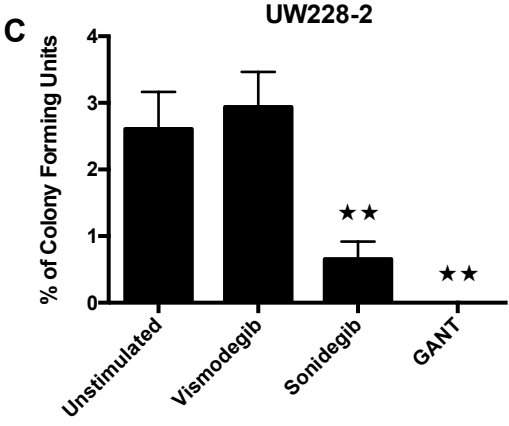
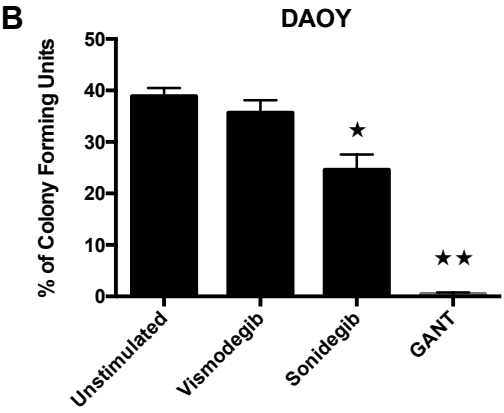
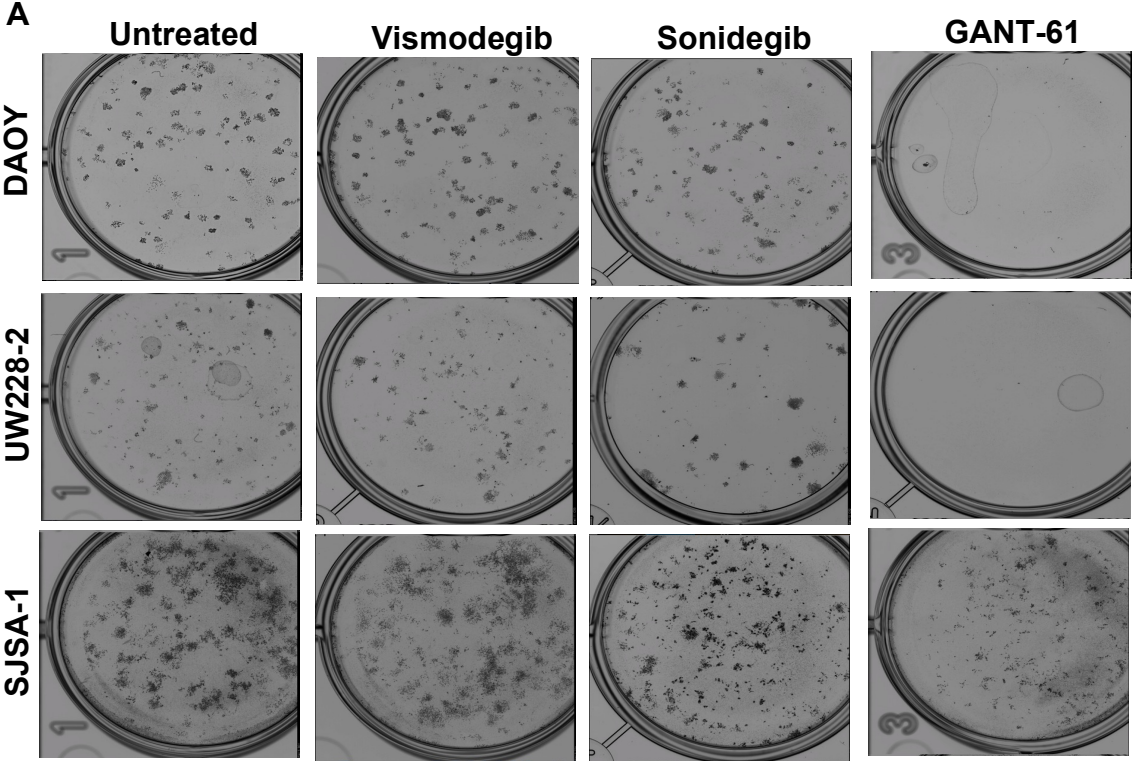


Figure 5.10: Colony forming cells are sensitive to GANT-61, but resistant to vismodegib.

*Colony-Forming Assays: Cells were seeded at a density of 75 cells/cm² for DAOY, 187.5 cells/cm² for UW228-2, and 125 cells/cm² for SJSA-1 cell lines in the presence or absence of Hh Antagonists for 7-12 days. (A) Representative images, (B) DAOY cell line treated with vismodegib, sonidegib and GANT-61, (C) UW228-2 cell line treated with vismodegib, sonidegib and GANT-61, (D) SJSA-1 cell line treated with vismodegib, sonidegib and GANT-61. All results are averages of at least four independent experiments, with three internal technical replicates for each condition. (n=4), Error bars represent SE mean, * represents $p<0.05$, ** represents $p<0.01$, t-test.*

5.2.7 Effect of Hh antagonist on 3D tumoursphere forming units

To determine whether Hh antagonists influence SC function, the % of tumoursphere forming units (TFUs) formed was calculated for each cell line. Both DAOY and UW228-2 cell lines grow in non-adherent conditions, however SJSA-1 does not and therefore was excluded. The cultured cells were treated for 24 hr before being passaged into non-adherent culture conditions and allowed to form spheres over 7 days, before enumeration and secondary passage.

Hh antagonists did not reduce the number of DAOY TFUs in both passage 1 and 2 (Figure 5.11A and B, respectively), instead there was a 2-fold increase in both the first and second passages following vismodegib treatment (1.4 ± 0.2 vs 2.2 ± 0.34 , $p<0.05$) and (2.3 ± 0.1 vs 7.1 ± 3.6 , $p<0.05$) respectively. An increase in the number of TFUs was also observed in both the first and second passages following sonidegib treatment (1.4 ± 0.2 vs 1.8 ± 0.6) and (2.3 ± 0.1 vs 4.4 ± 2.4) respectively. When assessing the impact of Hh antagonists on the relative TFU area, GANT-61 was found to reduce TFU size ($64.7\%\pm 18.9\%$; Figure 5.11C). This would suggest that both vismodegib and sonidegib treatment led to an increase in colony forming cells and therefore potential SCs.

In UW228-2 cells all three Hh antagonists had no effect on primary TFUs (Figure 5.12A), but secondary TFUs were reduced with vismodegib (2.4 ± 1.3 vs 1.5 ± 0.13) and GANT-61

(2.4 ± 1.3 vs 1.1 ± 0.5) (Figure 5.12B). Once more GANT-61 treatment was associated with smaller colonies ($60.0\% \pm 12.6\%$; Figure 5.12C). Thus UW228-2 cells demonstrated a reduction in secondary TFUs, suggesting that vismodegib and GANT-61 reduced SC numbers.

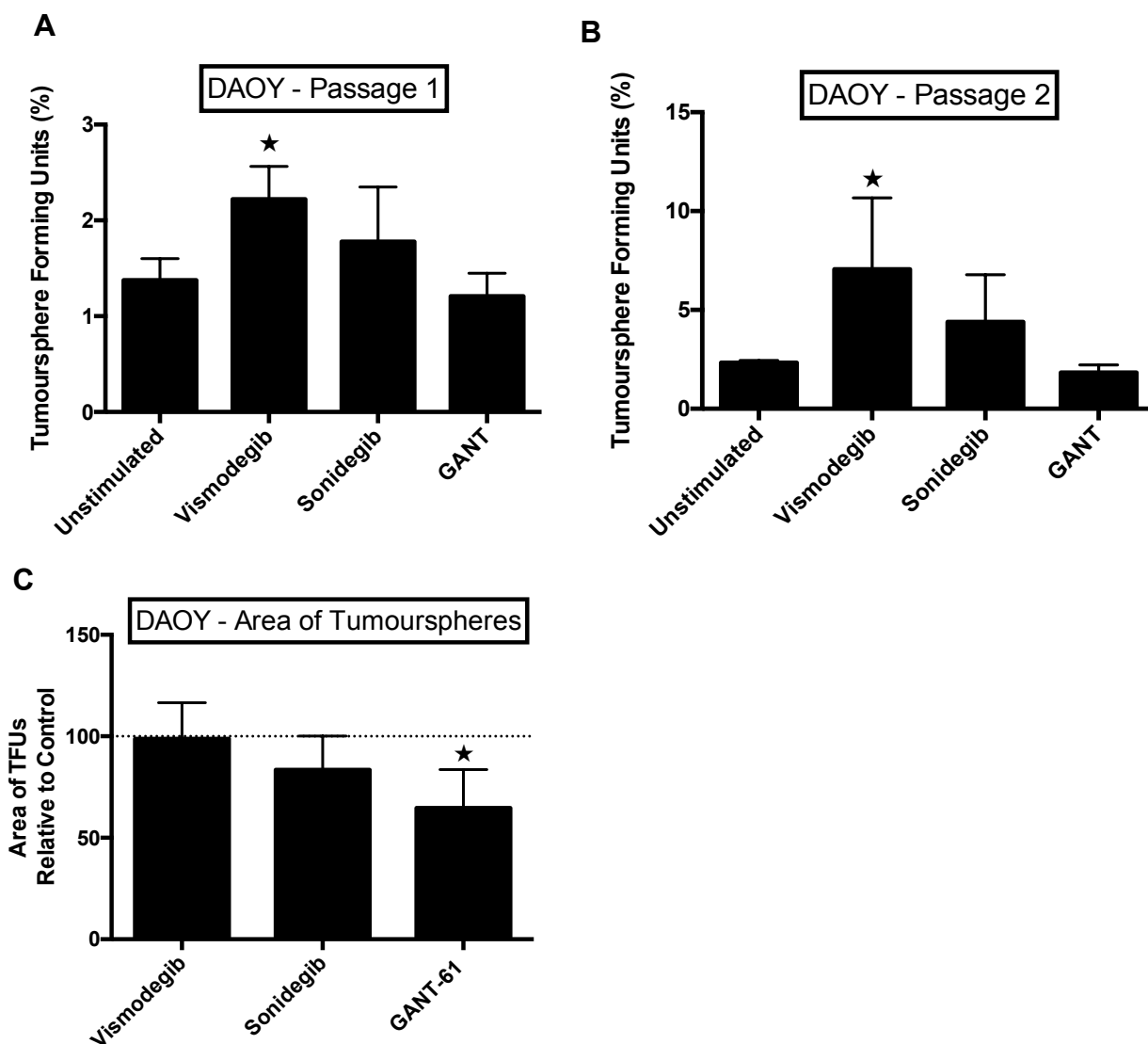


Figure 5.11: Tumoursphere-forming cells are sensitive to GANT-61, but not to vismodegib and sonidegib in DAOY cells.

Sphere-Forming Assays: Cells were seeded in 2D and allowed to adhere overnight before being treated with Hh antagonists (GANT-61, vismodegib, and sonidegib) for 24 hr. Following treatment cells were trypsinised and plated under sphere forming conditions at a density of 5 cells/ μ L and allowed to form spheres over 7 days before being enumerated (P1). Spheres were then dissociated and re-plated at a density of 5 cells/ μ L

allowed to grow for a further 7 days, before being finally enumerated (P2). **(A)** %TFUs at P1 in DAOY cells treated with Hh antagonists, **(B)** %TFUs at P2 in DAOY cells treated with Hh antagonists, **(C)** Area of DAOY TFUs treated with Hh antagonists relative to untreated control. Tumoursphere forming units (%) represents the number of spheres formed relative to the number of cells originally seeded. All results are averages of three independent experiments, with three internal technical replicates for each condition. ($n=3$), Error bars represent SE of mean, * represents $p<0.05$, ** represents $p<0.01$, t-test.

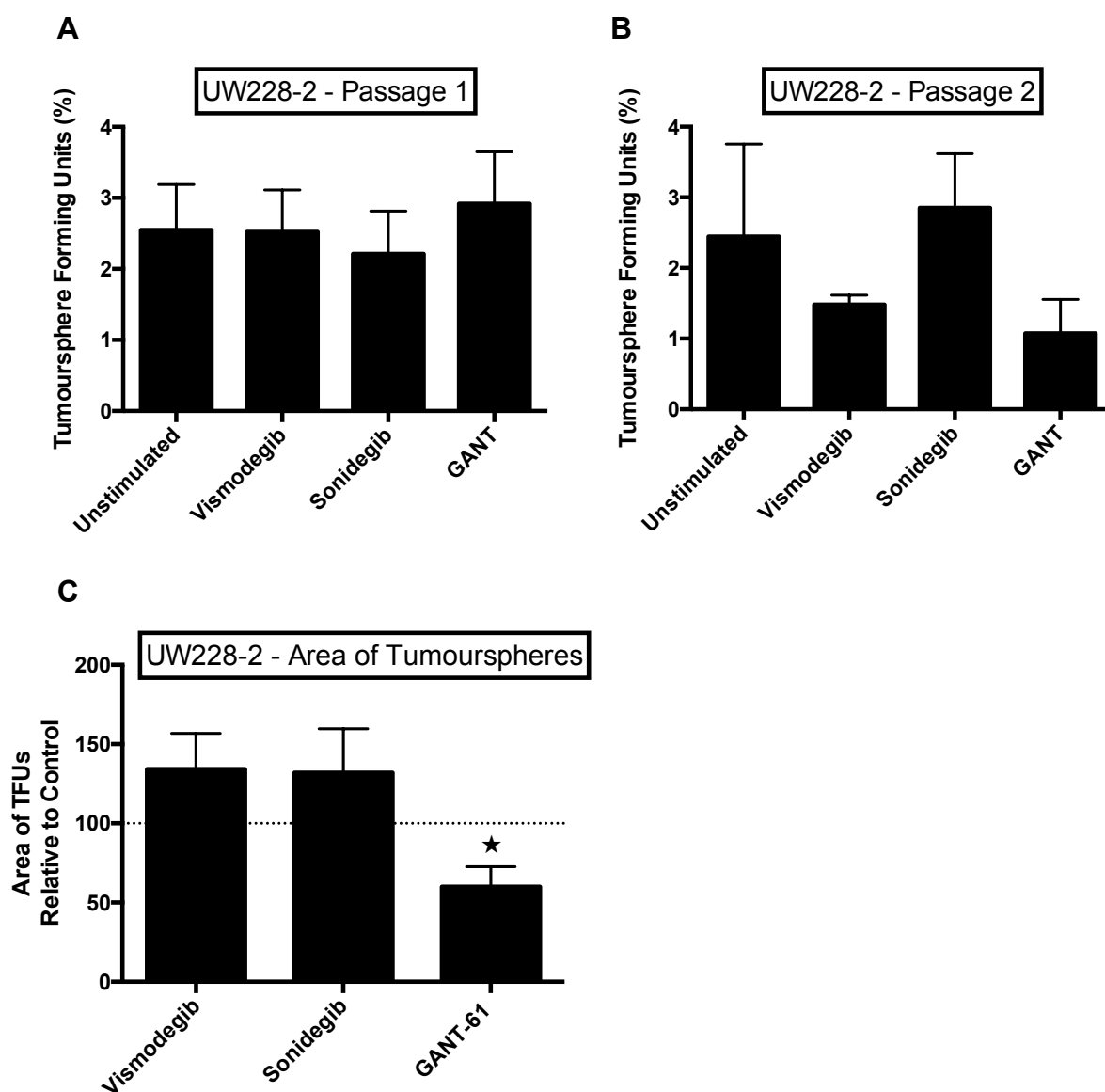


Figure 5.12: Tumoursphere-forming cells are sensitive to GANT-61, but not to vismodegib and sonidegib in UW228-2 cells.

*Sphere-Forming Assays: Cells were seeded in 2D and allowed to adhere overnight before being treated with Hh antagonists (GANT-61, vismodegib, and sonidegib) for 24 hr. Following treatment cells were trypsinised and plated under sphere forming conditions at a density of 5 cells/ μ L and allowed to form spheres over 7 days before being enumerated (P1). Spheres were then dissociated and re-plated at a density of 5 cells/ μ L allowed to grow for a further 7 days, before being finally enumerated (P2). (A) %TFUs at P1 in UW228-2 cells treated with Hh antagonists, (B) %TFUs at P2 in UW228-2 cells treated with Hh antagonists, (C) Area of UW228-2 TFUs treated with Hh antagonists relative to untreated control. Tumoursphere forming units (%) represents the number of spheres formed relative to the number of cells originally seeded. All results are averages of three independent experiments, with three internal technical replicates for each condition. (n=3), Error bars represent SE of mean, * represents $p < 0.05$, ** represents $p < 0.01$, t-test.*

5.2.8 Identifying genes that are TGF β regulated within Hh driven tumour cell lines

All three-tumour cell lines were treated with TGF β ligand for 1hr and the ALK5 antagonist (SB431542) for a further 3 hr, before performing qPCR on a panel of TGF β regulated genes in order to determine which genes are truly TGF β regulated (a response following agonist treatment which can be subsequently reversed following antagonist treatment) within each of the cell lines (Figure 5.13A-C). Summarised in Table 5.3.

In DAOY cells, following TGF β 1 agonist treatment, a decreased expression was observed for ADAM19 (-1.54 ± 0.13), ANGPTL4 (-2.89 ± 0.50), and CEBPD (-2.10 ± 0.22), whereas an increase in expression was observed for NEDD9 (0.93 ± 0.36), SERPINE1 (0.09 ± 0.10), and SKIL (0.06 ± 0.05) when compared to the untreated control (Figure 5.13A). Following SB431542 treatment in comparison to TGF β 1 treatment: no change in expression was observed for ADAM19, ANGPTL4, or NEDD9, whereas CEBPD increased (0.40 ± 0.44) in expression and both SERPINE1 (-4.91 ± 0.05) and SKIL (-3.09 ± 0.06) decreased in expression. Therefore, in the DAOY cell line, CEBPD, SERPINE1, and SKIL will be classified as TGF β regulated genes.

In UW228-2 cells, following TGF β 1 agonist treatment, a decreased expression was observed for CEBPD (-5.08 \pm 0.08), whereas an increase in expression was observed for ADAM19 (0.14 \pm 0.07), NEDD9 (1.15 \pm 0.13), SERPINE1 (1.89 \pm 0.27), and SKIL (0.28 \pm 0.09) when compared to the untreated control (Figure 5.13B). Following SB431542 treatment in comparison to TGF β 1 treatment: no change in expression was observed for ADAM19, SERPINE1, or SKIL, whereas NEDD9 (0.68 \pm 0.10) was shown to decrease in expression, and CEBPD was found to slightly increase (-4.63 \pm 0.05). Therefore, in the UW228-2 cell line, NEDD9 and CEBPD will be classified as TGF β regulated genes.

In SJSA-1 cells, following TGF β 1 agonist treatment, a decreased expression was observed for ANGPTL4 (-4.63 \pm 0.12), and CEBPD (-5.87 \pm 0.05), whereas an increase in expression was observed for NEDD9 (1.44 \pm 0.34), SERPINE1 (0.13 \pm 0.11), and SKIL (0.08 \pm 0.10) when compared to the untreated control (Figure 5.13C). Following SB431542 treatment in comparison to TGF β 1 treatment: no change in expression was observed for ANGPTL4, SERPINE1 or SKIL, whereas CEBPD increased (-0.04 \pm 0.39) in expression and NEDD9 (0.06 \pm 0.16) decreased in expression. Therefore, in the SJSA-1 cell line, CEBPD and NEDD9 will be classified as TGF β regulated genes.

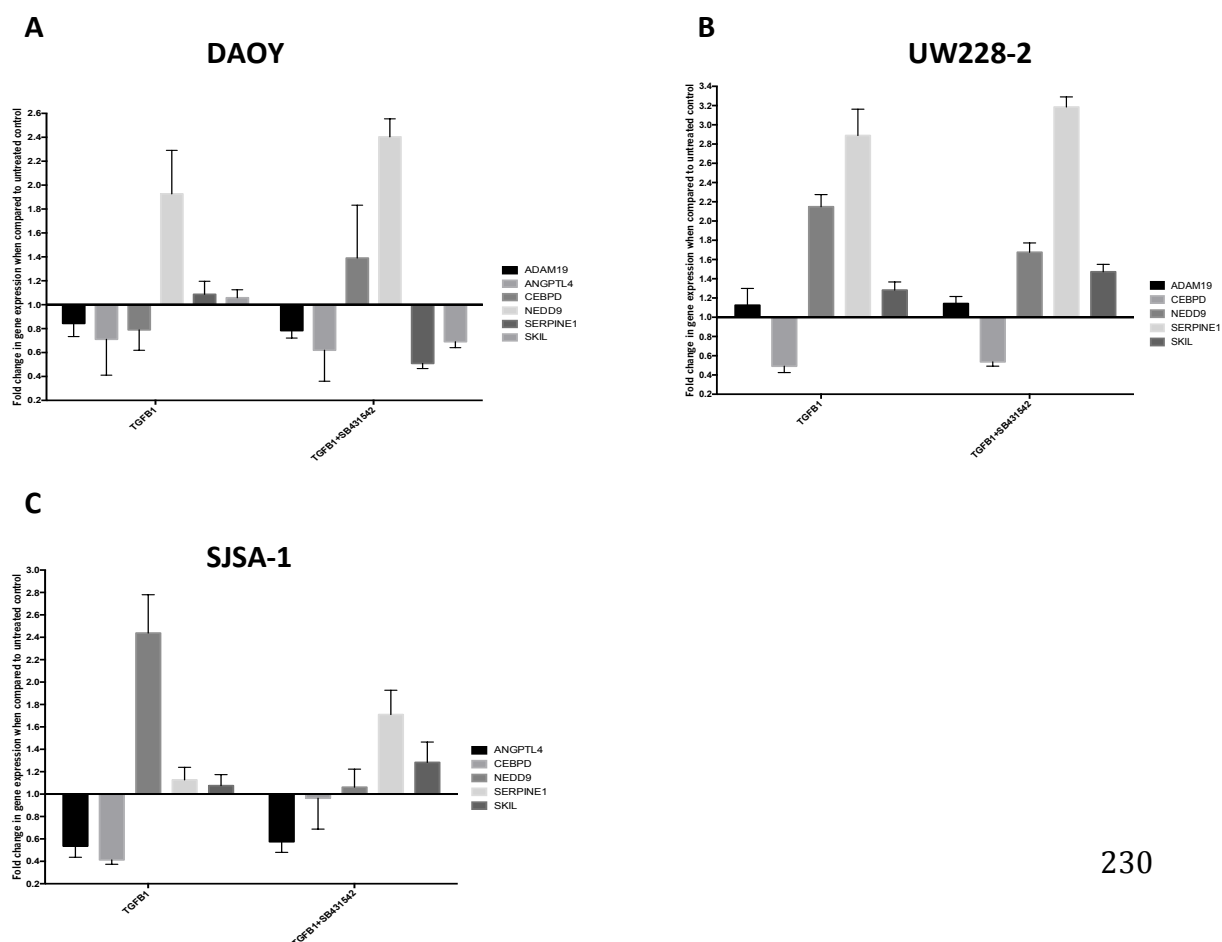


Figure 5.13: Identifying genes that are TGF β regulated within Hh driven tumour cell lines

Hh driven cell lines were cultured in the presence of TGF β 1 ligand for 1hr and the ALK5 antagonist (SB431542) for a further 3 hr, before performing qPCR on a panel of TGF β -regulated genes in (A) DAOY, (B) UW228-2, and (C) SJSA-1 cell lines. Expression values are based on the Log₁₀RQ, where a value of 1.0 represents a fold change of +10, and 0.1 represents a fold change of -10. All results are an average of two independent experiments (n=2). The qPCR assay was performed with three internal technical replicates and two endogenous controls.

Table 5.3: Identifying genes that are TGF β regulated within Hh driven tumour cell lines

*UP, represents genes that are upregulated; DOWN, represents genes that are downregulated; NC, represents no change in gene expression. All changes stated are in comparison to the untreated control. *=moderately up/downregulated; **=highly up/downregulated. ?=cannot determine based on the available data.*

Cell Line	TGF β Regulated Genes	TGF β 1 Agonist	SB431542	TGF β Regulated
DAOY	ADAM19	DOWN	DOWN	?
	ANGPTL4	DOWN	DOWN	?
	CEBPD	DOWN	UP	YES
	NEDD9	UP	UP	NO
	SERPINE1	UP	DOWN	YES
	SKIL	UP	DOWN	YES
UW228-2	ADAM19	UP	UP	NO
	CEBPD	DOWN**	DOWN*	YES
	NEDD9	UP**	UP*	YES
	SERPINE1	UP	UP	NO
	SKIL	UP*	UP*	NO
SJSA-1	ANGPTL4	DOWN	DOWN	NO
	CEBPD	DOWN	NC	YES
	NEDD9	UP	NC	YES
	SERPINE1	UP	UP	NO
	SKIL	UP	UP	NO

5.2.9 Hh antagonists induce SMAD3 phosphorylation and regulate TGF β gene expression

To determine if Hh antagonism could induce TGF β signalling, Western blot analysis was undertaken on protein lysates extracted from cells following a 4 hr treatment with Hh antagonists and quantified using ImageJ software. As a positive and negative control, cells were treated with TGF β 1 and SB431542, respectively. Using Western blot analysis, in the DAOY cell line, increased levels of pSMAD3 were observed following GANT-61 (140.4% \pm 12.7%), vismodegib (145.5% \pm 9.1%; $p < 0.05$), and sonidegib (132.14 \pm 10.7) (Figure 5.14A). In the UW228-2 cell line, increased levels of pSMAD3 were also observed following GANT-61 (123.1% \pm 2.7%; $p < 0.05$), vismodegib (156.5% \pm 33.8%; $p < 0.05$), and sonidegib (126.2 \pm 3.9; $p < 0.05$) (Figure 5.14B). Finally, this increase in pSMAD3 levels was also observed in primary BCC tissue, following treatment with GANT-61 (115.1% \pm 8.3%), vismodegib (122.6% \pm 9.5%), and sonidegib (112.4% \pm 1.8%; $p < 0.05$) (Figure 5.14C).

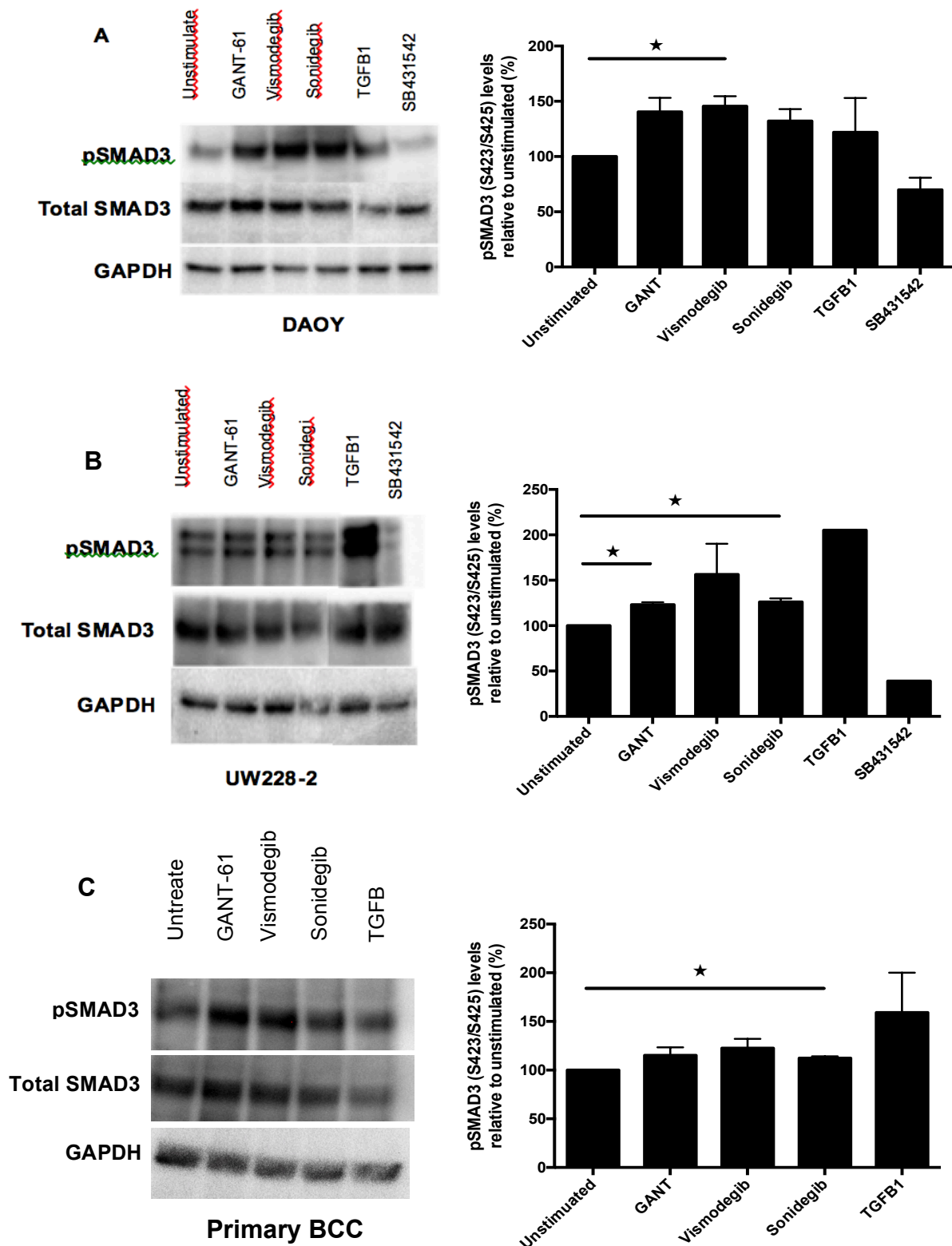


Figure 5.14: The TGF β signalling pathway is activated following treatment with Hh antagonists in Hh driven tumours

The tumour cell lines, DAOY and UW228-2, were cultured in normal growth medium in the presence of Hh antagonists at a concentration of 10 μ M for 4hr before lysing and extracting protein for Western blot analysis. Primary BCC adhered to the same drugging

*and protein extraction regime, but whole tissue was first dissociated into single cells and then plated before being drugged. Western Blotting and Densitometry analysis for (A) DAOY cells, (B) UW228-2 cells (C) Primary BCC cells. pSMAD3 bands were normalised firstly to total SMAD3, and then GAPDH. Experiments on the DAOY and UW228-2 cell lines were performed in triplicate (n=3), while experiment on primary BCC was performed in duplicate (n=2), Error bars represent SE of mean, * represents $p < 0.05$, t-test.*

To determine the impact of Hh antagonists on TGF β regulated genes (defined in section 5.2.8), cell lines were cultured with Hh antagonists for 24hr, and RNA subsequently extracted for a qPCR assay (summarised in Table 5.4).

In DAOY cells, as previously mentioned the cell specific TGF β regulated genes (TGF β 1-induced and ALK5 receptor kinase dependent), CEBPD, SERPINE1 and SKIL were found to decrease, increase and increase in expression, respectively, following TGF β 1 agonist treatment when compared to the untreated control (Figure 5.15A). Following Hh antagonist treatment in comparison to the untreated control: a reduction in CEBPD expression was found following treatment with vismodegib (-3.89 ± 0.11 ; $p < 0.05$), whereas GANT-61 showed no change in expression (0.02 ± 0.09), and sonidegib induced an increase in expression (1.43 ± 0.38 ; $p < 0.05$); a reduction was observed in SERPINE1 expression following vismodegib (-2.05 ± 0.09) and GANT-61 (-0.74 ± 0.08) treatment, whereas an increase was observed for sonidegib (1.70 ± 0.31) treatment; finally, a reduction was observed in SKIL expression following vismodegib (-1.82 ± 0.08) and GANT-61 (-0.87 ± 0.08) treatment, whereas an increase was observed for sonidegib (0.23 ± 0.08) treatment. Therefore, in the DAOY cell line, a TGF β 1 induced response was observed for: 1) vismodegib and CEBPD expression, 2) sonidegib and SERPINE1 and SKIL expression, and 3) GANT-61 and CEBPD expression.

In UW228-2 cells, as previously mentioned the cell specific TGF β regulated genes (TGF β 1-induced and ALK5 receptor kinase dependent), CEBPD and NEDD9 were found to decrease and increase in expression, respectively, following TGF β 1 agonist treatment when compared to the untreated control (Figure 5.15B). Following Hh antagonist

treatment in comparison to the untreated control: a reduction in CEBPD expression was found following treatment with vismodegib (-2.60 ± 0.45) and sonidegib (-3.62 ± 0.06 ; $p < 0.05$), but this however was not observed following GANT-61 treatment (0.33 ± 0.13); a reduction was observed in NEDD9 expression following vismodegib (-3.54 ± 0.04) and sonidegib (-5.70 ± 0.04 ; $p < 0.01$) treatment, whereas an increase was observed for GANT-61 (0.29 ± 0.07) treatment. Therefore, in the UW228-2 cell line, a TGF β 1 induced response was observed for: 1) vismodegib and CEBPD expression, 2) sonidegib and CEBPD expression, and 3) GANT-61 and NEDD9 expression.

In SJS-1 cells, as previously mentioned the cell specific TGF β regulated genes (TGF β 1-induced and ALK5 receptor kinase dependent), CEBPD and NEDD9 were found to decrease and increase in expression, respectively, following TGF β 1 agonist treatment when compared to the untreated control (Figure 5.15C). Following Hh antagonist treatment in comparison to the untreated control: an increase in CEBPD expression was found following treatment with sonidegib (0.41 ± 0.37) and GANT-61 (0.40 ± 0.26), whereas no change in expression was observed following vismodegib treatment (-1.39 ± 0.18); an increase was observed in NEDD9 expression following sonidegib (0.42 ± 0.17) treatment, whereas no change was observed for both vismodegib (0.12 ± 0.17) and GANT-61 (0.07 ± 0.05) treatment. Therefore, in the SJS-1 cell line, a TGF β 1 induced response was observed for: sonidegib and NEDD9 expression only.

Collectively these findings show that the response of each cell line is varied following Hh antagonist treatment. Sonidegib was shown to induce TGF β regulated genes in DAOY cells. Both sonidegib and vismodegib appeared to downregulate TGF β regulated genes in UW228-2 cells, a cell line known to be less sensitive to Hh antagonist treatment.

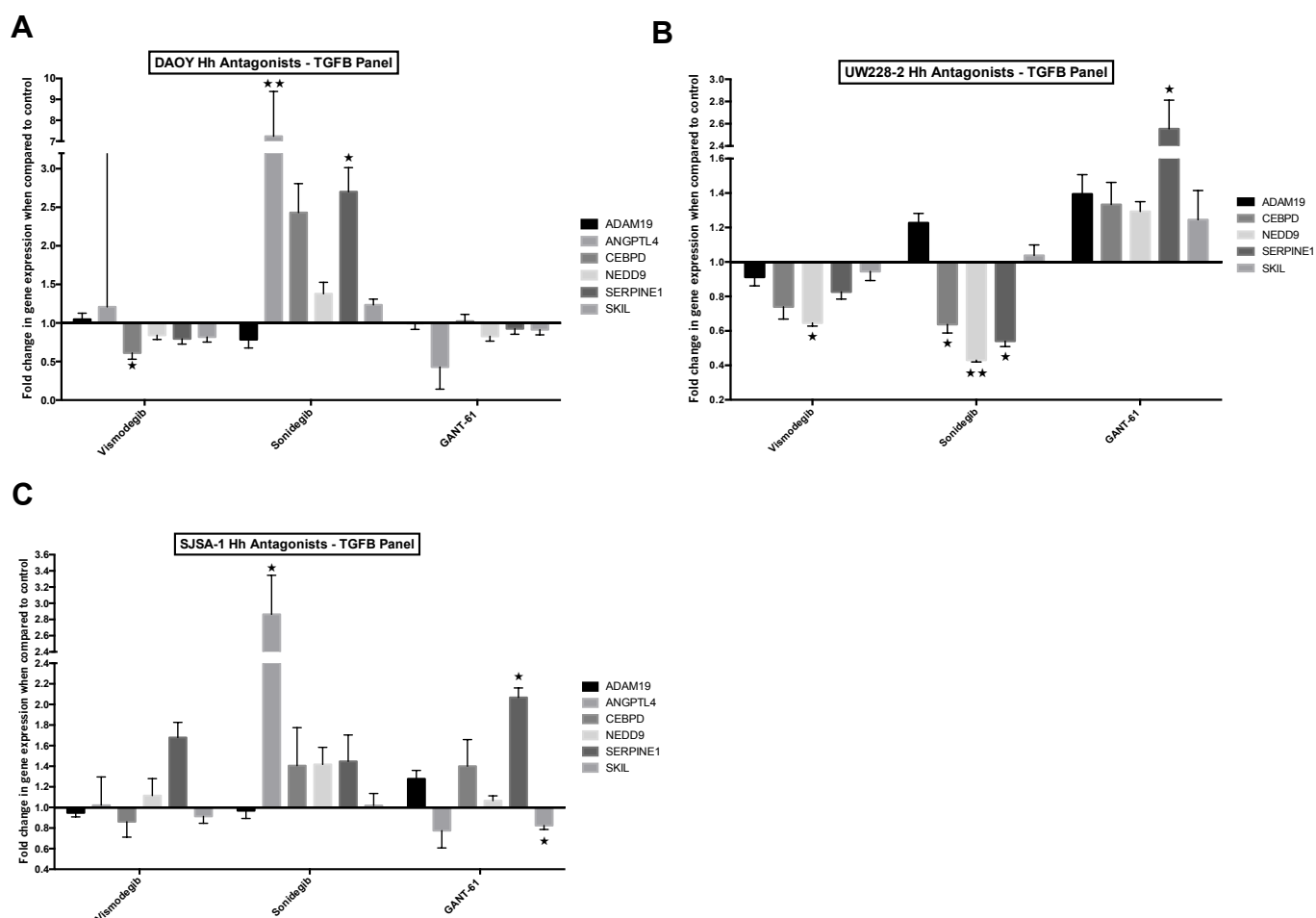


Figure 5.15: TGF β -regulated genes are induced following treatment with Hh antagonists in Hh driven tumours.

(A) HaCaT cells treated with TGF β 1 (+ve); blue bars shown genes upregulated in response to TGF β 1; red bars indicate genes downregulated in response to TGF β 1, **(B)** DAOY cell line treated with GANT-61, vismodegib and sonidegib, **(C)** UW228-2 cell line treated with vismodegib, sonidegib and GANT-61, and **(D)** SJS-1 cell line treated with vismodegib, sonidegib, and GANT-61. Expression values are based on the Log₁₀RQ, where a value of 10.0 represents a fold change of +10, and 0.1 represents a fold change of -10 in comparison to the control. All results are an average of two independent experiments. The qPCR assay was performed with three internal technical replicates and two endogenous controls. (n=2), Error bars represent SE of mean, * represents p<0.05, ** represents p<0.01.

Table 5.4: Impact of Hh antagonists on cell line specific TGF β regulated genes

*UP, represents genes that are upregulated; DOWN, represents genes that are downregulated; NC, represents no change in gene expression. All changes stated are in comparison to the untreated control. *=moderately up/downregulated; **=highly up/downregulated. ?=cannot determine based on the available data.*

Cell Line	TGF β Regulated Genes	Impact of TGF β 1	Impact of Vismodegib	Induction of TGF β Regulated Genes	Impact of Sonidegib	Induction of TGF β Regulated Genes	Impact of GANT-61	Induction of TGF β Regulated Genes
DAOY	CEBPD	DOWN	DOWN*	YES	UP	NO	DOWN	YES
	SERPINE1	UP	DOWN	NO	UP*	YES	DOWN	NO
	SKIL	UP	DOWN	NO	UP	YES	DOWN	NO
UW228-2	CEBPD	DOWN**	DOWN*	YES	DOWN**	YES	UP	NO
	NEDD9	UP	DOWN*	NO	DOWN*	NO	UP	YES
SJS-A-1	CEBPD	DOWN	DOWN/NC	YES/?	UP	NO	UP	NO
	NEDD9	UP	NC	NO/?	UP	YES	NC	NO

5.2.10 Blocking TGF β signalling

TGF β signalling can be blocked at the level of: TGF β receptor kinase activation (small molecule tyrosine kinase inhibitor SB431542), and signal transduction binding of phosphorylated SMAD3 with the co-SMAD, SMAD4 (by siRNA transcript knockdown).

Next the efficacy of the two approaches for blocking TGF β 1 signalling in our Hh driven tumour cell lines was determined by evaluating nuclear pSMAD3 accumulation using immunofluorescence and expression of a panel of TGF β responsive genes by qRT-PCR (already defined). As expected, immunofluorescence of pSMAD3 showed reduction of nuclear accumulation with SB431542 in all three Hh driven cell lines (Figure 5.16A). SMAD4 knockdown was achieved with siRNA to limit cell cytotoxicity before evaluation

of the effectiveness of *in vitro* TGF β signalling blockade. Optimisation of SMAD4 siRNA transfection was undertaken with varying concentrations of Lipofectamine and siRNA; and qPCR was performed to assess the level of SMAD4 transcript knockdown (Figure 5.16B). In both the DAOY and UW228-2 cell lines (data not available for SJS-1 cell line), when using 0.625 μ M of Lipofectamine with 0.3125 μ M of SMAD4 siRNA, a 10-fold and 4-fold downregulation of SMAD4 was achieved, respectively, when compared to the control. Furthermore, when knocking down SMAD4, there was a downregulation in most of the TGF β regulated genes in all three-cell lines (Figure 5.16C).

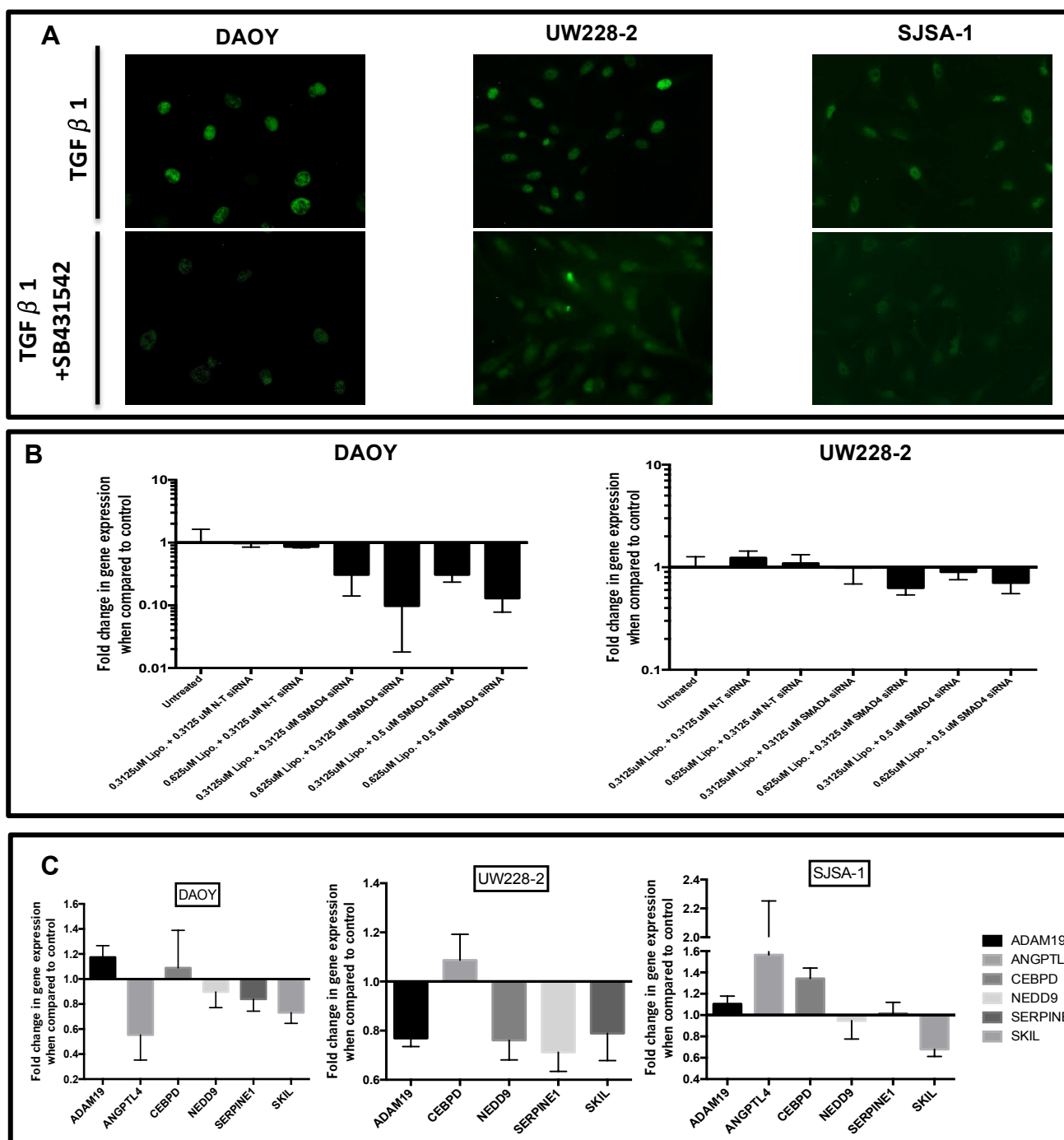


Figure 5.16: Blocking TGFβ signalling.

DAOY, UW228-2 and SJS-1 cell lines were cultured under normal growth conditions before being treated with 10 μM SB431542 for 24 hr and subsequently performing (A) Immunofluorescence for pSMAD3 nuclear labelling, with TGFβ1 used as a positive control (B) qPCR to show the downregulation of SMAD4 following optimisation of lipofectamine and siRNA concentrations in the DAOY and UW228-2 cells (data not

available for SJS-1 cell line). The core panel of genes was used on DAOY, UW228-2 and SJS-1 cells treated with (C) SMAD4 siRNA for 48 hr. Expression values are based on the Log_{10}RQ , where a value of 10.0 represents a fold change of +10, and 0.1 represents a fold change of -10. The qPCR assay was performed with three internal technical replicates and two endogenous controls. Error bars represent SE of mean.

5.2.11 Effect of Blocking TGF β Signalling on Hh-regulated Genes in Hh Driven Tumours

We next sought to test the impact of TGF β inhibitors (SB431542, and SMAD4 siRNA) on Hh-regulated genes (defined in section 5.2.3) using qPCR (Figure 5.17; summarised in Table 5.5). As previously mentioned numerous studies have demonstrated crosstalk between the TGF β and Hh signalling pathways, we therefore wanted to establish whether genes regulated through Hh signalling are impacted following the addition of TGF β inhibitors in our Hh driven cell lines.

In DAOY cells, as previously mentioned the cell specific Hh regulated genes (Hh-induced and Hh inhibitor responsive), GLI1, GLI2 and SMO were found to all increase in expression, following Hh agonist treatment when compared to the untreated control. Following SB43142 treatment, in comparison to the untreated control: a slight increase in SMO (0.10 ± 0.05) expression was found, but this however was not observed for GLI1 and GLI2 where there was no change in expression (0.09 ± 0.41) and (-0.63 ± 0.24), respectively. Following SMAD4 knockdown, in comparison to the untreated control: an increase in expression was observed for GLI1 (1.60 ± 0.8 ; $p<0.05$), GLI2 (0.27 ± 0.20) and SMO (1.42 ± 0.34 ; $p<0.05$). Therefore, in the DAOY cell line, a Hh induced response was observed for: 1) SB431542 and GLI1 and SMO expression, 2) SMAD4 knockdown and GLI1, 2, and SMO expression.

In UW228-2 cells, as previously mentioned the cell specific Hh regulated genes, GLI1, GLI2 and SMO were found to increase, decrease and decrease in expression,

respectively, following Hh agonist treatment when compared to the untreated control. Unfortunately data is not available for the impact of SB431542 on Hh regulated genes in this cell line. Following SMAD4 knockdown, in comparison to the untreated control: an increase in expression was observed for GLI1 (0.77 ± 0.74), no change in expression was observed for GLI2 (0.06 ± 0.31), while the expression of SMO decreased unchanged (-0.83 ± 0.05). Therefore, in the UW228-2 cell line, a Hh induced response was observed for: 1) SMAD4 knockdown and GLI1 and SMO expression.

In the SJSA-1 cell line, GLI2, PTCH, and SMO were classified as being Hh regulated. In SJSA-1 cells, all three genes were downregulated in response to SB431542 treatment, GLI2 (-3.97 ± 0.15 ; $p < 0.01$), PTCH1 (-3.37 ± 0.1 ; $p < 0.05$), and SMO (-1.10 ± 0.20) (Figure 5.17). Finally, following SMAD4 knockdown, no changes in gene expression were observed in any of the genes when compared to the untreated control (Figure 5.17). Therefore, in the SJSA-1 cell line, a Hh induced response was observed for: 1) SB431542 and GLI2, PTCH and SMO expression.

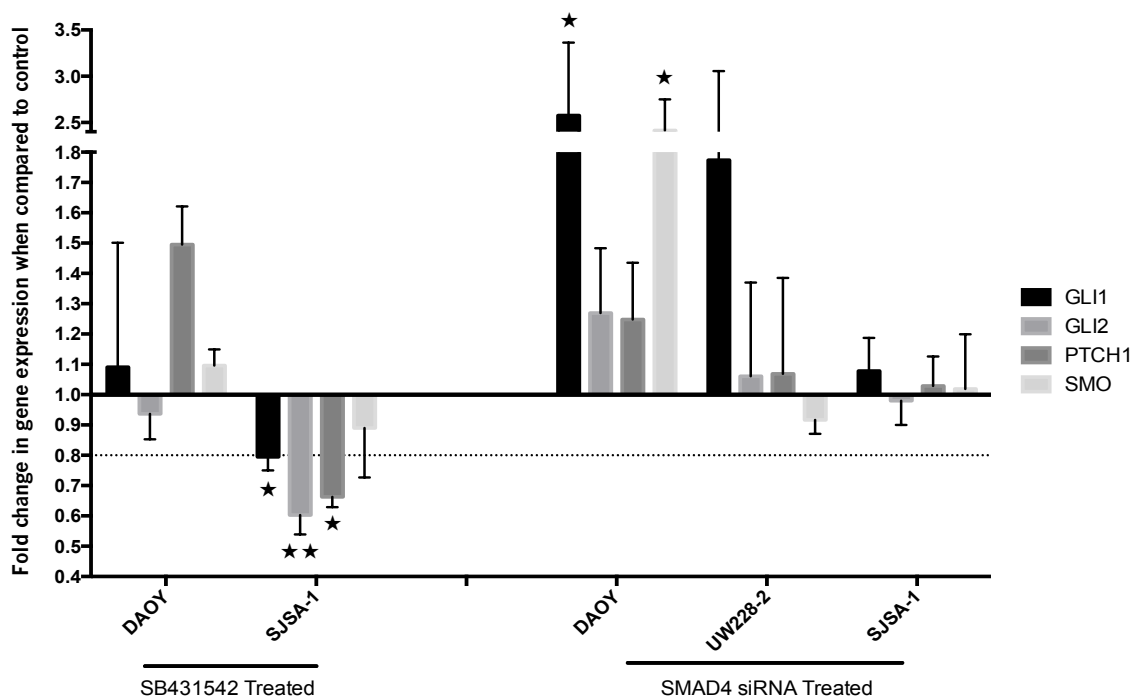


Figure 5.17: Effect of Blocking TGF β Signalling on Hh-regulated Genes in Hh Driven Tumours.

*Hh driven cell lines were cultured in the presence of the TGF β blocker SB431542 for 24 hr, and SMAD4 siRNA for 48 hr. RNA was extracted and assayed for a panel of Hh-regulated genes in DAOY, UW228-2, and SJSA-1 cells by qPCR. Expression values are based on the Log_{10}RQ , where a value of 10.0 represents a fold change of +10, and 0.1 represents a fold change of -10. All results are an average of two independent experiments. The qPCR assay was performed with three internal technical replicates and two endogenous controls. ($n=2$), Error bars represent SE of mean, *represents $p < 0.05$, ** represents $p < 0.01$, t-test.*

Table 5.5: Impact of TGF β inhibition on cell line specific Hh regulated genes

*UP, represents genes that are upregulated; DOWN, represents genes that are downregulated; NC, represents no change in gene expression. All changes stated are in comparison to the untreated control. *=moderately up/downregulated; **=highly up/downregulated. ?=cannot determine based on the available data.*

Cell Line	Hh Regulated Genes	Impact of Hh	Impact of SB431542	Induction of Hh Regulated Genes	Impact of SMAD4 siRNA	Induction of Hh Regulated Genes
DAOY	GLI1	UP	UP/NC	YES/?	UP*	YES
	GLI2	UP	DOWN/NC	?	UP	YES
	SMO	UP	UP	YES	UP*	YES
UW228-2	GLI1	UP	N/A	N/A	UP	YES
	GLI2	DOWN	N/A	N/A	NC	?
	SMO	DOWN	N/A	N/A	DOWN	YES
SJS-1	GLI2	DOWN	DOWN	YES	NC	NO
	SMO	DOWN	DOWN	YES	NC	NO
	PTCH	DOWN	DOWN	YES	NC	NO

5.2.12 Apoptosis after blocking TGF β signalling

In order to determine whether TGF β inhibition (SB431542 and SMAD4 siRNA) increased cell death in our Hh driven cell lines, we undertook flow cytometric analysis on cells treated for 4, 24, and 48 hours, then labelled with Annexin V and DAPI.

Figure 5.18 shows representative dot plots between untreated and TGF β antagonist treated cell lines over three time-points. Table 5.6 below outlines the effect of SB431542 and SMAD4 siRNA only treatments on early apoptosis (Annexin^{pos}/DAPI^{neg}),

late apoptosis (Annexin^{pos}/DAPI^{pos}) or necrosis (Annexin^{neg}/DAPI^{pos}) over three time-points (4, 24 and 48hr) in our Hh driven cell lines relative to the total cell population (100%).

As a percentage of the total cell population (100%) all three-cell lines demonstrated no significant difference in early apoptosis, late apoptosis or necrosis between untreated and SB431542 treatment over the three time-points, with the exceptions of DAOY cells, where the 48 hr treatment increased the percentage of cells in early apoptosis (3.70% vs 10.63%; $p < 0.05$); and in UW228-2 cells, where 24 and 48 hr treatments increased the percentage of cells in late apoptosis (0.63% vs 9.20%; $p < 0.05$ and 0.73% vs 5.64%; $p < 0.05$, respectively).

As a percentage of the total cell population (100%) all three-cell lines demonstrated no significant difference in early apoptosis, late apoptosis or necrosis between scrambled siRNA and SMAD4 siRNA treatment over the three time-points (Table 5.6).

In conclusion, the TGF β antagonists, SB431542 and SMAD4 siRNA had no effect on cell apoptosis or death in all three-cell lines.

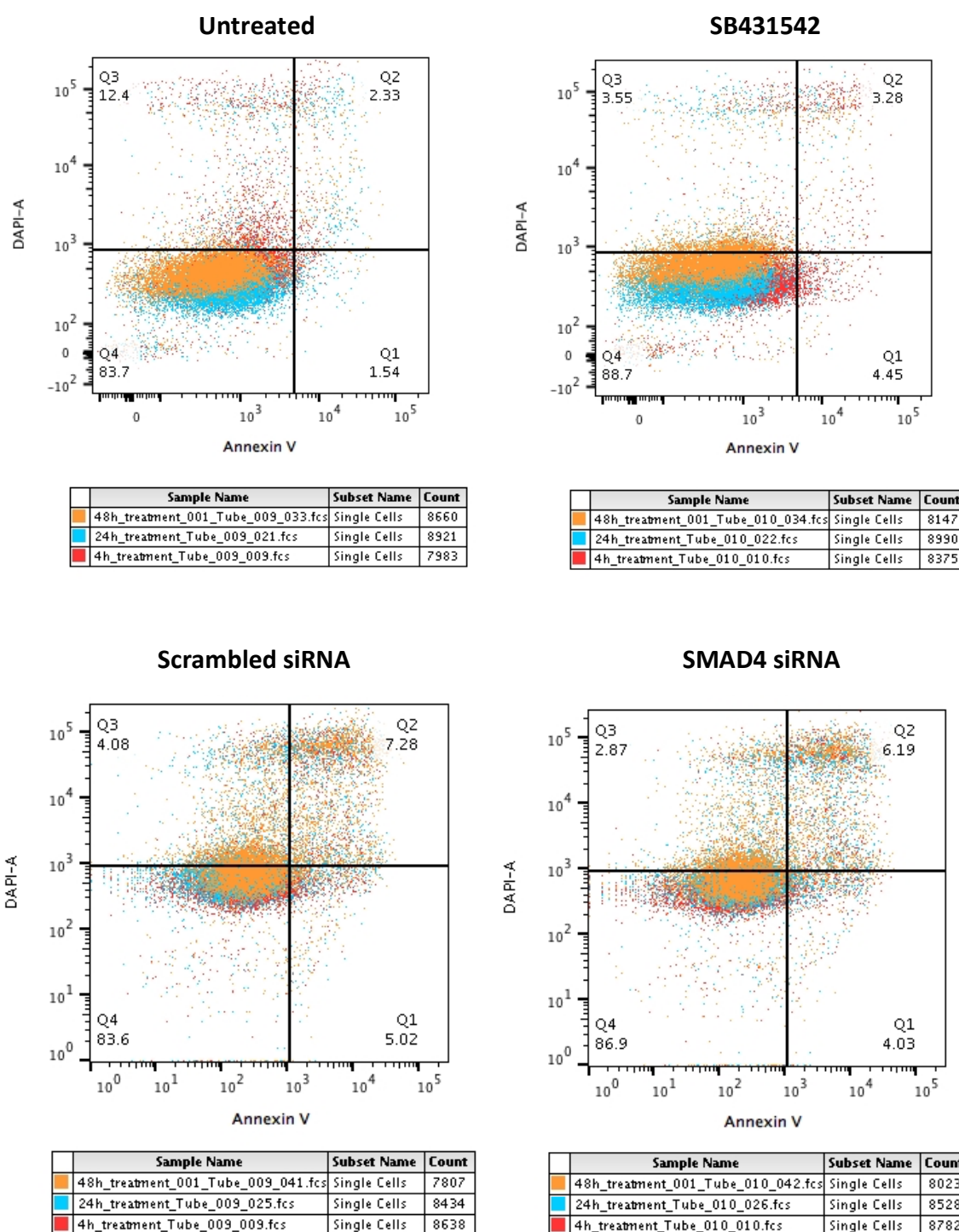


Figure 5.18: Impact TGF β antagonist only treatment on apoptosis in Hh driven tumour cell lines

Representative dot plot to show the effect of TGF β antagonists over the three time periods 4, 24, and 48 hours in Hh driven tumour cell lines. 4hr (red population), 24hr (blue population), and 48hr (orange population) treatments are merged on top of each other in order to display any shifts following treatment over the three time periods. Annexin V (apoptosis marker) and DAPI (dead cell marker) are on the X- and Y-axis,

respectively. Each quadrant represents as follows: Q1) early apoptosis, Q2) late apoptosis, Q3) necrosis, Q4) viable cells. Experiments were performed in duplicate ($n=2$), * represents $p<0.05$, t -test.

Table 5.6: Effect of TGF β antagonist treatment on inducing apoptosis in Hh driven cell lines.

#	Drug	Time Points (hr)	% Live Cells	% Early Apoptosis	% Late Apoptosis	% Necrosis
DAOY	Untreated	4	90.95	5.34	1.75	1.96
		24	89.55	5.72	2.75	1.99
		48	91.90	3.70	0.99	3.39
	SB431542	4	87.75	4.44	1.43	6.36
		24	86.60	7.71	3.22	2.46
		48	82.85	10.63	3.24	3.31
	Scrambled siRNA	4	88.35	3.41	4.72	3.50
		24	81.30	2.80	5.51	10.39
		48	65.15	3.59	11.65	19.64
	SMAD4 siRNA	4	90.25	2.66	3.84	3.25
		24	81.45	3.35	6.38	8.83
		48	67.20	2.81	10.37	19.65
UW228-2	Untreated	4	95.25	2.47	0.83	1.48
		24	95.50	1.46	0.63	2.42
		48	94.80	1.88	0.73	2.60
	SB431542	4	87.30	3.83	2.96	5.95
		24	82.15	3.82	9.20	4.84
		48	85.70	3.92	5.64	4.80
	Scrambled siRNA	4	85.20	0.77	4.63	9.38
		24	86.50	2.39	1.66	9.47
		48	81.30	2.95	4.08	11.70
	SMAD4 siRNA	4	95.50	0.83	0.70	2.97
		24	90.50	1.87	1.07	6.57
		48	86.30	2.81	2.02	8.85
Untreated	4	93.10	3.94	1.21	1.57	
	24	95.70	1.20	1.26	1.84	
	48	95.40	1.85	0.69	2.04	

SJS-1	SB431542	4	94.55	2.26	1.47	1.77
		24	94.05	2.88	1.34	1.74
		48	95.50	1.72	1.22	1.57
	Scrambled siRNA	4	82.40	8.75	3.76	5.08
		24	71.20	4.75	8.60	15.40
		48	30.10	8.88	33.00	28.00
	SMAD4 siRNA	4	88.20	5.12	2.18	4.49
		24	75.70	4.50	6.27	13.60
		48	39.00	8.97	25.40	26.70

5.2.13 Effect of Blocking TGF β signalling on cell viability

TGF β signalling blockade with SB431542 was evaluated by plating 10,000 cells into a 96-well flat-bottomed plate overnight then incubating with SB431542 for 24 hr, before evaluation of cell viability using cell titre glo assay on a CLARIOstar plate reader. These experiments were conducted in quadruplicate, in three separate experiments.

We observed no loss of viability in DAOY (98.8% \pm 3.7%), UW228-2 (107.0% \pm 1.9%), and SJS-1 (124.8% \pm 19.8%) cell lines in comparison to unstimulated control (100%) (Figure 5.19A). In conclusion, TGF β signalling blockade with the small molecule receptor tyrosine kinase inhibitor SB431542, although effective at blocking TGF β signalling, did not significantly affect cell viability significantly in these experiments.

TGF β signalling blockade with SMAD 4 siRNA was similarly evaluated by incubation with SMAD4 siRNA for 48 hr, before evaluating cell viability through the cell titre glo assay. These experiments were conducted in quadruplicate, in three separate experiments. We observed no loss of viability, in DAOY (106.0% \pm 6.4%), UW228-2 (102.5% \pm 1.9%), and SJS-1 (109.6% \pm 8.0%) cell lines in comparison to scrambled controls (100%) (Figure 5.19B).

In summary, the 2D culture growth and viability of Hh driven cell lines studied (DAOY, SJS-1 and UW228-2) was unaffected by TGF β blockade.

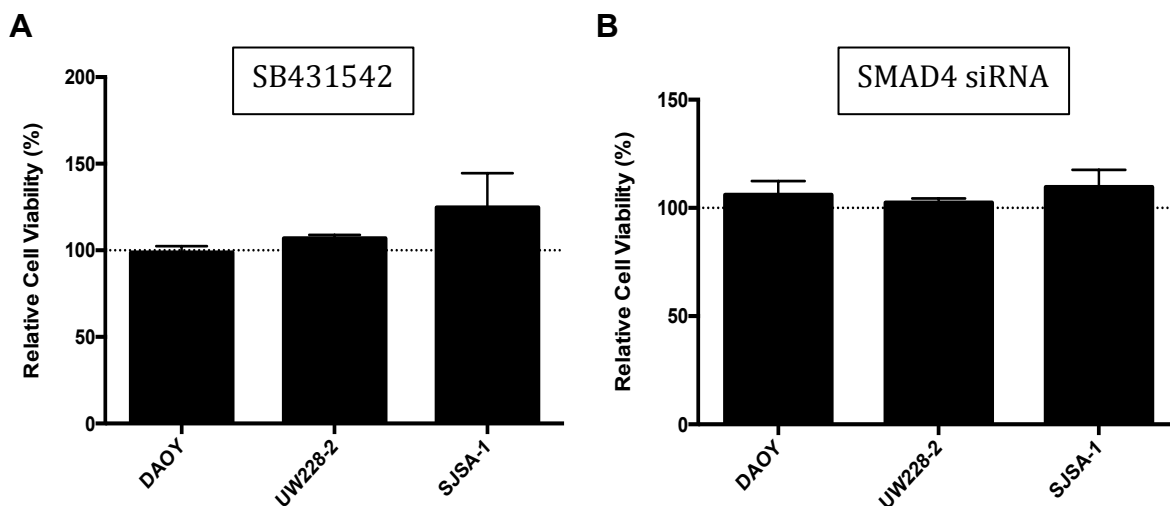


Figure 5.19: Blocking the TGF β signalling pathway at both the receptor and transcription factor level appears to have very little impact on relative cell viability in Hh driven cell lines.

DAOY, UW228-2 and SJSA-1 cell lines were cultured under normal conditions and treated with (A) 10 μ M SB431542 for 24hr and (B) SMAD4 siRNA for 48 hr. Graphs represent an average over three independent experiments, with each experiment having four internal technical replicates for each condition. (n=3). Error bars represent SE of mean.

5.2.14 Effect of TGF β blockade on 2D colony formation

As TGF β can regulate SC fate and cell viability, we next evaluated the effect of TGF β blockade on 2D Colony formation (Watabe *et al.*, 2009).

To evaluate the effects SB431542 on CFE, 75 (DAOY), 187.5 (UW228-2), and 125 (SJSA-1) cells/cm² were plated in a 12-well tissue culture plate and left to adhere overnight. Cells were then treated with SB431542 for 7 days and CFE was evaluated using GelCount (Oxford Optronix). Experiments were performed in triplicate, in four separate experiments. There was a reduction in CFE in all cell lines, DAOY (78.2% \pm 7.3%), UW228-2 (53.0% \pm 2.4%; $p < 0.01$) and SJSA-1 (65.1% \pm 6.9%; $p < 0.05$) in comparison to unstimulated controls (100%) (Figure 5.20B).

TGF β signalling blockade with SMAD4 siRNA was similarly evaluated for CFE, by first incubating with siRNA for 48 hr before trypsinising and plating SMAD4 siRNA and scramble cells at the same densities as before for 7 days. There was no difference in CFE compared to scrambled control for DAOY (92.1% \pm 7.1%) and UW228-2 (96.8% \pm 6.7%), while a reduction was observed for SJSA-1 (78.3% \pm 4.3%) (Figure 5.20C).

In summary, SB431542 led to a significant reduction in CFE in two cell lines (UW228-2 and SJSA-1). There was no reduction in CFE with SMAD4 knockdown in DAOY and UW228-2, whereas a slight reduction was observed in SJSA-1 cells.

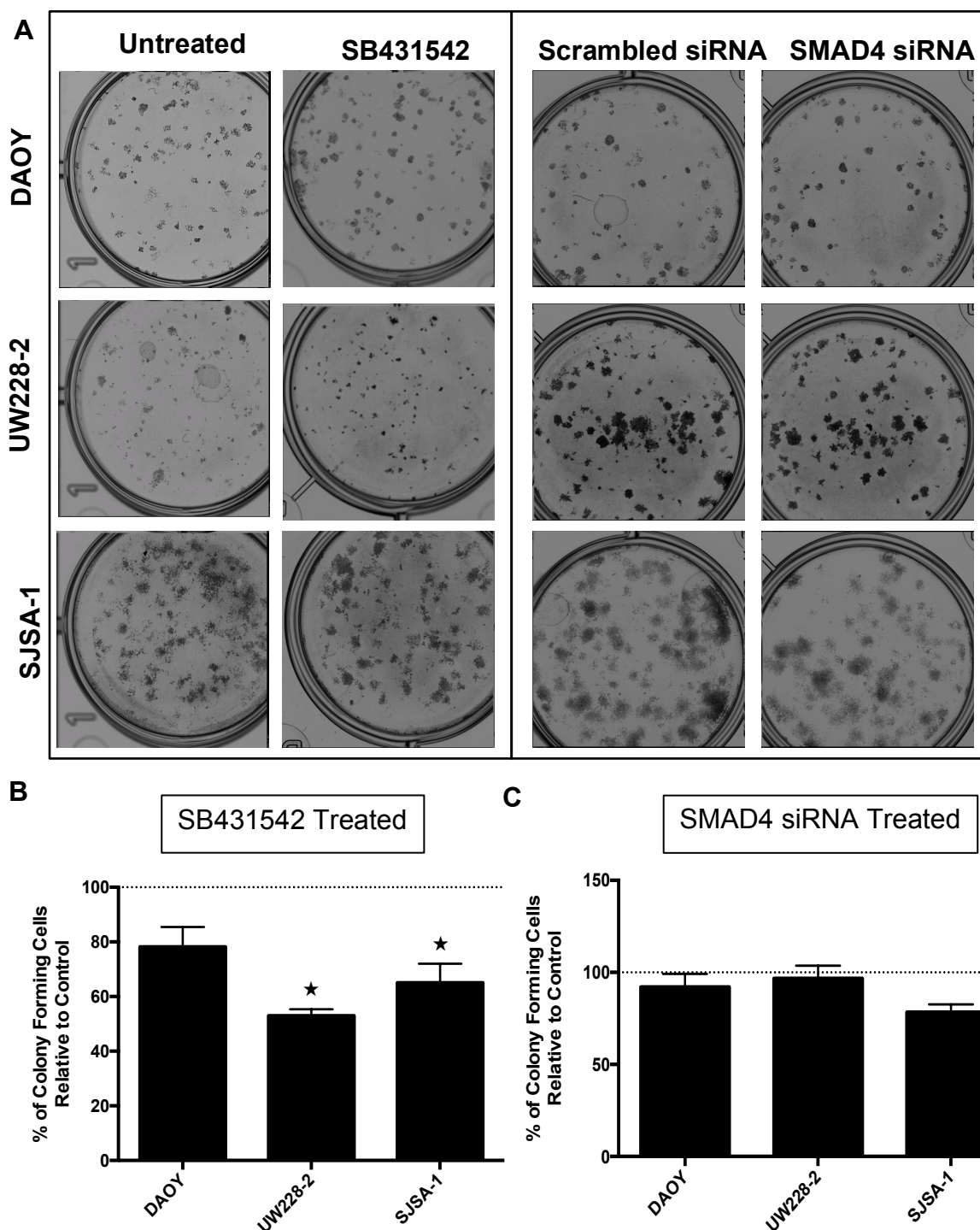


Figure 5.20: Effect of TGF β blockade on 2D colony formation: Colony-Forming Assays. Cells were seeded at a density of 75 cells/cm² for DAOY, 187.5 cells/cm² for UW228-2, and 125 cells/cm² for SJSA-1 cell lines in the presence or absence of TGF β Antagonists for 7-12 days. **(A)** Representative Images, **(B)** SB431542 treatment, **(C)** SMAD4 K-D. All results are averages of at least 4 experimental replicates, along with three internal technical replicates for each drugging condition. (n=4), Error bars represent SE of mean, * represents $p < 0.05$, t-test.

5.2.15 Effect of TGF β blockade on 3D tumoursphere forming units

To determine the effect of SB431542 on 3D TFUs, we treated cells in adherent culture for 24 hr before passaging them into non-adherent culture conditions at a density of 5 cells/ μ L for both DAOY and UW228-2 cell lines. After 7 days, spheres were counted using an inverted microscope (Passage 1) then dissociated into single cells and subsequently reseeded at 5 cells/ μ L and again allowed to form spheres over 7 days and counted (Passage 2).

After passage 1 there was no reduction of 3D TFUs following SB431542 treatment in comparison to the control: DAOY (127.8% \pm 11.3%) and UW228-2 (109.0% \pm 25.5%). At passage 2 3D TFUs were reduced in both cell lines although these changes were not significant: DAOY (72.7%) and UW228-2 (88.9%) (Figure 5.21A).

The effect of SMAD 4 knockdown on 3D TFUs was determined by incubating cultured cells with SMAD4 siRNA for 48 hr before trypsinising and plating at low density for 7 days. After 7 days, spheres were counted, dissociated and reseeded at the same density before being allowed to form spheres for another 7 days and counted again.

After passage 1, SMAD4 knockdown resulted in a reduction of 3D TFUs in DAOY cells (51.9% \pm 7.4%; $p < 0.05$), but not in the UW228-2 cells (100.0% \pm 14.0%). At passage 2 both cell lines demonstrated reduced 3D TFUs: DAOY (62.8% \pm 11.6%; $p < 0.05$) and UW228-2 (72.7% \pm 36.4%) (Figure 5.21B).

TGF β blockade did not impact on the size of the TFUs in either the DAOY or UW228-2 cell lines following both SB431542 treatment and SMAD4 K-D (Figure 5.21C).

In summary, TGF β blockade resulted in a partial effect on 3D TFUs, predominantly seen at passage 2, suggesting that TGF β was necessary for TFE and therefore SC self renewal/maintenance.

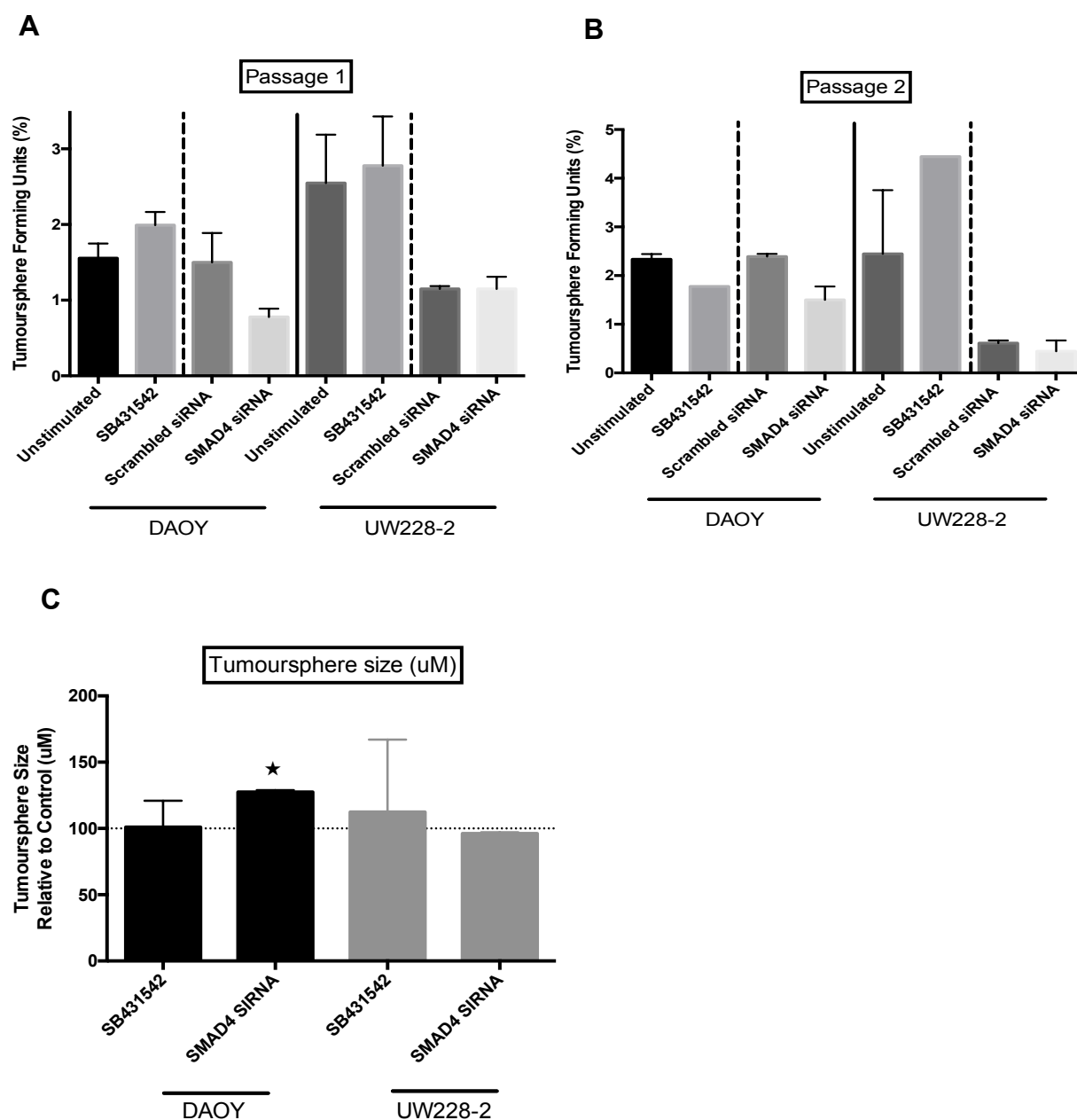


Figure 5.21: Effect of TGF β blockade on tumoursphere-forming cells: Sphere-Forming Assays.

Cells were seeded in 2D and allowed to adhere overnight before being treated with the TGF β antagonists, SB431542 and SMAD4 siRNA for 24 and 48hr, respectively. Following treatment cells were trypsinised and plated under sphere forming conditions at a density of 5 cells/ μ L for both DAOY and UW228-2 cell lines and allowed to form spheres over 7 days before being enumerated (P1). Spheres were then dissociated and re-plated at a density of 5 cells/ μ L and allowed to grow for a further 7 days, before being enumerated

(P2). **(A)** % TFUs at P1 in DAOY and UW228-2 cells treated with TGF β antagonists, **(B)** %TFUs at P2 in DAOY and UW228-2 cells treated with TGF β antagonists, **(C)** Area of DAOY and UW228-2 TFUs treated with TGF β antagonists relative to untreated control. (n=3), (n=1, for conditions lacking error bars), Error bars represent SE of mean, * represents $p < 0.05$, t-test.

5.2.16 Effect of combining TGF β and Hh antagonist on Hh- and TGF β -regulated genes

We sought to determine the expression of TGF β regulated genes by combining SB431542 with Hh-signalling inhibitors (Figure 5.22) and comparing gene expression levels to Hh antagonist only treated cells (Figure 5.15). Summarised in Table 5.7.

As highlighted in section 5.2.9, in the DAOY cell line, a TGF β 1 induced response was observed for: 1) vismodegib and CEBPD expression, 2) sonidegib and SERPINE1 and SKIL expression, and 3) GANT-61 and CEBPD expression. For SB431542 combination treatment (Figure 5.22A): in the combination treatment (SB431542+vismodegib) we observed an increase in expression for CEBPD (0.98 ± 0.24) in comparison to the vismodegib only treatment; in the combination treatment (SB431542+sonidegib) we observed a downregulation of SERPINE1 (-7.43 ± 0.10) and SKIL (-7.23 ± 0.11) when compared with the sonidegib only treatment; finally, in the combination treatment (SB431542+GANT-61) we observed an upregulation of CEBPD (2.03 ± 0.43) when compared to the GANT-61 only treatment. Therefore, SB431542 treatment appeared to reverse the induction of TGF β regulated genes for the respective Hh antagonist treatments.

As highlighted in section 5.2.9, in the UW228-2 cell line, a TGF β 1 induced response was observed for: 1) vismodegib and CEBPD expression, 2) sonidegib and CEBPD expression, and 3) GANT-61 and NEDD9 expression. For SB431542 combination treatment (Figure 5.22B): in the combination treatment (SB431542+vismodegib) we observed an increase in expression for CEBPD (0.34 ± 0.22) in comparison to the vismodegib only treatment; in the combination treatment (SB431542+sonidegib) we observed an increase in CEBPD (-

2.08±0.09) expression, and a downregulation of NEDD9 (-8.88±0.12) when compared with the sonidegib only treatment; finally, in the combination treatment (SB431542+GANT-61) we observed a downregulation of NEDD9 (-7.46±.11) when compared to the GANT-61 only treatment. Therefore, SB431542 treatment appeared to reverse the induction of TGFβ regulated genes for the respective Hh antagonist treatments.

As highlighted in section 5.2.9, in the SJSA-1 cell line, a TGFβ1 induced response was observed for: sonidegib and NEDD9 expression only. For SB431542 combination treatment (Figure 5.22C): in all three of the combination treatments (SB431542+vismodegib, SB431542+sonidegib and SB431542+GANT-61) we observed a decrease in expression of NEDD9 (-2.64±0.15, -2.61±0.14, -1.12±0.11, respectively) in comparison to the Hh antagonist only treatments. Therefore, SB431542 treatment appeared to reverse the induction of the TGFβ regulated gene, NEDD9, for all Hh antagonist treatments.

We next sought to determine the impact of SMAD4 K-D in combination with Hh antagonists on the expression of the TGFβ regulated genes in comparison to Hh antagonist only treatments (summarised in Table 5.8). Firstly however, when comparing the gene expression levels of the TGFβ-regulated genes between Hh antagonist only treatments (Figure 5.15) and scrambled siRNA+Hh antagonists only treatments, we found that gene expression values were all comparable between the treatments in all of our cell lines, therefore the control siRNA had no impact or minimal impact on the expression of our chosen genes.

As highlighted in section 5.2.9, in the DAOY cell line, a TGFβ1 induced response was observed for: 1) vismodegib and CEBPD expression, 2) sonidegib and SERPINE1 and SKIL expression, and 3) GANT-61 and CEBPD expression. For SMAD4 siRNA combination treatment (Figure 5.22D): in the combination treatment (SMAD4 siRNA+vismodegib) we observed a slight increase in expression for CEBPD (-2.09±0.14) in comparison to the vismodegib only treatment (-4.62±0.10); in the combination treatment (SMAD4 siRNA+sonidegib) we observed a downregulation of SERPINE1 (0.11±0.08) and a slight

upregulation/no change in SKIL (0.00 ± 0.12) when compared with the sonidegib only treatment (0.81 ± 0.14 and -0.89 ± 0.05 , respectively); finally, in the combination treatment (SMAD4 siRNA+GANT-61) we observed a upregulation of CEBPD (0.34 ± 0.09) when compared to the GANT-61 only treatment (-1.38 ± 0.08). Therefore, SMAD4 K-D appeared to reverse the induction of TGF β regulated genes for the respective Hh antagonist treatments, with the exception of SKIL in the sonidegib treated group.

As highlighted in section 5.2.9, in the UW228-2 cell line, a TGF β 1 induced response was observed for: 1) vismodegib and CEBPD expression, 2) sonidegib and CEBPD expression, and 3) GANT-61 and NEDD9 expression. For SMAD4 siRNA combination treatment (Figure 5.22E): in the combination treatment (SMAD4 siRNA+vismodegib) we observed an increase in expression for CEBPD (0.48 ± 0.17) in comparison to the vismodegib only treatment (-2.29 ± 0.04); in the combination treatment (SMAD4 siRNA+sonidegib) we observed no change in expression for CEBPD (-2.42 ± 0.21) in comparison to the sonidegib only treatment (-2.58 ± 0.04); finally, in the combination treatment (SMAD4 siRNA+GANT-61) we observed no change in NEDD9 expression (0.12 ± 0.08) when compared to the GANT-61 only treatment (0.01 ± 0.06). Therefore, SMAD4 K-D appeared to partially reverse the induction of TGF β regulated genes for the respective Hh antagonist treatments.

As highlighted in section 5.2.9, in the SJS-1 cell line, a TGF β 1 induced response was observed for: sonidegib and NEDD9 expression only. For SMAD4 siRNA combination treatment (Figure 5.22F): in all three of the combination treatments (SMAD4 siRNA+vismodegib, SMAD4 siRNA+sonidegib and SMAD4 siRNA+GANT-61) we observed a slight increase in expression of NEDD9 (-0.95 ± 0.20 , 0.15 ± 0.29 , -0.24 ± 0.20 , respectively) in comparison to the Hh antagonist only treatments (-2.36 ± 0.11 , 0.04 ± 0.22 , -1.45 ± 0.30 , respectively). Therefore, SMAD4 K-D did not appear to reverse the induction of TGF β regulated genes for the respective Hh antagonist treatments.

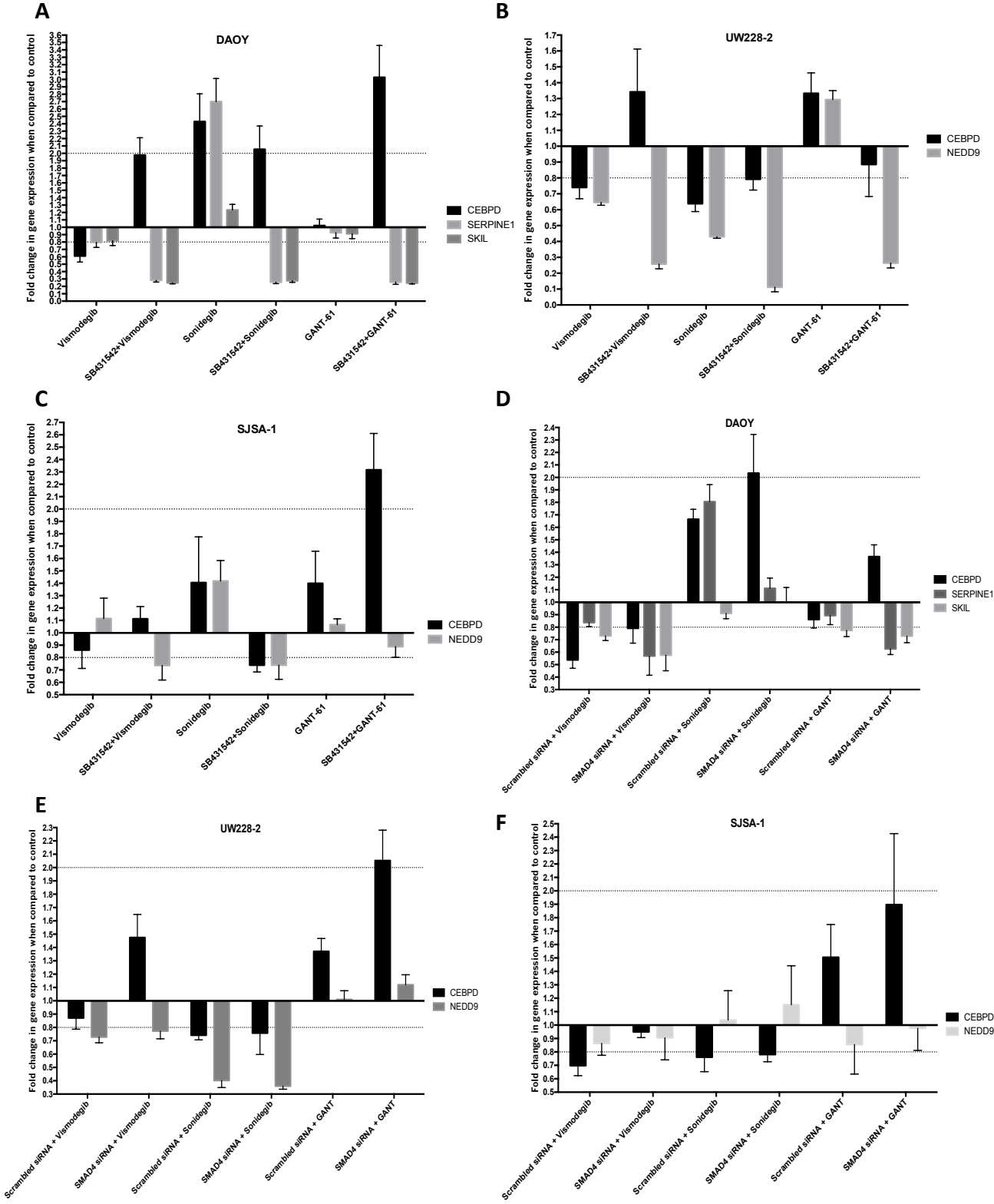


Figure 5.22: Effect of Blocking TGFβ- and Hh-signalling on TGFβ-regulated Genes in Hh Driven Tumours.

Hh driven cell lines were cultured in the presence of the TGFβ blocker SB431542 for 24hr, and SMAD4 siRNA for 48 hr, in combination with Hh antagonists (GANT-61, vismodegib,

sonidegib). RNA was extracted and assayed for a panel of TGF β -regulated genes following treatment with SB431542 in combination with Hh antagonists in **(A)** DAOY, **(B)** UW228-2, and **(C)** SJSA-1 cells, and treatment with SMAD4 siRNA in combination with Hh antagonists in **(D)** DAOY, **(E)** UW228-2, and **(F)** SJSA-1 cells by qPCR. Expression values are based on the Log₁₀RQ, where a value of 10.0 represents a fold change of +10, and 0.1 represents a fold change of -10. Results are an average of two independent experiments. The qPCR assay was performed with three internal technical replicates and two endogenous controls. (n=2). Error bars represent SE of mean.

Table 5.7: Impact of SB431542 combinational treatments on cell line specific TGF β regulated genes

UP, represents genes that are upregulated; DOWN, represents genes that are downregulated; NC, represents no change in gene expression. All changes stated are in comparison to the untreated control. *=moderately up/downregulated; **=highly up/downregulated. ?=cannot determine based on the available data.

Cell Line	TGF β Regulated Genes	Impact of Vismodegib	Impact of SB431542+ Vismodegib	Impact of Sonidegib	Impact of SB431542+ Sonidegib	Impact of GANT-61	Impact of SB431542+ GANT-61
DAOY	CEBPD	DOWN*	UP	UP	UP	DOWN	UP
	SERPINE1	DOWN	DOWN	UP*	DOWN	DOWN	DOWN
	SKIL	DOWN	DOWN	UP	DOWN	DOWN	DOWN
UW228-2	NEDD9	DOWN*	DOWN**	DOWN*	DOWN**	UP	DOWN**
	CEBPD	DOWN*	UP	DOWN**	DOWN*	UP	DOWN/NC
SJSA-1	CEBPD	DOWN/NC	UP/NC	UP	DOWN	UP	UP
	NEDD9	NC	DOWN	UP	DOWN	NC	DOWN/NC

Table 5.8: Impact of SMAD4 siRNA combinational treatments on cell line specific TGF β regulated genes

*UP, represents genes that are upregulated; DOWN, represents genes that are downregulated; NC, represents no change in gene expression. All changes stated are in comparison to the untreated control. *=moderately up/downregulated; **=highly up/downregulated. ?=cannot determine based on the available data.*

Cell Line	TGF β Regulated Genes	Impact of Vismodegib	Impact of SMAD4 siRNA+ Vismodegib	Impact of Sonidegib	Impact of SMAD4 siRNA+ Sonidegib	Impact of GANT-61	Impact of SMAD4 siRNA+ GANT-61
DAOY	CEBPD	DOWN**	DOWN*	UP	UP	DOWN	UP
	SERPINE1	DOWN**	DOWN**	UP	NC	DOWN	DOWN
	SKIL	DOWN**	DOWN**	DOWN	NC	DOWN	DOWN
UW228-2	NEDD9	DOWN	DOWN	DOWN	DOWN	NC	UP/NC
	CEBPD	DOWN	UP	DOWN	DOWN	UP*	UP**
SJS-A-1	CEBPD	DOWN	DOWN	DOWN	DOWN	UP	UP
	NEDD9	DOWN	DOWN/NC	NC	UP/NC	DOWN	NC

Next, we sought to determine the impact of combining TGF β - and Hh-signalling inhibitors on Hh-regulated genes when compared to Hh antagonist only treated cells. SB431542 combinational treatments are summarised in Table 5.9; whereas SMAD4 siRNA combinational treatments are summarised in Table 5.10.

As highlighted in section 5.2.3, in the DAOY cell line, a Hh induced response was observed for: 1) vismodegib and GLI1, GLI2 and SMO expression, 2) sonidegib and GLI1, GLI2 and SMO expression, and 3) GANT-61 and GLI1, GLI2 and SMO expression. For SB431542 combination treatment (Figure 5.23A): in the combination treatment (SB431542+vismodegib) we observed an increase in expression for GLI1 (-1.14 ± 0.42) and SMO (0.06 ± 0.03), whereas GLI2 (-0.16 ± 0.11) slightly increased in expression when compared to the vismodegib only treatment; in the combination treatment

(SB431542+sonidegib) we observed an increase in expression for GLI1 (0.10 ± 0.14) and SMO (0.08 ± 0.11), whereas GLI2 (-0.44 ± 0.10) expression remained unchanged when compared with the sonidegib only treatment; finally, in the combination treatment (SB431542+GANT-61) we again observed an increase in expression for GLI1 (0.11 ± 0.58) and SMO (0.02 ± 0.08), whereas GLI2 (0.03 ± 0.08) expression was reduced when compared with the the GANT-61 only treatment. Therefore, SB431542 treatment appeared to increase the expression of both GLI1 and SMO when combined with all three Hh antagonists.

As highlighted in section 5.2.3, in the UW228-2 cell line, a Hh induced response was observed for: 1) vismodegib and SMO expression, 2) sonidegib and GLI2 and SMO expression, and 3) GANT-61 and GLI2 and SMO expression. For SB431542 combination treatment (Figure 5.23B): in the combination treatment (SB431542+vismodegib) we observed no change in expression for SMO (-5.01 ± 0.15) when compared to the vismodegib only treatment; in the combination treatment (SB431542+sonidegib) we observed an increase in expression for GLI2 (0.15 ± 0.74) and SMO (0.13 ± 0.26) when compared with the sonidegib only treatment; finally, in the combination treatment (SB431542+GANT-61) we again observed an increase in expression for GLI2 (0.71 ± 1.72) and SMO (2.06 ± 0.17) when compared with the the GANT-61 only treatment. Therefore, SB431542 treatment appeared to increase the expression of both GLI1 and SMO when combined with sonidegib and GANT-61.

As highlighted in section 5.2.3, in the SJSA-1 cell line a Hh induced response was observed for: 1) vismodegib and GLI2, PTCH and SMO expression, 2) sonidegib and GLI2, PTCH and SMO expression, and 3) GANT-61 and GLI2, PTCH and SMO expression. For SB431542 combination treatment (Figure 5.23C): in the combination treatment (SB431542+vismodegib) we observed an increase in expression for SMO (0.27 ± 0.15), whereas GLI2 (-1.69 ± 0.11) and PTCH (-2.39 ± 0.05) decreased in expression when compared to the vismodegib only treatment; in the combination treatment (SB431542+sonidegib) we observed an increase in expression for SMO (0.37 ± 0.04), whereas GLI2 (-1.56 ± 0.09) and PTCH (-2.50 ± 0.06) decreased in expression when compared with the sonidegib only treatment; finally, in the combination treatment

(SB431542+GANT-61) we again observed an increase in expression for SMO (1.35 ± 0.39), whereas GLI2 (-3.20 ± 0.09) and PTCH (-1.80 ± 0.10) decreased in expression when compared with the GANT-61 only treatment. Therefore, SB431542 treatment appeared to decrease the expression of both GLI2 and PTCH and increase the expression of SMO when combined with all three Hh antagonists.

For SMAD4 siRNA combination treatment in the DAOY cell line (Figure 5.23D): in the combination treatment (SMAD4 siRNA+vismodegib) no change in expression was observed for GLI1, 2 and SMO when compared to the vismodegib only treatment; in the combination treatment (SMAD4 siRNA+sonidegib) we observed a downregulation of SMO (-2.49 ± 0.17), whereas no change was observed for both GLI1 (0.85 ± 0.65) and 2 (0.10 ± 0.13) when compared with the sonidegib only treatment (0.55 ± 0.18 , 1.06 ± 0.57 , -0.75 ± 0.15 , respectively); finally, in the combination treatment (SMAD4 siRNA+GANT-61) no change in expression was observed for GLI1, 2 and SMO when compared to the GANT-61 only treatment. Therefore, SMAD4 K-D appeared to have less impact than SB431542 on the Hh regulated genes when combined with Hh antagonists.

For SMAD4 siRNA combination treatment in the UW228-2 cell line (Figure 5.23E): in the combination treatment (SMAD4 siRNA+vismodegib) a decrease in expression was observed for SMO (-7.36 ± 0.16) when compared to the vismodegib only treatment (-1.82 ± 0.10); in the combination treatment (SMAD4 siRNA+sonidegib) we observed a downregulation of SMO (-3.31 ± 0.08), whereas no change was observed for GLI2 (-0.33 ± 0.63) when compared with the sonidegib only treatment (-0.19 ± 0.10 , 0.03 ± 0.08 , respectively); finally, in the combination treatment (SMAD4 siRNA+GANT-61) we observed a downregulation of SMO (-4.09 ± 0.10), whereas no change was observed for GLI2 (1.76 ± 0.54) when compared with the GANT-61 only treatment (0.83 ± 0.20 , 1.47 ± 0.52 , respectively). Therefore, SMAD4 K-D in combination with Hh antagonists appeared to have no impact on GLI2, but caused the downregulation of SMO when compared to Hh antagonist only controls.

For SMAD4 siRNA combination treatment in the SJSA-1 cell line, no change was observed between the combination treatments and the Hh antagonist only treatments on the expression of GLI2, PTCH and SMO (Figure 5.23F).

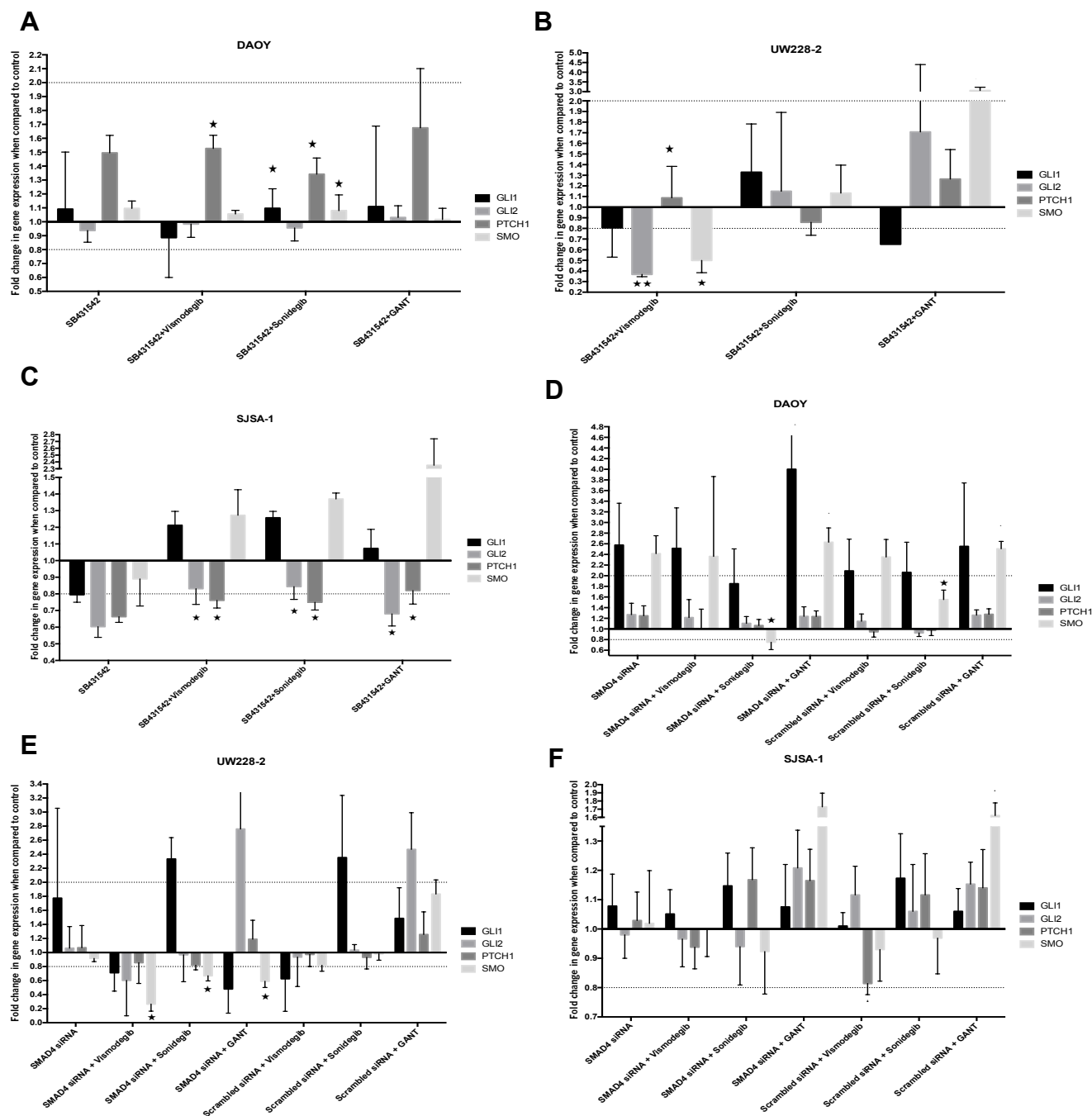


Figure 5.23: Effect of Blocking TGF β Signalling and Hh-signalling on Hh-regulated Genes in Hh Driven Tumours.

Hh driven cell lines were cultured in the presence of the TGF β blocker SB431542 for 24hr, and SMAD4 siRNA for 48hr, in combination with Hh antagonists (GANT-61, vismodegib,

sonidegib). RNA was extracted and assayed for a panel of Hh-regulated genes following treatment with SB431542 in combination with Hh antagonists in **(A)** DAOY, **(B)** UW228-2, and **(C)** SJS-1 cells, and treatment with SMAD4 siRNA in combination with Hh antagonists in **(D)** DAOY, **(E)** UW228-2, and **(F)** SJS-1 cells by qPCR. Expression values are based on the Log_{10}RQ , where a value of 10.0 represents a fold change of +10, and 0.1 represents a fold change of -10. Results are an average of two independent experiments. The qPCR assay was performed with three internal technical replicates and two endogenous controls. ($n=2$), Error bars represent SE of mean, * represents $p<0.05$, ** represents $p<0.01$, t-test.

Table 5.9: Impact of SB431542 combinational treatments on cell line specific Hh regulated genes

UP, represents genes that are upregulated; DOWN, represents genes that are downregulated; NC, represents no change in gene expression. All changes stated are in comparison to the untreated control. *=moderately up/downregulated; **=highly up/downregulated. ?=cannot determine based on the available data.

Cell Line	Hh Regulated Genes	Impact of Vismodegib	Impact of SB431542+ Vismodegib	Impact of Sonidegib	Impact of SB431542+ Sonidegib	Impact of GANT-61	Impact of SB431542+ GANT-61
DAOY	GLI1	UP	DOWN/NC	DOWN	NC	UP	UP/NC
	GLI2	NC	UP	DOWN	DOWN	DOWN	UP
	SMO	UP	UP/NC	DOWN	NC	UP	NC
UW228-2	GLI2	DOWN	DOWN*	DOWN	UP/NC	DOWN	UP
	SMO	DOWN	DOWN*	DOWN	UP/NC	DOWN	UP*
SJS-1	GLI2	UP	DOWN	UP	DOWN	UP	DOWN
	PTCH	UP	DOWN	UP	DOWN	UP	DOWN
	SMO	UP	UP	UP	UP	UP	UP

Table 5.10: Impact of SMAD4 siRNA combinational treatments on cell line specific Hh regulated genes

*UP, represents genes that are upregulated; DOWN, represents genes that are downregulated; NC, represents no change in gene expression. All changes stated are in comparison to the untreated control. *=moderately up/downregulated; **=highly up/downregulated. ?=cannot determine based on the available data.*

Cell Line	Hh Regulated Genes	Impact of Vismodegib	Impact of SMAD4 siRNA+ Vismodegib	Impact of Sonidegib	Impact of SMAD4 siRNA+ Sonidegib	Impact of GANT-61	Impact of SMAD4 siRNA+ GANT-61
DAOY	GLI1	UP	UP	UP	UP	UP	UP
	GLI2	NC	NC	DOWN/NC	NC	UP/NC	NC
	SMO	UP	UP	UP	DOWN	UP	UP
UW228-2	GLI2	NC	DOWN	NC	NC	UP	UP
	SMO	DOWN	DOWN	NC	DOWN	UP	DOWN
SJS-1	GLI2	NC	NC	NC	NC	NC	NC
	PTCH	DN	NC	NC	NC	NC	NC
	SMO	DN	NC	NC	NC	UP	UP

5.2.17 The effect of combining TGF β and Hh antagonists on apoptosis

In order to determine whether combining TGF β inhibition (through SB431542) with Hh inhibition (GANT-61, vismodegib and sonidegib) increased apoptosis in our Hh driven cell lines, we undertook flow cytometric analysis on cells treated for 4, 24, and 48 hours.

Figure 5.24 shows representative dot plots between TGF β antagonist only treated cells compared to combination treatment of TGF β antagonist with Hh antagonist over three time-points. As a percentage of the total cell population (100%) all three cell lines demonstrated no significant change in the percentage of cells in early apoptosis, late

apoptosis or necrosis between vismodegib treatment alone or in combination with SB431542 for any of the three time-points (Table 5.11).

As a percentage of the total cell population (100%) an increase in the percentage of cells in early apoptosis between sonidegib alone or in combination with SB431542 was observed for 24 and 48 hr in DAOY cells (0.53% vs 10.72%; $p < 0.05$ and 0.45% vs 16.28%; $p < 0.05$, respectively). A marginal increase was also observed in the percentage of cells in late apoptosis, although this was not statistically significant. Conversely no effect was observed in either UW228-2 or SJSA-1 cells following this treatment combination.

As a percentage of the total cell population (100%) all three-cell lines demonstrated no additive effect on the percentage of cells in early apoptosis, late apoptosis or necrosis between GANT-61 alone or in combination with SB431542 for any of the three time-points.

In conclusion, combining TGF β and Hh antagonists had minimal effect on apoptosis.

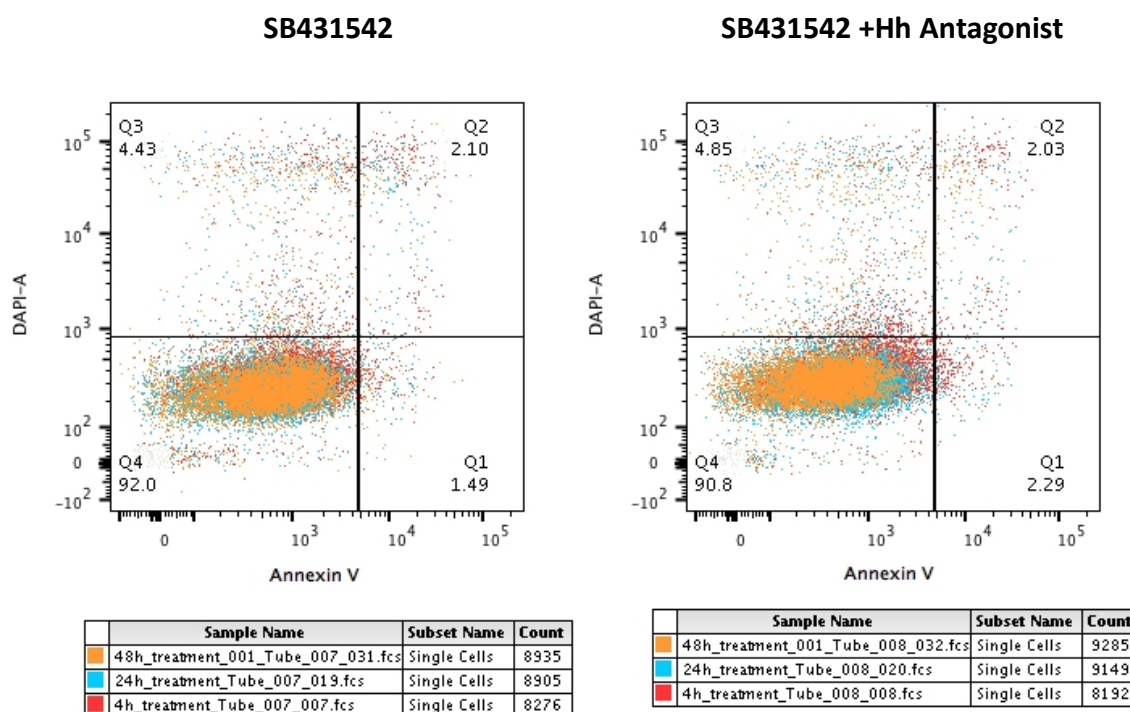


Figure 5.24: Impact of SB431542 in combination with Hh antagonists on apoptosis in Hh driven tumour cell lines

Representative dot plot to show the effect of combinational treatment over the three time periods 4, 24, and 48 hours in Hh driven tumour cell lines. 4hr (red population), 24hr (blue population), and 48hr (orange population) treatments are merged on top of each other in order to display any shifts following treatment over the three time periods. Annexin V (apoptosis marker) and DAPI (dead cell marker) are on the X- and Y-axis, respectively. Each quadrant represents as follows: Q1) early apoptosis, Q2) late apoptosis, Q3) necrosis, Q4) viable cells. Experiments were performed in duplicate (n=2), * represents $p < 0.05$, t-test.

Table 5.11: Effect of Combining TGF β - and Hh-Antagonist Treatment on inducing apoptosis in DAOY cells.

Cell Line	Drug	Time Points (hr)	% Live Cells	% Early Apoptosis	% Late Apoptosis	% Necrosis
DAOY	Untreated	4	90.95	5.34	1.75	1.96
		24	89.55	5.72	2.75	1.99
		48	91.90	3.70	0.99	3.39
	SB431542	4	87.75	4.44	1.43	6.36
		24	86.60	7.71	3.22	2.46
		48	82.85	10.63	3.24	3.31
	SB431542+ Vismodegib	4	94.55	2.07	0.87	2.52
		24	91.50	4.38	1.22	2.89
		48	88.20	7.96	1.30	2.57
	SB431542+ Sonidegib	4	87.30	6.09	3.66	2.95
		24	80.25	10.72	5.67	3.39
		48	75.15	16.28	5.46	3.11
	SB431542+ GANT-61	4	91.05	4.73	1.85	2.36
		24	88.95	6.96	1.51	2.55
		48	77.40	10.13	2.08	10.35
UW228-2	Untreated	4	95.25	2.47	0.83	1.48
		24	95.50	1.46	0.63	2.42

		48	94.80	1.88	0.73	2.60
		4	87.30	3.83	2.96	5.95
	SB431542	24	82.15	3.82	9.20	4.84
		48	85.70	3.92	5.64	4.80
	SB431542+ Vismodegib	4	92.05	5.58	0.86	1.48
		24	93.95	2.86	0.82	2.42
		48	91.80	3.48	0.96	3.75
	SB431542+ Sonidegib	4	89.45	2.94	2.57	5.06
		24	89.95	2.11	2.08	5.88
		48	84.25	4.89	5.02	5.83
	SB431542+ GANT-61	4	93.10	4.35	0.94	1.63
		24	91.65	3.94	1.08	3.32
		48	79.05	8.97	4.79	7.25
SJSA-1	Untreated	4	93.10	3.94	1.21	1.57
		24	95.70	1.20	1.26	1.84
		48	95.40	1.85	0.69	2.04
	SB431542	4	94.55	2.26	1.47	1.77
		24	94.05	2.88	1.34	1.74
		48	95.50	1.72	1.22	1.57
	SB431542+ Vismodegib	4	93.25	2.09	2.52	2.13
		24	93.20	3.76	1.12	1.91
		48	95.40	1.60	1.04	1.99
	SB431542+ Sonidegib	4	79.90	1.00	8.44	10.65
		24	84.00	4.16	7.88	4.00
		48	93.20	1.78	2.24	2.82
	SB431542+ GANT-61	4	94.95	1.49	1.64	1.97
		24	87.60	5.57	3.01	3.83
		48	88.35	1.73	1.81	8.15

In order to determine whether combining TGF β inhibition (through SMAD4 siRNA) with Hh inhibition (vismodegib, sonidegib and GANT-61) increased apoptosis in the Hh driven cell lines, DAOY (Table 5.12), UW228-2 (Table 5.13), and SJSA-1 (Table 5.14) we undertook flow cytometric analysis on cells treated for 4, 24, and 48 hours. Figure 5.25 shows representative dot plots between SMAD4 siRNA only treated cells compared to combination treatment of SMAD4 siRNA with Hh antagonist over three time-points.

As a percentage of the total cell population (100%) all three-cell lines demonstrated no increase in the % of apoptosis or necrosis between vismodegib, sonidegib or GANT-61 alone or in combination with SMAD4 siRNA for any of the three time-points (Table 5.12-5.14).

In conclusion, combining TGF β (SMAD4 siRNA) and Hh antagonists did not induce cell apoptosis.

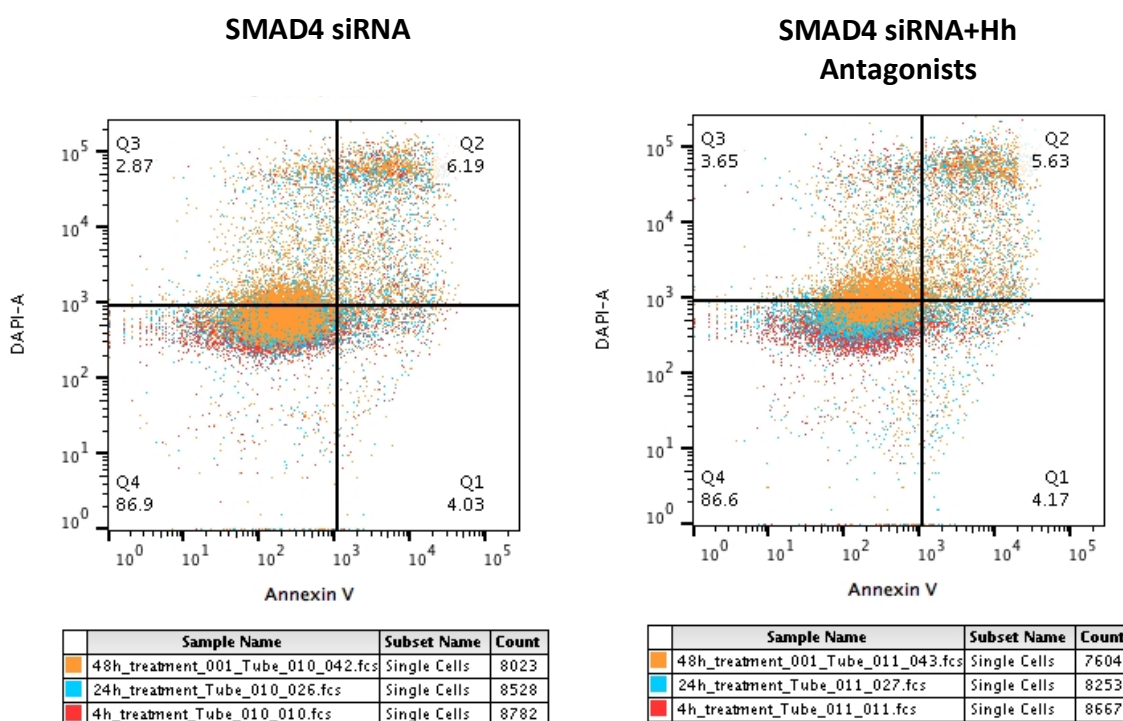


Figure 5.25: Impact of SMAD4 siRNA in combination with Hh antagonists on apoptosis in Hh driven tumour cell lines

*Representative dot plot to show the effect of combinational treatment over the three time periods 4, 24, and 48 hours in Hh driven tumour cell lines. 4hr (red population), 24hr (blue population), and 48hr (orange population) treatments are merged on top of each other in order to display any shifts following treatment over the three time periods. Annexin V (apoptosis marker) and DAPI (dead cell marker) are on the X- and Y-axis, respectively. Each quadrant represents as follows: Q1) early apoptosis, Q2) late apoptosis, Q3) necrosis, Q4) viable cells. Experiments were performed in duplicate (n=2), * represents $p < 0.05$, t-test.*

Table 5.12: Effect of Combining TGF β - and Hh-Antagonist Treatment on inducing apoptosis in DAOY cells.

Drug	Time Points (hr)	% Live Cells	% Early Apoptosis	% Late Apoptosis	% Necrosis
Scrambled+ Vismodegib	4	88.05	2.88	4.43	4.67
	24	73.80	3.88	9.61	12.72
	48	62.00	4.75	12.91	20.32
SMAD4+ Vismodegib	4	89.75	2.81	3.77	3.68
	24	80.70	2.73	6.54	10.06
	48	68.30	3.54	10.12	18.04
Scrambled+ Sonidegib	4	84.45	3.15	3.66	8.77
	24	74.05	3.49	6.73	15.75
	48	55.15	5.00	14.39	25.50
SMAD4+ Sonidegib	4	79.05	3.43	6.22	11.25
	24	79.65	3.33	6.63	10.40
	48	57.85	3.22	13.09	25.85
Scrambled+ GANT-61	4	88.20	2.86	3.88	5.05
	24	71.75	4.41	10.07	13.76
	48	48.75	3.62	15.86	31.75
SMAD4+ GANT- 61	4	90.40	2.89	3.59	3.18
	24	79.45	4.30	7.56	8.68
	48	54.75	3.82	15.64	25.80

Table 5.13: Effect of Combining TGF β - and Hh-Antagonist Treatment on inducing apoptosis in UW228-2 cells.

Drug	Time Points (hr)	% Live Cells	% Early Apoptosis	% Late Apoptosis	% Necrosis
Scrambled+ Vismodegib	4	66.80	1.34	19.90	11.90
	24	67.70	1.74	15.70	14.90
	48	55.70	5.71	15.90	22.60
SMAD4+ Vismodegib	4	95.10	1.37	0.90	2.59
	24	88.90	2.86	1.47	6.77
	48	83.40	1.44	1.34	13.80
Scrambled+ Sonidegib	4	67.30	1.02	20.00	11.70
	24	66.90	1.93	12.10	19.00
	48	63.00	4.12	19.70	13.20
SMAD4+ Sonidegib	4	86.20	0.68	3.67	9.44
	24	86.50	2.39	1.66	9.47
	48	86.20	1.80	2.54	9.41
Scrambled+ GANT-61	4	69.10	1.51	18.60	10.80
	24	50.90	3.95	23.80	21.40
	48	25.20	7.80	43.20	23.80
SMAD4+ GANT- 61	4	94.80	1.53	0.73	2.93
	24	84.80	3.29	1.91	9.97
	48	49.90	6.21	18.10	25.80

Table 5.14: Effect of Combining TGF β - and Hh-Antagonist Treatment on inducing apoptosis in SJSA-1 cells.

Drug	Time Points (hr)	% Live Cells	% Early Apoptosis	% Late Apoptosis	% Necrosis
Scrambled+ Vismodegib	4	85.40	5.18	3.16	6.23
	24	71.50	6.48	8.70	13.30
	48	35.50	8.87	27.50	28.10
SMAD4+ Vismodegib	4	86.20	4.53	3.44	5.83
	24	75.50	2.03	3.38	19.10
	48	46.60	7.34	18.40	27.70
Scrambled+ Sonidegib	4	86.50	3.49	2.73	7.24
	24	73.40	3.73	6.46	16.40
	48	30.90	9.01	30.40	29.70
SMAD4+ Sonidegib	4	85.80	3.85	3.25	7.10
	24	71.30	4.08	8.02	16.60
	48	36.20	8.36	26.50	29.00
Scrambled+ GANT-61	4	84.00	6.94	3.60	5.50
	24	66.10	6.22	11.00	16.70
	48	7.01	6.29	65.00	21.70
SMAD4+ GANT- 61	4	89.60	4.21	1.78	4.36
	24	70.80	4.95	8.59	15.70
	48	8.64	8.28	67.70	15.30

5.2.18 Effect of Hedgehog and TGF β blockade on cell viability

We observed no significant difference in cell viability in all three cell lines between vismodegib alone and vismodegib in combination with SB431542: DAOY (99.4% \pm 2.0% vs 96.9% \pm 4.4%), UW228-2 (103.8% \pm 1.2% vs 76.6% \pm 5.5%) and SJSA-1 (120.5% \pm 16.3% vs 131.4% \pm 26.6%) (Figure 5.26 A-C).

We observed no significant difference in cell viability in all three-cell lines between sonidegib alone and sonidegib in combination with SB431542: DAOY (87.9% \pm 7.4% vs 87.6% \pm 5.1%), UW228-2 (103.1% \pm 1.9% vs 99.4% \pm 3.0%) and SJSA-1 (118.0 \pm 14.0 vs 125.1% \pm 23.4%) (Figure 5.26 A-C).

We observed no significant difference in cell viability in all three-cell lines between GANT-61 alone and GANT-61 in combination with SB431542: DAOY (96.3% \pm 1.5% vs 95.0 \pm 2.2%), UW228-2 (81.5% \pm 4.4% vs 104.9% \pm 3.1%) and SJSA-1 (109.3% \pm 16.4% vs 118.3% \pm 23.4%) (Figure 5.26 A-C).

We observed no significant loss of cell viability in all three-cell lines between scrambled control siRNA, vismodegib + scrambled control siRNA and vismodegib + SMAD4 siRNA: DAOY (100% \pm 0.0% vs 121.8% \pm 15.9% vs 110.5% \pm 8.3%), UW228-2 (100.0 \pm 0.0% vs 108.8% \pm 3.2% vs 105.6% \pm 2.7%), and SJSA-1 (100% \pm 0.0% vs 114.6% \pm 5.5% vs 118.1% \pm 6.0%) (Figure 5.26 A-C).

We observed no significant loss of cell viability in all three-cell lines between scrambled control siRNA, sonidegib + scrambled control siRNA and sonidegib + SMAD4 siRNA: DAOY (100.0% \pm 0.0% vs 105.9% \pm 11.1% vs 106.4% \pm 10.2%), UW228-2 (100.0% \pm 0.0% vs 103.7% \pm 4.1% vs 104.1% \pm 1.7%), and SJSA-1 (100.0% \pm 0.0% vs 100.4% \pm 9.4% vs 111.1% \pm 6.0%) (Figure 5.26 A-C).

We observed no significant loss of cell viability in all three-cell lines between scrambled control siRNA, GANT-61 + scrambled siRNA control and GANT-61 + SMAD4 siRNA: DAOY (100.0% \pm 0.0% vs 96.1% \pm 14.8% vs 93.1% \pm 14.7%), UW228-2 (100.0% \pm 0.0% vs

85.9%±4.5% vs 87.2%±4.8%), and SJS-1 (100.0%±0.0% vs 86.3%±5.0% vs 80.9%±7.3%) (Figure 5.26 A-C).

Hence blocking TGF β signalling together with hedgehog antagonism did not adversely affect cell viability.

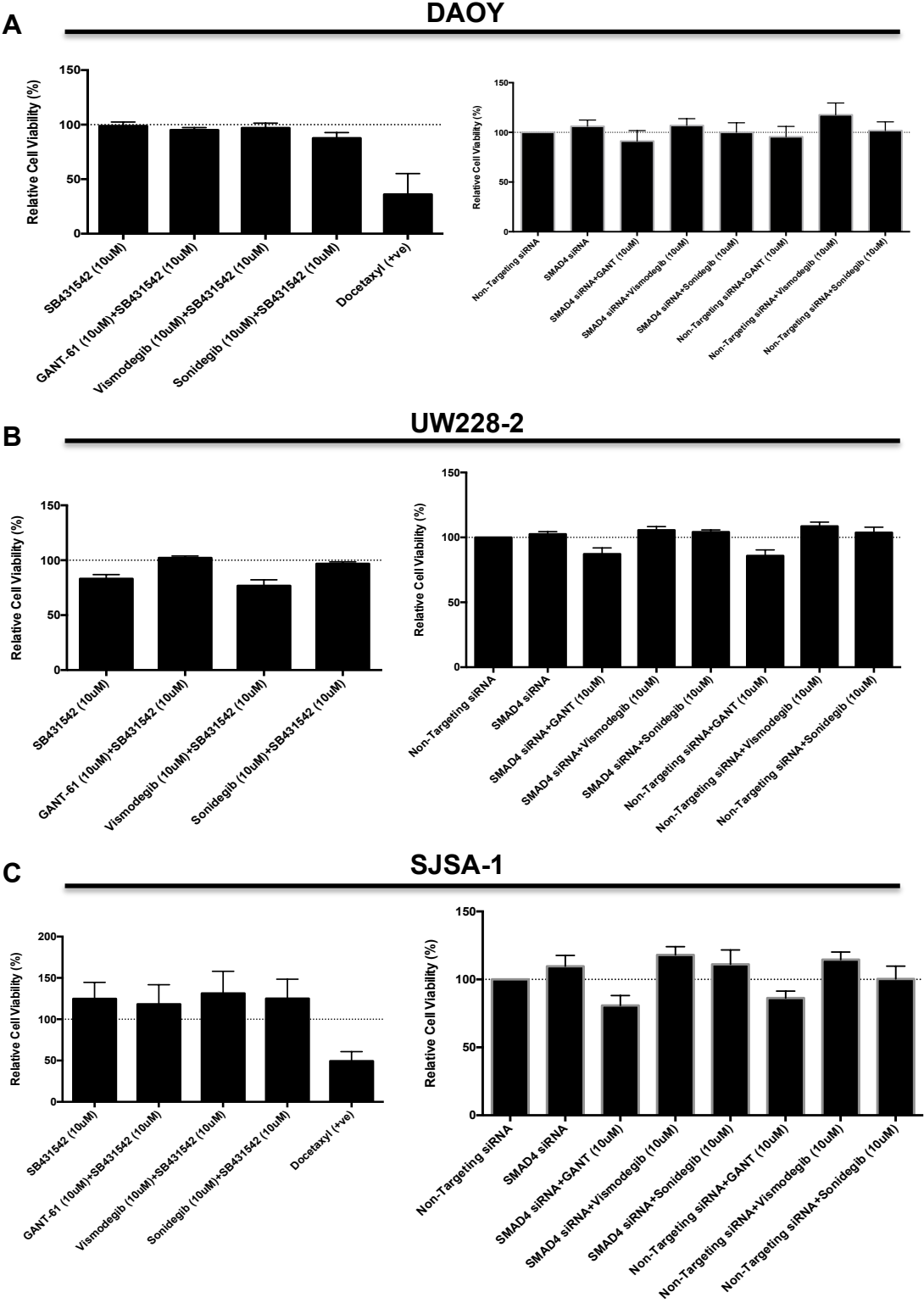


Figure 5.26: Effect of Combining TGF β and Hh Antagonist Treatment on Cell Viability in Hh Driven Tumours.

Combining TGF β and Hh antagonist treatments in the (A) DAOY cell line, (B) UW228-2 cell line, and (C) SJSA-1 cell line. Graphs represent an average over three independent experiments, with each experiment having four internal technical replicates for each condition. (n=3). Error bars represent SE of mean.

5.2.19 Effect of TGF β and Hh blockade on 2D colony forming efficiency

We observed no significant difference in CFE between vismodegib alone and vismodegib + SB431542: DAOY (91.8% \pm 6.2% vs 107.6% \pm 4.7%) and SJSA-1 (77.1% \pm 14.1% vs 75.8% \pm 14.6%). However vismodegib + SB431542 was associated with reduced viability in UW228-2 (112.7% \pm 20.1% vs 57.8% \pm 14.8%, $p < 0.05$) (Figure 5.27A).

We observed no significant difference in CFE between all three-cell lines between sonidegib alone and sonidegib + SB431542: DAOY (63.2% \pm 7.6% vs 73.8% \pm 10.3%), UW228-2 (25.1% \pm 10.1% vs 22.9% \pm 12.2%) and SJSA-1 (31.6% \pm 6.0% vs 59.1% \pm 14.9%) (Figure 5.27B).

We observed no significant difference in CFE between all three-cell lines between GANT-61 alone and GANT-61 + SB431542: DAOY (1.1% \pm 0.7% vs 3.7% \pm 1.6%), UW228-2 (0% \pm 0% vs 0% \pm 0%) and SJSA-1 (22.6% \pm 11.7% vs 21.1% \pm 9.9%) (Figure 5.27C).

We observed no significant loss of CFE in all three-cell lines between scrambled control siRNA, vismodegib + scrambled control siRNA and vismodegib + SMAD4 siRNA: DAOY (100.0% \pm 0.0% vs 90.1% \pm 13.8% vs 79.1% \pm 9.3%), UW228-2 (100.0% \pm 0.0% vs 79.1% \pm 9.3% vs 60.8% \pm 22.1%), and SJSA-1 (100.0% \pm 0.0% vs 44.4% \pm 10.4% vs 25.7% \pm 3.8%) (Figure 5.27A).

We observed no significant loss of CFE in all three-cell lines between scrambled control siRNA, sonidegib + scrambled control siRNA and sonidegib + SMAD4 siRNA: DAOY (100.0% \pm 0.0% vs 82.1% \pm 16.5% vs 88.3% \pm 9.2%), UW228-2 (100.0% \pm 0.0% vs 17.6% \pm 8.9% vs 19.6% \pm 8.8%), and SJSA-1 (100.0% \pm 0.0% vs 28.0% \pm 8.7% vs 43.2% \pm 14.7%) (Figure 5.27B).

We observed no significant loss of CFE in all three-cell lines between scrambled control siRNA, GANT-61 + scrambled siRNA control and GANT-61 + SMAD4 siRNA: DAOY (100.0% \pm 0.0% vs 11.8% \pm 7.1% vs 6.6% \pm 4.4%), UW228-2 (100.0% \pm 0.0% vs 0% \pm 0% vs 0% \pm 0%), and SJSA-1 (100.0% \pm 0.0% vs 14.8% \pm 5.2% vs 16.3% \pm 7.2%) (Figure 5.27C).

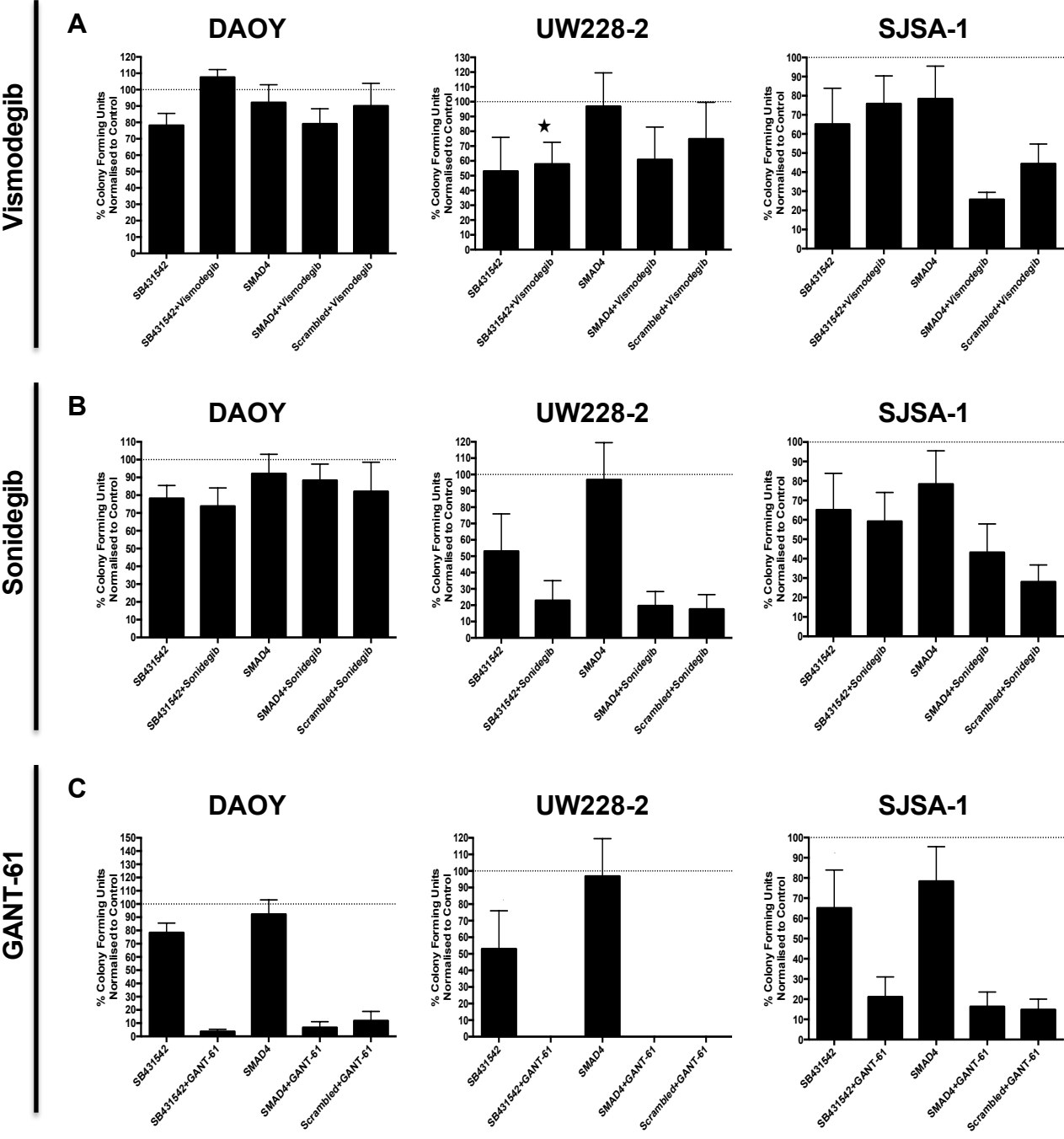


Figure 5.27: Effect of TGFβ and Hh blockade on 2D colony formation: Colony-Forming Assays.

Cells were seeded at a density of 75 cells/cm² for DAOY, 187.5 cells/cm² for UW228-2, and 125 cells/cm² for SJSJA-1 cell lines in the presence or absence of TGFβ antagonists for 7-12 days. **(A)** Vismodegib in combination with SB431542 and SMAD4 siRNA in DAOY, UW228-2 and SJSJA-1 cells, **(B)** Sonidegib in combination with SB431542 and SMAD4 siRNA in DAOY, UW228-2 and SJSJA-1 cells **(C)** GANT-61 in combination with SB431542 and SMAD4 siRNA in DAOY, UW228-2 and SJSJA-1 cells. All results are averages of at

least 4 experimental replicates, along with three internal technical replicates for each druging condition. ($n=4$), Error bars represent SE of mean, * represents $p<0.05$, t-test.

5.2.20 Effect of TGF β and Hh blockade on 3D tumoursphere forming units

To determine the effect of combined Hh and TGF β inhibition on 3D TFUs we evaluated the effect in a non-adherent colony forming efficiency assay over two passages. Both DAOY and UW228-2 cells were treated with TGF β blockade and or Hh antagonist for 24hr in adherent culture before passaging them into non-adherent culture conditions at low density.

Vismodegib or vismodegib + SB431542 after passage 1 demonstrated no reduction in 3D TFUs: DAOY (2.22 ± 0.34 vs 1.25 ± 0.32) and UW228-2 (2.52 ± 0.59 vs 2.91 ± 1.81). Also at passage 2 there were no reductions in 3D TFUs: DAOY (7.10 ± 0.11 vs 2.44) and UW228-2 (1.48 ± 0.13 vs 0.22) (Figure 5.28 A-D).

Sonidegib or sonidegib + SB431542 after passage 1 demonstrated no reduction in 3D TFUs: DAOY (1.78 ± 0.57 vs 2.06 ± 0.89) and UW228-2 (2.21 ± 0.61 vs 3.55 ± 0.98). Also at passage 2 there were reductions in 3D TFUs: DAOY (4.39 ± 2.39 vs 2.89) and UW228-2 (2.85 ± 0.77 vs 2.56) (Figure 5.28 A-D).

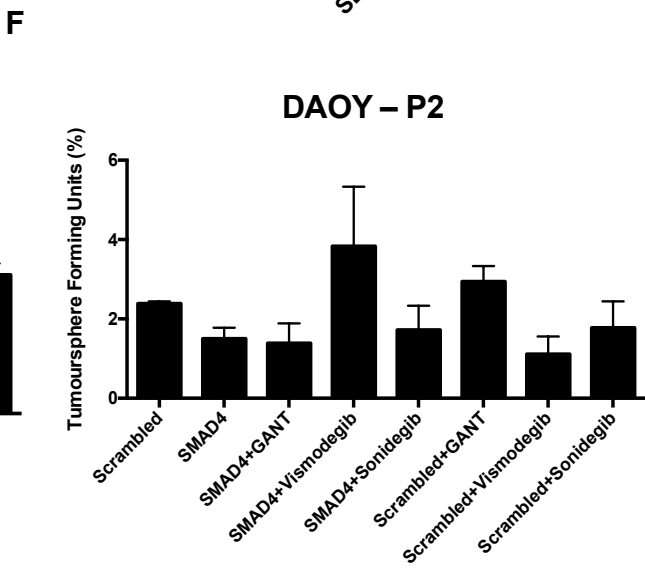
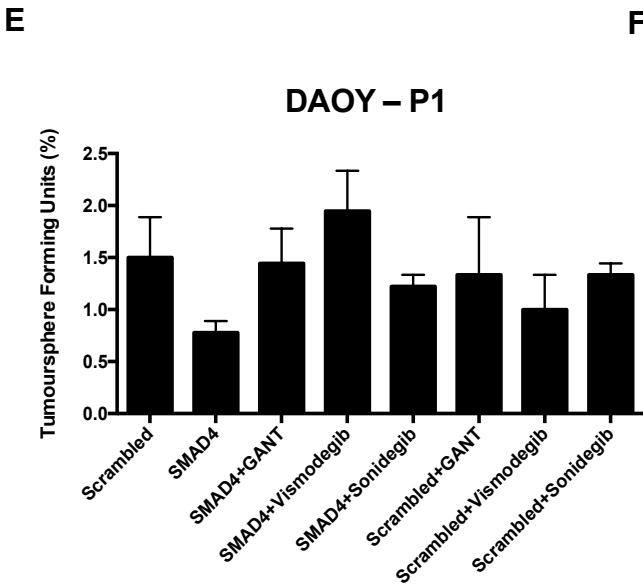
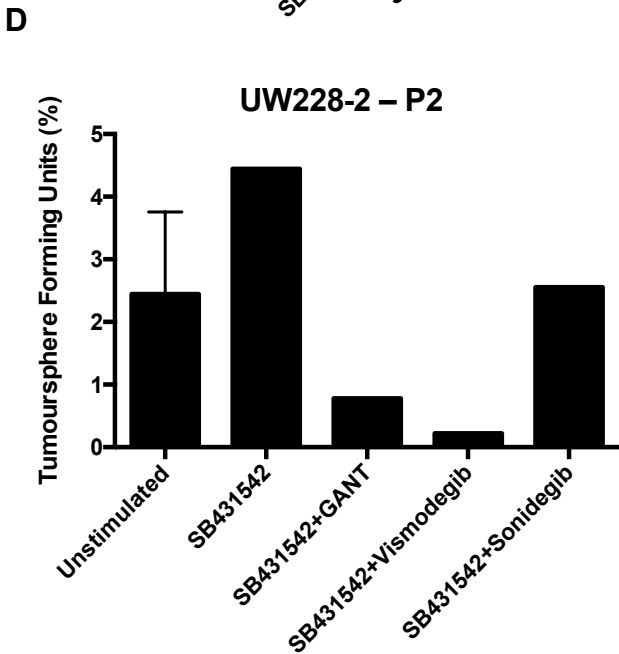
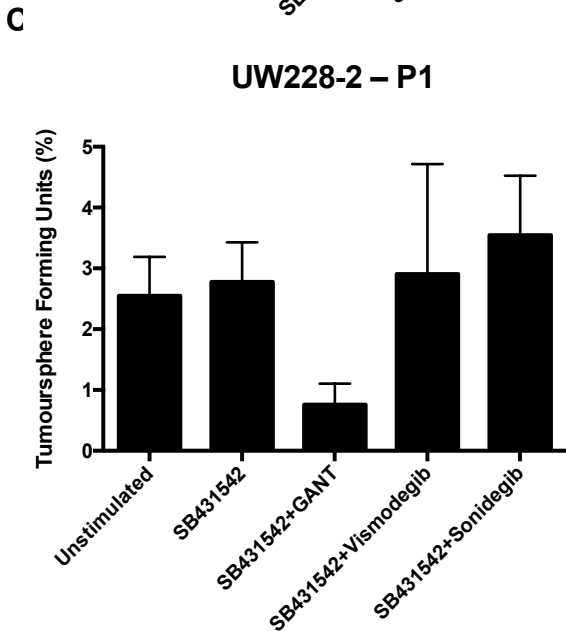
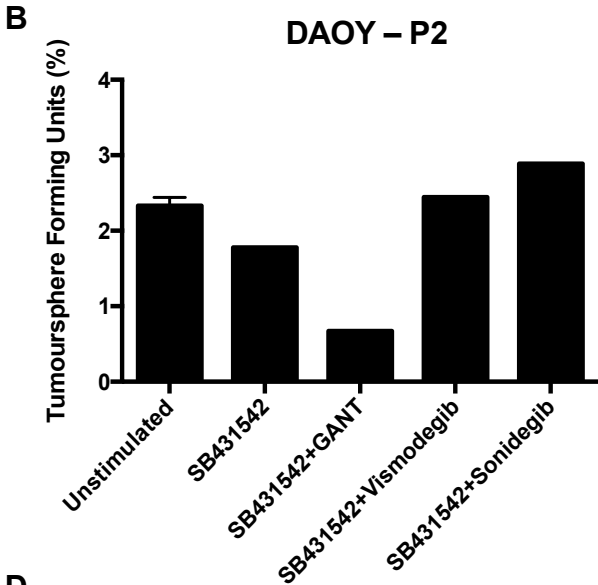
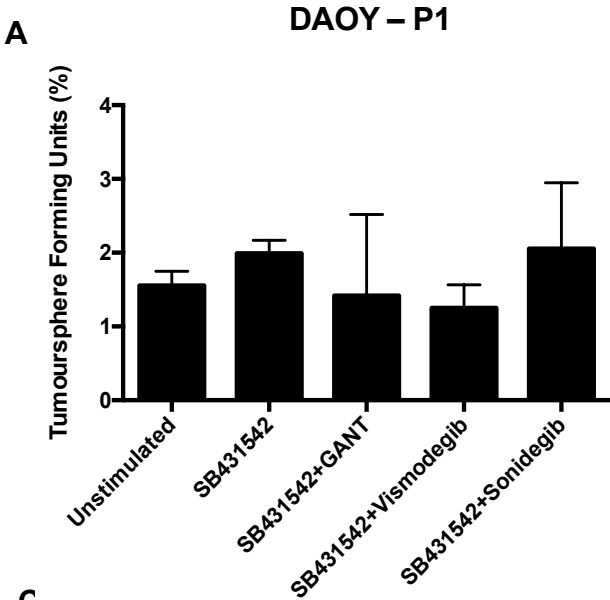
GANT-61 or GANT-61 + SB431542 after passage 1 demonstrated no reduction in 3D TFUs: DAOY (1.21 ± 0.24 vs 1.42 ± 0.18) and UW228-2 (2.92 ± 0.73 vs 0.76 ± 0.35). Also at passage 2 there were reductions in 3D TFUs: DAOY (1.83 ± 0.39 vs 0.67) and UW228-2 (1.07 ± 0.48 vs 0.78) (Figure 5.28 A-D).

Comparing vismodegib + scrambled siRNA or vismodegib + SMAD4 siRNA, no reduction of 3D TFUs was observed in at passage 1: DAOY (1.00 ± 0.00 vs 1.94 ± 0.39) and UW228-2 (1.78 ± 0.39 vs 1.74 ± 0.15). Also at passage 2 there was no reduction of 3D TFUs: DAOY (1.11 ± 0.44 vs 3.83 ± 1.5) and UW228-2 (1.50 ± 0.39 vs 0.89 ± 0.78) (Figure 5.28 E-H).

Comparing sonidegib + scrambled siRNA or sonidegib + SMAD4 siRNA, no reduction of 3D TFUs was observed in at passage 1: DAOY (1.33 ± 0.11 vs 1.22 ± 0.11) and UW228-2 (1.74 ± 0.44 vs 1.52 ± 0.38). Also at passage 2 there was no reduction of 3D TFUs: DAOY (1.78 ± 0.67 vs 1.72 ± 0.61) and UW228-2 (1.11 ± 1.11 vs 1.44 ± 0.56) (Figure 5.28 E-H).

Comparing GANT-61 + scrambled siRNA or GANT-61 + SMAD4 siRNA, no reduction of 3D TFUs was observed in at passage 1: DAOY (1.33 ± 0.56 vs 1.44 ± 0.33) and UW228-2 (1.00 ± 0.51 vs 1.19 ± 0.58). Also at passage 2 there was no reduction of 3D TFUs: DAOY (2.94 ± 0.39 vs 1.39 ± 0.50) and UW228-2 (0.67 ± 0.00 vs 0.61 ± 0.06) (Figure 5.28 E-H).

In summary, combined treatment with Hh and TGF β antagonists did not adversely affect 3D TFUs.



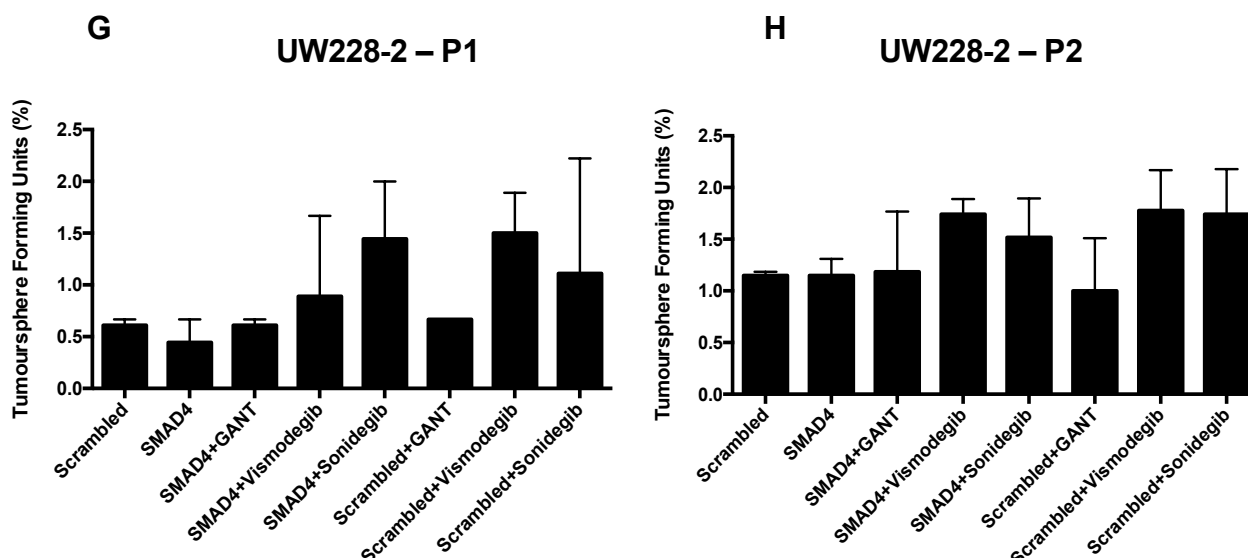


Figure 5.28: Effect of TGF β and Hh blockade on tumoursphere-forming cells: sphere-forming assays.

Cells were seeded in 2D and allowed to adhere overnight before being treated with TGF β (SB431542 and SMAD4 siRNA) in combination with Hh antagonists (GANT-61, vismodegib, sonidegib). Following treatment cells were trypsinised and plated under sphere forming conditions at a density of 5 cells/ μ L for both DAOY and UW228-2 cell lines and allowed to form spheres over 7 days before being enumerated (P1). Spheres were then dissociated and re-plated at a density of 5 cells/ μ L allowed to grow for a further 7 days, before being finally enumerated (P2). **(A)** %TFUs at P1 in DAOY cells treated with SB431542 in combination with Hh antagonists, **(B)** %TFUs at P1 in UW228-2 cells treated with SB431542 in combination with Hh antagonists, **(C)** %TFUs at P2 in DAOY cells treated with SB431542 in combination with Hh antagonists, **(D)** %TFUs at P2 in UW228-2 cells treated with SB431542 in combination with Hh antagonists, **(E)** %TFUs at P1 in DAOY cells treated with SMAD4 siRNA in combination with Hh antagonists, **(F)** %TFUs at P1 in UW228-2 cells treated with SMAD4 siRNA in combination with Hh antagonists, **(G)** %TFUs at P2 in DAOY cells treated with SMAD4 siRNA in combination with Hh antagonists, **(H)** %TFUs at P2 in UW228-2 cells treated with SMAD4 siRNA in combination with Hh antagonists. Tumoursphere forming units (%) represents the number of spheres formed relative to the number of cells originally seeded. All results are averages of three experimental replicates for P1 (with the exception of scrambled+GANT-61 for UW228-2) and P2 (with the exception of bars with no error bars where only one replicate was obtained), with three internal technical replicates for each drugging condition. (n=3). Error bars represent SE of mean.

5.3 Discussion

In this chapter, a range of functional assays have been used to evaluate the susceptibility of three Hh driven tumour cell lines and primary BCC tissue towards Hh antagonists at the level of the whole cell population and CSC population, along with the impact on these cell lines following TGF β antagonist treatment alone and in combination with Hh antagonists. Therefore, in order to identify the impact of both Hh and TGF β antagonists on the tumour cell lines, it was important to first identify the genes that are truly Hh regulated and TGF β regulated within each of the cell lines, since gene responses are context dependent and are likely to vary between different tumour types and cell lines. To do this all three-tumour cell lines were treated separately with: 1) Hh agonist alone 2) Hh agonist + Hh antagonist (vismodegib, sonidegib or GANT-61), 3) TGF β 1 agonist only, and 4) TGF β 1 agonist + TGF β antagonist (SB431542 or SMAD4 knockdown) in order to determine which genes within the panel of Hh- and TGF β regulated genes demonstrated a response following agonist treatment which could be subsequently reversed following antagonist treatment. Any genes that demonstrated this response were considered to be Hh-induced/SMO/GLI dependent and/or TGF β 1-induced/ALK5 receptor kinase dependent.

In the DAOY cell line 3 out of 4 of the Hh gene panel were classified as being Hh regulated, notably, GLI1, 2, and SMO. All three of these genes were upregulated following Hh agonist treatment, and decreased following addition of the Hh antagonists, vismodegib, sonidegib, or GANT-61. Therefore the DAOY cell line was found to be a SHh dependent cell line and, given the impact of the inhibitors, can be classified as SMO dependent (vismodegib and sonidegib) and GLI dependent (GANT-61). Therefore the DAOY cell line displayed a fully responsive canonical Hh signalling pathway. In the UW228-2 cell line, the response to agonist and antagonist treatments was more convoluted than that observed in the DAOY cell line. Only GLI1 was found to be upregulated following Hh agonist treatment, whereas GLI2, PTCH and SMO were all downregulated. Furthermore, Hh antagonists did not reverse this expression, but rather enhanced the effects observed in the Hh agonist treated cells by further downregulating GLI2, PTCH, and SMO, and upregulating GLI1. Therefore agonist and antagonist treatments were not found to perform reciprocal actions on these genes, and as a

consequence the UW228-2 cell line does not display a fully responsive canonical Hh signalling pathway. This is a little surprising as both DAOY and UW228-2 cell lines represent the two most cited medulloblastoma cell lines and have been well established as being Hh driven through a number of means including the demonstration of GLI transcriptional activity by luciferase-based reporter assays and overexpression of Hh-pathway genes (e.g. GLI1, PTCH1, SMO) (Di Marcotullio *et al.*, 2004; Triscott *et al.*, 2013; Arnhold *et al.*, 2016). However, although both are characterized as being Hh driven, they demonstrate different levels of expression of Hh pathway components, with the DAOY cell line shown to exhibit high levels of SHh, PTCH1, GLI1, and GLI2 expression, while UW228-2, demonstrates lower levels of SHh, PTCH1 and GLI2 (Arnhold *et al.*, 2016; Götschel *et al.*, 2013). Therefore, studies have shown that DAOY cells are more responsive to Hh signalling than UW228-2 cells (Arnhold *et al.*, 2016; Götschel *et al.*, 2013), which is consistent with our observations. Finally, in the SJSA-1 cells, Hh agonist treatment induced a similar response to that observed in UW228-2 cells in that an upregulation of GLI1 and downregulation of GLI2, PTCH and SMO was observed. However, unlike in the UW228-2 cells, SJSA-1 cells demonstrated a reversal in the expression of GLI2, PTCH and SMO following Hh antagonist treatment. Interestingly, however, was the observation that Hh agonist treatment resulted in the downregulation of these Hh target genes, indicating that they are negatively regulated in this cell line. Furthermore, the lack of impact on GLI1 expression following Hh antagonist treatment can potentially be explained by the fact that SJSA-1 cells have a 15-fold amplification of GLI1 (Khatib *et al.*, 1993).

Next we identified TGF β 1-induced/ALK5 receptor kinase dependent genes within each of our cell lines. In the DAOY cell line 3 out of 6 of the TGF β gene panel were classified as being TGF β regulated, notably CEBPD, SERPINE1 and SKIL. SB431542 treatment reverted the expression of these genes following TGF β 1 treatment, and therefore are ALK5 receptor kinase dependent. Furthermore, this same response was also observed following SMAD4 knockdown, so these three genes appear to be SMAD4 dependent also. In both the UW228-2 and SJSA-1 cell lines 2 out of 6 of the TGF β 1 genes were classified as being TGF β regulated, notably CEBPD and NEDD9. The expressions of both of these genes were again reverted following both SB431542 treatment and SMAD4

knockdown and therefore may be ALK5 receptor kinase dependent and SMAD4 dependent genes. This panel of TGF β regulated genes was identified from the panel of 27 genes defined in section 3.2.5, and was based on their expression levels in both HaCaT and primary BCC cells. However, as a future experiment, it will be important to run the entire panel of 27 genes against TGF β 1 treated cells with and without TGF β antagonists in each of the cell lines, in order to identify a more comprehensive cell line specific panel of TGF β regulated genes. This will inevitably allow more subtle changes that may be occurring within each cell line to be identified following treatment.

Once both Hh- and TGF β -regulated genes had been established in the cell lines we assessed the impact of Hh antagonists on TGF β regulated genes, and vice versa, in order to further elucidate the crosstalk between Hh and TGF β signalling. Our data so far points towards TGF β signalling being relevant in our model. As a consequence the assumption would be that when Hh signalling is abrogated, TGF β signalling would also diminish. However, we have shown that following Hh antagonist treatment, TGF β pathway activity increases in our Hh driven tumour cell lines, as evidenced through nuclear accumulation of pSMAD3 in all cell lines (for all Hh antagonists), and in some instances through the induction of downstream TGF β regulated genes in each of the cell lines. Of the TGF β regulated genes identified within each of the cell lines, CEBPD was induced following Hh antagonist treatment in all three cell lines, whereas SERPINE1 was induced following sonidegib and GANT-61 treatment in DAOY cells; NEDD9 was induced by GANT-61 and sonidegib in UW228-2 and SJSA-1 cells, respectively. This again highlights the importance of establishing a larger panel of TGF β regulated genes within each cell line as the induction of these genes following Hh antagonist treatment may have been more pronounced if the gene panel was more comprehensive. Interestingly, there appeared to be no difference between Hh antagonists in their ability to induce nuclear pSMAD3 in DAOY, UW228-2 (data not available for SJSA-1 cells), and primary BCC cells. Therefore, although the cell lines appear to have varied reliance on Hh signalling (based on the expression of Hh regulated genes), all cell lines exhibited nuclear pSMAD3 expression following Hh antagonist treatment, which could suggest that mechanisms downstream of the points of Hh inhibition are responsible for TGF β induction. Our results have also shown that TGF β signalling inhibition impacted the

expression of Hh regulated genes within the three cell lines, with SB431542 treatment (data not available for UW228-2 cells) and SMAD4 knockdown both shown to induce the same response as that of the Hh agonist treated cells. This contradicts findings by Dennler *et al.* (2007) who showed that TGF β 1 agonist treatment potently induced the expression of GLI2 and subsequently GLI1, whereas we have shown that TGF β signalling inhibition caused the induction of these Hh regulated genes in some instances within our cell lines. There are a couple of caveats, in that we have not yet assessed the impact of TGF β 1 agonist treatment on Hh regulated genes (and vice versa) in our cell lines, and Dennler *et al.* (2007) used different cell lines to us, and therefore a direct comparison cannot be made between the two. Nevertheless, our data indicates that these two pathways may be interlinked in that the inhibition of one leads to the induction of the other, within these cell lines. Furthermore, in a similar manner to using nuclear pSMAD3 labelling to identify active TGF β signalling, assessing GLI1 and 2 nuclear labelling of cells following TGF β inhibition will be important as a future experiment to determine Hh signalling pathway activity in a more robust manner.

When assessing the impact of Hh and TGF β antagonist only treatments in functional assays, our results showed that Hh antagonists (vismodegib, sonidegib and GANT-61) were largely ineffective at impacting cell viability or cell apoptosis, which is consistent with what has been found in some reports (Arnhold *et al.*, 2016; Infante *et al.*, 2016). However, sonidegib showed a slightly greater potency than vismodegib, with a reduction observed in cell viability for the DAOY cell line, however this was not seen in the other two cell lines. This could potentially be explained by the fact that the DAOY cell line has been characterized by us and other studies (Arnhold *et al.*, 2016; Götschel *et al.*, 2013) as having a fully functional canonical Hh signaling pathway and to be more sensitive to SHh driven proliferation, thus making it more susceptible to inhibition of SMO. The fact that this effect was seen for sonidegib but not vismodegib in this cell line could be because sonidegib is a more potent inhibitor of SMO than vismodegib, which has been documented in the clinical studies (Skvara *et al.*, 2011). Nevertheless, even though a small reduction in cell viability was observed, the ability of these two drugs to impact cell viability was poor. Finally, GANT-61 showed the greatest response of all three drugs, with slight reductions in viability observed for both DAOY and UW228-2 cell

lines, but not SJS-1 cells. The ineffectiveness of GANT-61 in SJS-1 cells could again be due to the fact that this cell line has higher levels of GLI1 transcript, which could therefore make it more resistant to GLI1 blockers such as GANT-61 due to the potential surplus of GLI1 and the presence of mechanisms that enhance the amplification of GLI1. Furthermore, this cell line appears to be less reliant on Hh signalling for its growth than the DAOY cell line, based on the literature, and our qPCR expression data. However, the increased effectiveness of GANT-61 on cell viability for DAOY and UW228-2 cells compared to the SMO antagonists may be due to the ability of these proteins to be activated by both SHh-ligand dependent and –independent mechanisms. This is interesting as it indicates that the inhibition of GLI transcription factors has impacted other neighboring pathways resulting in it being more effective in this assay. However, the apparent ability of TGF β signalling to respond to a reduction in Hh signalling following treatment suggests that this could be a survival mechanism that is preventing cell death following Hh antagonist treatment. When determining the effect of blocking TGF β signalling alone we found that SB431542 treatment and SMAD4 knockdown again did not induce apoptosis or significantly impact cell viability. The effectiveness of blocking TGF β signalling in Hh antagonist-resistant tumour cell lines has been previously demonstrated (Thayer *et al.*, 2003). In this study the ability of cyclopamine to induce apoptosis in a series of pancreatic cell lines (all shown to harbour elevated levels of GLI1), was demonstrated in 50% of the cell lines tested (Thayer *et al.*, 2003). A later study went on to demonstrate that in these cyclopamine-resistant cell lines, the basal expression of both GLI1 and 2, as well as their proliferative capacity was greatly inhibited by SB431542 (Dennler *et al.*, 2007). However, based on our findings, TGF β inhibition was capable of inducing Hh regulated genes in these cell lines which may potentially explain why no response was observed on cell viability and apoptosis. However, an important point to also note is that the cell viability and apoptosis assays were performed after 24 hr of Hh and/or TGF β antagonist treatment, and therefore it is possible that longer time points are required to observe any effect, therefore for future experiments, exposing the cells for longer time-points should be performed to discount this possibility.

Since both the Hh and TGF β signalling pathways appear to be induced following TGF β and Hh inhibition, respectively, our next step was to inhibit both of these pathways together and to assess the impact on each of the cell lines. Firstly, we assessed the impact of the combinational treatments on the expression of both TGF β and Hh regulated genes. In the DAOY cell line, SB431542 was capable of reversing Hh antagonist-induced CEBPD, whereas SERPINE1 and SKIL induction was reversed in the SB431542 and sonidegib combination group. This same effect was also observed by SMAD4 knockdown. In the UW228-2 cells, SB431542 was capable of reversing Hh antagonist-induced CEBPD and NEDD9 in combination with all Hh antagonists, whereas SMAD4 knockdown reversed CEBPD but not NEDD9. In the SJSA-1 cells, SB431542 reversed NEDD9 induction in combination with all Hh antagonists, while CEBPD was reversed in combination with sonidegib only. SMAD4 knockdown did not have an impact on either CEBPD or NEDD9. Therefore, inhibiting the TGF β signalling pathway both through SB431542 treatment and SMAD4 knockdown (not in the case of SJSA-1 cells) was capable of reverting the induction of TGF β regulated genes following Hh antagonist treatment. The discrepancy between the ability of NEDD9 induction to be reversed by SB431542 and SMAD4 knockdown in UW228-2 could be explained by the fact that NEDD9 was induced by GANT-61 and not vismodegib and sonidegib in the single treatments. However, the inability of SMAD4 to revert NEDD9 induction when combined with GANT-61 may suggest that the induction of NEDD9 by GANT-61 occurs independent of SMAD4 but dependent on ALK5 receptor kinase activity in UW228-2 cells. Furthermore, the inability of SMAD4 knockdown to revert Hh antagonist-mediated expression of TGF β regulated genes could be because they are induced in a manner that is independent of SMAD4. Both SMAD2 and 3 have the ability to freely diffuse in (Fink *et al.*, 2003) and out (Inman *et al.*, 2002a) of the nucleus independent of SMAD4; with a recent study by David *et al.* (2016) showing that SMAD2 and 3 can initiate TGF β responses independent of SMAD4. They went on to show that Sox4 was induced in a SMAD4 independent manner and could provide a mechanism through which TGF β promotes aggressiveness in SMAD4 null pancreatic ductal adenocarcinoma (David *et al.*, 2016). Hence these findings create a precedent demonstrating the ability of SMAD2/3 to induce TGF β transcriptional changes independent of SMAD4. However, SJSA-1 cells were particularly sensitive to knockdown using Lipofectamine, and as consequence a lot

of cell death was observed. As a consequence qPCR analysis to assess the level of SMAD4 mRNA was not possible due to technical issues with the qPCR; therefore, the level of SMAD4 knockdown achieved in SJSA-1 cells is not available. Furthermore, with regards to siRNA knockdown procedures, SMAD4 knockdown was achieved using SMARTpool siRNA (Dharmacon, GE Healthcare), which consists of a mixture of four different siRNAs. In an ideal situation, in the first instance, siRNA should be optimized by using individual siRNAs to determine which are capable of achieving the best levels of SMAD4 knockdown. Subsequently, based on these findings, either single siRNA or SMARTpool could be used (if at least 2 out of 4 are shown to be effective) (note: scrambled siRNA should always be used as a control).

In DAOY cells, when assessing the impact of combination treatment on Hh regulated genes, interestingly, SB431542 was shown to revert the effect of Hh antagonist treatment on Hh regulated genes, whereas no effect was observed for SMAD4 knockdown. This same effect was seen to varying degrees in the other two cell lines, with UW228-2 cells demonstrating that SB431542 could revert the effects on Hh regulated genes induced by sonidegib and GANT-61, but not vismodegib, while SMAD4 knockdown was shown to revert SMO but not GLI2 for all Hh antagonist treatments. Finally, in the SJSA-1 cell line, SB431542 was able to revert the expression of Hh antagonist-mediated GLI2 and SMO expression, whereas no effect was observed following SMAD4 knockdown. These observations are interesting as they suggest that although TGF β inhibitors are capable of reducing Hh antagonist-mediated TGF β regulated gene induction, they also seem to revert the Hh antagonist mediated response of Hh regulated genes, and thereby stimulate a Hh agonist induced response (when using the expression of Hh regulated genes as an output).

An important future experiment that needs to be performed is to assess the impact of combined treatments on the nuclear accumulation of pSMAD3, since assessing the ability of SB431542 treatment and SMAD4 knockdown to reduce the levels of Hh antagonist-induced accumulation of nuclear pSMAD3 will tell us if this accumulation is dependent on both ALK5 receptor kinase activity and SMAD4. However, the ability of these TGF β antagonists to in part reverse TGF β induced genes following Hh antagonist

treatment would indicate that the mechanism involved is at least partially dependent on ALK5 receptor kinase activity and SMAD4.

When assessing the impact of combining Hh and TGF β antagonist treatments in functional assays, our results showed that combinational treatments had no significant impact on cell viability or cell apoptosis. Therefore, inhibiting both of these pathways was not sufficient to impact cell viability, which as previously mentioned could be as a result of drugging for 24 hr, instead of longer time points; however, it could also indicate that other mechanisms beyond these two signalling pathways are responsible for cell survival.

Based on chapter 4, crosstalk between TGF β and Hh signalling pathways must also be considered in the cancer stem cell population. Our data show evidence that Hh antagonists mimicked the effects observed on cell viability and apoptosis in CSCs. Both GANT-61 and sonidegib were found to have an impact on colony-forming cells, however the effect of GANT-61 was far more pronounced, as nearly all colony-forming cells were killed in all three-cell lines. Conversely, no effect was observed on colony-forming cells following vismodegib treatment. For tumour-sphere forming cells, sonidegib was not found to have the same effects, with no impact observed on tumoursphere size or survival in anoikis-resistant cells (passage 1), nor self-renewing cells (passage 2). GANT-61 was capable of impacting tumoursphere size in passage 1 indicating that it is capable of reducing cell proliferation, along with being able to impact on self-renewal as evidence through the reduction of tumourspheres in passage 2. Like in the CFA, vismodegib was found to have no effect on tumoursphere forming cells. The resistance towards SMO antagonists identified in most assays corroborates what was reported by Colmont *et al.* (2013) whereby no effect was observed following vismodegib treatment in a primary BCC *in vitro* SC assay. However, with regards to GANT-61 although concentrations used were cited in numerous publications it is possible that under SC conditions the concentration was cytotoxic, or, given its ability to inhibit GLI proteins directly, there could be abrogation of GLI with other factors that contribute to off target effects. Nevertheless, it is important to note that GANT-61 did not have a significant

impact on the whole cell population as evidenced by cell viability and apoptosis assays indicating that maybe GANT-61 is a potent inhibitor of CSCs.

TGF β antagonists were found to have very little impact on tumoursphere formation either on anoikis-resistant cells (passage 1) or self-renewing cells (passage 2) in all three cell lines. SB431542 was found to reduce the number of colony forming cells in our cell lines which may be explained by the fact that TGF β signalling as previously described is involved in CSC maintenance. However, when both Hh and TGF β antagonists were combined, no additive impact was observed in either colony forming cells or tumourspheres. It is important to note however, that both the colony forming and sphere forming assays have their limitations, in that the colony forming assay measures the ability of a cell to grow in conditions where cell-cell contact is absent, and therefore is more of a progenitor like assay rather than a SC assay; whereas the sphere forming assay is a true SC assay as it measures the ability of a cell to grow in anoikis conditions (passage 1) and self renew (passage 2), although it only selects for SCs that divide and not for ones that are quiescent. For future work, if the CSC population is indeed important to cell survival, as potentially evidenced through GANT-61 (CFA and SFA) and SB431542 (CFA), then performing cell viability and apoptosis assays for longer time periods becomes even more important as no effect would be seen on the total cell population over short time periods if CSCs are effected following treatment, therefore longer time periods will be able to discern any potential effects of the drugs on the cell lines.

Thus blocking TGF β signalling at the level of the receptor and formation of intracellular SMAD heterodimers did not influence Hh driven cell survival upon Hh antagonist treatment. As a consequence it is increasingly apparent that other mechanisms may be in play that facilitate cell survival, and are possibly downstream of the inhibitors that we have been using. Therefore in chapter 6, we will attempt to explore the mechanisms that could potentially be involved. As a consequence, further exploration is required to test our hypothesis that TGF β signalling is responsible for the survival of Hh driven tumour cells following Hh antagonist treatment.

Chapter 6: Defining the Basis for Nuclear Translocation of SMAD3 Following Hh Antagonist Treatment

Chapter 6 Defining the Basis for Nuclear Translocation of SMAD3 Following Hh Antagonist Treatment

6.1 Introduction

We had hypothesised that resistance to Hh antagonists and Hh driven cancer cell survival was dependent upon TGF β signalling, based on preliminary microarray analysis. Consistent with the earlier published reports, Hh signalling was associated with an increase in TGF β signalling. Microarray gene set enrichment, RT-PCR profiling, Western blot analysis and immunofluorescence demonstrated enriched TGF β signalling at the tumour periphery and notably within the BCC CSC enriched population. In line with our hypothesis, Hh antagonist treatments, despite reducing Hh regulated genes, did not affect cell viability and simultaneously led to an increase in TGF β regulated genes.

Blocking TGF β signalling at the level of the receptor (tyrosine kinase inhibitor SB431542) and SMAD4 siRNA all led to a reduction in TGF β signalling with down-regulation of a TGF β core gene set in our *in vitro* assays. We observed that TGF β signalling blockade was capable of reversing the expression of Hh antagonist-induced TGF β regulated genes. However, when Hh driven cancer cells were treated with Hh antagonists together with either the tyrosine kinase inhibitor (SB431542) or SMAD4 siRNA there was no synergistic killing. Hence, pSMAD3 regulation of TGF β associated genes may still influence Hh driven cancer cell survival after Hh antagonist treatment.

SMAD proteins, similar to other intracellular signal transduction proteins, are sequestered in the cell cytoplasm bound to microtubules in the absence of active signalling (Dong *et al.*, 2000). The microtubule-organising centre is the connection between the microtubule network and nucleus and is crucial for both nuclear movement and intracellular signal transduction (Fletcher and Mullins, 2010). It has been shown that SMAD proteins use this microtubule scaffold to shuttle into the nucleus to effect gene regulation (Batut *et al.*, 2007). For example, the microtubular proteins kinesin-1 and the dynein light chain km23-1 are required for SMAD2 phosphorylation and translocation into the nucleus (Batut *et al.*, 2007; Jin *et al.*, 2007). Dong *et al.* (2000)

showed in several cell lines that endogenous SMAD2, 3, and 4 bind microtubules in the absence of TGF β stimulation (Dong *et al.*, 2000). Moreover, connexin43 can displace SMAD3 from microtubules as it competes for the same microtubular binding site (Dai *et al.*, 2007). Importantly, displacement of SMAD3 from microtubules by connexin43 led to expression of TGF β regulated genes. Thus, intracellular localisation of SMAD proteins including SMAD3 demonstrates their association with the microtubular network and their displacement can lead to TGF β ligand independent signalling.

Drugs that disrupt the microtubule network have been developed for the treatment of cancer and include nocodazole and colchicine. Nocodazole binds tubulin and blocks the formation of one of the two interchain disulphide linkages, which therefore blocks microtubule formation through polymerisation (Vasquez *et al.*, 1997). Dong *et al.* (2000) showed that nocodazole led to displacement and phosphorylation of SMAD2, with nuclear translocation and regulation of TGF β associated genes (Dong *et al.*, 2000). One proposed mechanism for nocodazole associated TGF β gene regulation, suggests that Rho/ROCK can facilitate SMAD2/3 phosphorylation (Samarakoon *et al.*, 2009). Hence we hypothesised that SMAD3 phosphorylation and nuclear translocation into the nucleus after Hh antagonists may result from Hh antagonist induced microtubular collapse. In order to determine this we will use primary BCC tissue and the DAOY cell line, which in chapter 5 was identified, as having an intact canonical Hh signalling pathway, whereas the UW228-2 and SJSA-1 cell lines did not.

6.2 Results

6.2.1 TGF β ligand expression is not induced by Hh antagonist

We sought to determine if Hh antagonist treatment could induce autocrine TGF β signalling by increasing expression of TGF β ligands. Consistent with the crosstalk between Hh and TGF β pathways, Hh antagonist treatments did not induce expression of TGF β ligands (Figure 6.1). After 24 hr treatment with vismodegib, both DAOY (-2.35 ± 0.02 ; $p < 0.05$) and UW228-2 (-2.85 ± 0.09 ; $p < 0.05$) cells showed downregulated expression of TGF β 2 (Figure 6.1 A & B). Sonidegib treatment was associated with downregulated expression of TGF β 2 in UW228-2 cells (-4.97 ± 0.04 ; $p < 0.05$) (Figure 6.1A & B). GANT-61 treatment led to downregulation of TGF β 2 and 3 in DAOY cells (-3.36 ± 0.04 ; $p < 0.05$ and -3.52 ± 0.06 ; $p < 0.05$ respectively), whereas UW228-2 cells showed downregulated expression of TGF β 1 and 3 (-2.98 ± 0.09 ; $p < 0.05$ and -8.74 ± 0.15 ; $p < 0.01$ respectively) (Figure 6.1 A & B). GANT-61 was associated with a small but significant increase in TGF β 2 in UW228-2 cells (1.67 ± 0.15 ; $p < 0.05$). Irrespective of the Hh antagonist, constitutive TGF β signalling in SJS-1 cells was not associated with an increase in TGF β ligand expression (Figure 6.1C). Consistent with the lack of response to concomitant TGF β blockade, Hh antagonists did not induce the expression of TGF β ligands and therefore pathway activation may be ligand independent.

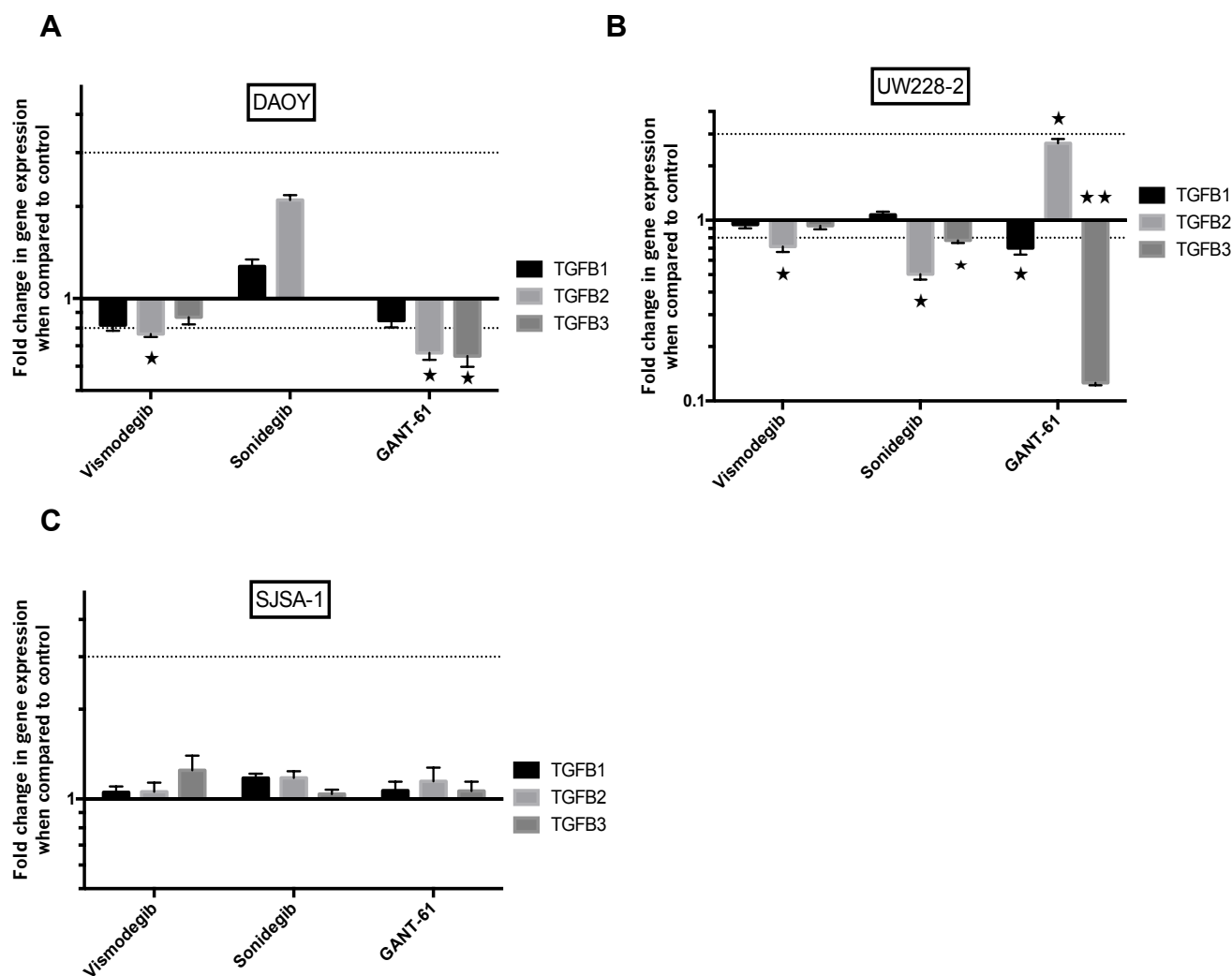


Figure 6.1: Hedgehog antagonist treatment in Hh driven tumour cell lines does not increase the expression of TGFβ ligands.

*Hh driven tumour cell lines (A) DAOY, (B) UW228-2, and (C) SJSA-1, were cultured in the presence of the Hh antagonists, vismodegib, sonidegib, and GANT-61 at a concentration of 10 μM for 24 hr, then analysed by qPCR for the expression of TGFβ1, 2, and 3 ligands. Expression values are presented as Log₁₀RQ, with an average of two independent experiments. The qPCR assay was performed with three internal technical replicates and two endogenous controls. Dotted lines represent a +2 or -2 fold change in gene expression in comparison to the control. (n=2), Error bars represent SE of mean, * represents p<0.05, ** represents p<0.01, t-test.*

6.2.2 Nocodozaole induced microtubule collapse leads to nuclear accumulation of pSMAD3

We next sought to determine if SMAD3 associated with microtubules in Hh driven cancer cell lines and if so whether disruption of the microtubule network could lead to nuclear translocation of pSMAD3. DAOY cells were cultured onto glass coverslips and subsequently treated with 1 μ M nocodazole for 8 and 24 hr, and immunofluorescence was performed to stain for α -tubulin and pSMAD3. Untreated DAOY cells formed an intricate microtubular cytoskeletal network with actin microfilaments and α -tubulin macrofilaments (Figure 6.2 upper row). After incubation with nocodazole the cytoskeletal collapse led to a change in morphology to more spindle shaped cells. The cell membrane bound actin filaments were lost, and the perinuclear clusters indicative of α -tubulin distribution were observed (Figure 6.2 lower row; 24hr time-point shown). All cells treated with nocodazole displayed similar changes in morphology and cytoskeletal protein re-distribution. Thus, the Hh driven medulloblastoma cell line DAOY, which has a cytoskeleton that is easy to visualise, also demonstrated microtubular collapse after treatment with nocodazole.

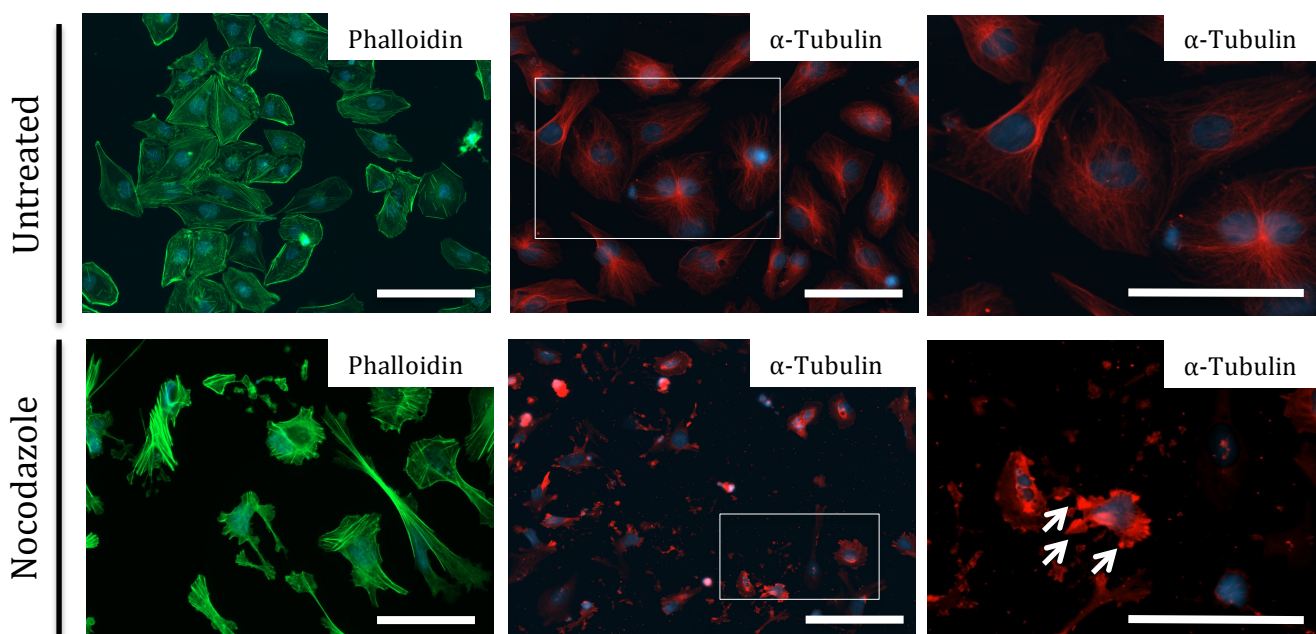


Figure 6.2: Nocodazole induced microtubule collapse

DAOY cell lines were cultured onto glass cover slips without (upper row) and with (lower row) nocodazole treatment for 24 hr. Nocodazole treatment resulted in redistribution of the cytoskeletal proteins, actin (labelled by phalloidin, left-hand-side images) and α -tubulin (centre and right-hand-side images). Cells are counterstained with the nuclear label DAPI. Scale bars = 50 μ M.

DAOY cells were cultured on glass cover slips and treated with 1 μ M nocodazole for 8 and 24 hrs. The cells were fixed in PFA, labelled with antibodies to α -tubulin and pSMAD3, and counterstained with DAPI. Collapse of the α -tubulin network was evident at both 8 and 24 hr (Figure 6.3). In contrast to untreated cells, pSMAD3 nuclear accumulation was also evident at both of these time points (Figure 6.3). The pattern of nuclear pSMAD3 resembled that observed previously after TGF β 1 treatment. Therefore, nocodazole achieved time dependent cytoskeletal collapse and nuclear translocation of pSMAD3 in the Hh driven tumour cell DAOY.

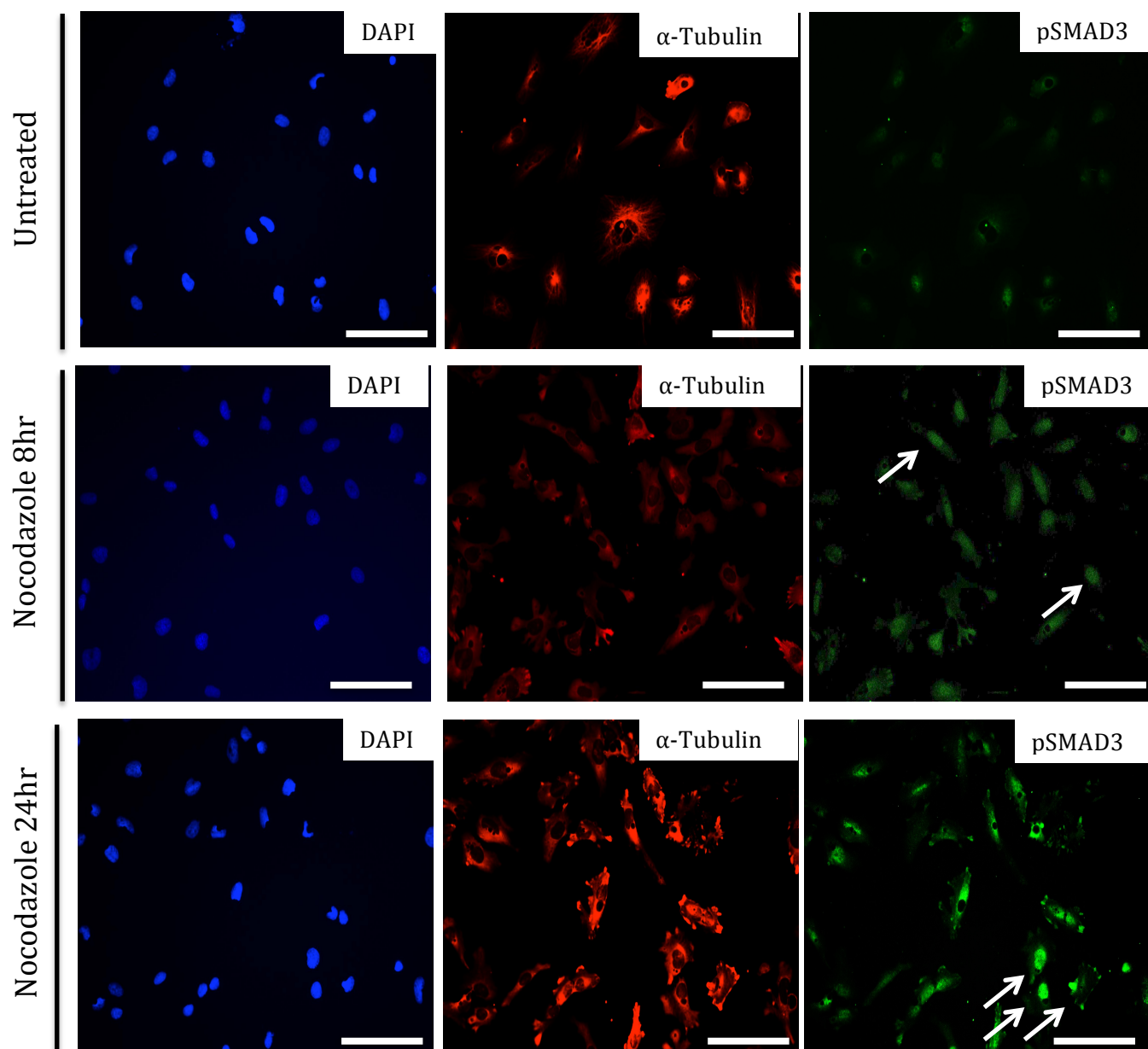


Figure 6.3: Nocodazole induced nuclear accumulation of pSMAD3 in Hh driven tumour cell line.

DAOY cells cultured on glass cover slips without (top row) and with nocodazole treatment for 8 hr (middle row) and 24 hr (bottom row). Cells were labelled with DAPI (left-hand-side) and antibodies to α -tubulin (middle) and pSMAD3 (right-hand-side). Cytoskeletal collapse and nuclear pSMAD3 was evident at both 8 and 24hr, but not in untreated cells. Scale bars = 50 μ M.

6.2.3 Primary BCC treated with Hh antagonist reduce acetylated tubulin

When incorporated into microtubules, tubulin accumulates a number of post-translational modifications that are important for its role in many biological and molecular functions, including acetylation. Catalyzed by α -tubulin acetyl-transferase, the acetylation of K40 on α -tubulin is a hallmark of stable microtubules (Friedmann *et al.*, 2012). To determine if Hh antagonist therapy of BCC could induce microtubular collapse, we undertook western blot analysis of vismodegib treated primary BCC cells at varying time points (Figure 6.4). As with nocodazole induced microtubular collapse, BCC cells treated with vismodegib for 24 hr resulted in loss of K40 acetylated α -tubulin (Figure 6.4). Hence, BCC treated with Hh antagonists also undergo time-dependent microtubule collapse.

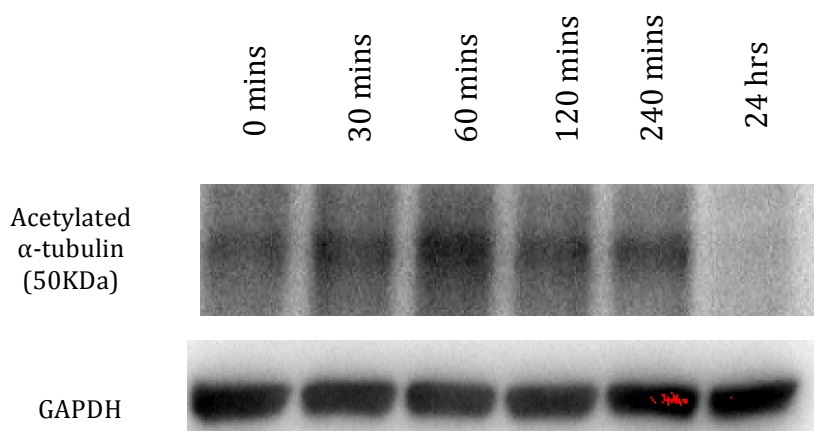


Figure 6.4: Hh antagonists induce microtubule destabilisation within primary human BCC

Primary BCC tissue was dissociated into single cells and cultured in the presence of 10 μ M vismodegib at varying time-points. Protein was then extracted and western blot performed using anti acetylated α -tubulin antibody, with GAPDH used as the loading control. Experiments were performed in duplicate.

6.2.4 Hh antagonists induce microtubule collapse and nuclear pSMAD3 accumulation

Next we sought to determine if Hh antagonist induced microtubular collapse was associated with pSMAD3 nuclear translocation. The Hh driven DAOY cell line was cultured onto glass coverslips and treated with vismodegib for 24 hrs. Cells were fixed and labelled for F-actin, α -tubulin, and pSMAD3. Vismodegib treatment led to a morphological change in DAOY cells, compared to untreated cells vismodegib treatment was associated with spindle shape transformation (Figure 6.5). Treated cells lost their ring of F-actin around the cell periphery (Figure 5.6 arrows), along with a reduction in α -tubulin in the cell cytoplasm. With vismodegib treatment, there was nuclear accumulation of pSMAD3 (Figure 6.6). Quantification of the relative fluorescence intensity of nuclear pSMAD3 staining within these cells revealed a 2-fold increase in treated cells ($4,031 \pm 567.0$) when compared to the untreated cells ($8,022 \pm 256.0$; $p < 0.01$; Figure 6.6B). Therefore, based on immunofluorescence staining, vismodegib treatment led to disruption of the microtubule network and was associated with an increase in the nuclear accumulation of pSMAD3.

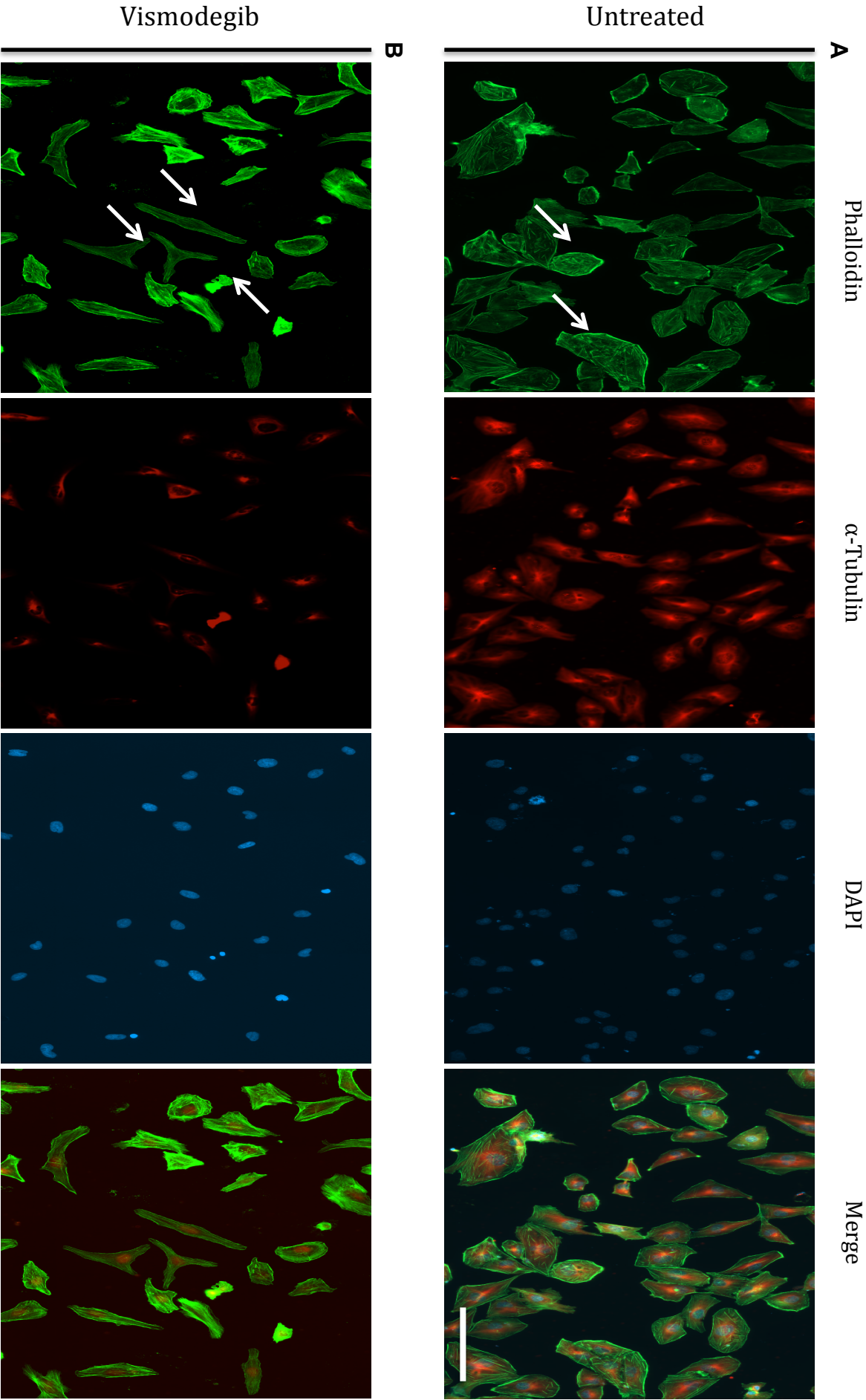


Figure 6.5: Hh antagonists induce microtubule changes in Hh driven tumour cell line.

DAOY cells cultured onto glass cover slips were treated with vismodegib at 10 μ M for 24 hr. Untreated and vismodegib treated DAOY cells were fixed and labelled with phalloidin-488 and α -tubulin. Scale bars are all = 50 μ M

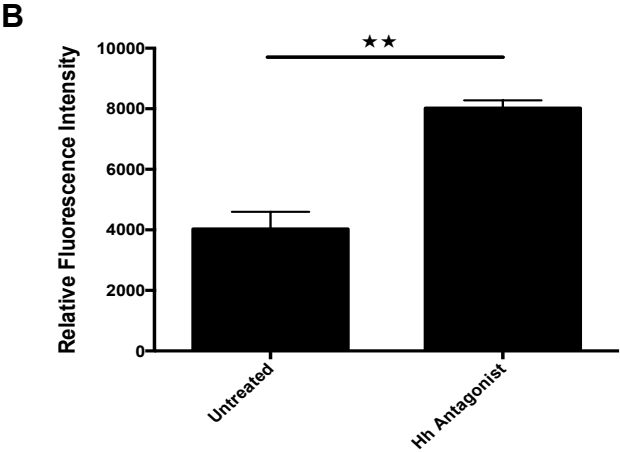
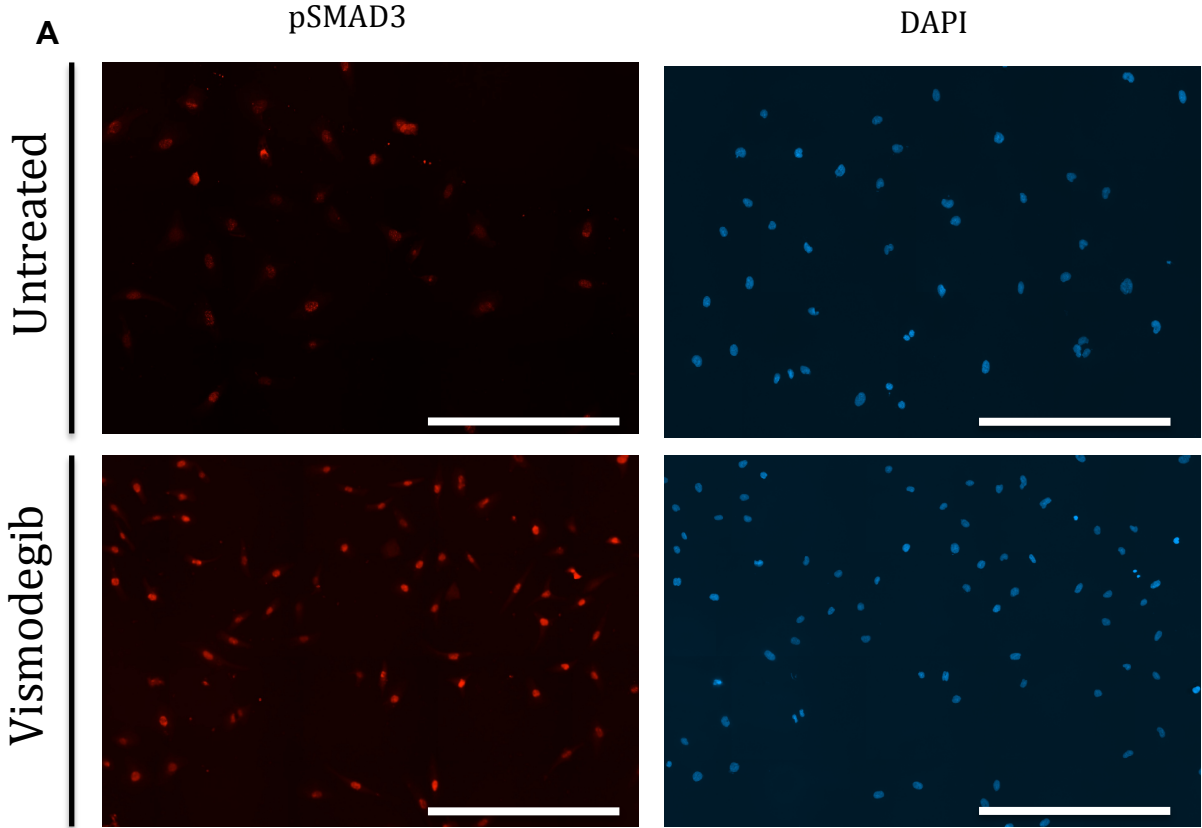


Figure 6.6: Hh antagonists induce nuclear accumulation of pSMAD3 in Hh driven tumour cell line.

DAOY cells were cultured onto glass cover slips and treated with 10 μ M vismodegib for 24 hr. (A) DAOY cells untreated and treated with vismodegib before being stained with pSMAD3, (B) relative fluorescent intensity (RFI) of nuclear pSMAD3 staining was

quantified using Image J software over three independent experiments. ($n=3$), Error bars represent SE of mean, ** represents $p<0.01$, t-test. Scale bars = 200 μM .

6.3 Discussion

In vertebrates, Hh signalling is coordinated by the primary cilium, a microtubule-based organelle that projects from the surface of most types of mammalian cells (Huangfu *et al.*, 2003; Goetz and Anderson, 2010). In the absence of Hh pathway activation, PTCH1 localizes to the primary cilium and inhibits SMO ciliary localisation (Rohatgi *et al.*, 2007). In the presence of Hh ligands, SMO accumulates in the cilium and activates the downstream Hh pathway (Corbit *et al.*, 2005). Similarly, other Hh pathway components, including SUFU and the GLI transcription factors, also localize to the cilium suggesting that the cilium is the subcellular site at which SMO interacts with its downstream targets (Haycraft *et al.*, 2005; Liu *et al.*, 2005). Hh signalling maintains the primary cilium through SMO mediated microtubule acetylation, and Hh antagonists have been previously reported to disrupt this microtubular network (Lee and Ko, 2016; Wu *et al.*, 2012). Our data corroborates these findings and has shown that in Hh driven tumour cells (where primary cilia is relevant), Hh antagonist treatment is capable of inducing microtubule collapse, evidenced through de-acetylation of α -tubulin (hallmark of microtubule collapse), and a reduction in the levels of phalloidin and α -tubulin filaments in primary BCC and DAOY cells, respectively. Our data shows that, following Hh antagonist treatment and therefore microtubule collapse, we get nuclear accumulation of pSMAD3. Interestingly, a study by Gu *et al.* (2016) determined that loss of α -tubulin acetylation was associated with TGF β induced EMT (Gu *et al.*, 2016). They reported that TGF β signalling increased the activity of HDAC6, which causes deacetylation of α -tubulin, and that treatment with the HDAC inhibitor, tubacin, or the ALK5 inhibitor, SB431542, restored the level of acetylated α -tubulin. An additional study by Korol *et al.* (2016), also identified TGF β induced cytoskeletal reorganisation through Rho/ROCK signalling as essential to the EMT of lens epithelial cells (Korol *et al.*, 2016). This therefore provides a mechanism through which Hh antagonists can induce microtubular changes, and therefore future experiments using tubacin or SB431542 in combination

with Hh antagonists will allow us to determine if the level of acetylated α -tubulin can be restored. Furthermore, a number of studies have highlighted the ability of Hh antagonists to modify the microtubular network, such as Lee and Ko, (2016), who showed that in mouse embryonic fibroblast cells (MEFs) activation of Hh signalling led to the acetylation of microtubules via SMO, which was subsequently abrogated upon treatment with the Hh antagonist, vismodegib. Based on the expression of TGF β ligands following Hh antagonist treatment in our Hh driven cell lines, Hh-antagonist induced TGF β signalling may not be ligand dependent, as no increase in TGF β ligand expression was observed following treatment. Therefore Hh antagonists are capable of impacting on the microtubular network, which is associated with the nuclear translocation of pSMAD3. This is not without precedent as it is becoming increasingly evident that SMAD signalling can be initiated through non-TGF β superfamily ligands, which in some instances is not entirely dependent on TGFBR1 (Samarakoon *et al.*, 2009; de Caestecker *et al.*, 1998). Although Hh antagonist treatment is associated with microtubular changes and nuclear accumulation of pSMAD3, it remained to be determined whether these two observations were linked. We therefore performed a proof of principle experiment using the microtubule destabilising agent, nocodazole, to confirm that microtubule collapse causes enhanced nuclear accumulation of pSMAD3. We found that nocodazole treated Hh driven DAOY cells demonstrated an increase in nuclear pSMAD3, which confirmed what other papers have shown using these destabilising agents (Samarakoon *et al.*, 2009; Samarakoon *et al.*, 2002; Samarakoon *et al.*, 2003; Ott *et al.*, 2003; Chaqour *et al.*, 2006; Muehlich *et al.*, 2007).

Although we have not currently elucidated a mechanism by which pSMAD3 is phosphorylated following Hh antagonist treatment, based on the literature there are several possibilities that could explain what we have observed. Microtubules and the molecules that interact with them can contribute to signal transduction by at least three distinct mechanisms: 1) microtubule sequestering and release, 2) microtubule delivery and 3) microtubule scaffolding of signalling molecules. For example, in order for SMAD2 to translocate to the nucleus it is required to associate with km23-1 and microtubules (Jin *et al.*, 2007); and in fact there is evidence to suggest that all SMADs interact with microtubules (Dong *et al.*, 2000). Furthermore, microtubules have been shown regulate

TGF β signalling by trapping SMADs in the cytoplasm (Dong *et al.*, 2000). Interestingly, in this study they demonstrated that by destabilising the microtubules with nocodazole or colchicine, TGF β signalling was increased through dissociation of the SMADs from the microtubules (Dong *et al.*, 2000), with a later study showing that this release could be regulated by connexin-43 (Dai *et al.*, 2007). More specifically, Samarakoon *et al.* (2009) implicated the potential role of the Rho-ROCK pathway, as they found that nocodazole treated cells were capable of activating Rho-GEFs which led to Rho-GTP loading and subsequent phosphorylation of SMAD3 and downstream expression of TGF β regulated genes (SERPINE1 and CTGF) (Samarakoon *et al.*, 2009). In fact the interaction between the TGF β and Rho/ROCK signalling pathways, and the subsequent impact on the microtubular network has been reported by a number of publications (Vardouli *et al.*, 2008; Xue *et al.*, 2012; Samarakoon *et al.*, 2009). The same group also demonstrated that blocking with the Rho/ROCK signalling pathway could inhibit TGFBR1 induced phosphorylation and subsequent nuclear accumulation of pSMAD2 (Samarakoon *et al.*, 2008a), and that this pathway could also modulate the duration of SMAD2/3 phosphorylation and subsequent nuclear accumulation (Samarakoon *et al.*, 2008b). Interestingly, non-canonical activation of R-SMADs has been shown after nocodazole treatment through the disassociation of R-SMADs from microtubules, which are subsequently phosphorylated by Mps1 kinase (Dong *et al.*, 2000; Zhu *et al.*, 2007); this therefore provides a good target for studying in our Hh driven tumour cells following Hh antagonist treatment. Therefore, these studies along with our findings suggest a role for microtubule dynamics in the regulation of SMAD signalling, and the ability of Hh antagonists to influence those dynamics.

In future work, elucidating the mechanisms through which nuclear pSMAD3 is induced following Hh antagonist treatment could be evaluated through a series of experiments. Initially, it will be necessary to determine whether or not it is ligand dependent and/or receptor kinase dependent. To do this TGF β 1, 2, 3 blockers should be administered in combination with Hh antagonist treatments to determine the effect on nuclear pSMAD3 levels, assessed by Western blot and immunofluorescence. Assessing receptor kinase dependence could be achieved through the use of the ALK5 inhibitor, SB431542, in combination with Hh antagonists, to again determine the impact on pSMAD3 levels. If

Hh induced pSMAD3 nuclear accumulation is dependent on ligand and/or receptor activity then it would be necessary to assess the ability of SB431542 to reverse Hh antagonist induced microtubule destabilisation, and to address the inability of TGF β blockade to impact cell viability in the Hh driven cell lines (Chapter 5). If Hh antagonist induced nuclear accumulation of pSMAD3 is not dependent on receptor kinase activity then alternative mechanisms will be explored through determining the effect of blocking the aforementioned potential targets, including the Rho/ROCK signalling pathway using the p160ROCK blocker, Y-27632. Additionally, the Rho/ROCK signalling cascade is transduced through transcription factors, such as serum response factor (SRF); therefore assessing the nuclear accumulation of SRF following treatment with Hh antagonist treatment and combination treatment with SB431542 will be of interest. Furthermore, in order to determine the importance of pSMAD3 and/or Rho/ROCK to impact the microtubular network, performing siRNA knockdowns of these proteins and then assessing the effect on the microtubular network will allow that to be determined.

In summary, we have confirmed that in Hh driven cancer cells, nocodazole induced microtubule collapse increases nuclear accumulation of pSMAD3 protein levels. Likewise, the Hh antagonist vismodegib also disrupted the microtubular network, with an accompanied increase in nuclear pSMAD3 in both primary BCC and a Hh driven tumour cell line. Hence our findings show that Hh antagonists disrupt the microtubular network in a time dependent manner, which in turn results in modulation of TGF β regulated genes. The broader implications of the research and future experiments will be discussed in more detail in chapter 7.

Chapter 7: General Discussion

Chapter 7 General Discussion

7.1 Discussion

Over the past 10 years the focus of drug discovery in oncology has evolved from empiric development to one of a rationale approach. Currently, emphasis is on the development of targeted therapeutic agents that have been identified through the discovery of genetic alterations in human cancers and the signalling pathways that they alter. In individuals with malignancies that are driven by dominant mutations, gene amplifications, or translocations (“oncogene addiction”), single agent therapies were initially shown to be effective, however the vast majority of tumours subsequently become refractory to treatment (e.g. through acquired resistance) and patients often succumb to disease progression. Molecular targets that have FDA approved therapeutic agents include: HER2 amplification in breast cancer (Perez *et al.*, 2017; Welslau *et al.*, 2014), epidermal growth factor receptor (EGFR) mutations in non-small cell lung cancer (Zhao *et al.*, 2017; Zhang, 2016), BCR-ABL translocations in chronic myeloid leukaemia (CML), c-Kit mutations within gastrointestinal stromal tumours (GIST) (Holohan *et al.*, 2013), and with relevance to Hh driven cancers (e.g. BCC and medulloblastoma), inactivating mutations in the receptor of PTCH and/or activating mutations in the GPCR SMO within basal cell carcinoma (Von-Hoff *et al.*, 2009). However, key to the successful development and application of targeted therapies is having a better understanding of resistance mechanisms, as most tumour types are either refractory to targeted therapies (intrinsic resistance), or become refractory following therapy (acquired resistance). There are several mechanisms that have been identified for such resistance to targeted therapies including, increases in the expression of transporters capable of drug efflux, alterations or mutations of drug targets, drug detoxification and inactivation, impact on apoptosis, and interference with DNA replication machinery. Table 7.1 provides a summary of resistance mechanisms to some common molecularly targeted agents. This project focused on elucidating the mechanism of drug resistance in Hh driven tumours, and since BCC and medulloblastoma are prototypical cancers for Hh signalling they served as perfect models for studying resistance mechanisms towards targeted therapies.

Table 7.1: Summary of resistance mechanisms to some common molecular targeted agents

Targeted Therapy	Cancer Type	Target	Mechanism of Resistance
Imatinib	CML, ALL	BCR-ABL1	Mutations of the target (Chen <i>et al.</i> , 2008); Increased MDR1 expression (Shervington and Lu, 2008; Bhatavdekar <i>et al.</i> , 1998; Pusztai <i>et al.</i> , 2005)
Trastuzumab	ERBB2-positive breast cancer	ERBB2	PTEN loss (Nagata <i>et al.</i> , 2004), Truncation of ERBB2 (Recupero <i>et al.</i> , 2013); Activating mutations in PIK3CA (Berns <i>et al.</i> , 2007)
Gefitinib	NSCLC	EGFR	EGFR kinase domain mutations (Coco <i>et al.</i> , 2012; Shin <i>et al.</i> , 2012; Morris <i>et al.</i> , 1995); MET amplifications (Van Schaeybroeck <i>et al.</i> , 2005)
Cetuximab	Head and neck cancer, colorectal cancer	EGFR	KRAS mutation (Lievre <i>et al.</i> , 2006); Increased ERBB family signalling (Kishida <i>et al.</i> , 2005)
Vemurafenib	Melanoma	BRAF-V600E	Elevated BRAF-V600E expression (Van Schaeybroeck <i>et al.</i> , 2008), Acquired mutations in KRAS, NRAS or MEK1 (Sunnarborg <i>et al.</i> , 2002; Lee <i>et al.</i> , 2003; Kyula <i>et al.</i> , 2010; Zhou <i>et al.</i> , 2006)
Bevacizumab	Colorectal cancer, NSCLC, glioblastoma	VEGF	Hypoxia induced autophagy (Hu <i>et al.</i> , 2013), Activation of alternative signalling pathway (Jahangiri <i>et al.</i> , 2013)
Bortezomib	Multiple myeloma	Proteasome	Mutation in the binding site (Oerlemans <i>et al.</i> , 2008)
Vismodegib and Sonidegib	Basal cell carcinoma	SMO	Mutations of the target (Yauch <i>et al.</i> , 2009; Sharpe <i>et al.</i> , 2015; Atwood <i>et al.</i> , 2015; Ridky <i>et al.</i> , 2015), Cancer SCs (Colmont <i>et al.</i> , 2013; Colmont <i>et al.</i> , 2013), Activation of alternative signalling pathway (Colmont <i>et al.</i> , 2013)

Work has already begun to establish possible mechanisms of resistance in BCC towards SMO antagonist therapy, with some groups showing that mutations within SMO have altered its structure meaning that vismodegib and sonidegib are no longer able to bind and have an effect (Yauch *et al.*, 2009; Sharpe *et al.*, 2015; Atwood *et al.*, 2015; Ridky *et al.*, 2015). However, these mutations have only been identified in approximately 50% of treatment-resistant BCC, which therefore strongly supports the existence of one or more unidentified pathways responsible for drug resistance in the remaining 50% of treatment-resistant BCCs. When looking at the previously identified mechanisms of resistance towards targeted therapies in other cancers (Table 7.1), there are three principle mechanisms that have been identified; 1) the activation of alternate signalling pathways that are capable of driving tumour growth, 2) target mutations that prevent drug activity, and more recently 3) the presence of CSCs which in certain settings has been attributed to drug resistance, on account of them being intrinsically resistant to a wide array of therapeutic approaches (Valent *et al.*, 2012). Work in our lab using an *in vitro* based colony forming assay has already shown that human BCC cells are resistant to conventional chemotherapeutics such as etoposide (Colmont *et al.*, 2013), which was associated with increased expression of the ABCB1 (p-glycoprotein multi-drug resistance protein 1) transporter in the BCC CD200+ CSC population following treatment (Colmont *et al.*, 2014). Furthermore, our lab also demonstrated that human BCC cells were resistant to the targeted therapeutic, vismodegib (Colmont *et al.*, 2013), with preliminary microarray analysis identifying an enrichment of the TGF β signalling pathway following treatment. This work therefore raised the possibility of the involvement of the CSC population in drug resistance within BCC and also the potential role of TGF β signalling in crosstalk with Hh signalling to compensate for Hh pathway inhibition.

Both TGF β and Hh signalling have been recognised in BCC. Direct interaction between these two pathways was established in BCC, with GLI2 being identified as an early gene target of the TGF β /SMAD3 cascade independent of Hh signalling (Dennler *et al.*, 2007). Additional work by the same group confirmed that, in response to TGF β , SMAD3 was rapidly recruited to distinct elements within the GLI2 promoter and enhanced its

transcription (Dennler *et al.*, 2009). They also found that GLI1 (a specific marker for Hh signalling activity) was induced in a GLI2-dependent manner following TGF β pathway activation. Our data in chapter 3 supports the role of TGF β signalling in Hh driven cancers since microarray analysis on whole BCC tissue identified the enrichment of Hh and TGF β signalling, along with the overrepresentation of TGF β regulated genes. Furthermore, we found that cells active for TGF β signalling resided predominantly at the tumour nodule periphery, which is important, as it is where proliferation and invasion occur, and where our lab previously identified the CSC population in BCC. In chapter 4, we isolated CSCs from whole BCC tissue and attempted to elucidate the mechanisms of resistance in Hh driven cancers. Previously our group has identified a CSC population within BCC and shown this population to express CD200 and be resistant to Hh antagonists (Colmont *et al.*, 2013). Consistent with a HF bulge SC basis as the cell of origin for BCC (Youssef *et al.*, 2010; Wang *et al.*, 2011), we have shown that BCC CSCs demonstrated active TGF β signalling, and that immunofluorescent labelling of BCC tissue confirmed the presence of BCC CSC at the tumour periphery. We also found that cells at the tumour nodule periphery active for TGF β signalling were not associated with proliferation, which raised the possibility that they may be involved with invasion. Interestingly, we also found that the CSC population demonstrated concordant expression of TGF β regulated EMT genes, which is also consistent with other cancer types, where the role of TGF β signalling has been identified in the CSC population and has been linked to EMT/invasion (Bruna *et al.*, 2012; Lo *et al.*, 2012; Bhola *et al.*, 2013; Shipitsin *et al.*, 2007, You *et al.*, 2010; Mima *et al.*, 2012, Ikushima *et al.*, 2009; Penuelas *et al.*, 2009, Oshimori *et al.*, 2015). Future studies for this chapter are outlined in section 7.2 below.

Our findings from chapter 4 raised two important questions: (1) is TGF β signalling an important CSC survival pathway?; and alternatively, (2) after Hh antagonist treatment is there an enrichment of active TGF β signalling in BCC/medulloblastoma? Therefore, in chapter 5 we recruited the use of three well-established Hh driven tumour cell lines, notably the two medulloblastoma cell lines DAOY, and UW228-2, and the osteosarcoma cell line, SJSA-1. These cell lines as previously mentioned were chosen as both medulloblastoma and osteosarcoma are relevant tumour types for studying Hh

signalling, and they enabled us to study the stem cell compartment, which wasn't possible with BCC cell lines. Our results showed that Hh antagonists (vismodegib, sonidegib and GANT-61) had no significant impact on cell viability, which is consistent with what has been found in some reports (Arnhold *et al.*, 2016; Infante *et al.*, 2016). Both DAOY and UW228-2 cell lines represent the two most cited medulloblastoma cell lines and have been well established as being Hh driven, however, our gene expression data suggested that the DAOY cell line had a functionally intact canonical Hh signalling pathway, whereas the UW228-2 and the SJSA-1 cell lines did not. We have shown that following Hh antagonist treatment, TGF β pathway activity increases in our Hh driven tumour cell lines, as evidenced through nuclear accumulation of pSMAD3 in all cell lines, and in some instances through expression of downstream TGF β regulated genes. This apparent ability of TGF β signalling to respond to a reduction in Hh signalling following treatment suggests that this could be a survival mechanism, and the fact that it occurred in both the DAOY and UW228-2 cell lines suggests that this increase in pSMAD3 levels is independent of having an intact canonical Hh signalling pathway. However, our work showed that SB431542 treatment alone did not induce apoptosis or significantly impact cell viability, although did appear to be capable of reversing the expression of the TGF β core gene set phenotype induced following Hh antagonist treatment in our cell lines. However, even though at the gene expression level there appeared to be an effect following SB431542 treatment and SMAD4 knockdown, this was not mirrored in the cell viability assays, as combining TGF β and Hh antagonist treatment again resulted in no induction of apoptosis or decrease in cell viability.

With regards to the impact of treatment on the CSC population, we found that SMO antagonists were largely ineffective either on colony forming cells or tumourspheres in all three Hh driven cell lines, which corroborates findings from our group whereby no effect was observed following vismodegib treatment in a primary BCC in an *in vitro* SC assay (Colmont *et al.*, 2013). However, the exception was GANT-61, which had a highly significant impact on colony forming cells and tumoursphere size in all of our cell lines. For future experiments, it will be interesting to compare the effects observed following GANT-61 treatment with the knockdown of GLI TFs using siRNA in order to assess the impact on CSCs in both the CFA and SFA, and to see if the effects observed following

GANT-61 treatment are due to cytotoxicity or targeted killing of CSC. The impact observed for GANT-61 could be abrogation of GLI with other factors that contribute to off target effects. We found that TGF β antagonists were found to have very little impact on tumoursphere formation in all three Hh driven cell lines, and when both Hh and TGF β antagonists were combined in these cell lines no additive or synergistic effect was observed in either colony forming cells or tumourspheres. Although treatment with SB431542 and SMAD4 siRNA was capable of impacting the expression of some of the TGF β regulated genes following Hh antagonist treatment in our cell lines, the fact that no effect was observed on cell viability following treatment with TGF β antagonists alone or in combination with Hh antagonists suggests that other mechanisms may be involved aside from Hh and TGF β signalling. However, for future studies, performing cell viability and apoptosis assays following longer exposure to Hh antagonists will be important, as cell lines were treated for no longer than 48 hr in our experiments, and it will allow us to determine if longer time periods are required in order to see any effects.

In chapter 6, we demonstrated that the microtubule destabilizer, nocodazole induced microtubule collapse and subsequently increased nuclear pSMAD3 protein levels. Likewise, we found that the Hh antagonist vismodegib also disrupted the microtubular network, with an accompanied increase in nuclear pSMAD3 in both primary BCC and the DAOY cell line, which in turn results in modulation of TGF β regulated genes. Therefore, we have shown that Hh antagonists are capable of altering the microtubule network in Hh driven tumour cells and that this change is associated with increased levels of nuclear pSMAD3. Finally, the mechanisms that underlie both the alterations in the microtubular network and increase in TGF β signalling activity following Hh antagonist treatment need to be explored in more detail in our cell lines (Section 7.2, below). Furthermore, both of these observations are associated with EMT, and therefore this connection will need to be explored in more detail.

The disruption of the microtubular network following Hh antagonist treatment and the subsequent increase in nuclear pSMAD3 implicates the Rho/ROCK signalling pathway as a major target for further investigation. Interestingly, a recent publication by Whitson *et al.* (2018) identified a non-canonical mechanism of Hh pathway activation driven by the

Rho/ROCK signalling TF, serum response factor (SRF), in drug-resistant basal cell carcinoma; and they found that SRF was induced by Rho/formin family member Diaphanous (mDia) activated cytoskeletal reorganisation.

Additionally, in order to gain further insight into the mechanisms involved in drug resistance it is important to study what is observed in the clinic. As mentioned previously, the mechanisms that underlie approximately 50% of treatment-resistant BCCs are yet to be elucidated. Interestingly, there have been several clinical cases of SCC arising from the same tumour bed as the original BCC during and after Hh antagonist treatment (Ransohoff *et al.*, 2015; Mohan *et al.*, 2016; Aasi *et al.*, 2013; Orouji *et al.*, 2014; Zhu *et al.*, 2014; Chang *et al.*, 2012). In these reported cases, BCC is shown to initially regress and then regrow into a more aggressive tumour, which may again potentially implicate SCs in this transformation process. Therefore, in this instance it appears that these cells have deployed mechanisms enabling them to acquire a more aggressive and invasive phenotype. It is possible to contextualise this observation with our own data, in that microtubule dynamics can also mediate EMT and therefore make cells more invasive. Since we see an increase in TGF β signalling following Hh antagonist treatment in BCC tissue, then it is likely that this is also observed in the clinic. During the inter-conversion of an epithelial cell to a mesenchymal cell, microtubules must undergo spatial reorganisation. In fact recent studies have shown that bladder and breast cancers treated with drugs that target microtubule dynamics demonstrate increased levels of E-cadherin and a reduction in mesenchymal markers (Aparicio *et al.*, 2014; Yoshida *et al.*, 2014). However, it is important to note that the opposite has also been demonstrated, whereby the stabilisation of microtubules using paclitaxel has attenuated TGF β induced morphological changes, phosphorylation of SMAD2, and expression of α -smooth muscle actin and collagen I (Tsukada *et al.*, 2013). Furthermore, treatment of breast cancer cells with an inhibitor of microtubule dynamics, eribulin mesilate, decreased TGF β induced changes in EMT markers and phosphorylation of SMAD2 and 3 (Yoshida *et al.*, 2014). Therefore there is data to suggest that microtubules are capable of influencing gene expression during TGF β -induced EMT and that they clearly play an important role in guiding cell fate and motility during EMT. Interestingly, SCC is strongly associated with TGF β signalling and as

a consequence there is reason to suggest that Hh antagonist treatment may lead to the destabilisation of microtubules, which in turn leads to TGF β -induced EMT/invasion in either the general cell population or SC population. Importantly, we are in the process of obtaining PFFA patient BCC tissue samples that have been unresponsive following treatment with vismodegib. This will therefore allow us to evaluate any changes in TGF β signalling and explore mechanisms that underlie this increase using immunofluorescence in relevant patient samples.

7.2 Future Directions

With regards to the BCC CSC population (chapter 4), future studies will need to be performed in order to elucidate the role of this population further. Of interest to us is performing RNA sequencing and subsequent gene expression profiling on the CSC population between samples that have been treated with and without Hh antagonists, in order to identify differences in pathways/processes between these two groups. Furthermore, exploring the relationship between the CSCs at the invasive edge with the surrounding stroma is of interest as a number of the studies mentioned above have highlighted the role that the local microenvironment plays on CSC function. Although they did not look at CSCs within BCC tissue, a recent study by Kuonen *et al.* (2018) identified a role for TGF β signalling in promoting local invasion through peritumoural fibronectin deposition in BCC (Kuonen *et al.*, 2018). Interestingly, this study showed that higher levels of fibronectin and CAFs were found at the tumour edge in BCC (Kuonen *et al.*, 2018). CAFs have already been shown to promote BCC invasion through the paracrine activation of mesenchymal epithelial transition receptor tyrosine kinase (c-MET) in BCC tumour cells (Marsh *et al.*, 2008; Tiju *et al.*, 2009). Furthermore, the role of CAFs in increasing the frequency of tumour initiating cells, and the fact that TGF β signalling dramatically enhances this process has also been demonstrated (Calon *et al.*, 2015). Therefore, exploring the potential roles of TGF β signalling in the CSC population and the interaction of this population with surrounding stromal elements, such as CAFs, will be of interest in future studies.

Figure 7.1 outlines several avenues that will need to be explored in more detail in order to elucidate the mechanism/s through which nuclear pSMAD3 levels increase following Hh antagonist treatment. Specifically, Figure 7.1A outlines the notion that Hh antagonist induced microtubule collapse leads to the regulation of SMAD phosphorylation through alternative kinases independent of TGFBR1. A number of publications (highlighted previously) have identified alternative kinases capable of phosphorylating SMAD proteins. Therefore there are commercially available pharmacological inhibitors that can be deployed including AG1478 (EGFR), c3 transferase (Rho), Y-27632 (p160ROCK) and PD98059 or U0126 (MEK), in combination with Hh antagonist treatment to test the impact on our Hh driven cell lines. Figure 7.1B highlights another potential mechanism through which SMAD proteins can be induced, and it involves the ability of nuclear phosphatases such as PPM1A and pyruvate dehydrogenase phosphatase to regulate nuclear SMAD complexes. It is possible that SB431542 treatment in combination with Hh antagonists did not have an impact on our cell lines as microtubule destabilisation has been shown to influence factors such as the Rho/ROCK pathway that subsequently regulate the activity of these phosphatases (Samarakoon *et al.*, 2009). Inhibition of these phosphatases through factors initiated by microtubule alterations serve to stabilise the phosphorylated SMADs in the nucleus which are then free to induce downstream effects for longer time periods. As the Rho/ROCK signalling pathway has been previously identified as a negative regulator of these phosphatases following microtubule reorganisation, it would be interesting to assess whether inhibiting this pathway leads to a reduction of pSMAD3 within the nucleus following Hh antagonist treatment. Since destabilisation of these microtubules is an early event responsible for the initiation of TGF β signalling, it will be important to determine whether using a drug capable of stabilising microtubules such as paclitaxel, would have a significant effect on the level of TGF β signalling in our Hh driven cell lines following Hh antagonist treatment. Another important point that also needs to be addressed is determining whether or not nuclear translocation of SMAD3 and subsequent downstream effects are responsible for conferring a survival mechanism to Hh driven cells after treatment. Therefore knocking down SMAD3 with siRNA will allow us to determine if cells can become sensitised to Hh antagonist treatment. Furthermore, our studies have focused on SMAD3; therefore it would be interesting to determine whether an increase in

nuclear pSMAD2 is observed in the same way as SMAD3 after treatment. Additionally in order to test the hypothesis that Hh driven tumour cells undergo TGF β -induced EMT following Hh antagonist treatment, there will be a need to obtain functional data on these cells rather than gene expression outputs alone. Therefore performing invasion and/or migration assays on our cell lines treated with Hh antagonists will help us better understand if these cells are indeed becoming more invasive following treatment.

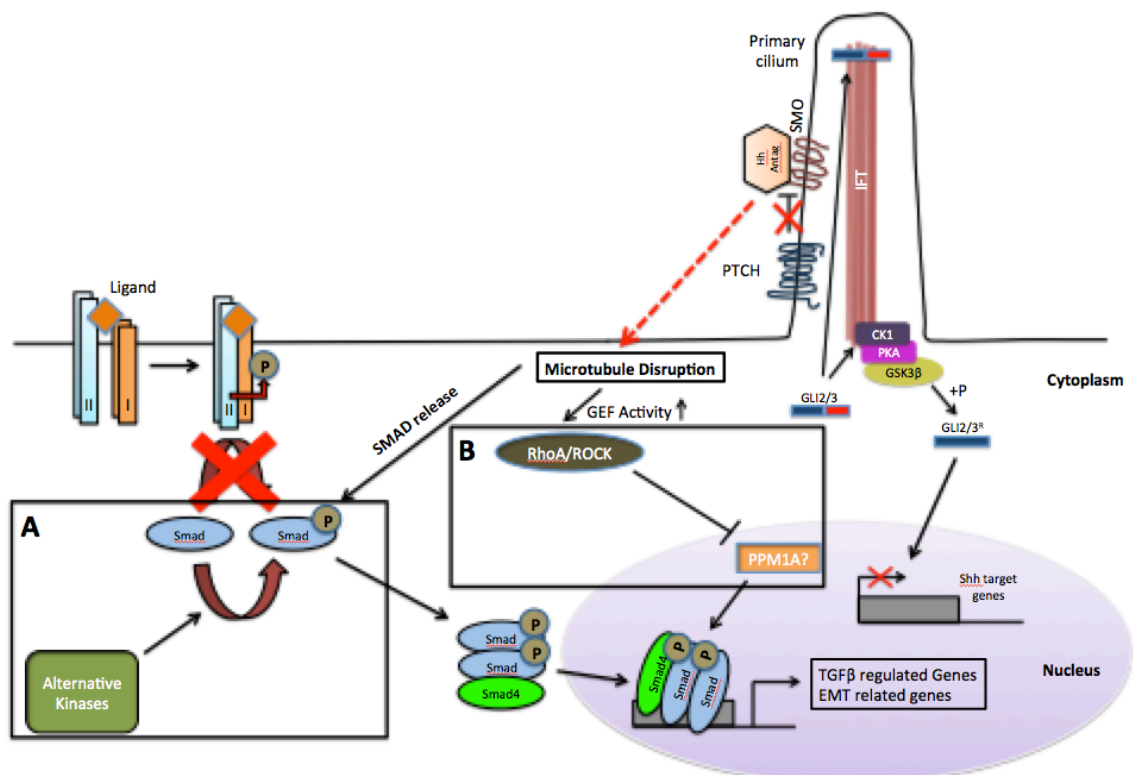


Figure 7.1: Microtubule destabilization can induce SMAD signalling through two potential mechanisms.

Drug-initiated microtubule disassembly mobilizes several signalling pathways that impact on SMAD signalling in two potential ways. (A) Ability of alternative kinases to phosphorylate and activate SMADs independent of TGFBR1 or (B) the induction of alternative pathways that negatively regulate phosphatases that are responsible for shuttling deactivating nuclear SMAD complexes.

Appendices

Appendix One: Driver genes affected by subtle mutations

Oncogenes	Core Pathway	Process	Tumour Suppressor Genes	Core Pathway	Process
CTNNB1	APC	Cell Fate	APC	APC	Cell Fate
GNAS	APC; PI3K; TGF- β , RAS	Cell Survival/Cell Fate	AXIN1	APC	Cell Fate
ABL1	Cell Cycle/Apoptosis	Cell Survival	CDH1	APC	Cell Fate
BCL2	Cell Cycle/Apoptosis	Cell Survival	FAM123B	APC	Cell Fate
CARD11	Cell Cycle/Apoptosis	Cell Survival	HNF1A	APC	Cell Fate
MYD88	Cell Cycle/Apoptosis	Cell Survival	NF2	APC	Cell Fate
NFE2L2	Cell Cycle/Apoptosis	Cell Survival	RNF43	APC	Cell Fate
PPP2R1A	Cell Cycle/Apoptosis	Cell Survival	SOX9	APC	Cell Survival
MED12	Cell Cycle/Apoptosis; TGF- β	Cell Survival	TRAF7	Apoptosis	Cell Survival
DNMT1	Chromatin Modification	Cell Fate	CASP8	Cell Cycle/Apoptosis	Cell Survival
DNMT3A	Chromatin Modification	Cell Fate	CDC73	Cell Cycle/Apoptosis	Cell Survival
EZH2	Chromatin Modification	Cell Fate	CDKN2A	Cell Cycle/Apoptosis	Cell Survival
H3F3A	Chromatin Modification	Cell Fate	CYLD	Cell Cycle/Apoptosis	Cell Survival
HIST1H3B	Chromatin Modification	Cell Fate	FUBP1	Cell Cycle/Apoptosis	Cell Survival
IDH1	Chromatin Modification	Cell Fate	NPM1	Cell Cycle/Apoptosis	Cell Survival
IDH2	Chromatin Modification	Cell Fate	RB1	Cell Cycle/Apoptosis	Cell Survival
SPOP	Chromatin Modification; HH	Cell Fate	TP53	Cell Cycle/Apoptosis; DNA Damage Control	Cell Survival
SETBP1	Chromatin Modification; Replication	Cell Fate	TNFAIP3	Cell Cycle/Apoptosis; MAPK	Cell Survival
SMO	HH	Cell Fate	ARID1A	Chromatin Modification	Cell Fate
GATA2	NOTCH, TGF- β	Cell Fate	ARID1B	Chromatin Modification	Cell Fate
AKT1	PI3K	Cell Survival	ARID2	Chromatin Modification	Cell Fate
PIK3CA	PI3K	Cell Survival	ASXL1	Chromatin Modification	Cell Fate
TSHR	PI3K; MAPK	Cell Survival	ATRX	Chromatin Modification	Cell Fate
ALK	PI3K; RAS	Cell Survival	KDM5C	Chromatin Modification	Cell Fate
CBL	PI3K; RAS	Cell Survival	KDM6A	Chromatin Modification	Cell Fate
CSF1R	PI3K; RAS	Cell Survival	MEN1	Chromatin Modification	Cell Fate
EGFR	PI3K; RAS	Cell Survival	MLL2	Chromatin Modification	Cell Fate
ERBB2	PI3K; RAS	Cell Survival	MLL3	Chromatin Modification	Cell Fate
MET	PI3K; RAS	Cell Survival	NCOR1	Chromatin Modification	Cell Fate
PDGFRA	PI3K; RAS	Cell Survival	PAX5	Chromatin Modification	Cell Fate
FGFR2	PI3K; RAS ; STAT	Cell Survival	PBRM1	Chromatin Modification	Cell Fate
FGFR3	PI3K; RAS ; STAT	Cell Survival	PRDM1	Chromatin Modification	Cell Fate
GNA11	PI3K; RAS; MAPK	Cell Survival	SETD2	Chromatin Modification	Cell Fate
KIT	PI3K; RAS; STAT	Cell Survival	SMARCA4	Chromatin Modification	Cell Fate
GNAQ	PI3K;RAS; MAPK	Cell Survival	SMARCB1	Chromatin Modification	Cell Fate
BRAF	RAS	Cell Survival	TET2	Chromatin Modification	Cell Fate
HRAS	RAS	Cell Survival	WT1	Chromatin Modification	Cell Fate
KRAS	RAS	Cell Survival	EP300	Chromatin Modification; APC; TGF- β ; NOTCH	Cell Survival/Fa

MAP2K1	RAS	Cell Survival	DAXX	Chromatin Modification; Cell Cycle/Apoptosis	Cell Fate
NRAS	RAS	Cell Survival	CREBBP	Chromatin Modification; Transcriptional Regulation	Cell Fate
PTPN11	RAS	Cell Survival	ATM	DNA Damage Control	Genome Maintenance
RET	RAS; PI3K	Cell Survival	BAP1	DNA Damage Control	Genome Maintenance
FLT3	RAS; PI3K; STAT	Cell Survival	BRCA1	DNA Damage Control	Genome Maintenance
CRLF2	STAT	Cell Survival	BRCA2	DNA Damage Control	Genome Maintenance
JAK1	STAT	Cell Survival	MLH1	DNA Damage Control	Genome Maintenance
JAK2	STAT	Cell Survival	MSH2	DNA Damage Control	Genome Maintenance
JAK3	STAT	Cell Survival	MSH6	DNA Damage Control	Genome Maintenance
MPL	STAT	Cell Survival	STAG2	DNA Damage Control	Genome Maintenance
FOXL2	TGF- β	Cell Fate	PTCH1	HH	Cell Fate
AR	Transcriptional Regulation	Cell Fate	STK11	mTOR	Cell Survival
SF3B1	Transcriptional Regulation	Cell Fate	FBXW7	NOTCH	Cell Fate
SRSF2	Transcriptional Regulation	Cell Fate	NOTCH1	NOTCH	Cell Fate
U2AF1	Transcriptional Regulation	Cell Fate	NOTCH2	NOTCH	Cell Fate
KLF4	Transcriptional Regulation; WNT	Cell Fate	GATA1	NOTCH, TGF- β	Cell Fate
			PIK3R1	PI3K	Cell Survival
			PTEN	PI3K	Cell Survival
			TSC1	PI3K	Cell Survival
			B2M	PI3K; RAS; MAPK	Cell Survival
			CEBPA	PI3K; RAS; MAPK	Cell Survival
			VHL	PI3K; RAS; STAT	Cell Survival
			CIC	RAS	Cell Survival
			NF1	RAS	Cell Survival
			MAP3K1	RAS; MAPK	Cell

			Survival
	SOCS1	STAT	Cell Survival
	ACVR1B	TGF-b	Cell Survival
	SMAD2	TGF-b	Cell Survival
	SMAD4	TGF-b	Cell Survival
	BCOR	Transcriptional Regulation	Cell Fate
	GATA3	Transcriptional Regulation	Cell Fate
	PHF6	Transcriptional Regulation	Cell Fate
	RUNX1	Transcriptional Regulation	Cell Fate

Bibliography

Bibliography

<http://www.cancerresearchuk.org/cancer-info/cancerstats/mortality/all-cancers-combined/newpagetemp>

Aasi, S., Silkiss, R., Tang, J.Y., Wysong, A., Liu, A. *et al.* (2013) New Onset of Keratoacanthomas After Vismodegib Treatment for Locally Advanced Basal Cell Carcinomas: A Report of 2 Cases. *JAMA Dermatol*, **149**(2):242-3

Abecassis, L., Rogier, E., Vazquez, A., Atfi, A. and Bourgeade, M. F. (2004) Evidence for a role of MSK1 in transforming growth factor- β -mediated responses through p38 α and SMAD signalling pathways. *J. Biol. Chem.*, **279**:30474-30479

Adams, J. (2002) Proteasome inhibition: a novel approach to cancer therapy. *Trends Mol Med.*, **8**(4 Suppl):S49-54.

Adams, J. (2004) The development of proteasome inhibitors as anticancer drugs. *Cancer Cell.*, **5**(5):417-21

Adams, J.M., and Cory, S. (2007). The Bcl-2 apoptotic switch in cancer development and therapy. *Oncogene*, **26**:1324–1337.

Al-Hajj, M., Wicha, M.S., Benito-Hernandez, A., Morrison, S.J. and Clarke, M.F. (2003) Prospective identification of tumorigenic breast cancer cell. *Proc Natl Acad Sci U S A*, **100**(7):3983–3988

Al-Othman, M.O., Mendenhall, W.M. and Amdur, R.J. (2001) Radiotherapy alone for clinical T4 skin carcinoma of the head and neck with surgery reserved for salvage. *Am J Otolaryngol*, **22**:387-90

Alarcón, C., Zaromytidou, A.-I., Xi, Q., Gao, S., Yu, J. *et al.* (2009) CDK8/9 drive SMAD transcriptional action, turnover and YAP interactions in BMP and TGF β pathways. *Cell*, **139**:757-769

Alcedo, J., Ayzenzon, M., Von Ohlen, T., Noll, M. and Hooper, J.E. (1996) The *Drosophila*

smoothened gene encodes a seven-pass membrane protein, a putative receptor for the Hedgehog signal. *Cell*, **86**:221–232

Allen, T.D. and Potten, C.S. (1974) Fine-structural identification and organization of the epidermal proliferative unit. *J Cell Sci.*, **15**:291–319

Allinen, M., Beroukhi, R., Cai, L., Brennan, C., Lahti-Domenici, J. *et al.* (2004) Molecular characterization of the tumor microenvironment in breast cancer. *Cancer Cell*, **6**:17-32

Alonso, L. and Fuchs, E. (2006) The hair cycle. *J Cell Sci*, **119**(3):391-3

Alsina, M., Trudel, S., Furman, R.R., Rosen, P.J., O'Connor, O.A. *et al.* (2012) A Phase I Single-Agent Study of Twice-Weekly Consecutive-Day Dosing of the Proteasome Inhibitor Carfilzomib in Patients with Relapsed or Refractory Multiple Myeloma or Lymphoma. *Clin. Cancer Res.* **18**:4830-4840.

An, H.X., Beckmann, M.W., Reifenberger, G., Bender, H.G. and Niederacher, D. (1999) Gene amplification and overexpression of CDK4 in sporadic breast carcinomas is associated with high tumor cell proliferation. *Am J Pathol.*, **154**(1):113-8

Andl, T., Ahn, K., Kairo, A. *et al.* (2004) Epithelial Bmpr1a regulates differentiation and proliferation in postnatal hair follicles and is essential for tooth development. *Development*, **131**:2257-68

Anido, J., Saez-Borderias, A., Gonzalez-Junca, A., Rodon, L., Folch, G. *et al.* (2010) TGF- β Receptor Inhibitors Target the CD44^{high}/Id1^{high} Glioma-Initiating Cell Population in Human Glioblastoma. *Cancer Cell*, **18**:655-668

Antonarakis, E.S., Chen, Y., Elsamanoudi, S.I., Brassell, S.A. *et al.* (2011) Long-term overall survival and metastasis-free survival for men with prostate-specific antigen-recurrent prostate cancer after prostatectomy: analysis of the Center for Prostate Disease Research National Database. *BJU Int.*, **108**(3):378-85.

Aparicio, L.A., Castosa, R., Haz-Conde, M., Rodriguez, M., Blanco, M. *et al.* (2014) Role of the microtubule-targeting drug vinflunine on cell-cell adhesions in bladder epithelial tumour cells. *BMC Cancer*; **14**:507

Aragon, E., Goerner, N., Zaromytidou, A.I., Xi, Q., Escobedo, A. *et al.* (2011) A Smad action turnover switch operated by WW domain readers of a phosphoserine code. **25**:1275-1288

Arendsdorf, A.M., Marada, S. and Ogden, S.K. (2016) Smoothened Regulation: A Tale of Two Signals. *Trends in Pharmacological Sciences*, **37**(1):62–72.

Armitage, P., Doll, R. (2004) The age distribution of cancer and a multi-stage theory of carcinogenesis. *Br J Cancer* **91**:1983-9

Arnhold, V., Boos, J. and Lanvers-Kaminsky, C. (2003) Targeting hedgehog signalling pathway in pediatric tumors: in vitro evaluation of SMO and GLI inhibitors. *Cancer Chemother Pharmacol.*, **77**(3):495-505

Artandi, S.E., and DePinho, R.A. (2010). Telomeres and telomerase in cancer. *Carcinogenesis*, **31**:9–18

Aszterbaum, M., Beech, J. and Epstein, E.H. Jr (1999) Ultraviolet radiation mutagenesis of hedgehog pathway genes in basal cell carcinomas. *J Investig Dermatol Symp Proc.*, **4**(1):41-5

Aszterbaum, M., Rothman, A., Johnson, R.L., Fisher, M., Xie, J. *et al.* (1998) Identification of mutations in the human PATCHED gene in sporadic basal cell carcinomas and in patients with the basal cell nevus syndrome. *Jr J Invest Dermatol.*, **110**(6):885-8

Athar, M., Li, C., Tang, X., Chi, S., Zhang, X. *et al.* (2004) Inhibition of smoothened signalling prevents ultraviolet B-induced basal cell carcinomas through regulation of Fas expression and apoptosis. *J Cancer Res.*, **64**(20):7545-52

Attisano, L., and Wrana, J.L. (2002). Signal transduction by the TGF-beta superfamily. *Science*, **296**:1646-1647.

- Atwood, S.X., Sarin, K.Y., Whitson, R.J., Li, J.R., Kim, G. *et al.* (2015) Smoothened variants explain the majority of drug resistance in basal cell carcinoma. *Cancer Cell*, **27**(3):342–353.
- BabuRajendran, N., Palasingam, P., Narasimhan, K., Sun, W., Prabhakar, S. *et al.* (2010) Structure of Smad1 MH1/DNA complex reveals distinctive rearrangements of BMP and TGF- β effectors. *Nucleic Acid Res.* **38**:3477-3488
- Baeriswyl, V., and Christofori, G. (2009). The angiogenic switch in carcinogenesis. *Semin. Cancer Biol.*, **19**:329–337
- Baish, J.W., Stylianopoulos, T., Lanning, R.M., Kamoun, W.S., Fukumura, D. *et al.* (2011) Scaling rules for diffusive drug delivery in tumor and normal tissues. *Proc Natl Acad Sci USA*, **108**(5):1799-1803
- Bakin, A.V., Tomlinson, A.K., Bhowmick, N.A., Moses, H.L. and Arteaga, C.L. (2000) Phosphatidylinositol 3-kinase function is required for transforming growth factor beta-mediated epithelial to mesenchymal transition and cell migration. *J Biol Chem*, **275**:36803–36810
- Bao, S., Wu, Q., McLendon, R.E., Hao, Y., Shi, Q. *et al.* (2006) Glioma SCs promote radioresistance by preferential activation of the DNA damage response. *Nature* **444**:756–60
- Bar, E.E. *et al.* (2007) Hedgehog signalling promotes medulloblastoma survival via Bc/II. *Am J Pathol.*; **170**(1):347-55.
- Barker, N., van Es, J.H., Kuipers, J. *et al.* (2007) Identification of SCs in small intestine and colon by marker gene Lgr5. *Nature*; **449**: 1003–1007. 104
- Barnfield, P.C., Zhang, X., Thanabalasingham, V., Yoshida, M. and Hui, C.C. (2005) Negative regulation of GLI1 and GLI2 activator function by Suppressor of Fused through multiple mechanisms. *Differentiation*, **73**:397–405

- Barranco, S.C., Ho, D.H., Drewinko, B., Romsdahl, M.M., and Humphrey, R.M. (1972) Differential sensitivities of human melanoma cells grown in vitro to ara- binosylcytosine. *Cancer Res.*, **32**:2733–2736
- Barrios-Rodiles, M., Brown, K.R., Ozdamar, B. *et al.* (2005) High-throughput mapping of a dynamic signalling network in mam-malian cells. *Science*, **307**:1621–1625
- Bates, S. and Peters, G. (1995) Cyclin D1 as a cellular proto-oncogene. *Semin Cancer Biol.*, **6**(2):73-82
- Batut, J., Howell, M. and Hill, C.S. (2007) Kinesin-mediated transport of SMAD2 is required for signalling in response to TGF-beta ligands. *Dev Cell*, **12**(2):261–274
- Beachy, P.A., Karhadkar, S.S. and Berman, D.M. (2004) Tissue repair and SC renewal in carcinogenesis. *Nature*, **432**:324-331
- Bean, J., Brennan, C., Shih, J.Y., Riely, G., Viale, A. *et al.* (2007) *MET* amplification occurs with or without *T790M* mutations in *EGFR* mutant lung tumors with acquired resistance to gefitinib or erlotinib. *PNAS December*, **104**(52):20932-20937
- Beck, B., Driessens, G., Goossens, S., Youssef, K.K., Kuchnio, A. *et al.* (2011) A vascular niche and a VEGF-Nrp1 loop regulate the initiation and stemness of skin tumours. *Nature*, **478**:399–403
- Becker, A. J., McCulloch, E. A., Till, J. E. (1963). "Cytological Demonstration of the Clonal Nature of Spleen Colonies Derived from Transplanted Mouse Marrow Cells". *Nature*. **197**(4866): 452–454.
- Bellomo, C., Caja, L. and Moustakas, A. (2016) Transforming growth factor β as a regulator of cancer stemness and metastasis. *Brit J Cancer*, **115**:761-769
- Bergers, G., and Benjamin, L.E. (2003). Tumorigenesis and the angiogenic switch. *Nat. Rev. Cancer*, **3**:401–410

- Berman, D.M., Karhadkar, S.S., Maitra, A., Montes De Oca, R., Gerstenblith, M.R. *et al.* (2003) Widespread requirement for Hedgehog ligand stimulation in growth of digestive tract tumours. *Nature*, **425**(6960):846-51
- Berns, K. *et al.* (2007) A functional genetic approach identifies the PI3K pathway as a major determinant of trastuzumab resistance in breast cancer. *Cancer Cell*; **12**: 395–402.
- Berx, G., and van Roy, F. (2009). Involvement of members of the cadherin superfamily in cancer. *Cold Spring Harb. Perspect. Biol.*, **1**(6):a003129
- Betschinger, J. and Knoblich, J.A. (2004) Dare to be different: asymmetric cell division in *Drosophila*, *C. elegans* and vertebrates. *Curr. Biol.*, **14**:674–685
- Bhaskar, P.T. and Hay, N. (2007) The two TORCs and Akt. *Dev Cell.*, **12**(4):487-502
- Bhatia, R., Holtz, M., Niu, N., Gray, R., Snyder, D.S. *et al.* (2003) Persistence of malignant hematopoietic progenitors in chronic myelogenous leukemia patients in complete cytogenetic remission following imatinib mesylate treatment. *Blood*, **101**(12):4701-7
- Bhatavdekar, J.M. *et al.* (1998) Overexpression of CD44: a useful independent predictor of prognosis in patients with colorectal carcinomas. *Ann. Surg. Oncol*; **5**: 495–501.
- Bhatia, N., Thiyagarajan, S., Elcheva, I., Saleem, M., Dlugosz, A. *et al.* (2006) Gli2 Is Targeted for Ubiquitination and Degradation by β -TrCP Ubiquitin Ligase. *Journal of Biological Chemistry*. **281**: 19320-19326.
- Bhola, N.E., Balko, J.M., Dugger, T.C., Kuba, M.G., Sanchez, V. *et al.* (2013) TGF- β inhibition enhances chemotherapy action against triple-negative breast cancer. *J Clin Invest*, **123**:1348–1358
- Bhowmick, N. A., Ghiassi, M., Aakre, M., Brown, K., Singh, V., and Moses, H. L. (2003) TGF β -induced RhoA and p160ROCK activation is involved in the inhibition of Cdc25A with resultant cell-cycle arrest. *Proc. Natl. Acad. Sci. U. S. A.*, **100**:15548-15553

- Bhowmick, N.A., Neilson, E.G., and Moses, H.L., (2004) Stromal fibroblasts in cancer initiation and progression. *Nature*, **432**(7015):332–337
- Bhowmick, N.A., Zent, R., Ghiassi, M., McDonnell, M. and Moses, H.L. (2001) Integrin beta 1 signalling is necessary for transforming growth factor-beta activation of p38MAPK and epithelial plasticity. *J Biol Chem*, **276**:46707–46713
- Bickenbach, J.R. (1981) Identification and behavior of label-retaining cells in oral mucosa and skin. *J Dent Res.*, **60**(Spec No C):1611–20
- Bickenbach, J.R. and Chism, E. (1998) Selection and Extended Growth of Murine Epidermal SCs in Culture. *Experimental Cell Research*, **244**:184–195
- Bird, A. (2002) DNA methylation patterns and epigenetic memory. *Genes Dev.*, **16**(1):6-21.
- Bitgood, M.J., Shen, L., and McMahon, A.P. (1996) Sertoli cell signalling by Desert hedgehog regulates the male germline. *Curr. Biol.*, **6**:298–304
- Blanpain, C., Lowry, W.E., Geoghegan, A., Polak, L. and Fuchs, E. (2004) Self-renewal, multipotency, and the existence of two cell populations within an epithelial SC niche. *Cell*, **118**:635–48
- Blanpain, C. (2013) Tracing the cellular origin of cancer. *Nat. Cell Biol.* **15**:126-134
- Blasco, M.A. (2005). Telomeres and human disease: ageing, cancer and beyond. *Nat. Rev. Genet.*, **6**:611–622
- Bleau, A.M., Hambardzumyan, D., Ozawa, T., Fomchenko, E.I., Huse, J.T. *et al.* (2009) PTEN/PI3K/Akt pathway regulates the side population phenotype and ABCG2 activity in glioma tumor stem-like cells. *Cell SC* **4**:226–35
- Boiko, A.D., Razorenova, O.V., van de Rijn, M. *et al.* (2010) Human melanoma initiating cells express neural crest nerve growth factor receptor CD271. *Nature*; **466**: 133-137
- Bollag, G., Tsai, J., Zhang, J., Zhang, C., Ibrahim, P. *et al.* (2012) Vemurafenib: the first

drug approved for BRAF-mutant cancer. *Nat Rev Drug Discov*, **11**(11): 873–886

Bonilla, X., Parmentier, L., King, B., Bezrukov, F., Kaya, G. (2016) Genomic analysis identifies new drivers and progression pathways in skin basal cell carcinoma. *Nature Genetics*, **48**:398-406

Bonnet, D. & Dick, J.E. (1997) Human acute myeloid leukemia is organized as a hierarchy that originates from a primitive hematopoietic cell. *Nat. Med.* **3**, 730–737

Boonyaratanakornkit, J.B., Yue, L., Strachan, L.R. *et al.* (2010) Selection of Tumorigenic Melanoma Cells Using ALDH. *J Invest Dermatol*; **130**: 2799–2808.

Borst, P. and Elferink, R.O. (2002) Mammalian ABC transporters in health and disease. *Annu. Rev. Biochem.*, **71**:537–592

Bossen, C., Ingold, K., Tardivel, A., Bodmer, J.L., Gaide, O., Hertig, S., Ambrose, C., Tschopp, J., and Schneider, P. (2006) Interactions of tumor necrosis factor (TNF) and TNF receptor family members in the mouse and human. *J. Biol. Chem.* **281**, 13964–13971

Bouchard, C., Thieke, K., Maier, A., Saffrich, R., Hanley-Hyde, J. *et al.* (1999) Direct induction of cyclin D2 by Myc contributes to cell cycle progression and sequestration of p27. *EMBO J.*, **18**(19):5321-33

Boyd, A.S., Shyr, Y. and King, L.E. (2002) Basal cell carcinoma in young women: an evaluation of the association of tanning bed use and smoking. *J Am Acad Dermatol*, **46**:706-9

Bozic, I., Antal, T., Ohtsuki, H., Carter, H., Kim, D. *et al.* (2010) Accumulation of driver and passenger mutations during tumor progression. *Proc Natl Acad Sci USA*, **107**(43):18545-50

Brand, F.X., Ravel, N., Gauchez, A.S. *et al.* (2006) Prospect for anti-her2 receptor therapy in breast cancer. *Anticancer Res*, **26**(1B):715-22

Brantsch, K.D., Meisner, C., Schönfisch, B. *et al.* (2008) Analysis of risk factors determining prognosis of cutaneous squamous-cell carcinoma: a prospective study. *Lancet Oncol*; **9**: 713-720.

Breier, G., (2000) Angiogenesis in embryonic development--a review. *Placenta*, **21**:Suppl A:S11-5.

Broadus, J. and Doe, C.Q. (1997) Extrinsic cues, intrinsic cues and microfilaments regulate asymmetric protein localization in *Drosophila* neuroblasts. *Curr. Biol.*, **7**:827–835

Brown, K.A., Pietenpol, J.A. and Moses, H.L. (2007) A tale of two proteins: Differential roles and regulation of Smad2 and Smad3 in TGF- β signaling. *Journal of Cellular Biochemistry*, **101**:

Brown, J.A., Yonekubo, Y., Hanson, N., Sastre-Perona, A., Basin, A. *et al.* (2017) TGF- β -Induced Quiescence Mediates Chemoresistance of Tumor-Propagating Cells in Squamous Cell Carcinoma. *Cell Stem Cell*. **21**:650-664

Brownell I., Guevara E., Bai C. B., Loomis C. A. and Joyner A. L. (2011). Nerve-derived sonic hedgehog defines a niche for hair follicle SCs capable of becoming epidermal SCs. *Cell SC*, **8**:552-565

Bruna, A., Greenwood, W., Le Quesne, J., Teschendorff, A., Miranda-Saavedra, D., Rueda, O.M. *et al.* (2012) TGF β induces the formation of tumour-initiating cells in claudin low breast cancer. *Nat Commun*, **3**:1055

Buchbinder, E.I. and Desai, A. (2016) CTLA-4 and PD-1 Pathways: Similarities, Differences, and Implications of Their Inhibition. *Am. J. Clin. Oncol.* **39**:98-106

Buckley, M.F., Sweeney, K.J., Hamilton, J.A., Sini, R.L., Manning, D.L. *et al.* (1993) Expression and amplification of cyclin genes in human breast cancer. *Oncogene*, **8**(8):2127-3.

- Buczacki, S.J. *et al.* (2013) Intestinal label-retaining cells are secretory precursors expressing Lgr5. *Nature*; **495**: 65–69.
- Buonamici, S., Williams, J., Morrissey, M., Wang, A., Guo, R. *et al.* (2010) Interfering with resistance to smoothed antagonists by inhibition of the PI3K pathway in medulloblastoma. *Sci Transl Med*, **2**:51ra70
- Burch, M. L., Yang, S. N., Ballinger, M. L., Getachew, R., Osman, N., and Little, P. J. (2010) TGF-beta stimulates biglycan synthesis via p38 and ERK phosphorylation of the linker region of SMAD2. *Cell. Mol. Life Sci.*, **67**:2077- 2090
- Burch, M., Zheng, W., and Little, P. (2011) SMAD linker region phosphorylation in the regulation of extracellular matrix synthesis. *Cell. Mol. Life Sci.* **68**:97-107
- Burger, H., van Tol, H., Boersma, A.W., Brok, M., Wiemer, E.A. *et al.* (2004) Imatinib mesylate (STI571) is a substrate for the breast cancer resistance protein (BCRP)/ABCG2 drug pump. *Blood*, **104**:2940–2942
- Burk, U., Schubert, J., Wellner, U., Schmalhofer, O., Vincan, E. *et al.* (2008) A reciprocal repression between ZEB1 and members of the miR-200 family promotes EMT and invasion in cancer cells. *EMBO Rep.*, **9**:582–9
- Burstein, H.J. (2005) The distinctive nature of HER2-positive breast cancers. *New Eng J Med*, **353**(16):1652–4
- Caccialanza, M., Percivalle, S. and Piccinno, R. (2004) Possibility of treating basal cell carcinomas of nevoid basal cell carcinoma syndrome with superficial x-ray therapy. *Dermatology*, **208**:60-3
- Caccialanza, M., Piccinno, R. and Grammatica, A. (2001) Radiotherapy of recurrent basal and squamous cell skin carcinomas: a study of 249 re-treated carcinomas in 229 patients. *Eur J Dermatol*, **11**:25-8
- Calon, A., Espinet, E., Palomo-Ponse, S., Tauriello, D.V., Iglesias, M. *et al.* (2012) Dependency of colorectal cancer on a TGF- β -driven program in stromal cells for

metastasis initiation. *Cancer Cell*, **22**:571-584

Calon, A., Lonardo, E., Berenguer-Llargo, A., Espinet, E., Hernando-Momblona, X. *et al.* (2015) Stromal gene expression defines poor-prognosis subtypes in colorectal cancer. *Nat. Genet.* **47**:320-329

Cao, Y., Liu, X., Zhang, W., Deng, X., Zhang, H. *et al.* (2009) TGF-beta repression of Id2 induces apoptosis in gut epithelial cells. *Oncogene*, **28**:1089-1098.

Cammareri, P., Rose, A., Vincent, D.F., Wang, J. *et al.* (2017) Inactivation of TGFβ receptors in stem cells drives cutaneous squamous cell carcinoma. *Nature Communications*, **7**: 12493.

Cavallaro, U., and Christofori, G. (2004). Cell adhesion and signalling by cad-herins and Ig-CAMs in cancer. *Nat. Rev. Cancer*, **4**:118–132.

Ceilley, R.I. and Del Rosso, J.Q. (2006) Current modalities and new advances in the treatment of basal cell carcinoma. *Int J Dermatol*, **45**:489-98

Cerutti, J.M., Ebina, K.N., Matsuo, S.E., Martins, L. Maciel, R.M. and Kimura E.T. (2003) Expression of SMAD4 and SMAD7 in human thyroid follicular carcinoma cell lines. *J. Endocrinol. Invest.*, **26**:516-521

Chan, L.H., Wang, W., Yeung, W., Deng, Y., Yuan, P. and Mak, K.K. (2014) Hedgehog signalling induces osteosarcoma development through Yap1 and H19 overexpression. *Oncogene*, **33**(40):4857-66

Chang, A.L. and Oro, A.E. (2012) Initial assessment of tumor regrowth after vismodegib in advanced basal cell carcinoma. *Arch Dermatol*, **148**:1324-1325

Chang, D.T., Lopez, A., von Kessler, D.P., Chiang, C., Simandl, B.K. *et al.* (1994) Products, genetic linkage and limb patterning activity of a murine hedgehog gene. *Development*, **120**: 3339–3353

Chapman, P.B., Hauschild, A., Robert, C. *et al.* (2011) BRIM-3 Study Group. Improved

survival with vemurafenib in melanoma with BRAF V600E mutation. *N Engl J Med*, **364**(26):2507–16

Chaqour, B., Yang, R., Sha, Q. (2006) Mechanical stretch modulates the promoter activity of the profibrotic factor CCN2 through increased actin polymerization and NF-kappaB activation. *J Biol Chem.*; **281**:20608–20622.

Chen, X., Weisberg, E., Fridmacher, V., Watanabe, M., Naco, G., Whitman, M. (1997) Smad4 and FAST-1 in the assembly of activin-responsive factor. *Nature*, **389**:85-89

Chen, C. R., Kang, Y., Siegel, P. M., and Massague, J. (2002). E2F4/5 and p107 as SMAD cofactors linking the TGFbeta receptor to c-myc repression. *Cell*, **110**:19-32.

Chen, J.K., Taipale, J., Cooper, M.K. and Beachy, P.A. (2002) Inhibition of Hedgehog signalling by direct binding of cyclopamine to Smoothed. *Genes Dev*, **16**:2743–8

Chen, W., Jin, W., Hardegen, N., Lei, K.J., Li, L. *et al.* (2003) Conversion of peripheral CD4+CD25- naive T cells to CD4+CD25+ regulatory T cells by TGF-beta induction of transcription factor Foxp3. *J. Exp. Med.*, **198**:1875-1886

Chen, M.L., Pittet, M.J., Gorelik, L., Flavell, R.A., Weissleder, R. *et al.* (2005) Regulatory T cells suppress tumor-specific CD8 T cell cytotoxicity through TGF-beta signals in vivo *Proc. Natl. Acad. Sci. USA*, **102**:419-424

Chen, J. *et al.* (2012) A restricted cell population propagates glioblastoma growth after chemotherapy. *Nature* **488**, 522–526

Chen, K., Rund, L. A., Beever, J. E., and Schook, L. B. (2006a) Isolation and molecular characterization of the porcine transforming growth factor beta type I receptor (TGFB1) gene. *Gene*, **384**:62-72 (A)

Chen, M.H., Wilson, C.W., Li, Y.J. *et al.* (2009) Cilium-independent regulation of GLI protein function by Sufu in Hedgehog signalling is evolutionarily conserved. *Genes Dev.*, **23**:1910–1928

- Chen, S., Crawford, M., Day, R. M., Briones, V. R., Leader, J. E., Jose, P. A., and Lechleider, R. J. (2006b) RhoA modulates SMAD signalling during transforming growth factor-beta-induced smooth muscle differentiation. *J. Biol. Chem.* **281**:1765-1770 (B)
- Chen, W., Ren, X.R., Nelson, C.D. *et al.* (2004) Activity-dependent internalization of Smoothed mediated by β -arrestin 2 and GRK2. *Science*, **306**:2257–2260
- Chen, Y. and Jiang, J. (2013) Decoding the phosphorylation code in Hedgehog signal transduction. *Cell Res*, **23**(2):186–200
- Chen, Y., Sasai, N., Ma, G. *et al.* (2011) Sonic Hedgehog dependent phosphorylation by CK1a and GRK2 is required for ciliary accumulation and activation of smoothed. *PLoS Biology*, **9**:e1001083
- Chen, Y., Yue, S., Xie, L., Pu, X.H., Jin, T. and Cheng, S.Y. (2011) Dual Phosphorylation of suppressor of fused (Sufu) by PKA and GSK3 β regulates its stability and localization in the primary cilium. *J Biol Chem.*, **286**:13502–13511
- Chen, Y. *et al.* (2008) Oncogenic mutations of ALK kinase in neuroblastoma. *Nature*; **455**: 971–974.
- Cheng, N., Chytil, A., Shyr, Y., Joly, A., and Moses, H.L., (2008) Transforming growth factor-beta signalling-deficient fibroblasts enhance hepatocyte growth factor signalling in mammary carcinoma cells to promote scattering and invasion. *Mol. Cancer Res.*, **6**(10)1521–1533
- Cheng, S.Y. and Bishop, J.M. (2002) Suppressor of Fused represses Gli-mediated transcription by recruiting the SAP18-mSin3 corepressor complex. *Proc Natl Acad Sci USA*, **99**:5442–5447
- Cheung, H.O., Zhang, X., Ribeiro, A. *et al.* (2009) The kinesin protein Kif7 is a critical regulator of GLI transcription factors in mammalian hedgehog signalling. *Sci Signal.*, **2**:ra29

Chiller, K., Passaro, D., McCalmont, T. *et al.* (2000) Efficacy of curettage before excision in clearing surgical margins of nonmelanoma skin cancer. *Arch Dermatol*, **136**:1327-32

Chng, Z., Teo, A., Pedersen, R.A. and Vallier, L. (2010) SIP1 Mediates Cell-Fate Decisions between Neuroectoderm and Mesendoderm in Human Pluripotent SCs. *Cell SC.*, **6**:59–70.

Chocron, S., Verhoeven, M.C., Rentzsch, F., Hammerschmidt, M. and Bakkers J. (2007) Zebrafish Bmp4 regulates left-right asymmetry at two distinct developmental time points. *Dev. Biol.*, **305**:577-588

Christenson, L.J., Borrowman, T.A., Vachon, C.M. *et al.* (2005) Incidence of basal cell and squamous cell carcinomas in a population younger than 40 years. *JAMA*, **294**:681-90

Chung, A.S. and Ferrara, N. (2011) Developmental and pathological angiogenesis. *Annu Rev Cell Dev Biol*, **27**:563-84

Ciccia, A., and Elledge, S.J. (2010). The DNA damage response: making it safe to play with knives. *Mol. Cell*, **40**:179–204.

Civenni G, Walter A, Kobert N, Mihic-Probst D, Zipser M, Belloni B, Seifert B, Moch H, Dummer R, van den Broek M, Sommer L. (2011) Human CD271-positive melanoma SCs associated with metastasis establish tumor heterogeneity and long-term growth. *Cancer Res*; **71**: 3098-3109

Civin, C.I., Almeida-Porada, G., Lee, M.J., Olweus, J., Terstappen, L.W., Zanjani, E.D. (1996) Sustained, retransplantable, multilineage engraftment of highly purified adult human bone marrow stem cells in vivo. *Blood*. **88**:4102–4109

Clarke, M.F., Dick, J.E., Dirks, P.B., Eaves, C.J., Jamieson, C.H. *et al.* (2006) Cancer stem cells--perspectives on current status and future directions: AACR Workshop on cancer stem cells. *Cancer Res*. **66**:9339–9344

Clark, A.G. and Vignjevic, D.M. (2015) Modes of cancer cell invasion and the role of the

microenvironment. *Curr. Opin. Cell Biol.* **36**: 13-22.

Claudinot, S., Nicolas, M., Oshima, H., Rochat, A., Barrandon, Y. (2005) Long-term renewal of hair follicles from clonogenic multipotent stem cells. *PNAS*, **102**:14677-14682.

Clayton, E. *et al.* (2007) A single type of progenitor cell maintains normal epidermis. *Nature*; **446**: 185–189.

Clement, V., Sanchez, P., de Tribolet, N., Radovanovic, I., Ruiz i Altaba, A. (2007) HEDGEHOG-GLI1 signalling regulates human glioma growth, CSC self-renewal, and tumorigenicity. *Curr Biol.*, **17**(2):165-72.

Clevers, H. (2005) SCs, asymmetric division and cancer. *Nature Genet.* **37**:1027–1028

Coco, S. *et al.* (2012) Identification of *ALK* germline mutation (3605delG) in pediatric anaplastic medulloblastoma. *J. Hum. Genet.*; **57**: 682–684.

Cojoc M, Mabert K, Muders MH, Dubrovskaja A. 2015. A role for CSCs in therapy resistance: cellular and molecular mechanisms. *Semin. Cancer Biol.* **31**:16–27

Collins, A.T., Berry, P.A., Hyde, C., Stower, M.J. and Maitland, N.J. (2005) Prospective identification of tumorigenic prostate cancer SCs. *Cancer Res*, **65**:10946–10951

Colmont, C.S., Benketah, A., Reed, S.H., Hawk, N.V., Telford, W.G. *et al.* (2013) CD200-expressing human basal cell carcinoma cells initiate tumor growth. *Proc Natl Acad Sci USA*, **110**(4):1434-9

Colmont, C.S. *et al.* (2014) Human basal cell carcinoma tumor-initiating cells are resistant to etoposide. *J Invest Dermatol.* **134**(3): 867-870

Colotta, F., Allavena, P., Sica, A., Garlanda, C., and Mantovani, A. (2009). Cancer-related inflammation, the seventh hallmark of cancer: links to genetic instability. *Carcinogenesis*, **30**:1073–1081.

- Comijn, J., Berx, G., Vermassen, P., Verschuere, K., van Grunsven, L. *et al.* (2001) The two-handed E box binding zinc finger protein SIP1 downregulates E-cadherin and induces invasion. *Mol Cell*, **7**:1267–78
- Corbit, K.C., Aanstad, P., Singla, V., Norman, A.R., Stainer, D.Y. and Reiter, J.F. (2005) Vertebrate Smoothed functions at the primary cilium. *Nature*, **437**:1018–1021
- Corona, R., Dogliotti, E., D'Errico, M. *et al.* (2001) Risk factors for basal cell carcinoma in a Mediterranean population: role of recreational sun exposure early in life. *Arch Dermatol*, **137**:1162-8
- Cotsarelis, G. and Millar, S.E. (2001) Towards a molecular understanding of hair loss and its treatment. *Trends Mol. Med.*, **7**:293–301
- Cotsarelis, G., Sun, T.T., and Lavker, R.M. (1990) Label-retaining cells reside in the bulge area of pilosebaceous unit: implications for follicular SCs, hair cycle, and skin carcinogenesis. *Cell*, **61**:1329–1337
- Coussens, L., Yang-Feng, T.L., Liao, Y.C., Chen, E., Gray, A. *et al.* (1985) Tyrosine kinase receptor with extensive homology to EGF receptor shares chromosomal location with neu oncogene. *Science*, **230**(4730):1132–9
- Cox, N.H., Eedy, D.J., Morton, C.A. (2006) Guidelines for management of Bowen's disease: update.
- Cozzio, A., Passegué, E., Ayton, P.M., Karsunky, H., Cleary, M.L., Weissman, I.L. (2003) Similar MLL-associated leukemias arising from self-renewing stem cells and short-lived myeloid progenitors. *Genes Dev.* **17**:3029–3035.
- Cui, W., Fowles, D. J., Bryson, S., Duffie, E., Ireland, H. *et al.* (1996) TGFbeta1 inhibits the formation of benign skin tumors, but enhances progression to invasive spindle carcinomas in transgenic mice. *Cell*, **86**:531-542.

Curley, M.D., Therrien, V.A., Cummings, C.L. *et al.* (2009) CD133 Expression Defines a Tumor Initiating Cell Population in Primary Human Ovarian Cancer SCs; **27**: 2875–2883.

Curiel, T.J. (2008) Regulatory T cells and treatment of cancer. *Curr. Opin. Immunol.* **20**:241-246

Curto, M., Cole, B.K., Lallemand, D., Liu, C.H., and McClatchey, A.I. (2007). Contact-dependent inhibition of EGFR signalling by Nf2/Merlin. *J. Cell Biol.*, **177**(5):893–903.

Dai, P., Nakagami, T., Tanaka, H., Hitomi, T. and Takamatsu, T. (2007) Cx43 Mediates TGF β Signalling through Competitive SMADs Binding to Microtubules. *Mol Biol Cell.*, **18**(6):2264–2273

Dalerba, P., Dylla, S.J., Park, I.K. *et al.* (2007) Phenotypic characterization of human colorectal cancer SCs. *Proc Natl Acad Sci U S A*; **104**: 10158–10163.

Danielson, K.G., Anderson, L.W. and Hosick, H.L. (1980) Selection and characterization in culture of mammary tumor cells with distinctive growth properties in vivo. *Cancer Res.*, **40**:1812–1819

David, D.J., Huang, Y-H., Chen, M. *et al.* (2016) TGF β Tumour Suppression through a Lethal EMT. *Cell*; **164**:1015-1030

David, D.J. and Massague, J. (2018) Contextual determinants of TGF β action in development, immunity and cancer. *Nature Reviews*, **19**:419-435

Davies, H., Bignell, G.R., Cox, C. *et al.* (2002) Mutations of the BRAF gene in human cancer. *Nature*, **417**(6892):949-54

Davies, M., Robinson, M., Smith, E., Huntley, S., Prime, S., and Paterson, I. (2005) Induction of an epithelial to mesenchymal transition in human immortal and malignant keratinocytes by TGF-beta1 involves MAPK, SMAD and AP-1 signalling pathways. *J Cell Biochem*, **95**:918-931.

Davies, M.A., and Samuels, Y., (2010) Analysis of the genome to personalize therapy for melanoma. *Oncogene*, **29**(41):5545–5555

Daya-Grosjean, L. and Couvé-Privat, S. (2005) Sonic hedgehog signalling in basal cell carcinomas. *Cancer Lett*, **225**:181-92

Davila, M.L. and Sadelain, M. (2016) Biology and clinical application of CAR-T cells for B cell malignancies. *Int J Hematol*, **104**:6-17.

de Caestecker, M.P. *et al.* (1998) SMAD2 transduces common signals from receptor serine-threonine and tyrosine kinases. *Genes Dev.*; **12**(11):1587-92.

De Smaele, E., Ferretti, E. and Gulino, A. (2010) Vismodegib, a small-molecule inhibitor of the hedgehog pathway for the treatment of advanced cancers. *Curr Opin Investig Drugs*, **11**:707–18

de Vries, E., Louwman, M., Bastiaens, M. *et al.* (2004) Rapid and continuous increases in incidence rates of basal cell carcinoma in the southeast Netherlands since 1973. *J Invest Dermatol*, **123**:634-8

De Wever, O. and Mareel, M. (2003) Role of tissue stroma in cancer cell invasion. *J. Pathol.*, **200**:429-447

Debatin, K. M. and Krammer, P.H. (2004) Death receptors in chemotherapy and cancer. *Oncogene* **23**:2950–2966

Deininger, M. (2008) Resistance and relapse with imatinib in CML: causes and consequences. *J Natl Compr Canc Netw*, **6**(Suppl 2):S11-S21.

Deininger, M., Buchdunger, E. and Druker, B.J. (2005) The development of imatinib as a therapeutic agent for chronic myeloid leukemia. *Blood*, **105**(7):2640-53

DeNardo, D.G., Andreu, P., and Coussens, L.M. (2010). Interactions between lymphocytes and myeloid cells regulate pro- versus anti-tumor immunity. *Cancer Metastasis Rev.*, **29**:309–316.

Denef, N., Neubuser, D., Perez, L. and Cohen, S.M. (2000) Hedgehog induces opposite

changes in turnover and subcellular localization of patched and smoothed. *Cell*, **102**:521–531

Deng, W., Vanderbilt, D.B., Lin, C-C., Martin, K.H., Brundage, K.M., Ruppert, M.J. (2015) SOX9 inhibits β -TrCP-mediated protein degradation to promote nuclear GLI1 expression and cancer stem cell properties. *J Cell Sci.* **128**:1123-1138

Denkler, S., André, J., Alexaki, I., Li, A., Magnaldo, T. *et al.* (2007) Induction of sonic hedgehog mediators by transforming growth factor-beta: SMAD3-dependent activation of GLI2 and GLI1 expression in vitro and in vivo. *Cancer Res.*, **67**(14):6981-6

Derheimer, F.A. and Kastan, M.B. (2010) Multiple roles of ATM in monitoring and maintaining DNA integrity. *FEBS Lett*, **584**(17):3675-81

Derynck, R., Akhurst, R. J., and Balmain, A. (2001) TGF β signalling in tumor suppression and cancer progression. *Nat. Genet.* **29**:117-129

Derynck, R., and Akhurst, R.J. (2007) Differentiation plasticity regulated by TGF-beta family proteins in development and disease. *Nat. Cell Biol.*, **9**:1000-1004

Derynck, R., and Zhang, Y. E. (2003). SMAD-dependent and SMAD-independent pathways in TGF-beta family signalling. *Nature*, **425**:577-584.

Derynck, R., Jarrett, J. A., Chen, E. Y., Eaton, D. H., Bell, J. R. *et al.* (1985). Human transforming growth factor-beta complementary DNA sequence and expression in normal and transformed cells. *Nature*, **316**:701-705.

Derynck, R., Zhang, Y., and Feng, X. H. (1998). SMADs: transcriptional activators of TGF-beta responses. *Cell*, **95**:737-740.

Deshpande, A., Sicinski, P., and Hinds, P.W. (2005). Cyclins and cdks in development and cancer: a perspective. *Oncogene*, **24**(17):2909–2915

Dexter, D.L., Fligiel, Z., Vogel, R., and Calabresi, P. (1979) Heterogeneity of Neoplastic-Cells from a Single Human-Colon Carcinoma. *Proc. Am. Assoc. Cancer Res.*, **20**:199–199

Dexter, D.L., Kowalski, H.M., Blazar, B.A., Fligel, Z., Vogel, R., and Heppner, G.H. (1978) Heterogeneity of tumor cells from a single mouse mammary tumor. *Cancer Res.*, **38**:3174–3181

Dhasarathy, A., Kajita, M., and Wade, P. A. (2007) The transcription factor snail mediates epithelial to mesenchymal transitions by repression of estrogen receptor-alpha. *Mol Endocrinol*, **21**:2907-2918.

Di Marcotullio, L., Ferretti, E., De Smaele, E., Argenti, B., Mincione, C. *et al.* (2004) REN(KCTD11) is a suppressor of hedgehog signalling and is deleted in human medulloblastoma. *Proc Natl Acad Sci USA*; **101**:10833–10838.

Diaz-Cano, S.J. (2012), Tumor Heterogeneity: Mechanisms and Bases for a Reliable Application of Molecular Marker Design. *Int J Mol Sci.*, **13**(2):1951–2011.

Dick, J.E. (2008) Stem cell concepts renew cancer research. *Blood*. **112**:4793–4807.

Diehn, M., Cho, R.W., Lobo, N.A., Kalisky, T., Dorie, M.J. *et al.* (2009). Association of reactive oxygen species levels and radioresistance in cancer SCs. *Nature* **458**:780–83

Diepenbruck, M. and Christofori, G. (2016) Epithelial-mesenchymal transition (EMT) and metastasis: yes, no, maybe? *Curr Opin Cell Biol.* **43**:7-13

Diepgen, T.L. and Mahler, V. (2002) The epidemiology of skin cancer. *Br J Dermatol*, **Suppl 61**:1-6

DiGiovanni, J. (1992) Multistage carcinogenesis in mouse skin. *Pharmacol Ther.*, **54**(1):63-128

Dijkgraaf, G.J., Alicke, B., Weinmann, L., Januario, T., West, K. *et al.* (2011) Small molecule inhibition of GDC-0449 refractory smoothed mutants and downstream mechanisms of drug resistance. *Cancer Res.*, **71**:435–44

Dikshit, R., Gupta, P.C., Ramasundarahettige, C., Gajalakshmi, V., Aleksandrowicz, L. *et al.* (2012) Cancer mortality in India: a nationally representative survey. *Lancet*, **379**(9828):1807-16

Ding, Q., Fukami, S., Meng, X. *et al.* (1999) Mouse suppressor of fused is a negative regulator of sonic hedgehog signalling and alters the subcellular distribution of GLI1. *Curr Biol.*, **9**:1119–1122

Doble, B.W. and Woodgett, J.R. (2003) GSK-3: tricks of the trade for a multi-tasking kinase. *J Cell Sci*, **116**:1175–1186

Doe, C.Q. and Bowerman, B. (2001) Asymmetric cell division: fly neuroblast meets worm zygote. *Curr. Opin. Cell Biol.*, **13**:68–75

Dong, C., Li, Z., Alvarez, R., Jr, Feng, X.H. and Goldschmidt-Clermont, P.J. (2000) Microtubule binding to SMADs may regulate TGF β activity. *Mol Cell*, **5**:27–34.

Doulatov, S., Notta, F., Laurenti, E. *et al.* (2012) Hematopoiesis: a human perspective. *Cell SC*; **10**: 120–136.

Doupé, D.P., Klein, A.M., Simons, B.D. & Jones, P.H. (2010) The ordered architecture of murine ear epidermis is maintained by progenitor cells with random fate. *Dev. Cell*; **18**: 317–323

Dowdy, S.C., Mariani, A., Reinholz, M.M., Keeney, G.L., Spelsberg, T.C., Podratz, K.C. and Janknecht R. (2005) Overexpression of the TGF-beta antagonist SMAD7 in endometrial cancer. *Gynecol. Oncol.*, **96**:368-373

Dowling, R.J., Pollak, M. and Sonenberg, N. (2009) Current status and challenges associated with targeting mTOR for cancer therapy. *BioDrugs.*, **23**(2):77-91.

Dranoff, G. (2005) The therapeutic implications of intratumoral regulatory T cells. *Clin Cancer Res*, **11**:822-8229

Driessens, G., Beck, B., Caauwe, A., Simons, B.D. & Blanpain, C. (2012) Defining the mode of tumour growth by clonal analysis. *Nature* **488**, 527–530

Drummond, C.J., Esfandiari, A., Liu, J., Lu, X., Hutton, C. *et al.* (2016) *TP53* mutant *MDM2*-amplified cell lines selected for resistance to *MDM2*-p53 binding antagonists retain sensitivity to ionizing radiation. *Oncotarget*, **7**(29): 46203–46218

Dvorak, H.F. (1986). Tumors: wounds that do not heal. Similarities between tumor stroma generation and wound healing. *N. Engl. J. Med.*, **315**:1650–1659.

Dvorak, H.F., Brown, L.F., Detmar, M. and Dvorak, A.M. (1995) Vascular permeability factor/vascular endothelial growth factor, microvascular hyperpermeability, and angiogenesis. *Am J Pathol.*, **146**(5):1029-39

Dyer, M.A., Farrington, S.M., Mohn, D., Munday, J.R., and Baron, M.H. (2001) Indian hedgehog activates hematopoiesis and vasculogenesis and can respecify prospective neurecto- dermal cell fate in the mouse embryo. *Development*, **128**:1717–1730

Eaves, C.J. (2008) Cancer SCs: Here, there, everywhere? *Nature*; **456**: 581-582.

Echelard, Y., Epstein, D.J., St-Jacques, B., Shen, L., Mohler, J. *et al.* (1993). Sonic hedgehog, a member of a family of putative signalling molecules, is implicated in the regulation of CNS polarity. *Cell*, **75**:1417–143

Edlund, S., Bu, S., Schuster, N., Aspenstrom, P., Heuchel, R. *et al.* (2003) Transforming growth factor- beta1 (TGF-beta)-induced apoptosis of prostate cancer cells involves SMAD7- dependent activation of p38 by TGF-beta-activated kinase 1 and mitogen-activated protein kinase kinase 3. *Mol Biol Cell*, **14**:529-544.

Edlund, S., Landstrom, M., Heldin, C.H. and Aspenstrom, P. (2002) Transforming growth factor-beta-induced mobilization of actin cytoskeleton requires signalling by small GTPases Cdc42 and RhoA. *Mol Biol Cell*, **13**:902–914

- Elmore, S. (2007) Apoptosis: A Review of Programmed Cell Death. *Toxicol Pathol.*, **35**(4):495–516.
- Embi, N., Rylatt, D.B. and Cohen, P. (1980) Glycogen synthase kinase-3 from rabbit skeletal muscle. Separation from cyclic-AMP-dependent protein kinase and phosphorylase kinase. *Eur J Biochem*, **107**(2):519-527.
- Endo, M., Fujii, K., Sugita, K. *et al.* (2012) Nationwide survey of nevoid basal cell carcinoma syndrome in Japan revealing the low incidence of basal cell carcinoma. *Am J Med Genet.*, **158A**:351–7
- Endoh-Yamagami, S., Evangelista, M., Wilson, D. *et al.* (2009) The mammalian Cos2 homolog Kif7 plays an essential role in modulating Hh signal transduction during development. *Curr Biol.*, **19**:1320–1326
- Engel, M.E., McDonnell, M.A., Law, B.K. and Moses, H.L. (1999) Interdependent SMAD and JNK signalling in transforming growth factor-beta-mediated transcription. *J Biol Chem*, **274**:37413–37420.
- Engelman, J.A., Zejnullahu, K., Mitsudomi, T., Song, Y., Hyland, C. *et al.* (2007) MET amplification leads to gefitinib resistance in lung cancer by activating ERBB3 signalling. *Science*, **316**(5827):1039-43
- Eppert, K., Takenaka, K., Lechman, E.R., Waldron, L., Nilsson, B. *et al.* (2011). Stem cell gene expression programs influence clinical outcome in human leukemia. *Nat. Med.* **17**:1086–93
- Epstein, E.H. (2008) Basal cell carcinomas: attack of the hedgehog. *Nat Rev Cancer*, **8**(10):743-54
- Eramo, A., Lotti, F., Sette, G. *et al.* (2008) Identification and expansion of the tumorigenic lung cancer SC population. *Cell Death Differ*; **15**: 504–514.
- Evangelista, M., Lim, T.Y., Lee, J. *et al.* (2008) Kinome siRNA screen identifies regulators

of ciliogenesis and hedgehog signal transduction. *Sci Signal.*, **1**:ra7

Evans, D.G., Ladusans, E.J., Rimmer, S. *et al.* (1993) Complications of the naevoid basal cell carcinoma syndrome: results of a population based study. *J Med Genet.*, **30**:460–4

Evans, R.A., Tian, Y.C., Steadman, R., Phillips, A.O. (2003) TGF- β 1-mediated fibroblast-myofibroblast terminal differentiation—the role of Smad proteins. *Exp Cell Res*, **282**: 90–100

Ewen, M. E., Oliver, C. J., Sluss, H. K., Miller, S. J., and Peeper, D. S. (1995). p53-dependent repression of CDK4 translation in TGF-beta-induced G1 cell-cycle arrest. *Genes Dev*, **9**:204-217.

Falk, S., Wurdak, H., Ittner, L.M. *et al.* (2008) Brain area-specific effect of TGF β signalling on Wnt-dependent neural SC expansion. *Cell SC*; **2**:472-483.

Fan, H., Oro, A.E., Scott, M.P. and Khavari P.A. (1997) Induction of basal cell carcinoma features in transgenic human skin expressing sonic hedgehog. *Nat Med*, **3**:788-792

Fan, L., Pepicelli, C.V., Dibble, C.C., Catbagan, W., Zarycki, J.L. *et al.* (2004) Hedgehog signalling promotes prostate xenograft tumor growth. *Endocrinology*, **145**(8):3961-70

Fan, Q., He, M., Sheng, T., Zhang, X., Sinha, M. *et al.* (2010) Requirement of TGFbeta signalling for SMO-mediated carcinogenesis. *J. Biol. Chem.*, **285**:36570–36576.

Fan, Q-W., Aksoy, O., Wong, R.A., Ilkhanizadeh, S., Novotny, C.J. *et al.* (2017) A Kinase Inhibitor Targeted to mTORC1 Drives Regression in Glioblastoma. *Cancer Cell*. **31**: 424-435.

Fang, D., Nguyen, T.K., Leishear, K., Finko, R., Kulp, A.N. *et al.* (2005) A tumorigenic subpopulation with SC properties in melanomas. *Cancer Res*, **65**:9328–9337

Feng, X.H. and Derynck, R. (2005) Specificity and versatility in tgf-beta signalling through SMADs. *Annu Rev Cell Dev Biol*, **21**:659-93

- Feron, O. (2009). Pyruvate into lactate and back: from the Warburg effect to symbiotic energy fuel exchange in cancer cells. *Radiother. Oncol.*, **92**:329– 333.
- Ferrara, N. (2009). Vascular endothelial growth factor. *Arterioscler. Thromb. Vasc. Biol.*, **29**:789–791
- Ferrara, N., Gerber, H.P. and LeCouter, J. (2003) The biology of VEGF and its receptors. *Nat Med.*, **9**(6):669-76
- Fidler, I.J. (2003). The pathogenesis of cancer metastasis: the 'seed and soil' hypothesis revisited. *Nat. Rev. Cancer*, **3**:453–458
- Fink, S.P., Mikkola, D., Willson, J.K., Markowitz, S. (2003) TGF-beta-induced nuclear localization of Smad2 and Smad3 in Smad4 null cancer cell lines. *Oncogene*, **22**:1317-1323
- Fletcher, D.A. and Mullins, R.D. (2010) Cell mechanics and the cytoskeleton. *Nature*, **463**(7280):485-492
- Florenes, V. A., Bhattacharya, N., Bani, M. R., Ben-David, Y., Kerbel, R. S., and Slingerland, J. M. (1996) TGF-beta mediated G1 arrest in a human melanoma cell line lacking p15INK4B: evidence for cooperation between p21Cip1/WAF1 and p27Kip1. *Oncogene*, **13**:2447-2457
- Foitzik, K., Lindner, G., Mueller-Roever, S., *et al.* (2000) Control of murine hair follicle regression (catagen) by TGF-beta1 in vivo. *FASEB J*, **14**:752-60
- Fojo, T. and Bates, S. (2003) Strategies for reversing drug resistance. *Oncogene*, **22**:7512–7523
- Fraser, H.M. and Lunn, S.F., (2000) Angiogenesis and its control in the female reproductive system. *Br Med Bull.*, **56**(3):787-97.
- Frey, R.S. and Mulder, K.M. (1997) TGFbeta regulation of mitogen-activated protein kinases in human breast cancer cells. *Cancer Lett*, **117**:41–50

Friedberg, E.C., Aguilera, A., Gellert, M., Hanawalt, P.C., Hays, J.B., Lehmann, A.R., Lindahl, T., Lowndes, N., Sarasin, A., and Wood, R.D. (2006). DNA repair: from molecular mechanism to human disease. *DNA Repair (Amst.)*, **5**:986–996.

Friedmann, D.R., Aguilar, A., Fan, J., Nachury, M.V. and Marmorstein, R. (2012) Structure of the α -tubulin acetyltransferase, α TAT1, and implications for tubulin-specific acetylation". *Proc. Natl. Acad. Sci. U.S.A.*, **109**(48):19655–19660.

Friese, M.A., Wischhusen, J., Wick, W., Weiler, M., Eisele, G., Steinle, A. and Weller M. (2004) RNA interference targeting transforming growth factor-beta enhances NKG2D-mediated antiglioma immune response, inhibits glioma cell migration and invasiveness, and abrogates tumorigenicity in vivo. *Cancer Res.*, **64**:7596-7603

Fuchs, E. (2016) Epithelial Skin Biology: Three Decades of Developmental Biology, a Hundred Questions Answered and a Thousand New Ones to Address. *Curr. Top Dev. Biol.* **116**:357-374.

Fuchs, E., and Chen, T. (2013) A matter of life and death: self-renewal in SCs *EMBO Rep*; **14**(1): 39–48.

Fuchs, E. and Nowak, J.A. (2008) Building epithelial tissues from skin SCs. *Cold Spring Harb Symp Quant Biol*, **73**:333-50

Fukunaga-Kalabis. M., Roesch, A., Herlyn, M. (2011) From cancer SCs to tumor maintenance in melanoma. *J Invest Dermatol*; **131**: 1600-4.

Fynan, T.M. and Reiss, M. (1993) Resistance to inhibition of cell growth by transforming growth factor-beta and its role in oncogenesis. *Crit Rev Oncog.*, **4**(5):493-540

Gailani, M.R., Stähle-Bäckdahl, M., Leffell, D.J., Glynn, M., Zaphiropoulos, P.G. *et al.* (1996) The role of the human homologue of *Drosophila* patched in sporadic basal cell carcinomas. *Nat Genet.*, **14**(1):78-81

- Gallagher, R.P., Bajdik, C.D., Fincham, S. *et al.* (1996) Chemical exposures, medical history, and risk of squamous and basal cell carcinoma of the skin. *Cancer Epidemiol Biomarkers Prev*, **5**:419-24
- Gallagher, R.P., Hill, G.B., Bajdik, C.D. *et al.* (1995) Sunlight exposure, pigmentary factors, and risk of nonmelanocytic skin cancer. I. Basal cell carcinoma. *Arch Dermatol*, **131**:157-63
- Gallico, G.G., O'Connor, N.E., Compton, C.C., Kehinde, O., Green, H. (1984) Permanent coverage of large burn wounds with autologous cultured human epithelium. *N Engl J Med*, **311**:448-451
- Gallagher, A.J. and Schiemann, W.P. (2007) Src phosphorylates Tyr284 in TGF-beta type II receptor and regulates TGF-beta stimulation of p38 MAPK during breast cancer cell proliferation and invasion. *Cancer Res*, **67**:3752–3758.
- Gambichler, T., Skrygan, M., Kaczmarczyk, J.M., Hyun, J., Tomi, N.S. *et al.* (2007) Increased expression of TGF-beta/SMAD proteins in basal cell carcinoma. *Eur J Med Res*, **12**(10):509-14
- Gao, S., Alarcon, C., Sapkota, G., Rahman, S., Chen, P-Y. *et al.* (2009) Ubiquitin ligase Nedd4L targets activated Smad2/3 to limit TGF β signaling. *Mol. Cell*. **36**:457-468
- Geng, Y., and Weinberg, R. A. (1993). Transforming growth factor beta effects on expression of G1 cyclins and cyclin-dependent protein kinases. *Proc Natl Acad Sci U S A*, **90**:10315-10319.
- Gerdes, M.J. and Yuspa, S.H. (2005) The contribution of epidermal stem cells to skin cancer. *Stem Cell Rev*. **1**:225–31.
- Ghazizadeh, S. and Taichman, L.B. (2001) Multiple classes of SCs in cutaneous epithelium: a lineage analysis of adult mouse skin. *EMBO J.*, **20**:1215–22
- Gilbert, C.W., Mulbal, S. and Lajtha, L.G. (1965) Rate of chromosome duplication at the end of the deoxyribonucleic acid synthetic period in human blood cells. *Nature*, **208**:159–61

Ginestier, C. *et al.* (2007) ALDH1 is a marker of normal and malignant human mammary SCs and a predictor of poor clinical outcome *Cell SC*; **1**(5): 555–567.

Glick, A., Ryscavage, A., Perez-Lorenzo, R., Hennings, H., Yuspa, S. and Darwiche, N. (2007) The high-risk benign tumor: evidence from the two-stage skin cancer model and relevance for human cancer. *Molecular Carcinogenesis*, **46**(8):605–610.

Glick, A.B. (2012) The Role of TGF β Signalling in Squamous Cell Cancer: Lessons from Mouse Models. *J Skin Cancer*, **2012**:249063

Glick, A.B., Lee, M.M., Darwiche, N., Kulkarni, A.B., Karlsson, S. and Yuspa, S.H. (1994) Targeted deletion of the TGF β 1 gene causes rapid progression to squamous cell carcinoma. *Genes and Devel.*, **8**(20):2429–2440

Go, C., He, W., Zhong, L. *et al.* (2000) Aberrant cell cycle progression contributes to the early-stage accelerated carcinogenesis in transgenic epidermis expressing the dominant negative TGFBRII. *Oncogene*, **19**(32):3623–3631.

Go, C., Li, P. and Wang, X.J. (1999) Blocking transforming growth factor β signalling in transgenic epidermis accelerates chemical carcinogenesis: a mechanism associated with increased angiogenesis. *Cancer Res*, **59**(12):2861–2868

Goetz, S.C. and Anderson, K.V. (2010) The primary cilium: a signalling centre during vertebrate development. *Nat Rev Genet.*, **11**:331–344

Gomis, R. R., Alarcon, C., He, W., Wang, Q., Seoane, J., *et al.* (2006) A FoxO-SMAD synexpression group in human keratinocytes. *Proc Natl Acad Sci USA*, **103**(34):12747-52

Goodwin, R.G., Holme, S.A. and Roberts, D.L. (2004) Variations in registration of skin cancer in the United Kingdom. *Clin Exp Dermatol*, **29**:328-30

Gorelik, L. and Flavell, R.A. (2000) Abrogation of TGF β signalling in T cells leads to spontaneous T cell differentiation and autoimmune disease. *Immunity*, **12**:171-181

Gorlin, R.J. and Goltz, R.W. (1960) Multiple nevoid basal-cell epithelioma, jaw cysts and bifid rib. A syndrome. *Engl J Med.*, **262**:908-12

Götschel, F. *et al.* (2013) Synergism between Hedgehog-GLI and EGFR Signalling in Hedgehog-Responsive Human Medulloblastoma Cells Induces Downregulation of Canonical Hedgehog-Target Genes and Stabilized Expression of GLI1. *PLoS One*. **8**(6):e65403

Gottesman, M. M., Fojo, T. and Bates, S.E. (2002) Multidrug resistance in cancer: role of ATP-dependent transporters. *Nature Rev. Cancer*, **2**:48–58

Grachtchouk, M., Mo, R., Yu, S., Zhang, X., Sasaki, H. *et al.* (2000) Basal cell carcinomas in mice overexpressing GLI2 in skin. *Nat Genet*, **24**:216-217

Grachtchouk, M., Pero, J., Yang, S.H., Ermilov, A.N., Michael, L.E. *et al.* (2011) Basal cell carcinomas in mice arise from hair follicle SCs and multiple epithelial progenitor populations. *J Clin Invest*, **121**(5):1768-1781

Graham, S.M., Jorgensen, H.G., Allan, E., Pearson, C., Alcorn, M.J. *et al.* (2002) Primitive, quiescent, Philadelphia- positive SCs from patients with chronic myeloid leukemia are insensitive to STI571 *in vitro*. *Blood*, **99**:319–325

Gray, J.M. and Pierce, G.B., Jr. (1964) Relationship between Growth Rate and Differentiation of Melanoma in Vivo. *J. Natl. Cancer Inst.*, **32**:1201–1210

Greco, V., Chen, T., Rendl, M. *et al.* (2009) A two-step mechanism for SC activation during hair regeneration. *Cell SC*, **4**:155-69

Gregory, P.A., Bert, A.G., Paterson, E.L., Barry, S.C., Tsykin, A. *et al.* (2008) The miR-200 family and miR-205 regulate epithelial to mesenchymal transition by targeting ZEB1 and SIP1. *Nat Cell Biol.*, **10**:593–601

Griffiths, R.W., Suvarna, S.K. and Stone, J. (2005) Do basal cell carcinomas recur after complete conventional surgical excision? *Br J Plast Surg*, **58**:795-805

Grothey, A. and Ellis, L.M. (2008) Targeting angiogenesis driven by vascular endothelial growth factors using antibody-based therapies. *Cancer J.*, **14**(3):170-7

Griewank, K.G., Murali, R., Schilling, B., Scholz, S., Sucker, A. (2013) *TERT* promoter mutations in ocular melanoma distinguish between conjunctival and uveal tumours. *British Journal of Cancer*, **109**:497-501

Grubisha, M.J., Cifuentes, M.E., Hammes, S.R., DeFranco, D.B. (2012) A Local Paracrine and Endocrine Network Involving TGF β , Cox-2, ROS, and Estrogen Receptor β Influences Reactive Stromal Cell Regulation of Prostate Cancer Cell Motility. *Molecular Endocrinology*, **26**:940-954

Gu, S., Liu, Y., Zhu, B., Ding, K., Yao, T.p *et al.* (2016) Loss of α -Tubulin Acetylation Is Associated with TGF- β -induced Epithelial-Mesenchymal Transition. *J Biol Chem.* **291**:5396-5405

Guasch, G., Schober, M., Pasolli, H.A., Polak, L., Conn, E.B. and Fuchs. E. (2007) Loss of TGF β signalling destabilizes homeostasis and promotes squamous cell carcinomas in stratified epithelium. *Cancer Cell.* **12**:313–327

Gulino, A., Ferretti, E. and De Smaele, E. (2009) Hedgehog signalling in colon cancer and SCs. *EMBO Mol Med.*, **1**:300–2

Guo, X. and Wang, X.F. (2009) Signalling cross-talk between TGF-beta/BMP and other pathways. *Cell Res*, **19**(1):71-88

Gupta, P.B. *et al.* (2011) Stochastic state transitions give rise to phenotypic equilibrium in populations of cancer cells. *Cell*; **146**: 633–644

Hahmann, C., and Schroeter, T. (2010) Rho-kinase inhibitors as therapeutics: from pan inhibition to isoform selectivity. *Cell. Mol. Life Sci.*, **67**:171-177

Hahn, H., Wicking, C., Zaphropoulos, P.G., Gailani, M.R., Shanley, S. *et al.* (1996) Mutations of the human homolog of *Drosophila* patched in the nevoid basal cell

carcinoma syndrome. *Cell*, **85**(6):841-5.

Halder, R.M. and Bang, K.M. (1988) Skin cancer in blacks in the United States. *Dermatol Clin*, **6**:397-405

Halilovic, E. and Solit, D.B. (2008). Therapeutic strategies for inhibiting oncogenic BRAF signalling. *Curr Opin Pharmacol*, **8**(4):419-26.

Hamerlik, P., Lathia, J.D., Rasmussen, R., Wu, Q., Bartkova, J. *et al.* (2012) Autocrine VEGF-VEGFR2- Neuropilin-1 signalling promotes glioma stem-like cell viability and tumor growth. *J. Exp. Med.* **209**:507–20

Hanafusa, H., Ninomiya-Tsuji, J., Masuyama, N. *et al.* (1999) Involvement of the p38 mitogen-activated protein kinase pathway in transforming growth factor-beta-induced gene expression. *J Biol Chem*; **274**:27161–27167.

Hanahan, D., and Folkman, J. (1996). Patterns and emerging mechanisms of the angiogenic switch during tumorigenesis. *Cell*, **86**:353–364

Haramis, A.P., Begthel, H., van den Born., M. *et al.* (2004) *De novo* crypt formation and juvenile polyposis on BMP inhibition in mouse intestine. *Science*; **303**:1684-1686.

Harper, J.W., and Elledge, S.J. (2007). The DNA damage response: Ten years after. *Mol. Cell*, **28**:739–745.

Haslehurst, A.M., Koti, M., Dharsee, M., Nuin, P., Evans, K. *et al.* (2012) EMT transcription factors snail and slug directly contribute to cisplatin resistance in ovarian cancer. *BMC Cancer*, **12**:91

Hata, A., Seoane, J., Lagna, G., Montalvo, E., Hemmati-Brivanlou, A., Massague, J. (2000) OAZ uses distinct DNA- and protein-binding zinc fingers in separate BMP-Smad and Olf signaling pathways. *Cell*, **100**:229-240

Hawinkels, L.J., Paauwe, M., Verspaget, H.W., Wiercinska, E., van der Zon, J.M. *et al.* (2014). Interaction with colon cancer cells hyperactivates TGF- β signaling in cancer-

associated fibroblasts. *Oncogene*, **33**:97-107

Haycraft, C.J., Banizs, B., Aydin-Son, Y., Zhang, Q., Michaud, E.J., Yoder, B.K. (2005) GLI2 and GLI3 localize to cilia and require the intraflagellar transport protein polaris for processing and function. *PLoS Genet.*, **1**:e53

He, X.C., Zhang, J., Tong, W.G. *et al.* (2004) BMP signalling inhibits intestinal SC self-renewal through suppression of Wnt- β -catenin signalling. *Nat Genet*; **36**:1117-1121.

Heldin, C.H. and Moustakas, A. (2012) Role of SMADs in TGFbeta signalling. *Cell Tissue Res*, **347**(1):21-36.

Hellemans, J., Coucke, P.J., Giedion, A., De Paepe, A., Kramer, P., *et al.* (2003) Homozygous mutations in IHH cause acrocapitofemoral dysplasia, an autosomal recessive disorder with cone-shaped epiphyses in hands and hips. *Am. J. Hum. Genet.*, **72**:1040–1046

Heller, E.R., Gor, A., Wang, D., Hu, Q., Lucchese, A. *et al.* (2013) Molecular signatures of basal cell carcinoma susceptibility and pathogenesis: A genomic approach. *Int J Oncol*, **42**(2):583-96

Hennings, H., Glick, A.B., Lowry, D.T., Krsmanovic, L.S., Sly, L.M. and Yuspa, S.H. (1993) FVB/N mice: an inbred strain sensitive to the chemical induction of squamous cell carcinomas in the skin. *Carcinogenesis*, **14**:2353–2358

Heppner, G.H. (1984). Tumor heterogeneity. *Cancer Res*. **44**, 2259–2265

Herrera, R. E., Makela, T. P., and Weinberg, R. A. (1996). TGF beta-induced growth inhibition in primary fibroblasts requires the retinoblastoma protein. *Mol Biol Cell*, **7**:1335-1342.

Higdon, R. *et al.* (2017) Integrated Proteomic and Transcriptomic-Based Approaches to Identifying Signature Biomarkers and Pathways for Elucidation of Daoy and UW228 Subtypes. *Proteomes*; **5**:5

Hill, C. S. (2009). Nucleocytoplasmic shuttling of SMAD proteins. *Cell Res*, **19**:36-46.

Hirano, F., Kaneko, K., Tamura, H., *et al.* (2005) Blockade of B7-H1 and PD-1 by monoclonal antibodies potentiates cancer therapeutic immunity. *Cancer Res.* **65**:1089–1096.

Hirotsu, M., Setoguchi, T., Sasaki, H., Matsunoshita, Y., Gao, H. *et al.* (2010) Smoothed as a new therapeutic target for human osteosarcoma. *Mol Cancer.*, **9**:5

Hnisz, D., Schuijers, J., Lin, C.Y., Weintraub, A.S., Abraham, B.J. *et al.* (2015) Convergence of developmental and oncogenic signaling pathways at transcriptional super-enhancers. *Mol Cell.* **58**:362-370

Hocevar, B.A., Brown, T.L. and Howe, P.H. (1999) TGF-beta induces fibronectin synthesis through a c-Jun N- terminal kinase-dependent, SMAD4-independent pathway. *EMBO J*, **18**:1345–1356

Hofmann, W-K., Komor, M., Wassmann, B., Jones, L.C., Gschaidmeier, H. *et al.* (2003) Presence of the BCR-ABL mutation Glu255Lys prior to STI571 (imatinib) treatment in patients with Ph+ acute lymphoblastic leukemia. *Blood*, **102**(2):659-61

Hogan, C.J., Shpall, E.J., Keller, G. (2002) Differential long-term and multilineage engraftment potential from subfractions of human CD34+ cord blood cells transplanted into NOD/SCID mice. *Proc Natl Acad Sci USA*, **99**:413–418.

Holmes, D.I.R. and Zachary, I. (2005) The vascular endothelial growth factor (VEGF) family: angiogenic factors in health and disease. *Genome Biol*, **6**(2):209.

Holohan, C., Van Schaeybroeck, S., Longley, D.B., Johnston, P.G. *et al.* (2013) Cancer drug resistance: an evolving paradigm *Nat Rev Cancer*; **13**(10):714-26.

Holt, P.J. (1988) Cryotherapy for skin cancer: results over a 5-year period using liquid nitrogen spray cryosurgery. *Br J Dermatol*, **119**:231-40

Holtz, M.S., Slovak, M.L., Zhang, F., Sawyers, C.L., Forman, S.J. and Bhatia, R. (2002) Imatinib mesylate (STI571) inhibits growth of primitive malignant progenitors in chronic

myelogenous leukemia through reversal of abnormally increased proliferation. *Blood*, **99**:3792–3800

Hooper, J.E. and Scott, M.P. (1989) The *Drosophila patched* gene encodes a putative membrane protein required for segmental patterning. *Cell*, **59**:751–765

Hori, S., Nomura, T. and Sakaguchi, S. (2003) Control of regulatory T cell development by the transcription factor Foxp3. *Science*, **299**:1057-1061

Horsley, V., O'Carroll, D., Tooze, R., Ohinata, Y., Saitou, M. *et al.* (2006) Blimp1 Defines a Progenitor Population that Governs Cellular Input to the Sebaceous Gland. *Cell*, **126**:597–609

Houghton, P. J., Germain, G.S., Harwood, F.C., Schuetz, J.D., Stewart, C.F. *et al.* (2004) Imatinib mesylate is a potent inhibitor of the ABCG2 (BCRP) transporter and reverses resistance to topotecan and SN-38 *in vitro*. *Cancer Res.*, **64**:2333–2337

Hosen, N., Park, C.Y., Tatsumi, N., Oji, Y., Sugiyama, H. *et al.* (2007) CD96 is a leukemic stem cell-specific marker in human acute myeloid leukemia. *Proc Natl Acad Sci USA*. **104**:11008–11013.

Hsu, P.P., and Sabatini, D.M. (2008). Cancer cell metabolism: Warburg and beyond. *Cell*, **134**:703–707.

Hsu, S.H., Zhang, X., Yu, C. *et al.* (2011) Kif7 promotes hedgehog signalling in growth plate chondrocytes by restricting the inhibitory function of Sufu. *Development*, **138**:3791–3801

Hsu, Y.-C., Li, L. and Fuchs, E. (2014) Transit-amplifying cells orchestrate SC activity and tissue regeneration. *Cell*, **157**:935-949

Hu, Y.L. *et al.* (2013) Hypoxia-induced autophagy promotes tumor cell survival and adaptation to antiangiogenic treatment in glioblastoma. *Cancer Res.*; **72**:1773–1783.

Huang, C.P., Tsai, M.F., Chang, T.H., Tang, W.C., Chen, S.Y. *et al.* (2013) ALDH-positive lung cancer SCs confer resistance to epidermal growth factor receptor tyrosine kinase

inhibitors. *Cancer Lett.* **328**:144–51

Huangfu, D. and Anderson, K.V. (2005) Cilia and Hedgehog responsiveness in the mouse. *Proc Natl Acad Sci USA.*, **102**:11325–11330

Huangfu, D., Liu, A., Rakeman, A.S., Murcia, N.S., Niswander, L. and Anderson, K.V. (2003) Hedgehog signalling in the mouse requires intraflagellar transport proteins. *Nature*, **426**(6962):83-7

Hui, C.C. and Angers, S. (2011) GLI proteins in development and disease. *Annu Rev Cell Dev Biol.*, **27**:513–537

Humke, E.W., Dorn, K.V., Milenkovic, L., Scott, M.P. and Rohatgi, R. (2010) The output of Hedgehog signalling is controlled by the dynamic association between suppressor of fused and the GLI proteins. *Genes Dev.*, **24**:670–682

Huntly, B.J., Shigematsu, H., Deguchi, K., Lee, B.H., Mizuno, S. *et al.* (2004) MOZ-TIF2, but not BCR-ABL, confers properties of leukemic stem cells to committed murine hematopoietic progenitors. *Cancer Cell.* **6**:587–596.

Hurwitz, H.I., Dowlati, A., Saini, S., Savage, S., Suttle, B. (2009) Phase I trial of pazopanib in patients with advanced cancer. *Clin Cancer Res.* **15**:4220-4227

Hynes, N.E. and Lane, H.A. (2005) ERBB receptors and cancer: the complexity of targeted inhibitors. *Nat Rev Cancer*, **5**(5):341

Iavarone, A., and Massague, J. (1997) Repression of the CDK activator Cdc25A and cell-cycle arrest by cytokine TGF-beta in cells lacking the CDK inhibitor p15. *Nature*, **387**:417-422

Ignatova, T.N., Kukekov, V.G., Laywell, E.D., Suslov, O.N., Vrionis, F.D. and Steindler, D.A. (2002) Human cortical glial tumors contain neural stem-like cells expressing astroglial and neuronal markers *in vitro*. *Glia*, **39**:193–206

Ikushima, H., and Miyazono, K. (2010). TGFbeta signalling: a complex web in cancer progression. *Nat. Rev. Cancer*, **10**(6):415–424

Ikushima, H., Todo, T., Ino, Y., Takahashi, M., Miyazawa, K. and Miyazono, K. (2009) Autocrine TGF- β signalling maintains tumorigenicity of glioma- initiating cells through Sry-related HMG-box factors. *Cell SC*, **5**:504–514

Ingallina, C. *et al.* (2016) Inhibition of Hedgehog-dependent tumors and cancer SCs by a newly identified naturally occurring chemotype. *Cell Death Dis.*; **7**(9):e2376.

Ingham, P.W. and McMahon, A.P. (2001) Hedgehog signalling in animal development: paradigms and principles. *Genes Dev.*, **15**(23):3059-87

Ingham, P.W. and McMahon, A.P. (2001) Hedgehog signalling in animal development: paradigms and principles. *Genes Dev.*, **15**:3059-3087

Ingham, P.W., Taylor, A.M. and Nakano, Y. (1991) Role of the *Drosophila patched* gene in positional signalling. *Nature*, **353**:184–187

Inman, G.J., Nicolas, F.J. and Hill, C.S. (2002) Nucleocytoplasmic shuttling of Smads 2, 3, and 4 permits sensing of TGF-beta receptor activity. *Mol. Cell.* **10**:283-294

Inman, G.J., Nicolas, F.J., Callahan, J.F., Harling, J.D., Gaster, L.M. (2002b) SB-431542 is a potent and specific inhibitor of transforming growth factor-beta superfamily type I activin receptor-like kinase (ALK) receptors ALK4, ALK5, and ALK7. *Mol Pharmacol.* **62**(1):65-74

Issa, J.P., Kantarjian, H.M. and Kirkpatrick, P. (2005) Azacitidine. *Nat Rev Drug Discov*, **4**(4):275-6

Ito, M., Liu, Y., Yang, Z., Nguyen, J., Liang, F. *et al.* (2005) SCs in the hair follicle bulge contribute to wound repair but not to homeostasis of the epidermis. *Nat Med.*, **11**:1351–4

Itoh, F., Asao, H., Sugamura, K., Heldin, C. H., ten Dijke, P., and Itoh, S. (2001) Promoting bone morphogenetic protein signalling through negative regulation of inhibitory SMADs. *EMBO J.*, **20**:4132-4142

Itoh, S., Itoh, F., Goumans, M.J. and Ten Dijke, P. (2000) Signalling of transforming growth factor family members through SMAD proteins. *Eur J Biochem*, **267**(24):6954-67

Itoh, S., Thorikay, M., Kowanetz, M. *et al.* (2003) Elucidation of SMAD requirement in transforming growth factor-beta type I receptor-induced responses. *J Biol Chem*, **278**:3751–3761.

Ivanov, D.P., Coyle, B., Walker, D.A. and Grabowska, A.M. (2016) In vitro models of medulloblastoma: Choosing the right tool for the job. *J Biotechnol.*, **236**:10-25

Jackson, S.P., and Bartek, J. (2009). The DNA-damage response in human biology and disease. *Nature*, **461**:1071–1078.

Jacob A (1827) Observations respecting an ulcer of peculiar character, which attacks the eyelids and other parts of the face. *Dublin Hospital Rep Commun Med Surg*, **4**:232-9.

Jacobsen, P.F., Jenkyn, D.J. and Papadimitriou, J.M (1985) Establishment of a human medulloblastoma cell line and its heterotransplantation into nude mice. *J. Neuropathol. Exp. Neurol.*, **44**:472-485

Jadrich, J.L., O'Connor, M.B. and Coucouvanis E. (2006) The TGF beta activated kinase TAK1 regulates vascular development *in vivo*. *Development*, **133**:1529–1541.

Jaffe, A.B. and Hall, A. (2005) Rho GTPases: biochemistry and biology. *Annu Rev Cell Dev Biol*, **21**:247– 269.

Jaffee, E.M., Hruban, R.H., Canto, M. and Kern, S.E. (2002) Focus on pancreas cancer. *Cancer Cell*, **2**:25-28

Jahangiri, A. *et al.* (2013) Gene expression profile identifies tyrosine kinase c-Met as a targetable mediator of antiangiogenic therapy resistance. *Clin. Cancer Res.*; **19**:1773–1783.

- Jaks, V., Barker, N., Kasper, M., van Es, J.H., Snippert, H.J. *et al.* (2008) Lgr5 marks cycling, yet long-lived, hair follicle SCs. *Nat Genet.*, **40**:1291–9
- James, D., Levine, A.J., Besser, D., Hemmati-Brivanlou, A. (2005) TGF β / activin/nodal signalling is necessary for the maintenance of pluripotency in human embryonic SCs. *Development*; **132**:1273-1282.
- Jansen-Dürr, P., Meichle, A., Steiner, P., Pagano, M., Finke, K. *et al.* (1993) Differential modulation of cyclin gene expression by MYC. *Proc Natl Acad Sci U S A.*, **90**(8):3685-9
- Jayaraman, L. and Massague, J. (2000) Distinct Oligomeric States of SMAD Proteins in the Transforming Growth Factor- β Pathway. *The Journal of Biological Chemistry*, **275**:40710-40717.
- Jayaraman, S.S., Rayhan, D.J., Hazany, S., Kolodney, M.S. (2014) Mutational Landscape of Basal Cell Carcinomas by Whole-Exome Sequencing. *Journal of Investigative Dermatology*, **134**: 213-220.
- Jemal, A., Siegel, R., Ward, E., Hao, Y., Xu, J. *et al.*, (2008) Cancer statistics,. *CA Cancer J Clin.* 2008 **58**(2):71–96
- Jennings, M.T. and Pietenpol, J.A. (1998) The role of transforming growth factor beta in glioma progression. *J. Neurooncol.*, **36**:123-140
- Jensen, K.B., Collins, C.A., Nascimento, E., Tan, D.W., Frye, M. *et al.* (2009) Lrig1 Expression Defines a Distinct Multipotent SC Population in Mammalian Epidermis. *Cell SC*, **4**:427–439
- Jensen, U.B., Yan, X., Triel, C., Woo, S.H., Christensen, R. and Owens, D.M. (2008) A distinct population of clonogenic and multipotent murine follicular keratinocytes residing in the upper isthmus. *J Cell Sci*, **121**:609–17
- Jensen, K.B., Jones, J., Watt, F.M. (2008) A SC gene expression profile of human squamous cell carcinomas. *Cancer Lett*; **272**: 23–31.
- Jiang, B.H., and Liu, L.Z., (2010) PI3K/PTEN signalling in angiogenesis and tumorigenesis.

Adv. Cancer Res., **102**:19–65

Jiang, J. and Hui, C.C. (2008) Hedgehog signalling in development and cancer. *Dev Cell.*, **15**(6):801-12

Jin, Q., Ding, W. and Mulder, K.M. (2007) Requirement for the dynein light chain km23-1 in a SMAD2-dependent transforming growth factor-beta signalling pathway. *J Biol Chem.*, **282**(26):19122–19132

Johnson, B.E. and Janne, P.A. (2006) Rationale for a phase II trial of pertuzumab, a HER-2 dimerization inhibitor, in patients with non-small cell lung cancer. *Clin Cancer Res.*, **12**(14 Pt 2):4436s-4440s

Johnson, G. L., and Lapadat, R. (2002) Mitogen-activated protein kinase pathways mediated by ERK, JNK, and p38 protein kinases. *Science*, **298**:1911- 1912

Johnson, R. L., Rothman, A.L., Xie, J., Goorich, L.V., Bare, J.W. *et al.* (1996) Human homolog of patched, a candidate gene for the basal cell nevus syndrome. *Science*, **272**:1668–1671

Johnson, T.M., Tromovitch, T.A. and Swanson, N.A. (1991) Combined curettage and excision: a treatment method for primary basal cell carcinoma. *J Am Acad Dermatol.*, **24**:613-7

Jones, P.H. and Watt, F.M. (1993) Separation of human epidermal SCs from transit amplifying cells on the basis of differences in integrin function and expression. *Cell*, **73**:713–724

Jones, R.G., and Thompson, C.B. (2009). Tumor suppressors and cell metabolism: a recipe for cancer growth. *Genes Dev.*, **23**:537–548.

Jordan, C.T., Upchurch, D., Szilvassy, S.J., Guzman, M.L., Howard, D.S. *et al.* (2000) The interleukin-3 receptor alpha chain is a unique marker for human acute myelogenous leukemia stem cells. *Leukemia*. **14**:1777–1784.

Kajita, M., McClinic, K.N., Wade, P.A. (2004) Aberrant expression of the transcription factors Snail and Slug alters the response to genotoxic stress. *Mol. Cell. Biol.* **24**:7559–7566.

Kalluri, R. and Weinberg, R. (2009) The basics of epithelial-mesenchymal transition. *J Clin Invest.*, **119**(6):1420-8

Kamaraju, A. K., and Roberts, A. B. (2005) Role of Rho/ROCK and p38 MAP kinase pathways in transforming growth factor-beta-mediated SMAD-dependent growth inhibition of human breast carcinoma cells in vivo. *J. Biol. Chem.*, **280**:1024-1036

Kamoto, D., Rostam, M. A., Piva, T. J., Babaahmadi Rezaei, H., Getachew, R. *et al.* (2014) Transforming growth factor β -mediated site-specific SMAD linker region phosphorylation in vascular endothelial cells. *J. Pharm. Pharmacol.*, **66**:1722- 1733

Kamimura, M., Bea, F., Akizawa, T., Katus, H. A., Kreuzer, J., and Viedt, C. (2004) Platelet-derived growth factor induces tissue factor expression in vascular smooth muscle cells via activation of Egr-1. *Hypertension*, **44**:944- 951

Kang, D.-H., Han, M.-E., Song, M.-H., Lee, Y.-S., Kim, E.-H. *et al.* (2009) The role of hedgehog signalling during gastric regeneration. *J. Gastroenterol.*, **44**:372-379

Kang, J.S., Liu, C. and Derynck, R. (2009) New regulatory mechanisms of TGF-beta receptor function. *Trends in cell biology*, **19**(8):385-394.

Kang, Y., Chen, C.-R. and Massague, J. A self-enabling TGF-b response coupled to stress signalling: SMAD engages stress response factor ATF3 for Id1 repression in epithelial cells. *Mol Cell*, **11**(4):915-26

Kang, Y., Siegel, P.M., Shu, W., Drobnjak, M., Kakonen, S.M. *et al.* (2003) A multigenic program mediating breast cancer metastasis to bone. *Cancer Cell*, **3**:537-549

Kang, Y., He, W., Tulley, S., Gupta, G.P., Serganova, I. *et al.* (2005) Breast cancer bone metastasis mediated by the Smad tumor suppressor pathway. *Proc Natl Acad Sci U S A.* **102**:13909–13914.

Kangsamaksin, T., Park, H.J., Trempus, C.S., Morris, R.J. (2007) A perspective on murine keratinocyte stem cells as targets of chemically induced skin cancer. *Mol Carcinog.* **46**:579–84.

Kantarjian, H., Giles, F., Wunderle, L., Bhalla, K., O'Brien, S. *et al.* (2006) Nilotinib in imatinib-resistant CML and Philadelphia chromosome-positive ALL. *N Engl J Med*, **354**(24):2542-51

Kantarjian, H., Issa, J.P., Rosenfeld, C.S. *et al.* (2006) Decitabine improves patient outcomes in myelodysplastic syndromes: results of a phase III randomized study. *Cancer*, **106**(8):1794-803.

Karagas, M.R., Stannard, V.A., Mott, L.A. *et al.* (2002) Use of tanning devices and risk of basal cell and squamous cell skin cancers. *J Natl Cancer Inst*, **94**:224-6

Karhadkar, S.S., Bova, G.S., Abdallah, N., Dhara, S., Gardner, D. *et al.* (2004) Hedgehog signalling in prostate regeneration, neoplasia and metastasis. *Nature*, **431**(7009):707-12

Karnoub, A.E., and Weinberg, R.A. (2006–2007). Chemokine networks and breast cancer metastasis. *Breast Dis.*, **26**:75–85.

Kastan, M.B. (2008). DNA damage responses: mechanisms and roles in human disease: 2007 G.H.A. Clowes Memorial Award Lecture. *Mol. Cancer Res.*, **6**:517–524.

Kastan, M.B., Onyekwere, O., Sidransky, D. *et al.* (1991) Participation of p53 protein in the cellular response to DNA damage. *Cancer Res*, **51**:6304-11

Kaur, P., and Potten, C.S. (2011) The interfollicular epidermal SC saga: sensationalism versus reality check. *Exp Dermatol*; **20**: 697–702.

Kavsak, P., Rasmussen, R. K., Causing, C. G., Bonni, S., Zhu, H. *et al.* (2000). SMAD7 binds to Smurf2 to form an E3 ubiquitin ligase that targets the TGF beta receptor for degradation. *Mol Cell*, **6**:1365-1375.

Keles, G.E., Berger, M.S., Srinivasan, J., Kolstoe, D.D., Bobola, M.S. and Silber, J.R. (1995) Establishment and characterization of four human medulloblastoma-derived cell lines. *Oncol. Res.*, **7**:493-503

Kemp CJ. (2005) Multistep skin cancer in mice as a model to study the evolution of cancer cells. *Semin Cancer Biol*, **15**:460–473

Kennedy, K.M., and Dewhirst, M.W. (2010). Tumor metabolism of lactate: the influence and therapeutic potential for MCT and CD147 regulation. *Future Oncol.*, **6**:127–148.

Kerbel, R.S. (2008) Tumor angiogenesis. *N Engl J Med*, **358**(19):2039-49

Khatib, Z.A., Matsushime, H., Valentine, M., Shapiro, D.N., Sherr, C.J and Look A.T. (1993) Coamplification of the CDK4 gene with MDM2 and GLI in human sarcomas. *Cancer Res*, **53**:5535 – 5541

Kogerman, P., Grimm, T., Kogerman, L., Krause, D., Uden, A.B. *et al.* (1999) Mammalian suppressor-of-fused modulates nuclear-cytoplasmic shuttling of Gli-1. *Nat. Cell Biol.* **1**: 312-319.

Kikushige, Y., Shima, T., Takayanagi, S., Urata, S., Miyamoto, T. *et al.* (2010) TIM-3 is a promising target to selectively kill acute myeloid leukemia stem cells. *Cell Stem Cell.* **7**:708–717.

Kim, J., Tang, J.Y., Gong, R., Kim, J., Lee, J.J. *et al.* (2010) Itraconazole, a commonly used antifungal that inhibits Hedgehog pathway activity and cancer growth. *Cancer Cell*, **17**:388–99

Kim, M.Y., Park, H.J., Baek, S.C., Byun, D.G. and Houh, D. (2002) Mutations of the p53 and PTCH gene in basal cell carcinomas: UV mutation signature and strand bias. *J Dermatol Sci.*, **29**(1):1-9

Kim, R., Emi, M., and Tanabe, K. (2007). Cancer immunoediting from immune surveillance to immune escape. *Immunology*, **121**:1–14.

- Kim, R., Emi, M., Tanabe, K. (2007) Cancer immunoediting from immune surveillance to immune escape. *Immunology*, **121**(1):1–14.
- Kimonis, V.E., Goldstein, A.M., Pastakia, B., Yang, M.L., Kase, R. *et al.* (1997) Clinical manifestations in 105 persons with nevoid basal cell carcinoma syndrome. *Am J Med Genet.*, **69**(3):299-308
- Kinzler, K.W. and Vogelstein, B. (1997). Cancer-susceptibility genes. Gatekeepers and caretakers. *Nature*, **386**(6627):761-763
- Kirkin, V., Joos, S. and Zörnig, M.. (2004) The role of Bcl-2 family members in tumorigenesis. *Biochim Biophys Acta*, **1644**(2-3):229-49.
- Kise, Y., Morinaka, A., Teglund, S. and Miki, H. (2009) Sufu recruits GSK3 β for efficient processing of GLI3. *Biochem Biophys Res Commun.*, **387**:569–574
- Kishida, O. *et al.* (2005) Gefitinib (“Iressa”, ZD1839) inhibits SN38-triggered EGF signals and IL-8 production in gastric cancer cells. *Cancer Chemother. Pharmacol.*; **55**:393–403.
- Knudson, A., (1971) Mutation and cancer: statistical study of retinoblastoma. *Proc Natl Acad Sci*, **68**:820-823
- Koleva, M., Kappler, R., Vogler, M., Herwig, A., Fulda, S. and Hahn, H. (2005) Pleiotropic effects of sonic hedgehog on muscle satellite cells. *Cell. Mol. Life Sci.*, **62**:1863-1870
- Kolterud, A., Grosse, A.S., Zacharias, W.J., Walton, K.D., Kretovich, K.E. *et al.* (2009) Paracrine Hedgehog signalling in stomach and intestine: new roles for hedgehog in gastrointestinal patterning. *Gastroenterology*, **137**:618-628
- Kool, M., Koster, J., Bunt, J., Hasselt, N.E., Lakeman, A. *et al.* (2008) Integrated genomics identifies five medulloblastoma subtypes with distinct genetic profiles, pathway signatures and clinicopathological features *PLoS One*, **3**(8):e3088
- Korol, A., Taiyab, A. and West-Mays, J.A (2016) RhoA/ROCK Signaling Regulates TGF β -

Induced Epithelial-Mesenchymal Transition of Lens Epithelial Cells through MRTF-A. *Mol Med.* **22**:713-723

Kovacs, J.J., Whalen, E.J., Liu, R. *et al.* (2008) β -arrestin-mediated localization of Smoothed to the primary cilium. *Science*, **320**:1777–1781

Kozar, S. *et al.* (2013) Continuous clonal labeling reveals small numbers of functional SCs in intestinal crypts and adenomas. *Cell SC*; **13**, 626–633.

Krauss, S., Concordet, J.P. and Ingham, P.W. (1993) A functionally conserved homolog of the *Drosophila* segment polarity gene Hh is expressed in tissues with polarizing activity in zebrafish embryos. *Cell*, **75**:1431–1444

Kretzschmar, M., Doody, J. and Massagué, J. (1997) Opposing BMP and EGF signalling pathways converge on the TGF β family mediator SMAD1. *Nature*, **389**:618-622.

Krivtsov, A.V., Twomey, D., Feng, Z., Stubbs, M.C., Wang, Y. *et al.* (2006) Transformation from committed progenitor to leukaemia stem cell initiated by MLL-AF9. *Nature*. **442**:818–822.

Kumar, P., Orton, C.I., McWilliam, L.J. *et al.* (2000) Incidence of incomplete excision in surgically treated basal cell carcinoma: a retrospective clinical audit. *Br J Plast Surg*, **53**:563-6

Kunkele, A., De Preter, K., Heukamp, L., Thor, T., Pajtler, K.W. *et al.* (2012) Pharmacological activation of the p53 pathway by nutlin-3 exerts anti-tumoral effects in medulloblastomas. *Neuro. Oncol.* **14**:859-869

Kuonen, F., Surbeck, I., Sarin, K.Y., Dontenwill, M., Ruegg, C. *et al.* (2018) TGF β , Fibronectin and Integrin α 5 β 1 Promote Invasion in Basal Cell Carcinoma. *J Invest Dermatol.* **S0022-202X**:31966-3

Kuperwasser, C., Chavarria, T., Wu, M., Magrane, G., Gray, J.W., Carey, L., Richardson, A., and Weinberg, R.A. (2004). Reconstruction of functionally normal and malignant

human breast tissues in mice. *Proc. Natl. Acad. Sci. USA* **101**: 4966–4971.

Kurisaki, A., Kose, S., Yoneda, Y., Heldin, C-H., Moustakas, A. (2001) Transforming Growth Factor- β Induces Nuclear Import of Smad3 in an Importin- β 1 and Ran-dependent Manner. *Mol Cell Biol.* **12**:1079-1091

Kurzrock, R., Kantarjian, H. M., Druker, B. J., Talpaz, M. (2003) Philadelphia chromosome-positive leukemias: From basic mechanisms to molecular therapeutics. *Annals of Internal Medicine*, **138**(10):819–830.

Kusanagi, K., Inoue, H., Ishidou, Y., Mishima, H.K., Kawabata, M., Miyazono, K. (2000) Characterization of a Bone Morphogenetic Protein-responsive Smad-binding Element. *Mol Cell Biol.* **11**:555-565.

Kvinlaug, B.T., Chan, W.I., Bullinger, L., Ramaswami, M., Sears, C. *et al.* (2011) Common and overlapping oncogenic pathways contribute to the evolution of acute myeloid leukemias. *Cancer Res.* **71**:4117–4129

Kwak, E.L, Bang, Y.J., Camidge, D.R., Shaw, A.T., Solomon, B. *et al.* (2010) Anaplastic lymphoma kinase inhibition in non-small-cell lung cancer. *N Engl J Med*, **363**(18):1693-703

Kyula, J.N. *et al.* (2010) Chemotherapy-induced activation of ADAM-17: a novel mechanism of drug resistance in colorectal cancer. *Clin. Cancer Res.*; **16**:3378–3389.

Labbe, E., Silvestri, C., Hoodless, P.A., Wrana, J.L., Attisano, L. (1998) Smad2 and Smad3 positively and negatively regulate TGF beta-dependent transcription through the forkhead DNA-binding protein FAST2. *Mol Cell.* **2**:109-120

Lacour J.P. (2002) Carcinogenesis of basal cell carcinomas: genetics and molecular mechanisms. *Br J Dermatol*, **146**:17-19

Lacroix, J., Schlund, F., Leuchs, B., Adolph, K., Sturm, D. *et al.* (2014) Oncolytic effects of parvovirus H-1 in medulloblastoma are associated with repression of master regulators

of early neurogenesis. *Int. J. Cancer*, **134**:703-716

Lal, H., Ahmad, F., Zhou, J., Yu, J. E., Vagnozzi, R. J. *et al.* (2014) Cardiac Fibroblast Glycogen Synthase Kinase-3 β Regulates Ventricular Remodeling and Dysfunction in Ischemic Heart. *Circulation*, **130**:419-430

Lammie, G.A., Fantl, V., Smmith, R., Schuurig, E., Brookes, S. *et al.* (1991) D11S287, a putative oncogene on chromosome 11q13, is amplified and expressed in squamous cell and mammary carcinomas and linked to BCL-1. *Oncogene*, **6**(3):439-4

Lamouille, S. and Derynck, R. (2007) Cell size and invasion in TGF-beta-induced epithelial to mesenchymal transition is regulated by activation of the mTOR pathway. *J Cell Biol*, **178**:437–451

Lamouille, S., Xu, J. and Derynck, R. (2014) Molecular mechanisms of epithelial–mesenchymal transition, *Nat Rev Mol Cell Biol.*, **15**(3): 178–196

Lane, S.W., Williams, D.A., and Watt, F.M. (2014) Modulating the stem cell niche for tissue regeneration. *Nat. Biotechnol.* **32**:795-803.

Lang, P.G. and Maize, J.C. (1986) Histologic evolution of recurrent basal cell carcinoma and treatment implications. *J Am Acad Dermatol*, **14**:186-96

Langer, C., Jurgensmeier, J. M., and Bauer, G. (1996) Reactive oxygen species act at both TGF-beta-dependent and -independent steps during induction of apoptosis of transformed cells by normal cells. *Exp Cell Res*, **222**:117-124.

Lapidot, T. *et al.* (1994) A cell initiating human acute myeloid leukaemia after transplantation into SCID mice. *Nature* **367**, 645–648

Lapouge, G., Youssef, K.K., Vokaer, B., Achouri, Y., Michaux, C. *et al.* (2011) Identifying the cellular origin of squamous skin tumors. *Proc Natl Acad Sci U S A.* **108**:7431–6

Laurie, N.A., Donovan, S.L., Shih, C.S. *et al.* (2006) Inactivation of the p53 pathway in

retinoblastoma. *Nature*, **444**:61-66

Lavker, R.M., Sun, T.T., Oshima, H., Barrandon, Y., Akiyama, M. *et al.* (2003). Hair follicle SCs. *J. Investig. Dermatol. Symp. Proc.*, **8**:28–38

Lawler, S., Feng, X.H., Chen, R.H. *et al.* (1997) The type II transforming growth factor-beta receptor autophosphorylates not only on serine and threonine but also on tyrosine residues. *J Biol Chem*, **272**:14850–14859

Leach, D.R., Krummel, M.F., Allison J.P. (1996) Enhancement of antitumor immunity by CTLA-4 blockade. *Science*. **271**:1734–1736.

Lear, J.T., Smith, A.G., Strange, R.C. *et al.* (1998) Patients with truncal basal cell carcinoma represent a high-risk group. *Arch Dermatol*, **134**:373

Lear, W., Dahlke, E. and Murray, C.A. (2007) Basal cell carcinoma: review of epidemiology, pathogenesis, and associated risk factors. *J Cutan Med Surg*, **11**:19-30

Lechler, T. and Fuchs, E. (2005) Asymmetric cell divisions promote stratification and differentiation of mammalian skin. *Nature*, **437**:275–280

Lee, D.C. *et al.* (2003) TACE/ADAM17 processing of EGFR ligands indicates a role as a physiological convertase. *Ann. NY Acad. Sci.*; **995**:22–38.

Lee, M.J., Hatton, B.A., Villavicencio, E.H. *et al.* (2012) Hedgehog pathway inhibitor saridegib (IPI-926) increases lifespan in a mouse medulloblastoma model. *Proc Natl Acad Sci U S A*, **109**(20):7859–7864

Lee, M.K., Pardoux, C., Hall, M.C. *et al.* (2007) TGF-beta activates Erk MAP kinase signalling through direct phosphorylation of ShcA. *EMBO J*; **26**:3957–3967.

Lee, S. J., and McPherron, A. C. (2001). Regulation of myostatin activity and muscle growth. *Proc Natl Acad Sci U S A*, **98**:9306-9311.

Lee, S., and Helfman, D. M. (2004) Cytoplasmic p21Cip1 Is Involved in Ras- induced Inhibition of the ROCK/LIMK/Cofilin Pathway. *J. Biol. Chem.*, **279**:1885-1891

Lemmon, M.A., and Schlessinger, J. (2010), Cell signalling by receptor tyrosine kinases. *Cell*, **141**(7):1117–1134

Lepper, C., Partridge, T.A., and Fan, C.-M. (2011). An absolute requirement for Pax7-positive satellite cells in acute injury-induced skeletal muscle regeneration. *Development*, **138**:3639–3646

Lessard, J. and Sauvageau, G. (2003) Bmi-1 determines the proliferative capacity of normal and leukaemic stem cells. *Nature*. **423**:255–260.

Levayer, R., and Lecuit, T. (2008) Breaking down EMT. *Nat Cell Biol*, **10**:757–759.

Levine, B., and Kroemer, G. (2008). Autophagy in the pathogenesis of disease. *Cell*, **132**:27–42

Levy, L. and Hill, C.S. (2006) Alterations in components of the TGF-beta superfamily signalling pathways in human cancer. *Cytokine Growth Factor Rev.*, **17**:41–58

Levy, V., Lindon, C., Harfe, B.D. and Morgan, B.A. (2005) Distinct SC Populations Regenerate the Follicle and Interfollicular Epidermis. *Developmental Cell*, **9**:855–861

Lewis, K.A., Gray, P.C., Blount, A.L., MacConell, L.A., Wiater, E., Bilezikjian, L.M., and Vale, W. (2000) Betaglycan binds inhibin and can mediate functional antagonism of activin signalling. *Nature*, **404**:411–414

Li, C., Heidt, D.G., Dalerba, P., Burant, C.F., Zhang, L. *et al.* (2007) Identification of pancreatic cancer SCs. *Cancer Res*, **67**:1030–1037

Li, M.O. and Flavell, R.A. (2008) TGF- β : A Master of All T Cell Trades. *Cell*, **134**:392–404

Li, L. and Clevers, H. (2010) Coexistence of quiescent and active adult stem cells in mammals. *Science*. **327**:542–5.

Li, S., Park, H., Trempus, C.S., Gordon, D., Liu, Y. *et al.* (2013) A keratin 15 containing stem cell population from the hair follicle contributes to squamous papilloma development in the mouse. *Mol. Carcinog.* **52**:751–759

Lichty, B. D., Keating, A., Callum, J., Yee, K., Croxford, R. *et al.* (1998) Expression of p210 and p190 BCR-ABL due to alternative splicing in chronic myelogenous leukaemia. *British J of Haem.* **103**(3):711–715.

Liem, K.F., Jr, He, M., Ocbina, P.J. and Anderson, K.V. (2009) Mouse Kif7/Costal2 is a cilia-associated protein that regulates Sonic hedgehog signalling. *Proc Natl Acad Sci USA*, **106**:13377–13382

Lievre, A. *et al.* (2006) KRAS mutation status is predictive of response to cetuximab therapy in colorectal cancer. *Cancer Res.*; **66**:3992–3995.

Lin, H.Y., Wang, X.F., Ng-Eaton, E., Weinberg, R.A. and Lodish, H.F. (1992) Expression cloning of the TGF-beta type II receptor, a functional transmembrane serine/threonine kinase. *Cell*, **68**(4):775-785.

Lim, X., Tan, S.H., Koh, W.L., Chau, R.M., Yan, K.S. *et al.* (2013) Interfollicular epidermal stem cells self-renew via autocrine Wnt signaling. *Science*, **342**:1226-1230

Liu, A., Wang, B. and Niswander, L.A. (2005) Mouse intraflagellar transport proteins regulate both the activator and repressor functions of GLI transcription factors. *Development*, **132**:3103–3111

Liu, Y., Festing, M., Thompson, J.C., Hester, M., Rankin, S. *et al.* (2004) Smad2 and Smad3 coordinately regulate craniofacial and endodermal development. *Developmental Biology*, **270**:411-426

Liu, F., and Matsuura, I. (2004) Inhibition of SMAD Antiproliferative Function by CDK Phosphorylation. *Cell Cycle*, **4**:63-66

Liu, F., Massagué, J. and Ruiz i Altaba, A. (1998) Carboxy-terminally truncated GLI3 proteins associate with SMADs. *Nat Genet.*, **20**(4):325-6

Liu, S., Dontu, G., Mantle, I.D., Patel, S., Ahn, N.S. *et al.* (2006) Hedgehog signalling and Bmi-1 regulate selfrenewal of normal and malignant human mammary SCs. *Cancer Res*, **66**:6063–6071

Liu, V.C., Wong, L.Y., Jang, T., Shah, A.H., Park, I. *et al.* (2007) Tumor Evasion of the Immune System by Converting CD4+CD25⁻ T Cells into CD4+CD25⁺ T Regulatory Cells: Role of Tumor-Derived TGF- β . *The Journal of Immunology*, **178**:2883-2892

Liu, T., Soong, L., Liu, G., Konig, R., Chopra, A.H. (2009) CD44 expression positively correlates with Foxp3 expression and suppressive function of CD4⁺ Treg cells. *Biol Direct*. **4**: 40

Liu, L., Liu, X., Ren, X., Tian, Y., Chen, Z. *et al.* (2016) Smad2 and Smad3 have differential sensitivity in relaying TGF β signaling and inversely regulate early lineage specification. *Scientific Reports*, **6**:21602

Ljungman, M. and Lane, D.P. (2004) Transcription – guarding the genome by sensing DNA damage. *Nat Rev Cancer*.**4**(9):727-37

Lo, P.K., Kanojia, D., Liu, X., Singh, U.P., Berger, F.G. *et al.* (2012) CD49f and CD61 identify Her2/neu-induced mammary tumor-initiating cells that are potentially derived from luminal progenitors and maintained by the integrin-TGF β signalling. *Oncogene*, **31**:2614–2626

Lomas, A., Leonardi-Bee, J. and Bath-Hextall, F. (2012) A systematic review of worldwide incidence of nonmelanoma skin cancer. *Br J Dermatol*, **166**:1069-80

Longley, D. B. and Johnston, P.G. (2005) Molecular mechanisms of drug resistance. *J. Pathol.*, **205**:275–292

Lonial, S., Waller, E.K., Richardson, P.G., Jagannath, S., Orłowski, R.Z. *et al.* (2005) Risk factors and kinetics of thrombocytopenia associated with bortezomib for relapsed, refractory multiple myeloma. *Blood*, **106**: 3777-3784.

Lopez-Garcia, C., Klein, A.M., Simons, B.D., Winton, D.J. (2010) Intestinal SC replacement follows a pattern of neutral drift. *Science* **330**: 822–825

LoRusso, P.M., Rudin, C.M., Reddy, J.C., Tibes, R. *et al.* (2011) Phase I Trial of Hedgehog Pathway Inhibitor Vismodegib (GDC-0449) in Patients with Refractory, Locally Advanced

or Metastatic Solid Tumors. *Clin Cancer Res.*, **17**(8): 2502–2511

Lowe, S. W., Cepero, E. and Evan, G. (2004) Intrinsic tumour suppression. *Nature*, **432**:307–315

Luo, Y., Dallaglio, K., Chen, Y., Robinson, W.A., Robinson, S.E. *et al.* (2012) ALDH1A isozymes are markers of human melanoma stem cells and potential therapeutic targets. *Stem Cells*, **30**:2100-2113.

Ma, L., Wang, D.D., Huang, Y., Yan, H., Wong, M.P. and Lee, V.H. (2015) EGFR Mutant Structural Database: computationally predicted 3D structures and the corresponding binding free energies with gefitinib and erlotinib. *BMC Bioinformatics*, **16**:85

Ma, W.W. and Adjei, A.A., (2009) Novel agents on the horizon for cancer therapy. *CA Cancer J Clin*, **59**(2):111-37.

Mac Gabhann, F., and Popel, A.S. (2008). Systems biology of vascular endothelial growth factors. *Microcirculation*, **15**:715–738

Mackenzie, I.C. (1969) Ordered structure of the stratum corneum of mammalian skin, *Nature*, **222**:881-882

Mackenzie, I.C. and Bickenbach, J.R. (1985) Label-retaining keratinocytes and Langerhans cells in mouse epithelia. *Cell Tissue Res.*, **242**:551–6

Madan, V., Lear, J.T. and Szeimies RM (2010) Non-melanoma skin cancer. *Lancet*, **375**:673- 85

Mahadevan, D., Cooke, L., Riley, C., *et al.*, (2007) A novel tyrosine kinase switch is a mechanism of imatinib resistance in gastrointestinal stromal tumors. *Oncogene*, **26**(27):3909-19

Maitah, M.Y., Shadan, A., Ahmad, A., Gadgeel, S., Sarker, F.H. (2011) Upregulation of sonic hedgehog contributes to TGF β 1-induced epithelial to mesenchymal transition in NSCLC cell. *PLOS One*, **13**;6(1):e16068

Malanchi, I., Peinado, H., Kassen, D., Hussenet, T., Metzger, D. *et al.* (2008) Cutaneous cancer stem cell maintenance is dependent on beta-catenin signalling. *Nature*, **452**: 650–653

Malanchi, I., Santamaria-Martinez, A., Susanto, E., Peng, H., Lehr, H.A. *et al.* (2011) Interactions between cancer stem cells and their niche govern metastatic colonization. *Nature*, **481**:85-89

Manasanch, E.E., Mathur, R., Lee, H.C., Weber, D.M., Patel, K.K. (2017) Pilot Study of Pembrolizumab for Immunoprevention in Smoldering Multiple Myeloma. *Blood*, **130**: 3089

Mancuso, M., Pazzaglia, S., Tanori, M., Hahn, H., Merola, P. *et al.* (2004) Basal cell carcinoma and its development: insights from radiation-induced tumors in PTCH1-deficient mice. *Cancer Res.*, **64**(3):934-41

Mani, S. A., Yang, J., Brooks, M., Schwaninger, G., Zhou, A. *et al.* (2007). Mesenchyme Forkhead 1 (FOXC2) plays a key role in metastasis and is associated with aggressive basal-like breast cancers. *Proc Natl Acad Sci U S A*, **104**:10069-10074.

Mani, S.A. Guo, W. Liao, M.J. Eaton, E.N. Ayyanan, A. *et al.* (2008) The epithelial-mesenchymal transition generates cells with properties of SCs. *Cell*, **133**:704-715

Mann, B.S., Johnson, J.R., Cohen, M.H., Justice, R. and Pazdur, R. (2007) FDA approval summary: vorinostat for treatment of advanced primary cutaneous T-cell lymphoma. *Oncologist*, **12**(10):1247-52

Mann, R.K. and Beachy, P.A. (2004) Novel lipid modifications of secreted protein signals. *Annu Rev Biochem.*, **73**:891-923

Manning, G., Whyte, D. B., Martinez, R., Hunter, T., and Sudarsanam, S. (2002). The protein kinase complement of the human genome. *Science*, **298**:1912-1934.

Mao, J.H., Saunier, E.F., de Koning, J.P., McKinnon, M.M., Higgins, M.N. *et al.* (2006) Genetic variants of *Tgfb1* act as context-dependent modifiers of mouse skin tumor susceptibility. *Proc Natl Acad Sci U S A.*, **103**:8125-30.

Marett, L.D., Prithwish, D., Airia, P. and Dryer, D., (2008) Cancer in Canada in 2008. *CMAJ*, **179**(11):1163–1170.

Mariathasan, S., Turley, S.J., Nickles, D., Castiglioni, A., Yuen, K. *et al.* (2018) TGF β attenuates tumour response to PD-L1 blockade by contributing to exclusion of T cells. *Nature*, **554**:544-548

Marks, R., Gebauer, K., Shumack, S. *et al.* (2001) Imiquimod 5% cream in the treatment of superficial basal cell carcinoma: results of a multicenter 6-week dose-response trial. *J Am Acad Dermatol*, **44**:807-13

Marks, R., Staples, M. and Giles, G.G. (1993) Trends in non-melanocytic skin cancer treated in Australia: the second national survey. *Int J Cancer*, **53**:585-90

Marsh, D., Dickinson, S., Neill, G.W., Marshall, J.F., Hart, I.R., Thomas, G.J. (2008) Alpha vbeta 6 Integrin promotes the invasion of morphoeic basal cell carcinoma through stromal modulation. *Cancer Res*, **68**:3295-3303

Marson, C.M. (2009) Histone deacetylase inhibitors: design, structure-activity relationships and therapeutic implications for cancer. *Anticancer Agents Med Chem.*, **9**(6):661-92.

Marti, E., Takada, R., Bumcrot, D.A., Sasaki, H., and McMahon, A.P. (1995) Distribution of Sonic hedgehog peptides in the developing chick and mouse embryo. *Development*, **121**:2537–2547

Martin-Malpartida, P., Batet, M., Kaczmarek, Z., Freier, R., Gomes, T. *et al.* (2017) Structural basis for genome wide recognition of 5-bp GC motifs by SMAD transcription factors. *Nat. Commun.* **8**: 2070

Mascre, G., Dekoninck, S., Drogat, B., Youssef, K.K., Brohee, S. *et al.* (2016) Distinct

contribution of stem and progenitor cells to epidermal maintenance *Nature*, **489**:257-262

Massague, J. (1998) TGF-beta signal transduction. *Annu. Rev. Biochem.* **67**:753-791

Massague, J. (2007) Sorting out breast-cancer gene signatures. *N. Engl. J. Med.*, **356**:294–297

Massagué, J. (2008). TGFbeta in cancer. *Cell*, 134(2):215–230

Massague, J., and Chen, Y. G. (2000). Controlling TGF-beta signalling. *Genes Dev*, **14**:627-644.

Massagué, J., and Wotton, D. (2000) New embo member's review: Transcriptional control by the TGFβ/SMAD signalling system. *EMBO J.* **19**:1745

Massague, J., Seoane, J. and Wotton, D. (2005) Smad transcription factors. *Genes & Dev.* **19**:2783-2810

Massagué, J., Seoane, J., and Wotton, D. (2005) SMAD transcription factors. *Genes Dev.*, **19**:2783-2810

Masson, N.M., Currie, I.S., Terrace, J.D. *et al.* (2006) Hepatic progenitor cells in human fetal liver express the oval cell marker Thy-1 *Am J Physiol Gastrointest Liver Physiol*; **291**: G45–G54.

Matei, C., Tampa, M., Poteca, T., Panea-Paunica, G., Georgescu, S.R. *et al.* (2013) Photodynamic therapy in the treatment of basal cell carcinoma. *J Med Life*, **6**(1):50-4

Mathew, R., Karantza-Wadsworth, V., and White, E. (2007). Role of autophagy in cancer. *Nat. Rev. Cancer*, **7**:961–967

Matsuura, I., Chiang, K.-N., Lai, C.-Y., He, D., Wang, G., *et al.* (2010) Pin1 Promotes Transforming Growth Factor-β-induced Migration and Invasion. *J. Biol. Chem.* **285**:1754-1764

- Matsuura, I., Denissova, N. G., Wang, G., He, D., Long, J., and Liu, F. (2004) Cyclin-dependent kinases regulate the antiproliferative function of SMADs. *Nature*, **430**:226-231
- McCartney-Francis, N. L., Frazier-Jessen, M., and Wahl, S. M. (1998) TGF- beta: a balancing act. *Int. Rev. Immunol.* **16**:553-580
- McKenzie, J.L., Gan, O.I., Doedens, M., Wang, J.C., Dick, J.E. (2006) Individual stem cells with highly variable proliferation and self-renewal properties comprise the human hematopoietic stem cell compartment. *Nat Immunol.* **7**:1225–1233
- McMahon, A.P., Ingham, P.W. and Tabin C.J. (2003) Developmental roles and clinical significance of hedgehog signalling. *Curr. Top. Dev. Biol.*, **53**:1-114
- Mechlin, C.W., Tanner, M.J., Chen, M., Buttyan, R., Levin, R.M. (2010) GLI2 expression and human bladder transitional carcinoma cell invasiveness. *J Urol*; **184**: 344–351.
- Meidhof, S., Brabletz, S., Lehmann, W., Preca, B.T., Mock, K. *et al.* (2015) ZEB1-associated drug resistance in cancer cells is reversed by the class I HDAC inhibitor mocetinostat. *EMBO Mol. Med.* **7**(6):831–47
- Meloni, A.R., Fralish, G.B., Kelly, P. *et al.* (2006) Smoothed signal transduction is promoted by G protein-coupled receptor kinase 2. *Mol Cell Biol.*, **26**:7550–7560
- Mercado-Pimentel, M.E. and Runyan R.B. (2007) Multiple transforming growth factor- β isoforms and receptors function during epithelial mesenchymal cell transformation in the embryonic heart. *Cells Tissues Organs*, **185**:146-156
- Merchant, M., Vajdos, F.F., Ultsch, M. *et al.* (2004) Suppressor of fused regulates GLI activity through a dual binding mechanism. *Mol Cell Biol.*, **24**:8627–8641
- Meric-Bernstam, F. and Gonzalez-Angulo, A.M. (2009) Targeting the mTOR signalling network for cancer therapy. *J Clin Oncol.*, **27**(13): 2278-87

Metcalfe, C. and de Sauvage, F.J. (2011) Hedgehog fights back: Mechanisms of acquired resistance against smoothed antagonists. *Cancer Res.*, **71**:5057–5061

Micke, P., Kappert, K., Ohshima, M., Sundquist, C., Scheidl, S. *et al.* (2007) *In Situ* Identification of Genes Regulated Specifically in Fibroblasts of Human Basal Cell Carcinoma. *Journal of Investigative Dermatology*, **127**:1516-1523

Miettinen, P. J., Ebner, R., Lopez, A. R., and Derynck, R. (1994) TGF-beta induced transdifferentiation of mammary epithelial cells to mesenchymal cells: involvement of type I receptors. *J Cell Biol*, **127**:2021-2036.

Miller, D.L. and Weinstock, M.A. (1994) Nonmelanoma skin cancer in the United States: incidence. *J Am Acad Dermatol*, **30**:774-8

Miller, F.R., Santner, S.J., Tait, L., Dawson, P.J. (2000) MCF10DCIS.com xenograft model of human comedo ductal carcinoma in situ. *J. Natl. Cancer Inst.*; **92**:1185-1186

Mima, K., Okabe, H., Ishimoto, T., Hayashi, H., Nakagawa, S. *et al.* (2012) CD44s regulates the TGF-b-mediated mesenchymal phenotype and is associated with poor prognosis in patients with hepatocellular carcinoma. *Cancer Res*, **72**:3414–3423

Mine, N., Anderson, R.M. and Klingensmith, J (2008) BMP antagonism is required in both the node and lateral plate mesoderm for mammalian left-right axis establishment. *Development*, **135**:2425-2434

Mitalipov, S. and Wolf, D. (2009) Totipotency, Pluripotency and Nuclear programming. *Adv Biochem Eng Biotechnol.* **114**:185-199.

Mitelman, F., Mark, J., Levan, G., and Levan, A. (1972) Tumor etiology and chromosome pattern. *Science*, **176**:1340–1341

Miyazono, K., Hellman, U., Wernstedt, C., and Heldin, C. H. (1988). Latent high molecular weight complex of transforming growth factor beta 1. Purification from human platelets and structural characterization. *J Biol Chem*, **263**:6407-6415.

Mizushima, N. (2007). Autophagy: process and function. *Genes Dev.*, **21**:2861– 2873

Mohan, S.V., Chang, J., Li, S., Henry, A.S., Wood, D.J. and Chang, A.L. (2016) Increased Risk of Cutaneous Squamous Cell Carcinoma After Vismodegib Therapy for Basal Cell Carcinoma *JAMA Dermatol.*, **152**(5):527-532

Morello, F., Perino, A., and Hirsch, E. (2009) Phosphoinositide 3-kinase signalling in the vascular system. *Cardiovasc. Res.*, **82**:261-271

Morgan, H., Benketah, A., Ord-McDermott, L., Rees, E., Mukhtar, A., Lanfredini, S., Olivero, C., Patel, G.K. (2018). Hair Follicle Telogen Differentiation in Human Basal Cell Carcinoma. *Journal of Investigative Dermatology* (manuscript under review)

Morgan, H., Olivero, C., Patel, G.K. (2018) Identification of human cutaneous basal cell carcinoma cancer SCs. *Methods in Molecular Biology*.

Morikawa, M., Koinuma, D., Tsutsumi, S., Vasilaki, E., Kanki, Y. *et al.* (2011) ChIP-seq reveals cell type-specific binding patterns of BMP-specific Smads and a novel binding motif. *Nucleic Acid Res.* **39**:8712-8727

Morisato, D. and Anderson, K.V. (1995) Signalling pathways that establish the dorsal-ventral pattern of the *Drosophila* embryo. *Annu. Rev. Genet.*, **29**:371-399

Morris, R.J., Fischer, S.M. and Slaga, T.J. (1985) Evidence that the centrally and peripherally located cells in the murine epidermal proliferative unit are two distinct cell populations. *J. Invest. Dermatol.* **84**:277 -281

Morris, R.J., Fischer, S.M. and Slaga, T.J. (1986) Evidence that a slowly cycling subpopulation of adult murine epidermal cells retains carcinogen. *Cancer Res.* **46**:3061

Morris, R.J., Haynes, A.C., Fischer, S.M., Slaga, T.J. (1991) Concomitant proliferation and formation of a stratified epithelial sheet by explant outgrowth of epidermal keratinocytes from adult mice. *In Vitro Cell Dev Biol.* **27A**:886–95

Morris, R.J., Coulter, K., Tryson, K., Steinberg, S.R. (1997) Evidence that cutaneous carcinogen-initiated epithelial cells from mice are quiescent rather than actively cycling. *Cancer Res.* **57**:3436–43.

Morris, R.J. and Potten, C.S. (1999) Highly persistent label-retaining cells in the hair follicles of mice and their fate following induction of anagen. *J Invest. Dermatol.* **112**:470-475.

Morris, R.J., Liu, Y., Marles, L., Yang, Z., Trempus, C. *et al.* (2004). Capturing and profiling adult hair follicle SCs. *Nat Biotechnol.*, **22**:411–7

Morris, S.W. *et al.* (1995) Fusion of a kinase gene, *ALK*, to a nucleolar protein gene, *NPM*, in non-Hodgkin's lymphoma. *Science*; **267**:316–317.

Morrison, S. J., Wright, D. and Weissman, I.L. (1997) Cyclophosphamide/granulocyte colony- stimulating factor induces hematopoietic SCs to proliferate prior to mobilization. *Proc. Natl Acad. Sci. USA*, **94**:1908–1913

Morrison, S.J. and Kimble, J. (2006) Asymmetric and symmetric stem-cell divisions in development and cancer. *Nature*, **441**(7097):1068-74

Morrison, S.J. and Spalding, A.C. (2008) Stem cells and niches: mechanisms that promote stem cell maintenance throughout life. *Cell*, **132**:598-611.

Moustakas, A., Souchelnytskyi, S. and Heldin, C.H. (2001) SMAD regulation in TGF β signal transduction. *J Cell Sci*, **114**(24):4359-69

Mross, K., Frost, A., Steinbild, S., Hedbom, S., Buchert, M. *et al.* (2012) A phase I dose-escalation study of regorafenib (BAY 73-4506), an inhibitor of oncogenic, angiogenic, and stromal kinases, in patients with advanced solid tumors. *Clin. Cancer Res.* **18**:2658-2667.

Mu, Y., Gudey, S.K. and Landstrom, M. (2012) Non-SMAD signalling pathways. *Cell Tissue Res*, **347**(1):11-20.

- Muehlich, S., Cicha, I., Garlich, C.D., Krueger, B., Posern, G. (2007) Actin-dependent regulation of connective tissue growth factor. *Am J Physiol Cell Physiol.*; **292**:C1732–1738.
- Mukherjee, S., Frolova, N., Sadlonova, A., Novak, Z., Steg, A. *et al.* (2006) Hedgehog signalling and response to cyclopamine differ in epithelial and stromal cells in benign breast and breast cancer. *Cancer Biol Ther.*, **5**:674–83
- Mulder, K.M. and Morris, S.L. (1992) Activation of p21ras by transforming growth factor beta in epithelial cells. *J Biol Chem*, **267**:5029–5031
- Mullen, A.C., Orlando, D.A., Newman, J.J., Loven, J., Kumar, R.M. *et al.* (2011) Master Transcription Factors Determine Cell-Type-Specific Responses to TGF- β Signaling. *Cell*, **147**:565-576.
- Musah, A., Gibson, J.E., Leonardi-Bee, J. *et al.* (2013) Regional variations of basal cell carcinoma incidence in the U.K. using The Health Improvement Network database (2004-10). *Br J Dermatol*, **169**:1093-9
- Nagata, Y. *et al.* (2004) PTEN activation contributes to tumor inhibition by trastuzumab, and loss of PTEN predicts trastuzumab resistance in patients. *Cancer Cell*, **6**: 117–127.
- Nakanishi, Y., Seno, H., Fukuoka, A., Ueo, T., Yamaga, Y. *et al.* (2013) Dclk1 distinguishes between tumor and normal SCs in the intestine. *Nat. Genet.* **45**:98–103
- Nanni, L., Ming, J.E., Bocian, M. and Steinhaus, K. (1999) The mutational spectrum of the sonic hedgehog gene in holoprosencephaly: SHH mutations cause a significant proportion of autosomal dominant holoprosencephaly. *Hum Mol Genet*, **8**(13):2479-88.
- Neel, D.S. and Bivona, T.G. (2017) Resistance is futile: overcoming resistance to targeted therapies in lung adenocarcinoma. *npj Precision Oncology*, **1**:3
- Negrini, S., Gorgoulis, V.G., and Halazonetis, T.D. (2010). Genomic instability—an evolving hallmark of cancer. *Nat. Rev. Mol. Cell Biol*, **11**:220–228.

Newick, K., O'Brien, S., Moon, E. and Albelda, S.M. (2017) CAR T Cell Therapy for Solid Tumors. *Annual Review of Medicine*, **68**:139-152

Nguyen, K.S., Kobayashi, S. and Costa, D.B. (2009) Acquired Resistance to Epidermal Growth Factor Receptor Tyrosine Kinase Inhibitors in Non–Small-Cell Lung Cancers Dependent on the Epidermal Growth Factor Receptor Pathway . *Clin Lung Cancer*, **10**(4):281-9

Nickel, J., Sebald, W., Groppe, J. C., and Mueller, T. D. (2009) Intricacies of BMP receptor assembly. *Cytokine Growth Factor Rev.* **20**:367-377

Nieto, M.A., Huang, R.Y., Jackson, R.A. and Thiery, J.P. (2016) EMT: 2016. *Cell*, **166**:21-45

Nieuwenhuis, E. and Hui, C.C. (2005) Hedgehog signalling and congenital malformations. *Clin. Genet.*, **67**:193-208

Nijhof, J.G., Braun, K.M., Giangreco, A., van Pelt, C., Kawamoto, H. *et al.* (2006) The cell-surface marker MTS24 identifies a novel population of follicular keratinocytes with characteristics of progenitor cells. *Development*, **133**:3027–37

Nolan-Stevaux, O., Lau, J., Truitt, M.L., Chu, G.C., Hebrok, M. *et al.* (2009) GLI1 is regulated through Smoothed-independent mechanisms in neoplastic pancreatic ducts and mediates PDAC cell survival and transformation. *Genes Dev.*, **23**(1):24-36

Nordling, C.O. (1953) A new theory on the cancer-inducing mechanism. *Br J Cancer*, **7**:68-72

Nowell, P.C. (1976) The clonal evolution of tumor cell populations. *Science*, **194**(4260):23-8

Nüsslein-Volhard, C. and Wieschaus, E. (1980) Mutations affecting segment number and polarity in *Drosophila*. *Nature*, **287**(5785):795-801

O'Brien, C.A., Pollett, A., Gallinger, S. *et al.* (2007) A human colon cancer cell capable of

initiating tumour growth in immunodeficient mice. *Nature*; **445**: 106–110.

O'Connor, M.B., Umulis, D., Othmer, H.G., and Blair, S.S. (2006) Shaping BMP morphogen gradients in the *Drosophila* embryo and pupal wing. *Development*, **133**:183-193

O'Connor, O.A., Stewart, K., Vallone, M., Molineaux, C.J., Kunkel, L.A. *et al.* (2009) A Phase 1 Dose Escalation Study of the Safety and Pharmacokinetics of the Novel Proteasome Inhibitor Carfilzomib (PR-171) in Patients with Hematologic Malignancies. *Clin Cancer Res.* **15**: 7085-7091.

O'Connor, O.A., Horwitz, S., Masszi, T., Van Hoof, A., Brown, P. *et al.* (2015) Belinostat in Patients With Relapsed or Refractory Peripheral T-Cell Lymphoma: Results of the Pivotal Phase II BELIEF (CLN-19) Study. *J. Clin. Oncol.* **33**:2492-2499

O'Driscoll, L., McMorrow, J., Doolan, P., McKiernan, Mehta, J.P. *et al.* (2006) Investigation of the molecular profile of basal cell carcinoma using whole genome microarrays. *Mol Cancer*, **5**:74

Oerlemans, R. *et al.* (2008) Molecular basis of bortezomib resistance: proteasome subunit $\beta 5$ (*PSMB5*) gene mutation and overexpression of PSMB5 protein. *Blood*; **112**:2489–2499.

Ogawa, K., Saito, A., Matsui H. *et al.* (2007) Activin/Nodal signalling is involved in propagation of mouse embryonic SCs. *J Cell Sci*; **120**:55-65.

Oida, T., Xu, L., Weiner, H.L., Kitani, A., Strober., W. (2006) TGF-beta-mediated suppression by CD4+CD25+ T cells is facilitated by CTLA-4 signaling. *J Immunol.* **177**:2331-2339

Okada, T., Lopez-Lago, M., and Giancotti, F.G. (2005). Merlin/NF-2 mediates contact inhibition of growth by suppressing recruitment of Rac to the plasma membrane. *J. Cell Biol.*, **171**(2):361–371

Omland, A.H., Wetterggren, E.E., Mollerup, S., Asplund, M., Mourier, T. *et al.* (2017)

Cancer associated fibroblasts (CAFs) are activated in cutaneous basal cell carcinoma and in the peritumoural skin. *BMC Cancer*, **17**:675

Ong, C.S., Keogh, A.M., Kossard, S. *et al.* (1999) Skin cancer in Australian heart transplant recipients. *J Am Acad Dermatol*, **40**:27-34

Oro, A.E. and Higgins, K. (2003) Hair cycle regulation of Hedgehog signal reception. *Dev. Biol.*, **255**:238-248

Oro, A.E., Higgins, K.M., Hu, Z., Bonifas, J.M., Epstein Jr., E.H. and Scott M.P. (1997) Basal cell carcinomas in mice overexpressing sonic hedgehog. *Science*, **276**: 817-821

Orouji, A., Goerdts, S., Utikal, J. and Leverkus, M. (2014) Multiple highly and moderately differentiated squamous cell carcinomas of the skin during vismodegib treatment of inoperable basal cell carcinoma. *Br J Dermatol.*, **171**(2):431-3

Oshima, H., Rochat, A., Kedzia, C., Kobayashi, K. and Barrandon, Y. (2001) Morphogenesis and renewal of hair follicles from adult multipotent SCs. *Cell*, **104**:233–45

Oshimori, N. and Fuchs, E. (2012) Paracrine TGF- signalling counterbalances BMP-mediated repression in hair follicle SC activation. *Cell SC*, **10**:63-75

Oshimori, N., Oristian, D. and Fuchs, E. (2015) TGF- β promotes heterogeneity and drug resistance in squamous cell carcinoma. *Cell*, **160**:963–976

Oskarsson, T., Batlle, E., Massague, J. (2014) Metastatic SCs: sources, niches, and vital pathways. *Cell SC* **14**:306–21

Otrock, Z.K., Hatoum, H.A., Awada, A.H., Ishak, R.S. and Shamseddine, A.I. (2009) Hypoxia-inducible factor in cancer angiogenesis: structure, regulation and clinical perspectives. *Crit Rev Oncol Hematol.*, **70**(2):93-102

Ott, C., Iwanciw, D., Graness, A., Giehl, K., Goppelt-Struebe, M. (2003) Modulation of the expression of connective tissue growth factor by alterations of the cytoskeleton. *J*

Biol Chem.; **278**:44305–44311.

Ozaki, T. and Nakagawara, A. (2011) Role of p53 in Cell Death and Human Cancers. *Cancers (Basel)*, **3**(1):994-1013

Ozdamar, B., Bose, R., Barrios-Rodiles, M. *et al.* (2005) Regulation of the polarity protein Par6 by TGFbeta receptors controls epithelial cell plasticity. *Science*, **307**:1603–1609

Padua, D., Zhang, X.H., Wang, Q., Nadal, C., Gerald, W.L. *et al.* (2008) TGFbeta primes breast tumors for lung metastasis seeding through angiopoietin-like 4. *Cell*, **133**:66-77

Pagan-Westphal, S.M. and Tabin, C.J. (1998) The transfer of left- right positional information during chick embryogenesis. *Cell*, **93**:25–35

Pages, F., Galon, J., Dieu-Nosjean, M.C., Tartour, E., Sautes-Fridman, C., and Fridman, W.H. (2010). Immune infiltration in human tumors: a prognostic factor that should not be ignored. *Oncogene*, **29**:1093–1102.

Pardoll, D.M. (2012) The blockade of immune checkpoints in cancer immunotherapy. *Nat. Rev. Cancer*, **12**:252-64

Pardali, K. and Moustakas, A. (2007) Actions of TGF-beta as tumor suppressor and pro-metastatic factor in human cancer. *Biochim Biophys Acta.*, **1775**: 21-62

Parsons, D.W., Li, M., Zhang, X., Jones, S., Leary, R.J. *et al.* (2011) The genetic landscape of the childhood cancer medulloblastoma. *Science*; **331**:435–439.

Patel, G.K., Terunuma, A., Telford, W. *et al.* (2012) Identification and characterization of tumor initiating cells in human primary cutaneous squamous cell carcinoma *J Invest Dermatol*; **132**: 401–409.

Patel, G.K., Yee, C.L., Yuspa, S.H., Vogel, J.C. (2012) A humanized stromal bed is required for engraftment of isolated human primary squamous cell carcinoma cells in immunocompromised mice. *J Invest Dermatol*; **132**(2):284-90.

- Paterson, S. C., Smith, K. D., Holyoake, T. L. and Jorgensen, H. G. (2003) Is there a cloud in the silver lining for imatinib? *Br. J. Cancer*, **88**:983–987
- Paus, R., and Cotsarelis, G. (1999) The biology of hair follicles. *N. Engl. J. Med.*, **341**:491–497.
- Peacock, C.D., Wang, Q., Gesell, G.S., Corcoran-Schwartz, I.M., Jones, E. *et al.* (2007) Hedgehog signalling maintains a tumor SC compartment in multiple myeloma. *Proc. Natl. Acad. Sci. U. S. A*, **104**:4048–4053
- Pecina-Slaus, N. (2003) Tumor suppressor gene E-cadherin and its role in normal and malignant cells. *Cancer Cell Int.*, **3**:17
- Pellegrini, C., Maturo, M.G., Nardo, L.D., Ciciarelli, V., Garcia-Rodrigo, C.G. and Fagnoli, M.C. (2017) Understanding the Molecular Genetics of Basal Cell Carcinoma. *Int J Mol Sci*, **18**(11):2485
- Penuelas, S., Anido, J., Prieto-Sanchez, R.M., Folch, G., Barba, I. *et al.* (2009) TGF- β increases glioma-initiating cell self-renewal through the induction of LIF in human glioblastoma. *Cancer Cell*, **15**:315–327
- Perez-Losada, J. and Balmain, A. (2003) Stem-cell hierarchy in skin cancer. *Nat Rev Cancer*. **3**:434–43.
- Perez-Roger, I., Kim, S.H., Griffiths, B., Sewing, A. and Land, H. (1999) Cyclins D1 and D2 mediate myc-induced proliferation via sequestration of p27(Kip1) and p21(Cip1). *EMBO J.*, **18**(19):5310-20
- Perez, E.A., Barrios, Eiermann, C. *et al.* (2017) Trastuzumab emtansine with or without pertuzumab versus trastuzumab plus taxane for human epidermal growth factor receptor 2-positive, advanced breast cancer: primary results from the phase III MARIANNE study *J Clin Oncol*; **35**:141-148

Perlman, R., Schiemann, W. P., Brooks, M. W., Lodish, H. F., and Weinberg, R. A. (2001) TGF-beta-induced apoptosis is mediated by the adapter protein Daxx that facilitates JNK activation. *Nat Cell Biol*, **3**:708-714.

Perona, R., (2006) Cell signalling: growth factors and tyrosine kinase receptors. *Clin. Transl. Oncol.*, **8**(2)77–82

Perrimon, N., Pitsouli, C. and Shilo, B.Z. (2012) Signalling mechanisms controlling cell fate and embryonic patterning. *Cold Spring Harb Perspect Biol*, **4**(8):a005975

Petersen, O.W., Polyak, K. (2010) SCs in the human breast *Cold Spring Harb Perspect Biol*; **2**: a003160.

Peterson, S.C., Eberl, M., Vagnozzi, A.N., Belkadi, A., Veniaminova, N.A. *et al.* (2015) Basal cell carcinoma preferentially arises from stem cells within hair follicle and mechanosensory niches. *Cell Stem Cell*. **16**:400-412

Petter, G., and Haustein, U.F. (1998) Squamous cell carcinoma of the skin- histopathological features and their significance for the clinical outcome. *J Eur Acad Dermatol Venereol*; **11**: 37-44.

Pierce, G.B. & Speers, W.C. (1988) Tumors as caricatures of the process of tissue renewal: prospects for therapy by directing differentiation. *Cancer Res*. **48**, 1996–2004

Pierce, G.B. & Wallace, C. (1971) Differentiation of malignant to benign cells. *Cancer Res*. **31**, 127–134

Pierce, D.F., Gorska, A.E., Chytil, A., Meise, K.S., Page, D.L. *et al.* (1995) Mammary tumor suppression by transforming growth factor beta 1 transgene expression. *Proc Natl Acad Sci U S A*, **92**:4254-8.

Pierceall, W.E., Goldberg, L.H., Tainsky, M.A., Mukhopadhyay, T., Ananthaswamy, H.N. (1991) *Ras* gene mutation and amplification in human nonmelanoma skin cancers. *Molecular Carcinogenesis*, **4**:196-202

- Pierreux, C.E., Nicolás, F.J. and Hill, C.S. (2000) Transforming growth factor β -independent shuttling of Smad4 between the cytoplasm and nucleus. *Mol. Cell. Biol.*, **20**:9041-9054
- Pittayapruek, P., Meehansan, J., Prapapan, O., Komine, M., Ohtsuki, M. (2016) Role of Matrix Metalloproteinases in Photoaging and Photocarcinogenesis. *Int J Mol Sci.* **17**:868
- Plaks, V., Kong, N., and Werb, Z. (2015) The Cancer Stem Cell Niche: How Essential is the Niche in Regulating Stemness of Tumor Cells? *Cell Stem Cell*, **16**:225-238.
- Pola, R., Ling, L.E., Aprahamian, T.R., Barban, E., Bosch-Marce M. *et al.* (2003) Postnatal recapitulation of embryonic hedgehog pathway in response to skeletal muscle ischemia. *Circulation*, **108**:479-485
- Pola, R., Ling, L.E., Silver, M., Corbley, M.J., Kearney, M. *et al.* (2001) The morphogen Sonic hedgehog is an indirect angiogenic agent upregulating two families of angiogenic growth factors. *Nat. Med.*, **7**:706-711
- Polyak, K., Lee, M. H., Erdjument-Bromage, H., Koff, A., Roberts, J. M. *et al.* (1994) Cloning of p27Kip1, a cyclin-dependent kinase inhibitor and a potential mediator of extracellular antimitogenic signals. *Cell*, **78**:59-66.
- Porter, P.L., Malone, K.E., Heagerty, P.J., Alexander, G.M., Gatti, L.A. *et al.* (1997) Expression of cell-cycle regulators p27Kip1 and cyclin E, alone and in combination, correlate with survival in young breast cancer patients. *JM Nat Med*, **3**(2):222-5
- Poste, G., Doll, J., Hart, I.R., and Fidler, I.J. (1980) In vitro selection of murine B16 melanoma variants with enhanced tissue-invasive properties. *Cancer Res.*, **40**:1636–1644
- Postigo, A.A., Depp, J.L., Taylor, J.J. and Kroll, K.L. (2003) Regulation of SMAD signalling through a differential recruitment of coactivators and corepressors by ZEB proteins. *EMBO J.*, **22**:2453–62
- Potten, C.S. (1974).The epidermal proliferative unit (EPU). The possible role of the

central basal cell. *Cell Tissue Kinet*, **7**:77-88

Potter, V.R. (1958). The biochemical approach to the cancer problem. *Fed. Proc.*, **17**:691–697.

Prince, M.E., Sivanandan, R., Kaczorowski, A. *et al.* (2007) Identification of a subpopulation of cells with cancer SC properties in head and neck squamous cell carcinoma. *Proc Natl Acad Sci U S A*; **104**: 973–978.

Puram, S.V., Tirosh, I., Parikh, A.S., Patel, A.P., Yizhak, K. *et al.* (2017) Single-Cell Transcriptomic Analysis of Primary and Metastatic Tumor Ecosystems in Head and Neck Cancer. *Cell*, **171**:1611-1624

Pusztai, L. *et al.* (2005) Phase II study of tariquidar, a selective P-glycoprotein inhibitor, in patients with chemotherapy- resistant, advanced breast carcinoma. *Cancer*; **104**: 682–691.

Qian, B.Z., and Pollard, J.W. (2010). Macrophage diversity enhances tumor progression and metastasis. *Cell*, **141**:39–51.

Quail, D.F., Taylor, M.J. and Postovit, L.M. (2012) Microenvironmental regulation of cancer SC phenotypes. *Curr SC Res Ther.*, **7**:197–216.

Quintana, E., Shackleton, M., Foster, H.R., Fullen, D.R., Sabel, M.S., Johnson, T.M., and Morrison, S.J. (2010). Phenotypic heterogeneity among tumorigenic melanoma cells from patients that is reversible and not hierarchically organized. *Cancer Cell* **18**: 510–523

Rajurkar, M., De Jesus-Monge, W.E., Driscoll, D.R., Appleman, V.A., Huang, H. *et al.* (2012) *PNAS*, **109**:E1038-E1047

Ramaswamy, B., Lu, Y., Teng, K-Y., Nuovo, G., Li, X. *et al.* (2012) Hedgehog Signaling Is a Novel Therapeutic Target in Tamoxifen-Resistant Breast Cancer Aberrantly Activated by PI3K/AKT Pathway. *Cancer Research* **72**:

Ransohoff, K.J., *et al.* (2013) Squamous Change in Basal-Cell Carcinoma with Drug Resistance. *N Engl J Med*, **373**:1079-1082

Ravani, A., Noonan, K.A., Pham, V., Bedi, R., Zhavoronkov, A. *et al.* (2018) Bifunctional immune checkpoint-targeted antibody-ligand traps that simultaneously disable TGF β enhance the efficacy of cancer immunotherapy. *Nature Communications*, **9**:741

Recupero, D. *et al.* (2013) Spontaneous and pronase-induced HER2 truncation increases the trastuzumab binding capacity of breast cancer tissues and cell lines.

J. Pathol; **229**: 390–399.

Reifenberger, J., Wolter, M., Weber, R.G., Megahed, M., Ruzicka, T. *et al.* (1998) Missense mutations in SMOH in sporadic basal cell carcinomas of the skin and primitive neuroectodermal tumors of the central nervous system. *Cancer Res.*, **58**(9):1798-803

Reifenberger J., Wolter M., Knobbe C.B., *et al.* (2005) Somatic mutations in the PTCH, SMOH, SUFUH and TP53 genes in sporadic basal cell carcinomas. *Br J Dermatol*, **152**:43-51

Rheinwald, J.G. and Green, H. (1975) Serial cultivation of strains of human epidermal keratinocytes: The formation of keratinizing colonies from single cells. *Cell*, **6**:331-343

Ricci-Vitiani, L., Lombardi, D.G., Pilozzi, E. *et al.* (2007) Identification and expansion of human colon-cancer-initiating cells. *Nature*; **445**: 111–115.

Rich, J. N., Zhang, M., Datto, M. B., Bigner, D. D., and Wang, X. F. (1999) Transforming growth factor-beta-mediated p15(INK4B) induction and growth inhibition in astrocytes is SMAD3-dependent and a pathway prominently altered in human glioma cell lines. *J Biol Chem*, **274**:35053-35058.

Richardson, P.G., Weller, E., Lonial, S., Jakubowiak, A.J., Jagannath, S. *et al.* (2010) Lenalidomide, bortezomib, and dexamethasone combination therapy in patients with newly diagnosed multiple myeloma. *Blood*, **116**:679-686.

- Riddle, R.D., Johnson, R.L., Laufer, E., and Tabin, C. (1993) Sonic hedgehog mediates the polarizing activity of the ZPA. *Cell*, **75**:1401–1416
- Ridky, T.W. and Cotsarelis, G. (2015) Vismodegib Resistance in Basal Cell Carcinoma: Not a Smooth Fit. *Cancer Cell*, **27**:315-316
- Riento, K. and Ridley, A.J. (2003) Rocks: multifunctional kinases in cell behaviours. *Nat Rev Mol Cell Biol.*, **4**(6):446–56
- Rippey, J.J. and Rippey, E. (1997) Characteristics of incompletely excised basal cell carcinomas of the skin. *Med J Aust*, **166**:581-3
- Robles A. I., Rodriguez-Puebla M. L., Glick A. B., Trempus C., Hansen L. *et al.* (1998) Reduced skin tumor development in cyclin D1-deficient mice highlights the oncogenic ras pathway *in vivo*. *Genes Dev.*, **12**:2469-2474
- Robson, C. N., Gnanapragasam, V., Byrne, R. L., Collins, A. T., and Neal, D. E. (1999) Transforming growth factor-beta1 up-regulates p15, p21 and p27 and blocks cell cycling in G1 in human prostate epithelium. *J Endocrinol*, **160**:257-266.
- Roche-Lestienne, C. Soenen-Cormu, V., Grardel-Duflos, N., Lai, J.L., Philippe, N. *et al.* (2002) Several types of mutations of the *Abl* gene can be found in chronic myeloid leukemia patients resistant to STI571, and they can pre-exist to the onset of treatment. *Blood*, **100**:1014–1018
- Rodrik-Outmezguine, V.S., Okaniwa, M., Yao, Z., Novotny, C.J., McWhirtner, C. *et al.* (2016) Overcoming mTOR resistance mutations with a new-generation mTOR inhibitor. *Nature*, **534**: 272-276.
- Roelink, H., Augsburger, A., Heemskerk, J., Korzh, V., Norlin, S. *et al.* (1994) Floor plate and motor neuron induction by vHh-1, a vertebrate homolog of hedgehog expressed by the notochord. *Cell*, **76**: 761–775
- Rohatgi, R., Milenkovic, L. and Scott, M.P. (2007) Patched1 regulates hedgehog signalling at the primary cilium. *Science*, **317**(5836):372–6.

Rohatgi, R., Milenkovic, L., Corcoran, R.B. and Scott, M.P. (2009) Hedgehog signal transduction by Smoothened: pharmacologic evidence for a 2-step activation process. *Proc Nat Acad Sci USA*, **106**(9):3196–201.

Rowe, D.E., Carroll, R.J. and Day, C.L. (1989) Mohs surgery is the treatment of choice for recurrent (previously treated) basal cell carcinoma. *J Dermatol Surg Oncol*, **15**:424-31

Rubin, A.I., Chen, E.H. and Ratner D (2005) Basal-cell carcinoma. *N Engl J Med*, **353**:2262-9

Rudin, C.M., Hann, C.L., Laterra, J., Yauch, R.L., Callahan, C.A. *et al.* (2009) Treatment of medulloblastoma with hedgehog pathway inhibitor GDC-0449. *N Engl J Med*, **361**:1173–8

Ruggeri, B., Caamano, J., Goodrow, T., DiRado, M., Bianchi, A. *et al.* (1991) Alterations of the p53 tumor suppressor gene during mouse skin tumor progression. *Cancer Res.*, **51**:6615–6621

Runyan, C. E., Schnaper, H. W. and Poncelet, A. C. (2004) The phosphatidylinositol 3-kinase/Akt pathway enhances SMAD3-stimulated mesangial cell collagen I expression in response to transforming growth factor- β 1. *J. Biol. Chem.*, **279**:2632-2639.

Rusnak, D.W., Lackey, K., Affleck, K. *et al.* (2001) The effects of the novel, reversible epidermal growth factor receptor/ErbB-2 tyrosine kinase inhibitor, GW2016, on the growth of human normal and tumor-derived cell lines in vitro and in vivo. *Mol Cancer Ther*; **1**:85-94

Sagai, T., Hosoya, M., Mizushina, Y., Tamura, M., and Shiroi-shi, T. (2005) Elimination of a long-range *cis*-regulatory module causes complete loss of limb-specific SHh expression and truncation of the mouse limb. *Development*, **132**:797–803

Salk, J.J., Fox, E.J., and Loeb, L.A. (2010). Mutational heterogeneity in human cancers: origin and consequences. *Ann. Rev. Pathol.*, **5**:51–75.

Samarakoon, R. and Higgins, P.J. (2002) MEK/ERK pathway mediates cell-shape-dependent plasminogen activator inhibitor type 1 gene expression upon drug-induced disruption of the microfilament and microtubule networks. *J Cell Sci.*, **115**(15):3093-103

Samarakoon, R. and Higgins, P.J. (2003) Pp60c-src mediates ERK activation/nuclear localization and PAI-1 gene expression in response to cellular deformation. *J Cell Physiol.* **195**:411-420

Samarakoon, R., Higgins, S.P., Higgins, C.E., Higgins, P.J. (2008a) TGF- β 1-induced plasminogen activator inhibitor-1 expression in vascular smooth muscle cells requires pp60c-src/EGFR^{Y845} and Rho/ROCK signaling. *J Mol Cell Cardiol.* **44**:527-538

Samarakoon, R. and Higgins, P.J. (2008b) Integration of non-SMAD and SMAD signaling in TGF- β 1-induced plasminogen activator inhibitor type-1 gene expression in vascular smooth muscle cells. *Thromb Haemost.* **100**:976-983.

Samarakoon, R., Higgins, C.E., Higgins, S.P. and Higgins, P.J. (2009) Differential requirement for MEK/ERK and SMAD signalling in PAI-1 and CTGF expression in response to microtubule disruption. *Cell Signal.*, **21**(6):986-95

Sampath, K., Cheng, A.M., Frisch, A., and Wright, C.V. (1997) Functional differences among *Xenopus* nodal-related genes in left-right axis determination. *Development*, **124**:3293–3302

San Miguel, J.F., Schlag, R., Khuageva, N.K. *et al.* (2008) Bortezomib plus melphalan and prednisone for initial treatment of multiple myeloma. *N Engl J Med.*, **359**(9):906-17

San-Miguel, J.F., Hungria, V.T., Yoon, S.S., Beksac, M., Dimopoulos, M.A *et al.* (2014) Panobinostat plus bortezomib and dexamethasone versus placebo plus bortezomib and dexamethasone in patients with relapsed or relapsed and refractory multiple myeloma: a multicentre, randomised, double-blind phase 3 trial. *Lancet Oncol.* **15**: 1195-1206

Sanchez-Danes, A., Hannezo, E., Larsimont, J.C., Liagre, M., Youssef, K.K. *et al.* (2016) Defining the clonal dynamics leading to mouse skin tumour initiation. *Nature*, **536**:298 – 303

Sanchez-Tillo, E., Liu, Y., de Barrios, O., Siles, L., Fanlo, L. *et al.* (2012) EMT-activating transcription factors in cancer: beyond EMT and tumor invasiveness. *Cell Mol Life Sci.* **69**:3429-3456

Sano, Y., Harada, J., Tashiro, S. *et al.* (1999) ATF-2 is a common nuclear target of SMAD and TAK1 pathways in transforming growth factor-beta signalling. *J Biol Chem*, **274**:8949–8957

Sansal, I., and Sellers, W. R. (2004) The biology and clinical relevance of the PTEN tumor suppressor pathway. *J. Clin. Oncol.*, **22**:2954-2963

Saqui-Salces, M. and Merchant, J.L. (2010) Hedgehog signalling and gastrointestinal cancer. *Biochim Biophys Acta*, **1803**(7):786-795

Santos D.C.C., Zaphiropoulos P.G., Neto C.F., *et al.* (2011) PTCH1 gene mutations in exon 17 and loss of heterozygosity on D9S180 microsatellite in sporadic and inherited human basal cell carcinomas. *Int J Dermatol*, **50**:838-843

Sasake, K., Sugai, T., Ishida, K., Osakabe, M., Amano, H. *et al.* (2018) Analysis of cancer-associated fibroblasts and the epithelial-mesenchymal transition in cutaneous basal cell carcinoma, squamous cell carcinoma, and malignant melanoma. *Human Pathology*, **79**:1-8

Sato, N., Leopold, P.L. and Crystal, R.G. (1999) Induction of the hair growth phase in postnatal mice by localized transient expression of Sonic hedgehog. *J. Clin. Invest.*, **104**:855-864

Sato, N., Leopold, P.L. and Crystal, R.G. (2001) Effect of adenovirus-mediated expression of Sonic hedgehog gene on hair regrowth in mice with chemotherapy-induced alopecia. *J. Natl Cancer Inst.*, **93**:1858–1864

Saylors, R.L., Sidransky, D., Friedman, H.S., Bigner, S.H., Bigner, D.D., Vogelstein, B. and

Brodeur G.M. (1991) Infrequent p53 gene mutations in medulloblastomas. *Cancer Res.*, **51**:4721-4723

Schatton, T., Murphy, G.F., Frank, N.Y., Yamaura, K., Waaga-Gasser, A.M. *et al.* (2008) Identification of cells initiating human melanomas. *Nature*, **451**:345-349

Schier, A.F. (2003) Nodal signalling in vertebrate development. *Annu. Rev. Cell Dev. Biol.*, **19**:589-621

Schilling, T.F., Concordet, J.P., and Ingham, P.W. (1999) Regulation of left–right asymmetries in the zebrafish by SHh and BMP4. *Dev. Biol.*, **210**:277–287

Schlange, T., Arnold, H.H. and Brand, T. (2002) BMP2 is a positive regulator of Nodal signalling during left-right axis formation in the chicken embryo. *Development*, **129**:3421-3429

Schober, M. and Fuchs, E. (2011) Tumor-initiating stem cells of squamous cell carcinomas and their control by TGF- β and integrin/focal adhesion kinase (FAK) signaling. *PNAS*, **108**:10544-10549

Schofield, R. (1978) The relationship between the spleen colony-forming cell and the haemopoietic SC. *Blood Cells*, **4**:7–25

Scott, G.A., Laughlin, T.S., and Rothberg, P.G. (2014) Mutations of the *TERT* promoter are common in basal cell carcinoma and squamous cell carcinoma. *Modern Pathology*, **27**:516-523.

Sekulic, A., Migden, M.R., Oro, A.E. *et al.* (2012) Efficacy and safety of vismodegib in advanced basal-cell carcinoma. *N Engl J Med.*, **366**:2171-2179

Semenza, G.L. (2008). Tumor metabolism: cancer cells give and take lactate. *J. Clin. Invest.*, **118**:3835–3837.

Semenza, G.L. (2010a). HIF-1: upstream and downstream of cancer metabolism. *Curr.*

Opin. Genet. Dev., **20**:51–56.

Senturk, S., Mumcuoglu, M., Gursoy-Yuzugullu, O., Cingoz, B., Akcali, K. C., and Ozturk, M. (2010). Transforming growth factor-beta induces senescence in hepatocellular carcinoma cells and inhibits tumor growth. *Hepatology*, **52**(3):966-74

Sequist, L.V., Bell, D.W., Lynch, T.J. and Haber, D.A. (2007) Molecular predictors of response to epidermal growth factor receptor antagonists in non-small-cell lung cancer. *J Clin Oncol.*, **25**(5):587-95.

Sergina, N.V., Rausch, M., Wang, D. *et al.* (2007) Escape from HER-family tyrosine kinase inhibitor therapy by the kinase-inactive HER3. *Nature*, **445**(7126):437-41.

Sethi, N., Dai, X., Winter, C.G., Kang, Y. (2011) Tumor-derived JAGGED1 promotes osteolytic bone metastasis of breast cancer by engaging notch signaling in bone cells. *Cancer Cell*, **19**:192-205

Seto, M., Ohta, M., Asaoka, Y., Ikenoue, T., Tada, M. *et al.* (2009) Regulation of the hedgehog signaling by the mitogen-activated protein kinase cascade in gastric cancer. *Molecular Carcinogenesis*, **48**:

Schatton, T., Murphy, G.F., Frank, N.Y. *et al.* (2008) Identification of cells initiating human melanomas. *Nature*; **451**: 345–349.

Schepers, A.G. *et al.* Lineage tracing reveals Lgr5+ SC activity in mouse intestinal adenomas. *Science* 337, 730–735 (2012)

Schmidt, P., Kopecky, C., Hombach, A. *et al.* (2011) Eradication of melanomas by targeted elimination of a minor subset of tumor cells *Proc Natl Acad Sci U S A*; **108**: 2474–2479.

Schroeder, K., Gururangan, S. (2014) Molecular variants and mutations in medulloblastoma. *Pharmgenom. Pers. Med.*; **7**:43–51.

- Shankaran V, Ikeda H, Bruce AT, White JM, Swanson PE, Old LJ, Schreiber RD.(2001) IFN γ and lymphocytes prevent primary tumour development and shape tumour immunogenicity. *Nature*, **410**:1107–11.
- Shapiro, J.R., Yung, W.K., and Shapiro, W.R. (1981) Isolation, karyotype, and clonal growth of heterogeneous subpopulations of human malignant gliomas. *Cancer Res.*, **41**:2349–2359
- Sharma, S.V., Bell, D.W., Settleman, J. and Haber, D.A. (2007). Epidermal growth factor receptor mutations in lung cancer. *Nat Rev Cancer*, **7**(3):169-81
- Sharpe, H.J., Pau, G., Dijkgraaf, G.J., Basset- Seguin, N., Modrusan, Z. *et al.* (2015) Genomic Analysis of Smoothed Inhibitor Resistance in Basal Cell Carcinoma. *Cancer Cell*, **27**:327–341.
- Shay, J.W. and Bacchetti, S.. (1997)_A survey of telomerase activity in human cancer. *Eur J Cancer.*, **33**(5):787-91.
- Shay, J.W. and Wright, W.E. (2011) Role of telomeres and telomerase in cancer. *Semin Cancer Biol.*, **21**(6):349–353.
- Shay, J.W., and Wright, W.E. (2000). Hayflick, his limit, and cellular ageing. *Nat. Rev. Mol. Cell Biol.*, **1**:72–76
- Sheahan, S., Bellamy, C. O., Harland, S. N., Harrison, D. J., and Prost, S. (2008) TGF β induces apoptosis and EMT in primary mouse hepatocytes independently of p53, p21Cip1 or Rb status. *BMC Cancer*, **8**:191
- Sherr, C.J., and McCormick, F. (2002). The RB and p53 pathways in cancer. *Cancer Cell*, **2**(2):103–112
- Shervington, A., Lu, C. (2008) Expression of multidrug resistance genes in normal and cancer SCs. *Cancer Invest*; **26**: 535–542.

Shi, Y., and Massague, J. (2003). Mechanisms of TGF-beta signalling from cell membrane to the nucleus. *Cell*, **113**:685-700.

Shi, Y., Hata, A., Lo, R. S., Massague, J., and Pavletich, N. P. (1997) A structural basis for mutational inactivation of the tumour suppressor SMAD4. *Nature*, **388**:87-93

Shi, Y., Wang, Y. F., Jayaraman, L., Yang, H., Massague, J., and Pavletich, N. P. (1998). Crystal structure of a SMAD MH1 domain bound to DNA: insights on DNA binding in TGF-beta signalling. *Cell*, **94**:585-594.

Shibuya, H., Yoneyama, M., Ninomiya-Tsuji, J., Matsumoto, K. and Taniguchi, T. (1992) IL-2 and EGF receptors stimulate the hematopoietic cell cycle via different signalling pathways: demonstration of a novel role for c-myc. *Cell*, **70**(1):57-67

Shien, K., Toyooka, S., Yamamoto, H., Soh, J., Jida, M. *et al.* (2013) Acquired resistance to EGFR inhibitors is associated with a manifestation of SC-like properties in cancer cells. *Cancer Res.* **73**:3051–61

Shim, J.H., Xiao, C., Paschal, A.E. *et al.* (2005) TAK1, but not TAB1 or TAB2, plays an essential role in multiple signalling pathways *in vivo*. *Genes Dev*, **19**:2668–2681

Shimokawa, M. *et al.* (2017) Visualization and targeting of LGR5+ human colon cancer SCs. *Nature*; **545**: 187–192

Shin, S., Kim, J., Yoon, S.O., Kim, Y.R., Lee, K.A. (2012) ALK-positive anaplastic large cell lymphoma with *TPM3-ALK* translocation. *Leuk. Res*; **36**: e143–e145.

Shin, I., Bakin, A.V., Rodeck, U., Brunet, A. and Arteaga, C.L. (2001) Transforming growth factor beta enhances epithelial cell survival via Akt-dependent regulation of FKHRL1. *Mol Biol Cell*, **12**:3328–3339

Shipitsin, M. Campbell, L.L. Argani, P. Weremowicz, S. Bloushtain-Qimron, N. *et al.* (2007) Molecular definition of breast tumor heterogeneity. *Cancer Cell*, **11**:259-273

Shlush, L.I., Zandi, S., Mitchell, A., Chen, W.C., Brandwein, J.M. *et al.* (2014)

Identification of pre-leukaemic haematopoietic SCs in acute leukaemia. *Nature* **506**:328–33

Shukla, A., Ho, Y., Liu, X., Ryscavage, A. and Glick, A.B. (2008) Cripto-1 alters keratinocyte differentiation via blockade of transforming growth factor-beta1 signalling: role in skin carcinogenesis. *Mol Cancer Res.*, **6**:509-16

Shukla, A., Edwrads, R., Yang, Y., Hahn, A., Folkers, K. *et al.* (2014) CLIC4 regulates TGF- β -dependent myofibroblast differentiation to produce a cancer stroma. *Oncogene*, **33**:842-850

Siebzehnruhl, F.A., Silver, D.J., Tugertimur, B., Deleyrolle, L.P., Siebzehnruhl, D. *et al.* (2013) The ZEB1 pathway links glioblastoma initiation, invasion and chemoresistance. *EMBO Mol. Med.* **5**:1196–212

Siegel, P.M. and Massague, J. (2003) Cytostatic and apoptotic actions of TGF-beta in homeostasis and cancer. *Nat Rev Cancer*, **3**:807-21

Sigal, A., and Rotter, V. (2000). Oncogenic mutations of the p53 tumor suppressor: the demons of the guardian of the genome. *Cancer Res.*, **60**:6788–6793.

Silverman, L.R., Demakos, E.P., Peterson, B.L. *et al.* (2002) Randomized controlled trial of azacytidine in patients Myelodysplastic syndrome: a study of the cancer and leukemia group B. *JCO*, **20**:2429-2440.

Siminovitch, L., McCulloch, E.A. and Till, J.E. (1963) The distribution of colony-forming cells among spleen colonies. *J. Cell. Physiol.* **62**: 327–336

Singh, S., Wang, Z., Liang Fei, D., Black, K.E., Goetz, J.A. *et al.* (2011) Hedgehog-producing cancer cells respond to and require autocrine Hedgehog activity. *Cancer Res.*, **71**:4454–63

Singh, S.K., Hawkins, C., Clarke, I.D., Squire, J.A., Bayani, J. *et al.* (2004) Identification of human brain tumour initiating cells. *Nature*, **432**:396–401

- Singh, A., Park, H., Kangsamaksin, T., Singh, A., Readio, N., Morris, R.J. (2012) Keratinocyte stem cells and the targets for nonmelanoma skin cancer. *Photochem. Photobiol.* **88**:1099-1110.
- Sinha, S., and Levine, B. (2008). The autophagy effector Beclin 1: a novel BH3- only protein. *Oncogene*, **27**(Suppl 1):S137–S148
- Sirard, C., de la Pompa, J.L., Elia, A, *et al.* (1998) The tumor suppressor gene *SMAD4/Dpc4* is required for gastrulation and later for anterior development of the mouse embryo. *Genes Dev*, 1998; **12**:107-119.
- Sjoblom, T., Jones, S., Wood, L.D., Parsons, D.W., Lin, J. *et al.* (2006) The consensus coding sequences of human breast and colorectal cancers. *Science*, **314**:268-274
- Skvara, H., Kalthoff, F., Meingassner, J.G., Wolff-Winiski, B., Aschauer, H. *et al.* (2011) Topical treatment of Basal cell carcinomas in nevoid Basal cell carcinoma syndrome with a smoothed inhibitor. *J Invest Dermatol*, **131**:1735–1744
- Smyth, M.J., Dunn, G.P., and Schreiber, R.D. (2006). Cancer immunosurveillance and immunoediting: the roles of immunity in suppressing tumor development and shaping tumor immunogenicity. *Adv. Immunol.*, **90**:1–50.
- Sneddon, J.B., Zhen, H.H, Montgomery, K. van de Rijn, M. Tward, A.D. *et al.* (2006) Bone morphogenetic protein antagonist gremlin 1 is widely expressed by cancer-associated stromal cells and can promote tumor cell proliferation. *Proc. Natl. Acad. Sci. USA*, **103**:14842-14847
- Sobinoff, A.P. and Pickett, H.A. (2017) Alternative Lengthening of Telomeres: DNA Repair Pathways Converge. *Trends Genet.* **33**:921-932
- Solanas, G. and Benitah, S. A. (2013) Regenerating the skin: a task for the heterogeneous SC pool and surrounding niche. *Nat. Rev. Mol. Cell Biol.*, **14**:737-748
- Sotiropoulou, P.A., Candi, A., Mascre, G., De Clercq, S., Youssef, K.K. *et al.* (2010) Bcl-2 and accelerated DNA repair mediates resistance of hair follicle bulge SCs to DNA-

damage-induced cell death. *Nat. Cell Biol.* **12**:572–82

Souchelnytskyi, S., Tamaki, K., Engstrom, U., Wernstedt, C., ten Dijke, O., Heldin, C.H. (1997) Phosphorylation of Ser465 and Ser467 in the C terminus of Smad2 mediates interaction with Smad4 and is required for transforming growth factor-beta signaling. *J Biol Chem.* **272**:28107-28115

Spender, L. C., O'Brien, D. I., Simpson, D., Dutt, D., Gregory, C. D. *et al.* (2009) TGF-beta induces apoptosis in human B cells by transcriptional regulation of BIK and BCL-XL. *Cell Death Differ.* **16**:593-602.

Stankic, M., Pavlovic, S., Chin, Y., Brogi, E., Padua, D. *et al.* (2013) TGFβ-Id1 Signaling Opposes Twist1 and Promotes Metastatic Colonization Via a Mesenchymal-to-Epithelial Transition. **5**:1228-1242

Stanton, B.Z., Peng, L.F., Maloof, N., Nakai, K. Wang, X. *et al.* (2009) A small molecule that binds Hedgehog and blocks its signalling in human cells. *Nat Chem Biol*, **5**:154-156

Steensma, D.P., Baer, M.R., Slack, J.L. *et al.* (2009) Multicenter study of decitabine administered daily for 5 days every 4 weeks to adults with myelodysplastic syndromes: the alternative dosing for outpatient treatment (ADOPT) trial. *J Clin Oncol.*, **27**(23):3842-8.

Steg, A.D., Bevis, K.S., Katre, A.A., Ziebarth, A., Dobbin, Z.C. *et al.* (2012) SC pathways contribute to clinical chemoresistance in ovarian cancer. *Clin. Cancer Res.*, **18**:869–881

Stephenson, J., Richards, D.A., Wolpin, B.M. and Becerra, C. (2011) The safety of IPI-926, a novel hedgehog pathway inhibitor, in combination with gemcitabine in patients (pts) with metastatic pancreatic cancer. *J Clin Oncol*, **15**:suppl4114

Stern, M.C., Benavides, F., LaCava, M. and Conti, C.J. (2002) Genetic analyses of mouse skin tumor progression susceptibility using SENCAR inbred derived strains. *Mol Carcinog.*, **35**:13–20

Stern, R.S. and Lange, R. (1988) Non-melanoma skin cancer occurring in patients treated with PUVA five to ten years after first treatment. *J Invest Dermatol*, **91**:120-4

Stone, D.M., Hynes, M. and Armanini, M. *et al.* (1996) The tumour-suppressor gene *Patched* encodes a candidate receptor for Sonic hedgehog. *Nature*, **384**:129–134

Straface, G., Aprahamian, T., Flex, A., Gaetani, E., Biscetti, F. *et al.* (2009) Sonic hedgehog regulates angiogenesis and myogenesis during post-natal skeletal muscle regeneration. *J. Cell. Mol. Med.*, **13**:2424-2435

Stratton, M.R., Campbell, P.J. and Futreal, P. A., (2009) The cancer genome. *Nature* 2009, **458**:719–724

Sun, P. D., and Davies, D. R. (1995;). The cystine-knot growth-factor superfamily. *Annu Rev Biophys Biomol Struct*, **24**:269-291.

Sunnarborg, S. W. *et al.* (2002) Tumor necrosis factor- α converting enzyme (TACE) regulates epidermal growth factor receptor ligand availability. *J. Biol. Chem.*; **277**:12838–12845.

Sussman, L.A. and Liggins, D.F. (1996) Incompletely excised basal cell carcinoma: a management dilemma? *Aust N Z J Surg*, **66**:276-8

Svard, J., Heby-Henricson, K., Persson-Lek, M. *et al.* (2006) Genetic elimination of suppressor of fused reveals an essential repressor function in the mammalian Hedgehog signalling pathway. *Dev Cell*, **10**:187–197

Swanton, C. (2012) Intratumor heterogeneity: evolution through space and time. *Cancer Res.*, **72**:4875–4882

Tabarestani, S. and Ghafouri-Fard, S. (2012) Cancer SCs and response to therapy. *Asian Pac J Cancer Prev*, **13**(12):5951-8

Takai, S., Schlom, J., Tucker, J., Tsang, K.Y., Greiner, J.W. (2013) Inhibition of TGF- β 1 signaling promotes central memory T cell differentiation. *J Immunol.* **191**:2299-2307

- Talmadge, J.E., and Fidler, I.J. (2010). AACR centennial series: the biology of cancer metastasis: historical perspective. *Cancer Res.*, **70**:5649–5669
- Tang, B., Yoo, N., Vu, M., Mamura, M., Nam, J.S. *et al.* (2007) Transforming growth factor- β can suppress tumorigenesis through effects on the putative cancer stem or early progenitor cell and committed progeny in a breast cancer xenograft model. *Cancer Res*, **67**:8643–8652
- Tang J.Y. (2011) Elucidating the role of molecular signaling pathways in the tumorigenesis of basal cell carcinoma. *Semin Cutan Med Surg*, **30**:S6-S9
- Tang, J.Y., Mackay-Wiggan, J.M., Asterbaum, M. and Yauch, R.L. (2012) Inhibiting the Hedgehog Pathway in Patients with the Basal-Cell Nevus Syndrome. *N Engl J Med.*, **366**:2180-2188
- Tani, H., Morris, R.J. and Kaur, P. (2000) Enrichment for murine keratinocyte SCs based on cell surface phenotype. *Proc Natl Acad Sci U S A*, **97**:10960–5.
- Tauriello, D.V.F., Palomo-Ponce, S., Strok, D., Berenguer-Llargo, A., Badia-Ramentol, J. *et al.* (2018) TGF β drives immune evasion in genetically reconstituted colon cancer metastasis. *Nature*, **554**:538-543
- Taussig, D.C., Pearce, D.J., Simpson, C., Rohatiner, A.Z., Lister, T.A. *et al.* (2005) Hematopoietic stem cells express multiple myeloid markers: implications for the origin and targeted therapy of acute myeloid leukemia. *Blood*. **106**:4086–4092
- Taussig, D.C., Miraki-Moud, F., Anjos-Afonso, F., Pearce, D.J., Allen, K. *et al.* (2008) Anti-CD38 antibody-mediated clearance of human repopulating cells masks the heterogeneity of leukemia-initiating cells. *Blood*. **112**:568–575
- Taylor, M. D., Liu, L., Raffel, C., Hui, C.C., Mainprize, T.G. *et al.* (2002) Mutations in SUFU predispose to medulloblastoma. *Nature Genet.*, **31**:306–310
- Teh M.-T., Blaydon D., Chaplin T., *et al.* (2005) Genomewide single nucleotide polymorphism microarray mapping in basal cell carcinomas unveils uniparental disomy

as a key somatic event. *Cancer Res*, **65**:8597-8603

Telfer, N.R., Colver, G.B. and Morton, C.A. (2008) Guidelines for the management of basal cell carcinoma. *Br J Dermatol*, **159**(1):35-48

Temple, S. (2001) The development of neural SCs. *Nature*; **414**:112-117.

Teng, M.W.L., Swann, J.B., Koebel, C.M., Schreiber, R.D., and Smyth, M.J. (2008). Immune-mediated dormancy: an equilibrium with cancer. *J. Leukoc. Biol.*, **84**:988–993.

Teramoto, H., and Gutkind, J. S. (2013) Mitogen-Activated Protein Kinase Family in Encyclopedia of Biological Chemistry, Waltham: Academic Press

Terpstra, W., Ploemacher, R.E., Prins, A., van Lom, K., Pouwels, K. *et al.* (1996) Fluorouracil selectively spares acute myeloid leukemia cells with long-term growth abilities in immunodeficient mice and in culture. *Blood*. **88**:1944–1950

Tetteh, P.W. *et al.* (2016) Replacement of lost Lgr5-positive SCs through plasticity of their enterocyte-lineage daughters. *Cell SC*; **18**: 203–213

Thayer, S.P., di Magliano, M.P., Heiser, P.W., Nielsen, C.M., Roberts, D.J. *et al.* (2003) Hedgehog is an early and late mediator of pancreatic cancer tumorigenesis. *Nature*, **425**(6960):851-6

Theunissen, J.W. and de Sauvage, F.J. (2009) Paracrine Hedgehog signalling in cancer. *Cancer Res.*, **69**(15):6007-10

Thomas, D.A and Massague, J. (2005) TGF-beta directly targets cytotoxic T cell functions during tumor evasion of immune surveillance. *Cancer Cell*, **8**:369-380

Thuault, S., Valcourt, U., Petersen, M., Manfioletti, G., Heldin, C. H., and Moustakas, A. (2006) Transforming growth factor-beta employs HMGA2 to elicit epithelial-mesenchymal transition. *J Cell Biol*, **174**:175-183.

Tian, H., Callahan, C.A., DuPree, K.J., Darbonne, W.C., Ahn, C.P. *et al.* (2009) Hedgehog signalling is restricted to the stromal compartment during pancreatic carcinogenesis.

Proc Natl Acad Sci U S A., **106**(11):4254-9

Tian, H. *et al.* (2011) A reserve SC population in small intestine renders Lgr5-positive cells dispensable. *Nature*; **478**: 255–259.

Till, J.E. and McCulloch, E.A. (1961). A direct measurement of the radiation sensitivity of normal mouse bone marrow cells. *Radiat. Res.* **14**: 213–222.

Tilli, C.M., Van Steensel, M.A., Krekels, G.A. *et al.* (2005) Molecular aetiology and pathogenesis of basal cell carcinoma. *Br J Dermatol*, **152**:1108-24

Tjiu, J.W., Chen, J.S., Shun, C.T., Lin, S.J., Liao, Y.H. *et al.* (2009) Tumor-associated macrophage-induced invasion and angiogenesis of human basal cell carcinoma cells by cyclooxygenase-2 induction *J Invest Dermatol*, **129**:1016-1025

Tomasetti, C., Vogelstein, B. and Parmigiani, G. (2013). Half or more of the somatic mutations in cancers of self-renewing tissues originate prior to tumor initiation. *Proc Natl Acad Sci USA*, **110**:1999.

Tone, Y., Furuuchi, K., Kojima, Y., Tykocinski, M.L., Greene, M.I. (2008) Smad3 and NFAT cooperate to induce Foxp3 expression through its enhancer *Nat. Immunol.*, **9**:194-202

Tosolini, M., Kirilovsky, A., Mlecnik, B., Fredriksen, T., Mauger, S. *et al.* (2011) Clinical impact of different classes of infiltrating T cytotoxic and helper cells (Th1, th2, treg, th17) in patients with colorectal cancer. *Cancer Res*, **71**:1263-1271

Tovar, C., Rosinski, J., Filipovic, Z., Higgins, B., Kolinsky, K. *et al.* (2006). Small-molecule MDM2 antagonists reveal aberrant p53 signalling in cancer: implications for therapy. *Proc Natl Acad Sci U S A.*, **103**:1888–93

Trempeus, C.S., Morris, R.J., Bortner, C.D., Cotsarelis, G., Faircloth, R.S. *et al.* (2003) Enrichment for living murine keratinocytes from the hair follicle bulge with the cell surface marker CD34. *J Invest Dermatol.*, **120**:501–11

- Triscott, J., Lee, C., Foster, C., Manoranjan, B., Pambid, M.R. *et al.* (2013) Personalizing the treatment of pediatric medulloblastoma: polo-like kinase 1 as a molecular target in high-risk children. *Cancer Res.*, **73**:6734-6744
- Trompouki, E., Bowman, T.V., Lawton, L.N., Fan, Z.P., Wu, D-C. *et al.* (2011) Lineage regulators direct BMP and Wnt pathways to cell-specific programs during differentiation and regeneration. *Cell*, **147**:577-589.
- Tsukada, T., Fushida, S., Harada, S., Terai, S., Yagi, Y. (2013) Low- dose paclitaxel modulates tumour fibrosis in gastric cancer. *Int J Oncol*; **42**:1167–1174.
- Tukachinsky, H., Lopez, L.V. and Salic, A. (2010) A mechanism for vertebrate Hedgehog signalling: recruitment to cilia and dissociation of SuFu-GLI protein complexes. *J Cell Biol.*, **191**:415–428
- Tumbar, T., Guasch, G., Greco, V., Blanpain, C., Lowry, W.E. *et al.* (2004) Defining the epithelial SC niche in skin. *Science*, **303**:359–63
- Turner, N. and Grose, R. (2010) Fibroblast growth factor signalling: from development to cancer. *Nat Rev Cancer*. **10**(2):116-29
- Tuson, M., He, M. and Anderson, K.V. (2011) Protein kinase A acts at the basal body of the primary cilium to prevent GLI2 activation and ventralization of the mouse neural tube. *Development*, **138**:4921–4930
- Uchida, N., Buck, D.W., He, D. *et al.* (2000) Identification of human brain tumour initiating cells. *Proc Natl Acad Sci U S A*; **97**: 14720–14725. 103
- Vajdic, C.M., and van Leeuwen, M.T. (2009). Cancer incidence and risk factors after solid organ transplantation. *Int. J. Cancer*, **125**:1747–1754.
- Valent, P., Bonnet, D., DeMaria, R., Lapidot, T., Copland, M. *et al.* (2012) Cancer SC definitions and terminology: the devil is in the details. *Nature Rev. Cancer*, **12**:767–775

Vallier, L., Alexander, M., Pedersen, R.A. (2005) Activin/Nodal and FGF pathways cooperate to maintain pluripotency of human embryonic SCs. *J Cell Sci*; **118**:4495-4509.

Van Cutsem, E., Lenz, H.J., Köhne, C.H., Heinemann, V., Tejpar, S., Melezínek, I. *et al.* (2015) Fluorouracil, leucovorin, and irinotecan plus cetuximab treatment and RAS mutations in colorectal cancer. *J Clin Oncol*, **33**(7):692-700.

van den Brink, G.R. (2007) Hedgehog signalling in development and homeostasis of the gastrointestinal tract. *Physiol. Rev.*, **87**:1343–1375

van den Brink, G.R., Hardwick, J.C.H., Nielsen, C., Xu, C., ten Kate, F.J. *et al.* (2002) Sonic hedgehog expression correlates with fundic gland differentiation in the adult gastrointestinal tract. *Gut*, **51**:628-633

van der Schroeff, J.G., Evers, L.M., Boot, A.J., Bos, J.L. (1990) Ras oncogene mutations in basal cell carcinomas and squamous cell carcinomas of human skin. *Journal of Investigative Dermatology*, **94**: 423-425

van Dop, W.A., Heijmans, J., Büller, N.V., Snoek, S.A., Rosekrans, S.L. *et al.* (2010) Loss of Indian Hedgehog activates multiple aspects of a wound healing response in the mouse intestine. *Gastroenterology*, **139**:1665-1676

van Dop, W.A., Uhmman, A., Wijgerde, M., Sleddens-Linkels, E., Heijmans, J. *et al.* (2009) Depletion of the colonic epithelial precursor cell compartment upon conditional activation of the hedgehog pathway. *Gastroenterology*, **136**:2195-2203

van-den-Heuval, M. and Ingham, P.W. (1996) *Smoothed* encodes a receptor-like serpentine protein required for *hedgehog* signalling. *Nature*, **382**:547–551

van Es, J.H. *et al.* (2012) Dll1+ secretory progenitor cells revert to SCs upon crypt damage. *Nat. Cell Biol.*; **14**: 1099–1104.

van Rhenen, A., Moshaver, B., Kelder, A., Feller, N., Nieuwint, A.W. *et al.* (2007) Aberrant marker expression patterns on the CD34+CD38- stem cell compartment in acute myeloid leukemia allows to distinguish the malignant from the normal stem cell

compartment both at diagnosis and in remission. *Leukemia*. **21**:1700–1707.

van Schaeybroeck, S. *et al.* (2005) Epidermal growth factor receptor activity determines response of colorectal cancer cells to gefitinib alone and in combination with chemotherapy. *Clin. Cancer Res.*: **11**:7480–7489.

van Schaeybroeck, S. *et al.* (2008) Src and ADAM-17- mediated shedding of transforming growth factor- α is a mechanism of acute resistance to TRAIL. *Cancer Res.*; **68**:8312–8321.

Vander Heiden, M.G., Cantley, L.C., and Thompson, C.B. (2009). Understanding the Warburg effect: the metabolic requirements of cell proliferation. *Science*, **324**:1029–1033.

Vandewalle, C., Comijn, J., De Craene, B., Vermassen, P., Bruyneel, E. *et al.* (2005) SIP1/ZEB2 induces EMT by repressing genes of different epithelial cell-cell junctions. *Nucleic Acids Res*, **33**:6566-6578.

Vasquez, R.J., Howell, B., Yvon, A.M., Wadsworth P. and Cassimeris L. (1997) Nanomolar concentrations of nocodazole alter microtubule dynamic instability in vivo and in vitro. *Mol. Biol. Cell*, **8**:973–985.

Verschueren, K., Remacle, J.E., Collart, C., Kraft, H., Baker, B.S. *et al.* (1999) SIP1, a novel zinc finger/homeodomain repressor, interacts with SMAD proteins and binds to 5'-CACCT sequences in candidate target genes. *J Biol Chem.*, **274**:20489–98

Vidal, D., Matías-Guiu, X. and Alomar A (2004) Efficacy of imiquimod for the expression of Bcl-2, Ki67, p53 and basal cell carcinoma apoptosis. *Br J Dermatol*, **151**:656-62

Vijayachandra, K., Lee, J. and Glick, A.B. (2003) SMAD3 regulates senescence and malignant conversion in a mouse multistage skin carcinogenesis model. *Cancer Res.*, **63**:3447-52

- Vinals, F. and Pouyssegur, J. (2001) Transforming growth factor beta1 (TGF-beta1) promotes endothelial cell survival during *in vitro* angiogenesis via an autocrine mechanism implicating TGF-alpha signalling. *Mol Cell Biol*, **21**:7218–7230
- Vogelstein, B., Papadopoulos, N., Velculescu, V.E., Zhou, S., Diaz, L.A., Kinzler, K.W. (2013) Cancer genome landscapes. *Science*, **339** (6127): 1546-58
- Vogelstein, B., Papadopoulos, N., Velculescu, V.E., Zhou, S., Diaz, L.A. and Kinzler, K.W. (2013) Cancer genome landscapes. *Science*, **339**(6127):1546-58.
- Von Hoff, D.D., LoRusso, P.M., Rudin, C.M., Reddy, J.C., Yauch, R.L. *et al.* (2009) Inhibition of the Hedgehog Pathway in Advanced Basal-Cell Carcinoma. *N Engl J Med.*, **361**:1164-1172
- Vortkamp, A., Lee, K., Lanske, B., Segre, G.V., Kronenberg, H.M., and Tabin, C.J. (1996) Regulation of rate of cartilage differentiation by Indian hedgehog and PTH-related protein. *Science*, **273**:613–622
- Wagers, A.J. and Weissman, I.L. (2004) Plasticity of adult stem cells. *Cell*, **116**:639-648.
- Wagle, N., Emery, C., Berger, M.F., Davis, M.J., Sawyer, A. *et al.* (2011) Dissecting therapeutic resistance to RAF inhibition in melanoma by tumor genomic profiling. *J Clin Oncol.*, **29**(22):3085-96
- Walker, P. and Hill, D. (2006) Surgical treatment of basal cell carcinomas using standard postoperative histological assessment. *Australas J Dermatol*, **47**:1-12
- Wang, B. and Li, Y. (2006) Evidence for the direct involvement of β TrCP in Gli3 protein processing. *PNAS*, **103**: 33-38.
- Wang, G.Y., Wang, J., Mancianti, M-L. and Epstein, E.H. (2012) Basal Cell Carcinomas Arise from Hair Follicle SCs in PTCH1+/- Mice. *Cancer Cell*, **19**(1):114-124
- Wang, G.Y., Wang, J., Mancianti, M.L. and Epstein, E.H. Jr (2011) Basal Cell Carcinomas Arise from Hair Follicle SCs in PTCH1+/- Mice. *Cancer cell*, **19**(1):114-24

- Wang, J.G., Nakhuda, G.S., Guarnaccia, M.M., Sauer, M.V. and Lobo, R.A. (2007) Mullerian inhibiting substance and disrupted folliculogenesis in polycystic ovary syndrome. *Am. J. Obstet. Gynecol.*, 196(1):77e1-5
- Wang, L.C., Liu, Z.-Y., Gambardella, L., Delacour, A., Shapiro, R. *et al.* (2000) Conditional disruption of hedgehog signalling pathway defines its critical role in hair development and regeneration. *J. Invest. Dermatol.*, **114**:901-908
- Wang, Y., Zhou, Z., Walsh, C.T. and McMahon, A.P. (2009) Selective translocation of intracellular Smoothed to the primary cilium in response to Hedgehog pathway modulation. *Proc Nat Acad Sci USA*, **106**(8):2623–8.
- Wang, Y., Krivtsov, A.V., Sinha, A.U., North, T.E., Goessling, W. *et al.* (2010) The Wnt/beta-catenin pathway is required for the development of leukemia stem cells in AML. *Science*. **327**:1650–1653.
- Warburg, O. (1956a). On the origin of cancer cells. *Science*, **123**:309–314.
- Warburg, O. (1956b). On respiratory impairment in cancer cells. *Science*, **124**:269–270.
- Warburg, O.H. (1930). The Metabolism of Tumours: Investigations from the Kaiser Wilhelm Institute for Biology, Berlin-Dahlem. *British J. Surgery*, **19**(73)
- Watabe, T., and Miyazono, K. (2008). TGF β family signalling in SC renewal and differentiation. In: Derynck R, Miyazono K, eds. The TGF β Family. Cold Spring Harbor Laboratory Press: New York:585-612.
- Watabe, T. and Miyazono, K. (2009) Roles of TGF-beta family signalling in SC renewal and differentiation. *Cell Res*, **19**(1):103-15
- Watkins, D.N., Berman, D.M., Burkholder, S.G., Wang, B., Beachy, P.A. and Baylin, S.B. (2003) Hedgehog signalling within airway epithelial progenitors and in small-cell lung cancer. *Nature*, **422**(6929):313-7

Watkins, S.J., Jonker, L. and Arthur, H.M. (2006) A direct interaction between TGFbeta activated kinase 1 and the TGFbeta type II receptor: implications for TGFbeta signalling and cardiac hypertrophy. *Cardiovasc Res*, **69**:432–439.

Weedon, M.N., Lango, H., Lindgren, C.M., Wallace, C., Evans, D.M. *et al.* (2008) Genome-wide association analysis identifies 20 loci that influence adult height. *Nat. Genet.*, **40**:575-583

Weinstein, I.B. (2002) Cancer. Addiction to oncogenes--the Achilles heel of cancer. *Science*, **297**(5578):63-4.

Welslau, M., Diéras, V., Sohn, J.H. *et al.* (2014) Patient-reported outcomes from EMILIA, a randomized phase 3 study of trastuzumab emtansine (T-DM1) versus capecitabine and lapatinib in human epidermal growth factor receptor 2-positive locally advanced or metastatic breast cancer *Cancer*; **120**:642-651

Wertz, I.E., and Dixit, V.M., (2010) Regulation of death receptor signalling by the ubiquitin system. *Cell Death Differ.*, **17**(1):14–24

Weston, C.R. and Davis, R.J. (2007) The JNK signal transduction pathway. *Curr Opin Cell Biol*, **19**:142–149.

White, E., and DiPaola, R.S. (2009). The double-edged sword of autophagy modulation in cancer. *Clin. Cancer Res.*, **15**:5308–5316

White, A.C., Tran, K., Khuu, J., Dang, C., Cui, Y. *et al.* (2011) Defining the origins of Ras/p53-mediated squamous cell carcinoma. *Proc Natl Acad Sci U S A*. **108**:7425–30

Whitson, R.J., Lee, A., Urman, N.M., Mirza, A., Yao, C.Y. *et al.* (2018) Noncanonical hedgehog pathway activation through SRF-MKL1 promotes drug resistance in basal cell carcinomas. *Nat. Med.* **24**:271-281

Whyte, W.A., Orlando, D.A., Hnisz, D., Abraham, B.J., Lin, C.Y. *et al.* (2013) Master Transcription Factors and Mediator Establish Super-Enhancers at Key Cell Identity Genes. **153**:307-319

Wieser, R., Wrana, J.L. and Massague, J. (1995) GS domain mutations that constitutively activate T beta R-I, the downstream signalling component in the TGF-beta receptor complex. *The EMBO journal*, **14**(10):2199-2208.

Wieser, R.J.; Oesch, F. (1986). Contact Inhibition of Growth of Human Diploid Fibroblasts by Immobilized Plasma Membrane Glycoproteins. *J Cell Biol*, **103**: 361–367.

Wijgerde, M., Ooms, M., Hoogerbrugge, J.W., and Grootegoed, J.A. (2005) Hedgehog signalling in mouse ovary: Indian hedgehog and desert hedgehog from granulosa cells induce target gene expression in developing theca cells. *Endocrinology*, **146**:3558–3566

Wilkes, M.C., Mitchell, H., Penheiter, S.G. *et al.* (2005) Transforming growth factor-beta activation of phosphatidylinositol 3-kinase is independent of SMAD2 and SMAD3 and regulates fibroblast responses via p21-activated kinase-2. *Cancer Res*, **65**:10431–10440

Wilkes, M.C., Murphy, S.J., Garamszegi, N. and Leof, E.B. (2003) Cell-type-specific activation of PAK2 by transforming growth factor beta independent of SMAD2 and SMAD3. *Mol Cell Biol*, **23**:8878– 8889

Wilkes, M.C., Repellin, C.E., Kang, J-H., Andrianifahanana, M., Yin, X., Leof, E.B. (2015) Sorting nexin 9 differentiates ligand-activated Smad3 from Smad2 for nuclear import and transforming growth factor β signaling. *Mol. Biol. Cell*, **26**:3879-3891

Wing, K., Onishi, Y., Prieto-Martin, P., Yamaguchi, T., Miyara, T. *et al.* (2008) CTLA-4 control over FoxP3+ regulatory T cell function. *Science*, **322**:271-275

Witsch, E., Sela, M., and Yarden, Y., (2010) Roles for growth factors in cancer progression. *Physiology (Bethesda)*, **25**(2)85–101

Witta, S.E., Gemmill, R.M., Hirsch, F.R., Coldren, C.D., Hedman, K. *et al.* (2006) Restoring E-cadherin expression increases sensitivity to epidermal growth factor receptor inhibitors in lung cancer cell lines. *Cancer Res*. **66**:944–50

Wolter, M., Reifenberger, J., Sommer, C., Ruzicka, T. and Reifenberger, G. (1997) Mutations in the human homologue of the *Drosophila* segment polarity gene patched

- (*PTCH*) in sporadic basal cell carcinomas of the skin and primitive neuroectodermal tumors of the central nervous system. *Cancer Res.*, **57**:2581–2585
- Wong, C.S., Strange, R.C. and Lear, J.T. (2003) Basal cell carcinoma. *BMJ*, **327**:794-8
- Wong, S.Y. and Reiter, J.F. (2011) Wounding mobilizes hair follicle SCs to form tumors. *Proc Natl Acad Sci U S A*, **108**(10):4093-8
- Woo, S.H., Stumpfova, M., Jensen, U.B., Lumpkin, E.A. and Owens, D.M. (2010) Identification of epidermal progenitors for the Merkel cell lineage. *Development*, **137**:3965–71
- Woodworth, C.D., Michael, E., Smith, L., Vijayachandra, K., Glick, A. *et al.* (2004) Strain-dependent differences in malignant conversion of mouse skin tumors is an inherent property of the epidermal keratinocyte. *Carcinogenesis*, **25**:1771–1778
- Wrana, J. L., Attisano, L., Carcamo, J., Zentella, A., Doody, J. *et al.* (1992). TGF beta signals through a heteromeric protein kinase receptor complex. *Cell*, **71**:1003-1014.
- Wrana, J.L., Attisano, L., Wieser, R., Ventura, F. and Massague, J. (1994) Mechanism of activation of the TGF-beta receptor. *Nature*, **370**(6488):341-347.
- Wrighton, K.H., Lin, X., and Feng, X.-H. (2009) Phospho-control of TGF β superfamily signalling. *Cell Res.*, **19**:8-20
- Wu, A.M., Till, J.E., Siminovitch, L., McCulloch, E.A. (1967) A cytological study of the capacity for differentiation of normal hemopoietic colony-forming cells. *J. Cell Physiol.* **69**:177-184.
- Wu, A.M., Till, J.E., Siminovitch, L., McCulloch, E.A. (1968) Cytological evidence for a relationship between normal hemotopoietic colony-forming cells and cells of the lymphoid system. *J. Exp. Med.* **127**: 455–464.
- Wu, G., Chen, Y. G., Ozdamar, B., Gyuricza, C. A., Chong, P. A. *et al.* (2000). Structural basis of SMAD2 recognition by the SMAD anchor for receptor activation. *Science*, **287**:92-97

- Wu, M.Y. and Hill, C.S. (2009) TGF β Superfamily Signalling in Embryonic Development and Homeostasis. *Dev Cell*, **16**(3):329-43
- Wu, V.M., Chen, S.C., Arkin, M.R. and Reiter, J.F. (2012) Small molecule inhibitors of Smoothed ciliary localization and ciliogenesis. *Proc Natl Acad Sci U S A.*, **109**(34):13644-9
- Wu, C., Thalhamer, T., Franca, R.F., Xiao, S., Wang, C. *et al.* (2014) Galectin-9-CD44 interaction enhances stability and function of adaptive regulatory T cells. *Immunity*, **41**:270-282
- Xiao, Z., Latek, R., and Lodish, H. F. (2003). An extended bipartite nuclear localization signal in SMAD4 is required for its nuclear import and transcriptional activity. *Oncogene*, **22**:1057-1069.
- Xiao, Z., Liu, X., Henis, Y. I., and Lodish, H. F. (2000). A distinct nuclear localization signal in the N terminus of SMAD 3 determines its ligand-induced nuclear translocation. *Proc Natl Acad Sci U S A*, **97**:7853-7858.
- Xie, J., Johnson, R.L., Zhang, X., Bare, J.W., Waldman, F.M. *et al.* (1997) Mutations of the PATCHED gene in several types of sporadic extracutaneous tumors. *Cancer Res.*, **57**:2369–2372
- Xie, J., Murone, M., Luoh, S.M., Ryan, A., Gu, Q. *et al.* (1998) Activating Smoothed mutations in sporadic basal-cell carcinoma. *Nature*, **391**:90–92
- Xie, J., Murone, M., Luoh, S.M., Ryan, A., Gu, Q. *et al.* (1998) Activating Smoothed mutations in sporadic basal-cell carcinoma. *Nature*, **391**(6662):90-2
- Xie, T. and Spradling, A.C. (2000) A niche maintaining germ line SCs in the Drosophila ovary. *Science*, **290**(5490):328-30
- Xu, L., Kang, Y., Col, S. and Massague, J. (2002) Smad2 nucleocytoplasmic shuttling by nucleoporins CAN/Nup214 and Nup153 feeds TGFbeta signaling complexes in the

cytoplasm and nucleus. *Mol. Cell.* **10**:271-282

Xu, J., Lamouille, S., and Derynck, R. (2009) TGF-beta-induced epithelial to mesenchymal transition. *Cell Res*, **19**:156-172.

Yamada, M., Kodama, K., Fujita, S. *et al.* (1996) Prevalence of skin neoplasms among the atomic bomb survivors. *Radiat Res*, **146**:223-6

Yamaguchi, K., Shirakabe, K., Shibuya, H. *et al.* (1995) Identification of a member of the MAPKKK family as a potential mediator of TGF-beta signal transduction. *Science*, **270**:2008–2011

Yamamoto, M., Saijoh, Y., Perea-Gomez, A., Shawlot, W., Behringer, R.R. *et al.* (2004) Nodal antagonists regulate formation of the anteroposterior axis of the mouse embryo. *Nature*, **428**:387-392

Yamashita, Y.M., Yuan, H., Cheng, J., and Hunt, A.J. (2010) Polarity in stem cell division: asymmetric stem cell division in tissue homeostasis. *Cold Spring Harb. Perspect Biol.* **2**:a001313.

Yan, Z., Winawer, S., Friedman, E. (1994) Two different signal transduction pathways can be activated by transforming growth factor beta 1 in epithelial cells. *J Biol Chem*, **269**:13231–13237.

Yang J. and Weinberg, R.A. (2008) Epithelial-mesenchymal transition: at the crossroads of development and tumor metastasis. *Dev. Cell*, **14**:818-829

Yao, H.B., Shaw, P.C., Wong, C.C. and Wan, D.C. (2002) Expression of glycogen synthase kinase-3 isoforms in mouse tissues and their transcription in the brain. *J Chem Neuroanat*, **23**(4):291-297.

Yao, H.H., Whoriskey, W., and Capel, B. (2002) Desert Hedge- hog/Patched 1 signalling specifies fetal Leydig cell fate in testis organogenesis. *Genes & Dev.*, **16**:1433–1440

Yarden, Y. and Sliwkowski, M.X., (2001) Untangling the ErbB signalling network. *Nat Rev*

Mol Cell Biol, **2**(2):127-37.

Yauch, R.L., Dijkgraaf, G.J., Alicke, B., Januario, T., Ahn, C.P. *et al.* (2009) Smoothened mutation confers resistance to a Hedgehog pathway inhibitor in medulloblastoma. *Science*, **326**:572–4

Yauch, R.L., Gould, S.E., Scales, S.J., Tang, T., Tian, H. *et al.* (2008) A paracrine requirement for hedgehog signalling in cancer. *Nature*, **455**(7211):406-10

Ye, X. and Weinberg, R.A. (2015) Epithelial-Mesenchymal Plasticity: A Central Regulator of Cancer Progression. *Trends Cell Biol.* **25**:675-686

Yi, J.Y., Shin, I. and Arteaga, C.L. (2005) Type I transforming growth factor beta receptor binds to and activates phosphatidylinositol 3-kinase. *J Biol Chem*, **280**:10870–10876

Yilmaz, O.H., Valdez, R., Theisen, B.K., Guo, W., Ferguson, D.O. *et al.* (2006) Pten dependence distinguishes haematopoietic stem cells from leukaemia-initiating cells. *Nature*. **441**:475–482

Yin, H., Price, F. and Rudnicki, M.A. (2013) Satellite cells and the muscle SC niche. *Physiol. Rev.*, **93**:23-67

Ying, H., Kimmelman, A.C., Lyssiotis, C.A., Hua, S., Chu, G.C, *et al.* (2012) Oncogenic Kras maintains pancreatic tumors through regulation of anabolic glucose metabolism. *Cell*, **149**(3):656-70

Yogi, A., Callera, G. E., Tostes, R. C., and Touyz, R. (2006) c-Src mediates angiotensin II but not endothelin-1-induced activation of MAP kinases in vascular smooth muscle cells. *Hypertension*, **48**:E83-E84

Yoo, Y.A., Kang, M.H., Kim, J.S. and Oh, S.C. (2008) Sonic hedgehog signalling promotes motility and invasiveness of gastric cancer cells through TGF-beta-mediated activation of the ALK5-SMAD 3 pathway. *Carcinogenesis*, **29**(3):480-90

- Yoon, S.J., Foley, J.W. and Baker, J.C. (2015) HEB associates with PRC2 and SMAD2/3 to regulate developmental fates. *Nat. Commun.* **16**:6546
- Yoshida, T., Ozawa, Y., Kimura, T., Sato, Y., Kuznetsov G. *et al.* (2014) Eribulin meso- late suppresses experimental metastasis of breast cancer cells by reversing phenotype from epithelial-mesenchymal transition (EMT) to mesenchymal-epithelial transition (MET) states. *Br J Cancer*; **110**:1497–1505.
- You, H.N., Ding, W. and Rountree, C.B. (2010) Epigenetic regulation of cancer SC marker CD133 by transforming growth factor- β . *Hepatology*, **51**:1635– 1644
- Youssef, K.K., Lapouge, G., Bouvree, K., Rorive, S., Brohee, S. *et al.* (2012) Adult interfollicular tumour-initiating cells are reprogrammed into an embryonic hair follicle progenitor-like fate during basal cell carcinoma initiation. *Nat. Cell Biol.*, **14**:1282-1294
- Youssef, K.K., Van Keymeulen, A., Lapouge, G., Beck, B., Michaux, C. *et al.* (2010) Identification of the cell lineage at the origin of basal cell carcinoma. *Nat Cell Biol.*, **12**(3):299-305
- Yu, F., Kuo, C.T. and Jan, Y.N. (2006) *Drosophila* neuroblast asymmetric cell division: recent advances and implications for SC biology. *Neuron*, **51**:13–20
- Yu, L., Hebert, M.C. and Zhang, Y.E. (2002) TGF- β receptor-activated p38 MAP kinase mediates SMAD- independent TGF- β responses. *EMBO J*, **21**:3749–3759
- Yuan, T.L., and Cantley, L.C., (2008) PI3K pathway alterations in cancer: variations on a theme. *Oncogene*, **27**(41):5497–5510
- Yue, J., and Mulder, K. M. (2001) Transforming growth factor- β signal transduction in epithelial cells. *Pharmacol. Ther.*, **91**:1-34
- Yue, S., Chen, Y. and Cheng, S.Y. (2009) Hedgehog signalling promotes the degradation of tumor suppressor Sufu through the ubiquitin-proteasome pathway. *Oncogene*, **28**:492–499

Yun, J., Rago, C., Cheong, I., Pagliarini, R., Angenendt, P. *et al.* (2009) Glucose deprivation contributes to the development of KRAS pathway mutations in tumor cells. *Science*, **325**:1555

Yuspa, S.H. (1994) The pathogenesis of squamous cell cancer: lessons learned from studies of skin carcinogenesis--thirty-third G. H. A. Clowes Memorial Award Lecture. *Cancer Res.* **54**:1178–1189

Yuspa, S.H. (1998) The pathogenesis of squamous cell cancer: lessons learned from studies of skin carcinogenesis. *J Dermatol Sci.*, **17**:1–7

Zacharias, W.J., Li, X., Madison, B.B., Kretovich K., Kao, J.Y. *et al.* (2010) Hedgehog is an anti-inflammatory epithelial signal for the intestinal lamina propria. *Gastroenterology*, **138**:2368-2377

Zavadil, J., and Bottinger, E. P. (2005) TGF-beta and epithelial-to-mesenchymal transitions. *Oncogene*, **24**:5764-5774.

Zawel, L., Dai, J. L., Buckhaults, P., Zhou, S., Kinzler, K. W. *et al.* (1998) Human SMAD3 and SMAD4 are sequence-specific transcription activators. *Mol Cell*, **1**:611-617.

Zhang, H. S., Postigo, A. A., and Dean, D. C. (1999). Active transcriptional repression by the Rb-E2F complex mediates G1 arrest triggered by p16INK4a, TGFbeta, and contact inhibition. *Cell*, **97**:53-61.

Zhang, J., He, X.C., Tong, W.G., Johnson, T., Wiedemann, L.M. *et al.* (2006) Bone morphogenetic protein signaling inhibits hair follicle anagen induction by restricting epithelial stem/progenitor cell activation and expansion. *Stem Cells*. **24**:2826–39.

Zhang, J., Yang, P.L. and Gray, N.S. (2009) Targeting cancer with small molecule kinase inhibitors. *Nat Rev Cancer*, **9**:28-39.

Zhang, J.L., Qiu, L.Y., Kotzsch, A. Weidauer, S., Patterson, L. *et al.* (2008) Crystal structure analysis reveals how the Chordin family member crossveinless 2 blocks BMP-2 receptor binding. *Dev. Cell*, **14**:739-750

Zhang, Y.V., Cheong, J., Ciapurin, N., McDermitt, D.J., and Tumber, T. (2009) Distinct self-Renewal and differentiation phases in the niche of infrequently dividing hair follicle SCs. *Cell SC*, **5**:267–278

Zhang, D.X. and Glass, C.K. (2013) Towards an understanding of cell-specific functions of signal-dependent transcription factors. *J Mol Endocrinol.* **51**:T37-T50

Zhang, H. (2016) Three generations of epidermal growth factor receptor tyrosine kinase inhibitors developed to revolutionize the therapy of lung cancer *Drug Des Devel Ther*; **2**:3867-3872

Zhao, Y., Tong, C. and Jiang, J. (2007) Hedgehog regulates Smoothed activity by inducing a conformational switch. *Nature*, **450**:252–258

Zhao, D., Chen, X., Qin, N. *et al.* (2017) The prognostic role of EGFR-TKIs for patients with advanced non-small cell lung cancer *Sci Rep*; **12**:40374

Zheng, X., Mann, R.K., Sever, N. and Beachy, P.A. (2010) Genetic and biochemical definition of the Hedgehog receptor. *Genes Dev.*, **24**:57–71

Zhao, D., Chen, X., Qin, N. *et al.* (2017) The prognostic role of EGFR-TKIs for patients with advanced non-small cell lung cancer *Sci Rep*; **12**:40374

Zhou, L., Opalinska, J., and Verma, A. (2007) p38 MAP Kinase Regulates SC Apoptosis in Human Hematopoietic Failure. *Cell Cycle*, **6**:534-537

Zhou, X.P., Woodford-Richens, K., Lehtonen, R., Kurose, K., Aldred, M. *et al.* (2001) Germline Mutations in BMPR1A/ALK3 Cause a Subset of Cases of Juvenile Polyposis Syndrome and of Cowden and Bannayan-Riley-Ruvalcaba Syndromes. *Am J Hum Genet*, **69**(4):704-11

Zhu, C., Anderson, A.C., Schubart, A., Xiong, H., Imitola, J. *et al.* (2005) The Tim-3 ligand galectin-9 negatively regulates T helper type 1 immunity. *Nat. Immunol.* **6**:1245–1252.

Zhu, G.A., Sundram, U. and Chang, A.L. (2014) Two different scenarios of squamous cell carcinoma within advanced basal cell carcinomas: cases illustrating the importance of serial biopsy during vismodegib usage. *JAMA Dermatol*, **150**:970-973

Zhu, S., Wang, W., Clarke, D.C., Liu, X. (2007) Activation of Mps1 promotes transforming growth factor-beta-independent SMAD signalling. *J Biol Chem.*; **282**:18327–18338.

Zhu, Q. Krakowski, A.R. Dunham, E.E. Wang, L. Bandyopadhyay, A. *et al.* (2007) Dual role of SnoN in mammalian tumorigenesis. *Mol. Cell. Biol.*, **27**:324-339

Zhukova, N., Ramaswamy, V., Remke, M., Pfaff, E., Shih, D.J. *et al.* (2013) Subgroup-specific prognostic implications of TP53 mutation in medulloblastoma. *J. Clin. Oncol.*; **31**:2927–2935.

Zhuo, W., Wang, Y., Zhuo, X., Zhang, Y., Ao, X., Chen, Z. (2008) Knockdown of Snail, a novel zinc finger transcription factor, via RNA interference increases A549 cell sensitivity to cisplatin via JNK/mitochondrial pathway. *Lung Cancer*, **62**:8-14

Zilfou, J.T. and Lowe, S.W. (2009). Tumor suppressive functions of p53. *Perspect Biol.*, **1**(5): a001883

Zomer, A., Ellenbroek, S.I., Ritsma, L., Beerling, E., Vrisekoop, N. *et al.* (2013) Intravital imaging of cancer SC plasticity in mammary tumors. *SCs* **31**:602–6

Zorn, A.M., and Wells, J.M. (2007) Molecular basis of vertebrate endoderm development, *Int. Rev. Cytol.*, **259**:49-111